# Acta Physiologica Hungarica

VOLUME 81, NUMBER 1, 1993



Akadémiai Kiadó, Budapest

ACTA PHYSIOL. HUNG. APHDUZ. 81(1) 1–108 (1993) HU ISSN 0231—424X

# ACTA PHYSIOLOGICA HUNGARICA

## A PERIODICAL OF THE HUNGARIAN ACADEMY OF SCIENCES

*Acta Physiologica Hungarica* publishes original reports of studies in English.
*Acta Physiologica Hungarica* is published in one volume (4 issues) per year by

AKADÉMIAI KIADÓ

Publishing House of the Hungarian Academy of Sciences

H-1117 Budapest, Prielle Kornélia u. 19—35.

Manuscripts and editorial correspondence should be addressed to

*Acta Physiologica Hungarica*

H-1445 Budapest, P.O. Box 294, Hungary

Editor: P. Bálint

Managing editor: J. Bartha

*Subscription information*

Orders should be addressed to

AKADÉMIAI KIADÓ

H-1519 Budapest, P.O. Box 245

Subscription price for Volume 81 (1993) in 4 issues US$ 92.00, including normal postage, airmail delivery US$ 20.00.

*Acta Physiologica Hungarica* is abstracted/indexed in Biological Abstracts, Chemical Abstracts, Chemie-Information, Current Contents-Life Sciences, Excerpta Medica database (EMBASE), Index Medicus, International Abstracts of Biological Sciences

CONTENTS

PRINTED IN HUNGARY

Akadémiai Kiadó és Nyomda Vállalat, Budapest

# ACTA PHYSIOLOGICA HUNGARICA



VOLUME 81

AKADÉMIAI KIADÓ BUDAPEST

1993

*Acta Physiologica Hungarica, Volume 81 (1), pp. 3–11 (1993)*

# CONTROL ENGINEERING FOR PLANNING DRUG THERAPY

T. DEUTSCH, A. SALI

COMPUTER CENTRE, SEMMELWEIS UNIVERSITY OF MEDICINE, BUDAPEST, HUNGARY

Received November 6, 1991
Accepted September 19, 1992

An optimal drug input may be defined as producing an ideal therapeutic effect as closely as possible without exceeding predetermined safety limits on any adverse drug effects. The intensity and time patterns of the drug-elicited response are functions of the pharmacodynamic properties of the drug in the patient. Drug input optimisation can be considered as a control problem and the different control engineering techniques may serve to assist in planning/implementing drug dosage regimens.

This paper reviews some problems associated with planning optimal drug therapy in different clinical context and illustrates the solution of such problems by clinical examples.

**Keywords**: drug therapy, control engineering, planning drug dosage regimens, open-loop control, drug delivery systems

Drugs are administered to achieve a therapeutic objective. Figure 1 shows a simplified block diagram of drug therapy. In any event, the levels of effect actually being observed in the patient are compared to the level of response being sought, and the difference (described as the error signal) is then fed into a controller that adjusts drug dose rate [3, 4].

For long-acting, relatively safe drugs, the function of the controller can be performed by a clinician in the hospital ward, for short-acting drugs, however, this function is best accomplished by a mechanical computerized device called a drug-delivery system.

The mathematical relationship between the drug dosage, D and the time course of drug-induced response intensity, R is given by the following formal expression:

$$R = F(D, t, p)$$

Correspondence should be addressed to
Tibor DEUTSCH
Semmelweis University of Medicine, Computer Centre
H–1089 Budapest, Kálvária tér 5, Hungary

*Akadémiai Kiadó, Budapest*

where p represents a set of patient-specific parameters, such as elimination rate constant and volume of distribution [3].

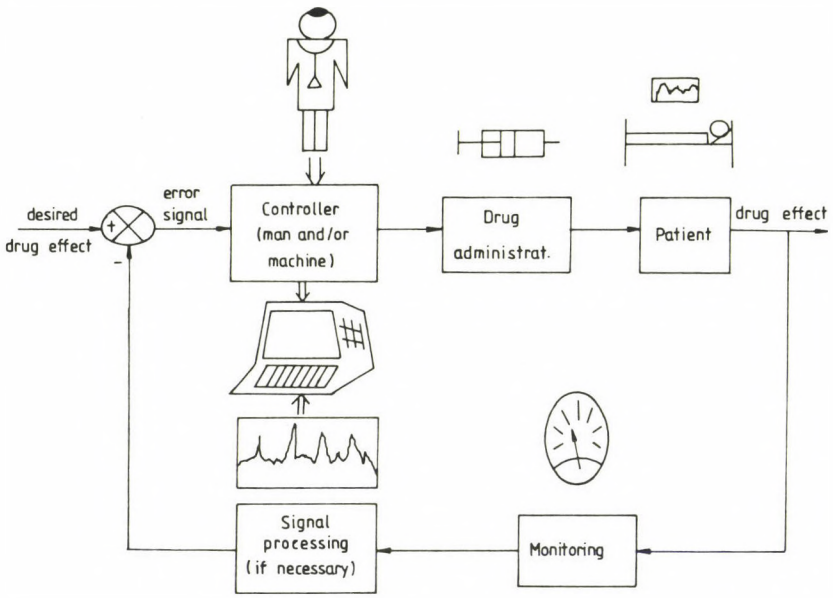


*Fig. 1.* Feedback control in drug therapy

Therapeutic objectives can be defined quantitatively by a "cost function" which depends on the measured response, target value or window and a penalty of not achieving the target. Drug input optimization means to determine the drug administration strategy which minimizes this cost function taking into account all constraints imposed by the clinical setting in which therapy should be applied.

*Drug administration as a control problem*

Drug dosage optimisation involves the operation of a feedback control loop in which the patient's response is measured following a known dosage, and a control algorithm is generated which optimizes the dose thereafter. Two types of control situations can be distinguished [5].

In the first case the patient's response to the current drug dosage is being sampled only infrequently or not at all. In these "data poor" situations the drug input is designed on the basis of information available before therapy started (open-loop control) or by occasional adjustment of drug administration when new data about the patient becomes available (open-loop feedback control).

In the second situation, in contrast, the drug dosage is a function of and directly related to the response of the patient; i.e. the rate of drug administration is continuously adjusted on those data to achieve selected targets (closed-loop control).

*Open-loop control (The target plasma level strategy)*

Once the characteristic parameters of drug kinetics are known in a particular patient (for example by applying a test dose before therapy started), an "a priori" dosage regimen may be determined that is consistent with the goals of the therapy.

For drugs with narrow therapeutic range, these dosage regimens, because of their lack of flexibility may lead either to unsatisfactory therapeutic responses and/or to unacceptable toxic effects. At least occasional monitoring of the patient's response to the current therapy is needed to ensure therapeutic objectives to be achieved.

The open-loop feedback strategy which realizes this objective consists of the following steps: (i) administration of a searching dosage based on patient-related data and general medical knowledge available prior to drug therapy such as serum creatinine level and population-based correlations between kinetic parameters in various disease states, (ii) monitoring the drug-elicited response with an optimal sampling strategy and (iii) adjust current therapy whenever the clinical status of the patient differs from the target one.

The target plasma level strategy constitutes the most widely used approach to calculate individualized dosage regimens. The underlying assumption is that a strong correlation exists between the level of drug in the plasma and the effect(s) induced.

For example, it is generally accepted that the blood level of antimicrobials used to treat bacterimias should exceed the minimum inhibitory concentration (MIC) while remaining below toxic levels.

The two principal reasons to obtain drug levels (monitoring) are (i) to see what they are and (ii) to get information to achieve levels we want the patient to have. Although the number of plasma level observations is never "enough", at some point we reach diminishing returns with further serum levels. As a rule of thumb, one should obtain at least 4 serum samples during a patient's course of therapy, spread over several dose intervals.

Monitored plasma levels allow pharmacokinetic models to be adjusted for individual patients. The precision of the parameter estimates will also depend on the proper selection of times at which blood samples are taken. Drug concentrations collected at optimal sampling times carry maximal information, i.e. these levels are most sensitive to (and changed by) a change in the value of the kinetic parameter to be determined.

For drugs obeying one-compartment kinetics at (or near) the peak is the best time to draw serum level to find most accurately the value representing the volume of

distribution and sampling at a time equal to 1/ln2 times the drug's half life is recommended to get the best estimate for the elimination rate constant [4].

The plasma concentration of a drug at a desired level over a prolonged period of time can be best maintained by continuous intravenous infusion. When the time to reach the steady state is appreciable, it may be desirable to administer a loading dose.

If a drug is administered in repetitive doses the fluctuations between peak and trough plasma levels depend on the dosing interval as shown in Fig. 2.

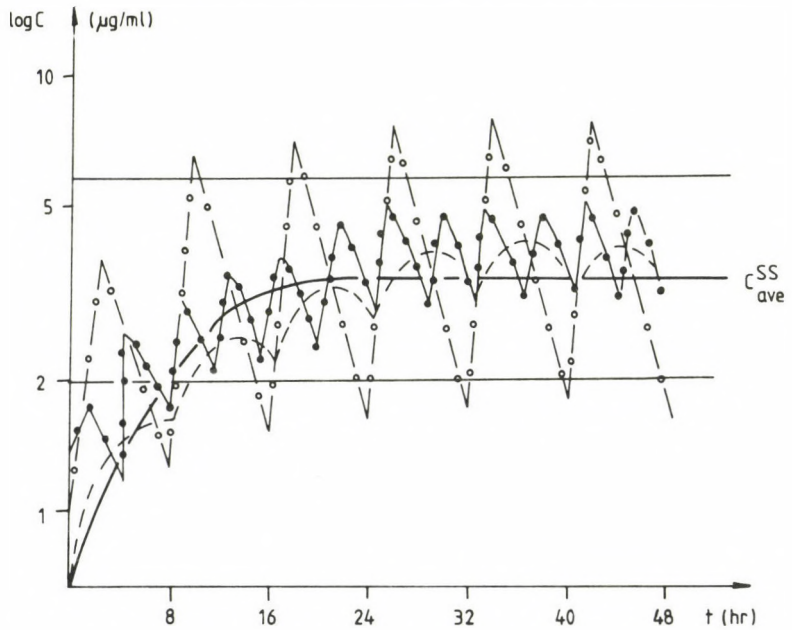


*Fig. 2.* Simulated serum levels of a hypothetical drug with different dosing interval

Among several factors that may affect the dosing rate (the dose administered per unit of time), the most important is the drug's clearance. Because this pharmacokinetic parameter is usually altered by diseases, it is important to determine its value for each subject.

For example, aminoglycoside antibiotics are mainly excreted via the kidneys, hence the elimination rate constants (ke) of these drugs, ke are correlated to the renal function characterized by the patient's creatinine clearance rate (Clcr):

$$ke = a + b\ Clcr$$

where a and b are regression coefficients for a given population of patients. Similarly the volume of distribution, Vd can be estimated using the patient's (lean) body weight.

The values of ke and Vd allow drug clearance to be computed as Cl = ke Vd, which in turn uniquely determines the total daily dose required to achieve a predefined average daily plasma level, $C^{ss}$:

$$D = C^{ss}\, Cl\, 24$$

Fluctuations can be kept within acceptable limits by adjusting the dosing frequency at which the total daily dosage is administered [2].

Cancer chemotherapy represents a more complex situation in which conflicting objectives such as maximizing cell kill at a tumor site, while minimizing damage elsewhere should be harmonised to obtain individually tailored drug regimes.

The kinetic model of the anticancer drug, methotrexate (MTX), incorporating the important enterohepatic circulation and the detailed compartmentalization of the gastro-intestinal tract and bile duct is shown in Fig. 3.

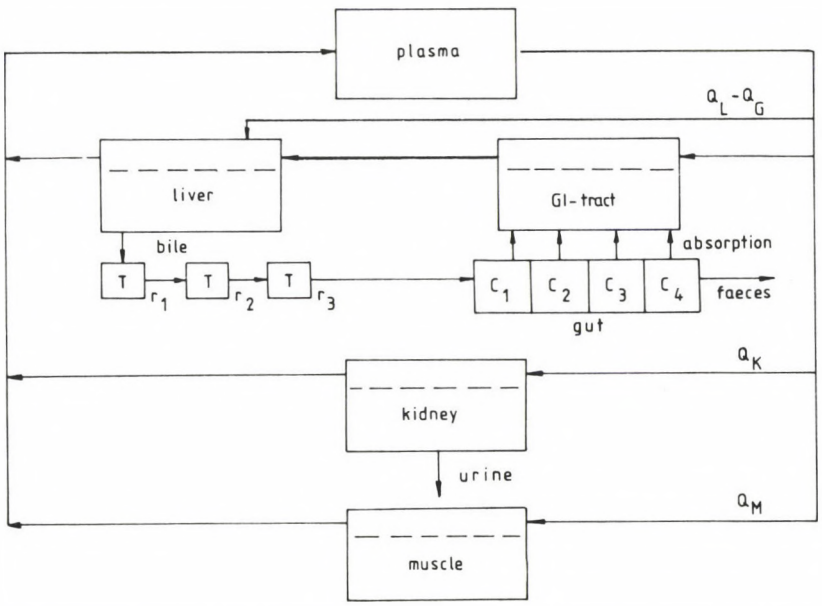


*Fig. 3.* Compartment model of MTX pharmacokinetics [2] ($Q_L$, $Q_K$, $Q_G$ refer to the hepatic, renal and intestinal blood flow rate, respectively. T denotes compartments in the bile duct while $r_1$, $r_2$ and $r_3$ represent transfer rate constants between the serially connected bile duct segments)

The tumor is assumed to be localized in the muscle compartment of the model in which a concentration, $c_m$ of $10^{-8}$ M is known to be sufficient to kill cancerous

cells *in vivo*. Thus the objective is to find an appropriate MTX infusion profile which will elevate $C_m$ to that critical level while maintaining drug level in other compartments such as liver, gut and kidneys as close to zero as possible. The optimal infusion rate vs time profile satisfying this criteria is shown in Fig. 4.

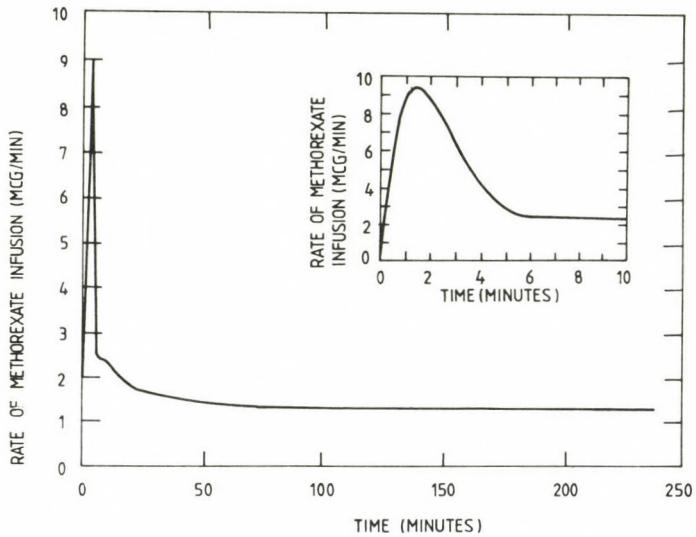


*Fig. 4.* Optimal MTX infusion rate vs time profile [2]

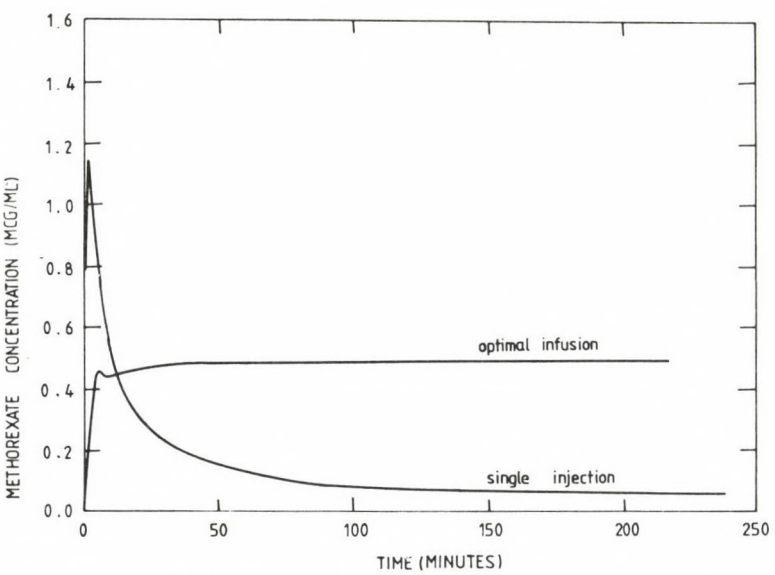


*Fig. 5.* The time course of MTX levels in the muscle following single injection and during the optimal infusion regime

Figure 5 presents a comparison of the drug concentrations over time in the muscle compartment during the optimal MTX infusion therapy and following a single injection of the drug.

As it is shown the drug concentration in the site of tumours quickly reaches the target level and in addition, the optimal drug input assures that the drug level can be maintained at the lethal level as long as desired.

On the other hand, the bolus therapy results in possibly toxic drug levels immediately after administration, moreover the therapeutic effect is expected to disappear 15–20 minutes after drug injection.

*Closed-loop drug delivery systems*

The continuous monitoring of the drug-elicited response and the use of this information for controlling drug input rate can produce clinical responses close to the desired profile. To achieve this objective a great variety of methods has been developed which differ in the extent to which they rely on models of drug pharmacodynamics.

The simplest class of methods do not refer to any model and apply on-off algorithms. One of these non-model-based algorithms turns on infusion if the measured variable differs from its desired level by more than a certain value, and turns off infusion when the output reaches the desired level. Such algorithms are generally safe and robust, but may cause considerable overshoot.

Other type of non-model-based algorithms are imbedded in controllers which compute drug infusion rate as function of the error and its rate of change. This algorithm is simple and very effective when the system is nearly time invariant and additional rules serve to assure that only safe levels of drugs are infused.

The third class of control algorithms involves the use of some mathematical model of the system to be controlled. Once a model of the controlled process is available, initial estimates of the controller parameters to yield satisfactory performance may be derived. Such model-based techniques also allow controller parameters to be updated as the system changes, leading to adaptive control [5].

Conventional insulin therapy consisting of two to four daily subcutaneous insulin injections seldom keeps a diabetic patient in near-normoglycaemic conditions. In the last two decades several efforts have been made to develop improved methods for achieving ideal blood glucose control in diabetic patients by means of external devices called artificial pancreas. This closed-loop system constitutes the first human imitation of a gland of internal secretion which determines the insulin infusion rate in accordance with monitored blood glucose levels as shown in Fig. 6 [1].

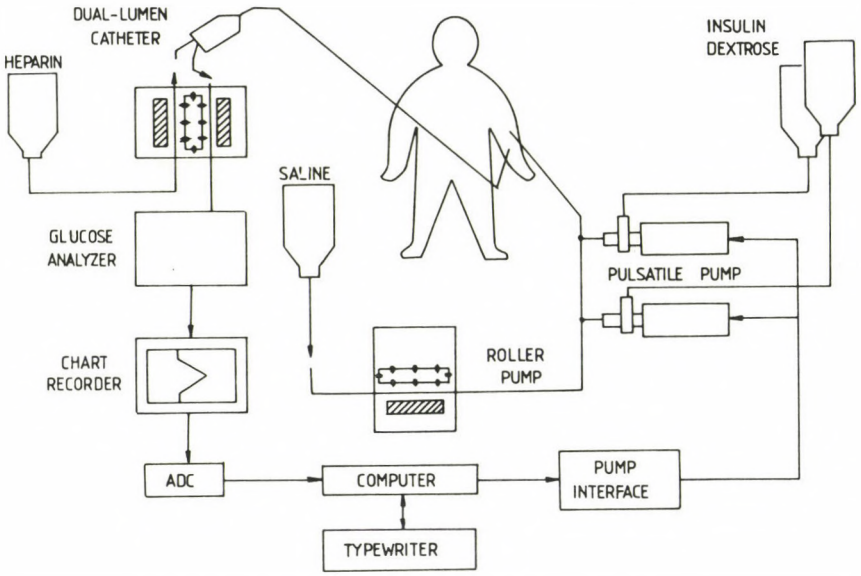


*Fig. 6.* The scheme of closed-loop control of blood sugar

Early versions of such devices have adopted control algorithms for insulin delivery based on the absolute value and rate of change of the deviation between measured and target blood glucose levels. More recent artificial beta cells, however, intensively use mathematical models of the glycoregulatory system for updating patient-specific model parameters in real-time and for adjusting insulin delivery in accordance with major changes and individual differences in the carbohydrate metabolism of patients.

Miniaturized closed-loop drug delivery systems (for example an implantable version of the artificial beta cell) are expected to play a dominant role in drug therapy in the future representing a new generation of drug products with individually tailored drug release characteristics.

**Acknowledgement**

The authors thank Cs. Stanka for his assistance in drawing the figures of this paper.

## REFERENCES

1. Albisser, A. M.: Intelligent instrumentation in diabetes management. CRC Critical Review in Biomedical Engineering **17**, 1–24 (1989), CRC Press Inc.
2. Dedrick, R. L.: Animal scale-up. Journal of Pharmacokinetics and Biopharmaceutics, **1**, 435–461 (1973).
3. Deutsch, T., Ludwig, E., Graber, H., Houin, J.: Fundamentals of clinical pharmacokinetics. In: Human Pharmacology. P. Kuemmerle, J. Shybuya and J.P. Tillement, eds, Elsevier Publ., Amsterdam 1991, pp. 291–485.
4. Jelliffe, R. W.: Clinical applications of pharmacokinetics and control theory. In: Selected Topics in Clinical Pharmacology. R. Maronde ed. Springer Verlag, New York 1986, pp. 26–82.
5. Vozeh, S. & Steimer, J.L. Control theory in drug therapy. Clinical Pharmacokinetics **10**, 457–476 (1986).

*Acta Physiologica Hungarica, Volume 81 (1), pp. 13–18 (1993)*

# PROTECTIVE EFFECTS OF THE INHIBITION OF THE RENIN-ANGIOTENSIN SYSTEM AGAINST GASTRIC MUCOSAL LESIONS INDUCED BY COLD-RESTRAINT IN THE RAT

F. ENDER, T. LABANCZ*, L. ROSIVALL**

*DEPARTMENT OF SURGERY SCHÖPF-MEREI HOSPITAL, AND **DEPARTMENT OF PATHOPHYSIOLOGY, SEMMELWEIS UNIVERSITY MEDICAL SCHOOL, DEPARTMENT OF SURGERY POSTGRADUATE MEDICAL UNIVERSITY, BUDAPEST, HUNGARY

Received February 12, 1992
Accepted September 8, 1992

Experiments were designed to examine whether inhibition of the renin-angiotensin system alters gastric mucosal damage in conscious rats subjected to restraint. Two hours immobilization resulted in an ulcer index of 46 ± 4 (n = 16) which was decreased by converting enzyme inhibitor (MK 422, enalaprilat) doses of 1 and 10 $mg \cdot kg^{-1} \cdot h^{-1}$ by 50 ± 16 (n = 8) and 66 ± 8% (n = 13), respectively ($p < 0.05$). Gastric blood flow measured by both the $^{99}Tc$-labelled frog erythrocytes and $^{86}Rb$-clearance methods was low in untreated rats and increased to more than three-fold in angiotensin converting enzyme inhibitor treated animals. Infusion of saralasin a specific angiotensin II receptor blocker (5 $\mu g \cdot kg^{-1} \cdot h^{-1}$, n = 25) also decreased the ulcer index by 40 ± 5% ($p < 0.05$). Thus inhibition of the renin-angiotensin system in conscious cold-restraint rat increased gastric blood flow and reduced mucosal damage. These results suggest that the renin-angiotensin system plays a significant role in the development of experimental gastric ulcer in the cold-restraint model.

**Keywords:** angiotensin converting enzyme inhibition, enalaprilat, gastric mucosa, saralasin, gastric blood flow, experimental stress-ulcer

The pathogenesis of stress-induced gastric lesions is far from being understood. A considerable body of laboratory and clinical evidence, however, indicates that mucosal, endocrine, vascular and neurogenic factors may be associated with this serious gastrointestinal disorder [4, 8].

The importance of the renin-angiotensin system (RAS) in the regulation of microcirculation in various organs under normal and particularly pathophysiological conditions is increasingly recognized [6]. It is also well established that impairment of

Correspondence should be addressed to
László ROSIVALL MD., PhD., DMSc.
Semmelweis University Medical School, Department of Pathophysiology
H–1445 Budapest, P.O. Box 370
1089 Budapest Nagyvárad tér 4, Hungary
Telephone: (36–1)–133–1939, Fax: (36–1)–113–8090

*Akadémiai Kiadó, Budapest*

local circulation plays a role in the development of mucosal damage in acute experimental gastric lesions induced by different manipulations [9]. Under extreme stress-conditions the RAS may be stimulated and levels of the vasoconstrictor angiotensin II may be increased.

It has been demonstrated that in cardiogen shock induced gastric mucosal laesions, converting enzyme inhibition decreased the severity of the mucosal damage [1]. In a recent study, however, the authors found opposite effects of converting enzyme inhibition on gastric stress ulcer, i.e. the high dose of Captopril worsened the lesions in immobilized cold-restraint model [5].

Our experiments have been designed to evaluate whether activation of RAS plays a role in the pathomechanism of gastric mucosal damage induced by cold-restraint. For this reason we studied the effects of inhibition of the RAS by an angiotensin converting enzyme inhibitor and a specific angiotensin II receptor antagonist.

## Material and methods

The experiments were carried out on male Wistar rats (200–250 g), deprived of food for 48 h but having free access to water. Under light ether anaesthesia tracheotomy was performed and a catheter was inserted into the right common carotid artery through which blood pressure was monitored by a mercury manometer. The right jugular vein was also catheterized for administration of drugs.

After recovery from anaesthesia the animals were immobilized in supine position by fixing their extremities to a wooden plate and they were kept in a cold room at 4 °C for two hours.

Renin-angiotensin system was inhibited MK 422 (enalaprilat, diacid form, Merck Sharp & Dohme, West Point, PA) and saralasin ($Sar^1$, $Ala^8$-Angiotensin II, SIGMA, St. Louis, Mo), respectively. The converting enzyme inhibitor was administered in a priming dose (1 or 10 $mg \cdot kg^{-1}$) intraperitoneally followed by intravenous infusion of 1 or 10 $mg \cdot kg^{-1} \cdot h^{-1}$ throughout the experiment. Angiotensin II receptor blocker was administered intravenously at a rate of 5 $\mu g \cdot kg^{-1} \cdot h^{-1}$. These doses of the inhibitors were demonstrated to minimize the pressor response to angiotensin I under different experimental conditions [7, 12, 13]. At the end of the experiments the animals were decapitated, the stomach was removed and opened along the greater curvature, rinsed quickly with cold water and carefully inspected by an observer unaware of the drug administered. Haemorrhagic areas and epithelial lesions were scored according to the following: petechiae = 1; erosions: 1 mm in length or diameter = 2; between 1 and 2 mm = 3; between 2 and 4 mm = 4; large than 4 mm = 5. The scores were then summed to obtain an ulcer index (UI) for the animal examined. Animals receiving vehicle (physiological saline) served as controls. Ulcer index of the treated animals was compared to those obtained from untreated rats at the same time.

In a separated group of animals at the end of the two-hour experimental period gastric mucosal blood flow was measured by $^{86}Rb$-clearance technique and by using $^{99}Tc$-labelled frog erythrocytes as described elsewhere [3, 11]. Two different methods were utilized for blood flow measurements because of the known inherent errors of the measuring techniques of the nutritive blood flow in tissues [11]. To avoid the error due to the usage of two gamma-radiating isotopes each measurement was carried out in different animals.

Data were analyzed by Wilcoxon's signed rank test. Differences were accepted as significant where P values were 0.05 or less. All results presented are means ± SE.

## Results

In conscious rats two-hour exposure to cold-restraint yielded a high ulcer index 46 ± 4 (n = 16). Following treatment with ACE inhibitor (MK 422) both at low- (1 $mg \cdot kg^{-1} \cdot h^{-1}$; n = 8) and in high-dose (10 $mg \cdot kg^{-1} \cdot h^{-1}$; n = 13) groups ulcer-index was significantly reduced by 50 ± 16 and 66 ± 8%, respectively (Fig. 1). Gastric blood flow was measured with two different techniques. Flow values obtained by both the $^{99}$Tc-labelled frog erythrocytes and $^{86}$Rb-clearance methods were low in untreated rats and increased by more than three times in ACE inhibitor treated animals while the mean systemic blood pressure was significantly reduced (Table I).

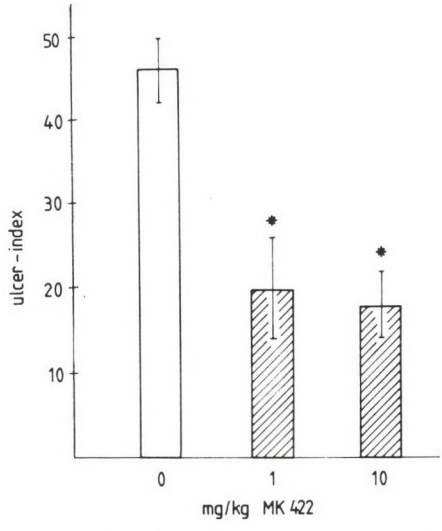


*Fig. 1.* Effects of angiotensin converting enzyme inhibitor (MK 422) in two different doses (1 and 10 $mg \cdot kg^{-1} \cdot h^{-1}$, i.p.) on gastric mucosal damage induced by cold-restraint in the rat. For determination of ulcer-index and further details see Methods. Groups included 16 (controls), 8 and 13 animals, respectively. Values are means ± SE, * $p < 0.05$

**Table I**

*Effects of ACE inhibition on gastric blood flow in cold-restraint rats*

| Group | BP mm Hg | Gastric blood flow $ml \cdot min^{-1} \cdot g^{-1}$ | |
|---|---|---|---|
| | | $^{86}$Rb-clearance | $^{99}$Tc-erythrocyte |
| Control | 110 ± 4 (9) | 0.030 ± 0.010 (5) | 0.045 ± 0.006 (4) |
| MK 422 | 89 ± 3* (10) | 0.103 ± 0.020* (6) | 0.170 ± 0.010* (4) |

BP = systematic arterial blood pressure; MK 422 = enalaprilat, diacid form; number of animals in parentheses; $\bar{x}$ ± SE; * $p < 0.05$. For further details see Methods.

To investigate further the role of the RAS in stress induced gastric ulceration, a specific angiotensin II receptor blocker was infused to animals (n = 25). Saralasin (5 $\mu g \cdot kg^{-1} \cdot h^{-1}$) also decreased ulcer index significantly by 40 ± 5%. Saralasin infusion decreased systemic blood pressure (132 ± 2 mm Hg) by 24 ± 3 mm Hg, while the spontaneous decrease in the untreated animals was 13 + 4 mm Hg during the two-hour observation period. The difference of these reductions was not statistically significant.

## Discussion

While it has become apparent that acute ulceration may follow a variety of stress conditions both in man and animals, the mechanisms by which the various disease states lead to acute ulceration remains at least partly unsolved. Several attempts have been made to study the acute stress ulceration induced by cold-restraint and to prevent it by vagotomy, anticholinergic and sympatholytic drugs, adrenalectomy, reduced intestinal bacterial flora, etc. A number of functional and morphological studies has been performed and concluded that local ischemia may play an important role in the development of gastric mucosal damage beside many other preconditioning or inducing factors [8, 14].

According to our latest knowledge appropriate investigations have not been carried out to examine the effects of the action of angiotensin II among the various putative aetiologic factors involved in the induction of gastric mucosal lesions in stress ulcer. Our experiment has been designed to find out whether or not inhibition of the RAS system has a protective effect against the development of gastric mucosal lesions in cold-restraint animals. Both the converting enzyme inhibitor and the specific angiotensin II receptor blocker reduced the mucosal gastric damage significantly and in a similar degree. These protective effects of ACE inhibitor were associated with a marked increase in gastric blood flow.

The $^{86}Rb$-clearance and the $^{99}Tc$-labelled frog erythrocyte methods that were used to measure the change in gastric blood flow due to the inhibition of renin-angiotensin system gave different absolute values as it was expected [11, 15] but the relative changes were similar.

Gastric blood flow measured in cold-restraint state was lower than the basal flow under normal conditions characterized by different methods [15] but it was similar to those obtained under different stress conditions [10]. These low blood flow values returned to the normal range during ACE inhibition. This could be caused by many different local and systemic, neurogenic and hormonal factors. The blood pressure response and the increase in local blood flow, however, suggest that under cold restraint the renin-angiotensin system is stimulated, and the gastric vasculature is responsive to angiotensin II.

The protective effects of ACE inhibition may be explained by maintaining normal blood supply. There are at least two different mechanisms which may lead to this vasodilation. One would be the decrease of the concentration of the vasoconstrictor peptide, angiotensin II, the other would be an increase in levels of vasodilator kinins secondary to inhibition of kininase activity [16]. The similar effects of the angiotensin II receptor blocker to those of enalaprilat suggest that the protection against gastric ulcer during ACE inhibition is, at least partly, due to the decreased formation of angiotensin II.

It is of interest that in a recent study when Captopril was administered in a dose of 100 times higher than that used in our study, it has been found that Captopril may worsen the gastric mucosal damage in restraint cold model [5]. It is known, however, that Captopril in a dose that exceeds 20–200 times the maximum human dose recommended increases the incidence of gastric mucosal erosion/ulceration in male rats [2]. The mechanism of this effect is not known but it may well be independent from the renin-angiotensin system.

In conclusion, we have demonstrated that ACE inhibition and saralasin treatment (i.e. inhibition of renin-angiotensin system) can reduce the gastric mucosal damage in cold-restraint animals. This suggests that the increased activity of renin-angiotensin system may contribute to the development of the acute gastric lesions induced by cold-restraint.

**Acknowledgements**

We are grateful to S. Adamkó for technical assistance and Merck, Sharp & Dohme for supplying MK 422. This work was supported by Grant OTKA-1093 from the Hungarian Research Foundation and Grant T 227/1990 from the Hungarian Ministry of Welfare.

## REFERENCES

1. Bailey, R. W., Buckley, G. B., Hamilton, S. R. et al.: The fundamental hemodynamic mechanism underlying gastric stress ulceration in cardiogenic shock. Ann. Surg. **205**, 597–600 (1987).
2. Physicians' desk reference. 42. Edition Med. Economic Co. Inc. New Jersey, pp. 2046–2048 (1988).
3. Buehler, R. W., Catanzaro, A. J., Stein, J. H., Hunter, W.: The radio-labelled frog red blood cell. A new marker of cortical blood flow distribution in the kidney of the dog. Circ. Res. **32**, 718–724 (1973).
4. Brooks, F. P.: The pathophysiology of peptic ulcer disease. Dig. Dis. and Sci. **30**, 15–27 (1985).
5. Cullen, J. J., Ephgrave, K. S.: Angiotensin-converting enzyme inhibition, kinin and stress ulceration. Current Surg. **452**, 485–499 1990.
6. Dzau, V. J.: Vascular effects of local angiotensin production. Am. J. Cardiol. **59**, 59A–65A (1987).
7. Fejes-Tóth, G., Zahajszky, T., Filep, J.: Renal response to AVP and DDAVP after angiotensin II blockade in the rat. Am. J. Physiol. (Renal Fluid Electrolyte Physiol.) **244**, F205–F209 (1983).
8. Goldmann, H., Rosoff, C. B.: Pathogenesis of acute gastric stress ulcers. Am. J. Pathol. **52**, 227–237 (1986).

8. Goldmann, H., Rosoff, C. B.: Pathogenesis of acute gastric stress ulcers. Am. J. Pathol. **52**, 227–237 (1986).
9. Guth, P. H., Hall, P.: Microcirculatory and mast cell changes in restraint-induced gastric ulcer. Gastroenterology **50**, 562–570 (1966).
10. Holm, H., Perry, M. A.: Role of blood flow in gastric acid secretion. Am. J. Physiol. **254**, (Gastrointest. Liver, Physiol. 17) G281–G293 (1988).
11. Rosivall, L., Hope, A., Clausen, G.: Incomplete and flow dependent extraction of 86Rb in the rat kidney. Pflügers Arch. **390**, 216–218 (1981).
12. Rosivall, L., Narkates, A. J., Oparil, S., Navar, G.: De novo intrarenal formation of angiotensin II during control and enhanced renin secretion. Am. J. Physiol. **252**, (Renal Fluid Electrolyte Physiol. 21) F1118–F1123 (1987).
13. Sweet, C. S., Arbegast, P. T., Gaul, S. L., Blaine, E. H., Gross, D. M.: Relationship between angiotensin I blockade and antihypertensive properties of single doses of MK-421 and captopril in spontaneous and renal hypertensive rats. European J. Pharmacol. **76**, 167–176 (1981).
14. Szabó, S.: Stress and gastroduodenal ulcers. Stress **1**, 25–36 (1980).
15. Szabó, G., Fazekas, Á., Rosivall, L., Pósch, E.: Measurement of regional blood flow with sulfanilamide (4-amino benzene sulfonamide). Res. Exp. Med. (Berl) **177**, 23–32 (1980).
16. Yang, H., Erdős, E., Levin, Y.: A dipeptidyl carboxipeptidase that converts angiotensin I and inactivates bradykinin. Biochem. Biophys. Acta **214**, 374–380 (1970).

*Acta Physiologica Hungarica, Volume 81 (1), pp. 19–28 (1993)*

# INFLUENCE OF SELECTIVE OPIATE ANTAGONISTS ON STRIATAL ACETYLCHOLINE AND DOPAMINE RELEASE

B. LENDVAI, N. T. SÁNDOR, A. SÁNDOR

INSTITUTE OF EXPERIMENTAL MEDICINE, DEPARTMENT OF PHARMACOLOGY,
HUNGARIAN ACADEMY OF SCIENCIES, BUDAPEST, HUNGARY

Received March 31, 1992
Accepted June 10, 1992

In the present study the effect of selective opiate antagonists on the release of acetylcholine (ACh) and dopamine (DA) was studied in striatal slices. β-funaltrexamine (β-FNA) a μ receptor antagonist, naltrindole (NTI) a δ receptor antagonist and a κ receptor antagonist nor-binaltorphimine (nor-BNI) were used to selectively block the different opioid receptor subpopulations located on the axon terminals. The receptor activation was examined on superfused slices from rat striatum previously labelled with [$^3$H]choline or [$^3$H]dopamine.

We found that both β-FNA and NTI significantly enhanced the evoked release of ACh using electrical field stimulation but it occurred only in those cases when dopaminergic input was impaired either by lesion of the nigrostriatal tract or by $D_2$ dopamine receptor blocade. By contrast, under these conditions the opiate antagonists had no modulatory effect on the release of DA.

Our data suggest that the release of ACh in the striatum is under the tonic control of endogenous opioid peptides. This effect is mediated via μ and δ opioid receptors. However the striatal DA release does not seem to be controlled tonically by opioid peptides.

**Keywords:** endogenous opioids, μ receptor, δ receptor, ACh release, DA release, non-synaptic interaction

Now it is widely accepted that the cholinergic interneurons of the corpus striatum are under control of DA released from the nigrostriatal tract which is believed the most important afferent projection of the striatum [1, 4, 11, 13, 19, 25, 41]. The receptors mediating this effect have been shown to be of the $D_2$ subtype which is apparently not coupled to adenylate cyclase [6, 40]. Low concentration of DA added to the perfusion fluid is able to enhance the stimulation evoked release of ACh from intact striatal slices [42]. This effect is due to a disinhibition of the dopaminergic control on the cholinergic neurons following a presynaptic

Correspondence should be addressed to
Balázs LENDVAI
Institute of Experimental Medicine
Department of Pharmacology
Hungarian Academy of Sciences
H–1450 Budapest, P.O. Box 67, Hungary

*Akadémiai Kiadó, Budapest*

autoreceptor mediated inhibition of the dopaminergic fibers [42]. In contrast, in case of destroyed dopaminergic bundle caused by 6-hydroxydopamine (6-OHDA) the evoked release of ACh was reduced by DA indicating that there is a direct presynaptic inhibitory control of DA over the cholinergic interneurons [42].

Conversely, ACh is capable of influencing the release of DA from nigrostriatal nerve terminals. The stimulated release of DA has been reported to be enhanced by ACh through both muscarinic and nicotinic presynaptic heteroreceptors [8, 9, 10, 33, 49]. In our laboratory nicotine has been shown to be ineffective on the release of ACh studied on striatal slices taken from intact rats but enhanced the release of ACh from slices when dopaminergic activity was impaired. This finding indicated that the dopaminergic inhibition of the ACh release overshadows the nicotinergic control over the cholinergic interneurons [32].

In addition it has been demonstrated that serotonin released from the raphestriatal axon terminals is able to control the release of ACh from striatal cholinergic interneurons via presynaptic 5-$HT_3$ receptors presumably [7, 43].

In this study we focused our interest on the interaction between cholinergic, dopaminergic and opioid peptide containing neurons. High level of enkephalin and the presence of β-endorphin and dynorphins have been found in the striatum. Enkephalinergic and dynorphinergic neurons as well as μ, δ and κ opioid receptors are present in this brain region [3, 15, 23, 24, 33, 36]. Although, opioid peptides, such as enkephalins and dynorphins may play important role in the modulation of the neuronal network, very little is known about their role in pathological conditions (e.g. Parkinson' syndrome).

Cholinergic interneurons of the striatum are modulated by opioid substances through μ and δ receptors [12, 18, 34]. These receptors are located on the cholinergic nerve terminals presynaptically and they have an inhibitory influence on the ACh release. We recently reported that there is an opioid receptor mediated tonic control on the striatal ACh release, most likely by endogenous enkephalins released from local neurons [31]. The other relevant target of the opioid peptides is the striatal dopaminergic nerve terminals. There is evidence that opioid agonists are able to directly inhibit the striatal DA release through presynaptic κ receptors [28, 35, 42, 48]. Following the activation of this receptor by U50,488H a selective κ agonist, an increase of ACh release was detected. The proper endogenous ligand for the κ receptors could be the dynorphin molecules released from the soma and/or the dentrites of the striatonigral prodynorphinergic fibers. Indeed, a certain level of dynorphins has been demonstrated in rat striatum [20, 21]. Finally, several lines of evidence suggest that nigrostriatal dopaminergic activity modulates the enkephalinergic neurons of the striatum [22]. Chronic treatment with a non-selective DA antagonist, haloperidol produced an increase in the level of enkephalins [14], proenkephalin A and their precursor mRNA levels [30, 38]. Similarly the reduction of

the striatal DA content caused by 6-OHDA pretreatment also increased the level of enkephalins [2, 26, 29, 37]. These results suggest that DA tonically inhibits the enkephalin biosynthesis in rat striatum [27]. While $D_2$ receptors are responsible for the inhibitory effect of DA on enkephalin biosynthesis, through $D_1$ receptors this process can be enhanced [16, 20, 21].

The neuronal network in the striatum makes multiple synaptic and non-synaptic interactions at the presynaptic level influencing the release of neurotransmitters [5, 17, 44, 45, 46, 47]. In the present study an attempt has been made to examine the effect of selective opiate antagonists on the striatal ACh and DA release. We found μ and δ antagonists to be effective in modulating the release of ACh. This finding suggests that the striatal ACh release is tonically controlled by endogenous opioids. However, the release of DA was not affected by endogenous opioid peptides. Neither nor-BNI nor naloxone had modulatory property on DA release.

## Materials and methods

All experiments were performed at 37 °C in modified Krebs solution containing (mM) NaCl: 118, KCl: 4.7, $CaCl_2$: 2.5, $KH_2PO_4$: 1.2, $MgSO_2$: 1.2, $NaHCO_3$: 25, and glucose: 12.5, continuously saturated with carbogen gas (95% $O_2$ + 5% $CO_2$).

The experiments were carried out on two groups of male Wistar rats (body weight 180–220 g): untreated rats and those pretreated by intracerebroventricular (icv) injection of 6-hydroxydopamine (6-OHDA). Five days before the experiments cannula was implanted icv and two doses of 250 μg 6-OHDA were administered. Three days elapsed between the two doses of 6-OHDA. The animals were killed 2 days after the second dose of 6-OHDA by decapitation, corpora striata were removed from the skull, cleaned of blood with ice cold saline and sliced into pieces (2 × 0.4 × 1.2 mm) with a McIlwain tissue chopper. The slices were incubated with [$^3$H]choline chloride 10 μCi/ml (specific activity: 78 Ci/mmol) or [$^3$H]dopamine ([$^3$H]DA) 10 μCi/ml (specific activity: 42 Ci/mmol) at 37 °C for 40 min in Krebs solution.

After the loading period the slices were washed five times with 10 ml of Krebs solution. Five slices were placed into a micro-volume perfusion chamber. After a 60-min preperfusion (flow rate: 0.5 ml/min) the effluent was collected in 3-min samples. During the collection of the 3rd and the 15th samples, the slices were stimulated ($S_1$ and $S_2$) for 2-min periods of square wave impulses by an Eltron stimulator of 2-msec duration at 2 Hz and 20 V (240 shocks).

Drugs were administered between the two stimulations thus the fractional release evoked by the first stimulation ($FRS_1$) served as an internal control. Drugs were usually applied 15 minutes before $S_2$, and maintained until the end of the experiments. Sulpiride was present in the Krebs solution from the end of the preperfusion period (15 min prior to $S_1$) to the end of the experiment.

At the end of each experiment the radioactive content of the slices was determined. The slices were homogenized in 1 ml of trichloroacetic acid. 100 μl aliquots of the supernatants of the tissue homogenizate were added to 6 ml of scintillation cocktail containing dioxane and assayed for radioactivity by liquid scintillation spectrometry.

Radioactivity of the samples was expressed in terms of disintegration per gram of tissue (Bq/g). High performance liquid chromatography (HPLC) and biochemical separation of labelled choline from ACh [41] indicated that mainly [$^3$H]ACh and in case of DA release [$^3$H]DA are responsible for radioactivity released by field stimulation from the striatum, prelabelled with [$^3$H]choline or [$^3$H]DA.

Therefore the fractional release (FR) of ACh and DA was calculated as a percentage of the total radioactivity present in the tissue at the beginning of the stimulation. Basal release was determined during the collection period before and after the stimulation period.

HPLC combined with electrochemical detection was used to measure DA content of the striatum.

The effect of drugs on the release of ACh or DA was expressed as the ratio of $FRS_2$ over $FRS_1$ ($FRS_2/FRS_1$). The statistical significance of the results was determined by Student's t-test or two-way analysis of variance with subsequent comparisons by Dunn's test; $p < 0.05$ was considered significant. Data presented in this paper are means ± S.E.M.

Methyl-[$^3$H]choline chloride (78 Ci/mmol) and [7,8-$^3$H]dopamine (42 Ci/mmol) were purchased from Amersham. Naltrindole hydrochloride (NTI), nor-binaltorphimine dihydrochloride (nor-BNI) and β-funaltrexamine hydrochloride (β-FNA) were from RPI (Research Biochemicals Incorporated). All other chemicals were purchased from Sigma Chemical. Drugs were freshly prepared on the day of use.

## Results

### *Effect of 6-hydroxydopamine pretreatment on striatal dopamine content*

After two doses of 6-OHDA the striatal DA content measured by HPLC reduced to 7 ± 2% of control (from 7.27 ± 0.49 to 0.51 ± 0.13 μg/g tissue). Therefore it was concluded that the dopaminergic nigrostriatal tract was fully destroyed. In this group the total amount of [$^3$H]ACh released from striatal slices was significantly higher compared to control (data not shown).

### *Influence of selective opiate antagonists on striatal acetylcholine release*

In control experiments 4.62 ± 0.65% of the radioactivity in the tissue was released by the first stimulation and 3.23 ± 0.37% by the second. The $FRS_2/FRS_1$ ratio was 0.84 ± 0.12 ($n = 6$) in the control experiments without 6-OHDA pretreatment. None of the selective antagonists applied between $S_1$ and $S_2$ changed this ratio indicating they had no effect on the release of ACh in slices taken from the control animals.

However, when the effect of β-FNA or NTI was studied on DA deficient rats (6-OHDA pretreated), they significantly enhanced the stimulation evoked release of ACh (Fig. 1). Nor-BNI did not cause any significant change in the $FRS_2/FRS_1$ ratio (Fig. 1). The 6-OHDA pretreated slices examined alone showed a value of 0.85 ± 0.11 ($n = 7$) without significant change compared to control.

FIG. 1/A

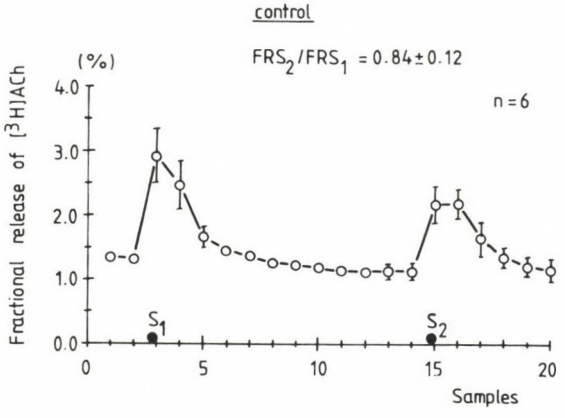


FIG. 1/B

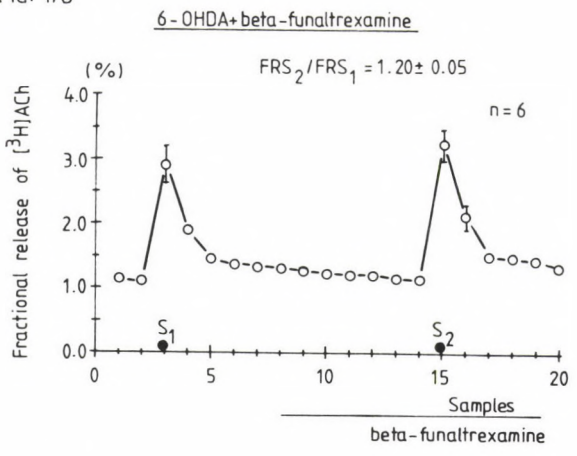


FIG. 1/C

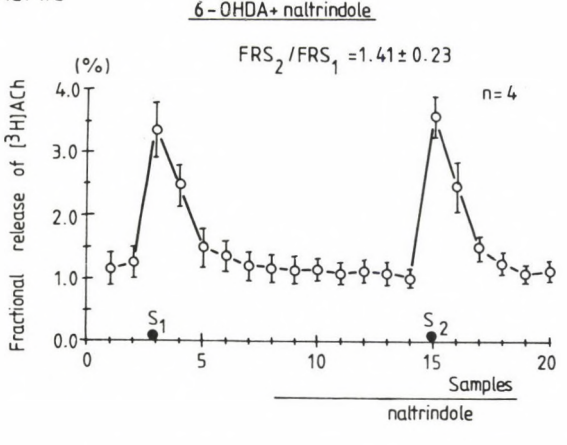


FIG. 1/D

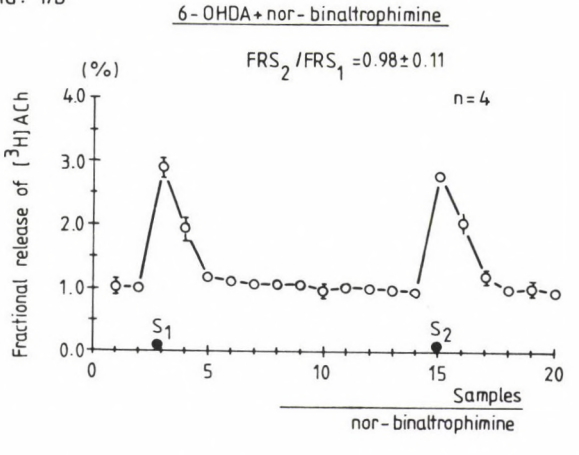


*Fig. 1.* Stimulatory effect of μ and δ receptor antagonists on the release of ACh. 1 μM of β-funaltrexamine (Fig. 1/B) and naltrindole (Fig. 1/C) enhanced the ACh release from striatal slices pretreated with 6-OHDA (see Methods). Nor-binaltrophimine was ineffective (Fig. 1/D). The $S_1$ and the $S_2$ correspond to the fractional release due to the first and the second electrical field stimulation, respectively

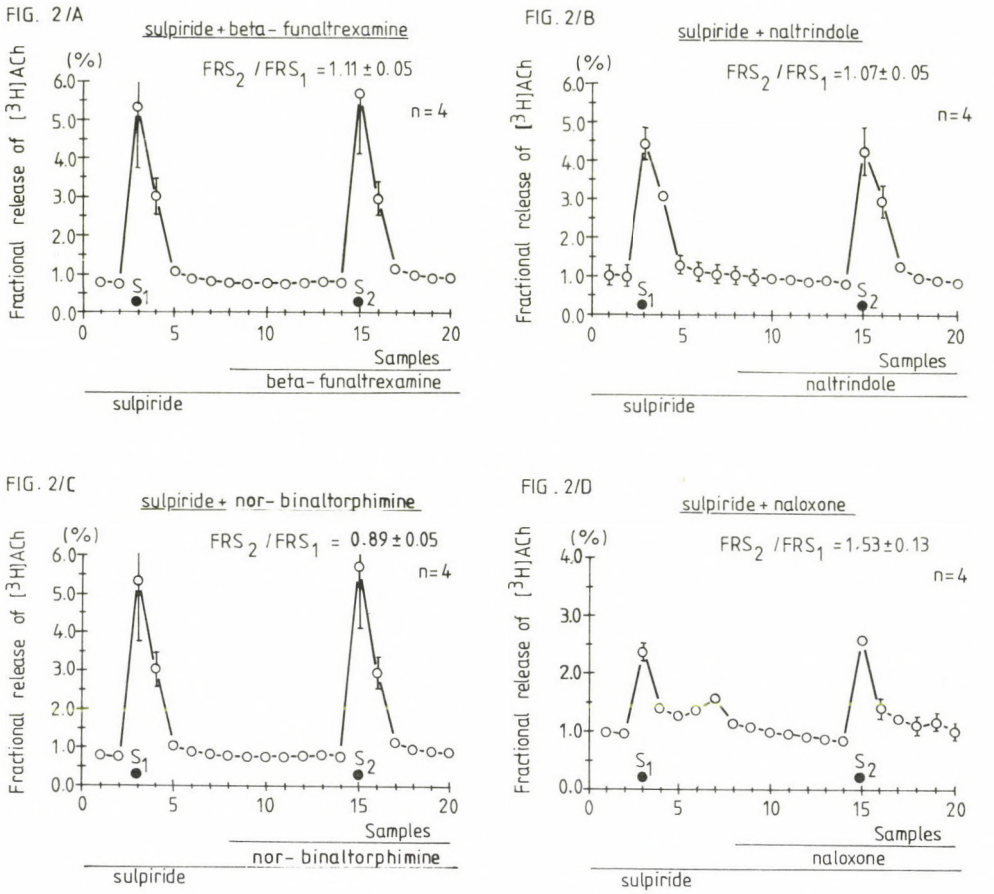


*Fig. 2.* Effect of selective opioid receptor antagonists on the release of ACh from striatal slices in the presence of a $D_2$ dopamine-receptor antagonist, sulpiride (10 μM). β-funaltrexamine (1 μM), a selective μ receptor antagonist (Fig. 2/A) and naltrindole (1 μM), a δ antagonist (Fig. 2/B) enhanced the release of ACh, while nor-binaltorphimine a K receptor antagonist (Fig. 2/C) did not cause significant change in the transmitter release. Note that the effect of naloxone (1 μM), a non-selective opiate antagonist (Fig. 2/D) was significantly higher compared to the effect of β-funaltrexamine or naltrindole

To prevent the effect of $D_2$ dopamine-receptor stimulation, sulpiride, a selective $D_2$ receptor antagonist was added to the perfusion solution 15 min prior to $S_1$. If sulpiride was present alone the total amount of ACh released from striatal slices showed a significant increase compared to control (data not shown) but the $FRS_2/FRS_1$ ratio did not change significantly (0.81 ± 0.06, n = 6). Under this condition the selective μ and δ antagonists enhanced the striatal ACh release but nor-BNI was ineffective in the presence of sulpiride either (Fig. 2). These data correspond well with the result obtained on slices taken from rats pretreated with 6-OHDA. Naloxone, a non-selective opioid receptor antagonist also enhanced the [$^3$H]ACh release from striatal slices but it caused significantly higher release of ACh than β-FNA or NTI alone (Fig. 2).

*Effect of opiate antagonists on striatal dopamine release*

The electrical stimulation evoked the release of [$^3$H]DA from striatal slices. In the control experiments 5.57 ± 0.34% of radioactivity present in the tissue was released by the first ($S_1$) and 3.79 ± 0.22% by the second stimulation ($S_2$). The $FRS_2/FRS_1$ ratio was 0.79 ± 0.05 (n = 4). Neither the selective κ antagonist, nor-BNI ($FRS_2/FRS_1$ = 0.77 ± 0.13; n = 4), nor the general opiate antagonist naloxone ($FRS_2/FRS_1$ = 0.80 ± 0.03; n = 4) modulated the stimulation evoked release of DA from nigrostriatal nerve endings.

## Discussion

In certain neurodegenerative diseases it seems theoretically to be possible that a change in the interneuronal communication is responsible for the symptoms [45, 47], at least at the onset of the disease. In case of the Parkinson's syndrome the missing factor is the dopaminergic tonic inhibition of ACh release in the striatum. Our recent observations [31] and the data presented in this paper suggest that the lack of enkephalinergic control on cholinergic interneurons may also be involved.

The effects of opioid peptide receptor antagonists, that they enhanced the release of ACh indicate that there is an endogenous substance tonically inhibiting the release of ACh. In our experiments μ and δ antagonists but not the κ receptor antagonist are able to affect the ACh release in rats pretreated with 6-OHDA. In contrast, none of the antagonists was effective in influencing the release of DA from striatal slices indicating the lack of a tonic effect of opioid peptides on DA release. Since κ receptors and the presence of dynorphins have been demonstrated in the striatum [28, 42, 48], a non-tonic effect of endogenous opioids cannot be ruled out. The physiological role of dynorphinergic neurons in the striatum is still unclear and

needs further investigations. The fact that μ and δ receptor antagonists as well as naloxone were found to be effective in modulating the striatal ACh release further supports the view that μ and δ receptors may be situated in a functional receptor complex on the striatal cholinergic axon terminals [35].

The question remained to be answered why the endogenous opioid peptides control the cholinergic interneurons of the striatum only in those cases when the dopaminergic input is impaired. One of the possible explanations is that the dopaminergic tonic control over the cholinergic neurons simply overshadows the peptidergic control. The second possible explanation is that there may be a presynaptic DA mediated inhibition of the striatal enkephalinergic neurons possibly using non-synaptic pathways [45, 47]. In this case in rats with intact dopaminergic input DA inhibits the release of enkephalin in the striatum, thus we could not observe any effect of opiate antagonists. However, a decrease in the striatal DA content may result in an increase of the release of enkephalin, thereby increasing the peptidergic inhibition of the release of ACh.

## REFERENCES

1. Agid, Y., Guyenet, P., Glowinski, J., Beaujouan, J. C., Javoy, F.: Inhibitory influence of nigrostriatal dopamine system on the striatal cholinergic neurons in rat. Brain Res. **86**, 488–492 (1975).
2. Angulo, J. A., Davis, L. G., Burkhart, B. A., Chritoph, G. R.: Reduction of striatal dopaminergic transmission elevates striatal proenkephalin mRNA. Eur. J. Pharmacol. **130**, 341–343 (1986).
3. Atweh, S. F., Kuhar, M. J.: Autoradiographic localization of opiate receptors in rat brain. Brain Res. **134**, 393–405 (1977).
4. Chesselet, M. F.: Presynaptic regulation of neurotransmitter release in the brain: Facts and hypothesis. Neuroscience **12**, 347–375 (1984).
5. Dimova, R., Vuillet, J., Seite, R.: Study of the rat neostriatum using a combined Golgi-electron microscope technique and serial sections. Neuroscience **5**, 1581–1596 (1980).
6. Garcia-Sainz, J. A.: Inhibitory receptors and ion channel effectors. Trends Pharmac. Sci. **9**, 271–272 (1988).
7. Gillet, G., Ammor, S., Fillion, G.: Serotonin inhibits acetylcholine release from rat striatum slices: evidence for presynaptic receptor-mediated effect. J. Neurochem. **45/6**, 1687–1691 (1985).
8. Giorguieff, M. F., Le Floc'h, M. L., Westfall, T. C., Glowinski, J., Besson, M. J.: Nicotinic effect of acetylcholine on the release of newly synthesized [$^3$H]dopamine in rat striatal slices and cat caudate nucleus. Brain Res. **106**, 117–131 (1976).
9. Giorguieff, M. F., Le Floc'h, M. L., Glowinski, J. L., Besson, M. J.: Involvement of cholinergic presynaptic receptors of nicotinic and muscarinic types in the control of the spontaneous release of dopamine from striatal dopaminergic terminals in the rat. J. Pharmacol. Exp. Ther. **200**, 535–544 (1977).
10. Goodman, F. R.: Effects of nicotine on distribution and release of $^{14}$C-norepinephrine and $^{14}$C-dopamine in rat brain striatum and hypothalamus. Neuropharmacology **3**, 1025–1032 (1974).
11. Guyenet, P., Agid, J., Javoy, F., Beaujouan, J. C., Rossier, J., Glowinski, J.: Effect of dopaminergic receptor agonists and antagonists on the activity of neostriatal cholinergic system. Brain Res. **84**, 227–244 (1976).
12. Hársing, L. G. Jr., Vizi, E. S., Knoll, J.: Increase by enkephalin of acetylcholine release from striatal slices of the rat. Pol. J. Pharmacol. **30**, 387–395 (1978).

13. Hertting, G., Zumstein, A., Jackisch, R., Hoffman, I., Starke, N.: Modulation by endogenous dopamine of the release of acetylcho'ine in the caudate nucleus of the rabbit. Naunyn Schmiedebergs Arch. Pharmacol. **315**, 111–117 (1980).
14. Hong, J. S., Tang, HY-T, Fratta, W., Costa, E.: Rat striatal methionine-enkephalin content after chronic treatment with cataleptogenic and noncataleptogenic antischizophrenic drugs. J. Pharmacol. Exp. Ther. **205**, 141–147 (1978).
15. Hughes, J., Kosterlitz, H. W., Smith, T. W.: The distribution of methionine-enkephalin and leucine-enkephalin in the brain and periferial tissue. Br. J. Pharmacol. **61**, 639–647 (1977).
16. Jiang, H. K., McGinty, J. F., Hong, J. S.: Differential modulation of striatonigral dynorphin and enkephalin by dopamine receptor subtypes. Brain Res. **507**, 57–64 (1990).
17. Kemp, J. M., Powell, T. P. S.: The structure of the caudate nucleus of the cat: light and electron microscopy. Phil. Trans. R. Soc. Ser. B. **262**, 383–401 (1971).
18. Lapchak, P. A., Araujo, D. M., Collier, B.: Regulation of endogenous acetylcholine release from mammalian brain slices by opiate receptors: hippocampus, striatum and cerebral cortex of guinea-pig and rat. Neuroscience **31**, 313–325 (1989).
19. Lehmann, J., Langer, S. Z.: The striatal cholinergic interneuron: synaptic target of dopaminergic terminals. Neuroscience **10**, 1105–1120 (1983).
20. Li, S. J., Sivam, S. P., Hong, J. S.: Regulation of the concentration of dynorphin-A (1–8) in the striatonigral pathway by the dopaminergic system. Brain Res. **398**, 390–392 (1986).
21. Li, S. J., Sivam, S. P., McGinty, J. F., Jiang, H. K., Douglass, J., Calavetta, L., Hong, J. S.: Regulation of the metabolism of striatal dynorphin by the dopaminergic system. J. Pharmacol. Exp. Ther. **246**, 403–408 (1988).
22. Loh, H. H., Brase, D. A., Sampath-Khanna, S., Mar, J. B., Way, E. L.: β-Endorphin: in vitro inhibition of striatal dopamine release. Nature Lond. **264**, 567–568 (1976).
23. Mansour, A., Khachaturian, H., Lewis, M. E., Akil, H., Watson, J.: Anatomy of CNS opioid receptors. Trends Neurosci. **11**, 308–314 (1988).
24. Martin, W. R.: Pharmacology of opioids. Pharmacol. Rev. **35**, 283 (1984).
25. Miller, J. C. and Friedhoff, A. J.: Dopamine receptor-coupled modulation of the $K^+$-depolarized overflow of [$^3$H]acetylcholine from rat striatal slices: alterations after chronic haloperidol and alpha-methyl-p-tyrosine pretreatment. Life Sci. **25**, 1249–1256 (1979).
26. Mocchetti, I., Schwartz, J. P. Costa, E.: Use of mRNA hybridization and radioimmunoassay to study mechanisms of drug-induced accumulation of enkephalins in rat brain structures. Mol. Pharmacol. **28**, 86–91 (1985).
27. Morris, B. J., Herz, A., Hollt, V.: Localization of striatal opioid gene expression, and its modulation by mesostriatal dopamine pathway: an in situ hybridization study. J. Mol. Neurosci. **1**, 9–18 (1989).
28. Mulder, A. H., Wardeh, G., Hogenboom, F., Frankhuyzen, A. L.: κ and δ opioid receptor agonists differentially inhibit striatal dopamine and acetylcholine release. Nature **308**, 278 (1984).
29. Normand, E., Popovici, T., Onteniente, B., Fellmann, D., Piatier-Tonneau, D., Auffray, C., Bloch, B.: Dopaminergic neurons of the substantia nigra modulate proenkephalin A gene expression in rat striatal neurons. Brain Res. **439**, 39–46 (1988).
30. Sabol, S. L., Yoshikawa, K., Hong, J. S.: Regulation of methionin-enkephalin precursor messenger RNA in rat striatum by haloperidol and lithium. Biochem. Biophys. Res. Commun. **113**, 391–399 (1983).
31. Sándor, N. T., Kiss, J., Sándor, A., Lendvai, B., Vizi, E. S.: Naloxone enhances the release of acetylcholine from cholinergic interneurons of the striatum if the dopaminergic input is impaired. Brain Res. **552**, 343–345 (1991).
32. Sándor, N. T., Zelles, T., Kiss, J., Sershen, H., Töröcsik, A., Lajtha, Á., Vizi, E. S.: Effect of nicotine on dopaminergic-cholinergic interaction in the striatum. Brain Res. **567**, 313–316 (1991).
33. Sar, M., Stumpf, W. E., Miller, R. J., Chang, K. J., Cuatrecasas, P.: Immunohistochemical localization of enkephalin in rat brain and spinal cord. J. Comp. Neurol. **182**, 17–38 (1978).

34. Schoffelmeer, A. N. M., Hanssen, H. A., Stoof, J. C., Mulder, A. H.: Blockade of $D_2$ dopamine receptors strongly enhances the potency of enkephalins to inhibit dopamine-sensitive adenylate cyclase in rat neostriatum: involvement of δ- and μ-opioid receptors. J. Neurosci. **6**, 22–35 (1986).
35. Schoffelmeer, A. N. M., Rice, K. C., Jacobson, A. E., Van Gulderen, J. G., Hogenboom, F., Heijna, M. H., Mulder, A. H.: μ-, δ- and K-opioid receptor-mediated inhibition of neurotransmitter release and adenylate cyclase activity in rat brain slices: studies with fentanyl isothiocyanate. Eur. J. Pharmacol. **154**, 169–178 (1988).
36. Schwartz, J. C., Pollard, H., Llorens, C., Malfroy, B., Gros, C., Pradelles, P. H., Dray, F.: Endorphins and endorphin receptors in striatum: relationship with dopaminergic neurons. In: Advances in Biomechanical Psychopharmacology, eds E. Costa and M. Trabucchi Vol. 18. Raven Press, N. Y. 1978, pp. 245–264.
37. Sivam, S. P., Breese, G. R., Napier, T. C., Mueller, R. A., Hong, J. S.: Dopaminergic regulation of proenkephalin-A gene expression in the basal ganglia. Natl. Inst. Drug Abuse Res. Monograph Ser. **75**, 389–392 (1986).
38. Sivam, S. P., Breese, G. R., Krause, J. E., Napier, T. C., Mueller, R. A., Hong, S. J.: Neonatal and adult 6-hydroxydopamine-induced lesions differentially alter tachykinin and enkephalin gene expression. J. Neurochem. **49**, 1623–1633 (1987).
39. Somogyi, P., Priestley, J. V., Cuello, A. C., Smith, A. D., Takagi, H.: Synaptic connections of enkephalin-immunoreactive nerve terminals in the neostriatum: a correlated light and electron microscopic study. J. Neurocytol. **11(5)**, 779–807 (1982).
40. Stoof, J. C., Kebabian, J. W.: Independent in vitro regulation by the $D_2$ dopamine receptor of dopamine-stimulated efflux of cyclic AMP and $K^+$-stimulated release of acetylcholine from rat neostriatum. Brain Res. **250**, 263–270 (1982).
41. Vizi, E. S., Rónai, A. Z., Hársing, L. G. Jr., Knoll, J.: Inhibitory effect of dopamine on acetylcholine release from caudate nucleus. Pol. J. Pharmacol. Pharm. **29**, 201–211 (1977).
42. Vizi, E. S., Hársing, L. G. Jr., Knoll, J.: Presynaptic inhibition leading to disinhibition of acetylcholine release from interneurons of caudate nucleus: effect of dopamine, β-endorphin and D-$Ala^2$-$Pro^5$-enkephalinamide. Neuroscience **2**, 953–961 (1977).
43. Vizi, E. S., Hársing, L. G. Jr., Zsilla, G.: Evidence of the modulatory role of serotonin in acetylcholine release from striatal interneurons. Brain Res. **212**, 89–99 (1981).
44. Vizi, E. S.: Presynaptic modulation of neurochemical transmission. Prog. Neurobiol. **12**, 181–290 (1979).
45. Vizi, E. S.: Non-synaptic interactions between neurons: Modulation of neurochemical transmission. In: Pharmacological and Clinical Aspects. John Wiley and Sons, Chichester, New York, 1985.
46. Vizi, E. S.: Non-synaptic inhibitory signal transmission between axon terminals: physiological and pharmacological evidence. In: Transmission in the brain: novel mechanisms for neuronal transmission, eds K. Fuxe and L. F. Agnati, Raven Press Ltd, New York, 1991, pp. 89–96.
47. Vizi, E. S., Lábos, E.: Non-synaptic interactions at presynaptic level. **37**, 145–163 (1991).
48. Werling, L. L., Frattali, A., Portoghese, P. S., Takemori, A. E., Cox, B. M.: Kappa receptor regulation of dopamine release from striatum and cortex of rats and guinea pigs. J. Pharmacol. Exp. Ther. **246**, 282–286 (1988).
49. Westfall, T. C.: Effect of nicotine and other drugs on the release of $^3$H-norepinephrine and $^3$H-dopamine from rat brain slices. Neuropharmacology **13**, 693–700 (1974).

*Acta Physiologica Hungarica, Volume 81 (1), pp. 29–35 (1993)*

# RESPONSE OF HEPATIC DRUG-METABOLIZING ENZYMES TO IMMOBILIZATION STRESS IN RATS OF VARIOUS AGES

Anna NAGYOVA, E. GINTER

INSTITUTE OF PREVENTIVE AND CLINICAL MEDICINE, BRATISLAVA, CZECHO-SLOVAKIA

Received March 31, 1992
Accepted July 8, 1992

The effects of acute two-hour immobilization stress in hepatic microsomal drug-metabolizing enzyme activities, liver and blood serum zinc and copper levels, content of vitamin C in adrenals, were studied in rats of three age categories (4, 12, 24 months old). Immobilization stress resulted in marked reduction in the concentrations of vitamin C in adrenals of all age categories. In stressed animals, the activities of microsomal aniline hydroxylase, p-nitroanisol 0-demethylase, and the hepatic concentrations of microsomal protein were significantly increased in young 4-month-old rats, especially. In these rats increased levels of zinc in blood serum and copper in the liver, were seen. The levels of zinc and copper in older rats after immobilization stress were apparently unchanged. Age-dependent decrease in the activities of hepatic microsomal monooxygenases and adrenal vitamin C content in control rats were observed.

**Keywords**: cytochrome P-450, acute immobilization stress, vitamin C, zinc, copper

Stress is considered one of the risk factors in aging and the development of many diseases due to its interference with many biochemical reactions in the organism. It is known that different forms of stress conditions cause changes in the metabolism of hormones, vitamins, trace elements etc. A characteristic biochemical expression of stress in an abrupt increase in adrenal corticosteroids in blood plasma which is always preceeded by a release of vitamin C by the adrenals. Changes in plasma corticosteroids may affect the levels of serum Zn and Cu [1].

Another aspect of the influence of stress may be the changes of the activities of hepatic cytochrome P-450-dependent monooxygenase system [12], which is responsible for the metabolism of drugs and xenobiotics as well as endogenous substrates. Cytochrome P-450 is affected by both exogenous factors (drugs, environmental chemicals, stress, diet) and endogenous factors (sex, age, genetic disposition). Steroid hormones including corticosteroids affect the metabolism of drugs by stimulating or inhibiting the activities of hepatic drug-metabolizing enzymes

Correspondence should be addressed to
Anna NAGYOVA
Institute of Preventive and Clinical Medicine
833 01 Bratislava, Limbova 14, Czecho-Slovakia

*Akadémiai Kiadó, Budapest*

[5]. There are very few references concerning this aspect of immobilization stress influence.

We have therefore examined the influence of immobilization stress in rats of different ages on hepatic microsomal drug-metabolizing enzymes (cytochrome P-450, aniline hydroxylase, p-nitroanisol 0-demethylase). We have simultaneously determined adrenal vitamin C, liver and blood serum Zn and Cu levels as important components of the antioxidant system involved in adaptation reactions to a stress.

## Materials and methods

Male Wistar rats of three different age categories (4, 12, 24 months old), weighing 300–500 g were used in the experiment. The control and experimental groups were given commercial laboratory diet and drinking water ad libitum. The rats of all age categories were divided into control and immobilized groups (immobilization lasting 2 hours). The animals were decapitated after 16-hour fasting and 2-hour immobilization stress. The number of rats in each group was 6. The livers were quickly removed, chilled, weighed and one part was homogenized using a Potter–Elvenjem homogenizer with Teflon pestle to prepare liver microsomes [15]. Another part of the liver was stored at −27 °C until analyzed for Zn and Cu content. Analyses were performed after prior dry mode mineralization and solubilization by using flame atomic absorption spectrophotometer Perkin–Elmer model 5 000. Blood serum levels of Zn and Cu were determined directly after dilution [22]. In liver microsomes protein concentration [16], aniline hydroxylase activity [10], p-nitroanisole, O-demethylase activity [17] and cytochrome P-450 [18] were determined. For the determination of cytochrome P-450 a dual wavelength spectrophotometer UV/VIS Pye Unicam SP 8–100 was used. Vitamin C in the adrenals was also determined [20]. The results were statistically evaluated by Student's *t*-test.

## Results

### *Hepatic microsomal enzymes*

The influence of aging and immobilization stress on the activity of hepatic microsomal monooxygenases is given in Table I. The content of microsomal proteins and the activity of aniline hydroxylase were significantly increased in 4-month-old rats, while no changes were seen in old rats. The content of cytochrome P-450 was slightly increased in all age categories of stressed rats, but the difference was significant in the oldest rats only (increase 26%, $P < 0.05$). Activity of 0-demethylase was increased after acute immobilization stress in all age categories. Its activities in 4- and 12-month-old rats were 21% and 35% of the control value respectively. An age-dependent decrease in the activities of hepatic microsomal monooxygenases in control and stressed rats, were observed. Content of cytochrome P-450 and the activity of aniline hydroxylase in 24-month-old control rats were 26% ($P < 0.01$) and 17% of those in 4-month-old control rats.

**Table I**

*Effect of immobilization stress on the activity of hepatic microsomal enzymes in rats of various ages*

| Age | Group | Microsomal protein (mg/g liver) | Cytochrome P-450 (nmol/mg protein) | Cytochrome $b_5$ (nmol/mg protein) | Aniline hydroxylase (nmol/min/mg protein) | p-nitroanisol 0-demethylase (nmol/min/mg protein) |
|---|---|---|---|---|---|---|
| 4 months | control | 12 ± 3 | 0.53 ± 0.08 | 0.35 ± 0.05 | 0.41 ± 0.09 | 0.53 ± 0.16 |
| | stress | 16 ± 2[a] | 0.60 ± 0.12 | 0.35 ± 0.05 | 0.62 ± 0.15[a] | 0.67 ± 0.07[a] |
| 12 months | control | 15 ± 1 | 0.50 ± 0.06 | 0.35 ± 0.05 | 0.39 ± 0.09 | 0.47 ± 0.13 |
| | stress | 15 ± 3 | 0.55 ± 0.14 | 0.39 ± 0.05 | 0.42 ± 0.07 | 0.72 ± 0.11[a] |
| 24 months | control | 13 ± 1 | 0.39 ± 0.03[b] | 0.33 ± 0.03 | 0.34 ± 0.05 | 0.50 ± 0.16 |
| | stress | 15 ± 1 | 0.53 ± 0.14[a] | 0.38 ± 0.05 | 0.39 ± 0.08 | 0.58 ± 0.15 |

Data represent means ± SD from 6 rats in each group. [a] significantly different from control, $P < 0.05$; [b] significantly different from 4-month-old control, $P < 0.01$

*Vitamin C*

The content of vitamin C in adrenals of rats of various ages after acute immobilization stress is shown in Fig. 1. Adrenal vitamin C concentration was markedly affected by immobilization stress in all age categories. The greatest decrease in adrenal vitamin C concentration was observed in 12-month-old rats (59%, $P < 0.001$). The concentration of vitamin C in adrenals decreased almost linearly with age.

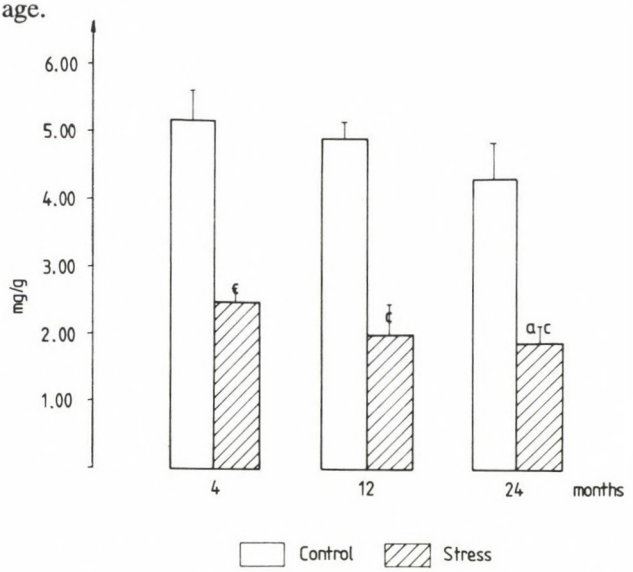


*Fig. 1.* Vitamin C content in adrenals of rats of various ages after acute immobilization stress. Data represent means ± SD from 6 rats in each group. [a] Significantly different from 4-month-old stressed group, $P < 0.05$; [c] significantly different from control, $P < 0.001$

*Zinc and copper*

Changes in the levels of Zn and Cu in blood serum and the liver after acute immobilization stress of rats of different age are given in Table II. Levels of zinc in blood serum and copper in the liver were significantly increased in 4-month-old rats after immobilization stress (16–20%, $P < 0.01$).

**Table II**

*Blood serum and liver levels of Zn and Cu in rats of various ages after acute immobilization stress*

| Age | Group | serum | | liver | |
|---|---|---|---|---|---|
| | | Zn (μg/ml) | Cu (μg/ml) | Zn (μg/g) | Cu (μg/g) |
| 4 months | control | 1.25 ± 0.09 | 1.40 ± 0.10 | 89.2 ± 9.6 | 12.8 ± 0.9 |
| | stress | 1.49 ± 0.12[a] | 1.40 ± 0.05 | 94.5 ± 10.1 | 15.3 ± 1.1[a] |
| 12 months | control | 1.25 ± 0.13 | 1.89 ± 0.33[b] | 84.1 ± 12.7 | 12.9 ± 1.6 |
| | stress | 1.32 ± 0.09 | 1.82 ± 0.12 | 90.3 ± 7.1 | 14.5 ± 0.9 |
| 24 months | control | 1.26 ± 0.10 | 2.19 ± 0.67[b] | 81.1 ± 12.6 | 12.9 ± 1.2 |
| | stress | 1.39 ± 0.08 | 2.08 ± 0.10 | 90.7 ± 6.1 | 14.5 ± 1.1 |

Data represent means ± SD from 6 rats in each group. [a] significantly different from control, $P < 0.01$; [b] significantly different from 4-month-old control, $P < 0.05$

Only slight effect of immobilization stress on the levels of Zn and Cu in blood serum and the liver in older rats, was observed. Levels of Cu in blood serum of control and stressed rats increased as a consequence of aging ($P < 0.05$). The levels of Zn in blood serum were not affected by aging, while its levels in the liver showed decreasing tendency with age.

## Discussion

The effect of various forms of stress upon microsomal drug-metabolizing enzymes is not uniform [12]. The response of these enzymes to pain, cold, oxidative stress, isolation stress or other stressful stimuli have been studied. For example, isolation stress increased in *in vitro* experiments, the activity of some microsomal enzyme system concerned with benzo(a)pyrene activation [4], while combinations of oxidative stress and exhaustive physical exercise or hyperoxia caused marked decreases in cytochrome P-450 content [23]. Similarly emotional-pain stress caused the decline in cytochrome P-450 content in liver microsomes [25]. Stress (cold exposure) elevated the rate of metabolism of aniline and ethylmorphine [24] and short term stress, such as hind limb ligation caused a decrease in hexobarbital

sleeping time [6]. It has been shown that liver microsomal drug-metabolizing enzymes are involved in metabolic deactivation of the endogenous steroid hormones and their activity may be increased by stress or administration of corticosteroids. In corticosterone-treated rats kept on protein-deficient diet increase of the activity of hepatic microsomal biphenyl 4-hydroxylase was observed. The authors postulated that the increases in the hepatic drug-metabolizing enzymes in energy-deficient animals were mediated either directly or indirectly through the endogenous corticosteroids which play a central role in the adaptive response to dietary protein insufficiency [3]. The same authors found increase in hepatic biphenyl 4-hydroxylase, and increase in plasma corticosterone in rats kept on a diet deficient in protein and calories [2]. The response of animals to various forms of stress is often measured by plasma corticosteroid levels [21] and its increased levels were also observed in rats after acute immobilization stress [8]. This study has demonstrated that a 2-hour immobilization stress does affect cytochrome P-450 content and the microsomal metabolism of aniline and p-nitroanisole. Since stress significantly enhanced the activity of these enzymes and in parallel experiments it maximally elevated plasma corticosteroids [8], our results suggest that the increases observed in the activity of hepatic drug-metabolizing enzymes in stressed rats could be related with increased plasma corticosteroids levels.

In general, the activity of all biotransformation reaction declines in old age. The diminished activities of hepatic microsomal drug metabolizing enzymes in both, old male and female rats were demonstrated [13, 14, 19]. Age-dependent decrease in cytochrome P-450 and aniline hydroxylase in our study is similar to that observed by above-mentioned authors. In addition, the present results support previous findings, demonstrating that adrenal vitamin C content is diminished in old age. Vitamin C is known to play a vital role in many cytochrome P-450 dependent detoxication reactions in animals [26] and humans [7]. Thus, old organism could became more susceptible to deleterious effect of drugs and xenobiotics.

In our previous study serum Zn levels after chronic immobilization stress during 7 days were not changed [11]. However the results presented here indicate significant increase in serum Zn levels in 4-month-old rats (19%, $P < 0.01$) after an acute 2-hour immobilization stress. These conflicting results could be explained as a dependence on the duration of stress. Stress has been reported to induce metallothionein (MT) synthesis in the liver which is known to control distribution of Zn and Cu.

Eighteen hours of immobilization stress in rats resulted in an increase of liver MT, but its changes were not apparently related to changes in cytosolic Zn [9]. Acute stress-induced responses in liver Cu levels observed in this study have shown higher levels in stressed rats of all age categories (12–20%), with the maximum in young 4-month-old animals ($P < 0.01$). Increased Cu and Zn levels in the liver of stressed

rats probably depend on liver metallothionein induction. Our results also demonstrate the accumulation of Cu in blood serum of old rats what is in agreement with the free radical theory of aging.

Acute stress-induced changes in biochemical parameters studied were more evident in younger than in older rats and could be considered as an adaptive response to a stressor, probably via plasma corticosteroid levels, which may alter the metabolism of xenobiotics including drugs and physiologically important substances.

## REFERENCES

1. Balasch, J., Flos, R.: Plasmatic variation of factors related to iron metabolism in stress. Agressologie **16**, 89–93 (1975).
2. Basu, T. K., Dickerson, J. W. T., Parke, D. V.: The effect of diet on rat plasma corticosteroids and liver aromatic hydroxylase activity. Biochem. J. **125**, 16 (1971).
3. Basu, T. K., Dickerson, J. W. T., Parke, D. V.: Effect of protein energy nutrition on rat plasma corticosteroids and liver microsomal hydroxylase activity. Nutr. Metabol. **18**, 49–54 (1975).
4. Capel, I. D., Jenner, M., Pinnock, M. H., Dorrell, H. M., Williams, D. C.: The effect of isolation stress on some hepatic drug and carcinogen-metabolising enzymes in rats. J. Environm. Pathol. Toxicol. **4/2**, 3, 337–344 (1980).
5. Conney, A. H.: Pharmacological implications of microsomal enzyme induction. Pharmacol. Rev. **19**, 317–366 (1967).
6. Driever, C. W., Bosquet, W. F., Miya, T. S.: Stress stimulation of drug metabolism in the rat. Int. J. Neuropharmac. **5**, 199–205 (1966).
7. Ginter, E., Vejmolova, J.: Vitamin C-status and pharmacokinetic profile of antipyrine in man. Br. J. Clin. Pharmac. **12**, 256–258 (1981).
8. de Goeij, D. C. E., Kvetnansky, R., Whitnall, M. H., Jezova, D., Berkenbosch, F., Tilders, F. J. H.: Repeated stress-induced activation of corticotropin-releasing factor neurons enhances vasopressin stores and colocalization with corticotropin-releasing factor in the median eminence of rats. Neuroendocrinology **53**, 150–159 (1991).
9. Hidalgo, J., Borras, M., Garvey, J. S., Armario, A.: Liver, brain and heart metallothionein induction by stress. J. Neurochem. **55**, 651–654 (1990).
10. Holtzman, J. L., Gillette, J. R.: Effect of dietary orotic acid and adenine sulfate on hepatic microsomal enzymes in male and female rats. Biochem. Pharmacol. **18**, 1927–1933 (1969).
11. Kadrabova, J., Kaldy, A., Sviatko, P., Balazova, E., Gratzlova, J., Balaz, V.: Changes in zinc and copper levels in serum and organs following chronic immobilization stress in rats of different ages. Cas. Lék. ces. **125**, 708–711 (1986). In Slovak.
12. Kato, R.: Drug metabolism under pathological and abnormal physiological states in animals and man. Xenobiotica **7**, 25–92 (1977).
13. Kato, R., Takanaka, A.: Effect of phenobarbital on electron transport system, oxidation and reduction of drugs in liver microsomes of rats of different age. J. Biochem. (Tokyo) **63**, 406–408 (1968).
14. Kato, R., Vassanelli, P., Frontino, G., Chiesara, E.: Variation in the activity of liver microsomal drug-metabolizing enzymes in rats in relation to the age. Biochem. Pharmacol. **13**, 1037–1051 (1964).
15. Kupfer, D., Levin, E.: Monooxygenase drug metabolizing activity in $CaCl_2$-aggregated hepatic microsomes from rat liver. Biochem. Biophys. Res. Commun. **47**, 611–618 (1972).
16. Lowry, O. H., Rosebrough, N. J., Farr, A. L., Randall, R. J.: Protein measurement with the Folin phenol reagent. Biol. Chem. **193**, 265–275 (1951).

17. Netter, K. J., Seidel, G.: An adaptively stimulated O-demethylating system in rat liver microsomes and its kinetic properties. J. Pharmacol. Exp. Ther. **146**, 61–65 (1964).
18. Omura, T., Sato, R.: The carbon monoxide-binding pigment of liver microsomes. J. Biol. Chem. **239**, 2370–2378 (1964).
19. Rikans, L. E.: Effects of ethanol on microsomal drug metabolism in aging female rats. I. Induction. Mech. Ageing Dev. **48**, 267–280 (1989).
20. Roe, J. H., Kuether, C. A.: Determination of ascorbic acid in whole blood and urine trough the 2,4-dinitrophenylhydrazine derivate of dehydroascorbic acid. J. Biol. Chem. **147**, 399–406 (1943).
21. Rosecrans, J. A., Watzman, N., Buckley, J. P.: The production of hypertension in male albino rats subjected to environmental stress. Biochem. Pharmacol. **15**, 1707–1718 (1966).
22. Salmela, S., Vuori, E.: Improved direct determination of copper and zinc in a single serum dilution by atomic absorption spectrophotometry. Atomic Spectr. **5**, 146–149 (1984).
23. Serbinova, E. A., Kadiiska, M. B., Bakalova, R. A., Koynova, G. M., Stoyanovsky, D. A., Karakashev, P. C., Stoytchev, Ts. S., Wolinsky, I., Kagan, V. E.: Lipid peroxidation activation and cytochrome P-450 decrease in rat liver endoplasmic reticulum under oxidative stress. Toxicol. Lett. **47**, 119–123 (1989).
24. Stitzel, R. E., Furner, R. L.: Stress-induced alterations in microsomal drug metabolism in the rat. Biochem. Pharmacol. **16**, 1489–1494 (1967).
25. Ugolev, A. T., Dudchenko, A. M., Belonsova, V. V., Lukjianova, L. D.: Effects of emotional-pain stress on induction of P-450 cytochrome in the rat liver. Biull. Eksp. Biol. Med. **108(7)**, 48–50 (1989). In Russian.
26. Zannoni, V. G., Flynn, E. J., Lynch, M.: Ascorbic acid and drug metabolism. Biochem. Pharmacol. **2**, 1377–1392 (1972).

*Acta Physiologica Hungarica, Volume 81 (1), pp. 37–43 (1993)*

# PHOSPHOLIPID ASYMMETRY IN MICROSOMAL MEMBRANES OF HUMAN BRAIN TUMORS

A. LEDWOŻYW, K. LUTNICKI*

DEPARTMENT OF PATHOPHYSIOLOGY, THE VETERINARY FACULTY OF AGRICULTURAL ACADEMY and
*DEPARTMENT OF PATHOPHYSIOLOGY, FACULTY OF MEDICINE, MEDICAL ACADEMY, LUBLIN, POLAND

Received April 2, 1992
Accepted July 8, 1992

Phospholipid topology in human brain tumor microsomes was investigated by the use of specific aminophospholipid tracer, trinitrobenzenesulfonic acid, and by phospholipase hydrolysis method.

In non-neoplastic brain cortex and white matter the outer leaflet of the bilayer contains predominantly phosphatidylcholine and the inner leaflet mostly phosphatidylethanolamine and phosphatidylserine. Sphingomyelin is equally distributed between the two leaflets.

In microsomes from glioma and meningioma tumors, a significant decrease in phosphatidylcholine and sphingomyelin at the outer surface was observed.

**Keywords**: microsomes, phospholipid asymmetry, brain tumors

Perhaps one of the most salient features of biological membranes recognized in the last decade is that they are highly asymmetric structures both with respect to their proteins and their lipids. This recognition forms an important supplement of the fluid mosaic membrane model, in which membrane proteins are considered as being attached to or embedded in a fluid lipid bilayer [26]. Although this model is presumably correct for most natural membranes, each membrane must be considered as a special case being highly specific in molecular structure. Insight into the topology of membrane constituents will certainly aid the understanding of specific membrane functions. This is particularly true for functions attributed to membrane proteins since the nonrandom distribution of the proteins across the membrane is absolute. Proteins linked to phospholipid polar head groups or embedded in hydrophobic domains of the lipid bilayer are never located on both sides of the same membrane [9]. For lipids the situation is more complex. Not only are the functional aspects less specifically defined, but their asymmetric distribution is also less

Correspondence should be addressed to
Andrzej LEDWOŻYW
Department of Pathophysiology,
The Veterinary Faculty of Agricultural Academy
20-033 Lublin, Akademicka 12, Poland

*Akadémiai Kiadó, Budapest*

extreme, i.e. certain phospholipids are present on both membrane sides but to a different extent [5].

Localization of lipids in biological membranes is carried out by measuring the extent to which phospholipids are available on either side of the membrane to different classes of reagents, i.e. nonpermeable group-specific reagents, phospholipases and phospholipid exchange proteins. These experiments require that when the reagents react with one side of the membrane, none of lipids present at the other membrane side participate in the reaction. Phospholipases have the advantage over chemical reagents, that the combination of them can in principle attack all the phospholipid classes. The disadvantage may be that they disturb bilayer integrity more easily than labels or exchange proteins do.

With the exception or erythrocytes, there are limitations in preparing membrane derivatives in which only the inside can be exposed to the agent. Therefore sidedness experiments with other cells or subcellular organelles usually involve a reaction with intact cells (membrane outside) and lysed cells or subcellular structures (both membrane sides), and the lipids that react in the latter case and not in the former, are assigned to the cytoplasmic surface of the membrane.

Since Barnett et al. [1] discovered that the cellular transformation was associated with some changes in lipid constituents and membrane fluidity, almost all types of tumor cells, such as lymphoma [25], leukaemia [21] or cancer cells [19] have been revealed to have a fluid membrane. However, there are no investigations regarding the membrane of brain tumors, although fluidity of lipid–protein model membranes prepared from bovine brain white matter were performed [11].

In this study, using a specific aminophospholipid marker, trinitrobenzenesulfonic acid (TNBS), and phospholipase hydrolysis we have analysed phospholipid distribution in microsome membranes of human brain tumors.

## Materials and methods

Eighteen brain tumors, including 8 gliomas (5 glioblastomas and 3 astrocytomas) and 10 meningiomas (3 meningotheliomatous, 5 transitional and 2 fibroblastic) were obtained during surgery. The diagnosis in each case was confirmed morphologically. Portions of adjacent normal-appearing cortex and white matter were obtained for control study.

The frozen brain samples were weighed and homogenized with aliquots of 20 mM Tris-HCl buffer, pH = 7.2, The microsomal fraction was prepared according to Sellinger and Boreas [23].

Phospholipase C from *Clostridium welchii* and sphingomyelinase from *Staphylococcus aureus* were purchased from Sigma, St. Louis, USA.

For phospholipase experiments 2.5 mg of microsomal protein was suspended in 5 ml of 10 mM glycylglycine buffer containing 100 mM KCl, 50 mM NaCl, 0.25 mM $Mg^{2+}$, 0.25 mM $Ca^{2+}$ and 44 mM sucrose, pH = 7.4. Ten IU of phospholipase C or 10 IU of sphingomyelinase was then added to the sample and the incubations were continued for 60, 120 or 180 min. Since calcium is required for phospholipase activity, the degradation of phospholipids was terminated by washing the microsomes with phosphate-buffered saline containing 5 mM EDTA. Lipids were extracted according to Folch et al. [6].

Phospholipids were separated by thin-layer chromatography on precoated silica gel G plates (E. Merck, Darmstadt, Germany) according to Roelofsen and Zwaal [22]. Chromatograms were visualized by iodine vapours, spots were scraped off the plate and the quantity of phospholipids was determined by measuring the amount of phosphorus according to Bartlett [2].

The percentage of phospholipid hydrolyzed following treatment of microsomes with phospholipase C was determined by measuring the ratio of remaining diacylglycerophospholipid to the corresponding lyso-derivative. For the determination of sphingomyelin degradation by sphingomyelinase, the absolute and relative quantity of sphingomyelin recovered from the sample was compared to the absolute and relative quantity of sphingomyelin recovered from the non-treated control sample.

In order to confirm the results obtained in phospholipase experiments, microsomes (2 mg protein) were incubated for 3 hr with 1 mM TNBS under penetrating and non-penetrating conditions, as described by Takahashi and Kako [27].

## Results

The rate of microsomal lipid hydrolysis did not increase between 1 and 3 hours. However, with a microsomal lipid extract more than 90% of the phospholipids were hydrolysed. Thus, it can be assumed, that phospholipase C does not lyse the membrane, and that 50% of the phospholipids accessible to the phospholipase C are located on the outer side of the microsome. The determination of the extent of hydrolysis of the different phospholipids shows that about 80% of phosphatidylcholine in grey and white matter microsomes, and about 55% of this phospholipid in glioma and meningioma tissue microsomes was digested. The amounts of phosphatidylethanolamine digested by phospholipase C in microsomes were about 35% in normal brain tissue and about 50% in neoplasms. Phosphatidylserine was digested to the extent of 20% and 40%, respectively, the amount of sphingomyelin hydrolyzed by sphingomyelinase were near 50% and 30%, respectively (Table I).

**Table I**

*Hydrolysis of brain microsomal phospholipids with phospholipase C and sphingomyelinase*

| | % of hydrolysis | | | |
|---|---|---|---|---|
| | Grey matter | White matter | Glioma | Meningioma |
| | $\bar{x} \pm SD$ | $\bar{x} \pm SD$ | $\bar{x} \pm SD$ | $\bar{x} \pm SD$ |
| Phosphatidylcholine | 78.3 ± 6.5 | 75.3 ± 6.6 | 56.1 ± 4.2 | 54.2 ± 5.1 |
| Phosphatidylethanolamine | 35.2 ± 2.4 | 33.7 ± 2.5 | 51.3 ± 4.0 | 52.6 ± 4.6 |
| Phosphatidylserine | 22.8 ± 1.9 | 21.2 ± 2.0 | 42.1 ± 3.1 | 40.0 ± 3.5 |
| Sphingomyelin | 52.3 ± 4.5 | 50.6 ± 4.4 | 32.1 ± 2.5 | 34.6 ± 3.1 |
| Total phospholipids | 49.6 ± 4.4 | 51.5 ± 4.4 | 50.7 ± 4.4 | 52.2 ± 4.7 |

In order to confirm the results for aminophospholipids, microsomes were incubated with TNBS in penetrating and non-penetrating conditions. When TNBS was allowed to penetrate the membrane, about 90% of different aminophospholipids both in "control" and neoplastic microsomes reacted with this reagent. However, under non-penetrating conditions only 35% of phosphatidylethanolamine in "normal" brain microsomes and about 40% of this phospholipid in tumor microsomes were accessible to the reagent. Accessibility of ethanolamine plasmalogen to the reagent was in these conditions 30% and 35%, respectively. Phosphatidylserine was accessible to the extent of 20% and 30%, respectively (Table II).

**Table II**

*Percent of brain microsomal aminophospholipid reacting with trinitrobenzenesulfonate under non-penetrating conditions*

| | % of reacting phospholipids | | | |
|---|---|---|---|---|
| | Grey matter | White matter | Glioma | Meningioma |
| PE diacyl | 35 ± 4 | 34 ± 4 | 41 ± 4 | 45 ± 6 |
| PE alkenylacyl | 27 ± 3 | 29 ± 4 | 34 ± 4 | 36 ± 4 |
| PS diacyl | 21 ± 2 | 22 ± 3 | 29 ± 3 | 34 ± 4 |

Mean values ± S.D. PE – phosphatidylethanolamine. PS – phosphatidylserine

These results are in good agreement with those obtained with phospholipase C and suggest that under these conditions, only the phospholipids of the outer leaflet of the microsomal vesicle were available for the chemical marker and enzymatic digestion.

Assuming that all external phospholipids were accessible, the distribution on each side of the bilayer could be evaluated. In non-neoplastic tissue microsomes of the outer leaflet of the bilayer contains predominantly phosphatidylcholine and of the inner leaflet mostly phosphatidylethanolamine and phosphatidylserine. Sphingomyelin is equally distributed between the two leaflets. Phosphatidylinositol is not hydrolyzed by phospholipase C from *Clostridium welchii*, but since the hydrolyzed lipids account for 50% of the total phospholipids, phosphatidylinositol can be tentatively assigned to the inner leaflet of the bilayer.

However, significant differences were observed in phospholipid distribution of neoplastic tissue microsomes. A significant decrease in phosphatidylcholine which occupied the outer leaflet of the membrane was observed. Similar changes were observed in sphingomyelin distribution. On the contrary, phosphatidylethanolamine and phosphatidylserine were dislocated to the outer leaflet of the bilayer in meningioma and glioma microsomes (Table III).

**Table III**

*Distribution of phospholipids (mole %) on either side of the bilayer of control brain and neoplastic microsomal membranes*

| Sidedness | Grey matter | | White matter | | Glioma | | Meningioma | |
|---|---|---|---|---|---|---|---|---|
| | Outer | Inner | Outer | Inner | Outer | Inner | Outer | Inner |
| PC | 31.6 ± 1.5 | 8.0 ± 0.6 | 33.0 ± 2.1 | 8.5 ± 0.8 | 23.1 ± 2.0 | 12.3 ± 1.3 | 20.1 ± 1.8 | 11.4 ± 1.0 |
| PE diacyl | 5.6 ± 0.4 | 12.0 ± 0.9 | 5.3 ± 0.5 | 10.2 ± 1.1 | 7.1 ± 0.6 | 9.4 ± 0.8 | 7.3 ± 0.8 | 8.5 ± 0.9 |
| PE alkenylacyl | 5.0 ± 0.5 | 14.7 ± 1.2 | 4.8 ± 0.5 | 12.1 ± 1.3 | 7.0 ± 0.8 | 11.3 ± 1.2 | 7.5 ± 0.6 | 12.0 ± 1.3 |
| PS | 2.5 ± 0.2 | 8.3 ± 0.9 | 2.8 ± 0.3 | 7.8 ± 0.8 | 3.6 ± 0.4 | 6.0 ± 0.7 | 4.0 ± 0.4 | 6.3 ± 0.7 |
| Sph | 3.6 ± 0.4 | 3.0 ± 0.3 | 3.8 ± 0.4 | 3.3 ± 0.4 | 2.1 ± 0.2 | 5.2 ± 0.6 | 2.5 ± 0.3 | 4.8 ± 0.5 |

Mean values ± S.D. PC – phosphatidylcholine, PE – phosphatidylethanolamine, PS – phosphatidylserine, Sph – sphingomyelin

## Discussion

In recent years the phospholipids are regarded as the major components of the biomembranes, which have dynamic structure and they not only act as a barrier, but they also appear to function in initiating a variety of cell functions. The importance of biological membrane fluidity has been implicated in patch and cap formation in lymphocytes [14], sugar transport [15], membrane enzymatic protein activity [3], clustering of particles [18], temperature [20], platelet aggregation [28] and diabetes mellitus [17]. Asymmetrical distribution of phospholipids in chicken brain microsomal membranes has been shown by Freysz and co-workers [9]. According to these authors, the outer leaflet of the microsomal vesicles contained about 75% of the choline phospholipids and about 25% of the aminophospholipids, whereas an opposite distribution was observed for the inner leaflet. Similar results were also reported for ethanolamine phosphoglycerides in synaptosomal plasma membranes by Fontaine et al. [7].

Hattori and co-workers [10] have shown, that meningioma and metastatic cancers of the brain had more fluid membranes than the control brain, while glioma was more rigid than the cortex, nevertheless being more fluid than the white matter.

The alteration in membrane fluidity of brain tumors may be responsible in determining aspects of each of its major behavioural characteristics. In a metastatic tumor which had more fluid membrane, increasing fluidity may somehow relate to the mechanism of distant metastasis.

This increase in fluidity of brain tumor microsomal membranes may be due to the increase of unsaturated fatty acid content. However, there are many other factors modulating membrane fluidity besides the content of phospholipid and fatty acid

composition [24], including the ratio of lipid to protein, quality of membrane proteins [13], and protein-lipid interactions [4]. The content of cholesterol also makes the membrane rigid [12].

To our knowledge, this is a first evidence, that phospholipid asymmetry in brain tumor microsomes is profoundly disturbed. These disturbances can provide an explanation for the changes in membrane functions, although the precise relationship between phospholipid topology and any specific functional alteration remains to be defined.

## REFERENCES

1. Barnett, R. E., Furcht, L. T., Scott, R. E.: Differences in membrane fluidity and structure in contact-inhibited and transformed cells. Proc. Natl. Acad. Sci. USA **71**, 1992–1994 (1974).
2. Bartlett, G. R.: Phosphorus assay in column chromatography. J. Biol. Chem. **234**, 466–468 (1959).
3. Bösterling, B., Stier, A.: Specificity in the interaction of phospholipids and fatty acids with vesicle reconstituted cytochrome P-450: a spin label study. Biochim. Biophys. Acta **729**, 258–266 (1983).
4. Chapman, D., Gomez-Ferninadez, J. C., Goni, F. M.: Intrinsic protein-lipid interactions: physical and biochemical evidence. FEBS Lett. **98**, 211–223 (1979).
5. Drenthe, E. H. S., Klompmakers, A. A., Bonting, S. L., Daemen, F. J. M.: Transbilayer distribution of phospholipids in photoreceptor membrane studied with trinitrobenzene sulfonate alone and in combination with phospholipase D. Biochim. Biophys. Acta **603**, 130–141 (1980).
6. Folch, J., Lees, M., Sloane-Stanley, G. H.: A simple method for the isolation and purification of total lipids from animal tissues. J. Biol. Chem. **226**, 497–509 (1957).
7. Fontaine, R. N., Harris, R. A., Schroeder, F.: Aminophospholipid asymmetry in murine synaptosomal plasma membrane. J. Neurochem. **34**, 269–277 (1980).
8. Freysz, L., Dreyfus, J., Vincendon, G., Binaglia, L., Roberti, L., Porcellati, G.: Asymmetry of brain microsomal membrane correlation between the asymmetric distribution of phospholipids and the enzymes involved in their synthesis. In: Phospholipids in the nervous system, ed. Horrocks, L. Raven Press, New York 1982, vol. 1, p. 37.
9. Freysz, L., Horth, S., Dreyfus, H.: Topographic distribution of enzymes synthesizing phosphatidylcholine and phosphatidylethanolamine in chicken brain microsomes. J. Neurochem. **38**, 582–587 (1982).
10. Hattori, T., Andoh, T., Sakai, N., Yamada, H., Kameyama, Y., Ohki, K., Nozawa, Y.: Membrane phospholipid composition and membrane fluidity of human brain tumor: a spin label study. Neurol. Res. **9**, 38–43 (1987).
11. Hemmings, M. A., Post, J. F. M.: Lipid-protein interactions in model membranes from bovine brain white matter: an ESR, spin label and electron microscopy study. Biochim. Biophys. Acta **436**, 222–234 (1976).
12. Inbar, M., Shinitzky, M.: Cholesterol as a bioregulator in the development and inhibition of leukemia. Proc. Natl. Acad. Sci. USA **71**, 4229–4231 (1974).
13. Jähnig, F.: Structural order of lipids and proteins in membranes: evaluation of fluorescence anisotrophy data. Proc. Natl. Acad. Sci. USA **76**, 6361–6365 (1979).
14. Klausner, R. D., Bhalla, D., Draysten, P., Hoover, R. L., Karnovsky, M. J.: Model for capping derived from inhibition of surface receptor capping by free fatty acids. Proc. Natl. Acad. Sci. USA **77**, 437–441 (1979).

15. Linden, C. D., Wright, K. L., McConnel, H. M., Fox, C. F.: Lateral phase separations in membrane lipids and the mechanism of sugar transport in *Eschierichia coli*. Proc. Natl. Acad. Sci. USA **70**, 2271–2275 (1973).
16. Lowry, O. H., Rosebrough, N. J., Farr, A. L., Randall, R. J.: Protein measurement with the Folin phenol reagent. J. Biol. Chem. **193**, 265–275 (1951).
17. Lupu, F., Calb, M., Fixman, A.: Alterations of phospholipid asymmetry in the membrane of spontaneously aggregated platelets in diabetes. Thromb. Res. **50**, 605–616 (1988).
18. Nicolson, G. L.: Topography of membrane concavalin A sites modified by proteolysis. Nature **239**, 193–196 (1980).
19. Nicolson, G. L., Poste, G.: The cancer cell: dynamic aspects and modifications in cell-surface organization. N. Engl. J. Med. **295**, 253–258 (1976).
20. Ohki, K., Kasai, R., Nozawa, Y.: Correlation between fluidity and fatty acid composition of phospholipid species in *Tetrahymena pyriformis* during temperature acclimation. Biochim. Biophys. Acta **558**, 273–281 (1979).
21. Petitou, M., Tuy, F., Rosenfeld, C., Mishal, Z., Paintrand, M., Jasnin, C., Mathe, G., Inbar, M.: Decreased microviscosity of membrane lipids in leukemic cells: two possible mechanisms. Proc. Natl. Acad. Sci. USA **75**, 2306–2310 (1978).
22. Roelofsen, B., Zwaal, R. F. A.: The use of phospholipases in the determination of asymmetric phospholipid distribution in membranes. Meth. Membr. Biol. **7**, 147–158 (1976).
23. Sellinger, O. Z., Boreas, R. N.: Zonal density gradient electrophoresis of intracellular membranes of brain cortex. Biochim. Biophys. Acta **173**, 176–184 (1969).
24. Shinitzky, M.: Membrane fluidity in malignancy: adversative and recuperative. Biochim. Biophys. Acta **738**, 251–261 (1984).
25. Shinitzky, M., Inbar, M.: Difference in microviscosity induced by different cholesterol levels in the surface membrane lipid layer of normal lymphocytes and malignant lymphoma cells. J. Mol. Biol. **85**, 603–615 (1974).
26. Singer, S. J., Nicolson, G. L.: The fluid mosaic model of the structure of cell membranes. Science **175**, 720–731 (1972).
27. Takahashi, K., Kako, K. J.: The effects of myocardial ischemia and nisoldipine pretreatment on the asymmetric distribution of phosphatidylethanolamine in a canine heart sarcolemmal preparation. Biochem. Med. Metab. Biol. **35**, 308–321 (1986).
28. Zwaal, R. F. A., Bevers, E. M.: Platelet phospholipid asymmetry and its significance in hemostasis. Subcell. Biochem. **9**, 299–334 (1983).

*Acta Physiologica Hungarica, Volume 81 (1), pp. 45–57 (1993)*

# EVIDENCE FOR THE PRE-SYNTHESIZED STATE OF SECRETED MACROPHAGE ARGINASE: ARGINASE ACTIVITY CANNOT BE MODIFIED IN SHORT-TERM CULTURES

A. HRABÁK, F. ANTONI, Ildikó CSUKA

1ST DEPARTMENT OF BIOCHEMISTRY, SEMMELWEIS UNIVERSITY MEDICAL SCHOOL, BUDAPEST, HUNGARY

Received April 3, 1992
Accepted June 3, 1992

The arginase produced by peritoneal macrophages is not synthesized *de novo* in short-term (3 h) cultures after harvesting the cells. In long-term cultures the arginase synthesis is restored. In contrast to arginase lysozyme is continuously synthesized in short-term cultures. These statements were proved by the following experimental results:

1. Protein synthesis inhibitor and lysosomotropic agents did not alter the arginase level.

2. Arginine and its analogue, canavanine and ornithine were not able to change the arginase activity.

3. The product of an alternative metabolic pathway of arginine, sodium nitrite, did not affect arginase activity.

4. Effectors influencing the synthesis of cyclic nucleotides (cAMP, cGMP), indomethacin, sodium nitroprusside and an analogue of cAMP had no effect on the arginase activity.

5. Arginase activity could not be significantly modified either by an *in vitro Micrococcus luteus* treatment or by changing the adherence period of peritoneal exudate cells.

6. When arginase was produced in murine peritoneal macrophages at various periods with medium change, the total arginase released into the media from murine and rat macrophages did not exceed the original intracellular arginase content of the adhered cells during the first 6 hours.

**Keywords**: macrophages, arginase, lysozyme, protein synthesis inhibitors, medium change

Fishman [9] reported that murine peritoneal macrophages contained a much higher arginase activity than rat peritoneal cells. We have already demonstrated [12–14] that this difference can also be observed in casein-elicited peritoneal macrophages and the *in vitro* secretion of arginase was maximal 1–6 hours after their

Correspondence should be addressed to
András HRABÁK
Semmelweis University Medical School, 1st Department of Biochemistry
H-1444 P.O. Box 260, Puskin u. 9, Hungary

*Akadémiai Kiadó, Budapest*

adherence, if expressed in specific activity units. The arginase activity of elicited murine macrophages was also higher than that of resident cells. It was also proved that this difference cannot be due to the $Ca^{2+}$-ion concentration, the energy supply, the different cell types of the peritoneal cavity of the two species [14]. Arginase production of macrophages was studied in LPS (lipopolysaccharide)-treated cells and the role of a cAMP-mediated system in the activation of the arginase production was observed [6]. Recently other investigators found that arginine is serving as a source of another important synthetic process: the synthesis of nitric oxide (NO) and nitrite ($NO_2$) is also realized by using arginine [21, 22]. It is very likely that the produced NO has important functions in the tumoricid effect of macrophages [8, 10, 11], the self-killing during immunological processes, and the focal vasodilatation caused by the endothelium derived NO [1, 2, 17, 20].

All the processes mentioned above were carried out *in vitro* long-term murine macrophage cultures. Our earlier observations concerning the difference in short-term murine and rat macrophage cultures cannot be explained by these investigations. For this reason we performed a series of experiments to explore the cause of this difference and the possible regulation of the arginase production. Several protein synthesis inhibitors, proteolysis inhibitors, effectors of the cAMP and cGMP-dependent systems, arginine and its derivatives were applied for modifying arginase activity. Lysozyme was always measured as a reference enzyme for macrophages.

## Materials and methods

*Animals and cells*

CFLP male mice and Wistar male rats (LATI, Gödöllő, Hungary) were injected i.p. with 1 ml and 5 ml 2% dephosphorylated casein, respectively. Animals were sacrified on the fourth day, cells were removed from the peritoneal cavity by using a $Ca^{2+}$ and $Mg^{2+}$-free Hanks medium and centrifuged at 500 g. The isolated PEC (peritoneal exudate cells) were then resuspended in Hanks medium containing $Ca^{2+}$ and $Mg^{2+}$ and left to be adhered for 30–60 min in plastic petri dishes (Linbro). The adhered cells were considered as macrophages.

*Treatments with protease inhibitor*

10–100 µl 4 mg/ml PMSF (phenyl-methyl-sulfonyl-fluoride) dissolved in IPA (isopropanol) was added to 1.0 ml of culture media. Macrophages were treated with PMSF for various culturing periods and arginase and lysozyme activities were determined directly from the supernatants or from cell lysates. These latter were prepared from the cells after removing the supernatant and adding 1.0 ml water for 1 h at room temperature. The eventual precipitate was removed by centrifugation.

The damage of macrophages by this treatment was checked by using PMSF solution and identical amount of IPA as control on metabolically labelled ($^{14}$C-leucine) macrophages. The metabolic labelling was performed as reported earlier [5]. The direct effect of IPA and PMSF on enzyme activities was also checked.

*Cultures in the presence of various drugs*

Various drugs capable of inhibiting protein synthesis or having lysosomotropic properties were studied to show their effect on enzyme activities in macrophages. Emetine (100 nM – 1 mM), cycloheximide and puromycine (1 μM – 1 mM) were used as protein synthesis inhibitors and chloroquine (1 μM – 1 mM), ammonium chloride and LeuOMet (L-leucine-O-methyl ester, 0.1 – 10 mM) were applied as lysosomotropic agents in the cultures of murine and rat macrophages during the incubation period. Enzyme activities were determined directly both from supernatants and cell lysates. The effects of these drugs on cell damage and on the enzyme activities were also checked as in the case of IPA and PMSF. Several other compounds were tested because of their known effect on cAMP or the cGMP-dependent intracellular processes. $Bt_2$cAMP ($N^6$, $O^2$-dibutyryl-adenosine-3':5' cyclic monophosphate) was used at 1 mM, sodium nitroprusside at 0.1 and 0.01 mM final concentration. Sodium nitrite as a final product of the arginine deiminase pathway was used at 50 – 200 μM concentration.

*Adding of exogenous arginine, ornithine and canavanine to the cultures*

Elicited murine and rat macrophages were cultured in the presence of 0.6, 6.0 and 30.0 mM arginine in Hanks medium for 3 h at 37 °C. Arginase was measured directly from the supernatants and cell lysates. Ornithine was added at 1 – 20 mM final concentration, while L-canavanine, an arginine analogue was applied at 0.6 – 3.0 mM final concentration. Enzyme activities were determined in each case.

*Study of the effect of M. luteus bacteria on the arginase activity*

$10^8 - 5 \times 10^8$ *M. luteus* bacteria were added to the adhered peritoneal macrophages for 60 min. Then the bacteria were removed by washing three times and Hanks medium was added for 3 h at 37 °C. In some experiments *M. luteus* cells were present during 3 h and after the treatment the enzyme activities were measured.

*Determination of enzymes and amount of protein*

Arginase activity was detected on the basis of urea formation. Urea was measured by a spectrophotometric reaction [7]. Several times the enzyme was also detected on the basis of ornithine production by ion exchange thin layer chromatography [16]. Lysozyme activity was measured spectrophotometrically according to Jolles [18]. Protein concentration was determined according to Lowry et al. [19]

*Release of arginase and lysozyme from cells cultured for various periods*

Macrophages were cultured and their medium was changed at 3 h, 6 h, 24 h and 48 h. Enzyme activities were measured in the media at each time interval in the removed medium. Hanks' medium was used for 3 h and 6 h, Eagle's medium containing 10% FCS (foetal calf serum) was used for 24 h and 48 h. Control urea levels in the serum-containing media were subtracted from each individual sample.

*Measuring of cAMP content*

Cells were harvested, adhered and cultured for 3 h. The cAMP content of the adhered cells and macrophages cultured for 3 h was determined by a cAMP-measuring kit of Amersham.

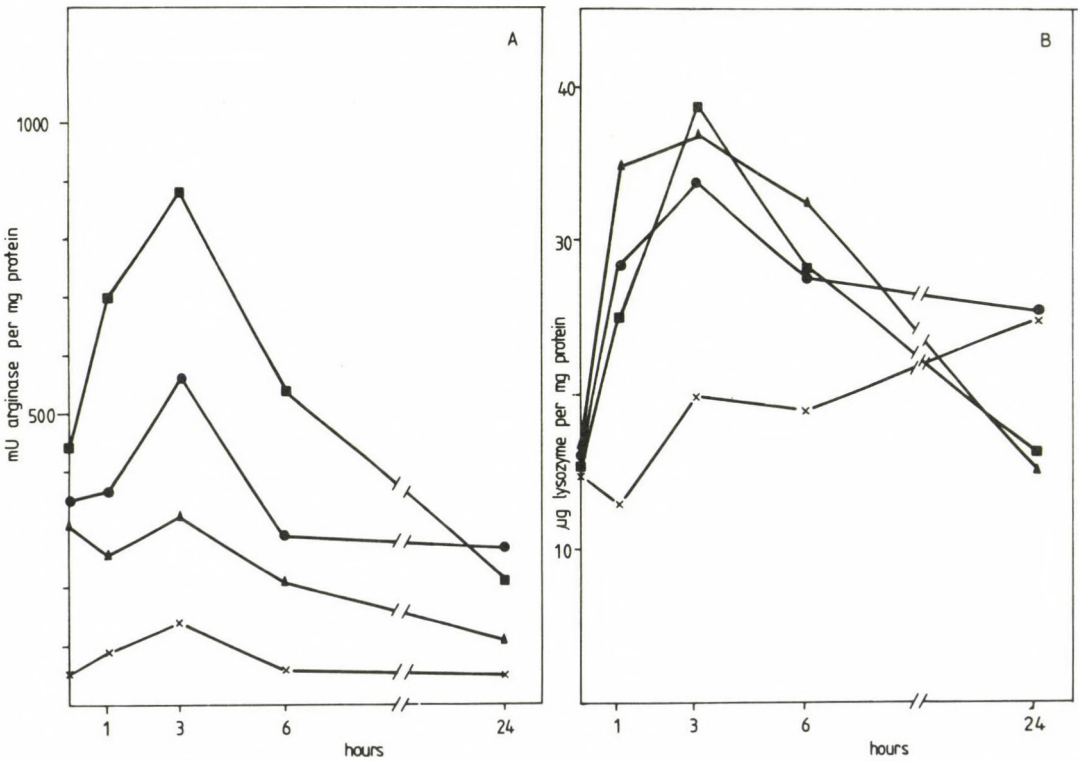


*Fig. 1.* The effect of protease inhibitor on macrophage arginase and lysozyme. PMSF did not enhance the arginase (A) and lysozyme (B) activity in macrophage supernatants during the first 6 h of culture. ▲ = murine casein-elicited macrophages without treatment, ■ = murine casein-elicited macrophages in the presence of 5% IPA, ● = murine casein-elicited macrophages in the presence of 0.2 mg/ml PMSF–5% IPA, × = rat casein-elicited macrophages in the presence of 0.2 mg/ml PMSF–5% IPA. Cells were cultured at 37 °C in Hanks (0–6 h) or in Eagle (24 h) medium

## Results and discussion

### *The effect of the protease inhibitor*

PMSF did not have any significant enhancing effect on the arginase activity during the first 6 hours. The elevated arginase activity in the cell supernatants can be attributed to the presence of IPA (the solvent of PMSF) that can damage the plasma membrane in certain extent leading to a higher release of arginase from the cells (Fig. 1). IPA and PMSF showed a direct effect on metabolically labelled macrophages: 26.8±4.1% of labelling was released from control cells and 52.4±7.7% was released from IPA- and PMSF-treated cells, respectively, during 3 h at 37 °C

(data not shown). The high sensitivity of macrophage membrane compared to lymphocytic plasma membrane was observed earlier [15]. In contrast, lysozyme release was not affected by IPA and PMSF treatment (Fig. 1) suggesting a different secretion mechanism (e.g. a selective leakage).

This result suggested that the difference between short-term arginase release of murine and rat cells cannot be explained by the different proteolytic activity in peritoneal cells.

*The effect of protein synthesis inhibitors*

Emetine, cycloheximide and puromycine are known as effective blockers of eukaryotic protein synthesis. These drugs had not any decreasing effect on the murine arginase activities (Table I). At the same time both $^{14}C$-labelled leucine and arginine incorporation were inhibited by these drugs either in murine or in rat macrophages (data not shown) and emetine was found to be able to inhibit the phagocytosis in rat peritoneal macrophages [4]. This observation proved that arginase had to be produced before adding the drugs.

**Table I**

*The effect of various treatments on the murine and rat macrophage arginase*

| Samples | Secreted | Intracellular |
|---|---|---|
| Murine | | |
| control | 240 ± 69 | 191 ± 11 |
| 0.1 mM emetine | 294 ± 91 | 218 ± 27 |
| 0.1 mM cycloheximide | 346 ± 37 | 179 ± 67 |
| 0.1 mM puromycine | 286 ± 88 | 163 ± 71 |
| 0.1 mM chloroquine | 242 ± 91 | 168 ± 71 |
| 1.0 mM $NH_4Cl$ | 242 ± 146 | 129 ± 92 |
| 1.0 mM LeuOMet | 239 ± 33 | 305 ± 78 |
| 0.1 mM $NaNO_2$ | 269 ± 62 | 171 ± 71 |
| 0.1 mM Na nitroprusside | 270 ± 70 | 165 ± 21 |
| 1.0 μM indomethacin | 219 ± 34 | 238 ± 53 |
| 1.0 mM $Bt_2cAMP$ | 221 ± 42 | 200 ± 62 |
| $5 \times 10^8$ M. luteus | 222 ± 63 | 182 ± 85 |
| Rat | | |
| control | 17 ± 10 | 45 ± 16 |
| 1.0 mM $Bt_2cAMP$ | 39 ± 20 | 54 ± 16 |
| $5 \times 10^8$ M. luteus | 54 ± 47 | 54 ± 35 |

Specific activity is expressed in mU arginase per mg protein. 1 mU = 1 nmol urea released per min. S.E.M. values were calculated from 4 simultaneous experiments

*The effect of various lysosomotropic agents*

Chloroquine, ammonium chloride and LeuOMet were added to the cultures at their effective lysosomotropic concentrations. These agents had no effect on the arginase level both in the secreted and in the intracellular (lysate) macrophage fractions. The slight enhancing effect of LeuOMet on the intracellular arginase cannot be considered as a significant effect (Table I). Lysosomotropic agents like chloroquine and LeuOMet were also found to be potent inhibitors of protein synthesis and phagocytosis in peritoneal macrophages [4, 5]. Consequently, these results also support the hypothesis that arginase was synthesized in the cells *in vivo*, before their harvesting from the peritoneal cavity.

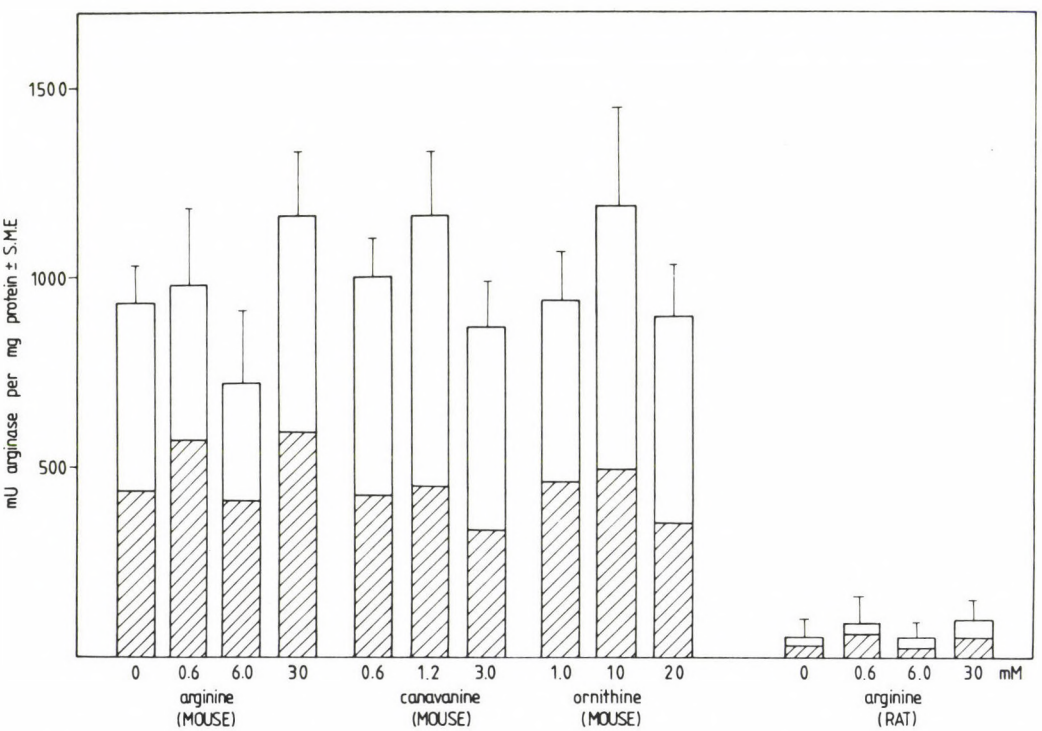


*Fig. 2.* The effect of arginine, its analogue and derivative on macrophage arginase activity. Arginine, canavanine and ornithine did not influence the arginase activity either in the secreted (▨) or in the intracellular (□) fraction. Neither has total macrophage arginase changed. Cells were cultured for 3 h at 37 °C

*Arginine, its analogue canavanine and ornithine are not the inducers or repressors of arginase in short-term cultures*

Arginine was used at various concentrations in the cultures to provoke arginase synthesis. Neither 0.6 mM (the arginine level of Eagle medium) nor 30 mM did cause any significant effect on the enzyme activity. Ornithine, the product of arginase reaction and canavanine, an analogue of arginine could not affect the enzyme production during 3 h either (Fig. 2). It is well known that liver arginase can be induced *in vivo* by adding a high amount of protein in the food, i.e. arginase is an inducible enzyme in the liver. Our results may be explained in two ways: 1. in culture macrophage arginase cannot be induced by its substrate and its analogues or derivatives; 2. more likely, the enzyme induction is not observed in short-term cultures. This latter explanation is in good agreement with the hypothesis that arginase is not synthesized *de novo* during the first 3 hours. On the other side, the induction of arginase in liver *in vivo* also requires a long time (days and not hours). Nitrite, the oxidized product of another pathway of arginine metabolism [1, 2, 8, 10–12, 20–22] is not able to influence the arginase activity in macrophages within a short time (Table I). M. luteus bacteria are readily ingested by isolated murine and rat macrophages [4, 23, 24] showing that the cells are metabolically active: the exposure of the cells to M. luteus bacteria for the first hours did not cause any change in arginase activity.

*Effectors of cAMP and cGMP dependent mechanisms had no effect on arginase activity*

The hydrolysis of arginine into urea and ornithine in LPS-induced macrophages (24 h in vitro) was regulated, at lease, partly, by a cAMP dependent mechanism [5]. For checking the possibility to influence the arginase activity in short-term cultures, indomethacin, a potent inhibitor of cyclooxygenase and consequently the adenylate cyclase by decreasing the $PGE_2$ level and $Bt_2cAMP$, the hydrophobic permeable dibutyryl derivative of cAMP were used to study the arginase activity in the presence of these compounds. Neither indomethacin nor $Bt_2cAMP$ exerted effect on the short-term arginase (Table I) supporting that the formation of arginase was not altered during this period i.e. the enzyme had to be pre-synthesized in the cells before isolation. The cAMP level of freshly isolated and adhered macrophages was also measured in resident and casein-elicited murine and rat macrophages supposing that the different arginase activities may be attributed to different cAMP levels, but cAMP levels were too low to be measured in any macrophage sample. Possibly, the cyclic nucleotide was metabolized completely before harvesting the cells.

Sodium nitroprusside, an activator of guanylate cyclase [3] did not influence the arginase level (Table I).

*Released arginase during the first 3–6-h culture period does not exceed the enzyme activity of adhered cells*

Murine and rat peritoneal cells were harvested and allowed to be adhered for 30 min. Adhered cells were then cultured for 3 h in Hanks' medium. After this time, medium was changed for a fresh Hanks' medium. After 3 h the medium was changed again for Eagle's medium containing 10% FCS and cells were cultured further for 24 h. Then the medium was changed again for Eagle's medium containing serum and culturing was continued for 48 h. Sterile conditions were provided by adding 100 IU/ml penicilline and 0.1 mg/ml streptomycine into the media. Arginase and lysozyme activities were determined in each removed supernatant and in the cells after 48 h and the total secreted arginase was compared to the arginase content of the adhered cells. The results of this experiments show (Table II) that in the first 6 hours the amount of secreted arginase did not exceed the arginase activity in the adhered cells but additional arginase was measured in long-term cultures. Our former experiments showed that the greater part of arginase was released during the adherence of cells, but the specific activity was higher in the first 3-h cultures [14] because other proteins were also secreted during the adherence period decreasing the specific activity. In contrast to arginase, lysozyme release was higher in 3-h cultures than during adherence and short-term cultures showed an excess above the content of the adhered cells indicating that this enzyme is constitutively produced and secreted.

**Table II**

*Arginase and lysozyme release from murine and rat macrophages and the effect of medium change*

| Sample | Murine | | Rat | |
|---|---|---|---|---|
| | arginase | lysozyme | arginase | lysozyme |
| PEC before adherence | 3.07 ± 1.01 | 0.12 ± 0.04 | 1.30 ± 0.48 | 0.37 ± 0.02 |
| Release during adherence | 2.81 ± 0.88 | 0.17 ± 0.10 | 0.86 ± 0.13 | 0.25 ± 0.06 |
| Adhered macrophages | 3.28 ± 0.45 | 0.09 ± 0.03 | 0.79 ± 0.22 | 0.15 ± 0.04 |
| 3 h release (adhered) | 1.81 ± 0.47 | 0.44 ± 0.08 | 0.20 ± 0.03 | 0.34 ± 0.04 |
| 3 + 3 h release | 1.66 ± 0.36 | 0.13 ± 0.02 | 0.29 ± 0.15 | 0.07 ± 0.02 |
| 3 + 3 + 24 h release | 3.97 ± 0.99 | 0.53 ± 0.05 | 0.97 ± 0.10 | 0.25 ± 0.07 |
| 3+3+24+24 h release | 2.48 ± 0.48 | 0.14 ± 0.06 | 0.28 ± 0.04 | 0.06 ± 0.02 |
| 3+3+24+24 h intracel. | 2.34 ± 0.16 | 0.04 ± 0.03 | 0.85 ± 0.15 | 0.02 ± 0.02 |

Arginase activity is expressed in mU arginase per $10^6$ cells, lysozyme activity in μg lysozyme per $10^6$ cells. Media were changed at the time points indicated above. Hanks' medium was used for short-term experiments (3 and 3+3 h) and Eagle's medium (containing 10% FCS) was used for 24 and 48 h (24+24 h) experiments. Intracellular enzyme was determined only at the final stage. Released enzymes were measured directly from the removed supernatants

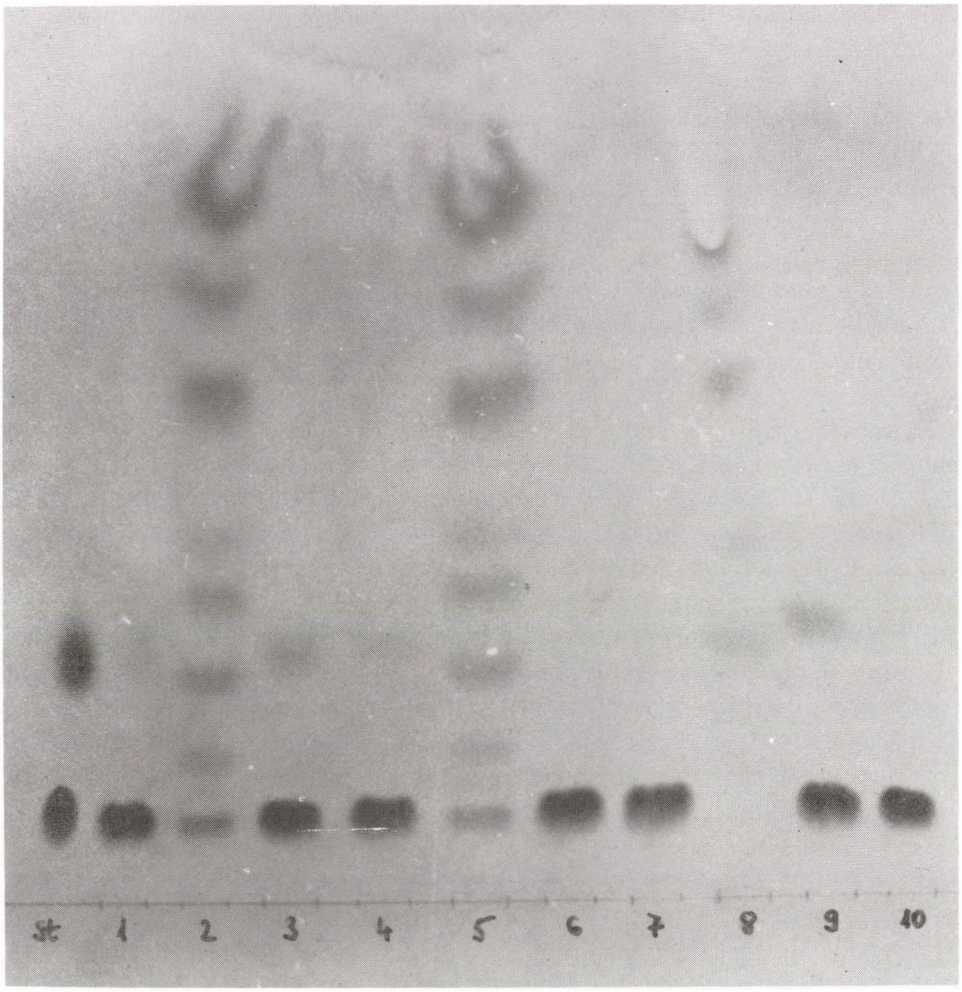


*Fig. 3.* Thin layer ion exchange chromatography of various murine macrophage cultures. Supernatants of samples cultured in Eagle (30 μl) were chromatographed immediately. Samples cultured in Hanks were stopped at the given time, 100 μl samples and 100 μl 0.1 M Arg were incubated at 37 °C for 180 min and 30 μl samples were chromatographed. Samples: St = standard amino acids, Arg, Lys and Orn (increasing $R_f$), 1 = 3H + 3H sup., 2 = 3E sup., 3 = 3H sup., 4 = 3E + 3H sup., 5 = 3E + 3E sup., 6 = 24EF + 3H sup., 7 = control, 8 = 24EF sup., 9 = 3H int., 10 = 3H + 3H int. Abbreviations: H and E = Hanks and Eagle media used for culture, F = foetal calf serum 10%, + indicates change of medium at the time given (3 or 24 h). sup. = supernatant, int. = intracellular Chromatography was made of the last supernatant or cell lysate. Control: 0.05 M Arg incubated for 180 min at 37 °C

A similar experiment summarized in Fig. 3 showed that all short-term cultures (including samples with changed medium) contained arginase (ornithine spots are visible) independently of the culturing medium. If culture was performed for 24 h in Eagle's medium and then changed for Hanks for 3 h, ornithine was not found in this second supernatant. This investigation also has supported the hypothesis that arginase was pre-synthesized in isolated macrophages, the greatest part of the enzyme was secreted in the first 6 hours and additional arginase must be synthesized *de novo* requiring long-term (24 h) culture. This arginase formation, in contrast to the short-term release could be inhibited by emetine and cycloheximide [13]. Figure 3 also shows that the original arginine content of Eagle medium was metabolized into ornithine indicating a high arginase activity in the long-term culture supernatant.

Two additional experiments were performed to prove that the failure to affect the arginase activity in short-term macrophage cultures cannot be due to the low number of macrophages in the adhered fraction or to the short adherence period. Cells were harvested and then fractionated on a Ficoll-Paque gradient before adherence. Mononuclear cells are enriched in the interphase and this fraction contains higher arginase and lysozyme activity than the pelleted cells in both species (data not shown). Figure 4 shows that the enzyme activities were not significantly different in the cells adhered for various periods from 15 – 180 min.

As to our experiments arginase is not *de novo* synthesized in peritoneal macrophages during short-term cultures. The enzyme should be synthesized during 72 h between the casein injection and the killing of the animal. The differences in enzyme activities at various time points [13, 14] may be attributed to the differences in the release of the enzyme. This statement was proved by the following facts: the enzyme activity was not changed in the presence of protein synthesis inhibitors. Enzyme activity cannot be influenced by arginine and its derivatives, exposing to bacterial loading and using various effectors of cAMP and cGMP dependent systems. The enzyme activity is independent on the adherence time period. Fishman [9] could not detect arginase after a 3-h incubation in the medium even in murine macrophages. In our experiments the enzyme was found both in the secreted and the intracellular fractions and the results summarized above supported a hypothesis that the arginase must be synthesized before harvesting the cells from the peritoneal cavity. Our results in good agreement with Fishman's observations [9] also suggested that in long-term experiments a *de novo* arginase synthesis may be observed (Table II). The lack of arginase synthesis in short-term murine macrophage cultures and in rat peritoneal macrophages may be caused by a down modulation of the arginase synthesis after harvesting the cells in short-term cultures. The reappearance of the arginase in long-term (24 h) cultures may be explained by the oscillation of the production of various enzymes: different enzymes are synthesized in the different

periods of the cell cycle. Experiments are in progress to study the nature and the regulation of this long-term synthetic process.

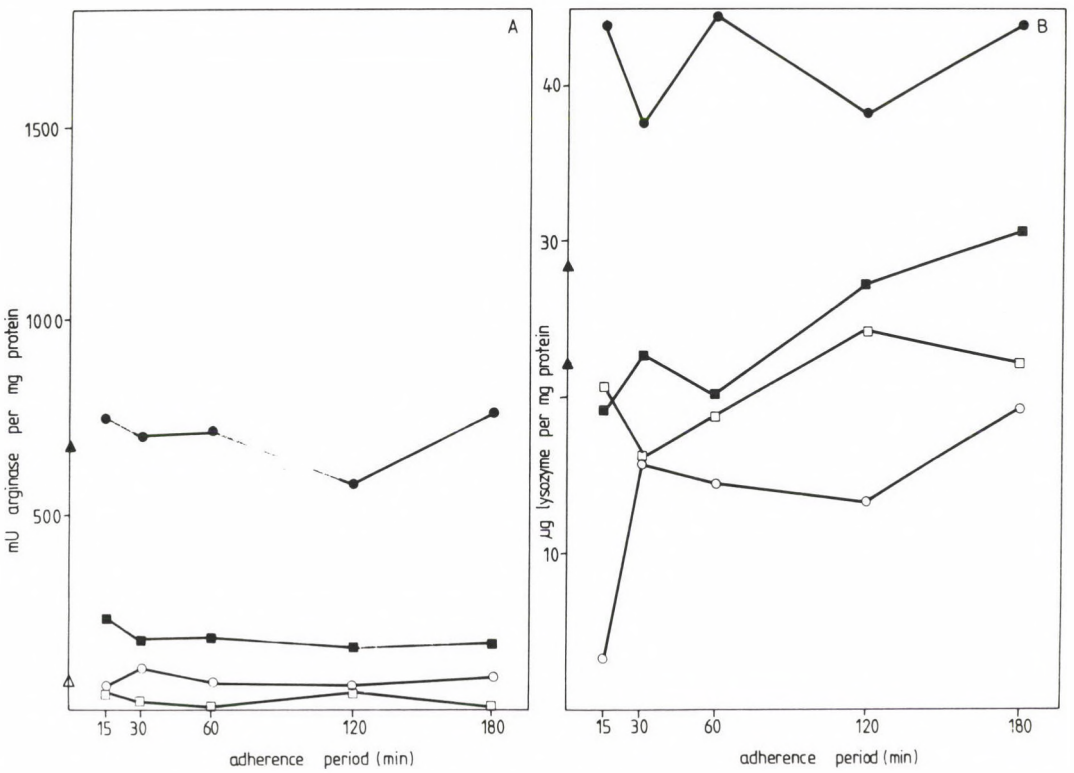


*Fig. 4.* The effect of adherence period on macrophage arginase and lysozyme. Arginase (A) and lysozyme (B) specific have not changed by varying the adherence period. ▲ = murine, Δ = rat PEC before adherence, ■ = murine, □ = rat PEC after adherence, • = murine, o = rat adherent cells at 3 h. Cells were left to adhere in Hanks medium for 15–180 min at 37 °C. After adherence cells were washed twice and cultured in fresh Hanks medium for 3 h at 37 °C

## Acknowledgement

The authors wish to express their thank to F. A. Antoni to the helpful discussion and grammatical checking, to Mrs. Ágnes Gerencsér and Miss Judit Szabó to the skillful technical assistance.

This work was supported by the grant (ETK 5-179) of the Hungarian Ministry of Welfare.

## REFERENCES


1. Albina, J. E., Caldwell, M. D., Henry, W. L. Mills, C. D.: Regulation of macrophage functions by L-arginine. J. Exp. Med. **169**, 1021–1029 (1989).
2. Albina, J. E., Mills, C. D., Henry, W. L., Caldwell, M. D.: Regulation of macrophage physiology by L-arginine. J. Immunol. **143**, 3641–3646 (1989).
3. Antoni, A. F., Dayanithi, G.: Guanosine 3':5' monophosphate and activators of guanylate cyclase inhibit secretagogue-induced corticotropin release by rat anterior pituitary. Biochem. Biophys. Res. Commun. **158**, 824–830 (1989).
4. Antoni, F., Hrabák, A., Csuka, I.: Effects of emetine and chloroquine on phagocytic processes of rat macrophages. Biochem. Pharmacol. **35**, 2869–2874 (1986).
5. Antoni, F., Csuka, I., Hrabák, A., Temesi, Á., Szende, B., Lapis, K.: The effect of L-leucine-methyl ester on the phagocytosis and amino acid incorporation in murine peritoneal cells. Acta Biochim. Biophys. **24**, 299–311 (1989).
6. Benninghoff, B., Dröge, W., Lehmann, V.: The lypopolysaccharide-induced stimulation of peritoneal macrophages involves at least two signal pathways. Partial stimulation by lipid A precursors. Eur. J. Biochem. **179**, 589–594 (1989).
7. Coulombe, J. J., Favreau, L.: A new simple method for colorimetric determination of urea. Clin. Chem. **9**, 102–108 (1963).
8. Drapier, J.-C., Hibbs, J. B.: Differentiation of murine macrophages to express nonspecific cytotoxicity for tumor cells results in L-arginine dependent inhibition of mitochondrial iron-sulfur enzymes in macrophage effector cells. J. Immunol. **140**, 2829–2838 (1988).
9. Fishhman, M.: Functional heterogeneity among peritoneal macrophages. III. No evidence for the role of arginase in the inhibition of tumor cell growth by supernatants from macrophages or macrophage subpopulation cultures. Cell. Immunol. **55**, 174–184 (1980).
10. Hibbs, J. B. Jr., Vavrin, Z., Taintor, R. R.: L-arginine is required for expression of the activated macrophage effector mechanism causing metabolic inhibition in target cells. J. Immunol. **138**, 550–565 (1987).
11. Hibbs, J. R. Jr., Taintor, R. R., Vavrin, Z.: Macrophage cytotoxicity: role for L-arginine deiminase and imino nitrogen oxidation to nitrite. Science **235**, 473–476 (1987).
12. Hrabák, A., Antoni, F., Csuka, I.: The influence of various chemicals on arginase production in peritoneal macrophages. 14th IUB Congress, Prague, abstr. 520 (1988).
13. Hrabák, A., Antoni, F., Csuka, I.: Down-modulated expression of secreted arginase production in peritoneal macrophages. 20th FEBS Meeting, Budapest, abstr. 088 (1990).
14. Hrabák, A., Antoni, F., Csuka, I.: Differences in the arginase activity produced by resident and stimulated murine and rat peritoneal macrophages. Int. J. Biochem. **23**, 997–1003 (1991).
15. Hrabák, A., Antoni, F., Szabó, M. T., Csuka, I.: Differences and similarities in the sensitivity of lymphocytic and macrophage plasma membrane to deoxycholate. Acta Microbiol. Hung. **38**, 233–242 (1991).
16. Hrabák, A., Ferenczi, S.: Thin layer ion-exchange chromatography on resin-coated chromatoplates. IV. Determination of ornithine in biological fluids. Acta Biochim. Biophys. Acad. Sci. Hung. **6**, 383–384 (1971).
17. Ignarro, L. J.: Endothelium-derived nitric oxide: actions and properties. FASEB Journal **3**, 31–36 (1989).
18. Jolles, P.: Lysozymes from rabbit spleen and dog spleen. Methods in Enzymol. **5**, 137–140 (1962).
19. Lowry, O. H., Rosembrough, N. J., Farr, A. L., Randall, R. J.: Protein measurement with the Folin phenol reagent. J. Biol. Chem. **193**, 265–275 (1951).
20. Marletta, M. A.: Nitric oxide: biosynthesis and biological significance. Trends Biochem Sci. **14**, 488–492 (1989).

21. Stuehr, D. J., Marletta, M. A.: Mammalian nitrate biosynthesis: Mouse macrophages produce nitrate and nitrite in response to Escherichia Coli lipopolysaccharide. Proc. Natl. Acad. Sci. USA **82**, 7738–7742 (1985).
22. Stuehr, D. J., Marletta, M. A.: Induction of nitrite/nitrate synthesis in murine macrophages by BCG infection. J. Immunol. **139**, 518–525 (1987).
23. Vray, B., Hoebeke, J., Saint-Guillain, M., Leloup, R., Strosberg, A. D.: A new quantitative fluorimetric assay for phagocytosis of bacteria. Scand. J. Immunol. **11**, 147–153 (1980).
24. Vray, B., Saint-Guillain, M., Leloup, R., Hoebeke, J.: Kinetic and morphologic studies of rat macrophage phagocytosis. J. Reticuloend. Soc. **29**, 307–319 (1981).

*Acta Physiologica Hungarica, Volume 81 (1), pp. 59–70 (1993)*

# EFFECTS OF MAGNESIUM AND ETHMOZIN ON VENTRICULAR TACHYCARDIA INDUCED BY OUABAIN AND VENTRICULAR PACING IN CONSCIOUS DOGS WITH COMPLETE ATRIOVENTRICULAR BLOCK

T. FAZEKAS,* M. A. VOS, J. D. M. LEUNISSEN, H. J. J. WELLENS

DEPARTMENT OF CARDIOLOGY, UNIVERSITY OF LIMBURG, MAASTRICHT, THE NETHERLANDS

Received April 15, 1992
Accepted October 7, 1992

A study was made of whether the administration of magnesium or ethmozin to conscious dogs with normal plasma Mg levels (0.75 ± 0.06 mmol/l) terminates ouabain-induced ventricular tachycardia, an arrhythmia which is dependent on triggered activity resulting from delayed afterdepolarizations. Sustained monomorphic ventricular tachycardia was induced by programmed ventricular pacing during the continuous iv. infusion of ouabain to animals with a formaldehyde-induced permanent complete AV block. A single dose of $MgSO_4$ (100 mg/kg b.w. iv.) abolished only those ventricular tachycardias with cycle lengths > 325 ms (inverse use-dependency); ventricular tachycardias with cycle lengths < 320 ms were merely slowed, despite the fact that the increase in plasma Mg levels was considerable and comparable in both groups (3.9 ± 1.6 and 4.8 ± 1.9 mmol/l). In contrast, ethmozin (2 mg/kg b.w. iv.) terminated both fast and slow ventricular tachycardias. It is concluded that ethmozin (moricizine) is more effective than the traditionally used $MgSO_4$ in terminating ventricular tachycardia resulting from cardiac glycoside toxicity.

**Keywords:** ouabain toxicity, ventricular tachycardia, magnesium, ethmozin, conscious dog

Although the frequency of iatrogenic cardiac glycoside intoxication has decreased during the past decade as a consequence of the less extensive and more rational application of the digitalis glycosides, it is not rare even now; 5–10% of the inpatients treated with such drugs suffer from digitalis intoxication [35]. The cardiotoxic effect of a digitalis overdosage, inducing extreme bradycardia, was mentioned in the classic book by Withering as long ago as 1785, but the mechanism

Correspondence should be addressed to
Tamás FAZEKAS
Veterans Affairs Medical Center, Department of Medicine,
Cardiovascular Section, Oklahoma University Health Sciences Center,
151F, 921 N.E. 13th Oklahoma City/Oklahoma 73104, USA

*European Society of Cardiology Research Fellow (on leave from the 1st Department of Medicine, Albert Szent-Györgyi University Medical School, Szeged, Hungary)

*Akadémiai Kiadó, Budapest*

of tachycardias/tachyarrhythmias provoked by cardiotonic steroids has become known only during the past 15 years [1, 13, 18, 20, 33, 37].

The emergence and perpetuation of clinical arrhythmias were earlier ascribed to reentry, enhanced automaticity or a combination of these two phenomena. In the past two decades, however, it has become clear that there is also a third arrhythmia mechanism, which may play a pathogenetic role in the development of specific clinical tachycardias: *afterdepolarization*, an electrophysiological phenomenon that takes place at a cellular level; the sustained/repetitive activity based on this is referred to as a *triggered rhythm* [1, 4, 25, 26, 50, 53]. Afterdepolarization is a transient depolarization that occurs during the phase (2nd or 3rd) of repolarization of the cardiac action potential (*e*arly *a*fter*d*epolarization = EAD) or, after this has been completed, in the 4th diastolic phase (*d*elayed *a*fter*d*epolarization = DAD; Fig. 1). Both can induce a propagating triggered impulse if the amplitude of the afterdepolarization is sufficient for the threshold potential to be reached, and if this is followed by further, similar ones, so that a sustained rhythmic activity, a triggered tachycardia, emerges [6, 10, 25, 26, 44]. We speak about a 'triggered' activity (TA) because the development of such a rhythm/arrhythmia is initiated by EAD or DAD assuming the advance of the *previous* action potential [33]. The pathomechanism of EAD and DAD differ. The former is the arrhythmia mechanism of the 'torsades de pointes' ventricular tachycardia (VT) accompanying the congenital or acquired long QT/QTU syndromes, whereas the digitalis-induced tachyarrhythmias (atrial tachycardia with AV block, non-paroxysmal AV junctional tachycardia, ventricular extrasystole/bigeminy, VT, bidirectional VT) can be attributed to TA based on DAD [6, 9, 10, 13, 29, 33, 38, 41, 53]. The primary cause of DAD is the $Ca^{2+}$-overload of the heart cells. Cardiac glycosides with a positive inotropic effect block the sarcolemmal $Na^+$-$K^+$-ATPase, which leads to an increase in the intracellular $Na^+$ concentration; this latter stimulates the $Na^+$:$Ca^{2+}$ exchanger to an enhanced functioning, which is accompanied by the removal of $Na^+$ from within the cell, but the intracellular level of $Ca^{2+}$ increases [25, 33]. The latter mobilizes further $Ca^{2+}$ from the sarcoplasmic reticular (SR) and mitochondrial stores, and finally the increase in the free cytosolic $Ca^{2+}$ concentration and the oscillatory intracellular $Ca^{2+}$ release from the SR activates a non-selective *t*ransient *i*nward cation current ($I_{ti}$) responsible for DADs [13].

The TA based on DAD is characterized by overdrive enhancement (overdrive acceleration), which means that up to a certain limit, increase of the rate of electrical stimulation is accompanied by an increase in the amplitude of DAD, a shortening of the coupling interval of the first triggered action potential ('first postpacing interval') and an acceleration of the induced tachycardia [14, 16, 17, 23, 46, 48, 50]. In contrast, the pacemaker cells of the heart firing by spontaneous diastolic depolarization (sinus

rhythm, idioventricular escape rhythm) are characterized by overdrive suppression [7, 24].

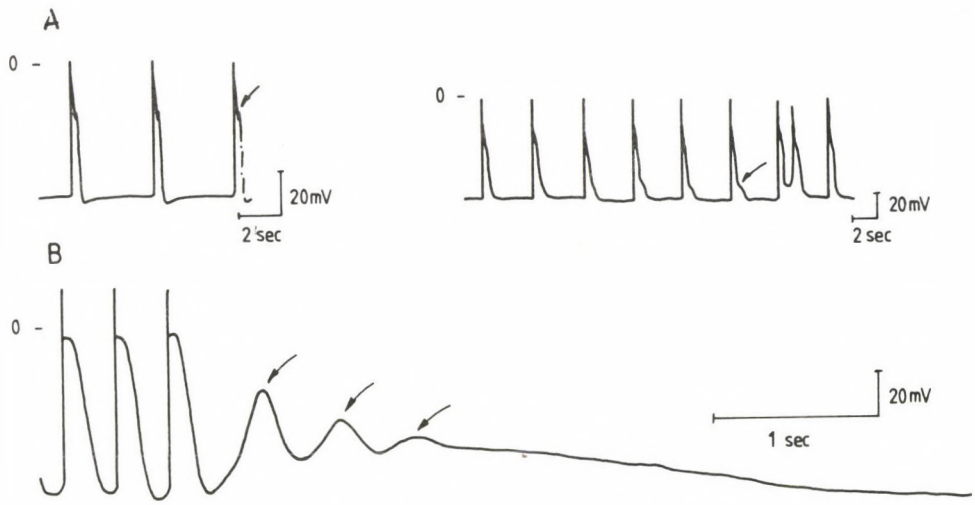


*Fig. 1.* Panel A: early afterdepolarization (EAD) observed in the 2nd (left) and 3rd (right) phases of the cardiac action potential. Panel B: three delayed afterdepolarizations (DADs, arrows) after the driven action potentials (by permission of Michael R. Rosen [33])

The goal of the present work was an *in vivo* study of the drug sensitivity of sustained monomorphic VT (SMVT) induced by systemic (iv.) ouabain intoxication, based on DAD. The effectivities of an old (magnesium [54]) and a more recent (ethmozin = moricizine [8, 34]) antiarrhythmic agent were compared in the conscious dog model developed in Maastricht [17, 44–50].

## Methods

The experiments were performed on mongrel dogs of either sex, weighing 18–34 kg. In a preliminary surgery, right thoracotomy was followed by the induction of a permanent complete AV block by the injection of 37% formaldehyde [35]. At the same time, pacing electrodes were inserted into the basal portion of the right ventricle and the apex of the left ventricle, and these were then exteriorized to the back through the skin of the neck. Spontaneous VTs occur during the first week after induction of the heart block, and the experiments on the conscious dogs were therefore performed only 2–3 weeks postoperatively. Six ECG leads were registered continuously (limb bipolar and unipolar leads; Siemens Elema Mingograf 1604), and the events were also recorded on a tape recorder (Ampex). VT was induced by ouabain administration and programmed electrical stimulation (PES) of the ventricle [14, 20, 23, 44]. Ouabain was injected in an iv. bolus during 2 minutes (43 ± 7 μg/kg; 30–50 μg/kg); the correlation found between the body weight and the ouabain dose required to induce SMVT is depicted in Fig. 2 [46]. Eight minutes following administration of the bolus, continuous iv. ouabain infusion was begun (0.054–0.09 μg/kg/min) and was maintained throughout the experiment. The PES was performed with a

computerized stimulator suitable for continuous on-line measurement and display of the RR intervals [40]. The strength of the stimulus was twice the diastolic threshold, the duration of stimulation trains was 4, 10 or 20 sec, and the interstimulus interval was 200, 300 or 400 msec. The different pacing trains were delivered randomly in repeated 15-minute periods until SMVT appeared (79 ± 47 min).

Twenty minutes after induction of SMVT, $MgSO_4$ was administered (n = 8) in a dose of 100 mg/kg b.w. in an iv. bolus during 1–2 minutes [15, 21, 30]. If the $MgSO_4$ terminated VT, SMVT was reinduced by pacing, and ethmozin was administered (2 mg/kg b.w. iv. in 2 min; n = 7) at least 60 min after the injection of $MgSO_4$. The VT cycle length, calculated as the average of ten consecutive RR intervals, was measured every minute. The Mg concentration of the blood plasma of the dogs was determined in the control state and after $MgSO_4$ injection. The Student one- and two-tailed *t*-tests were applied for statistical analysis (means ± SD).

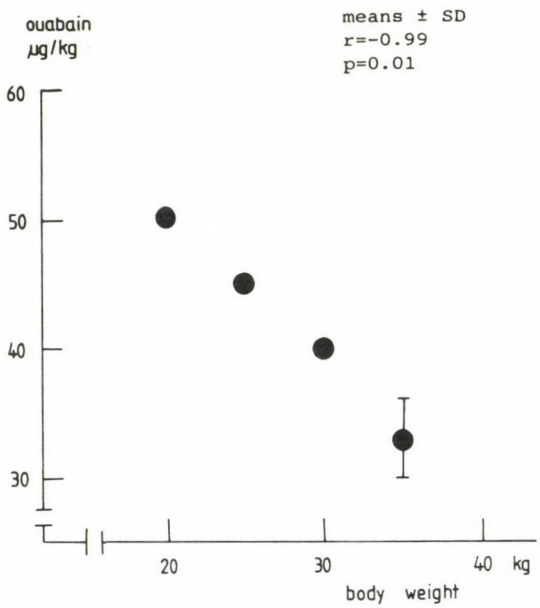


*Fig. 2.* Correlation between body weight of dogs and ouabain dose needed to induce sustained monomorphic ventricular tachycardia (n = 28)

## Results

$MgSO_4$ slowed every VT (310 ± 25 ms → 355 ± 30 ms, $p < 0.05$); this effect was more marked at longer cycle length (> 325 ms) than for faster VTs (< 320 ms) [16% vs 10%; $p < 0.01$]. Only VTs with a cycle length > 325 ms were ceased by Mg (3/8), and the faster ones (< 320 ms; 5/8) were merely slowed, despite the blood plasma Mg level increase being considerable and comparable in both groups (control 0.75 ± 0.06 mmol/l, after $MgSO_4$ administration 3.9 ± 1.6 or 4.8 ± 1.9 mmol/l;

Fig. 3). In contrast, ethmozin stopped both fast and slow VTs: the arrhythmia was terminated within 1–2 minutes after the injection in 6–7 animals (Fig. 4).

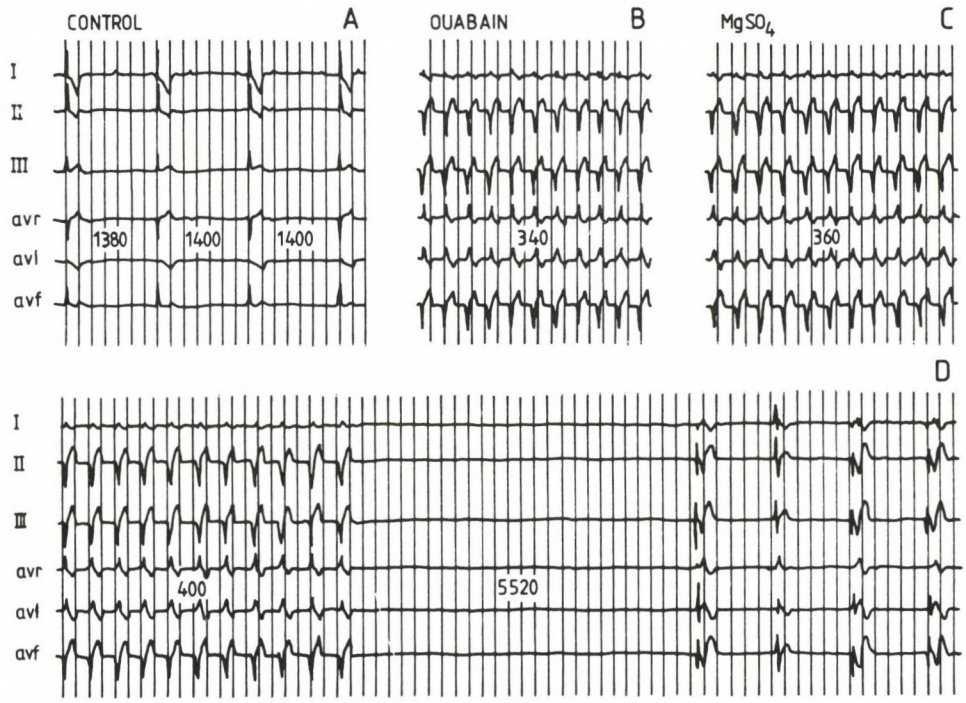


*Fig. 3.* Termination of ouabain-induced sustained monomorphic ventricular tachycardia (SMVT) with magnesiumsulfate. Panel A: idioventricular rhythm accompanying complete AV block. Panel B: ouabain-induced SMVT with mean cycle length (CL) of 340 ms. Panel C: the SMVT slows after the administration of magnesium (100 mg/kg iv.; CL = 360 ms). Panel D: SMVT stops 1.5 sec after the injection following a further RR interval increase (400 ms)

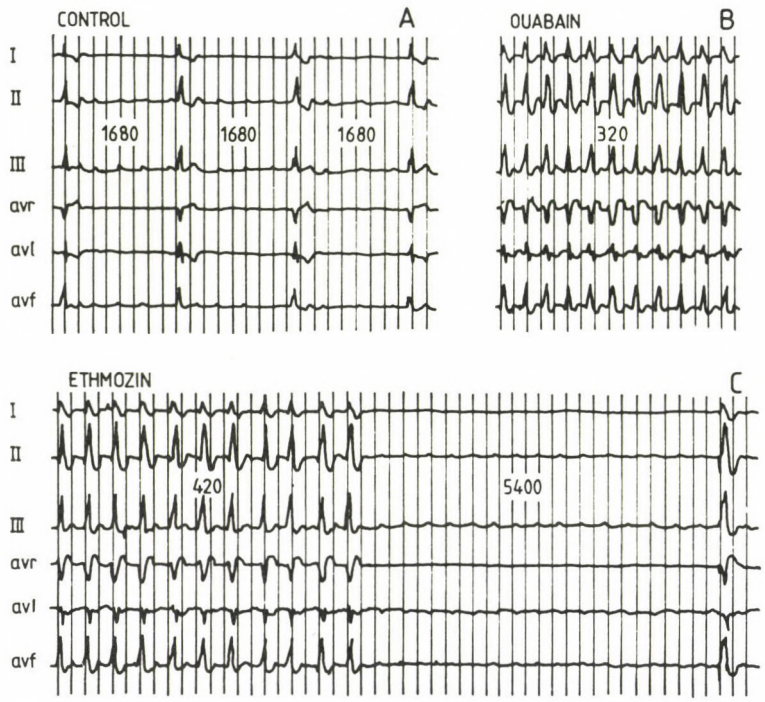


*Fig. 4.* Panel A: complete AV block before cardiac glycoside administration. Panel B: SMVT with a CL of 320 msec, induced by ouabain and ventricular pacing. Panel C: after the injection of ethmozin (moricizine, 2 mg/kg iv.) the SMVT slows and then stops

## Discussion

The short duration of action of an iv. bolus of Mg (< 45 min) allowed a comparison of the effects of $MgSO_4$ and ethmozin (moricizine) on VT induced by ouabain intoxication [11, 46]. The antiarrhythmic effect of iv. magnesium ($MgSO_4$, $MgCl_2$) was first observed in digitalis intoxication [54], and it has subsequently found extensive empirical use for the treatment of different atrial and ventricular clinical arrhythmias [15, 29, 30, 38, 52]. The mechanism of its antiarrhythmic action seems to be complex. The electrophysiological effect of Mg in inhibiting the slow inward $Ca^{2+}$ current ($Ca^{2+}$ antagonism) is best known [9, 11, 31, 52]. It is assumed that $Mg^{2+}$ inhibits $Ca^{2+}$ influx in part directly, and in part by stimulating the enzymes (phosphatases) that dephosphorylate the Ca channels [31]. The automatic cells of the sinoatrial and AV nodes are characterized by a $Ca^{2+}$-dependent depolarization of 'slow response' type, which is in accord with observations indicating that Mg acts particularly on these myocardial structures [32, 52]. The Mg-induced negative

chronotropism and prolongation of the sinus-node recovery time (SNRT/CSNRT) can be traced back to behaviour of Mg in depressing sinus nodal automaticity. In spite of these observations we did not experience the arrest of the sinus nodal activity in our experiments: the atrial depolarizations (P waves) originating from the sinus node returned immediately after the termination of VT (Fig. 3). Mg acts on the AV-nodal conduction in a dose (concentration)-dependent manner: PQ/PR and AH interval prolongations must primarily be expected if the serum Mg level exceeds 2.5 mmol/l [32]. In humans and conscious mammals, contributions to the direct effect of Mg on the AV node are made by the indirect antiadrenergic and vagomimetic actions of the cation [52]. On the above basis, it is understandable that the fast iv. injection of Mg stops AV-nodal and AV-reciprocating (accessory pathway using) supraventricular tachycardias via its 'verapamil-like' and autonomic nervous system effects [11, 52]. It does not influence the electrical activity of the myocardial regions activated by fast $Na^+$-dependent depolarization (normal atrial and ventricular working muscle, His-Purkinje system): it does not affect the QRS and HV intervals or the QT/$QT_c$ duration [32]. Naturally, this latter does not contradict the fact that in drug-induced long QT/QTU syndrome Mg shortens the QT interval and makes the process of ventricular repolarization more homogenous [10, 29]. The slow idioventricular rhythm (IVR) associated with complete heart block can be ascribed to the fast, $Na^+$-dependent depolarization of the ventricular cells possessing normal (−90 mV) resting potential ('normal automaticity' [7, 24]), but the effect of Mg on the IVR of our ouabain-intoxicated conscious dogs was not studied systematically. Ventricular ectopic activity and spontaneous VT accompanying the 16–24-hour myocardial infarction (MI) presumably based on abnormal automaticity (originating from surviving subendocardial Purkinje cells with low diastolic membrane potentials) or reentry are suppressed by Mg in both MI-patients and Harris-dogs [7, 18, 21]. The ventricular arrhythmias induced by barium (Ba) have a multifarious pathogenetic scenario: a role is played in their development not only by abnormal automaticity, but also by EAD- and DAD-induced TA [7]. It was earlier demonstrated that both clinical (poisoning-induced) and experimental Ba-arrhythmias can be stopped and prevented by iv. $MgSO_4$ administration [30]. There can be no doubt, however, that the reason why Mg recently came into the focus of interest of theoreticians and clinicians dealing with cardiac electrophysiology was the discovery that the experimental EAD and the triggered clinical tachycardia emerging very likely from EAD (i.e. the 'torsades de pointes' VT), can be abolished/prevented by the *in vitro* superfusion or *in vivo* injection of Mg [2, 6, 10, 27, 29]. EAD can be in part attributed to the *re*activation of the L-type $Ca^{2+}$ channels, associated with the prolongation of the cardiac action potential duration (APD). The $Ca^{2+}$ antagonist property of Mg explains why it extinguishes EAD arising at membrane potentials more positive than −60 mV during the 2nd plateau phase of the action potential

[2, 6]. Recent studies also reveal that Mg also suppresses EADs induced by agents, which inhibit repolarizing $K^+$-currents (cesium, quinidine, 4-aminopyridine), at membrane potentials more negative than −60 mV during the 3rd phase of action potential, probably due to the attenuation of the tetrodotoxin-sensitive $Na^+$ 'window'-currents [2, 28]. Accurate elucidation of the mechanism of antiarrhythmic action of Mg is a task for the future. Nevertheless, the view is already extensively accepted that iv. Mg is the choice of drug in the treatment of 'torsades de pointes' VT occurring in *acquired/drug-induced* long QT/QTU syndromes [6, 10, 12, 29].

Interestingly, analysis of the effects of Mg on EAD and 'torsades de pointes' VT has distracted attention from study of the Mg therapy of triggered tachycardias based on DAD, and the number of such investigations is relatively low [5, 37]. One reason why this is surprising is that the practice of the iv. Mg treatment of digitalis-induced arrhythmias has a past of several decades [38, 54]. It is undoubted, however, that the traditionally recommended iv. $MgSO_4$ treatment had only a modest efficacy in the conscious dog model we used: only 3 of 8 ouabain-induced VTs were stopped. The observation of the *inverse use-dependent* antiarrhythmic action of Mg in ouabain-induced VT, however, was not described earlier. Further study of this interesting pharmacological effect might lead closer to an understanding of the pathomechanism of TA based on DADs: the possibility is not excluded that Mg acts on the dynamics of uptake and release of intracellular/myoplasmic $Ca^{2+}$, by influencing the sarcoplasmic reticular, ryanodine-sensitive $Ca^{2+}$ channels. At any event, the results presented here and those published earlier permit the conclusion that Mg suppresses this arrhythmia mechanism (DAD/TA) more weakly than ethmozin, lidocaine, verapamil or flunarizine [47, 49, 53].

Ethmozin (moricizine) is a Ic $Na^+$ channel blocking antiarrhythmic drug of phenothiazine structure. It was recently explored that, similarly to flecainide and encainide (CAST), it increases the mortality of post-MI patients suffering from ventricular premature beats. It was previously believed to cause proarrhythmia more rarely than the other Ic agents [3, 12, 39, 51]. Ethmozin has a complex cardiac electrophysiological effect too. It blocks the upstroke velocity ($V_{max}$) of the cardiac action potential by inhibiting the fast inward $Na^+$ current ($I_{Na+}$) in a concentration- and use-dependent manner [34]. Ethmozin was reported to block predominantly the inactivated $Na^+$ channels in rat ventricular myocytes and it also decreases $I_{Ca2+}$ in frog ventricular cells [42]. Ethmozin slows the spreading of the impulse in all parts of the myocardium, which may manifest in the prolongation of the PR and QRS intervals [3, 34, 42, 43, 50]. It is very likely that the proarrhythmic action of ethmozin can be ascribed to its marked depressant action on impulse conduction [43]. Ethmozin shortens APD in Purkinje fibers but either does not change or slightly lengthens APD in ventricular muscle fibers [42]. It suppresses the abnormal automaticity and ventricular arrhythmias supposed to be due to this mechanism (e.g.

16–24 post-MI; [3, 8]). By shortening of the APD of Purkinje fibers it eliminates EADs evoked with a $Ca^{2+}$-agonist (BayK 8644; [27]). There is no clinical experience relating to the ethmozin therapy of 'torsades' VT. *In vitro*, it reduces the amplitude of DAD induced in Purkinje fibers by ouabain, and prolongs the first postpacing interval [22]. The *in vivo* data presented in this study also clearly demonstrate that ethmozin (moricizine) strongly suppresses TA based on DAD in the intact dog heart.

Overall, the present results, clinical experience and the literature data permit the statement that triggered VT based on DAD and provoked by overdosage of cardiac glycoside can be treated more effectively with lidocaine or ethmozin than with iv. $MgSO_4$. The latter is rather of specific value in the therapy of 'torsades de pointes' VT generated by EAD [10, 11, 29].

## REFERENCES


1. Aronson, R. S.: Delayed afterdepolarizations and pathological states. In: Cardiac electrophysiology: a textbook. eds Rosen, M. R., Janse, M. J., Wit, A. L. Futura Publishing Co., Mount Kisco, New York, 1990, pp. 303–322.
2. Bailie, D. S., Inoue, H., Kaseda, S., Ben-David, J., Zipes, D. P.: Magnesium suppression of early afterdepolarizations and ventricular tachyarrhythmias induced by cesium in dogs. Circulation **77**, 1395–1402 (1988).
3. Bigger, J. T.: Cardiac electrophysiological effects of moricizine hydrochloride. Am. J. Cardiol. **65**, 15D–20D (1990).
4. Brugada, P., Wellens, H. J. J.: The role of triggered activity in clinical ventricular arrhythmias. PACE **7**, 260–271 (1984).
5. Cohen, L., Kitzes, R.: Magnesium sulfate and digitalis-toxic arrhythmias. JAMA **249**, 2808–2810 (1983).
6. Cranefield, P. F., Aronson, R. S.: Torsades de pointes and early afterdepolarizations. Cardiovasc. Drug Therap. **5**, 531–538 (1991).
7. Dangman, K. H., Danilo, P. Jr.: Intact animal models of automatic rhythms. In: Cardiac electrophysiology: a textbook. eds Rosen, M. R., Janse, M. J., Wit, A. L. Futura Publishing Co., Mount Kisco, New York, 1990, pp. 223–233.
8. Dangman, K. H., Hoffman, B. F.: Antiarrhythmic effects of ethmozin in cardiac Purkinje fibers: suppression of automaticity and abolition of triggering. J. Pharmacol. Exp. Therap. **227**, 578–586 (1983).
9. Fazekas, T.: Antiaritmás kezelés $Ca^{++}$ antagonistákkal. Orv. Hetil. **130**, 1195–1200 (1989).
10. Fazekas, T.: Kinidin-syncope "torsades de pointes" kamrai tachycardiával. In: Klinikai betegbemutatások. Válogatott fejezetek a belgyógyászatból. eds Varró, V., Fazekas, T. Medicina Könyvkiadó, Budapest, 1989, pp. 7–34 (In Hungarian).
11. Fazekas, T.: A magnézium és a szív. Antiaritmiás kezelés magnéziummal. In: A magnézium forrásai és jelentősége az élővilágban. eds Fazekas, T., Selmeczi, B., Stefanovits, P. Akadémiai Kiadó, Budapest, 1992, pp. 188–200 (In Hungarian).
12. Fazekas, T., Smeets, J. L. R. M., Wellens, H. J. J.: Az antiaritmiás gyógyszerek aritmogén hatása. A proaritmiák korszerű szemlélete. Orv. Hetil. **132**, 2243–2248 (1991) (In Hungarian).
13. Ferrier, G. R.: Digitalis arrhythmias: role of oscillatory afterdepolarizations. Prog. Cardiovasc. Dis. **19**, 459–474 (1977).

14. Furukawa, T., Kimura, S., Castellanos, A., Bassett, A. L., Myerburg, R. J.: In vivo induction of "focal" triggered ventricular arrhythmias and responses to overdrive pacing in the canine heart. Circulation **82**, 549–559 (1990).
15. Ghani, M. F., Rabah, M.: Effect of magnesium chloride on electrical stability of the heart. Am. Heart J. **94**, 600–602 (1977).
16. Goldberger, J. J., Aronson, R. S.: Effects of verapamil on ventricular tachycardia induced by ouabain in guinea pigs. PACE **15**, 162–170 (1992).
17. Gorgels, A. P. M.: Ventricular impulse formation and the influence of digitalis intoxication. (thesis) Schrijen-Lippertz BV, Voerendaal, The Netherlands, 1985.
18. Gorgels, A. P. M., Vos, M. A., Brugada, P., Wellens, H. J. J.: The clinical relevance of abnormal automaticity and triggered activity. In: Cardiac arrhythmias: where to go from here? eds Brugada, P., Wellens, H. J. J. Futura Publishing Co., Mount Kisco, New York, 1987, pp. 147–169.
19. Gorgels, E. P. M., Vos, M. A., Smeets, J. L. R. M., Kriek, E., Brugada, P., Wellens, H. J. J.: Delayed afterdepolarizations and atrial and ventricular arrythmias. In: Cardiac electrophysiology: a textbook. eds Rosen, M. R., Janse, M. J., Wit, A. L. Futura Publishing Co., Mount Kisco, New York, 1990, pp. 341–354.
20. Hariman, R. J., Gough, W. B.: Delayed afterdepolarization-induced triggered activity as a mechanism of ventricular arrhythmias in vivo. In: Cardiac electrophysiology: a textbook. eds Rosen, M. R., Janse, M. J., Wit, A. L. Futura Publishing Co., Mount Kisco, New York, 1990, pp. 323–332.
21. Harris, A. S., Estandia, A., Smith, H. T., Olsen, R. W., Ford, T. J., Tillotson, R. F.: Magnesium sulfate and chloride in suppression of ectopic ventricular tachycardia accompanying acute myocardial infarction. Am. J. Physiol. **172**, 251–258 (1953).
22. Hewett, K., Gessman, L., Rosen, M. R.: Effects of procaine amide, quinidine and ethmozin on delayed afterdepolarizations. Eur. J. Pharmacol. **96**, 21–28 (1983).
23. Iinuma, H., Sekiguchi, A., Kato, K.: The response of digitalized canine ventricle on programmed stimulation: a study on triggered activity arrhythmias in the whole heart. PACE **12**, 1331–1346 (1989).
24. Ilvento, J. P., Provet, J., Danilo, P. Jr., Rosen, M. R.: Fast and slow idioventricular rhythms in the canine heart: a study of their mechanism using antiarrhythmic drugs and electrophysiologic testing. **49**, 1909–1916 (1982).
25. January, C. T., Fozzard, H. A.: Delayed afterdepolarizations in heart muscle: mechanisms and relevance. Pharmacol. Reviews **40**, 219–227 (1988).
26. January, C. T., Makielski, J. C.: Triggered arrhythmias, new insights into basic mechanisms. Curr. Opinion Cardiol. **5**, 65–68 (1990).
27. January, C. T., Riddle, J. M., Salata, J. J.: A model of early afterdepolarizations: induction with the $Ca^{2+}$ channel agonist Bay K 8644. Circ. Res. **62**, 563–571 (1988).
28. Kaseda, S., Gilmour, R. F., Zipes, D. P.: Depressant effect of magnesium on early afterdepolarizations and triggered activity induced by cesium, quinidine, and 4-aminopyridine in canine cardiac Purkinje fibers. Am. Heart J. **118**, 458–466 (1989).
29. Keren, A., Tzivoni, D.: Torsades de pointes: prevention and therapy. Cardiovasc. Drugs Therap. **5**, 509–514 (1991).
30. Kiss, Z., Fazekas, T.: Szívritmuszavarok báriummérgezésben. Magy. Belorv. Arch. **32**, 297–303 (1979) (In Hungarian).
31. Reinhart, R. A.: Clinical correlates of the molecular and cellular actions of magnesium on the cardiovascular system. Am. Heart J. **121**, 1513–1521 (1991).
32. Rogiers, Ph., Vermeier, W., Kesteloot, H., Stroobandt, R.: Effect of infusion of magnesium sulfate during atrial pacing on ECG intervals, serum electrolytes, and blood pressure. Am. Heart J. **117**, 1278–1283 (1989).

33. Rosen, M. R.: Delayed afterdepolarizations induced by digitalis. In: Cardiac electrophysiology: a textbook. eds Rosen, M. R., Janse, M. J., Wit, A. L. Futura Publishing Co., Mount Kisco, New York, 1990, pp. 273–281.
34. Rosenshtraukh, L. V., Anyukhovsky, E. P., Nesterenko, V. V., Undrovinas, A. I., Shugushev, Kh., Portnov, V. F., Burnashev, N. A.: Electrophysiological aspects of moricizine HCl. Am. J. Cardiol. **60**, 27F–34F, 1987.
35. Scherlag, B. J., Kosowsky, B. D., Damato, A. N.: A technique for ventricular pacing from the His bundle of the intact heart. J. Appl. Physiol. **22**, 584–587 (1967).
36. Smith, T. W.: Digitalis. Mechanism of action and clinical use. New Engl. J. Med. **318**, 358–365 (1988).
37. Specter, M., Schweizer, E., Goldman, R. H.: Studies on magnesium's mechanism of action in digitalis-induced arrhythmias. Circulation **52**, 1001–1005 (1975).
38. Székely, P., Wynne, N. A.: The effects of magnesium on cardiac arrhythmias caused by digitalis. Clin. Sci. **10**, 241–247 (1951).
39. Task Force of the WG on Arrhythmias of the ESC: CAST and beyond. Implications of the Cardiac Arrhythmia Suppression Trial. Consensus statement. Circulation **81**, 1123–1127 (1990).
40. Van der Steld, A., Dassen, W. R. M., Gorgels, A. P. M., Beekman, H. D. M., Wellens, H. J. J.: Flexible multiprocessor system to support electrophysiological investigation in animals. Comput. Cardiol. 525–528 (1984).
41. Vanagt, E. J., Wellens, H. J. J.: The electrocardiogram in digitalis intoxication. In: What's new in electrocardiography. eds Wellens, H. J. J., Kulbertus, H. S. Martinus Nijhoff Publishers, The Hague, 1981, pp. 315–343.
42. Varró, A., Surawicz, B.: Effect of antiarrhythmic drugs on membrane channels in cardiac muscle. In: Cardiac electrophysiology and arrhythmias. eds Fisch, C., Surawicz, B. Elsevier, New York/Amsterdam/London/Tokyo, 1991, pp. 277–296.
43. Vaughan Williams, E. M.: Classification of the antiarrhythmic action of moricizine. J. Clin. Pharmacol. **31**, 216–221 (1991).
44. Vos, M. A.: New observations to identify abnormal impulse formation in the intact heart. (thesis) Datawyse, Maastricht, The Netherlands, 1989.
45. Vos, M. A., Gorgels, A. P. M., Drenth, J. P. H., Leunissen, J. D., Wellens, H. J. J.: Termination of ouabain-induced ventricular tachycardia by flunarizine in conscious dogs. Eur. J. Pharmacol. **165**, 139–145 (1989).
46. Vos, M. A., Gorgels, A. P. M., Leunissen, J. D. M., van Deursen, R. T. A. M., Wellens, H. J. J.: Significance of the number of stimuli to initiate ouabain-induced arrhythmias in the intact heart. Circ. Res. **68**, 38–44 (1991).
47. Vos, M. A., Gorgels, A. P. M., Leunissen, J. D. M., Wellens, H. J.J.: Discriminative power of drugs to identify arrhythmogenic mechanisms in vivo. Cardiovasc. Drugs Therap. **5**, Suppl. 3, 402 (1991).
48. Vos, M. A., Gorgels, A. P. M., Leunissen, J. D. M., Wellens, H. J. J.: The in vivo response of ouabain-induced arrhythmias to pacing: acceleration instead of termination. Am. Heart J. **120**, 604–611 (1990).
49. Vos, M. A., Gorgels, A. P. M., Leunissen, J. D. M., Wellens, H. J. J.: Flunarizine allows differentiation between mechanisms of arrhythmias in the intact heart. Circulation **81**, 343–349 (1990).
50. Vos, M. A., Gorgels, A. P. M., de Wit, B., Drenth, J. P. H., van Deursen, R. T. A. M., Leunissen, J. D. M., Wellens, H. J. J.: Premature escape beats. A model for triggered activity in the intact heart? Circulation **82**, 213–224 (1990).
51. Wechsler, M. E., Steinberg, J. A., Giardina, E. E-G.: Time course of moricizine's effect on signal-averaged and 12 lead electrocardiograms: insights into mechanism of action. J. Am. Coll. Cardiol. **17**, 1626–1633 (1991).
52. Wesley, R. C., Haines, D. E., Lerman, B. B., DiMarco, J. P., Crampton, R. S.: Effect of intravenous magnesium sulfate on supraventricular tachycardia. Am. J. Cardiol. **63**, 1129–1131 (1989).

53. Zipes, D. P.: Monophasic action potentials in the diagnosis of triggered arrhythmias. Prog. Cardiovasc. Dis. **33**, 385–396 (1991).
54. Zwillinger, L.: Über die Magnesiumwirkung auf das Herz. Klin. Wochenschr. **14**, 1429–1433 (1935).

*Acta Physiologica Hungarica, Volume 81 (1), pp. 71–86 (1993)*

# HYPERTENSION AND ALCOHOLISM*

Veronika MORVAI, Györgyi KONDOROSI*, GY. UNGVÁRY**, Edit SZÉPVÖLGYI**

SECOND DEPARTMENT OF MEDICINE, SEMMELWEIS UNIVERSITY MEDICAL SCHOOL,
*GYULA NYIRŐ HOSPITAL AND **NATIONAL INSTITUTE OF OCCUPATIONAL HEALTH, BUDAPEST, HUNGARY

Received June 2, 1992
Accepted August 24, 1992

Blood pressures of 122 patients, undergoing alcohol withdrawal treatment in hospital, were taken at admission and one and two weeks after admission, and various laboratory tests that are thought to be the markers of alcoholism (gamma glutamyltransferase – GGT, mean corpuscular volume – MCV, serum uric acid) were performed (by the authors).

At admission 27% of the patients had hypertension. The GGT and MCV exceeded the upper level of the normal range in 75% and 68% respectively of the group studied. 70% of the high MCV values was between 96–100 fl, it was closed to normal value. Out of 122 alcoholics 8 patients had serum uric acid levels higher than the upper limit (420 μmol/l), and in 14% of the alcoholics this level was found near the upper limit (350–420 μmol/l).

Among the laboratory markers of alcoholism and the alcohol-associated parameters there was a relationship only between the GGT and daily alcohol consumption, so 13% of the change in GGT value was explained by the daily dose of alcohol consumption.

There was a significant interaction between GGT and systolic blood pressure, as well as between serum uric acid and systolic blood pressure. These laboratory markers give explanation for the blood pressure change in 16% of the cases. From the two laboratory markers only the effect of GGT proved to be significant: above 200 GGT value the probability of high systolic blood pressure increases.

It was also found, that alcohol withdrawal after two weeks decreased blood pressure in the majority of alcoholics, and after two weeks the average of systolic and diastolic blood pressure was significantly lower than at admission.

**Keywords:** alcohol-induced hypertension, laboratory markers of alcoholism, alcohol withdrawal, multiple linear regression

In the past years a number of clinical and epidemiological studies have been published on the relationship between alcohol consumption and hypertension. Most of these have reported that the frequency of hypertension in alcoholics significantly surpasses that of the population [1, 8, 11, 13, 20, 22].

Correspondence should be addressed to
Veronika MORVAI
Second Department of Medicine,
Semmelweis University Medical School
H–1088 Budapest, Szentkirályi u. 46, Hungary

*Supported by grant T–192/1990 form the Hungarian Ministry of Welfare

Alcoholism frequently remains unrecognised, even during hospital treatment [2, 12, 21, 33], thus numerous attempts have been made to elaborate clinical laboratory tests which help the diagnosing of alcoholism. As a result of these, the increase of the serum gamma glutamyltransferase (GGT), the mean corpuscular volume (MCV), and the serum uric acid level are regarded as markers of alcoholism [5, 7, 27, 34, 35].

Our aims in the present study was to find out:

1. What is the frequency of hypertension and the markers typical of alcoholism (increase of GGT, MCV, serum uric acid levels) among alcoholics?

2. Is there a correlation between the hypertension of alcoholics and the frequency of the mentioned indirect signs (abnormal values of MCV, GGT and serum uric acid) or other parameters, directly characteristic of alcoholism (e.g. daily dose of alcohol consumed, duration of alcoholism)?

3. What effect does alcohol withdrawal treatment have on hypertension?

## Patients and methods

Hundred and twenty-two male patients undergoing withdrawal treatment were examined, their daily consumption of alcohol exceeded 80 g. According to the WHO diagnostic criteria, all patients were alcohol-dependent. During the alcohol withdrawal regimen, all patients were treated with meprobamat (Andaxin), and 37.5% of them also took clometiazol (Heminevrin) for the alleviation of the serious withdrawal symptoms. Members of the studied population were given this latter drug only for the first 3 days. Data describing alcohol consumption (duration, quantity of drinking) were obtained by interviewing the patients. At admission and two weeks after admission, the patients' blood pressure was taken, following a 10 minute sitting period, in a sitting position, with a mercury manometer (according to WHO requirements). Routine physical, standard biochemical, and haematological laboratory and other routine (e.g. ECG) examinations were performed at admission.

During the statistical processing of the selected parameters (age, duration of alcohol exposure, daily consumption of alcohol, systolic and diastolic blood pressure, CGT, MCV, serum uric acid), the one-variable distributions (mean, SE, mode, median, standard deviation, variation, range) were prepared first and analysed according to Kolmogorov-Smirnov. One-way-ANOVA (or Kruskal-Wallis test), multiple-way analysis of variance (ANOVA) and loglinear model were used to test the effect of alcohol on GGT, MCV and serum uric acid level and the blood pressure. One of the aims of this study was to test whether there was a connection among the laboratory markers of alcoholism and the alcohol-associated parameters (daily dose and duration of alcohol consumption) as well as the age of the patients. To investigate this question we used the multiple linear regression (Backward) method. The main aim of the examination was to clarify the relationship among the blood pressure of alcoholics and above-mentioned laboratory markers (GGT, MCV, serum uric acid) of alcoholism.

Using the one-way-ANOVA method* the Scheffe's test we investigated the difference between the mean systolic and diastolic blood pressure in each group of GGT, MCV and serum uric acid. We examined which groups can cause the difference.

Change of blood pressure during the two weeks was tested with one sample method $t$-test (Wilcoxon test).

*In case the conditions of the method were not available, the Kruskal-Wallis test was used.

## Results

*Patients*

122 male patients undergoing withdrawal treatment were examined, the average daily consumption of alcohol among the patients prior to admission was 217 ± 8.4 g (range: 80–410 g/day). More than twice of the average daily consumption of alcohol, at least 400 g characterized 11% of the patients (more than daily 400 g alcohol was consumed by 2% of the patients). The average age of all examined patients was 37 ± 0.6 years and 43% of them was 35 years old or younger. Because of their young age the average duration of their alcohol consumption was 13 ± 0.4 years. 46% of them were drinking for a shorter time than 10 years.

*Blood pressure at admission*

Out of 122 patients 33 (27%) had systolic blood pressure of 160 mm Hg and 31 (25.4%) had diastolic blood pressure of 95 mm Hg. Both systolic and diastolic blood pressure were increased in 25 patients. The average of the systolic blood pressure of 122 patients was 142 ± 1.7 mm Hg and the diastolic blood pressure was 89 ± 1.0 mm Hg. The patients with hypertension were mainly in the lower level range because only 6 of them had systolic blood pressure higher than 170 mm Hg and 17 of them had diastolic blood pressure higher than 100 mm Hg.

*The laboratory markers of alcoholism*

In the group examined the average of GGT was 90 ± 8.6 U/l, this was three times more than the normal value. The dispersion around the mean was high: the coefficients of variation (standard deviation/GGT mean) were 105%, the range (max-min) was 564 U/l. The MCV of 71% of the alcoholics was higher more than the upper level of the MCV (MCV = 95 fl), but out of 84 patients 61 the MCV was between 96 and 100 fl, it was close to the normal value. The average of MCV was 96 ± 0.5 fl.

The average of serum uric acid was 297 ± 6.9 μmol/l, it was under the upper limit (420 μmol/l) of normal range. An uric acid level near the upper limit of the normal value (at least 350 μmol/l) was found in one fifth of the alcoholics (Table I).

**Table I**

*Descriptive statistics*

| Parameters | Mean | Standard error | Mode | Median | Minimum | Maximum |
|---|---|---|---|---|---|---|
| 1. Age (year) | 36.7 | ± 0.58 | 32 | 37 | 23 | 50 |
| 2. Dose of alcohol (g/day) | 217.1 | ± 8.42 | 150 | 200 | 80 | 410 |
| 3. Duration of alcohol consumption (year) | 12.8 | ± 0.43 | 10 | 12 | 5 | 25 |
| 4. GGT (U/l) | 90.3 | ± 8.59 | 24 | 51 | 8 | 572 |
| 5. Serum uric acid (μmol/l) | 297.2 | ± 6.87 | 269 | 287.5 | 140 | 551 |
| 6. MCV (fl) | 96.4 | ± 0.52 | 96 | 96 | 76 | 110 |
| 7. Systolic blood pressure at admission (mm Hg) | 142.5 | ± 1.73 | 140 | 140 | 110 | 190 |
| 8. Diastolic blood pressure at admission (mm Hg) | 89.2 | ± 1.04 | 80 | 90 | 70 | 120 |

*Correlation among the laboratory markers of alcoholism and alcohol-associated parameters*

We have not found any relationship among daily consumption of alcohol, duration of alcoholism, age of the patients, and MCV or serum uric acid values. There was relationship ($p < 0.01$) between the GGT[1] and the duration of alcoholism

$$\lg 10\ GGT = (1443 + 1.39)\cdot 10^{-3}\ \text{alcohol (g/day)}$$
$$(SEE = 0.34)$$

The square of correlation coefficient was 0.13, 13% of the change in GGT value is explainable by the daily dose of alcohol consumption (Table II).

The GGT skew distribution was transformed with the help of logarithmic transformation to normal distribution.

**Table II**

*Regression results (GGT*)*

Regression equation:

lg 10 GGT = (1443 + 1.39) × $10^{-3}$ alcohol (g/day)

| Independent variables | Beta | SE Beta | t | p value | Correlation coefficient (R) and SEE |
|---|---|---|---|---|---|
| Dose of alcohol (g/day) | 0.35 | ± 0.088 | 4.013 | 0.0001 | R = 0.35 |
| | | | | | $R^2$ = 0.13 |
| Duration of alcohol consumption (year) | | Variables not in the equation | | | SEE = 0.34 |
| Age (year) | | | | | |

*lg 10 GGT = The logarithmic value of GGT was used for calculations

*Correlation between the laboratory markers of alcoholism and blood pressure*

There was no correlation between the MCV and blood pressure. According to the GGT values the population was divided into two groups (1:GGT < 30.2:GGT > 30). There was no difference between the two groups in the mean blood pressure values (Figs 1 and 2). The question arises, whether the group of high GGT patients is homogenous or not? The systolic blood pressure increased in patients with high (> 200) GGT (Table III) the average of blood pressure was significantly higher in this group than in the patients with GGT under a value of 70 or between 71 and 200. There was no connection between GGT and diastolic blood pressure.

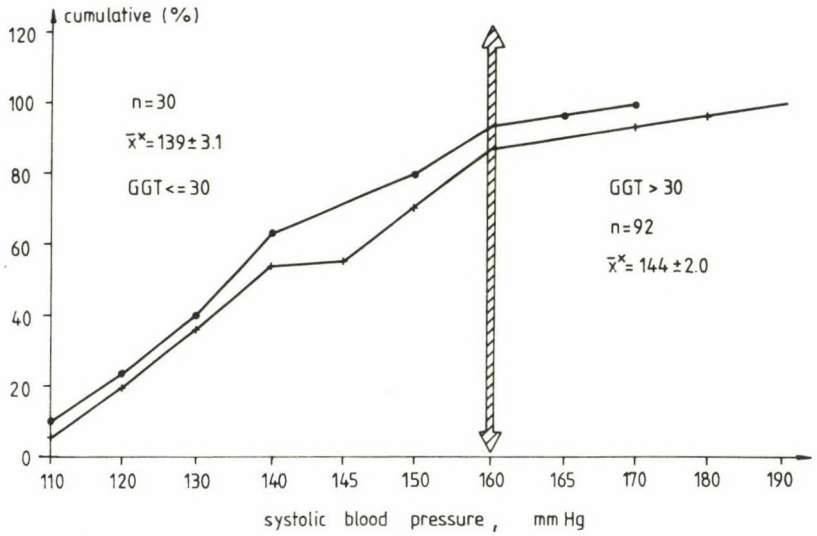


*Fig. 1.* Cumulative percent of systolic blood pressure in the group of patients with normal ($\leq$ 30 U/l) (•—•—•) and high ( > 30 U/l) (⊢—•—⊣) GGT value. *There is no significant difference between the means at the 0.05 level

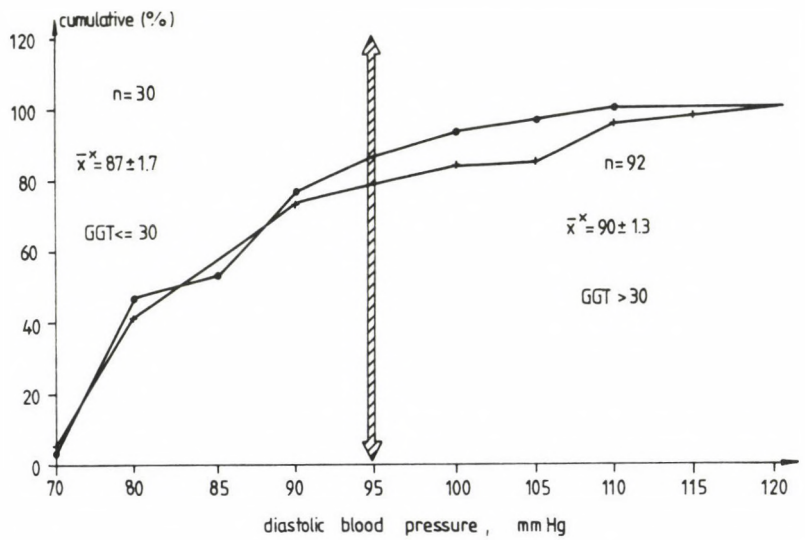


*Fig. 2.* Cumulative percent of diastolic blood pressure in the groups of patients with normal ( $\leq$ 30 U/l) (•—•—•) and high (> 30 U/l) (⊢—•—⊣) GGT value. *There is no significant difference between the means at the 0.05 level

**Table III**

*Results of one-way-ANOVA*

| Groups | n | Systolic blood pressure (mm Hg) | Diastolic blood pressure (mm Hg) | Serum-uric-acid (μmol/l) | MCV (fl) | Age (year) | Dose of alcohol (g/day) | Duration of alcohol consumption (year) |
|---|---|---|---|---|---|---|---|---|
| | | mean ± SE | mean ± SE | mean ± SE | mean ± SE | mean ± SE | mean ± SE | mean ± SE |
| GGT (U/l) | | | | | | | | |
| I. < = 70 | 78 | 139 ± 2.1 | 87 ± 1.2 | 288 ± 7.6 | 97 ± 0.6 | 36 ± 0.8 | 197 ± 9.9 | 12 ± 0.6 |
| II. 71 – 200 | 30 | 144 ± 3.3 | 91 ± 2.2 | 293 ± 12.5 | 96 ± 1.2 | 37 ± 1.1 | 257 ± 16.9 | 13 ± 0.8 |
| III. > 200 | 14 | 159 ± 4.5 | 95 ± 3.9 | 359 ± 29.3 | 96 ± 2.1 | 39 ± 1.4 | 246 ± 25.2 | 14 ± 1.5 |
| p value | – | 0.001 | 0.115+ | 0.004 | 0.710 | 0.284 | 0.004 | 0.421 |
| Results of Scheffe's tests++ | – | I and III<br>II and III | – | I and III<br>II and III | – | – | I and II | |

+ Result of Kruskal-Wallis test;
++Denotes pairs of groups significantly different at the 0.05 level

**Table IV**

*Results of one-way-ANOVA*

| Groups | n | Systolic blood pressure (mm Hg) | Diastolic blood pressure (mm Hg) | GGT (U/l)- | MCV (fl) | Age (year) | Dose of alcohol (g/day) | Duration of alcohol consumption |
|---|---|---|---|---|---|---|---|---|
| | | mean ± SE | mean ± SE | mean ± SE | mean ± SE | mean ± SE | mean ± SE | mean ± SE |
| Serum uric acid (μmol/l) | | | | | | | | |
| I. < = 350 | 97 | 140 ± 1.9 | 87 ± 1.1 | 77,5 ± 7.5 | 96 ± 0.6 | 36 ± 0.7 | 213 ± 9.6 | 13 ± 0.5 |
| II. 351 – 420 | 17 | 151 ± 4.3 | 94 ± 2.2 | 97.1 ± 24.6 | 96 ± 1.3 | 39 ± 1.1 | 250 ± 17.4 | 15 ± 1.2 |
| III. > 420 | 8 | 157 ± 6.6 | 100 ± 5.0 | 231.8 ± 63.1 | 97 ± 2.5 | 35 ± 1.9 | 194 ± 37.5 | 12 ± 1.9 |
| p value | – | 0.007 | 0.001+ | 0.029+ | 0.843 | 0.208 | 0.249 | 0.212 |
| Difference between two groups | – | I and III++ | I and II+<br>I and III | I and III+<br>II and III | – | – | – | – |

+ Results of Kruskal-Wallis and Mann Whitney test;
++Results of Scheffe's tests: denotes pairs of groups significantly different at the 0.05 level

Investigating the relationship between serum uric acid level and blood pressure (Table IV) there was a difference between the systolic and diastolic blood pressure in different groups; over 250 μmol/l serum uric acid value blood pressure increased.

The values of GGT and serum uric acid change similarly, as it can be seen on the former tables, so it was necessary to investigate the interaction between the two variables. Using multivariables variant analysis we investigated the common effect of GGT and serum uric acid on systolic blood pressure. The effect of the age is not significant, so it can be left from the variables. There was no interaction between GGT and serum uric acid value (Table V), and the systolic blood pressure correlated mainly with the GGT values. (According to the multiple classification analysis the partial beta value is GGT: 0.30, serum uric acid: 0.20.) By the serum uric acid the p value is higher than 0.05 but smaller than 0.1.

The above-mentioned laboratory markers explain the change in blood pressure of 16% of the blood pressure changing. A loglinear model was used for the investigation of the linear interaction among the variables. With this model we have studied the effect of GGT and serum uric acid value on the proportion of low and high blood pressure. Using different loglinear models similarly to the former method, it was shown, that the interaction between GGT and serum uric acid value did not change significantly the proportion of low and high blood pressure. The effects in the model are: blood pressure, GGT-blood pressure, serum uric acid-blood pressure.

Our model gives a good estimation of empiric incidence (standard residual value $< 1.96$ or $> -1.96$), but the value of parameters is not significant in each group (Table VI). On the base of the model it can be seen that the GGT effects on the systolic blood pressure are at 5% significance level: above 200 GGT value the probability of high systolic blood pressure increases (Table VI/a).

**Table V**

*ANOVA*
*(Dependent: systole at admission)*

| Source of variation | Df | Mean square | F | p | Beta+ | R and $R^{2+}$ |
|---|---|---|---|---|---|---|
| Main effects | | | | | | |
| GGT | 2 | 2580.49 | 8.21 | 0.000 | 0.30 | |
| Serum uric acid | 2 | 835.21 | 2.66 | 0.075 | 0.20 | |
| Interactions | | | | | | R = 0.394 |
| GGT-Serum uric acid | 4 | 414.06 | 1.32 | 0.268 | – | |
| Residual | 113 | 314.38 | – | – | – | $R^2 = 0.155$ |
| Total | 121 | 363.74 | | | | |
| N = 122 | | | | | | |

Grouping:
- Serum uric acid: -350, 351 - 420, 421 -
- GGT: - 70, 71 - 200, 201 -

+Results of multiple classification analysis

**Table VI**

*Results of log-linear model*

| Factor | Observed | | Expected | | Std. | Adj. |
|---|---|---|---|---|---|---|
| | n | percent | n | percent | residuals | |
| **I. Systolic blood pressure (mm Hg) < 160** | | | | | | |
| 1. *GGT (U/l) < = 70* | | | | | | |
| Serum-u.-a. (μmol/l) < = 350 | 55 | 83.33 | 54.62 | 82.75 | 0.052 | 0.406 |
| Serum-u.-a. (μmol/l) 351 – 420 | 6 | 60.00 | 6.80 | 68.02 | −0.307 | −0.927 |
| Serum-u.-a. (μmol/l) > 420 | 2 | 99.99 | 1.58 | 79.15 | 0.331 | 0.853 |
| 2. *GGT (U/l) = 71 – 200* | | | | | | |
| Serum-u.-a. (μmol/l) < = 350 | 16 | 66.67 | 17.58 | 73.23 | −0.376 | −1.789 |
| Serum-u.-a. (μmol/l) 351 – 420 | 4 | 80.00 | 2.74 | 54.81 | 0.761 | 1.538 |
| Serum-u.-a. (μmol/l) > 420 | 1 | 99.99 | 0.68 | 68.40 | 0.382 | 0.758 |
| 3. *GGT (U/l) > 200* | | | | | | |
| Serum-u.-a. (μmol/l) < = 350 | 4 | 57.14 | 2.81 | 40.13 | 0.711 | 1.734 |
| Serum-u.-a. (μmol/l) 351 – 420 | 0 | 0.00 | 0.46 | 22.91 | −0.677 | −0.876 |
| Serum-u.-a. (μmol/l) > 420 | 1 | 20.00 | 1.73 | 34.66 | −0.557 | −1.324 |
| **II. Systolic blood pressure (mm Hg) > = 160** | | | | | | |
| 1. *GGT (U/l) < = 70* | | | | | | |
| Serum-u.-a. (μmol/l) < = 350 | 11 | 16.67 | 11.38 | 17.25 | −0.114 | −0.406 |
| Serum-u.-a. (μmol/l) 351 – 420 | 4 | 40.00 | 3.20 | 31.98 | 0.448 | 0.927 |
| Serum-u.-a. (μmol/l) > 420 | 0 | 0.00 | 0.42 | 20.85 | −0.646 | −0.853 |
| 2. *GGT (U/l) = 71 – 200* | | | | | | |
| Serum-u.-a. (μmol/l) < = 350 | 8 | 33.33 | 6.42 | 26.77 | 0.622 | 1.789 |
| Serum-u.-a. (μmol/l) 351 – 420 | 1 | 20.00 | 2.26 | 45.19 | −0.838 | −1.538 |
| Serum-u.-a. (μmol/l) > 420 | 0 | 0.00 | 0.32 | 31.60 | −0.562 | −0.758 |
| 3. *GGT (U/l) > 200* | | | | | | |
| Serum-u.-a. (μmol/l) < = 350 | 3 | 42.86 | 4.19 | 59.87 | −0.582 | −1.734 |
| Serum-u.-a. (μmol/l) 351 – 420 | 2 | 99.99 | 1.54 | 77.09 | 0.369 | 0.876 |
| Serum-u.-a. (μmol/l) > 420 | 4 | 80.00 | 3.27 | 65.34 | 0.406 | 1.324 |

Likelihood Ratio Chi Square = 6.27595 p = 0.179
Pearson Chi Square = 5.02075 p = 0.285

**Table VI/a**

*Results of log-linear model*

*Estimates for parameters*

| Parameters | Coefficients | SE (±) | Z-values | 95% confidencia intervallum | |
|---|---|---|---|---|---|
| **Systolic blood pressure** | 0.188 | 0.163 | 1.155 | −0.131 | 0.507 |
| *Systolic BP by GGT* | | | | | |
| GGT < = 70 | 0.422 | 0.158 | 2.661 | 0.111 | 0.732 |
| GGT 71−200 | 0.141 | 0.177 | 0.795 | −0.206 | 0.488 |
| GGT > 200 | −0.563 | 0.227 | −2.482 | −1.007 | −0.118 |
| *Systolic BP by Serum uric acid* | | | | | |
| Ser.-u.a. < = 350 | 0.175 | 0.187 | 0.935 | −0.192 | 0.541 |
| Ser.-u.a. 351−420 | −0.232 | 0.229 | −1.016 | −0.680 | 0.216 |
| Ser.-u.a. > 420 | 0.0576 | 0.303 | 0.190 | −0.537 | 0.652 |

*The effect of alcohol withdrawal on blood pressure*

The patients' blood pressure decreased significantly during the period of alcohol withdrawal. A week after withdrawal was started, the systolic blood pressure proved to be > 160 or = 160 mm Hg in only 5.7% of the group studied, two weeks after in only 2.5%.

At the end of the second week of withdrawal, the proportion of 110 mm Hg (hypotension) systolic blood pressure was significant – approx. 37% – because blood pressure decreased even in the majority of normotension alcoholics.

The diastolic blood pressure was 95 mm Hg also in fewer cases, namely in 16.4% of the alcoholics studied, at the end of the first week. At the end of the second week of alcohol withdrawal the average of the systolic blood pressure decreased from 142.5 (± 1.3) mm Hg to 122.5 (± 1.3) mm Hg and that of the diastolic blood pressure from 89.2 (± 1.0) mm Hg to 80.7 (± 0.8) mm Hg. The decrease of both values was significant (Table VII).

**Table VII**

*Change of the systolic and diastolic blood pressures after two weeks*

| Systole | | Diastole | |
|---|---|---|---|
| Result of one-sample t-test | | Result of Wilcoxon-test | |
| ($sys^2 - sys^1$) | mean = −19.92 | | |
| | SE = 1.27 | | |
| | t = −15.72 | | |
| | Df = 121 | Mean rank | Cases |
| | (n ∓ 122) | 25.00 | 6 − Ranks ($dia^1 < dia^2$) |
| | | 43.32 | 77 + Ranks ($dia^1 > dia^2$) |
| | | | 39 Ties ($dia^1 = dia^2$) |
| 2-tailed p. = 0.000 | | 122 total | |
| | | z = −7.2324 | 2-tailed p. = 0.000 |

$sys^1$ and $dia^1$ = systole and diastole at admission; $sys^2$ and $dia^2$ = systole and diastole two weeks after admission

## Discussion

Consumption of alcohol in large doses is thought to be responsible for 20−30% of essential hypertensions [19] although the correlation between the quantity and duration of alcohol consumption and hypertension has not been proved by all groups of authors [13] those individuals consuming moderate amounts (less than 40 g/day) of alcohol, do not have higher blood pressure than abstinents, indeed, their blood pressures can even be lower than that of the latter. The frequency of hypertension in the Hungarian population is 10−15%, but it is significantly greater, approximately twice (27%) as our results show in the alcoholic population studied, above a daily alcohol consumption of 80 g up to the maximal consumption of 400 g/day − which is the upper limit quantity for humans to metabolise [16].

The mechanism of the hypertension caused by alcohol is unknown. Acute alcohol administration has either no effect on blood pressure [26] or (especially in animal experiments) reduces it [6, 23, 25, 37].

Many symptoms of alcohol withdrawal are like that of a hyperadrenergic state [4] and can be treated with beta adrenergic-blocking drugs [38]. Although increased sympathetic activity may be a cause of permanent hypertension, other mechanisms can also be responsible for the increase in blood pressure.

Cushing syndrome, caused by alcohol [30] with a high plasma cortisol level which could not be completely suppressed with dexamethason, was found in patients who consumed alcohol and its cessation was experienced two or three weeks after the

withdrawal of alcohol. Increased corticosteroid level was often found in alcoholics without Cushing syndrome too [31], in these cases the highest level was found during alcohol withdrawal, especially when the symptoms were the most serious. The activation of the renin-angiotensin system can also play a role in the development of hypertension, since production of renin and aldosterone is increased during the period following acute alcohol consumption [17]. Hypertension can be partly connected with the increase of the total body water and blood volumes – as a result of increased corticosteroid and mineralocorticoid production – although the demonstrated increase of blood volume in alcoholics is relatively small, about 5% [3]. The higher sodium content of alcoholic drinks, e.g. beer, must also be taken into account [18].

We think, that the phenomenon that alcohol causes in the coronary artery system, in its microvasculature [9, 24], undoubtedly deserves attention in the explanation of alcoholic hypertension. Namely: as a result of the various neuroactive – vasoconstrictor – substances the progressive construction of the vascular lumen can lead to hypertension in mammals – but also in humans – after prolonged periods of alcohol consumption. The findings we described in connection with the coronary artery system raise the hypothesis, if increasing vasotonia in the microvasculature of the other regions of the systemic circulation (skeletal musculature, skin, kidneys, etc.), may develop hypertension too. However, as to our previous study in rats long periods of alcohol consumption were consistently accompanied by hypotension [24].

Blood pressure that was reduced to normal in the course of detoxication, in most patients remained normal for at least a year if the patient kept abstinence after leaving the hospital [28]. So the normalisation of the blood pressure is not the result of the response to admission to hospital and medical treatment. In the treatment of "heavy drinker" hypertonic patients, the above mentioned must be taken into consideration. Saunders et al. [28] found that as a result of abstinence, long lasting reduction in blood pressure occurs, even in those patients who previously had to be treated with antihypertensive drugs. According to their observations traditional treatment with drugs is usually unsuccessful in patients with hypertension caused by alcohol – probably because of the antagonistic effects of continuous alcohol consumption. In our present studies – except for a few cases – alcohol withdrawal always – not only in hypertonics – had a reducing effect of blood pressure. No increase in blood pressure has occurred in any case during withdrawal [10, 14, 15, 29, 32].

A series of epidemiological studies prove that the mortality due to cerebrovascular diseases increases in individuals consuming large quantities of alcohol, which can be connected directly with their high blood pressure. The disease, unfortunately, affects young people more and more often [10, 15, 32]. Since

cerebrovascular catastrophes constitute one important cause of mortality, the early recognition of reversible hypertension which makes one susceptible to stroke would be essential.

Hypertension can be diagnosed safely and in time with regular screening. Considering, however, that excessive alcohol consumption is often negated in alcoholics not-yet diagnosed – the recognition of the alcoholic origin of hypertension is important. What calls attention to this, among other things is, that abnormal GGT and MCV values are found in 75 and 68% of alcoholics.

Recently it was found [36] that blood pressure levels, as well as the prevalence and incidence of hypertension were higher in subjects with serum gamma-glutamyl transpeptidase levels above 50 units/l than in those with normal levels. Thus, elevated serum gamma glutamyl transpeptidase activity may identify drinkers being at higher risk for the development of alcohol-related hypertension [36].

The significance of the diagnosis of alcoholic hypertension is obvious. Firstly, alcoholic hypertension is quickly normalised after the cessation of drinking. Secondly, in the case of hypertonic patients we must reckon with all the diseases resulting from hypertension – ischaemic cardiac disease (sudden cardiac death), stroke, etc. – regardless of the cause of it, since the occurrence of hypertension in the population compared to any kind of general morbidity is more frequent.

## REFERENCES

1. Altura, B. M., Altura, B. T.: Alcohol, the cerebral circulation and strokes. Alcohol **1**, 325–331 (1984).
2. Barcha, R., Stewart, M. A., Guze, S. B.: The prevalence of alcoholism among general hospital ward patients. Am. J. Psychiatry **125**, 681–684 (1968).
3. Beard, J. D., Knott, D. H.: Fluid and electrolyte balance during acute withdrawal in chronic alcoholic patients. JAMA **204**, 135–139 (1968).
4. Carlsson, C., Haggendahl, J.: Arterial noradrenaline levels after ethanol withdrawal. Lancet **2**, 889–890 (1967).
5. Chan, A. W. K., Welte, J. W., Whitney, R. B.: Identification of alcoholism in young adults by blood chemistries. Alcohol **4**, 175–179 (1987).
6. Conway, N.: Hemodynamic effects of ethyl alcohol in patients with coronary heart disease. Br. Heart J. **30**, 638–644 (1968).
7. Drum, D. E., Goldman, P. A., Jankowski, C. B.: Elevation of serum uric acid as a clue to alcohol abuse. Arch. Intern. Med. **141**, 477–479 (1981).
8. Harburg, E., Ozgoren, F., Hawthorne, V. M., Schork, M. A.: Community norms of alcohol usage and blood pressure: Tecumseh, Michigan Am. J. Public Health **70**, 813–820 (1980).
9. Hermann, H.-J., Morvai, V., Ungváry, Gy., Norden, C., Mühlig, P.: Long-term effects of ethanol on coronary microvessels of rats. Microcirc. Endoth. Lymphat. **1**, 589–610 (1984).
10. Hillbom, M., Kaste, M.: Does ethanol intoxication promote brain infarction in young adults? Lancet **2**, 1181–1183 (1978).
11. Jackson, R., Stewart, A., Beaglehole, R., Scragg, R.: Alcohol consumption and blood pressure. Am. J. Epidemiol. **122**, 1037–1044 (1985).

12. Jankowski, C. B., Drum, D. E.: Criteria for the diagnosis of alcoholism. Arch. Intern. Med. **137**, 1532–1536 (1977).
13. Klatsky, A. L., Friedman, G. D., Siegelaub, A. B., Gerard, M. F.: Alcohol consumption and blood pressure. N. Engl. J. Med. **296**, 1194–1200 (1977).
14. Kozarevic, D., McGee, D., Vojvodic, N., Racic, Z., Dawber, T., Gordon, T., Zukel, W.: Frequency of alcohol consumption and morbity and mortality. Lancet **1**, 613–616 (1980).
15. Lee, K.: Alcoholism and cerebrovascular thrombosis in the young. Acta Neurol. Scand. **59**, 270–274 (1979).
16. Lieber, C. S., Jones, D. P., Mendelson, J., DeCarli, L. M.: Fatty liver, hyperlipaemia, and hyperuricaemia produced by prolonged alcohol consumption despite adequate dietary intake. Trans. Ass. Am. Physicians **76**, 289–300 (1963).
17. Linkola, J., Fyhrquist, F., Ylikahri, R.: Renin, aldosterone and cortisol during ethanol intoxication and hangover. Acta Physiol. Scand. **106**, 75–82 (1979).
18. MacLeod, A. M.: Beer. In: Rose, A. H. ed. Alcoholic beverages. Academic Press, London, pp. 43–137 (1977).
19. Mathews, J. D.: Alcohol use, hypertension and coronary heart disease. Clin. Sci. Mol. Med. **51**, $661_s$–$663_s$ (1976).
20. Mohácsi, G., Sonkodi, S., Ábrahám, G., Lovas, S., Boda, K., Csirik, J., Remes, P., Varró, V.: A tartós alkoholfogyasztás hatása a vérnyomásra. Orv. Hetil. **132**, 63–68 (1991). (In Hungarian).
21. Moore, R. A.: The prevalence of alcoholism in a community general hospital. Am. J. Phychiatry **128**, 130–131 (1971).
22. Morvai, V., Kondorosi, Gy., Szendrő, Z., Ungváry, Gy.: Hipertónia és az alkoholizmus. Egészségtudomány **34**, 74–83 (1990). (In Hungarian).
23. Morvai, V., Nádházi, Z., Ungváry, Gy., Folly, G.: Akut alkohol-bevitel kardiovaszkuláris hatásai szubakut alkohol-mérgezésben. Kísérl. Orvostud. **32**, 257–265 (1987). (In Hungarian).
24. Morvai, V., Ungváry, Gy., Herrmann, H. J., Kühne, C.: Effects of quantitative undernourishment, ethanol and xylene on coronary microvessels of rats. Acta Morph. Hung. **35**, 199–206 (1987).
25. Morvai, V., Nádházi, Z., Molnár, Gy., Ungváry, Gy., Folly, G.: Acute effects of low doses of alcohol on the cardiovascular system in young men. Acta Med. Hung. **45**, 339–348 (1988).
26. Riff, D., Jain, A., Doyle, J.: Acute hemodynamic effect of ethanol on normal human volunteers. Am. Heart J. **78**, 592–597 (1969).
27. Ryback, R. S., Rawlings, R., Faden, V., Negron, G. L.: Laboratory test changes in young abstinent male alcoholics. Am. J. Clin. Pathol. **83**, 474–479 (1985).
28. Saunders, J. B., Beevers, D. G., Paton, A.: Alcohol-induced hypertension. Lancet **2**, 653–656 (1981).
29. Shaper, A. G., Phillips, A. N., Pocock, S. J., Walker, M., Macfarlane, P. W.: Risk factors for stroke in midde aged British men. Br. Med. J. **302**, 1111–1115 (1991).
30. Smalls, A. G., Kloppenborg, P. W., Njo, K. T., Knochen, J. M., Roland, C. M.: Alcohol-induced Cushingoid syndrome. Br. Med. J. **2**, 1298 (1976).
31. Stokes, P. E.: Adrenocortical activation in alcoholics during chronic drinking. Ann. N. Y. Acad. Sci. **215**, 77–83 (1973).
32. Taylor, J. R., Coombs-Orme, T.: Alcohol and strokes in young adults. Am. J. Psychiatry **142**, 116–118 (1985).
33. Umbricht-Schneiter, A., Santora, P., Moore, R. D.: Alcohol abuse: comparison of two methods for assessing its prevalence and associated morbidity in hospitalized patients. Am. J. Med. **91**, 110–118 (1991).
34. Vanclay, F., Raphael, B., Dunne, M., Whitfield, J., Lewin, T., Singh, B.: A community screening test for high alcohol consumption using biochemical and haematological measures. Alcohol-Alcohol **26**, 337–346 (1991).
35. Whitfield, J. B., Heusley, W. J., Bryden, D., Gallagher, H.: Some laboratory correlates of drinking habits. Ann. Clin. Biochem. **15**, 297–303 (1978).

36. Yamada, Y., Ishizaki, M., Kido, T., Honda, R., Tsuritani, I., Ikai, E., Yamaya, H.: Alcohol, high blood pressure, and serum gamma-glutamyl transpeptidase level. Hypertension **18**, 819–826 (1991).
37. Zeiner, A. R., Parades, A., Christensen, H. D.: The role of acetaldehyde in mediating to an acute dose of ethanol among different racial groups. (Abstr.) Alcoholism **37**/2, 193 (1978).
38. Zilm, D. H., Jacob, M. S., MacLeod, S. M., Sellers, E. M., Ti, T. Y.: Propranolol and clordiazepoxide effects on cardiac arrhythmias during alcohol withdrawal. Alcoholism: Clin. Exper. Res. **4**, 400–405 (1980).

*Acta Physiologica Hungarica, Volume 81 (1), pp. 87–93 (1993)*

# THE EFFECTS OF SELENIUM SUPPLEMENTATION ON ANTIOXIDATIVE ENZYME ACTIVITIES AND PLASMA AND ERYTHROCYTE SELENIUM LEVELS

Belma TURAN, Nejat DALAY, Lale AFRASYAP*, Ertan DELILBASI**, Zeynep SENGÜN**, Ahmet SAYAL**, Askin ISIMER***

DEPARTMENT OF BIOPHYSICS, FACULTY OF MEDICINE, ANKARA UNIVERSITY, TURKEY
*I. U. ONCOLOGY INSTITUTE, ISTANBUL UNIVERSITY, TURKEY
**DEPARTMENT OF ORAL SURGERY, FACULTY OF DENTISTRY, GAZI UNIVERSITY, TURKEY
***DEPARTMENT OF PHARMACOLOGY AND TOXICOLOGY, GÜLHANE MILITARY MEDICAL ACADEMY, TURKEY

Received June 6, 1992
Accepted October 27, 1992

Plasma and erythrocyte selenium levels in rabbits supplemented with therapeutic doses of selenium were studied by Zeeman graphite furnace atomic absorption spectrometry using a new palladium-ascorbic acid chemical modifier in order to achieve a higher precision. An improved coupled test procedure was used to determine the glutathione peroxidase (GSH-Px) activities. Superoxide dismutase activities were measured employing a method for the clinical assay of the enzyme. The selenium levels and GSH-Px activities both in the plasma and erythrocytes were higher in the supplemented group when compared to the controls. The SOD activities were increased in the erythrocytes but remained unchanged in the plasma. On the other hand, a higher copper/zinc ratio was found both in the plasma and erythrocytes of the supplemented group. These findings support the importance of the dietary selenium intake in terms of the principal role of selenium in the cellular antioxidative mechanisms and imply that measurements of plasma selenium levels may be a notable sensitive indicator of the short-term selenium status.

**Keywords**: selenium, antioxidative enzyme activities, erythrocyte, plasma, copper, zinc, atomic absorption spectrometry, glutathione peroxidase, superoxide dismutase

Despite many similarities with sulphur, selenium occupies a unique position among metals and nonmetals. Its strong tendency to change its oxidation level has been utilized in organic chemical synthesis where redox reactions are involved [17]. Hydrogen peroxide ($H_2O_2$), the hydroxyl radical ($OH^-$) and the superoxide radical ($O_2^-$) are toxic to the cells and can cause tissue damage by oxidizing the DNA, proteins and lipids. Intracellular defence mechanisms to detoxify these reacti

Correspondence should be addressed to
Nejat DALAY
Basic Oncology Department, I. U. Oncology Institute
34390 Capa, Istanbul, Turkey

oxygen species include the enzymatic systems like superoxide dismutase (SOD) and glutathione peroxidase (GSH-Px).

Each of these enzymes requires an essential mineral as a cofactor for its catalytic activity. The activities of these enzymes within mammalian cells are the result of a complex interplay between the availability of the cofactor and the regulation of the enzyme synthesis and degradation rates [5]. Studies have revealed that tissue Cu, Zn-SOD and GSH-Px activities decrease during copper and selenium deficiencies [14]. However, there are still contradictory results on the antioxidant enzyme activities induced by metal deficiencies.

Human plasma GSH-Px has been shown to be a glycosylated selenoprotein structurally, enzymatically and antigenically distinct from known cellular GSH-Px [2]. Several findings indicate that plasma GSH-Px is a unique selenoenzyme.

With the growing appreciation of the role of dietary selenium in cardiac disease and cancer a considerable number of reports has appeared where low selenium levels were associated with a wide variety of diseases. Cónsequently, if a decline in the selenium level and the associated GSH-Px activity is likely to be considered as an aetiological factor in a particular disease it might be expected that selenium supplementation should reverse at least some of the disease symptoms. Studies conducted in Turkey have revealed that the mean selenium levels are lower in the Turkish population when compared to the developed countries [8, 12].

The aims of the study were to a) show the relationship between the activities of membrane-bound GSH-Px and SOD in response to selenium supplementation, b) determine the effects of the increase in dietary selenium on the plasma and erythrocyte selenium levels by a modified Zeeman graphite furnace atomic absorption spectrometry using a new palladium-ascorbic acid chemical modifier and c) investigate whether the high level of dietary selenium intake should affect the copper/zinc ratio in the plasma and erythrocytes.

## Materials and methods

Twenty male New Zealand white rabbits with an overall mean weight of 2600 g were kept by pairs in stainless steel wire mesh cages. The rabbits were fed on the same standard diet before selenium supplementation for one week. After the completion of the week blood samples were collected in heparinized plastic tubes and stored at −70 °C after being frozen in liquid nitrogen. A solution containing 50 μg selenium/ml per kg body weight was administered daily by gastric intubation while a group of 10 rabbits were kept as the control group. Gastric intubation was accomplished by a plastic cannula of 3 mm diameter. After 15 days of supplementation all animals were sacrificed by decapitation and exsanguination. Blood samples were collected in heparinized plastic tubes in the same manner as described above.

Selenium in the plasma and erythrocytes was determined by graphite furnace atomic absorption spectrometry (Varian AA-30/40 Spectrometer, GTA-96 graphite tube atomizer) using a palladium-ascorbic acid chemical modifier instead of the nickel modifier [13]. The palladium modifier (Sigma: P-6901) was injected into the graphite tube prior to adding the plasma and erythrocyte samples. The

samples were prediluted with a solution of 0.5% Triton X-100 and the reducing agent, 0.125% L-ascorbic acid. Calibration was achieved by the standard additions method using a selenium standard stock solution with the additions made automatically by an autosampler.

The copper and zinc levels were determined colorimetrically with deproteinization. The absorbance readings for copper and zinc were made at 436 and 560 nm.s, respectively.

The plasma and erythrocyte GSH-Px activities were determined by using an improved coupled test procedure [10]. In order to measure the SOD activities the method for the clinical assay of SOD was employed [18].

The significance levels of the results with respect to the controls were determined by the Student t-test.

## Results and discussion

Rabbit consuming diets supplemented with 50 μg Se/kg body weight daily did not gain more weight during the feeding period than did rabbits whose diet was not containing selenium.

Table I shows the selenium, copper and zinc levels as well as the plasma and erythrocyte GSH-Px and SOD activities (as mean ± SD) before selenium supplementation. The element levels and enzyme activities in the supplemented and control groups are given in Table II. No significant differences are observed between the values in the control group and the values before supplementation.

**Table I**

*The mean (SD) values of parameters before experiment*

| Samples | Selenium (ng/ml) | Copper (μg/dl) | Zinc μg/dl) | GSH-Px (U/ml) | SOD (μg/l and mg/l) |
|---|---|---|---|---|---|
| Plasma | 65.08 ± 6.12 | 397.72 ± 19.58 | 194.32 ± 44.26 | 0.409 ± 0.079 | 83.33 ± 35.54 |
| Erythrocyte | 555.90 ± 67.64 | 205.34 ± 76.74 | 209.98 ± 61.86 | 17.94 ± 5.04 | 136.91 ± 15.13 |

Both the plasma and erythrocyte selenium levels and GSH-Px activities in the supplemented group (Table II) are higher than those in the controls ($p < 0.05$). The SOD activity is also increased ($p < 0.05$) in the erythrocytes while it remains unchanged in the plasma (Table III) with respect to the controls. Approximately a four-fold increase in the copper/zinc ratio with respect to the control group was found both in the plasma and the erythrocytes of the experimental group.

**Table II**

*The mean (±SD) values of parameters after selenium supplementation*

| Samples | Plasma | | Erythrocyte | |
|---|---|---|---|---|
| | Control | Experiment | Control | Experiment |
| Selenium (ng/ml) | 65.12 ± 5.70 | 200.45 ± 5.71 | 553.43 ± 30.30 | 975.06 ± 78.53 |
| Copper (μg/dl) | 402.90 ± 30.85 | 1135.64 ± 317.46 | 208.84 ± 56.74 | 525.59 ± 76.14 |
| Zinc (μg/dl) | 190.52 ± 10.54 | 167.38 ± 12.08 | 216.03 ± 92.73 | 136.77 ± 55.62 |
| GSH-Px (U/ml) | 0.412 ± 0.073 | 0.576 ± 0.097 | 19.08 ± 5.64 | 35.34 ± 5.62 |
| SOD (μg/l and mg/l) | 85.46 ± 21.10 | 91.90 ± 28.98 | 157.5 ± 18.15 | 228.89 ± 16.80 |

**Table III**

*The significance levels of differences between the mean values of experimental and control groups*

| Parameters | Plasma | Erythrocyte |
|---|---|---|
| Selenium | $p < 0.05$ | $p < 0.05$ |
| Copper: Zinc | $p < 0.05$ | $p < 0.05$ |
| GSH-Px | $p < 0.05$ | $p < 0.05$ |
| SOD | $p < 0.05$ | $p < 0.05$ |

In our study a new Zeeman graphite furnace system was used for the determination of selenium in plasma and erythrocytes. Since palladium is reduced to the metallic state in the graphite tube the use of a palladium-ascorbic acid chemical modifier provided additional thermal stability and a higher sensitivity for selenium when compared to the commonly used nickel modifier.

Different studies point to the fact that the GSH-Px activity may depend on the selenium content of the diet [9]. Dietary selenium intake greatly affects the GSH-Px activity in different tissues in rats, chicken and sheep [17]. Approximately, 36% of total selenium is estimated to be in association with Se–GSH-Px in rat liver and the selenium status is highly correlated with the activity of this fraction [6]. Tissue GSH-Px activities would appear to be a sensitive indicator of the blood selenium levels in animal models [9]. Previous reports have revealed a linear relationship between dietary selenium supply and blood selenium concentration in human [3, 15]. Baker and Cohen [3] have shown that a significant correlation exists between the

blood and erythrocyte selenium levels and the GSH-Px activities up to 140 μg selenium per liter of erythrocyte, the level at which the enzymatic activity reaches a plateau. Plasma selenium is consistently lower than erythrocyte selenium and is more rapidly influenced by dietary supply modifications of by the selenium status than erythrocyte selenium [15]. In our work we observed a 200% increase in the plasma selenium levels while the erythrocyte selenium levels increased by 77%. Thus, plasma selenium appears to be a more sensitive indicator of the short-term selenium status.

According to Simmons et al. [16] the biochemical function of selenium, which affects the peroxidation in houseflies and rats independent of GSH-Px is unknown. Seleno-compounds other than GSH-Px are also believed to be involved in the process. It has been shown that seleno-amino acids such as seleno-cysteine, -cystine, -cystamine and -methionine can catalyze the reduction of peroxidase *in vitro* and may also act as antioxidants *in vivo* [4, 11]. A different form of selenoprotein P in rats was reported to contain more plasma selenium than does GSH-Px [1].

In a selenium supplementation study Xia et al. [19] have shown that although the selenium status did not affect the SOD and catalase activities in red blood cells, supplementation resulted in elevated plasma selenium concentrations and higher GSH-Px activities. However, the differences in the GSH-Px activities were relatively small when compared to those in the selenium levels. These results speak for the presence of additional plasma forms of selenium besides the GSH-Px. Our results are in good agreement with reported data. Following supplementation the selenium and GSH-Px levels in plasma and red blood cells are observed to increase with respect to the controls. The erythrocyte SOD levels were also increased while the plasma SOD level did not change. The increases in the plasma (% 200) and erythrocyte (% 77) selenium levels were highly significant. The activity of the selenium dependent enzyme GSH-Px was also significantly higher both in the plasma (% 40) and erythrocytes (% 85). The activity of a further important cellular antioxidative enzyme, not directly associated with selenium were also increased by % 50. These results underline the importance of selenium in the cellular antioxidative mechanism.

The intra- and extracellular copper/zinc ratio was higher in the supplemented group. Distribution and retention of zinc in presence of cadmium and copper has been studied in rats exposed repeatedly to these metals [7]. It was found that whole body retention of zinc under the influence of cadmium is lower when compared to animals treated with zinc alone. However, the same study has revealed that administration of copper may lead to a twofold increase in the whole body retention of zinc while cadmium induces the accumulation of zinc only in the nuclear fraction of kidneys and the soluble fraction in the liver. Apparently there are complex interactions between the chemically similar metals cadmium, copper, zinc and selenium which can significantly affect the metabolism of the individual metals.

There has been evidence that variations in the nutritional intake of selenium may affect the function of the immune system, although the mechanisms involved are still unclear. It is evident, therefore that this area merits more research not only in terms of maintaining the status of general good health but also in terms of the control and prevention of many disorders. Further studies should be devoted to the influence of the marginal deficiency in this trace element whose optimal requirement does not seem to be adequate by the usual dietary intake.

## REFERENCES

1. Avissar, N., Whitin, J. C., Allen, P. Z., Palmer, I. S., Cohen, H. J.: Antihuman plasma glutathione peroxidase antibodies: Immunologic investigations to determine plasma glutathione peroxidase protein and selenium content in plasma. Blood **73**, **1**, 318–323 (1989).
2. Avissar, N., Whitin, J. C., Allen, P. Z., Wagner, D. D., Liegey, P., Cohen, H. J.: Plasma selenium dependent glutathione peroxidase, cell of origin and secretion. J. Biol. Chem. **264**, 15850–15855 (1989).
3. Baker, S. S., Cohen, H. J.: Increased sensitivity of H 202 in glutathione peroxidases-deficient rat granulocytes. J. Nutr. **114**, 2003–2008 (1984).
4. Behne, D., Walter, W.: Distribution of selenium and glutathione peroxidase in the rat. J. Nutr. **113**, 456–469 (1983).
5. Bettger, W. J., Bray, T. M.: Effect of dietary zinc or copper deficiency on catalase, glutathione peroxidase and superoxide dismutase activities in the rat heart. Nutr. Res. **9**, 319–326 (1989).
6. Chen, L. C., Borges, T., Glauert, H. P., Knight, S. A. B., Sunde, R. A., Schramm, H., Oesch, F., Chow, C. K., Robertson, L. W.: Modulation of selenium dependent glutathione peroxidase by perfluorodecanoic acid in rats: Effect of dietary selenium. J. Nutr. **120**, 298–304 (1990).
7. Chmielnicka, J., Komsta-Szumska, E., Zareba, G.: Effects of interaction between zinc cadmium and copper in rats. Biol. Trace Elem. Res. **17**, 285–291 (1988).
8. Delilbaşi, E., Turan, B., Yücel, E., Şaşmaz, K., Işimer, A. Sayal A.: Selenium and Behçet's disease. Biol. Trace Elem. Res. **28**, 21–25 (1991).
9. Dhur, A., Galan, P., Hercberg, S.: Relationship between selenium immunity and resistance against infection. Com. Biochem. Physiol. **96 C**, **2**, 271–280 (1990).
10. Günzler, W. A., Kremers, H., Flohe, L.: An improved coupled test procedure for glutathione peroxidase (EC 1.11.1.9) in blood. Z. Klin. Chem. Klin. Biochem. **12**, 444–448 (1974).
11. Hawkes, W. C., Wilhemsen, E. C., Tappel, A. L.: Abundance and tissue distribution of selenocysteine-containing proteins in the rat. J. Inorg. Biochem. **23**, 77–92 (1985).
12. Hincal, F., Yetgin, S., Basaran, N., Ataçeri, N.: Selenium status in turkey. Serum selenium levels of children and adults living in Ankara. In: Trace elements in health and disease. eds G. T. Yüregir, O. Donma, L. Kayrin. pp. 183–187, Ankara, Turkey (1991).
13. Knowles, M. B., Brodie, K. G.: Determination of selenium in blood by Zeeman graphite furnace atomic absorption spectrometry using a palladium-ascorbic acid chemical modifier. J. Anal. Atomic Spect. **3**, 511–516 (1988).
14. Prohaska, J. R., Gutsch, D. E.: Development of glutathione peroxidase activity during dietary and genetic copper deficiency. Biol. Trace Elem. Res. **5**, 35–45 (1983).
15. Rea, H. M., Thomson, C. D., Campbell, D. R., Robinson, M. F.: Relation between erythrocyte selenium concentrations and glutathione peroxidase activities of New Zealand residents and visitors to New Zealand. Brit. J. Nutr. **42**, 201–210 (1979).

16. Simmons T. W., Jamal, I. S., Lockshin, R. A.: Selenium modulates peroxidation in the absence of glutathione peroxidase in *Musca domestica*. Biochem. Biophys. Res. Commun. **165**, 158–163 (1989).
17. Stadtman, T. C.: Selenium biochemistry. Ann. Rev. Biochem. **59**, 111–125 (1990).
18. Sun, Y. I., Oberley, Y. W. and Li, Y.: A simple method for clinical assay of superoxide dismutase. Clin. Chem. **343**, 497–500 (1988).
19. Xia, Y., Hill, K. E., Burk, R. F.: Biochemical studies of a selenium deficient population in China: Measurement of selenium glutathione peroxidase and other oxidant defence indices in blood. J. Nutr. 1318–1326 (1989).

*Acta Physiologica Hungarica, Volume 81 (1), pp. 95–99 (1993)*

# THRYROIDECTOMY AND THYROXINE ADMINISTRATION ALTER SERUM CALCIUM LEVELS IN RAT

K. O. ADENIYI, O. O. OGUNKEYE*, C. O. ISICHEI*

DEPARTMENTS OF HUMAN PHYSIOLOGY AND *CHEMICAL PATHOLOGY, UNIVERSITY OF JOS, JOS, NIGERIA

Received July 23, 1992
Accepted October 7, 1992

The effects of thyroidectomy and thyroxine on serum calcium concentration were studied in adult albino Wistar strain rats using the technique described by Baginski et al. (1973) as used by Lorentz [10]. Thyroidectomy decreased serum calcium concentration from 2.28 ± 0.02 mmol/l to 1.61 ± 0.01 mmol/l. Chronic administration of thyroxine (6–8 μg/100 g body wt/day) for 35 days caused an increased serum calcium concentration from 2.28 ± 0.02 mmol/l to 2.98 ± 0.05 mmol/l.

These findings suggest that thyroidectomy and the dose of thyroxine used affected calcium metabolism in rats.

**Keywords:** thyroid gland, thyroid hormones, thyroidectomy, thyroxine, serum calcium, calcium metabolism

Calcium activation of muscle contraction involves calcium binding to troponin-C and the subsequent alteration of thin filament proteins. Thus, the interaction between troponin-1 and actin decreases [15]. Activation, therefore, may be brought about by an increase in calcium occupancy of troponin-C due to either an increased myoplasmic calcium ion concentration or to an increased calcium affinity for troponin-C at a given calcium ion concentration [11]. Calcium is therefore very important in promoting excitation concentration coupling in skeletal, smooth and cardiac muscles [12].

It was recently reported that thyroidectomy and thyroxine administration affected the contractility of the diaphragm and uterine muscles [4, 5]. These authors interpreted their findings to mean that thyroidectomy and thyroxine administration might be influencing calcium metabolism in the body. The present study therefore examines the effect of thyroidectomy and chronic thyroxine administration on serum calcium levels in rat.

Correspondences should be addressed to
Kayode O. ADENIYI
Department of Human Physiology, Faculty of Medical Sciences
University of Jos
Jos, P. M. B. 2084, Nigeria

*Akadémiai Kiadó, Budapest*

## Materials and methods

*Animals*

Forty adult male Wistar strain rats weighing between 120 g and 140 g were used. They were divided into four groups:

1. control;
2. thyroidectomized;
3. thyroidectomized rats treated with thyroxine;
4. thyroxine treated.

The rats in the last two groups were given daily dose of thyroxine (6–8 μg/100 g body weight/day. A. H. Cox and Co, Barnstaple U. K.) for 35 days.

The thyroxine tablets which were properly ground and well mixed, were given through the drinking water. The drinking water containing thyroxine was changed three times daily to ensure relative stability of the thyroxine. The drinking habit of the rats was also monitored closely to ensure that each rat received the required daily dose of thyroxine as described previously [1].

Rats in all the groups were provided with rat chow and tap water *ad libitum* for 35 days.

Under general anaesthesia using ether, the thyroid glands of rats in the appropriate groups were surgically removed by thermocautry with extra care and skill making sure the external parathyroids were left intact. These rats were also left for 35 days.

Clinical evaluation of thyroid state was confirmed by carrying out morphological studies on the thyroid glands from the control and thyroxine-treated rats as previously described [2, 3].

*Determination of serum calcium levels*

Following the expiration of 35 days blood samples were collected from all the rats under general anaesthesia directly from the heart. The blood samples were centrifuged and serum was collected for spectrophotometric analysis of calcium using spectrophotometer SP6 (Model 450 Pye Unicam Philips). Orthocresolphtalein complexone was used for the assay [8, 10]. The assay was based on the principle that metal complexing dye orthocresolphtalein complexone (CPC) forms a chromophore with calcium in alkaline solution. The colour produced was then measured spectrophotometrically at 575 nm. The chromogen reagent contained 8 hydroxyquinoline to mask interfering cations such as magnesium. The intensity of colour developed by the calcium-CPC complex increased proportionately with an increase in pH and was also dependent on the buffer species employed. Diethernolamine (DEA) was added to enhance the colour intensity. The pH was maintained between 10 and 12.

After measuring the developed colour, an excess of calcium chelator EDTA, was added to correct for haemolysis. This treatment dissociated the calcium–chromogen complex but the heamoglobin–chromogen complex remained undissociated. The absorbance due to this haemoglobin–chromogen complex was subtracted from the total absorbance to give calcium absorbance.

All reagents used were of analytical grade.

*Reagents used*

A stock standard was prepared freshly using 250 mg dry $CaCO_3$ and HCl. The solution was made up to 100 ml, pH 3.0 and allowed to stand for about 12 hours.

Working standard solution was obtained by diluting the stock standard 1 in 10 using distilled water.

Cresolphtalein complexone (CPC) was prepared using 10 mg CPC dissolved in 1.0 ml concentrated HCl and a few drops of distilled water. 100 ml di-methylsulfoxide and 2.5 g 8-hydroxyquinoline were later added.

DEA buffer was prepared using 500 mg KCl and 40 ml diethylamine diluted to 100 ml with distilled water.

EDTA was prepared by dissolving 0.5 g EDTA in 90 ml of distilled water.

*Experimental protocol*

Serum calcium concentrations were determined using the technique described by Baginski et al. (1973) as used by Lorentz [10].

2.5 ml CPC and 2.5 ml DEA buffer were added into three test tubes each containing 0.05 ml serum (Test), 0.05 ml standard (Standard) and 0.05 ml distilled water (Blank). The contents of the test tubes were properly mixed and read at 575 nm (A total). After this, 0.05 ml EDTA was added to each of the test tubes. The contents were properly mixed and read again at 575 nm (A after EDTA). The blank was always used to zero in the instrument.

*Calculations*

Serum calcium concentration was calculated as follows: calcium (mmol/l) = A unknown (Test) = A total − A after EDTA.

$$\text{Calcium (mmol/l)} = \text{A unknown/A standard} \times 2.5$$

*Statistics*

All results are expressed as means ± SEM. Statistical comparisons between the experimental groups were performed using the Student's two tailed test for unpaired data.

## Results

The results (Table I) show that the serum calcium concentration of control rats (2.28 ± 0.02 mmol/l) was not significantly different from the value obtained for thyroidectomized rats treated with thyroxine (2.30 ± 0.16 mmol/l). The value

**Table I**

*Serum calcium concentration*

| Type of rats | Initial body weight (g) | Body weight of rats after 35 days | Serum calcium concentration (mmol/l) |
|---|---|---|---|
| Control, (10) | 133.8 ± 3.30 | 250.48 ± 6.23 | 2.28 ± 0.02 |
| Thyroidectomized, (10) | 133.0 ± 3.38 | 225.32 ± 6.11 | 1.61 ± 0.01* |
| Thyroidectomized rats treated with thyroxine, (10) | 133.8 ± 3.80 | 252.67 ± 5.42 | 2.30 ± 0.16 |
| Thyroxine-treated, (10) | 133.8 ± 3.88 | 261.32 ± 6.03 | 2.98 ± 0.05* |

Values are means ± S.E.M.: Number of rats is shown in parentheses. *$p < 0.001$ compared with value for control rats.

obtained for thyroidectomized rats (1.61 ± 0.1 mmol/l) was significantly lower than the control value ($P < 0.001$). Thyroxine administration on the other hand significantly increased the serum calcium concentration from 2.28 ± 0.02 mmol/l to 2.98 ± 0.05 mmol/l ($P < 0.001$).

## Discussion

The method used presently in determining the serum calcium concentration was found to be reliable despite the few disadvantages inherent in the technique [6, 9, 14, 16]. In fact by using 8-hydroxyquinoline in the study, interfering cations such as magnesium were masked and the readings were objective [7]. Moreover, the fact that there are consistent differences between serum calcium concentration of control and thyroidectomized rats and for that matter between control and thyroxine treated rats argues that the differences in serum calcium concentrations of these different types of rats are intrinsic and caused mainly by the differences in the status of thyroid hormones between the rats.

The current study shows clearly that thyroidectomy decreases while thyroxine administration increases serum calcium concentration. This confirms and extends previous observations that thyrotoxicosis is associated with hypercalcaemia due to direct effect on calcium resorption from bones [13]. The fact that thyroidectomy decreased serum calcium concentration could therefore be interpreted to mean that thyroidectomy inhibits calcium resorption from bones. It could therefore be concluded that thyroidectomy and the dose by thyroxine used in this study affected calcium metabolism in rats. The observed effects of thyroidectomy and thyroxine administration on the contractility of the diaphragm and uterine muscles [4, 5] could therefore be due to the effects of these parameters on calcium metabolism in those rats.

## Acknowledgements

The authors acknowledge with deep gratitude, the help given by Mr. Daniel Ishaku. We also wish to thank Mr. Albert Buba for typing the manuscript.

## REFERENCES


1. Adeniyi, K. O., Olowookorun, M. O.: Haematological values in normal, thyroidectomized and thyroxine treated rats. Nig. J. Physiol. Sci. **4**, 64–66 (1988).
2. Adeniyi, K. O., Olowookorun, M. O.: Gastric acid secretion and parietal cell mass; effects of thyroidectomy and thyroxine. Am. J. Physiol. 256 (Gastrointest. Liver Physiol.) **19**, G975–G978 (1989).
3. Adeniyi, K. O., Olowookorun, M. O., Adeyemo, M. O., Oyejide, O.: Effect of exogenous thyroxine on the morphology and activity of the thyroid gland. Him. J. Env. Zool. **4**, 111–115 (1990).
4. Adeniyi, K. O., Ogunkeye O.O., Senok S. S., Udoh, F. V.: The effect of thyroidectomy and thyroxine on the reactivity of rat diaphragm muscle to electrical stimulation in vitro. Acta Physiol. Hungarica, In Press (1992).
5. Adeniyi, K. O., Ogunkeye, O. O., Senok, S. S., Udoh, F. V.: The effect of thyroidectomy and thyroxine on the reactivity of rat uterine muscle to electrical stimulation in vitro J. Pathophysiol. In Press (1992).
6. Besozzi, M., Franzini, C., Senaldi, Y.: Evaluation of cresolpthalein complexone and methylthymol blue direct methods for the determination of serum calcium. Quad. sclavo Diagn. Clin. Lab. **17**, 182–197 (1981).
7. Connerty, H. V., Briggs, A. R.: Determination of serum calcium by means of 0-cresolpthalein complexone. Am. J. Chin. Pathol. **45**, 290–296 (1966).
8. Fraser, D., Jones, G., Kooh, S. W., Raddel, C.: In: Textbook of clinical chemistry (Tietz NW ed). Philadelphia: Saunders, 1321–1351 (1986).
9. Goslin, P.: Analytical reviews in clinical biochemistry: Calcium measurement. Ann. clin. Biochem. **23**, 146–156 (1986).
10. Lorentz, K.: Improved determination a serum calcium with 2-cresolphtalein complexone. Clin. Chim. Acta **126**, 327–334 (1982).
11. Morano, I., Isac, M., Blentz, C., Wojciechowski, R., Ruegg, J. C.: Perhexiline increases calcium-activated force in skinned psoas fibres by raising calcium affinity of troponin-C. Biomed. Biochim. Acta **48**, 5/6, 5329–5334 (1989).
12. Morkin, B., LaRaia, P. J.: Excitation contraction coupling of muscles. New England Journal of Medicine **290**, 445–450 (1974).
13. Potts, J. T. Jr., Deftos, L. J.: Parathyroid hormone, calcitonin, vitamin D, bone and bone mineral metabolism. In: Duncan's Diseases of Metabolism Endocrinology. 7th ed In ed. P. K. Bondy and
    L. E. Rosenberg. W. B. B. Saunders, Philadelphia 1974, p. 1225.
14. Price, C. P., Spencer, K.: Multiple wavelength spectrophotometry and the centrifugal analyses. In: Centrifugal Analysers in Clinical Chemistry. New York: Praeger. pp. 213–229 (1980).
15. Ruegg, J. C.: Calcium: Muscle Contraction. A comparative approach. J. C. Ruegg ed. Springer–Verlag, Berlin–Heidelberg 1986, pp. 201–231.
16. Smale, T. A.: A modified cresolphtalein complexone method for manual calcium estimation. NZJ Med. Lab. Technol. **35**, 72–75 (1981).

*Acta Physiologica Hungarica, Volume 81 (1), pp. 101–108 (1993)*

# LOW CONCENTRATION OF TRITON X-100 INHIBITS DIACYLGLYCEROL ACYLTRANSFERASE WITHOUT MEASURABLE EFFECT ON PHOSPHATIDATE PHOSPHOHYDROLASE IN THE HUMAN PRIMORDIAL PLACENTA

G. GIMES, M. TÓTH*

2ND DEPARTMENT OF OBSTETRICS AND GYNECOLOGY AND
*1ST INSTITUTE OF BIOCHEMISTRY, SEMMELWEIS MEDICAL UNIVERSITY, BUDAPEST, HUNGARY

Received September 1, 1992
Accepted October 4, 1992

Agents causing accumulation of endogenous diacylglycerols (DAG) may be helpful in studies on the intracellular regulatory effects and on the mechanisms of attenuation of this putative second messenger. In a previous study (Tóth et al., BBA 921 (1987) 417–425) we have shown a marked stimulatory effect of low micellar concentration (0.05%, v/v) of Triton X-100 on the labelling of phosphatidic acid with ($^{32}$P)phosphate in minced human primordial placenta. The present results demonstrate that 0.05% Triton X-100 inhibits nearly completely the conversion of ($^{3}$H)diacylglycerols into ($^{3}$H)triacylglycerols in placenta fragments incubated with ($^{3}$H)glucose. However, this concentration of the detergent does not have any effect on the appearance of label in the sum of acylglycerols (comprising mono-, di- and triacylglycerols) and phosphatidylcholine, indicating a lack of effect on phosphatidate phosphohydrolase. The about 5-fold elevation of ($^{3}$H)diacylglycerols was attended by an approximately 3-fold rise in ($^{3}$H)phosphatidic acid and a 1.3-fold increase in the labelling of phosphatidylcholine. These findings provide supportive evidence that 1,2-DAG was formed due to inhibition of DAG-acyltransferase and suggest that some of the DAG was transformed into phosphatidic acid by diacylglycerol-kinase.

**Keywords:** diacylglycerol, diacylglycerol acyltransferase, Triton X-100, diacylglycerol kinase, primordial placenta (human)

In a previous paper [15] we have reported that a low micellar concentration (0.05%, v/v) of the nonionic detergent, Triton X-100 increases 4-6-fold the amount of ($^{32}$P)phosphatidic acid in minced human primordial placenta (chorion frondosum) incubated *in vitro* with ($^{32}$P)phosphate (($^{32}$P)$P_i$). This response could not be demonstrated by submicellar concentrations of Triton and was attended by a marked decrease in the labelling of phosphatidylcholine. Several findings have suggested that

Correspondence should be addressed to
Miklós TÓTH
Semmelweis Medical University, 1st Institute of Biochemistry
H–1088 Budapest, Puskin u. 9, Hungary

*Akadémiai Kiadó, Budapest*

Triton induces an accumulation of 1,2-diacylglycerols and diacylglycerol kinase activity may be involved in the abrupt rise of phosphatidic acid, but the origin of diacylglycerol serving as substrate for diacylglycerol kinase remained uncertain.

There are at least two aspects that make the elucidation of the source of diacylglycerols mobilized by Triton interesting. First, it is now widely held that diacylglycerols may be important signal molecules involved in the regulation of cellular proliferation and tissue growth [2, 6, 9, 10–13]. The primordial human placenta obtained from 2–3 month old pregnancies contains rapidly growing tissues, therefore the pathways of the formation and elimination of diacylglycerols in these tissues deserve attention. The diacylglycerol-mobilizing effect of Triton offers a possibility for the demonstration that diacylglycerol kinase plays "an attenuating role" when it eliminates elevated concentrations of endogenous diacylglycerols [1–3, 8]. Second, in rat lung microsomes [16] and adipocytes [17] Triton X-100 was shown to be inhibitory on $Mg^{2+}$-dependent phosphatidate phosphohydrolase, the key enzyme in cellular synthesis of new triacylglycerols and phosphatidylcholine [14, 16]. It seemed intriguing therefore, to test experimentally whether such an inhibitory effect of Triton X-100 applied in 0.05% (v/v) concentration contributes or not to the accumulation of phosphatidic acid in the placenta.

## Materials and methods

*Radioactive isotope*

(2-$^3$H)glucose (20 Ci/mmol) was obtained from Amersham International (England).

*Chemicals*

Diolein and monoolein were purchased from Sigma (St. Louis, MO), Silicagel H was from Merck (Darmstadt, Germany). Hepes was from Calbiochem (La Jolla, CA), various phospholipids were from Serva (Heidelberg, Germany). Triolein, Triton X-100, oleic acid and other chemicals were from Reanal (Budapest).

*Tissues*

Primordial placenta fragments were collected during legal instrumental interruptions of normal, 8–10 weeks-old pregnancies at the 2nd Department of Obstetrics and Gynecology, Semmelweis University of Medicine, Budapest. The tissue was rinsed and then suspended in ice-cold 0.9% NaCl, 40 mM Hepes-Na (pH 7.4), 1 mg/ml glucose solution and transported promptly to the site of experiment.

*Incubation and lipid extraction*

Tissue fragments were rinsed several times with 0.9% NaCl, minced with a pair of scissors and incubated in 2 ml Hanks medium containing no glucose added. The Hanks medium was buffered with 40 mM Hepes-Na (pH 7.4). Incubations were initiated by adding the label (10 μCi ($^3$H)glucose). Where

indicated, Triton X-100 (dissolved in 100 μl 0.9% NaCl) was added at 30 min of the incubation to give a final concentration of 0.05% (v/v). Control solutions were given the solvent at the same time. Incubations were carried out in open vials shaken continuously in a 37 °C water bath for 60 min. During this period the rate of incorporation of label from ($^3$H)glucose into various neutral and phospholipids was linear with time. Incubations were terminated and lipids extracted as reported [15]. Lipid extraction occurred according to a modified method [15] of Bligh and Dyer [4]. Extracted lipids were dissolved in 5.0 ml chloroform/methanol (1:1, v/v) and 0.5 ml portions were taken to determine the total extracted radioactivity. Following evaporation of the solvent, lipids were dissolved in 200 μl chloroform/methanol (2:1, v/v) and aliquots of this were used for TLC analysis.

*Radio-TLC of neutral and phospholipids*

For separation Silicagel-H thin layers and various solvent systems were used. For separation of neutral lipids petroleum ether or n-hexane/diethylether/acetic acid (70:30:1) solvent system [7] was employed. This gave a better separation of 1,3-diacylglycerols, 1,2-diacylglycerols and monoacylglycerols than the system we used earlier [15]. Separation of phosphatidic acid was achieved with chloroform/pyridine/formic acid (100:60:14) solvent system [15]. This system was also useful to determine the labelling of the acylglycerol fraction (containing mono-, di- and triacylglycerols). For separation of phosphatidylcholine, phosphatidylinositol and phosphatidylethanolamine chloroform/methanol/acetic acid/water (100:50:14:6) solvent mixture was used [15]. All of the above proportions are given in v/v.

Lipids, carrier and marker compounds were visualized by iodine vapor. Gel portions were scraped off into counting "mini" vials and after adding 2 ml scintillation solution [15] the radioactivity was counted using a Beckman LS 7800 liquid scintillation spectrometer.

*Calculation of results*

Following TLC run total cpm attached to the gel along the path of migration was determined. Using this figure then the percentage distribution of radioactivity among the various separated lipids could be calculated. Finally, from the percentage value and the total extracted cpm, the cpm value present in a particular lipid was computed. For the determination of the percentage distribution of cpm among acylglycerols, the site of application of the sample on the gel used for separation of neutral lipids (i.e. the origin which contained all of the phospholipids) was omitted from the calculation and the total amount of cpm present in acylglycerols was taken from the TLC for phosphatidic acid separation (see above). Determinations were carried out in triplicates and the experiment was repeated twice. In order to calculate the effect of a treatment relative to control, mean value of control incubations was taken as a unit and the average cpm value obtained with test incubations was divided by this unit.

## Results

When tissue mince was incubated with 5 μCi/ml ($^3$H)glucose for 60 min, Triton X-100 added in 0.05% (v/v) final concentration at 30 min of incubation inhibited the synthesis of triacylglycerols with a concomitant elevation in the rate of formation of diacylglycerol and phosphatidic acid (Figs 1 and 2). As a rule the response in phosphatidic acid was smaller than in 1,2-diacylglycerols and the gain of radioactivity recovered in 1,2-diacylglycerols roughly equalled the loss of radioactivity from triacylglycerols. Further analysis of the conversion of label from ($^3$H)glucose into various phospholipids (Fig. 2) revealed slight increases in the labelling of

phosphatidylinositol and phosphatidylcholine. Phosphatidylethanolamine was not found to contain appreciable amount of label. It is noteworthy, that Triton did not reduce the sum of labels present in acylglycerols + phosphatidylcholine below the control value (Table I), indicating that phosphatidate phosphohydrolase was not inhibited by the detergent.

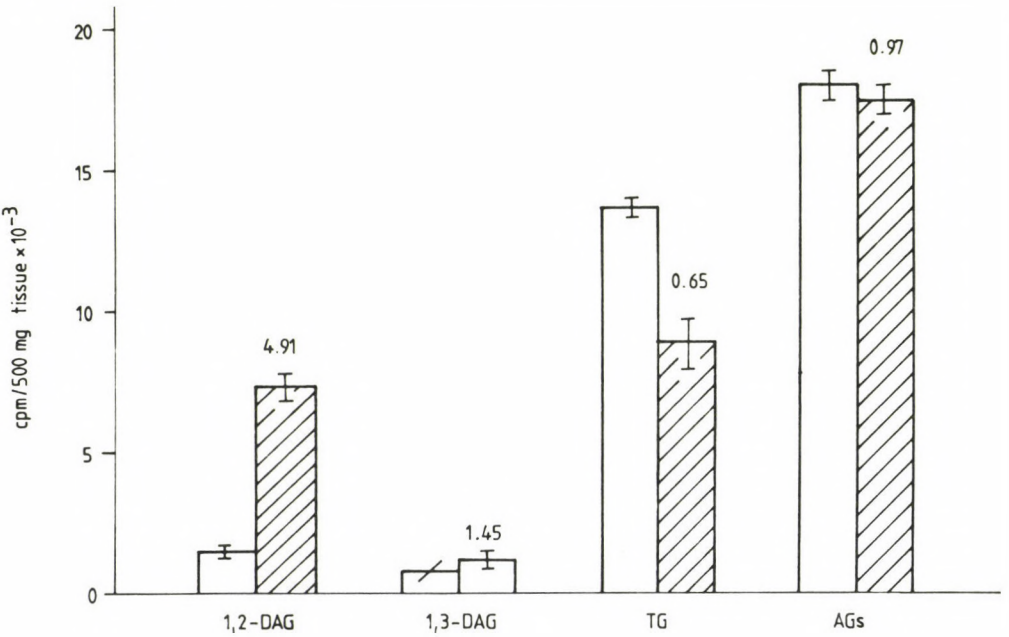


*Fig. 1.* Effect of Triton X-100 on rate of conversion of ($^3$H)glucose into various acylglycerols of the primordial placenta. Tissue mince (500 mg) was incubated in 2 ml Hanks medium (prepared without glucose) with 10 μCi ($^3$H)glucose at 37 °C for 60 min in open vials shaken continuously. Triton X-100 (final conc.: 0.05%, v/v) was added at 30 min of incubation. Control incubates received the solvent (0.1 ml 0.9% NaCl) at the same time. Following extraction and separation of lipids, radioactivity associated with the various lipids was counted. Mean values ± SE (n=3) are presented from three experiments with triplicate incubations each. Open bars: controls, hatched bars: incubations with Triton, numbers above the hatched bars: effect of Triton relative to the control. DAG = diacylglycerols, TG = triacylglycerols, AGs = acylglycerols (i.e. sum of radioactivites present in mono-, di- and triacylglycerols)

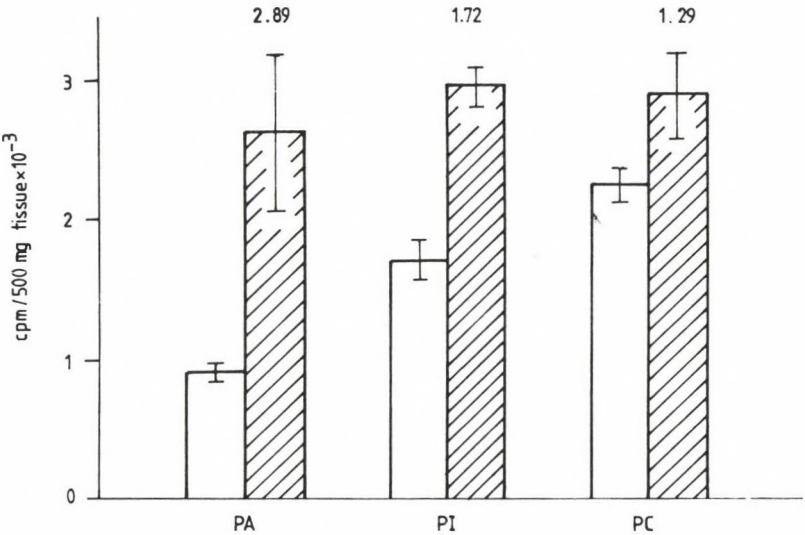


*Fig. 2.* Effect of Triton X-100 on the rate of conversion of ($^3$H)glucose into phosphatidic acid (PA), phosphatidylinositol (PI) and phosphatidylcholine (PC) of the primordial placenta. Tissue mince was incubated as outlined in the legend to Fig. 1. Open bars = controls, hatched bars = incubations with Triton, numbers above the hatched bars = effect of Triton relative to control

**Table I**

*Effect of Triton X-100 on the labelling of acylglycerols (AGs) plus phosphatidylcholine (PC) in the presence and absence of Triton X-100*

| | cpm/500 mg tissue ± SE | | |
|---|---|---|---|
| | control (C) | +Triton X-100 (T) | T/C |
| AGs + PC | 20287 ± 609 | 20400 ± 406 | 1.01 |

Data were taken from the experiments in Figs 1 and 2. Mean values ± SE (n=3) are presented from 3 experiments with triplicate incubations each

## Discussion

The results presented here provide supportive evidence that a low micellar concentration of Triton X-100 promotes the accumulation of diacylglycerols synthesized from glucose, that is via the de novo synthetic pathway of triacylglycerols and phospholipids (Fig. 3). The increase of labelled diacylglycerol was attended by a nearly equivalent reduction of triacylglycerols indicating that Triton – even in the

low concentration applied in this study – inhibits efficiently the activity of DAG-acyltransferase in this human tissue. The about 5-fold increase in the labelling of 1,2-DAG was accompanied by an almost 3-fold enhancement in the labelling of phosphatidic acid. Since accumulation of phosphatidate cannot be ascribed to an inhibition of phosphatidate phosphohydrolase activity, it is reasonable to assume that phosphatidate was synthesized from accumulating diacylglycerols acted upon by diacylglycerol kinase. Considering the precursor-product relationship between phosphatidic acid and phosphatidylinositol, the enhanced rate of synthesis of phosphatidylinositol is not surprising. On the other hand, the small but definite increase of label in phosphatidylcholine is contradictory to our previous finding with ($^{32}$P)phosphate, which was shown to be incorporated scarcely into phosphatidylcholine in the presence of Triton X-100 [15]. Assuming the increase of the specific radioactivity of DAG, it is plausible to believe that the slight increase in the rate of labelling of phosphatidylcholine is an apparent effect, reflecting an increased labelling rather than an enhanced rate of synthesis of phosphatidylcholine.

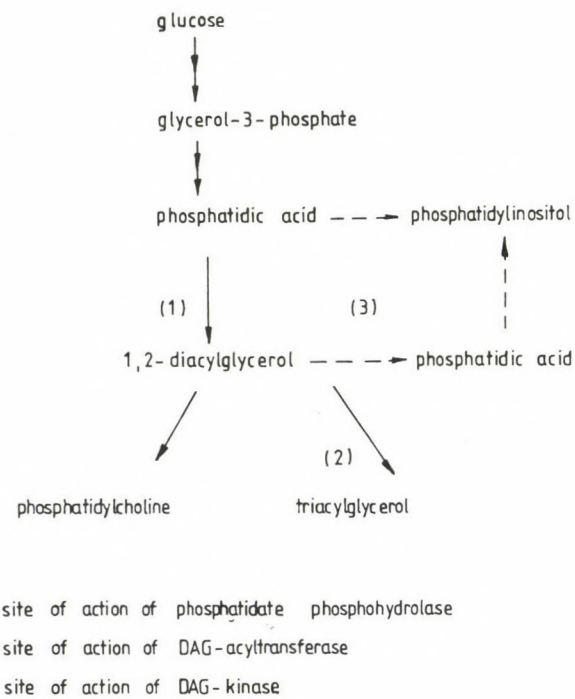


*Fig. 3.* Pathways of biosynthesis of neutral and phospholipids from glucose [14]

The primordial placenta is unique in the sense that it is composed of rapidly growing tissues. Our previous [15] and present results indicate a characteristic response to low micellar concentration of Triton in these tissues: the accumulation of phosphatidic acid.

The present findings suggest that inhibition of the activity of diacylglycerol acyltransferase may primarily be involved in this effect whereas the contribution of a diminished activity of phosphatidate phosphohydrolase seems improbable. Apparently, chorionic tissues respond to Triton X-100 differently as compared to rat lung [16] and adipose tissue [17], where inhibition of phosphatidate phosphohydrolase dominates. It is of interest that in rat hepatocytes cationic amphiphiles (like chlorpromazine) inhibit about 10-fold more efficiently the activity of phosphatidate phosphohydrolase than that of diacylglycerol acyltransferase [5]. Whether stimulated breakdown of some phospholipids present in cell membranes of primordial placenta contributes or not to the Triton-stimulated labelling of phosphatidic acid with ($^{32}$P)phosphate remains to be elucidated. Nevertheless the present results provide evidence of a Triton-provoked diacylglycerol accumulation taking place at the expense of triacylglycerol synthesis in the primordial placenta. This effect of Triton offers a method matching the microinjection of diacylglycerols [13] into trophoblastic cells and could perhaps be utilized for the study of activation of protein kinase C as well as the metabolism of diacylglycerols in the rapidly growing chorionic tissue.

**Acknowledgements**

The authors are grateful to Irene Szabó and Eszter Bérczi for the conscientious and expert technical assistance.

## REFERENCE

1. Bishop, W. R., Bell, R. M.: Attenuation of sn-1,2-diacylglycerol second messengers. J. Biol. Chem., **261**, 12513–12519 (1986).
2. Bishop, W. R., Bell, R. M.: Functions of diacyglycerol in glycerolipid metabolism, signal transduction and cellular transformation. Oncogene Research **2**, 205–218 (1988).
3. Bishop, W. R., Ganong, B. R., Bell, R. M.: Attenuation of sn-1,2-diacyglycerol second messengers by diacylglycerol kinase. J. Biol. Chem. **261**, 6993–7000 (1986).
4. Bligh, E. G., Dyer, W. J.: A rapid method of total lipid extraction and purification. Can. J. Biochem. Physiol. **37**, 911–917 (1959).
5. Brindley, D. N., Bowley, M.: Drugs affecting the synthesis of glycerides and phospholipids in rat liver. Biochem. J. **148**, 461–469 (1975).
6. Exton, J. H.: Signaling through phosphatidylcholine breakdown. J. Biol. Chem. **265**, 1–4 (1990).
7. Kates, M.: Techniques of lipidology. Isolation, analysis and identification of lipids. Elsevier Biomedical Press, Amsterdam, 1986, p. 327.

8. Kato, M., Kawai, S., Takenawa, T.: Defect in phorbol acetate-induced translocation of diacylglycerol kinase in erb 8-transformed fibroblast cells. FEBS Letters, **247**, 247–250 (1989).
9. Lacal, J. C., Moscat, J., Aaronson, S. A.: Novel source of 1,2-diacylglycerol elevated in cells transformed by Ha-ras oncogene. Nature **330**, 269–272 (1987).
10. Nishizuka, Y.: The role of protein kinase C in cell surface signal transduction and tumor promotion. Nature **308**, 693–698 (1984).
11. Plevin, R., Cook, S. J., Palmer, S., Wakelam, M. J. O.: Multiple sources of sn-1,2-diacylglycerol in platelet-derived-growth-factor-stimulated Swiss 3T3 fibroblasts. Biochem. J. **279**, 559–565 (1991).
12. Rozengurt, E.: Early signals in the mitogenic response. Science **234**, 161–166 (1986).
13. Suzuki-Sekimori, R., Matuoka, K., Nagai, Y., Takenawa, T.: Diacylglycerol, but not inositol 1,4,5-trisphosphate, accounts for platelet-derived growth factor-stimulated proliferation of BALB 3T3 cells. J. Cellular Physiology **140**, 432–438 (1989).
14. Tijburg, L. B. M., Geelen, M. J. H., van Golde, L. M. G.: Regulation of the biosynthesis of triacylglycerol, phosphatidylcholine and phosphatidylethanolamine in the liver. Biochim. Biophys. Acta **1004**, 1–19 (1989).
15. Tóth, M., Gimes, G., Hertelendy, F.: Triton X-100 promotes the accumulation of phosphatidic acid and inhibits the synthesis of phosphatidylcholine in human decidua and chorion frondosum tissues in vitro. Biochim. Biophys. Acta **921**, 417–425 (1987).
16. Walton, P. A., Possmayer, F.: The effects of Triton X-100 and chlorpromazine on the $Mg^{2+}$-dependent and $Mg^{2+}$-independent phosphatidate phosphohydrolase activities of rat lung. Biochem. J. **261**, 673–678 (1989).
17. Wells, G. N., Osborne, L. J., Jamdar, S. C.: Isolation and characterization of multiple forms of $Mg^{2+}$-dependent phosphatidate phosphohydrolase from rat adipose cytosol. Biochim. Biophys. Acta **878**, 225–237 (1986).

# INSTRUCTIONS TO AUTHORS

*Form of manuscript*

Two complete copies of the manuscript including all tables and illustrations should be submitted. Manuscripts should be typed double-spaced with margins at least 3 cm wide. Pages should be numbered consecutively.

Manuscripts should include the title, authors' names and short postal address of the institution where the work was done.

An abstract of not more than 200 words should be supplied typed before the text of the paper. The abstract should be followed by (no more than) five key-words.

*Abbreviations* should be spelled out when first used in the text. *Drugs* should be referred to by their WHO code designation (Recommended International Nonproprietary Name): the use of proprietary names is unacceptable. The *International System of Units* (SI) should be used for all measurements.

*References*

References should be numbered in alphabetical order and only the numbers should appear in the text [in brackets]. The list of references should contain the name and initials of all authors (the use of et al. instead of authors' name in the reference list is not accepted): for journal articles the title of the paper, title of the journal abbreviated according to the style used in Index Medicus, volume number, first and last page number and year of publication, for books the title followed by the publisher and place of publication.

Examples:

Székely, M., Szelényi, Z.: Endotoxin fever in the rat. Acta physiol. hung. **53,** 265–277 (1979).

Schmidt, R. F.: Fundamentals of Sensory Physiology. Springer Verlag, New York–Heidelberg–Berlin 1978.

Dettler, J. C.: Biochemical variation. In: Textbook of Human Genetics, eds Fraser, O., Mayo, O., Blackwell Scientific Publications, Oxford 1975, p. 115.

*Tables and illustrations*

Tables should be comprehensible to the reader without reference to the text. The headings should be typed above the table.

Figures should be identified by number and authors' name. The top should be indicated on the back. Their approximate place should be indicated in the text. Captions should be provided on a separate page.

*Proofs and reprints*

Reprints and proofs will be sent to the first author unless otherwise indicated. Proofs should be returned within 48 hours of receipt. Fifty reprints of each paper will be supplied free of charge.

# Acta Physiologica Hungarica

VOLUME 81, NUMBER 2, 1993




Akadémiai Kiadó, Budapest

ACTA PHYSIOL. HUNG. APHDUZ. 81 (2) 109–218 (1993) HU ISSN 0231—424X

# ACTA PHYSIOLOGICA HUNGARICA

## A PERIODICAL OF THE HUNGARIAN ACADEMY OF SCIENCES

*Acta Physiologica Hungarica* publishes original reports of studies in English.
*Acta Physiologica Hungarica* is published in one volume (4 issues) per year by

AKADÉMIAI KIADÓ

Publishing House of the Hungarian Academy of Sciences

H-1117 Budapest, Prielle Kornélia u. 19—35.

Manuscripts and editorial correspondence should be addressed to

*Acta Physiologica Hungarica*

H-1445 Budapest, P.O. Box 294, Hungary

Editor: P. Bálint

Managing editor: J. Bartha

*Subscription information*

Orders should be addressed to

AKADÉMIAI KIADÓ

H-1519 Budapest, P.O. Box 245

Subscription price for Volume 81 (1993) in 4 issues US$ 92.00, including normal postage, airmail delivery US$ 20.00.

*Acta Physiologica Hungarica* is abstracted/indexed in Biological Abstracts, Chemical Abstracts, Chemie-Information, Current Contents-Life Sciences, Excerpta Medica database (EMBASE), Index Medicus, International Abstracts of Biological Sciences

CONTENTS

PRINTED IN HUNGARY
Akadémiai Kiadó és Nyomda Vállalat, Budapest

*Acta Physiologica Hungarica, Volume 81 (2), pp. 109–110 (1993)*

# FOREWORD

The present special issue of our Journal Acta Physiologica Hungarica is dedicated to the 25th anniversary of the Department of Comparative Physiology of the Attila József University of Szeged. Quarter of Century seems to be a rather short period of time in the history of European higher Education, taking into account the long-long history of the well-known medieval Universities – Bologne, Paris, Vienna, Prague – or even that of the oldest Hungarian University founded in 1367 in Pécs by Louis the Great of Hungary. However in the history of the Szeged University, which did not reach even its hundredth anniversary, these twenty five years represent a respectful phase worth of commemoration.

The foundation of this Department has fulfilled an urgent need in the sixties, since the Szeged University, similarly to other non-medical Universities in Hungary, has inherited an incomplete structure from the pre-war period, biology being represented merely by the so-called "traditional" disciplines like Botany, Zoology, or Animal Morphology. The initiation came from "above", namely the Biological Section of the Hungarian Academy of Sciences has urged the modernization of Biology Curriculum of all three non-medical Universities, namely Budapest, Debrecen and Szeged. Budapest has been the first: several new Departments have been founded in the late fifties and in the sixties. Comparative Physiology among others. The Department of Comparative Physiology of Szeged followed closely the establishment of the sister institution of the Capital.

Personally I happened to be fortunate enough to witness the first steps of organizing, since our first difficulties, worries and successes have been the same! The invitation of my good friend Dr. Ottó Fehér, then associate professor in Debrecen, to organize and to chair the new Department was really an excellent idea.

Professor Fehér has a rich and honorable scientific personal history. Member of a rather restricted generation of Hungarian after-war graduated Physiologists, he displayed early his theoretical and technical motivations and skills. No wonder that the Search Committee of the Szeged University had discovered just him in Debrecen! Dr. Fehér was one of the most gifted pupils of the late István Went, who has founded a powerful and at that time influential physiological school in Debrecen. This serious, all-round educated and dedicated scholar had and still has the talent and the power to attract young scientists to join him. No marvel that by now the Szeged Department has developed into an internationally recognized community of active and creative Neurophysiologists.

*Akadémiai Kiadó, Budapest*

The specificity of this powerful team (under the leadership of Lajos Erdélyi now) can be formulated as follows: it is a typical "interface" community on the borderline of neurochemistry and classical neuronal electrophysiology, being prominent in the sophisticated neuronal analysis of delicate brain processes. The nine papers presented in this volume reflect (unfortunately only partly) this complexity of approaches. I would be more satisfied if some additional papers would cover such important contributions of the Szeged team like neuronal analysis of learning phenomena, experimental epilepsy, etc. But the reader of the present special issue will be able even reading only these 9 studies to construct a very positive and evocative picture about this sympathetic and erudite community celebrating its jubilee. Much success dear colleagues and friends!

Professor György Ádám, MD, D. Sc.
Eötvös Loránd University, Budapest

*Acta Physiologica Hungarica, Volume 81 (2), pp. 111–120 (1993)*

# ZINC BLOCKS THE A-TYPE POTASSIUM CURRENTS IN *HELIX* NEURONS

L. ERDÉLYI

DEPARTMENT OF COMPARATIVE PHYSIOLOGY, JÓZSEF ATTILA UNIVERSITY, SZEGED, HUNGARY

Received May 4, 1992
Accepted May 13, 1992

The effects of $Zn^{++}$ on the A-current in neurons of *Helix pomatia L.* were examined using the current- and voltage-clamp technique. $I_A$ was significantly depressed by zinc (Kd = 1.8 mM at −30 mV, $n_H$ = 0.6) applied in the perfusate. This depressive effect resulted in a depolarizing shift of the activation curve, associated with reduction of the maximum conductance. $Zn^{++}$ also caused a depolarizing shift of the steady-state inactivation curve. A dose-response curve for the depolarizing shift of the activation and inactivation curves of $I_A$, as a function of $Zn^{++}$ concentration, could be fitted by a single binding-site model with an apparent dissociation constant of approximately 1.8 mM. The modulatory action of $Zn^{++}$ on the A-currents was potential-dependent, being more effective near the resting membrane potential, and decreased with depolarization. In contrast to its effect on $I_A$, zinc caused a slight change in the delayed rectifier K-current but evoked an appreciable attenuation of the leak potassium conductance (Kd = 1.9 mM, $n_H$ = 1.1). Zinc suppressed the Ca-currents, too. Addition of zinc caused an increase in the time-to-peak and prolonged the decay time constant of the A-currents in a dose-dependent way (Kd = 1.7 mM, $n_H$ = 1.4).

In close correlation with the voltage-clamp experiments, $Zn^{++}$ depolarized the studied neurons, prolonged the action potential duration, suppressed the spike amplitude and increased the firing rate.

The results show that $Zn^{++}$ can evoke a depolarizing shift of both the activation and inactivation fates controlling $I_A$.

This modulatory effect of $Zn^{++}$ on gating of $I_A$ appears to reflect binding to a specific, saturable site.

**Keywords:** zinc, fast outward current, snail neurons, voltage-clamp

Various metal ions interfere with membrane functions that are normally regulated by $Ca^{++}$. Some metal ions are known to permeate through voltage-dependent $Ca^{++}$ channels, whereas others block $Ca^{++}$ currents and are widely used

Correspondence should be addressed to
L. ERDÉLYI
Department of Comparative Physiology, József Attila University
H-6726 Szeged, Középfasor 52, Hungary

*Akadémiai Kiadó, Budapest*

as inorganic $Ca^{++}$ antagonists [8]. Among divalent cations, $Zn^{++}$ is reported as a potent blocker of the voltage-activated $Ca^{++}$ channel in *Aplysia* neurons [2], the large conductance calcium activated potassium, and the transient outward currents in rat sympathetic neurons [3] and isolated ventricular myocytes [1]. In squid axon, $Zn^{++}$ alters the kinetics of sodium and potassium currents [6, 7]. Kawa (1979) and Oyama et al. (1982) have reported that $Zn^{++}$ can carry charges through the membrane $Ca^{++}$ channels in molluscan neurons and may support action potentials. $Zn^{++}$ is also known to block N-methyl-D-aspartate and GABA mediated responses in mammalian neurons [15, 18, 21].

The fast outward potassium currents have been studied in Helix neuron preparations [12, 13, 20]. Recently, it has been assumed, that the molluscan fast outward potassium channel is identical to members of the *Drosophila* Shaker $K^+$ channel family [16].

The effects of $Zn^{++}$ on resting membrane potential, action potential and membrane ionic currents have been investigated with the aid of current- and voltage-clamp methods.

The results suggest that $Zn^{++}$ markedly modulates the A-currents in *Helix* neurons but its action is not specific because leak current and $Ca^{++}$ currents are also modified in the same neurons.

## Materials and Methods

The ganglionic mass of the land snail *Helix pomatia* L. was dissected and incubated in physiological saline containing 80 mM NaCl, 4 mM KCl, 7 mM $CaCl_2$, 8 mM $MgCl_2$, and 5 mM Tris-HCl at pH 7.4.

After 10–15 min, the ganglionic mass was pinned to a Sylgard-coated chamber (about 5 ml volume) and desheathed with a small piece of razor blade and fine scissors to expose the neuronal cell bodies. The ganglionic preparation was equilibrated for 10–15 min before penetrating neurons. Cells were identified by soma location, action potential pattern and response to nerve stimulation.

The neurons were impaled with a low-resistance microelectrode (about 2 MOhm) and dialyzed with an intracellular saline containing 80 mM KCl, 0.02 mM $CaCl_2$, 1 mM EGTA, 20 mM Tris-HCl, at pH = 7.2. The cells were voltage-clamped using a home-built sample-and-hold amplifier connected with a Labmaster DMA and an IBM 286 computer equipped with Tl-l-125 interface (Axon Instruments, Inc.) and acquisition software. The data were printed out on a Hewlett Packard Desk Jet 500 printer or photographed from the screen of a Hitachi VC-6025 digital storage oscilloscope.

A-currents were isolated under spike threshold voltages in physiological saline or Na-free media by use of the conditioning hyperpolarization protocol.

$ZnCl_2$ was freshly dissolved in the extracellular solutions and applied in the perfusate. The experiments were made at room temperature (22–24 °C).

## Results

### *$Zn^{++}$ induced actions on the A-type potassium currents*

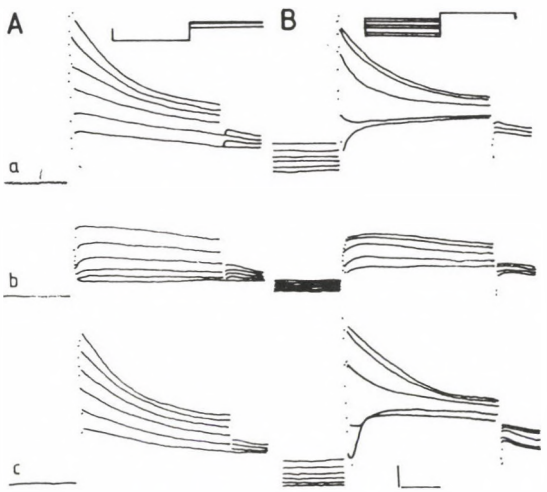


*Fig. 1.* Activation (A) and inactivation (B) of the A-type potassium currents recorded in Na-free (TRIS) solution (a), in 3 mM $Zn^{++}$ containing medium (b) and after 25 min washing (c). For $I_A$ activation voltage steps from −50 mV to 0 mV were applied following pre-pulses of 500 ms duration to −100 mV. For $I_A$ inactivation voltage was stepped to −10 mV following a series of pre-pulse potentials (−50 to −100 mV). Calibrations: 100 ms, 30 nA (A) and 20 nA (B)

As it can be seen in Figure 1, $Zn^{++}$ suppressed the peak amplitude of the A-currents, increased the time-to-peak and decreased the rate of inactivation. These actions of $Zn^{++}$ on the fast outward currents were similar when activation (A) and inactivation (B) protocols were studied. For $I_A$ activation voltage steps from −50mV to 0 mV were applied following pre-pulses of 500 ms duration to −100mV. For $I_A$ inactivation voltage was stepped to −10 mV following a series of pre-pulse potentials from −50 mV to −100 mV. As seen in Figure 1B, $Zn^{++}$ modulated the A-currents, by decreasing simultaneously the leak conductance and an inward Ca-current component of the studied neuron.

*$Zn^{++}$ actions on the voltage dependence and steady-state activation and inactivation of the A-currents*

Figure 2 shows the voltage dependence of activation and inactivation of the A-currents recorded in Na-free (TRIS) solution under control conditions and in the presence of 1.5 mM $Zn^{++}$ in the 10th min of application.

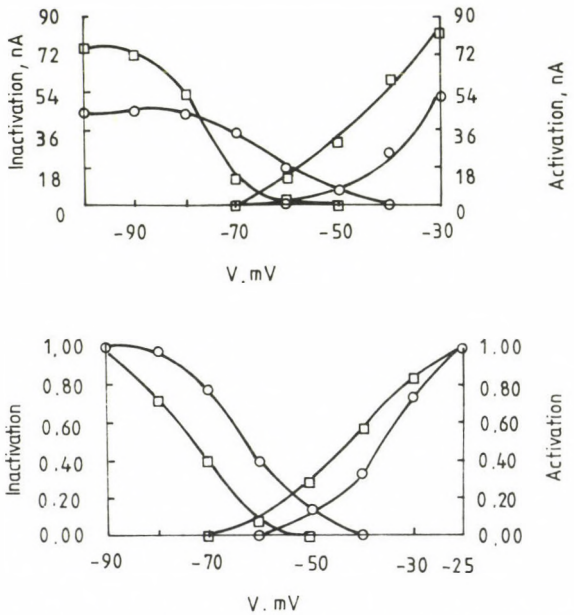


*Fig. 2.* $Zn^{++}$ causes a positive shift of the voltage dependence of activation and inactivation of the A-currents recorded in Na-free (TRIS) medium (open squares) and 1.5 mM $Zn^{++}$ containing solution (open circles)

Both current records and normalized curves show shifts of the voltage dependence of activation and inactivation of the A-currents towards more positive potential values in the presence of $Zn^{++}$. These actions of $Zn^{++}$ on the potential dependence of both activation and inactivation gates controlling $I_A$ were dose-dependent between 0.5 and 5 mM $Zn^{++}$ in the extracellular solution.

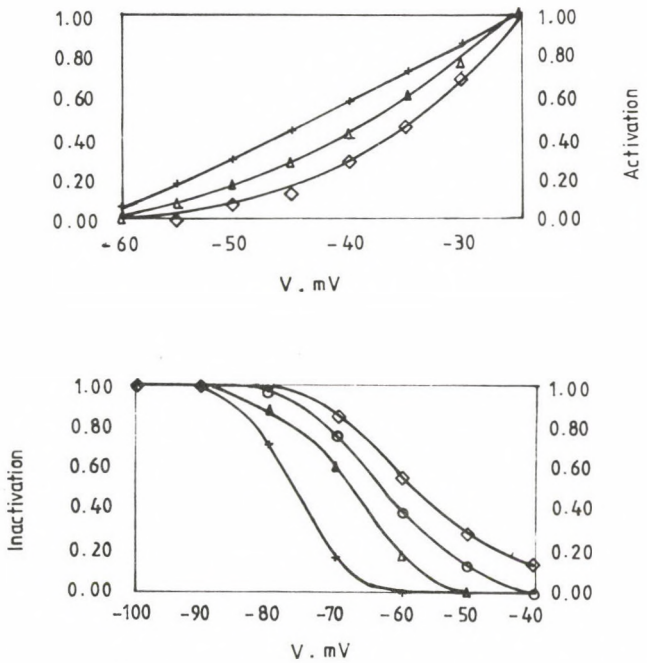


*Fig. 3.* $Zn^{++}$ causes a dose-dependent shift of the steady-state activation and inactivation curves for $I_A$. Crosses are control values. Values are recorded for 0.74 mM (open triangles), 1.5 mM (open circles) and 3 mM $Zn^{++}$ solutions (open squares) respectively

Figure 3 presents a family of curves recorded in Na-free (TRIS) solution 0.74 mM, 1.5 mM and 3 mM $Zn^{++}$ containing media respectively. As can be seen in Fig. 3, a more pronounced action of $Zn^{++}$ on the steady-state inactivation curves of the A-currents was observed. Furthermore, $Zn^{++}$ has a potential-dependent action on the peak amplitude of the studied A-currents. This is shown in Figure 4 A, where relative amplitudes of A-currents vs. $Zn^{++}$ doses are presented at −50mV, −40 mV, −30 mV and −20 mV command potentials. $Zn^{++}$ is more effective on the A-currents which have been activated near the resting membrane potential and the sensitivity sharply decreases with increasing command potentials. The $K_d$ of $Zn^{++}$ is an exponential function of the command potential by which $I_A$ was activated (Fig. 5A). In three different experiments, the $K_d$ of $Zn^{++}$ was 1.8 ± 0.4 (mean ± S. D.) mM at −30 mV membrane potential and the Hill coefficient (nH) was 0.61 ± 0.04 (mean ± S. D.).

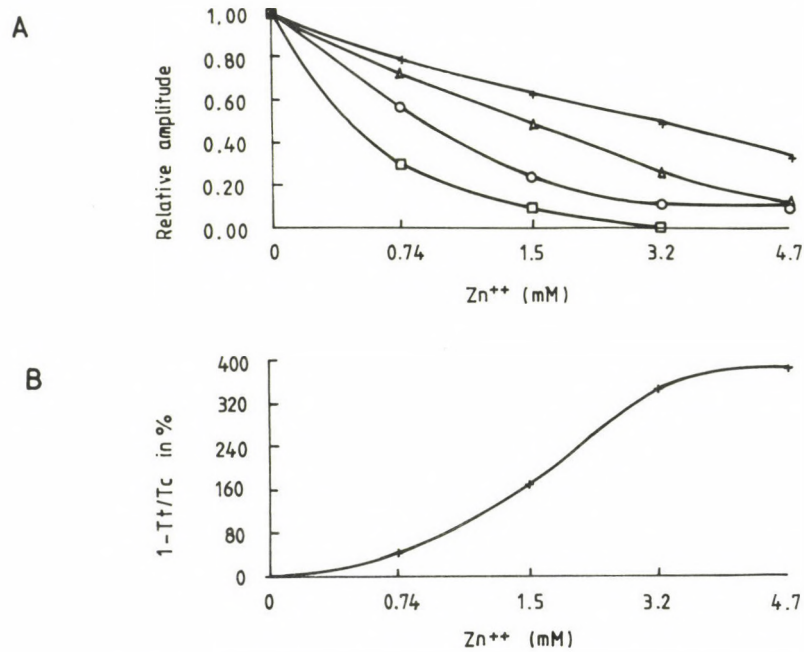


*Fig. 4.* A. Dose-response relationship for $Zn^{++}$ action on the peak amplitude of the A-currents activated at −50 mV (open squares), −40 mV (open circles), −30 mV (open triangles) and −20 mV (crosses) step potentials respectively. B. $Zn^{++}$ prolongs the time constant of decay of the A-currents in dose-dependent way

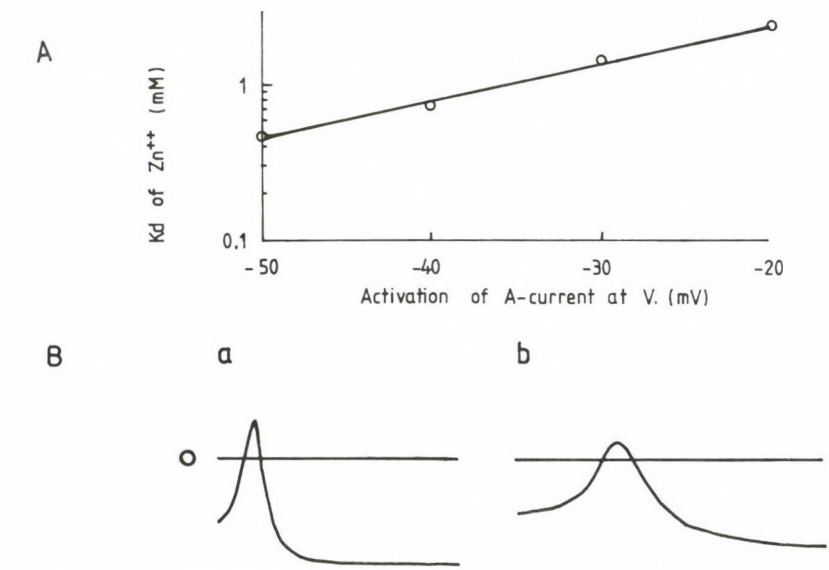


*Fig. 5.* A. The half-blocking dose for $Zn^{++}$ increases exponentially with increasing step depolarization where $I_A$ is activated. B. $Zn^{++}$ (1.5 mM) decreases the resting membrane potential, attenuates the spike amplitude and prolongs the action potential duration in normal solution. Calibration: 20 mV, 2 ms

The action of $Zn^{++}$ on the kinetics of the A-currents is a dose-dependent phenomenon as well. The dose-response relationship of the time constant of decay of the A-currents vs. $Zn^{++}$ dose is shown in Fig. 4B. The $K_d$ of $Zn^{++}$ was 1.7 mM and nH was 1.4 in this case.

*$Zn^{++}$ actions on the resting membrane potential and action potential*

$Zn^{++}$ decreased the resting membrane potential, suppressed the peak amplitude of the spikes and prolonged the action potential duration in current-clamp experiments (Fig. 5B). Additionally, it increased the membrane input resistance in the studied neurons. All these effects are in close correlation with attenuation of the leak conductance and the peak $Ca^{++}$ currents in voltage-clamped neurons.

*$Zn^{++}$ actions on other membrane curves*

Figure 6 shows the actions of 1.5 mM and 3 mM $Zn^{2+}$ on the leak currents which gradually decreased in the $Zn^{++}$-containing solution in comparison with the control Na-free (TRIS) medium. The action of $Zn^{2+}$ on the leak current is a dose-

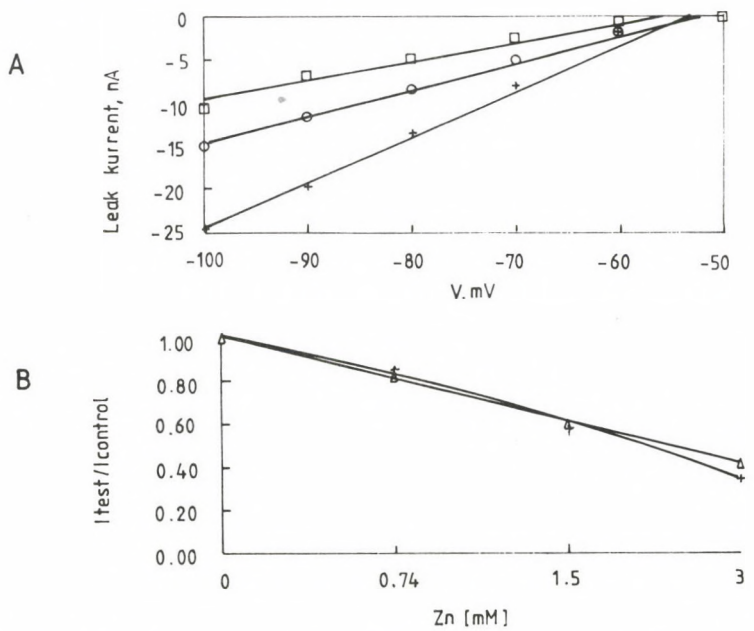


*Fig. 6.* $Zn^{++}$-induced depolarization is in close correlation with a decrease of the leak conductance (A). Leak currents are recorded in Na-free (TRIS) solution (crosses) in the presence of 1.5 mM (open circles) and 3 mM $Zn^{++}$ containing solutions (open squares). B. $Zn^{++}$ decreases the leak conductance in dose-dependent way but the action is not potential dependent. Leak currents are activated at −90 mV (crosses) and −100 mV (open triangles) from −50 mV holding potential

dependent event. Figure 6B shows the dose-response relationship of $Zn^{2+}$ action on the leak currents recorded at −90 mV and −100 mV step potentials from −50 mV holding potential. The $K_d$ of $Zn^{++}$ on the leak currents was 1.9 mV and the Hill coefficient was 1.1.

$Zn^{++}$ slightly attenuated the delayed outward current but it blocked the inward Ca-current (Fig. 7).

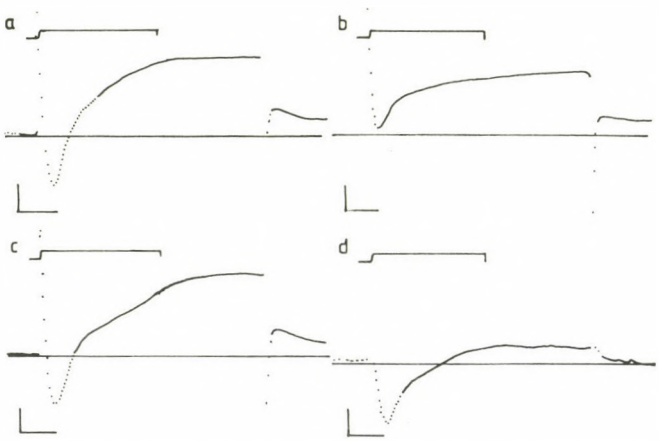


Fig. 7. $Zn^{++}$ attenuates the Ca-current but hardly influences the delayed outward current in Na-free (TRIS) solution. Membrane ionic current is activated by a step potential from −50 mV holding level to −10 mV in control solution (a), in the presence of 3.2 mM $Zn^{++}$ (b) and after 20 min washing (c). Difference of currents (a−b) shows the $Zn^{++}$ attenuated inward and outward current components (d). Calibration: 10 ms and 30 nA

## Discussion

A study of the actions of $Zn^{++}$ on voltage gated membrane ionic currents of identified *Helix* neurons clearly showed an attenuation of the fast outward, leak and Ca currents. The effects of $Zn^{++}$ on Ca currents have already been examined both in Aplysia and Helix neurons and remained out of the interest of this study [2, 10]. However, $Zn^{++}$-induced actions have been analysed both on the fast outward and leak currents.

The amplitudes of the fast outward and leak currents were suppressed by $Zn^{++}$ in dose-dependent manner, with equal sensitivity ($K_d$ = 1.8 mM). However, a potential-dependent suppression of the fast outward and a potential-independent modulation of the leak currents can be mentioned as differential actions for $Zn^{++}$. The Hill coefficient (nH) of the dose-inhibition curves gave different values for the stoichiometry of $Zn^{++}$ binding on or around the fast outward and leak current

channels because they were 0.61 and 1.1 respectively. That is modulation of the A-current channel needs zinc ion cooperativity while suppression of the leak current is a simple 1:1 ratio of $Zn^{++}$ binding to the recognition site. Comparable actions of $Ni^{++}$ and $Ca^{++}$ with $Zn^{++}$ were reported on the amplitude of the fast outward and leak currents in the same identified (LPa, RPa 1–3) neurons earlier [4]. The results together suggest that a common binding site may be involved when A-currents are modulated, however, the affinity of the supposed binding sites varies from cation to cation. Thus, the efficacy is a function of the cation species and the transmembrane potential gradient. The overall sequence of efficacy was as follows:

$$Zn^{++} > Ni^{++} > Ca^{++}.$$

Similar observations were reported with $Zn^{++}$ and other metal ions on the A-currents of cultured rat sympathetic [3] and sensory neurons [11]. Thus, it looks like, that the extracellular binding site for the various cations have common characteristics both in the membrane of rat and Helix neurons. Theoretical binding sites for metal ions in proteins are at the centre of high hydrophobic contrast [22]. This possibility looks like to be real for molluscan A-channel proteins as well [16]. The actions of $Zn^{++}$ on the kinetics of the A-currents suggests another binding site which is different from that where the conductance of the A-channel currents has been modulated. The sensitivity of the two supposed recognition sites is similar but the binding stoichiometries are different. Furthermore, the two targets of actions are pharmacologically distinct on the A-channel in the same identified Helix neurons [5]. Also, the conductance and kinetical mutants of Drosophila Shaker gene represents different protein structures [18]. The action of $Zn^{++}$ on the voltage gated ionic currents of various molluscan neurons and nerves are nonspecific because modulations of Na-, K-, Ca- and H-currents have already been reported [1–3, 6, 7, 10, 19]. However, the most sensitive transmembrane ionic component is the H-current in Helix neurons [10]. These observations suggest that the binding site for $Zn^{++}$ can be a common structure of some channel proteins. The overall actions of $Zn^{++}$ on Helix neurons are excitatory because zinc decreases the leak conductance which causes depolarization of the neuron membranes attenuation of the A-current channel decreases the interspike interval by giving rise to high frequency spike discharges.

## Acknowledgement

I wish to thank Dr. Alan Brafield for his comments on the manuscript. The work was supported by the Hungarian Academy of Sciences, Grant OTKA, 99/6541.

## REFERENCES


1. Agus, Z. S., Dukes, I. D., Morad, M.: Divalent cations modulate transient outward current in isolated rat ventricular myocytes. J. Physiol. Lond. **418**, 28P (1989).
2. Büsselberg, D., Evans, M. L., Rahmann, H., Carpenter, D. O.: Lead and zinc block a voltage-activated calcium channel of *Aplysia* neurons. J. Neurophys. **65**, 786–795 (1991).
3. Constanti, A., Smart, T. G.: Zinc blocks the A-current in cultured rat sympathetic neurones. J. Physiol. Lond. **396**, 159P (1988).
4. Erdélyi, L.: Effects of extracellular Ca and Ca-channel blockers on A-currents in snail brain neurons. Acta Biol. Hung. **38** (3–4), 299–314 (1987).
5. Erdélyi, L.: Effects of hydroxybenzenes on the A-currents in molluscan neurons. Comp. Biochem. Physiol. **96C**, 411–418 (1990).
6. Gilly, W., Armstrong, C. M.: Slowing of sodium channel opening kinetics in squid axon by extracellular zinc. J. Gen. Physiol. **79**, 935–964 (1982).
7. Gilly, W., Armstrong, C. M.: Divalent cations and the activation kinetics of potassium channels in squid giant axons, J. Gen. Physiol. **79**, 965–996 (1982).
8. Hagiwara, S., Byerly, L.: Calcium channel. Annu. Rev. Neurosci. **4**, 69–125 (1981).
9. Kawa, K.: Zinc-dependent action potentials in giant neurons of the snail, *Euhadra quaestia*. J. Membr. Biol. **49**, 325–344 (1979).
10. Mahaut-Smith, M. P.: The effect of zinc on calcium and hydrogen ion currents in intact snail neurons. J. Exp. Biol. **145**, 455–464 (1989).
11. Mayer, M. L., Sugiyama, K.: A modulatory action of divalent cations on transient outward current in cultured rat sensory neurons. J. Physiol. Lond. **396**, 417–433 (1988).
12. Neher, E.: Two fast transient current components during voltage clamp on snail neurons. J. Gen. Physiol. **58**, 36–53 (1971).
13. Neher, E. I., Lux, H. D.: Differential action of $TEA^+$ and two $K^+$-current components of a molluscan neuron. Pflügers Arch. ges. Physiol. **336**, 87–100 (1972).
14. Oyama, Y., Nishi, K., Yatani, A., Akaike, N.: Zinc current in *Helix* soma membrane. Comp. Biochem. Physiol. **72C**, 403–410 (1982).
15. Peters, S. Koh, J., Choi, D. W.: Zinc selectively blocks the action of N-methyl-D-aspartate on cortical neurons. Science Wash. D. C. **236**, 589–593 (1987).
16. Pfaffinger, P. J., Furukawa, Y., Zhao, B., Dugan, D., Kandel, E. R.: Cloning and expression of an *Aplysia* $K^+$ channel and comparison with native *Aplysia* $K^+$ currents. J. Neurosci. **11** (4), 918–927 (1991).
17. Salkoff, L. B., Tanouye, M. A.: Genetics of ion channels. Physiol. Rev. **66**, 301–329 (1986).
18. Smart, T. G.: Uncultured lobster muscle, cultured neurons and brain slices: the neurophysiology of zinc. J. Pharm. Pharmacol. **42**, 377–387 (1990).
19. Stanfield, P. R.: The effect of zinc ions on the gating of the delayed potassium conductance of frog sartorius muscle. J. Physiol. Lond. **251**, 711–735 (1975).
20. Taylor, P. S.: Selectivity and patch measurements of A-current channels in *Helix aspersa* neurones. J. Physiol. Lond. **388**, 437–447 (1987).
21. Westbrook, G. L., Mayer, M. L.: Micromolar concentrations of $Zn^{++}$ antagonize NMDA and GABA responses of hippocampal neurons. Nature **328**, 640–643 (1987).
22. Yamashita, M. M., Wesson, L., Eisenman, G., Eisenberg, G.: Where metal ions bind in proteins. Proc. Nat. Acad. Sci. USA. **87**, 5648–5652 (1990).

*Acta Physiologica Hungarica, Volume 81 (2), pp. 121–135 (1993)*

# DEEP SENSIBILITY OF THE MYSTACIAL PAD IN THE RAT AND ITS CORTICAL REPRESENTATION

O. FEHÉR, Andrea ANTAL, J. TOLDI, J. R. WOLFF*

DEPARTMENT OF COMPARATIVE PHYSIOLOGY, JÓZSEF ATTILA UNIVERSITY, SZEGED, HUNGARY
*ABTEILUNG FÜR KLINISCHE NEUROANATOMIE UND ENTWICKLUNGSNEUROBIOLOGIE, ZENTRUM ANATOMIE, GÖTTINGEN, GERMANY

Received March 10, 1992
Accepted April 29, 1992

The cortical representation of the rat's mystacial pad was examined with the aid of evoked field potentials and recording of single cell activity. Mechanical bending of the vibrissae activated the well-known area within the somato-sensory cortex. Electrical stimulation of the mystacial pad with inserted needle electrodes, bi- and monopolarly, caused a widespread activation extending practically to the whole exposed cortex, including visual, acoustic and motor areas (MSS potentials). The evoked field potentials were accompanied by well-recordable unit activity, mainly in the upper 1000 μm of the cortical depth.

Capsaicin, injected into the mystacial pad on the 8th–10th postnatal day heavily impaired the MSS potentials as recorded at 2 months of age, and only moderately acted on the mechanically evoked potentials. So did also the acutely injected capsaicin. Peak latency of the MSS potentials seemed to be in correlation with the distance from the punctum maximum. The latencies of unit potentials, however, did not show such dependence, they were between 8 and 10 ms. MSS potentials are thought to represent cortical projection mainly of thermo- and nociceptive fibers, which play an important role in the early postnatal life.

**Keywords**: somatosensory system, vibrissae, cortical representation, capsaicin sensitive receptors

In an earlier series of experiments dynamic interrelations of the visual and somatosensory fields of the rat cerebral cortex was studied after mono- and binocular enucleation [11]. In this connection arose among others the necessity to delineate the cortical representation of the mystacial pad including not only that of the vibrissal hairs and common fur but of all the receptors (thermoreceptors, nociceptors etc.) being housed in this exceptionally complex sensory area. In view of activation of all

Correspondence should be addressed to
OTTÓ FEHÉR
Department of Comparative Physiology, József Attila University
H-6701 Szeged P. O. B. 533, Hungary

*Akadémiai Kiadó, Budapest*

receptors resp. nerve endings connected to them electric stimulation seemed to be most practicable. To this aim steel needles were introduced into the medial and lateral border of the mystacial pad and cortical field and unit potentials were recorded when delivering single electric shocks to it. Special attention was paid to the areal distribution of the potentials evoked in this way. It turned out, that the representation of the mystacial pad on the cortical surface is unexpectedly wide, much larger than that of the vibrissal hairs. It was attempted to identify the receptors being able to evoke this widespread activation of the cerebral cortex. The field potentials evoked via electric stimulation of the mystacial pad will be called mystacial somatosensory (MSS) potential in this paper.

## Materials and methods

Seventy female CFY rats were used, anesthetized with 1.3 g/kg urethane, given intraperitoneally in light ethyl-ether anesthesia. The skull of the animal was fixed in a stereotaxic frame. The cerebral hemisphere was exposed on one or on both sides. The dura was removed only if microelectrode recording was aimed.

*Stimulation and recording.* For stimulation of the mystacial region two steel needles of 0.3 mm diameter were pierced into the skin of the upper lip; one immediately besides the nose, and the other about 1 cm behind, at the posterior border the mystacial region (see Fig. 5). Stimuli of 1–2 mA of 300 microsecond duration were given via a stimulus isolation unit, fed by a WPI Accupulser. The stimulating pulses were supramaximal in view of the cortical potentials but they evoked only minimal muscle twitches in the circumoral muscles. At examination of the deep sensibility of other regions (lower lip, eyelids, back of the nose, ear, hindlimb), the stimulus strength was adjusted so as to evoke maximal field potentials, but the electrode distance was kept at 1 cm. Stimulus repetition rate was 1/s.

Cortical field potentials were recorded monopolarly with a ball tipped silver wire electrode, attached to a differential amplifier. The frequency domain ranged from 0.1 Hz to 10 kHz. The indifferent electrode was clipped to the skin of the neck. Blocks of 10–50 evoked potentials were collected and averaged by computer and drawn by an X–Y plotter. The electric signals were visualized on the screen of a storage oscilloscope and recorded simultaneously on magnetic tape together with the trigger pulses.

Mapping of distribution of evoked potentials was carried out on the basis of the cortical map constructed by Zilles and Wree [13]. Records, taken from points of a millimeter grid, were averaged, normalized to the maximal value and plotted to Zilles's cortical map, or (as in case of bar diagrams) to a rectilinear coordinate system.

Single or multi-unit potentials were recorded extracellularly with metal microelectrodes. Their resistance was between 10 and 15 megohms. The microelectrode was moved with the aid of a Narishige hydraulic micromanipulator. The amplifier system was conventional with 1 kHz lower and 30 kHz upper limiting frequency. The unit potentials were evaluated by the same computer; post-stimulus histograms were constructed with 2 ms resolution for 500 ms each.

Visual stimulation was carried out with light flashes conducted by fiber optics to the right eye. The illumination was diffuse enough to evoke activity over the whole visual cortex. The repetition rate was 1/s in this case, too. Acoustic stimuli were applied to the right ear from a small loudspeaker, situated at 5 cm distance. Clicks of 1 ms duration were produced by a square wave stimulator so as to be supramaximal.

For mechanical stimulation of the vibrissal hair receptors a device was constructed (Mechanostim) for bending hairs with variable amplitude and frequency, in one or in both directions. Square wave, trapezoid and sinus shaped deflections were programmable. The device was synchronized with the oscilloscope and deflections of the stimulating arm could be visualized on one beam (not used in the present experiments).

*Treatment with capsaicin.* Newborn rats at 9–10 days of age were injected with 0.03 ml 200 μM capsaicin solution at the vibrissal pad on one side. Their MSS potentials were studied at 2 months of age and the untreated side served as control. In experiments with acute capsaicin treatment the drug was injected in 5 mg/ml concentration into the mystacial pad. The recording commenced after one hour.

## Results

Electric stimulation of the vibrissal pad evoked electrically recordable activity on the whole contralateral hemisphere (Fig. 1). MSS field potentials could be led off not only from the somato-sensory area but also from the visual, acoustic and motor areas. Maximal amplitudes were seen in the cortical representation of the vibrissal hairs, but amplitudes, obtained in the visual and acoustic fields were comparable or even higher than the respective specific sensory evoked potentials (see also Figs 7, 8 and 9).

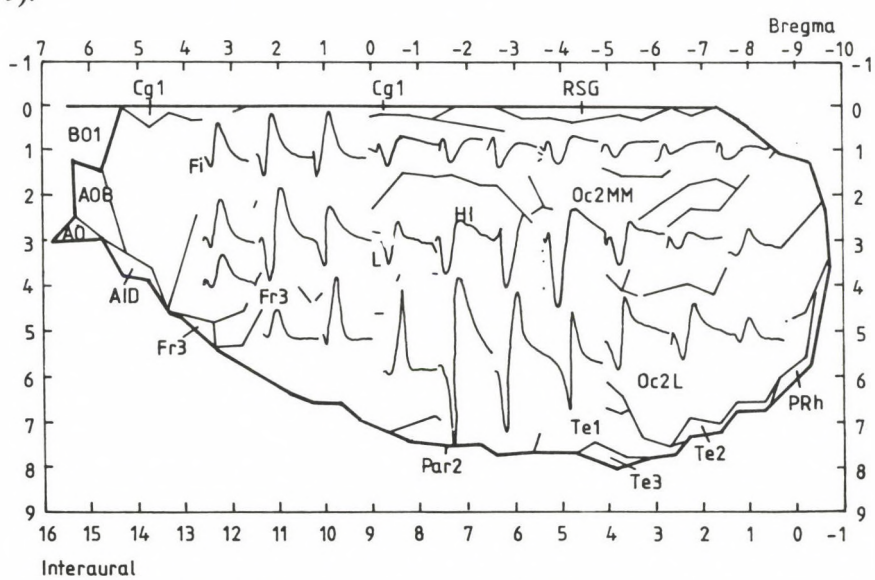


*Fig. 1.* Distribution of MSS potentials on the left cerebral hemisphere of the rat. The plot was superimposed on the map of Zilles and Wree (1979). Column at 0 mm (bregma) and rows at 2, 4 and 6 mm were omitted. Potentials at −2/5, −3/5 and −4/5 are presented with half amplification. Antero-posterior distances here and in other Figures are determined in relation to the bregma (upper abscissa)

Because of the widespread distribution of the MSS potentials, it appeared reasonable to examine, in what relation and proportion they stand with those recordable during mechanical bending of the vibrissae. Making use of the Mechanostim we stimulated the sinus hairs of the right side and recorded the evoked field potentials from the contralateral hemisphere. Their distribution is presented in Figure 2A, normalized to the maximum found at point −4/5 (4 mm behind bregma and 5.5 mm from midline). The area, covered by this kind of somato-sensory potentials proved to be far greater, than that delineated by Welker [12] with the aid of unit recording. It shows a considerable overlapping with the visual area and extends also to the motor cortex.

With this kind of presentation, the distribution of MSS potentials can be seen in Fig. 3A. MSS potentials seem to spread more medially and rostrally than those evoked by hair bending.

This mode of distribution of MSS potentials on the cortex suggested that electric stimulation is exciting not only mechanoreceptive but also other nerve fibers, mediating pain and/or thermal sensations.

Since Jancsó et al. [6], Faulkner and Growcott [4], Saumet and Duclaux [10], Nagy and van der Kooy [9] observed heavy impairment of nociceptive and heat sensibility, mediated by A-delta- and C-fibres after neonatal treatment with capsaicin, it seemed reasonable to examine the consequences of acute and neonatal capsaicin application to the vibrissal pad. Injection of 5 mg/ml capsaicin solution into the vibrissal pad, resulted, under acute conditions, in the effects, presented in Fig. 2 on the mechanically and in Figure 3 on the electrically evoked potentials. Capsaicin seemed to depress somewhat the mechanical responses (Fig. 2) but heavily impaired the MSS potentials both in view of amplitude and area of distribution (Fig. 3B) as compared to the control (Fig. 3A). Essentially the same was observed in rats, injected with 0.03 μM-300 μM capsaicin on the tenth postnatal day and recorded at 2 months of age (Fig. 4). Mechanically evoked potentials were far less impaired in these animals (not presented here).

It seems therefore justified to conclude, that electric stimulation activated most nerve fibers and among them nociceptive and thermoreceptive ones, having higher threshold. These fibers have an exceptionally wide representation on the cortical surface, disregarding boundaries of specific sensory areas.

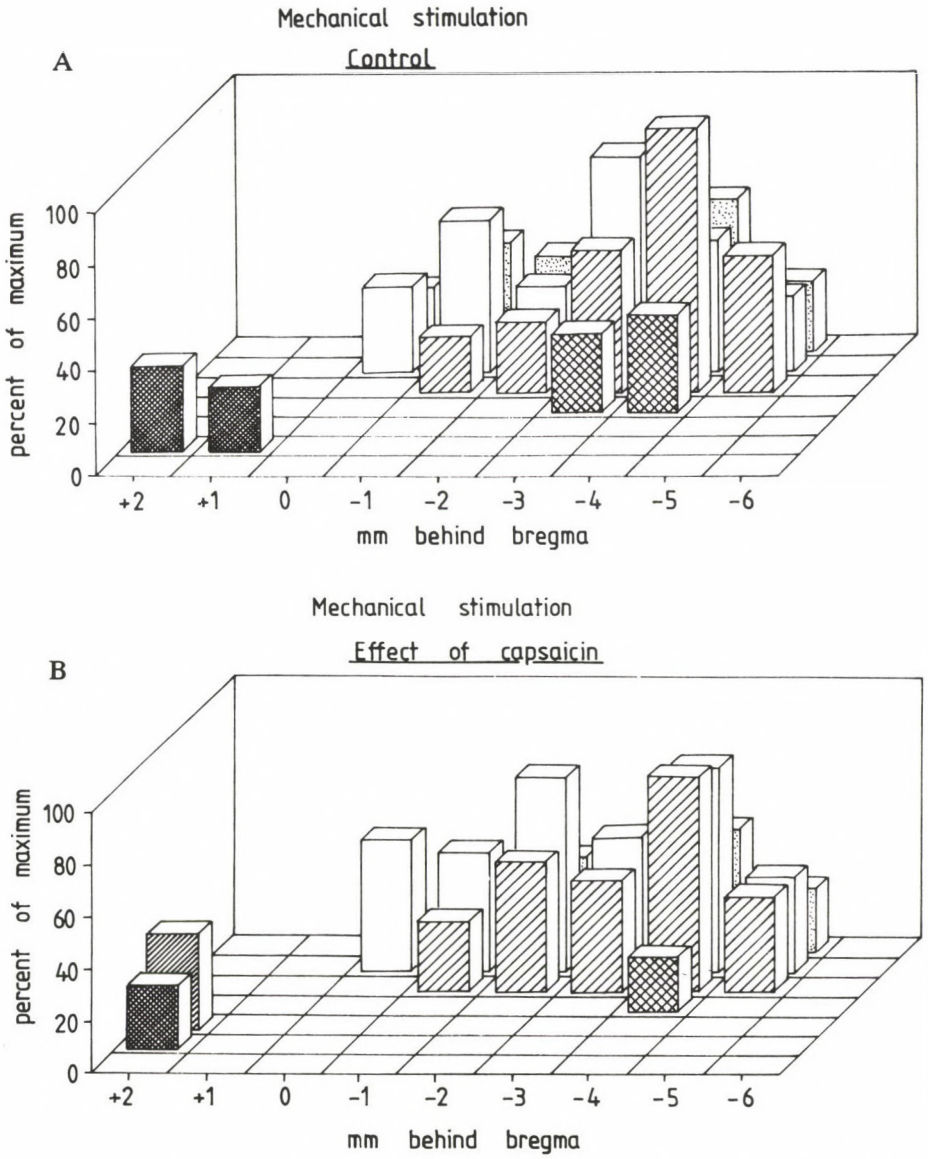


*Fig. 2. A*: Distribution of cortical field potentials evoked by bending of 20 vibrissal hairs with 1/s frequency in the horizontal plain. Amplitudes were normalized to the maximal one, recorded at −4/7 mm, taken as 100 percent. *B*: the same recorded at 1 hour after injection of 5 mg/ml capsaicin into the right vibrissal pad. Amplitudes are normalized to the maximum of the control side

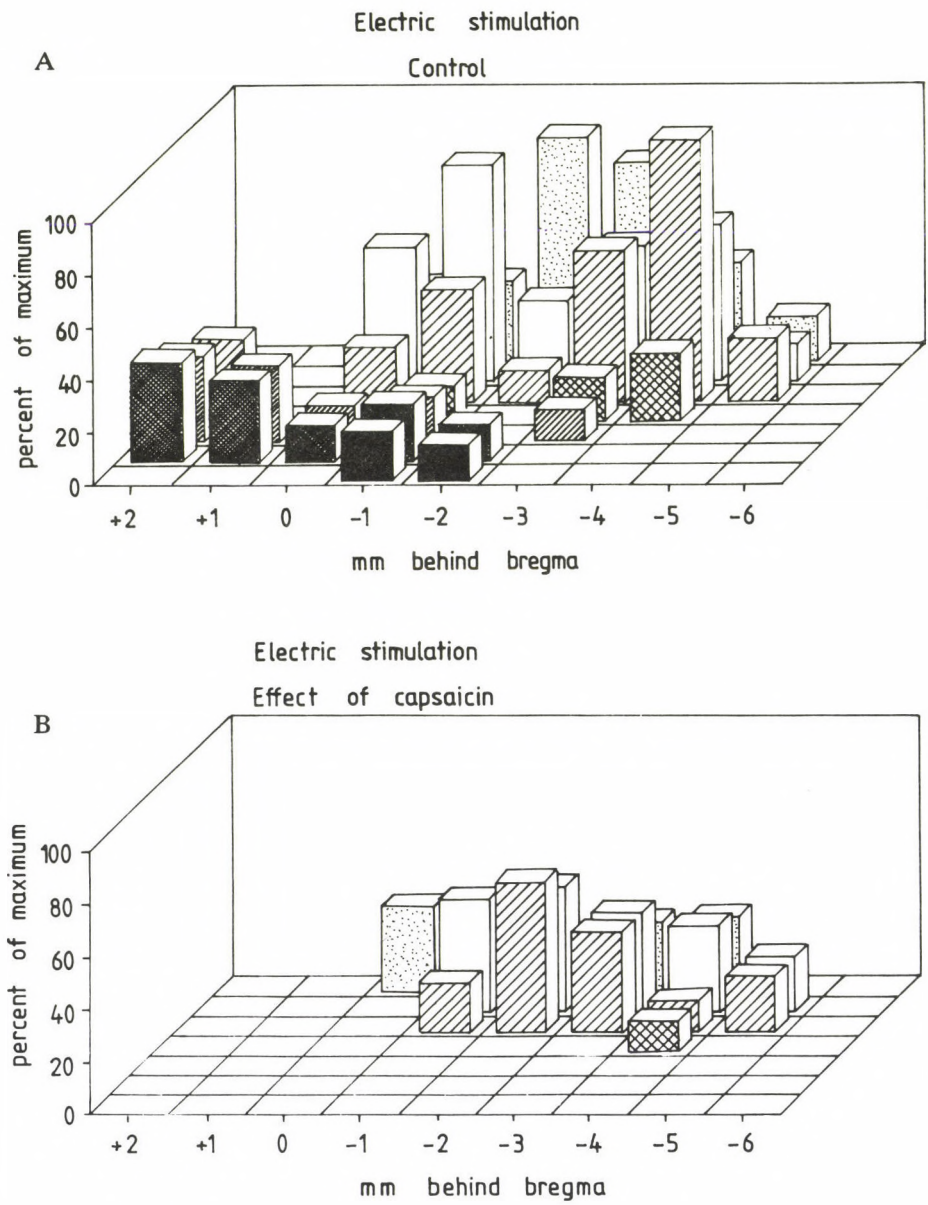


*Fig. 3. A*: Distribution of MSS potentials on the left hemisphere (control side). *B*: The same, after injection of 5 mg/ml capsaicin solution into the right vibrissal pad. Amplitudes are normalized to the maximum of the control side

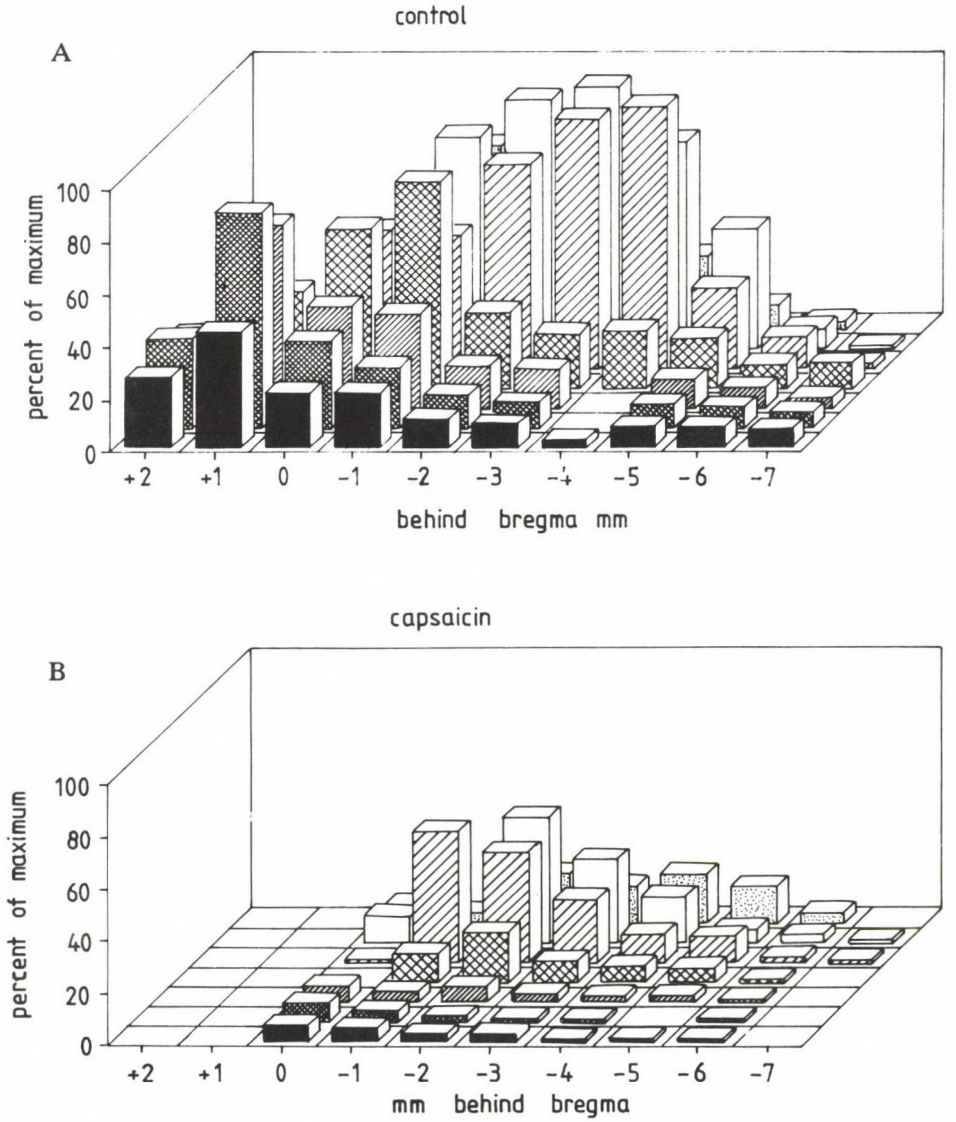


*Fig. 4. A*: Distribution of MSS potentials on the right hemisphere of a rat. Control record. *B*: Distribution of the MSS potentials on the left hemisphere of the same rat. On the 10th postnatal day 0.03 μl-300 μl capsaicin was injected into the right vibrissal pad. Amplitudes were normalized to the maximum of the control side. Plot of this side is presented as a mirror image in order to make comparison easier. Recording was carried out at 2 months of age

The question had now been raised, if this wide representation was the consequence of the stimulation paradigm. Two electrodes, 1 cm apart may stimulate a high number of receptors, densely packed in the vibrissal pad and this may lead to some facilitatory effects, irradiation in the cortex. Therefore several series of records were made with monopolar stimulation. The stimulating electrode was introduced into the nasal or lateral edge of the mystacial pad (see insert of Fig. 5), and the indifferent one was placed to the skin of the back or on the face skin of the other side. The effects of stimulation of a nasal (Fig. 5A) or a lateral point (Fig. 5B) do not seem to differ remarkably. The lateral point seems to excite some more rostral regions than the nasal one, but the surface area activated monopolarly was not smaller than in case bipolar stimulation. This shows, that the mode of stimulation did not influence the spread of excitation in the cerebral cortex.

In a parallel series of experiments the representations of the midline of nose, lower lip, eyelid, ear and hindlimb were determined with similarly placed bipolar electrode arrangement. The activated spots restricted themselves to those, detected by Welker [12] with detailed microelectrode mapping.

The latency of MSS potentials appeared to depend on the site of recording. In the punctum maximum, the latency of the first (usually positive) peak, was between 8 and 9 ms, and lengthened roughly proportionally with the distance up to 18 ms, in all directions. The correlation coefficient between latency and distance ranged between 0.62 and 0.79. One of the scatter diagrams with the fitting straight line is to be seen in Fig. 6. The lengthening of the latency includes also the smoother rise of potentials recorded at greater distances; the time to onset did not vary as much. The latencies of the unit discharges, however, rarely exceeded 10 ms, also in cases when peak latency of the field potential was longer.

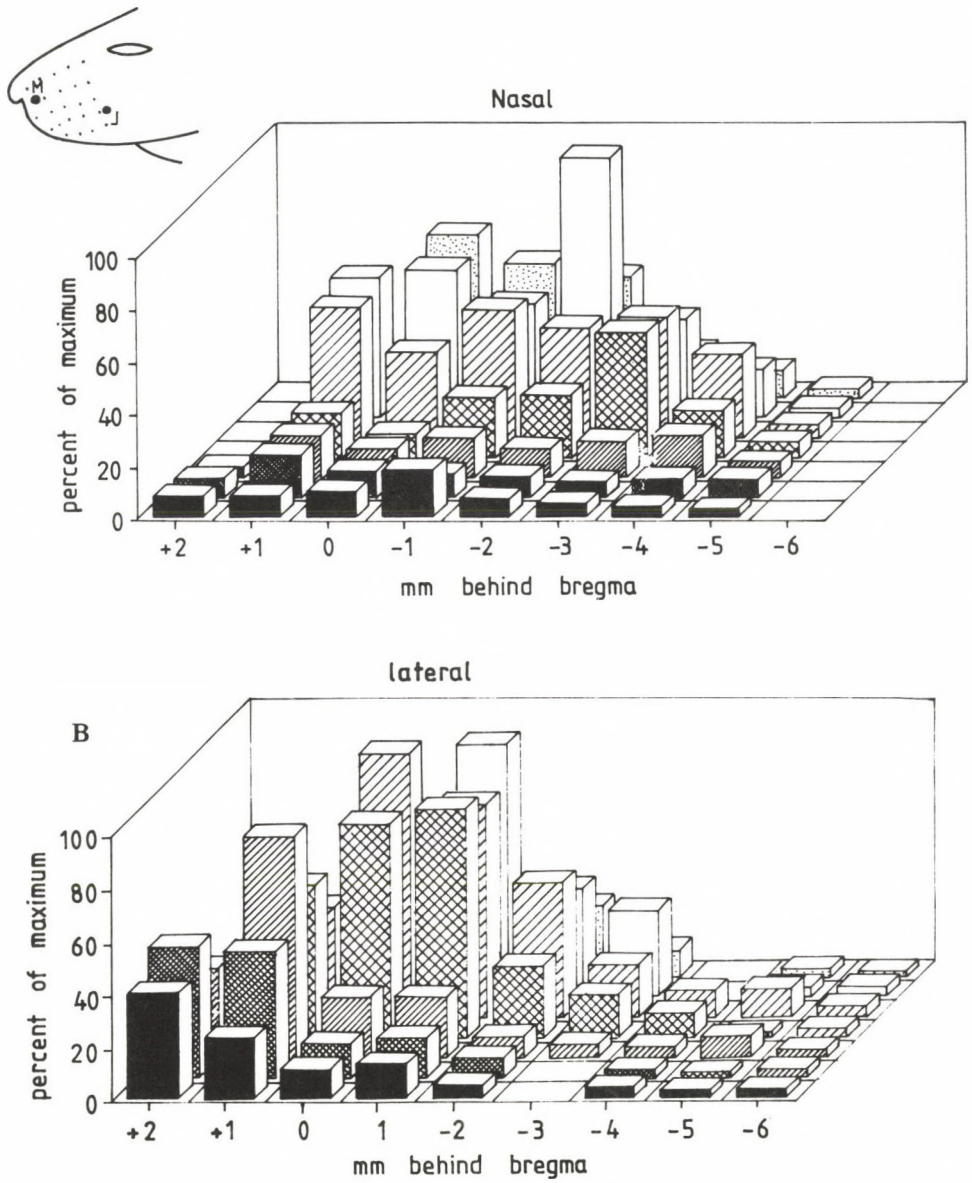


*Fig. 5. A*: Distribution of MSS potentials evoked by monopolar stimulation by an electrode introduced into the vibrissal pad, immediately at the nose. *B*: The same, evoked from a lateral electrode position, 1 cm posteriorly from the nasal one (electrode positions see in the insert)

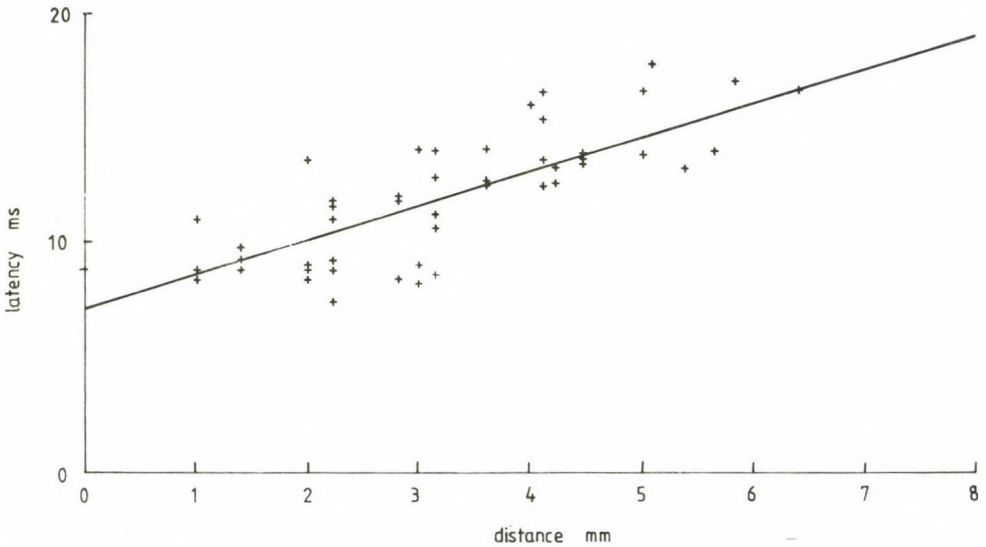


*Fig. 6.* Correlation between latency time of MSS potentials (ordinate) and the distance from the punctum maximum (abscissa). Correlation coefficient: 0.783, SE: ±1.77, f(x) = 6.91 + 1.56x

MSS stimulation evoked well detectable single and multi-unit activity, most part in the upper 1 mm of the cortical depth, irrespective of the area examined. Visual and MSS field potentials with post-stimulus histograms of unit activity are presented in Fig. 7, as recorded from point −6/4. The co-existence of the specific (visual) and MSS potentials at a locus, belonging unequivocally to the visual area could be demonstrated not only by records of field potentials but also by post-stimulus histograms of unit discharges collected over 50 sweeps at each record in the insert. The peak latency of the visual field potential was about 65 ms. The group of units recorded here was found at a depth of 675 um. MSS potentials, evoked in the auditory cortex (Te1, 2, point −5/7) together with multi-unit activity can easily be differentiated from the acoustic field potentials, evoked by click stimulus with 50 ms delay. The cells discharging to the acoustic stimulus were situated at a depth of 1130 μm. MSS potentials of high amplitude could also be recorded from the motor cortex (Figure 9). The responding cells were recorded at a distance 875 μm from the surface.

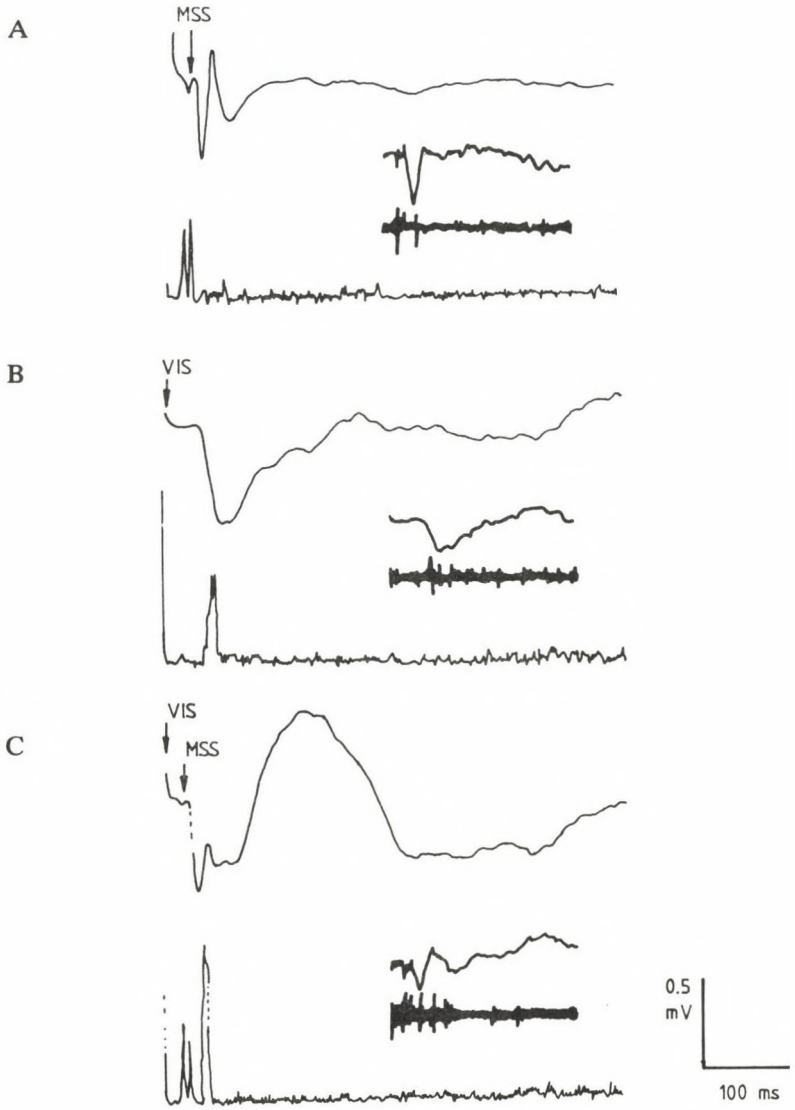


*Fig. 7.* A: Upper line: averaged MSS potentials led off from point −6/4 situated in the visual cortex. Lower line: post-stimulus histogram units found at a depth of 675 μm. Insert: MSS potential with unit discharge in single sweep record. B: The same in case of visual stimulaion. C: The same in case of combined (visual and electric) stimulation

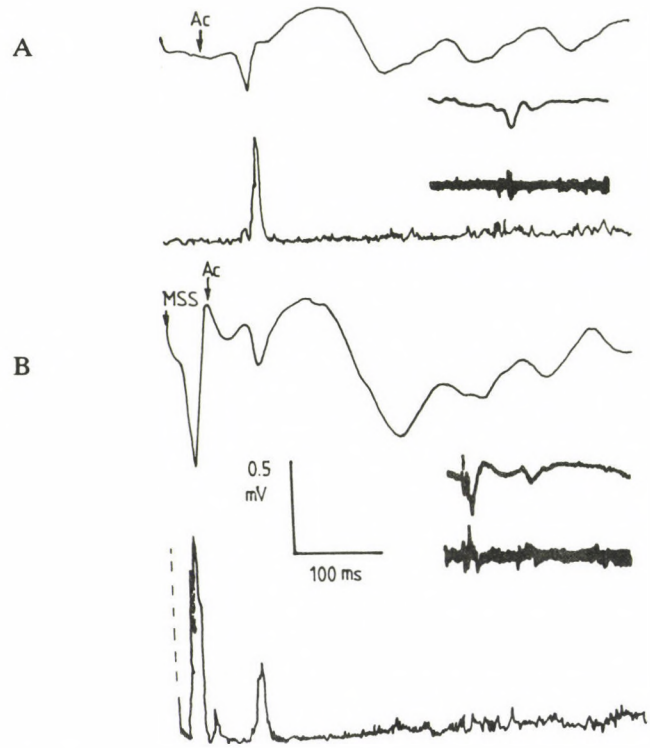


*Fig. 8. A*: Averaged MSS potentials led off from point −5/7 within the auditory area. Lower line: post-stimulus histogram of units, situated at 1130 μm cortical depth. The acoustic stimulus (Ac) was delayed by 50 ms. Inserts: single sweep records of MSS field and unit potentials. *B*: Record of combined MSS and acoustic stimulation. Acoustic stimulus was delayed by 50 ms

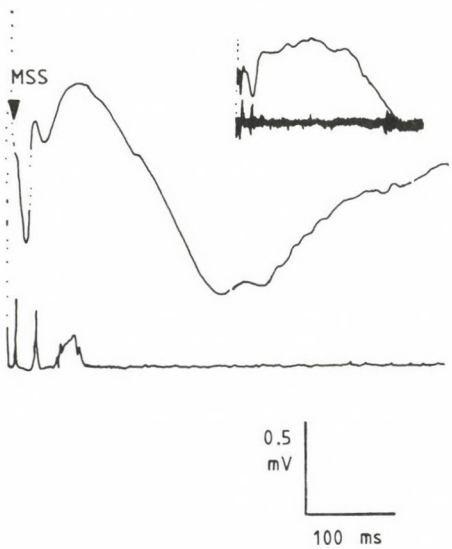


*Fig. 9.* MSS potential (upper line) and post-stimulus histogram of unit activity (lower line) as recorded from the motor cortex. Units were found at a depth of 875 μm

## Discussion

The central representation of different kinds of receptors has been examined with physiological and morphological methods, mainly in view of those reporting about vibrissal hairs and common fur, respectively. In mice, Nussbaumer and van der Loos (1985) found that the representation of common fur covers the anterior part of the barrel field while the posterior part was devoid of it. Common fur representation was concentrated in thin stripes around the posterior barrels. It must be noted, however, that the authors selected for examination only neurons of layer IV. Sharp et al. (1988), using 2-D-deoxyglucose and WGA-HRP method report, that vibrissal and common fur representation appears to be well distinguishable on spinal, thalamic and cortical levels. In the cortex common fur becomes represented in a zone, between SI and SII areas, by exciting neurons in all layers of the cortex. As to the cortical representation of thermal and nociceptive modalities no detailed comparative study is available. It would not be surprising, if their localization and extension showed remarkable differences from those of the mechanical senses.

There are, however, some relevant studies in other species which report about differences between representations and other properties of different sensory modalities of other somatic regions. For deep sensations Adey and Kerr [1] found bilateral representation in a marsupial and in the rabbit. The latency of the homolateral field potentials was longer. Creutzfeldt et al. [2] were able to activate units in the cat's visual cortex not only with optic but also with electric stimuli delivered to the intralaminar nuclei. Lomo and Mollica [7] detected acoustically and somatosensorily responsive cells in the visual cortex of the waking rabbit. Part of these responded also to photic stimuli. They suggested that this interaction took its source in the subcortical structures. Murata et al. [8] found neurons in the cat's visual cortex which could be activated also by acoustic and somatosensory stimuli. This responsiveness was preserved after spinal transection and proved to be bilateral. In transmission of these impulses the reticular formation and the intralaminar nuclei of the thalamus were suggested as possible relay stations. In the newly discovered visual area of the cat (at the ectosylvian gyrus and the insula) Hicks et al. [5] found cells responding not only to photic but also to somatosensory and acoustic stimuli especially frequently, if the latter were "unphysiological"; it means that somatosensory stimulation consisted in electric stimulation of the radial nerve and acoustic stimuli (as in our experiments) were clicks. Many of such cells proved to be polymodal.

In evaluating our experiments the first question to be answered is: what is stimulated by the electric pulses in the mystacial pad? The sensory innervation of the vibrissa region has been examined recently with light microscopic methods by Rice et al. (1986), Rice and Munger (1986) and Munger and Rice (1986). They found six varieties of sensory nerve endings, bearing differences in morphology and

localization. Merkel and Ruffini endings, lanceolate and free nerve endings have been found to participate in the innervation of both the mystacial hairs, guard hairs and common fur, at five different levels. Merkel endings are thought to be rapidly adapting, Ruffini endings slowly adapting mechanoreceptors. Free nerve endings are brought in connection with thermal and nociceptive function (Rice and Munger, 1986). Rapidly and slowly adapting mechanical receptors and thermoreceptors seem to play an outstanding role in the sensory functions of this area mostly in subprimate mammals. In primates where the forelimb helps to get more information, the importance of this area has become reduced (see ref. 3).

In our experiments electric stimuli activated probably nerve fibers of various destinations and thresholds rather than the receptors themselves; differences in conducting velocities may be reflected by latencies of their central representations. Since the stimulus intensities were adjusted so as to evoke maximal field potentials, we suppose that MSS potentials are the central reflections of excitation of all receptors housed in this region. However, the capsaicin sensitivity of MSS potentials indicated that they are built up mostly by impulses arriving via thermal and nociceptive fibers. The most intriguing question remains in this respect: why do not MSS potentials keep their cortical representation within the borders of the somatosensory area, as do vibrissal hairs? The cause of this exceptional occupancy may rest upon their special biological significance. These receptors (mainly touch- and thermoreceptors) are functioning already in the first postnatal days and represent the first functioning sensory modalities of the puppies. These receptors may help them to find the mother, induce reflex movements, orienting head and neck, enhancing activity of the limbs. This might account also for the intensive projection to the motor cortex.

**Acknowledgement**

This study was supported by collaboration grant of the Hungarian Academy of Sciences and the Deutsche Forschungsgemeinschaft (Project Wo 279/8-1)

## REFERENCES

1. Adey, W. R., Kerr, D. I. B.: The cerebral representation of deep somatic sensibility in the marsupial phalanger and the rabbit; an evoked potential and histological study. J. comp. Neurol. **100**, 597–625 (1954).
2. Creutzfeldt, O., Baumgartner, G., Jung, R.: Convergence of specific and unspecific afferent impulses on neurons of the visual cortex. Electroenceph. clin. Neurophysiol. **8**, 163–164 (1956).
3. Darian-Smith: The Trigeminal System. In: Handbook of Sensory Physiology. Vol. II. ed. A. Iggo, Springer Verlag, Berlin, 1973, pp. 271–277.

4. Faulkner, D. C., Growcott, J. W.: Effects of neonatal capsaicin administration on the nociceptive responses of the rat to mechanical and chemical stimuli. J. Pharm. Pharmacol. **32**, 656–657 (1980).
5. Hicks, T. P., Benedek, Gy., Thurlow, G. A.: Modality specifity of neuronal responses within the cat's insula. J. Neurophysiol. **60**, 422–437 (1988).
6. Jancso, G., Kiraly, E., Jancso-Gabor, A.: Pharmacologically induced selective degeneration of chemosensitive primary sensory neurones. Nature (London) **270**, 741–742 (1977).
7. Lomo, T., Mollica, A.: Activity of single units in the primary optic cortex in the unanaesthetized rabbit, during visual, acoustic, olfactory and painful stimulation. Arch. ital. Biol. **100**, 86–120 (1962).
8. Murata, K., Cramer, H., Bach-y-Rita, P.: Neuronal convergence of noxious, acoustic and visual stimuli in the visual cortex of the cat. J. Neurophysiol. **28**, 1223–1239 (1965).
9. Nagy, J. I., Vander Kooy, D.: Effects of neonatal capsaicin treatment on nociceptive thresholds in the rat. J. Neurosci. **3**, 1145–1150 (1983).
10. Saumet, J.-L., Duclaux, R.: Analgesia induced by neonatal capsaicin treatment in rats. Pharmacol. Biochem. Behav. **16**, 241–243 (1982).
11. Toldi, J., Joó, F., Fehér, O., Wolff, J. R.: Modified distribution patterns of responses in rat visual cortex induced by monocular enucleation. Neuroscience **24**, 59–66 (1988).
12. Welker, C.: Receptive fields of barrels in the somatosensory cortex of the rat. J. Comp. Neurol. **166**, 173–190 (1976).
13. Zilles, K., Wree, A.: Areal and laminar structure of the rat cortex. In: The Rat Nervous System. Vol. 1. Forebrain and Midbrain. Ed. Paxinos G., Academic Press, Sydney (1985).

*Acta Physiologica Hungarica, Volume 81 (2), pp. 137–145 (1993)*

# DIFFERENCE BETWEEN MALE AND FEMALE RATS IN VASOPRESSOR RESPONSE TO ARGININE VASOPRESSIN+

F. A. LÁSZLÓ, CS. VARGA*, A. PAPP, I. PÁVÓ,** F. FAHRENHOLZ***

*DEPARTMENT OF COMPARATIVE PHYSIOLOGY, JÓZSEF ATTILA UNIVERSITY OF SCIENCES, AND **ENDOCRINE UNIT, FIRST DEPARTMENT OF MEDICINE, ALBERT SZENT-GYÖRGYI MEDICAL UNIVERSITY, SZEGED, HUNGARY, AND ***MAX-PLANCK INSTITUTE FOR BIOPHYSICS, FRANKFURT AM, GERMANY

Received March 5, 1992
Accepted April 29, 1992

A study was carried out how the sexual difference influences the increase in blood pressure (BP) induced by arginine vasopressin (AVP), and how the binding characteristics of $^3$H-labelled AVP on membranes prepared from the vascular bed were affected. After the administration of various doses of AVP, a significantly higher BP increase was observed in male rats than in females. The vasopressor effect of AVP was reduced in males following orchidectomy or administration of the antiandrogen cyproterone acetate. The vasopressin (VP) antagonist d($CH_2$)$_5$Tyr(Me)AVP diminished the BP response to AVP in both sexes. The plasma AVP level was found to be much higher in males than in females, but it was decreased to the level of females after orchidectomy. The density of AVP-binding sites in the aorta membrane preparation was smaller in females, and in orchidectomized or cyproterone acetate-treated male rats than in the control males.

The results demonstrate that testosterone upregulates the number of AVP-binding sites, leading to an increase in the pressor response to AVP in the rat vascular bed.

**Keywords**: blood pressure, AVP, $V_1$ antagonist, orchidectomy, cyproterone acetate, aorta membrane preparation, AVP binding site

Sexual hormones have been shown to be involved in regulation of the biological action of vasoactive agents [2, 14]. We previously demonstrated that VP can induce a considerable renal vasospasm in rats treated with oestrogen [5, 8], and renal cortical necrosis can develop as a consequence of the vasoconstriction [7, 14].

Correspondence should be addressed to
F. A. LÁSZLÓ
Department of Comparative Physiology, József Attila University of Sciences
H-6726 Szeged, P. O. B. 533, Hungary

+Some parts of this work were presented at the XIth International Congress of Pharmacology (Amsterdam, The Netherlands, 1990).

*Akadémiai Kiadó, Budapest*

The renal arteries can be sensitized by oestrogen against the vasoconstrictive action of VP. A similar sensitizing effect was observed in rats treated with testosterone, but the renal cortical necrosis was more pronounced following VP administration in testosterone-pretreated rats than in rats treated with oestrogen. In the present work, a study was made of how sexual difference influences the increase in BP induced by AVP, and the binding characteristics of $^3$H-labelled AVP on membranes prepared from the rat aorta. In the third experimental series, the effects of the VP antagonist d$(CH_2)_5$Tyr(Me)-AVP on the BP increase produced in male and female rats were examined.

## Materials and Methods

The experiments were carried out on Wistar rats of the same age (12–14 weeks old), the females weighing 180–220 g and the males 250–300 g. The animals were anaesthetized with pentobarbital, administered i.p. in a dose of 45 mg/kg body weight (b.w.). After the anaesthetization, a cannula was inserted into the trachea, the left common carotid artery was prepared in the neck, the vagal nerve was separated from the vessel, and 0.1 ml physiological saline containing 5 U heparin was administered via a polyethylene cannula (outer diameter/inner diameter 0.8/0.5 mm) inserted into the carotid lumen, to inhibit blood clotting. The cannula was connected to a Hellige electromanometer, and the BP was recorded on a Biocomp five-channel polyphysiograph. Following the cervical preparation, phentolamine (Regitin, Ciba-Geigy) was administered i.p. in a dose of 10 mg/kg b.w. AVP (376 IU/mg) (0.02, 0.06, 0.18 μg/kg b.w.) was injected in a logarithmically increasing dose through a small syringe fixed into the lateral tail vein.

The effect on the BP was always measured continuously after AVP administration, and the BP increase was expressed as a percentage of the initial value. The VP antagonist [1-(β-mercapto-ββ-cyclopentamethylenepropionic acid)-2-0-methyltyrosine]AVP, d$(CH_2)_5$Tyr(Me)AVP, was injected in a dose of 0.2 μg/kg into the lateral tail vein 20 min before AVP administration. The dose of the antagonist was calculated as an effective antipressor dose (0.16 nmol/kg = 184 ng/kg), defined as the quantity which halves the pressor effect observed 20 min after i.v. administration of 2.0 IU AVP [9]. The method of BP measurement and detection of the effectiveness of the VP antagonist on the BP were described in detail in an earlier study [15].

Bilateral orchidectomy was carried out under ether anaesthesia 10 days before the experimentation. The efficiency of orchidectomy was controlled via the measurement of plasma testosterone (RIA). The antiandrogen cyproterone acetate (Androcur, Schering) was administered through a gastric tube in an oral dose of 2.5 mg/day once daily for 10 days. Testosterone (Retandrol, Richter) was injected s.c. in a dose of 2.5 mg/day once daily for 10 days.

Tissue preparation: Rat aorta plasma membrane was prepared by a two-step centrifugation procedure, according to the method of Pearlmutter et al. [19] with some modifications. The rats were decapitated, and the aorta was removed with forceps and placed in homogenizing buffer (100 mM TRIS/HCl, Ph 7.4, 10 mM $MgCl_2$). The tissue was cut into small pieces and homogenized with a teflon homogenizator. The liquid suspension was centrifuged at 1000 × g for 10 min at 4 °C. The supernatant was centrifuged at 100,000 × g for 60 min. The pellett was resuspended in homogenizing buffer and stored at −70 °C until further use.

Binding assay: A membrane suspension (containing 100 μg protein) in 100 ml binding buffer (50 mM TRIS/HCl, pH 7.4, 5 mM $MgCl_2$) containing 10 nM $^3$H-AVP in the presence of various

concentrations of unlabelled AVP was incubated at 30 °C for 30 min. To terminate the binding tests, the mixtures were diluted with 5 ml ice-cold washing buffer (10 mM TRIS/HCl, pH 7.4, 2 mM $MgCl_2$ and 0.05% BSA), immediately filtered under vacuum through Whatman GF/F filters, and rinsed twice with 5 ml ice-cold washing buffer. The filters were placed into counting vials with scintillation liquid and analysed by liquid scintillation spectrometry. Protein was determined by means of a modified fluorescamine assay [24]. $B_{max}$ and $K_D$ values were determined by the method of Fahrenholz et al. [3]: Binding curves were fitted to a logistic function with a weighed iterative least-squares procedure based on the method of steepest descent.

Biometric analysis was carried out with the two-tailed Student test.

## Results

Following the administration of various doses of AVP, a significantly higher BP increase was observed in males than in females (Fig. 1). After injection of the V1 antagonist $d(CH_2)_5Tyr(Me)AVP$ in a dose of 0.06 μg/kg b.w., the pressor response to AVP was substantially reduced in both sexes, but the reduction was more pronounced in males than in females. The effects of testosterone, orchidectomy and cyproterone acetate administration on the BP changes induced by AVP are demonstrated in Fig. 2. The reactivity of the vascular bed to AVP in male rats was not enhanced by the administration of testosterone. The vasopressor effect of AVP was less pronounced 10 days after bilateral orchidectomy. The BP response to AVP in males was also reduced after administration of the antiandrogen cyproterone acetate. In this case the pressor activity of AVP was the same in the two sexes. The plasma AVP level proved much higher in males than in females (Fig. 3). Following

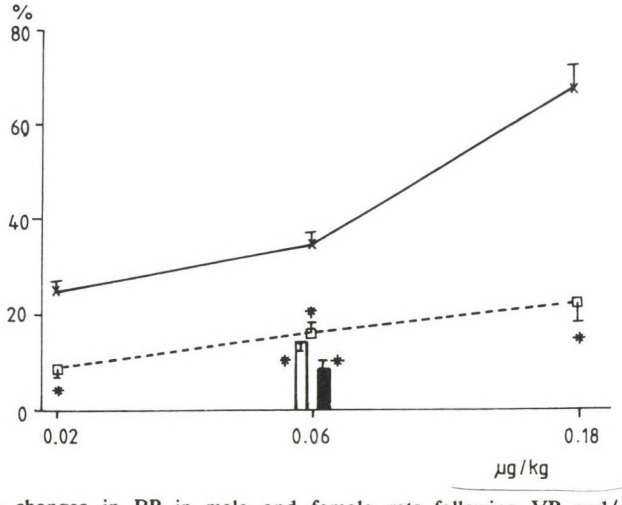


*Fig. 1.* Percentage changes in BP in male and female rats following VP and/or $V_1$ antagonist administration. X: male, VP (n:24); □: female, VP (n:25); ■: male, VP + $V_1$ antagonist (n:24); ▪: female, VP + $V_1$ antagonist (n:25). Mean ± S. E. M. *: significant difference

orchidectomy, the AVP concentration was reduced to the level of females. Cyproterone acetate treatment did not influence the AVP level in males. The plasma testosterone level was diminished by orchidectomy and remained unchanged after cyproterone acetate treatment.

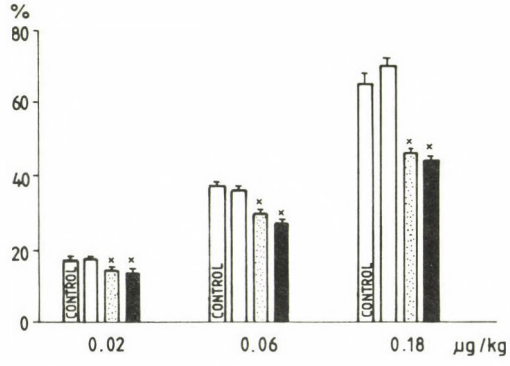


*Fig. 2.* Percentage changes in BP following VP administration in male rats treated with testosterone, cyproterone acetate or orchidectomy. ⊡: untreated control (n:12); □: testosterone treatment (n:10); ▨: orchidectomy (n:12); ■: cyproterone acetate treatment (n:11). Mean ± S. E. M. *: significant difference

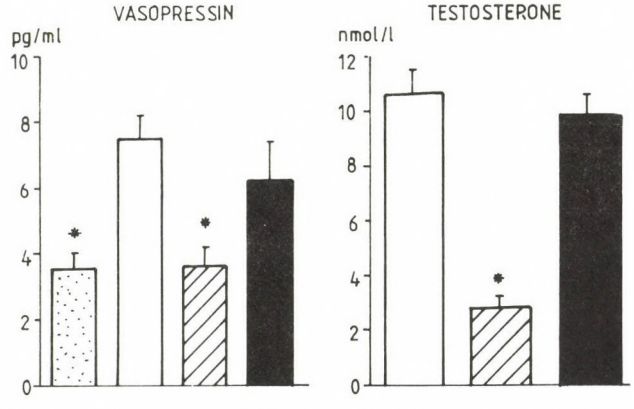


*Fig. 3.* Plasma AVP and testosterone levels following orchidectomy or cyproterone acetate treatment. ⊡: untreated female (n:20); □: untreated control male (n:20); ▨: orchidectomy (n:12); ■: cyproterone acetate treatment (n:11). Mean ± S. E. M. *: significant difference vs. control

In comparison with females or with orchidectomized or cyproterone acetate-treated males, male rats displayed an increase in the density of AVP-binding sites in the aorta membrane preparation (Table I). The maximum observed binding capacity ($B_{max}$) of $^3$H-AVP was significantly smaller in females, and in orchidectomized or cyproterone acetate-treated male rats than in control males. The ligand affinity of

untreated male rats proved to be moderately reduced in comparison with the other goups. The experiment on the specific binding of $^3$H-AVP resulted in a much flatter saturation curve for female (Fig. 4) than for male (Fig. 5) rat aorta crude membranes.

**Table I**

*Specific $^3$H-AVP binding to rat aorta membranes in different groups*

| Group | No. of animals | Maximal binding capacity ($B_{max}$) fmol/mg protein | Ligand concentration ($K_D$) nM |
|---|---|---|---|
| 1. Controls, male | 16 | 115 ± 14.5+ | 5.7 ± 0.7 |
| 2. Controls, female | 16 | 65 ± 6.0* | 3.6 ± 0.3* |
| 3. Orchidectomized, male | 14 | 77 ± 8.0* | 3.8 ± 0.2* |
| 4. Cyproterone acetate treatment, male | 15 | 80 ± 8.5* | 2.9 ± 0.6* |

mean ± S. E. M.
*: significant difference vs. control males

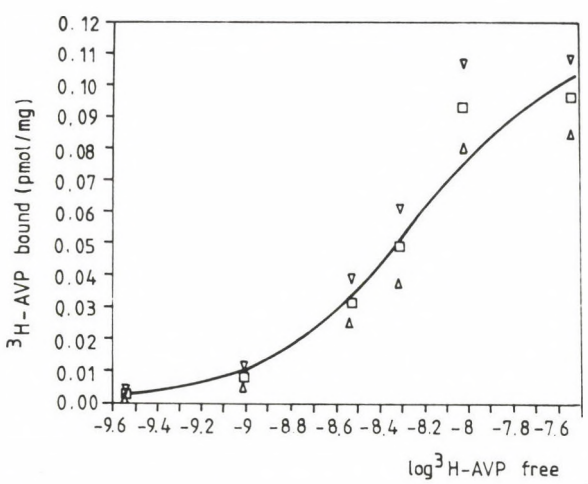


*Fig. 4.* Saturation curve of the specific binding of $^3$H-AVP to male rat aorta crude membranes

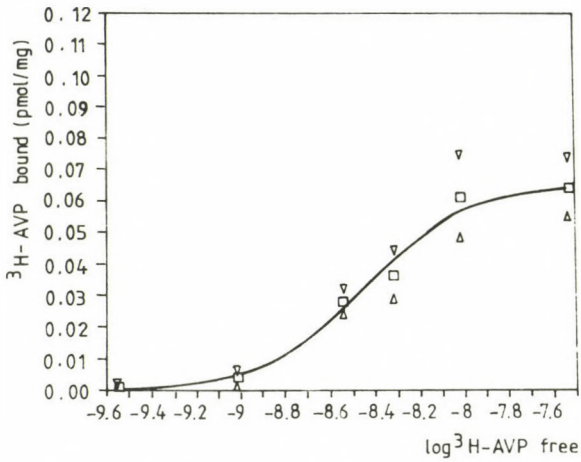


*Fig. 5.* Saturation curve of the specific binding of $^3$H-AVP to female rat aorta crude membranes

## Discussion

This investigation demonstrates that different doses of AVP induce a significantly higher BP in males; the vasopressor effect of AVP is less pronounced in male rats after orchidectomy and following administration of the antiandrogen cyproterone acetate; the density of AVP-binding sites in the aorta membrane preparation was found to be lower in females, and in orchidectomized or cyproterone acetate-treated male rats than in the control males. However, the ligand affinity was moderately smaller in untreated control male group.

We earlier observed a similar phenomenon in connection with renal vessels. VP administration after testosterone pretreatment induced renal cortical necrosis in rats, the histological picture pointing to the hypoxic origin of the change [18]. Testosterone sensitizes the renal arteries to the vasoconstrictive effect of VP [6]; renal cortical necrosis cannot be observed following the injection of VP alone, without testosterone pretreatment. Cyproterone acetate prevented the sensitizing effect of testosterone: as a result of the administration of cyproterone acetate simultaneously with testosterone, the subsequent administration of a large dose of VP did not result in renal cortical necrosis. This circumstance permits the conclusion that the sensitizing effect of testosterone is manifested through the mediation of the androgen receptors [6, 18]. This assumption is supported by observations proving the presence of androgen receptors in the kidney [1, 16, 22, 25].

The sensitizing effect of testosterone has also been detected in another region of the blood supply. In an earlier study we demonstrated that endogenous VP is of great importance in the pathogenesis of gastric haemorrhagic lesions induced by a

high concentration of ethanol [12, 13]. Recent observations revealed that ethanol generates more severe lesions in the gastric mucosa of male rats than in females. Orchidectomy and cyproterone acetate treatment each reduced the extent of ethanol-induced gastric erosions in male rats [10, 11].

The present results can be compared with findings of investigations of the relationship between the plasma testosterone level and the number of kidney AVP receptors in aged rats. A decreased number of renal binding sites for AVP in the aged rat was demonstrated both by a membrane-binding assay [4, 17] and by an immunocytochemical staining procedure [20]. An increasing functional impairment of the hypothalamo-neurohypophyseal system with aging was described by Turkington and Everitt [23], Sladek et al. [21] and Zbuzek et al. [26]. At the same time, the plasma testosterone concentration was found to be reduced in aged rats [4, 20], and testosterone treatment increased the number of AVP-binding sites in the aged kidney [4].

In conclusion, the vasopressor effect of AVP has been shown to be more pronounced in male rats than in females. After orchidectomy or the administration of cyproterone acetate, the BP increase induced by AVP in males was reduced to the level of females. This sensitizing effect of testosterone is developed via an increase in the AVP-binding sites found in the walls of the vascular beds.

## Acknowledgements

The authors are grateful to Prof. Maurice Manning (Department of Biochemistry, Toledo, Ohio, USA) for supplying the vasopressin antagonist, and to Dr. György Falkay (Department of Obstetrics and Gynaecology, Albert Szent-Györgyi Medical University, Szeged, Hungary) for the determination of plasma testosterone. This work was supported by the Hungarian Research Foundation (No. OTKA 1902, I/1) and the Hungarian Academy of Sciences (AKA No. 88-0-556).

## REFERENCES

1. Bullock, L. P., Bardin, C. W.: Androgen receptors in mouse kidney. A study of male, female and androgen-sensitive (tfm/y) mice. Endocrinology, **94**, 746–756 (1974).
2. Crofton, J. T., Ratliff, D. L., Brooks, D. P., Share, L.: The metabolic clearance rate and pressor responses to vasopressin in male and female rats. Endocrinology, **118**, 1777–1781 (1986).
3. Fahrenholz, F., Boer, R., Crause, P., Fritzsch, G., Grzonka, Z.: Interactions of vasopressin agonists and antagonists with membrane receptors. Eur. J. Pharmacol. **100**, 47–58 (1984).
4. Herzberg, N. H., Goudsmit, E., Kruisbrink, J., Boer, G. J.: Testosterone treatment restores reduced vasopressin binding sites in the kidney of the ageing rat. J. Endocrin. **123**, 59–63 (1989).
5. Kocsis, J., Szabó, E., László, F. A.: Serio-angiographic study of renal cortical necrosis induced by administration of estrin + vasopressin in rats. Invest. Radiol. **14**, 295–299 (1979).

6. Kocsis, J., Szabó, E., László, F. A.: Serio-angiographic study of protective action of cyproterone acetate against renal vasospasm following testosterone plus vasopressin administration in rats. Invest. Radiol. **17**, 254–258 (1982).
7. Kovács, K., Dávid, M. A., László, F. A.: Effect of hypophysectomy on the development of renal cortical necrosis induced by posterior pituitary extract in oestron pretreated rats. Br. J. Exp. Pathol. **45**, 415–418 (1964).
8. Kovács, K., László, F. A., Sövényi, E., Kocsis, J.: Angio-renographic studies in living rats during the development of renal cortical necrosis. Br. J. Radiol. **38**, 148–151 (1965).
9. Kruszynski, M., Lammek, B., Manning, M., Seto, J., Haldar, J., Sawyer, W. H.: [1–(beta-mercapto-beta-cyclopentamethylenepropionic acid)2–(0-methyl) tyrosine] arginine vasopressin and [1–(beta-mercapto-beta, betacyclopentamethylenepropionic acid)] arginine-vasopressin, two highly potent antagonists of the vasopressor response to arginine vasopressin. J. Med. Chem. **23**, 364–368 (1980).
10. László, F., Amani, E., Náfrádi, J., Karácsony, G., Szabó, E., Rengei, B., Lengyel, Z., László, F. A.: Ethanol generates more severe gastric mucosal damage in male than in female rats. The possible role of vasopressin in the phenomenon. Exp. Clin. Gastroenterol. Introductory Issue 35–36 (1990).
11. László, F., Amani, E., Varga, Cs., László, F. A.: Influence of sex hormones on ethanol-induced gastric haemorrhagic erosions in rats. Acta Physiol. Hung. (1992) in press.
12. László, F., Karácsony, G., Náfrádi, J., Rengei, B., Vecsernyés, M., Laczi, F., Szarvas, F., Lengyel, Z., László, F. A.: A high dose of ethanol releases vasopressin and simultaneously induces lesions in the rat stomach – the role of vasopressin in gastric cytoprotection. In: New Aspects of Morphology, Function and Regulation. Proceedings of the 4th Conference on Neurohypophysis, Copenhagen, 1989, pp. 159–161, Oxford University Press, Oxford, England, 1989.
13. László, F., Karácsony, G., Szabó, E., Láng, J., Baláspiri, L., László, F. A.: The role of vasopressin in the pathogenesis of ethanol-induced gastric hemorrhagic erosions in rats. Gastroenterology, **101**, 1242–1248 (1991).
14. László, F. A.: Renal cortical necrosis. Experimental induction by hormones. S. Karger, Basel, 1981.
15. László, F. A., Leprán, I., Baláspiri, L.: Cardiovascular effects of vasopressin agonists and an antagonist in rats. Exp. Clin. Endocrinol. (Life Sci. Adv.) **7**, 237–241 (1988).
16. Li, J. J., Cuthbertson, T. L., Li, S. A.: Specific androgen binding in the kidney and estrogen-dependent renal carcinoma of the Syrian hamster. Endocrinology, **101**, 1006–1015 (1977).
17. Miller, M. A., Dorsa, D. M.: Age-related changes of vasopressin receptors in the rat. Proc. of the 15th Annual Meeting of the Society for Neuroscience, Dallas, Texas, USA, abstr. No. 124.15.
18. Mónus, Z., László, F. A.: Cyproterone acetate-promoted prevention of renal cortical necrosis following testosterone + vasopressin administration. Br. J. Exp. Pathol. **60**, 72–75 (1979).
19. Pearlmutter, A. F., Szkrybalo, M., Pettibone, G.: Specific arginine vasopressin binding in particulate membrane from rat aorta. Peptides, **6**, 427–431 (1985).
20. Ravid, R., Fliers, E., Swaab, D. F., Zurcher, C.: Changes in vasopressin and testosterone in the senescent Brown-Norway (BN/Bi Rij) rat. Gerontology, **33**, 87–98 (1987).
21. Sladek, C. D., McNeill, T. H., Gregg, C. M., Blair, M. L., Baggs, R. B.: Vasopressin and renin response to dehydration in aged rats. Neurobiology of Ageing, **2**, 293–302 (1981).
22. Suzuki, K., Tamaoki, B.: Testosterone metabolism and 5-alpha-dihydrotestosterone-binding macromolecule in rat kidney. Steroids Lipids Res. **4**, 266–276 (1973).
23. Turkington, M. R., Everitt, A. V.: The neurohypophysis and ageing with special reference to the antidiuretic hormone. In: Hypothalamus, Pituitary and Ageing. Eds.: Everitt, A. V. and Burgess, J. A., Springfield, USA, pp. 123–136, 1976.

24. Van Frank, R. M.: Adaptation of fluorescent protein assay for use with cell fractions and homogenates. Anal. Biochem. **65**, 552–555 (1975).
25. Verhoeven, G., Heyns, W., De Moor, P.: Ammonium sulfate precipitation as a tool for the study of androgen receptor proteins in rat prostate and mouse kidney. Steroids, **26**, 149–167 (1975).
26. Zbuzek, V. K., Zbuzek, V., Wu, W. W.: Age-related differences in the incorporation of $^{3}$H-arginine into vasopressin in Fischer 344 rats. Experimental Gerontology, **22**, 113–125 (1987).

*Acta Physiologica Hungarica, Volume 81 (2), pp. 147–157 (1993)*

# PROTEIN KINASE C ACTIVATION IN *APLYSIA* NEURONS BY PHORBOL DIACETATE: COMPARISON OF EFFECTS FOLLOWING EXTRACELLULAR OR INTRACELLULAR APPLICATION

A. PAPP*, M. R. KLEE

DEPARTMENT OF NEUROPHYSIOLOGY, MAX PLANCK INSTITUTE FOR BRAIN RESEARCH, FRANKFURT/M., GERMANY

Received March 10, 1992
Accepted April 29, 1992

The effects of protein kinase C activation on electrophysiological phenomena of neurons in *Aplysia californica* ganglions were studied. The enzyme was activated by phorbol-12,13-diacetate applied either extracellularly by perfusion, or by intracellular pressure injection. In both forms of application, an increase in the potential upstroke speed and amplitude as well as a reduction of the depolarization evoked by extracellular acetylcholine application was found. A protein kinase C blocker, H-7, had opposite effects on the action potential. All observed actions of the phorbol ester were consistently faster in intracellular application than extracellular.

**Keywords**: *Aplysia* neuron, protein kinase C, phorbol diacetate, H-7, action potential, acetylcholine response

Phosphorylating processes are of great importance in regulating nerve cell functions. One of the key enzymes, protein kinase C (PKC), has been detected in a wide variety of nerve cells and tissues including *Aplysia* neurons [8]. The activity level of PKC influences several electrophysiological phenomena of the neurons depending either on voltage-gated or agonist-gated ion channels.

Alterations of the action potential were observed in central and peripheral neurons of vertebrates and neurons of invertebrates. In *Aplysia*, DeRiemer et al. [9] found – working on the so-called bag cells – that the spike, being purely Ca-dependent in these cells, was increased in its amplitude by phorbol ester treatment or

Correspondence should be addressed to
András PAPP
József Attila University, Department of Comparative Physiology
H-6701 Szeged, P. O. B. 533, Hungary

*On leave from Department of Comparative Physiology, József Attila University, Szeged, Hungary

*Akadémiai Kiadó, Budapest*

by intracellular PKC injection. This effect turned out to be a recruitment of a normally inactive Ca channel population [29]. In the visceral ganglion neurons of *Aplysia*, the spike is Na- and Ca-dependent to various proportions [17]. Previous studies on these neurons showed that the increase of spike amplitude and upstroke speed after treatment with a phorbol ester resulted mostly from increase of the fast $Na^+$ current, while $Ca^{2+}$ currents showed no change or a slight decrease [18], with the exception of an increased L-type current in a group of burster neurons (a "dual action" similar to that seen in cultured mouse neurons [32]). Outward currents in visceral ganglion cells, including the $Ca^{2+}$-activated $K^+$ current, were reduced after PKC activation [27].

In vertebrate neurons, the activation of PKC caused either increase or decrease in various membrane currents. On one hand, an increase of both the fast $Na^+$ current and the Ca-activated $K^+$ current was found in cat spinal motoneurons [33]. Similarly, in neurons of the cat motor cortex, the spike overshoot and the fast afterhyperpolarization were increased while the slow afterhyperpolarization was decreased by intracellular phorbol ester injections [2]. On the other hand, an inhibition or reduction of currents was found in several mammalian preparations. Extracellularly applied phorbol esters abolished the spike afterhyperpolarization in rat hippocampal cells [24], and reduced the calcium currents both in chicken dorsal root ganglion cells [14, 25] and guinea pig hippocampal neurons [10]. In mouse neuroblastoma cells, a reduction of $Na^+$ and $Ca^{2+}$ currents [20] was found and in cultured mouse neurons a reduction of $Ca^{2+}$ and $K^+$ currents [32] was observed. The $Na^+$ current and the fast $K^+$ current through mammalian ion channels, which had been expressed in *Xenopus* oocytes, were inhibited by PKC activation or direct injection of the enzyme [7, 21].

PKC activity has important influence on the synaptic transmission, a process where agonist-gated channels have a central role. In smooth muscles from different mammalian organs, the transmitter action was either decreased or increased by PKC activation [1]. An increase of EPSPs and decrease of IPSPs by presumably postsynaptic action was found by Baranyi et al. [3] after injecting phorbol ester into pyramidal neurons. In the case of the nicotinic acetylcholine (ACh) receptor, phosphorylation by PKC and the resulting desensitization were directly demonstrated [26]. Receptors of this type have been described from *Aplysia* neurons by Kehoe [16]. In other preparations, the enhancement of EPSPs was presumably of presynaptic origin, for example at the neuromuscular junction [28] or on the RC-EPSP in neuron R-15 of *Aplysia* [19].

In this study, the effects of a PKC activating phorbol ester, phorbol-12,13-diacetate (PDAc), on *Aplysia* central neurons were investigated. Effects on the action potential and the response evoked by extracellular ACh injection were observed and compared in case of extracellular versus intracellular application of PDAc. A PKC

inhibitor, 1-[5-isoquinolinylsulfonyl]-methylpiperazine (H-7, [13]) was used to prove that the actions of PDAc are PKC-mediated.

## Materials and Methods

*Preparation*

The experiments were carried out on neurons of isolated central ganglia of *Aplysia californica*. Identified neurons in the visceral ganglion [12] as well as unidentified ones in the pleural and pedal ganglia were used. Prepared single ganglions were fixed to the Sylgard bottom of the recording chamber by needles and were continuously perfused with artificial sea water (ASW). The composition of ASW was (in mM): NaCl, 480; KCl, 10; $CaCl_2$, 10; $MgCl_2$, 20; $MgSO_4$, 15; HEPES, 5. The pH was set to 7.8; the chamber and inflowing ASW were kept at a constant temperature of 16 °C.

*Recording*

The cells were impaled with a single microelectrode of 2–6 MOhm resistance, which was filled with 3 M KCl or a special injecting solution (see below). An AXOCLAMP 2 device was used in all experiments. Action potentials were recorded in bridge mode, and responses to extracellular ACh injections in current or voltage clamp mode. Action potentials and their first derivatives (dV/dt) were visualized and plotted by a Philips digital storage scope. ACh responses were directly written out by a chart recorder and stored in a Nicolet digital scope with disk memory.

*Substances and pressure injections*

Organic substances were obtained from Sigma, inorganic salts from Merck. Phorbol diacetate (PDAc) was made up to a 5.6 mM stock solution in 10% dimethyl sulfoxide (DMSO) – 90% distilled water. This was added for perfusion to the ASW to give 2.5–10 μM final concentration (the final DMSO concentration was thus maximally 0.02%, i.e. only 1/15 of that necessary to induce direct DMSO effects, [10]). For intracellular injection normal recording electrodes were filled with a solution containing PDAc, 0.5 mM; KCl, 2 M; Fast Green dye, 2 mg/ml. H-7 was dissolved in distilled water and was applied solely by the perfusion in 5–50 μM concentration. Extracellular ACh application was performed by ejecting 1 M ACh-Cl solution from broad-tipped pipettes (5–10 μm). Injections were done with ca. 200 kPa (~30 psi) pressure yielded by a pulse-controlled injection device (Neuro-Phore, Medical Systems Corp., USA). Before penetrating a neuron, the recording electrode was set under steady pressure and was pushed against the connective tissue around the ganglion until a fine trace of filling was forced out through the tip. The electrode now had about 2 MOhm resistance and was suitable both for recording and injection. The dyeing of the cytoplasm by Fast Green was used to determine the appropriate amount of injection. Moderate injections with only a light green staining around the electrode tip gave good effects, stronger ones caused a general impairment of the neuron.

## Results

### *Effects of PDAc on the action potential*

Treatment with PDAc caused a change in several features of the action potential, and the effects were qualitatively the same in either form of application. When applying the drug by perfusion, a consistent increase of the spike upstroke speed was found on a total of about 100 neurons including all neuron types in the ganglions. Figure 1 demonstrates this increase, indicated by the first time derivative (dV/dt) as an increase of the positive peak (Fig. 1C and D vs. A). An increase of the spike amplitude and the negative dV/dt peaks, although usually present, was less characteristic. Intracellular application of PDAc by pressure injection exerted its effect also mainly on the positive dV/dt peak as shown in Fig. 2 (parts C and D vs. A). In a fully developed state, i.e. over 20 min for extracellular and at 10 min for intracellular application (see below), the positive dV/dt peak increased to 122.00 ± 14.57% of the control in extracellular and 121.88 ± 15.91% in intracellular application of PDAc (mean ± S.D.; calculated from 14 and 8 neurons, respectively). To prove the PKC-dependence of the above changes, we treated the neurons with the known and potent PKC inhibitor, H-7, in several experiments. The alterations seen

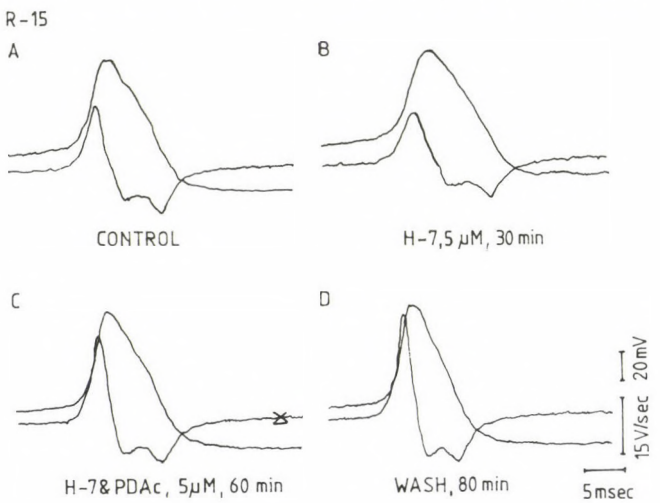


*Fig. 1.* Effects of PKC blocking and activation on parameters of the spike if PDAc is added to the ASW. Neuron R-15 in the visceral ganglion. Upper trace: action potential, lower trace: first time derivative (dV/dt). A: Control state. B: In presence of the PKC blocker H-7 both the first, positive peak of dV/dt and the spike amplitude are reduced. C: PDAc in the perfusion medium completely abolishes the effects of H-7. An increase of dV/dt and spike amplitude typical to PDAc action is seen. D: The action of PDAc is further increased by washing with ASW. The effects of H-7 could be washed out while those of PDAc were irreversible

under H-7 influence were opposite to those caused by PDAc both on the spike amplitude and speed (part B in Figs 1 and 2). They could, however, be reversed by subsequent PDAc administration, either extra- or intracellularly. The effects seen in the presence of both drugs were as described for PDAc above, but attenuated by the H-7 (part C in Figs 1 and 2). Washing out H-7 relieved the block and intensified the PDAc actions (part D in Figs 1 and 2). The changes of the spike had a characteristic difference in their time course for extracellular and intracellular application, as can be seen in column A of Figs 3 and 4. While the increase of dV/dt took always at least 25 min to develop when PDAc was added extracellularly, the effect of an intracellular PDAc injection was immediate and reached its peak in 10 minutes.

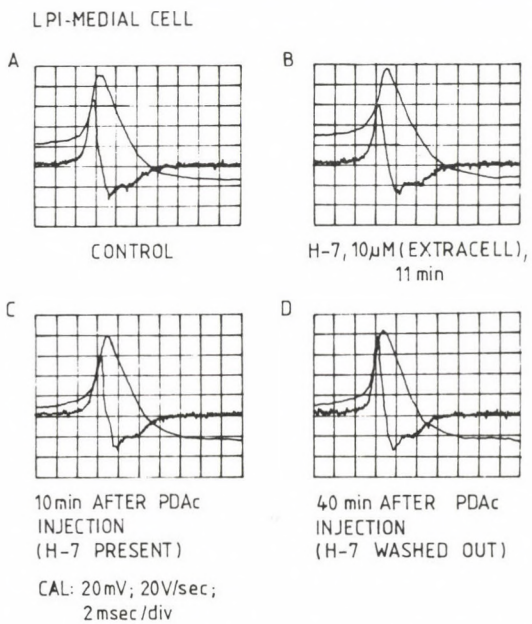


*Fig. 2.* Effects of PDAc blocking and activation in case of intracellular PDAc injection. Medial neuron in the left pleural ganglion. Same display as in Fig. 1. A: Control state. B: Treatment with H-7 decreases dV/dt and spike amplitude. C: After a moderate PDAc injection, the effects of PDAc were seen on the dV/dt peak and spike amplitude despite the presence of H-7. D: Washing out H-7 made the PDAc effects more pronounced

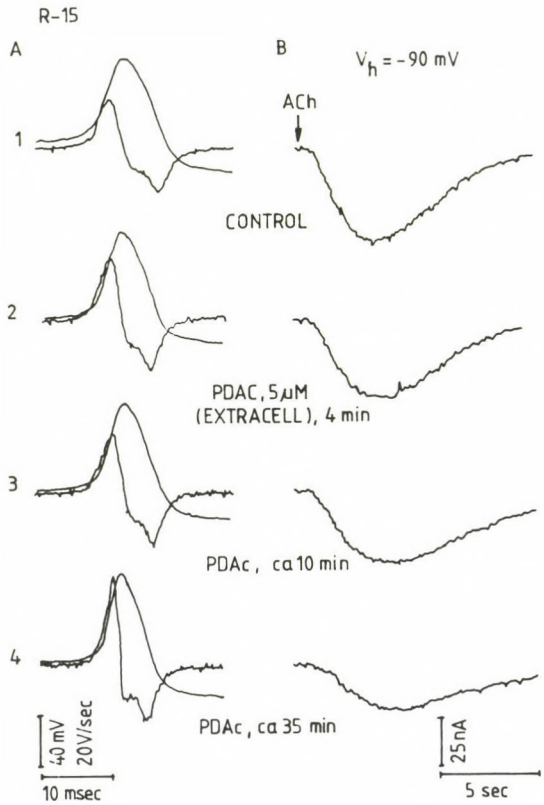


*Fig. 3.* Effect of extracellular PDAc on the ACh response and time course of PDAc effects. Neuron R-15. Column A: Spikes and dV/dt, meaning of traces like in Fig. 1. Column B: Inward currents corresponding to depolarizations evoked by 180 ms long ACh pulses recorded in voltage clamp (holding potential −90 mV). 1: Control state. In ASW containing 5 μM PDAc the spike shows alterations similar to those in Figs 1 and 2, and the ACh response is reduced. These changes could be seen already after 4 min (2) but reached full strength only after more than 30 min (3, 4)

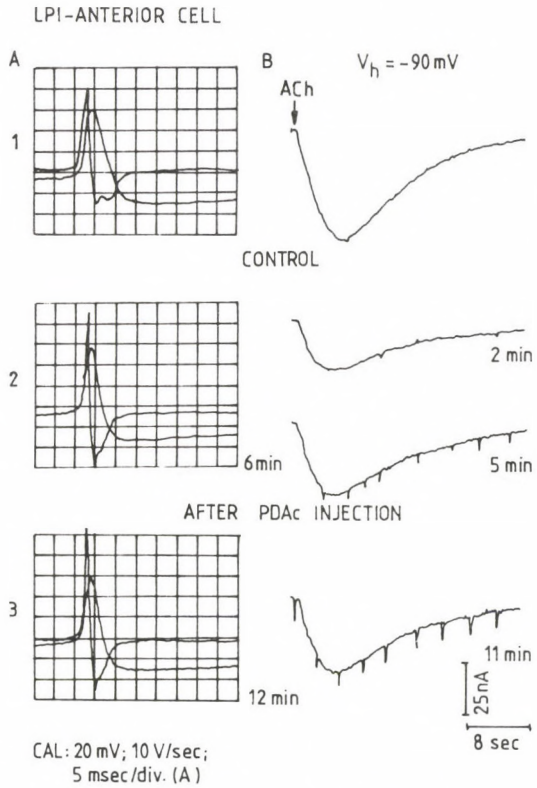


*Fig. 4.* Effect on the ACh response and time course of the effects in case of intracellular PDAc injection. Anterior cell in the left pleural ganglion. Column A: Spikes and dV/dt. Column B: Inward currents evoked by 2 s long ACh pulses recorded in voltage clamp (holding potential −90 mV). 1: Control state. Within 6 minutes after PDAc injection (2) the changes in the spike were just beginning while the reduction of the ACh response had already passed its maximum at 2 min. In the 12th min after injection (3), the increase of dV/dt was even stronger. At about the same time, the reduction of the ACh response was less strong but present and usually showed no further changes

### *Effects on responses evoked by ACh*

PDAc had another characteristic influence on the depolarizations or hyperpolarizations elicited by extracellularly applied ACh (acting mostly on nicotinic receptors, [16]). In the present study, depolarizing responses recorded from certain neurons in the visceral ganglion, from the anterior neurons [16] in the pleural ganglion, or from neurons in the pedal ganglion were used. The ACh injections were repeated every 3 or 4 min and their size was set individually to achieve a clear and stable depolarizing wave. Treatment with PDAc resulted in a marked decrease in the ACh response [19]. On either extra- or intracellular application, a maximal decrease

to about 60% of the control (58.50 ± 22.87% in extracellular, 59.36 ± 32.76% in intracellular PDAc application – mean ± S.D. – on 14 neurons each) was found (column B in Figs 3 and 4). The time course of the change of ACh response was very different in the two modes of PDAc application, as seen on the spike. When giving PDAc extracellularly (Fig. 3), the decrease began quite early but needed at least ca. 30 min to reach its maximal value (Fig. 3 B2 to B4). However, when PDAc was injected intracellularly, the decrease was rapid and reached its maximum in 2–5 minutes (Fig. 4 B2). After that, the response showed a recovery but remained, with few exceptions, diminished (Fig. 4 B3, B4).

## Discussion

As a result of the experiments presented, one can conclude that the effects induced by PDAc are almost identical for extra- and intracellular application except for their different time courses. The only major difference is seen in the effect of PDAc on the ACh D-response. While in extracellular PDAc application the response decreases continually, in intracellular application the initial reduction is maximal followed by a partial recovery. The data concerning spike alterations presented here show a similarity to those of DeRiemer et al. [9] made on bag cell neurons. Increased amplitude and upstroke speed can enhance the excitability of the soma, as described for mammalian neurons [2, 33] and for *Aplysia* [18]. PDAc, however, did not change spike afterhyperpolarization, as it does in mammalian neurons [2, 33]. In the bag cells, the main inward current is carried by $Ca^{2+}$, and the activity level of PKC influences the neuropeptide secretion of these cells. In the central ganglion neurons of *Aplysia*, the action potentials are at least partly Na-dependent [17]. The observed increase of the EPSPs after PDAc treatment [19] is similar to that found on the neuromuscular junction by Shapira et al. [28]. This effect can, despite of the differences between the cells, be likened to the enhanced secretion and might be the base of synaptic modifications. A PKC-dependent enhancement of excitatory postsynaptic potentials resulting from enhanced transmitter release has, in fact, been described in *Aplysia* by Fossier et al. [11] and in mammalian hippocampus by Malenka et al. [23]. The decrease of ACh-induced membrane potential changes after phorbol ester treatment looks, in relation to the above-mentioned increase of the postsynaptic potential, controversial. It should be stressed, however, that the reduction of the response evoked by ACh pulses directed on the soma reflects the activity of (extrasynaptic) receptors and is in no way connected to possible presynaptic changes. A similar reaction was observed on rat $GABA_B$ receptors which showed a PKC-mediated inhibition of the agonist response [31]. Likewise, from cerebellar Purkinje cells, a reduction of glutamate sensitivity by phorbol esters has been reported [6]. Although H-7 binds to the catalytic domain of PKC, and not to the

regulatory one, which is the site of action of phorbol esters [15], it is a rather effective blocker of phorbol ester actions. In extracellular application, H-7 reduces the slope of the action potential upstroke (Figs 1 and 2) and the peak amplitude of EPSPs in *Aplysia* neurons [19]. It also reduces the spike amplitude in *Aplysia* bag cells (in high concentration, [4]), blocks the potentiation of field potentials in the dentate gyrus [22] and blocks the IPSPs in rat CA1 neurons [5]. When applied intracellularly, H-7 causes a reduction of the spike amplitude but has only a weak effect on postsynaptic potentials [30].

The general similarity between the effects achieved by extracellular or intracellular PDAc application, on one hand, and their sensitivity to H-7, on the other hand, indicates that these effects are in fact mediated by PKC. Comparing an activating and a non-activating phorbol ester, Doerner et al. [10] used the same argumentation supplemented by the fact that effects of the non-activating substance were not antagonized by H-7. Using diacylglycerol (DAG) analogues, Hockberger et al. [14] found a decrease in $Ca^{2+}$ current in chick embryonal neurons only for extracellular application. As the effect was abrupt and not antagonized by different PKC blockers, they concluded that this action of DAG was not PKC-mediated. In our experiments, the antagonism between PDAc and H-7 was asymmetric, i.e. the effect of H-7 was reversed by PDAc (Figs 1 and 2) whereas that of PDAc was only minimally influenced by H-7, as demonstrated also on the monosynaptic RC-EPSP in neuron R-15 of *Aplysia* [19]. Despite these differences, one can conclude that the effects of PDAc on cellular electrophysiological phenomena in *Aplysia* neurons described here are PKC-mediated.

## REFERENCES

1. Baraban, J. R., Gould, R. J., Peroutka, S. J., Snyder, S. H.: Phorbol ester effects on neurotransmission: interaction with neurotransmitters and calcium in smooth muscle. Proc. Natl. Acad. Sci. USA **82**, 604–607 (1985).
2. Baranyi, A., Szente, M. B., Woody, C. D.: Intracellular injection of phorbol ester increases the excitability of neurons of the motor cortex of awake cats. Brain Res. **424**, 396–401 (1987).
3. Baranyi, A., Szente, M. B., Woody, C. D.: Activation of protein kinase C induces long-term changes of postsynapic currents in neocortical neurons. Brain Res. **440**, 341–347 (1988).
4. Conn, J. P., Strong, J. A., Azhderian, E. M., Nairn, A. C., Greengard, P., Kaczmarek, L. K.: Protein kinase inhibitors selectively block phorbol ester- or forskolin-induced changes in excitability of *Aplysia* neurons. J. Neurosci. **9**, 473–479 (1989).
5. Corradetti, R., Pugliese, A. M., Ropert, N.: The protein kinase C inhibitor 1-(5-isoquinolinesulphonyl)-2-methylpiperazine (H-7) disinhibits CA1 pyramidal cells in rat hippocampal slices. Br. J. Pharmacol. **98**, 1376–1382 (1989).
6. Crepel, F., Krupa, M.: Selective depression of the glutamate sensitivity of Purkinje cells by phorbol esters. An in vitro study on the rat cerebellar slice. J. Physiol. **406**, 17P (1988).

7. Dascal, N., Lotan, I.: Activation of protein kinase C alters voltage dependence of a $Na^+$ channel Neuron **6**, 165–175 (1991).
8. DeRiemer, S. A., Greengard, P., Kaczmarek, L. K.: Calcium/phosphatidylserine/-diacylglycerol-dependent protein phosphorylation in the *Aplysia* nervous system. J. Neurosci. **5**, 2672–2676 (1985).
9. DeRiemer, S. A., Strong, J. A., Albert, K. A., Greengard, P., Kaczmarek, L. K.: Enhancement of calcium current in *Aplysia* neurones by phorbol ester and protein kinase C. Nature **313**, 313–316 (1985).
10. Doerner, D., Abdel-Latif, M., Rogers, T. B., Alger, B. E.: Protein kinase C-dependent and -independent effects of phorbol esters on hippocampal calcium channel current. J. Neurosci. **10**, 1699–1706 (1990).
11. Fossier, P., Baux, G., Tauc, L.: Activation of protein kinase C by presynaptic FLRFamide receptors facilitates transmitter release at an *Aplysia* cholinergic synapse. Neuron **5**, 479–486 (1991).
12. Frazier, W. T., Kandel, E. R., Kupfermann, I., Waziri, R., Coggeshall, R. E.: Morphological and functional properties of identified neurons in the abdominal ganglion of *Aplysia californica*. J. Neurophysiol. **30**, 1288–1351 (1967).
13. Hidaka, H., Hagiwara, M., Chijiwa, T.: Molecular pharmacology of protein kinases. Neurochem. Res. **15**, 431–434 (1990).
14. Hockberger, P., Toselli, M., Swandulla, D., Lux, H-D.: A diacylglycerol analogue reduces neuronal calcium currents independently of protein kinase C activation. Nature **388**, 340–342 (1989).
15. Huang, K-P.: The mechanism of protein kinase C activation. TINS. **12**, 425–432 (1989).
16. Kehoe, J.: Three acetylcholine receptors in *Aplysia* neurones. J. Physiol. (Lond.) **225**, 115–146 (1972).
17. Klee, M. R.: TEA and 4-AP affects separate potassium and calcium channels differently in *Aplysia* S and F cells. Brain Res. Bull. **4**, 162–166 (1979).
18. Klee, M. R.: Different effects of a phorbol ester on membrane properties of *Aplysia* neurons. J. Bas. Clin. Physiol. Pharmacol. **1**, 119–124 (1990).
19. Klee, M. R., Hoyer, J.: Action of a phorbol ester in the presence of two PKC blockers. In: Klee M.R., Speckmann, E.-J., Lux H.-D. (eds) Physiology, Pharmacology and Development of Epileptogenic Phenomena. Springer, pp. 119–122 (1991).
20. Linden, D. J., Routtenberg, A.: Cis-fatty acids, which activate protein kinase C, attenuate $Na^+$ and $Ca^{2+}$ currents in mouse neuroblastoma cells. J. Physiol. **419**, 95–119 (1989).
21. Lotan, I., Dascal, N., Naor, Z., Boton, R.: Modulation of vertebrate brain $Na^+$ and $K^+$ channels by subtypes of protein kinase C. FEBS Letters **267**, 25–28 (1990).
22. Lovinger, D. M., Wong, K. L., Murakami, K., Routtenberg, A.: Protein kinase C inhibitors eliminate hippocampal long-term potentiation. Brain Res. **436**, 177–183 (1987).
23. Malenka, R. C., Ayoub, G. S., Nicoll, R. A.: Phorbol esters enhance transmitter release in rat hippocampal slices. Brain Res. **403**, 198–203 (1987).
24. Malenka, R. C., Madison, D. V., Andrade, R., Nicoll, R. A.: Phorbol esters mimic some cholinergic actions in hippocampal pyramidal neurons. J. Neurosci. **6**, 475–480 (1986).
25. Rane, S. G., Dunlap, K.: Kinase C activator 1,2-oleoylacetylglycerol attenuates voltage-dependent calcium current in sensory neurons. Proc. Natl. Acad. Sci. USA **83**, 184–188 (1986).
26. Safran, A., Provenzano, C., Sagi-Eisenberg, R., Fuchs, S.: Phosphorylation of membrane-bound acetylcholine receptor by protein kinase C: characterization and subunit specificity. Biochemistry **29**, 6730–6734 (1990).

27. Sawada, M., Ichinose, M., Maeno, T.: Protein kinase C activators reduce the inositol trisphosphate-induced outward current and the $Ca^{2+}$-activated outward current in identified neurons of *Aplysia*. J. Neurosci. Res. **22**, 158–166 (1989).
28. Shapira, R., Silberberg, S. D., Ginsburg, S., Rahamimoff, R.: Activation of protein kinase C augments evoked transmitter release. Nature **325**, 58–60 (1987).
29. Strong, J. A., Fox, A. P., Tsien, R. W., Kaczmarek, L. K.: Stimulation of protein kinase C recruits covert channels in *Aplysia* bag cell neurons. Nature **325**, 714–717 (1987).
30. Szente, M. B., Baranyi, A., Woody, C. D.: Effects of protein kinase C inhibitor H-7 on membrane properties and synaptic responses of neocortical neurons of awake cats. Brain Res. **506**, 281–286 (1990).
31. Taniyama, K., Takeda, K., Ando, H., Kuno, T., Tanaka, C.: Expression of the $GABA_B$ receptor in Xenopus oocytes and inhibition of the response by activation of protein kinase C. FEBS Letters **278**, 222–224 (1991).
32. Werz, M. A., Macdonald, R. L.: Dual actions of phorbol esters to decrease calcium and potassium conductances of mouse neurons. Neurosci. Lett. **78**, 101–106 (1987).
33. Zhang, L., Krnjevic, K.: Effects of intracellular injections of phorbol ester and protein kinase C on cat spinal motoneurons in vivo. Neurosci. Lett. **77**, 287–292 (1987).

*Acta Physiologica Hungarica, Volume 81 (2), pp. 159–174 (1992)*

# EFFECTS OF INTRACELLULARLY APPLIED AMINOPYRIDINE ON FIRING ACTIVITIES AND SYNAPTIC RESPONSES OF ELECTROPHYSIOLOGICALLY IDENTIFIED CELL TYPES IN THE MOTOR CORTEX OF CATS

Magdolna B. SZENTE, A. BARANYI

JÓZSEF ATTILA UNIVERSITY, DEPARTMENT OF COMPARATIVE PHYSIOLOGY, SZEGED, HUNGARY

Received March 10, 1992
Accepted April 29, 1992

Effects of 3-aminopyridine (3-Ap) applied intracellularly into electrophysiologically identified cortical neurons in the cat motor cortex were studied. Actions on the membrane and firing activity properties, excitatory and inhibitory postsynaptic responses were investigated. Intracellular microelectrode techniques and single electrode voltage clamp methods were used in experiments on anesthetized and chronic nonanesthetized cats. In addition to changes in neuronal excitability and firing activity properties the evoked postsynaptic responses were significantly altered. Augmentation of EPSPs was accompanied by increases of the total duration and amplitude of the second slow component of IPSPs without influencing the early fast IPSP component. It is concluded that most actions of 3-Ap reported here are derived from direct effects of 3-Ap on the postsynaptic membrane.

**Keywords**: aminopyridine, firing activities, synaptic response, electrophysiology, motor cortex

We have been dealing with the mechanisms of convulsive actions of locally applied 3-aminopyridine (3-Ap) as an experimental model of focal epileptic phenomena in the neocortex for fifteen years.

In earlier papers we have characterized ECoG patterns of 3-Ap-induced seizure activity and accompanying, seizure-related intracellular events both in the primary and mirror foci of anesthetized cats [1, 26, 27, 41–44].

In this report we describe effects of intracellularly applied 3-Ap on the membrane and firing activity properties, excitatory and inhibitory postsynaptic responses of electrophysiologically identified neurons in the cat motor cortex.

Aminopyridine is a relatively specific blocker of the early, transient $K^+$ current or A-current [11, 15, 17, 33, 35, 48, 49] although other evidences suggest it might

Correspondence should be addressed to
Magdolna B. SZENTE
József Attila University, Department of Comparative Physiology
H–6701 Szeged, P.O.B. 533, Hungary

*Akadémiai Kiadó, Budapest*

affect $Ca^{2+}$ currents as well [33–35]. In the soma-dendritic region, these postsynaptic effects may decrease the threshold and latency of action potentials [34], whereas at presynaptic terminals they facilitate neurotransmitter release [47]. Therefore, the aim of the present work was, to investigate the local, mainly postsynaptic actions of intracellularly applied 3-Ap into the recorded neurons.

## Materials and Methods

Experiments were performed on the motor cortex of anesthetized acute or conscious chronic cats.

*Preparation of acute cats for intracellular recording*

Adult cats weighing 2.5–3.5 kg were anesthetized with sodium pentobarbital (35 mg/kg; i.p.). The femoral vein was cannulated and an endotracheal tube inserted. The pericruciate cortex was exposed on both sides and covered with warm paraffin oil to prevent drying. The body temperature of animals was kept at 38 °C. An active bridge was used to inject currents and drugs into the recorded cells. Intracellular injection of 3-Ap was carried out by depolarizing current injection via the recording electrode (0.2–2.0 Hz, 200–500 ms, 2–3 nA for 2–8 min). The electrodes were filled with 100 mM 3-Ap dissolved in 0.5 M K-citrate. Intracellular signals and field potentials were stored on a 4-channel FM tape recorder (DC, 10 kHz) and photographed from the screen of a Tektronix storage oscilloscope. Other details concerning recording and stimulating circumstances were similar to those used in chronic experiments (see below).

*Preparation of cats for chronic intracellular recording*

The animals were prepared initially under sodium pentobarbital anesthesia (35 mg/kg i.p.) for subsequent intracellular recordings [4, 7, 45, 49]. Bipolar stimulating electrodes (SNEX–200, Rhodes Medical Inns., U.S.A.) were inserted stereotaxically in pedunculus cerebri (F: 6.5, L: 6.0, H: –5.0) and ventrolateral (VL) thalamic nucleus (F: 10.5, L: 4.0, H: 1.5), and fixed permanently to the skull [4, 7, 45]. On the day of surgery and on a 3–4 days basis postoperatively, the cats received Crysticillin Penicillin G (200,000 units) and Bicillin Penicillin G (150,000 units). During recordings the animals were awake, undrugged, and their bodies were loosely restrained in a cloth bag. The head of the cat was affixed to a David Kopf stereotaxic frame by means of four previously implanted stainless steel bolts. A small (1 mm diam.) orifice made above area 4 gamma under local anesthesia allowed insertions of the recording microelectrode into the motor cortex. After insertion the orifice was closed with steril agar (41 °C, 4%, in 0.9% NaCl). During experiments the behaviour of animals was continuously observed, and the studies were discontinued if the animals gave any signs of discomfort. These experiments were carried out according to guidelines of the Amer. Physiol. Society, the Society for Neuroscience and the University of California.

*Intracellular recordings, and data acquisition techniques*

Micropipettes were pulled from 1.5 mm (O.D>) theta- or omegadot capillaries and filled (in different experiments) with the following solutions: 1 M K-citrate, 20–50 mM QX-314 (N-(2,6-dimethylphenylcarbamoylmethyl-) triethylammonium bromide, Astra Pharmaceutical Product Inc., Worchester, MA), 50 or 100 mM 3-aminopyridine (3-Ap, Sigma), these solutions were made up in 1 M K-citrate. In chronic cat experiments 3-Ap and other drugs were injected intracellularly by pressure. The tips of microelectrodes were broken to < 0.5 μm (tip resistance: 20–40 MOhm) to permit intracellular recordings and pressure injection (5–7 $Kg/cm^2$ for 0.5–1.0 s) of a 3–6 μm (diam.) droplet of electrode

content [4, 7, 45]. In an average size neuron (30–40 μm diam.) a droplet of about 3 μm (diam.) of electrode content (50 mM 3-Ap in 1 M K-citrate) resulted in about 0.5 mM 3-Ap concentration.

Neuronal activity was fed through an Ag/AgCl wire to a Dagan 8100-1 DC electrometer amplifier. Electrodes that showed polarization during ± 5.0 nA, 50–100 ms current steps were discarded. Prior to and after cell penetrations the bridge was carefully balanced. With optimal capacity compensation the duration of capacitive artifacts of the voltage responses were < 0.3 ms and symmetrical at the make and break points of ± 1.0 nA constant current pulses. Resting membrane potential ($V_r$) and other parameters were measured 2–5 min after penetration. Spike threshold ($T_{50}$) was measured by injecting depolarizing constant current pulses (50–100 ms at 0.1–0.5 Hz), and voltage deflections were measured from $V_r$ to the initiation point of the spike. The whole neuron apparent input resistance ($R_N$) was measured by small hyperpolarizing constant current pulses (–0.2–1.0 nA, 50–200 ms at 0.1–0.5 Hz) at $V_r$, and the steady-state amplitude of 5–10 averaged voltage responses was used to calculate $R_N$. Membrane time constant ($T_m$) was calculated from the slope of log dV/dt vs. t after a regression line was fitted to semilog plots of averaged voltage records [7]. Spike amplitude was measured from threshold to peak, and spike duration at half amplitude. The amplitude of fast and slow afterhyperpolarizations of action potentials (fAHP, sAHP respectively) were measured from the firing threshold to the peak of AHPs.

For voltage clamp recording electrodes were connected to a Dagan 8100-1 custom-modified single channel voltage clamp (SEVC) amplifier through Ag/AgCl wires. Electrode rectification was tested in the cortex with currents of ± 5 nA. Care was taken to use microelectrodes with suitable resistances (15–30 MOhm). Capacitance compensation and switching frequency (5–7 kHz, using a duty cycle of 50%) were adjusted to allow the charging transients of electrode voltage to settle completely between oscillations [4, 45, 49]. These were achieved by (i) monitoring the headstage output as reasonably square [13]; (ii) checking that the amount of current flow was identical under current-clamp and voltage-clamp mode as measured with rectangular pulses of ± 2 nA [11]; and (iii) by increasing the gain together with adjustment of the phase until the desired holding potential was reached. Current and voltage records were displayed on an oscilloscope and stored on FM tape (DC-5 KHz band pass).

During experiments voltage and current signals were continuously monitored on a Tektronix storage oscilloscope and stored on magnetic tape (DC–5 kHz bandpass) for subsequent analysis. Averages of the records were made off-line by a PDP–11 computer at a rate of 20 kHz AD conversion. Statistical calculations were carried out on a Hewlett-Packard HP-28 S computer with general statistical programs. Experimental values are expressed as mean ± standard deviation (S.D.) of measurement. Null hypothesis was rejected when $p > 0.05$ was found using a two-tailed Student's *t*-test.

*Electrophysiological identifications of neurons and their synaptic responses*

PT (pyramidal tract) neurons were identified by their antidromic spikes to peduncular stimulation. Fast (fPT) and slow (sPT) PT neurons were also distinguished by the latency of their antidromic responses (< 2 ms in fPT, > 2 ms in sPT cells), as well as by other electrophysiological criteria [2, 3, 30]. All other cells were considered as non-pyramidal tract (nPT) neurons. Four classes of neurons were distinguished on the bases of patterns of firing: 1) regular-spiking (rsp; PT and nPT cells); 2) inactivating bursting (ib; PT and nPT cells); 3) non-inactivating bursting (nib; PT and nPT cells) and 4) fast-spiking (fsp; nPT) neurons (cf. [5, 6]).

Synaptic responses were elicited by stimulation of VL (0.2–0.7 mA; 0.1 ms; 0.3 Hz) and PT (0.2–0.5 mA; 0.1 ms; 0.3 Hz). The latency of onset and peak latency of excitatory postsynaptic potentials (EPSPs) were measured from the middle of stimulus artifact to the onset and the peak, respectively. The duration of EPSPs ($T_{EPSP}$) was measured at half amplitude.

## Results

Since no consistent differences were found in the effects of intracellularly applied 3-Ap in awake and anesthetized animals, the results are treated together.

The effects started within 0.5–1 min, reached their maximal level 2–6 min after injection and lasted for the end of intracellular recordings (about 40–50 min in most cases).

In voltage clamp experiments the early, rapidly activated outward currents, resembled to those of A-currents were consistently reduced or eliminated by intracellular application of 3-Ap (Fig. 1; cf. [49]).

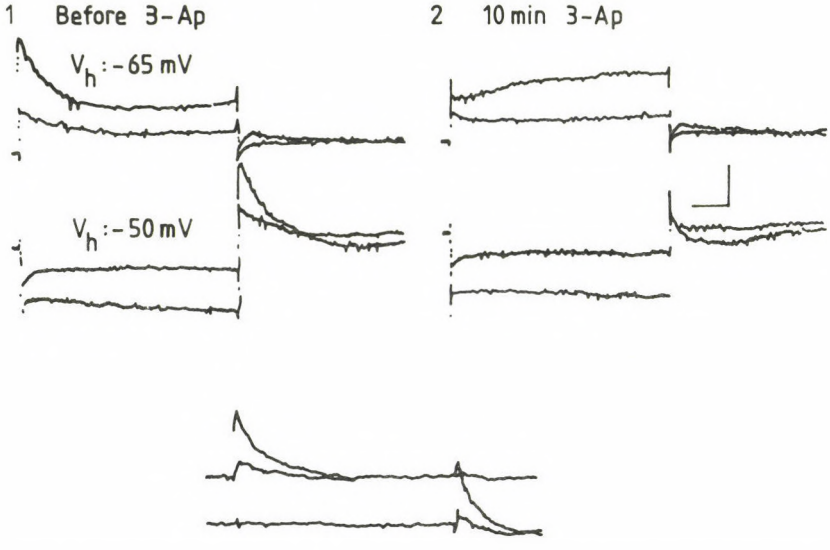


Fig. 1. Changes of membrane currents in PT cells after intracellular injection of 3-Ap and QX-314. *1*: Voltage clamp record 4 min after penetration with an electrode containing 25 mM QX-314 and 50 mM 3-Ap. A transient, fast-activating and inactivating outward current was observed at the onset of depolarizing command pulses of +20 and +40 mV, stepped from −65 mV holding potential ($V_h$). Hyperpolarizing command pulses of −20 and −40 mV stepped from −50 mV of $V_h$ reactivated the fast outward current at their offsets (superimposed records). *2*: 10 min after 3-Ap (and QX-314) injection the fast outward current was reduced and the firing activity was suppressed. The net current blocked by 3-Ap (below) was given by subtracting current measurements before and after injection of 3-Ap. Calibrations: 2 nA, 20 ms

3-Ap did not produce significant changes in the $V_r$ of $T_m$ of different cell types (Table I). The $R_N$ showed only moderate (< 20%) increases, mostly in cells with repeated 3-Ap injection (n = 21 neurons).

**Table I**

| | regular spiking control 3-Ap | bursting control 3-Ap | fast spiking control 3-Ap | |
|---|---|---|---|---|
| n | 165 | 120 | 42 | cells |
| | 26 | 22 | 9 | |
| $V_r$ | 65.3 ± 3.3 | 66.2 ± 3.2 | 63.6 ± 41 | mV |
| | 64.6 ± 4.4 | 65.5 ± 4.2 | 62.2 ± 4.3 | |
| $R_N$ | 8.8 ± 2.7 | 12.9 ± 2.8 | 19.9 ± 2.1 | MOhm |
| | 9.8 ± 2.6 | 13.4 ± 2.2 | 20.6 ± 2.7 | |
| $T_m$ | 12.8 ± 2.4 | 12.7 ± 2.2 | 7.2 ± 1.4 | ms |
| | 13.0 ± 1.8 | 12.1 ± 3.1 | 7.1 ± 3.1 | |
| $T_{50}$ | 53.9 ± 1.0 | 53.9 ± 2.1 | 54.3 ± 2.8 | mV |
| | 57.2 ± 2.0 | 58.2 ± 3.3 | 53.8 ± 2.1 | |
| ampl. of | 74.5 ± 4.2 | 75.0 ± 3.9 | 72.2 ± 2.3 | mV |
| action p. | 72.6 ± 3.1 | 74.3 ± 4.0 | 73.3 ± 1.8 | |
| dur. of | 0.68 ± 0.12 | 0.62 ± 0.11 | 0.25 ± 0.14 | ms |
| action p. | 0.75 ± 0.16 | 0.92 ± 0.17 | 0.26 ± 0.22 | |
| ampl. of | 8.7 ± 5.1 | 5.4 ± 1.7 | 12.2 ± 2.6 | mV |
| fAHP | 8.4 ± 4.1 | 5.7 ± 2.1 | 13.1 ± 3.1 | |
| ampl. of | 7.3 ± 4.3 | 7.3 ± 51 | – | mV |
| sAHP | 10.6 ± 3.8 | 10.2 ± 4.1 | | |
| dur. of | 66.9 ± 22.5 | 68.8 ± 16.5 | – | ms |
| sAHP | 73.0 ± 26.3 | 76.0 ± 17.6 | | |

Parameters were measured as described in section Materials and Methods.
Values are means ± S.D. –: lacks property

The duration of action potentials did not change significantly in most rsp/fPT, nib (PT and nPT) and fsp neurons (Fig. 2 A, C) whereas it increased in rsp/sPT and ib/nPT neurons (Fig. 2 and Table I). 3-Ap had little effects on the shape of action potentials in fsp neurons. The depolarizing afterpotentials following action potentials enhanced in nib/PT, ib/PT and rsp/nPT neurons (Figs 2; 3A). The summated and increased spike DAPs induced slow spikes with high threshold, resembling calcium-spikes (Fig. 4 A2). Summations of DAPs and slow spikes frequently resulted in depolarizing plateau potentials that were similar to paroxysmal depolarization shift (PDS), described in previous studies that representing the cellular correlate of interictal spikes [12, 25]. Depolarizing plateau potentials were usually followed by afterhyperpolarization and inhibition of neural firing activity (Fig. 4 A3).

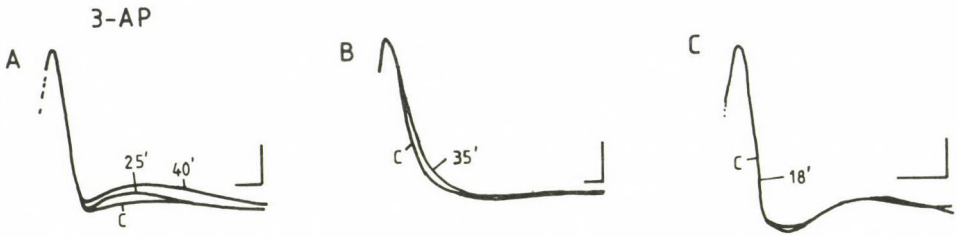


*Fig. 2.* Effects of intracellularly injected 3-Ap on the shape of action potentials. A: fPT regular spiking and non-inactivating bursting neurons; B: sPT regular spiking and inactivating bursting neurons; and C: nPT fast spiking cells. Records marked by C show action potentials before 3-Ap injection; Numbers indicate minutes after injections of 3-Ap. Oscilloscope was triggered by the action potentials. Calibrations: 20 mV; 0.5 ms

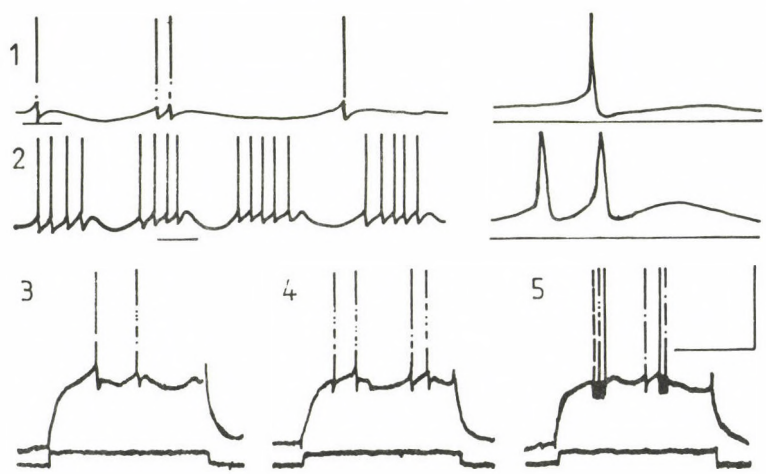


*Fig. 3.* Effect of intracellularly injected 3-Ap on the firing pattern of two nPT cells. *1*: spontaneous firing activity before 3-Ap injection and *2*: 7 min after 3-Ap injection. The firing activity increased and bursts of action potentials developed. Right part: records at higher speed from the underlined parts of 1, 2. The repolarizing phase of the action potentials slightly increased, and depolarizing afterpotential developed; *3–5*: Records taken from an another cell, before (3), and 4 or 9 mins after injection of 3-Ap (4, 5). Depolarizing pulses of 80 ms, 1.05 nA and 0.2 Hz were given to measure membrane excitability changes. Injection of 3-Ap increased the excitability of the cell and induced bursts of action potentials. Calibration: 50 mV, 10 nA and 75 ms, 40 ms (3–5)

The amplitude and duration of slow afterhyperpolarizations (sAHP) following action potentials or bursts were increased by 3-Ap. (Table I and Fig. 5; ib and nib cells). No consistent changes in fAHPs and in the amplitude of action potentials were observed after 3-Ap injection.

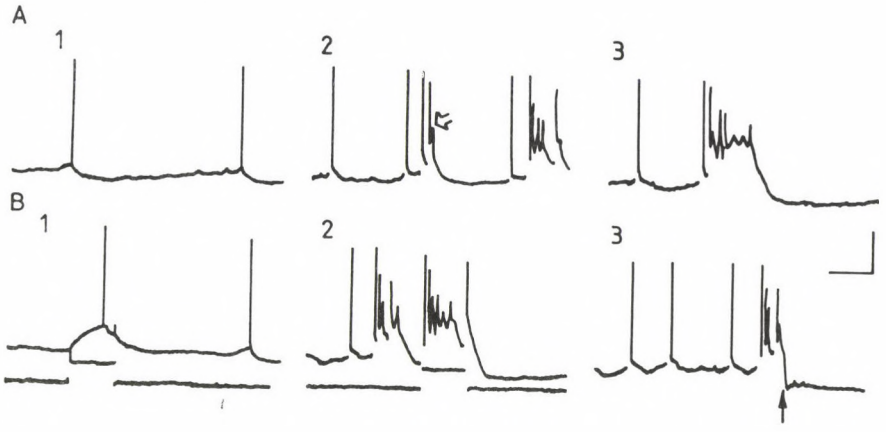


*Fig. 4.* Intracellular records from a slow PT neuron before and 10–12 min after injection of 3-Ap (150 mM). A1 and B1 are controls before pressure injection. Ten minutes after injection (A2, B2), slow spikes with small amplitudes and high-threshold were generated as a result of increased spike DAPs (marked by open arrowhead). Summations of DAPs and slow spikes resulted in depolarizing plateau potentials. Depolarizing plateau potentials could also be elicited by intracellular injection of depolarizing current pulses (B2), and terminated by VL IPSPs (B3, VL stimulation is marked arrow). Calibration: 30 mV, 2 nA, 60 ms

The firing activity increased after injection of 3-Ap and action potentials occurred in doublets and triplets (Fig. 3A1, 2). Burst generation both spontaneously and in response to depolarizing current steps were induced in the different cell types (Figs 3 A3–5 and 5). fsp/nPT cells did not show significant changes in these parameters to 3-Ap. The depolarizing envelopes underlying bursts of action potentials gradually increased in ib cells, and small, inactivating action potentials of long duration occurred on their tops. Increases in the depolarizing envelope of bursts, both in duration and in amplitude often resulted in depolarizing plateau potentials (Fig. 6B, C).

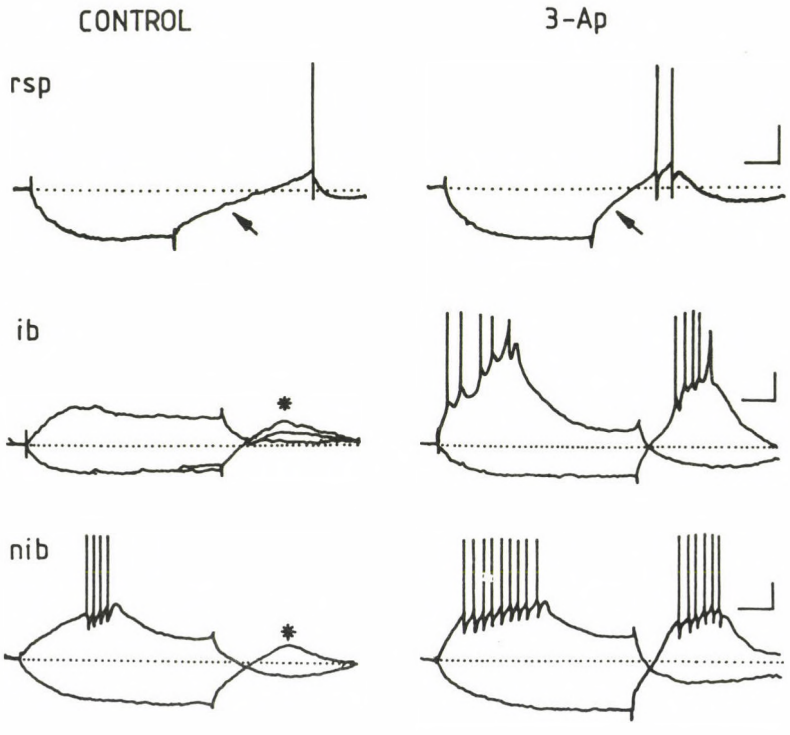


*Fig. 5.* Effects of intracellularly injected 3-Ap on the membrane and firing properties of different types of cells. Before injection (control) an outward rectification (due to activation of A-current (oblique arrows) or an inward rectification (in bursting cells, marked by stars, due to activation of Ca-conductance) are shown. After injection of 3-Ap (10 min) the outward rectification was reduced, the firing activity increased parallel with decreases of the firing threshold. Note increases of spike depolarizing afterpotential especially in sPT and bursting neurons. Calibration: 10 mV for rspneuron, 20 mV for others, 20 ms for all recordings. The amplitude of action potentials are truncated at higher amplifications

The effects of 3-ap on voltage responses to intracellular current injections were characteristic in different cell types (Figs 3A and 5). The number of spikes increased and the latency of the first action potential to depolarizing pulses decreased (Table I). The fast outward rectification, due to the activation of A current at the beginning of depolarizing voltage response and after hyperpolarizing current pulses were regularly suppressed after 3-Ap injection (Fig. 5). In bursting cells, small hyperpolarizing current pulses (<1.0 nA) were not followed by bursts if the same

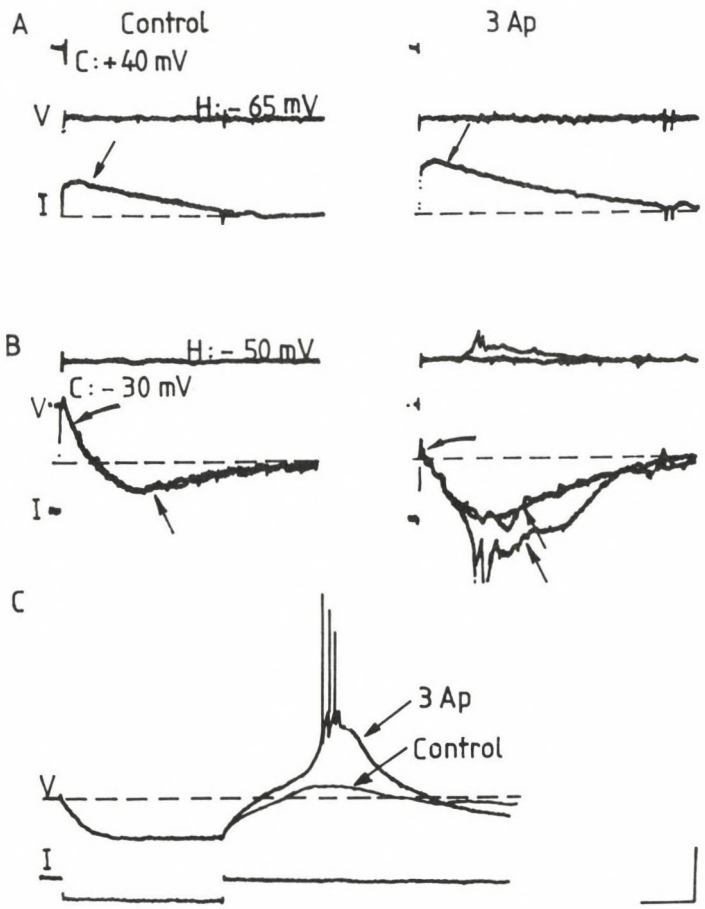


*Fig. 6.* Actions of intracellularly injected 3-Ap. Single electrode voltage clamp (A, B) and bridge records (C) were taken before (control) and 10 min after injection of 3-Ap. Inward currents are downward, outward currents are upward. V indicates voltage- and I-current records. A: current records from a PT neuron. The slow outward current (arrows) which appeared at the offset of +40 mV command steps (C) from a holding potential (H) of −65 mV increased after injection of 3-Ap. B: current records from a bursting nPT neuron. Three subsequent records are superimposed. Curved arrows at the offset of hyperpolarizing commands indicate the fast outward current which was reduced after injection of 3-Ap; straight arrows show the concurrent inward current occurring after the end of hyperpolarizing commands. This current was disclosed and enlarged as the fast outward current was reduced after injection of 3-Ap. The largest action potential-related conductances (lowest current record) could not be controlled completely by the SEVC. Spike currents are truncated. Dashed lines give zero current reference in A and B. C: voltage records from the neuron illustrated in B. 3-Ap facilitated a low-threshold depolarizing conductance appearing at the offset of hyperpolarizing pulses (control) which triggered bursts of action potentials after injection of 3-Ap. Dashed lines indicate resting membrane potential of −62 mV. Calibration: 2 nA, 20 ms in A and B, 2 nA, 20 mV, 20 ms in C [42]

depolarizing current pulse did not induce burst (Fig. 5 marked by stars at ib and nib cells). After 3-Ap injection burst was usually induced at the end of hyperpolarizing pulses of the same small intensity.

In voltage clamp experiments we have observed an inward current, at the offset of hyperpolarizing commands corresponding to the depolarizing envelope of bursts. Inward currents of this type were observed only if voltage steps were longer than 60–80 ms and the holding potentials were more positive than the resting potential [41] (Fig. 6). The coexistence of activation of this inward current simultaneously with the A current, even at subthreshold depolarizing membrane potentials, was found most frequently in bursting neurons. After injection of 3-Ap the inward current increased and the concurrent A current decreased.

In 3-Ap injected cells it was possible to induce depolarizing plateau potentials by depolarizing current pulses [41] (Fig. 4 B1, 2). Depolarizing plateau appearing spontaneously or induced by intracellular current injection in 3-Ap injected cells had features similar to those appearing spontaneously in cells of epileptic foci (Fig. 4 B2–3).

*Effects of 3-Ap on the synaptic responses*

*Excitatory postsynaptic responses*

The amplitude of EPSPs significantly increased (up to 178 ± 12%) in 38 of 73 3-Ap injected cells (Fig. 7A). In the rest of the cells, the amplitude increases in EPSPs amounted < 120% of the control values. These represent only a moderate increase of about 1 mV (control EPSP amplitude was 3–5 mV). The effects culminated within 2–6 min after injection and lasted until the end of the recordings. The extrapolated reversal potential of the EPSPs (−5 ± 2.1 mV, n = 18 cells) did not change significantly by 3-Ap. The increases in amplitudes were detected not only at $V_r$ but also during 1–2 nA de- or hyperpolarizing current injection (not shown). This observation suggests that the blockage of voltage-dependent A channels by 3-Ap did not contribute directly and significantly to the amplitude increases of EPSPs.

In voltage clamp measurements increases in the amplitude and slope of the raising phase of excitatory postsynaptic currents (EPSCs) were measured after 3-Ap injection (Fig. 7B). In 16 cells we could measure the reversal potential of EPSC before and after injection of 3-Ap. 3-Ap did not induce significant changes in the reversal potential of EPSCs (Fig. 7B). These results confirmed our observations on the EPSPs in voltage recording experiments (see above). Parallel with increases in amplitude, the duration of EPSCs was almost doubled. In about 50% of the cells EPSCs was not significantly changed by 3-Ap in spite of definite block of A current.

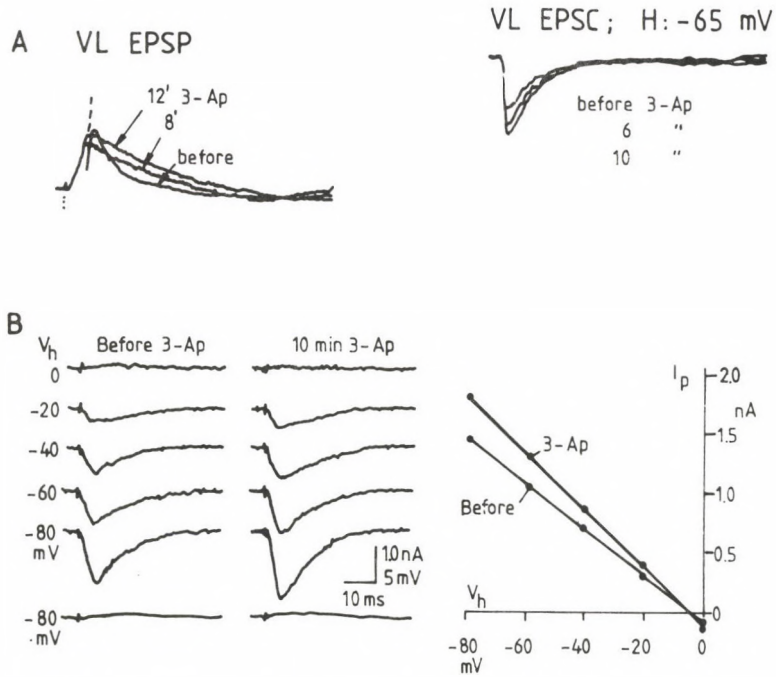


*Fig. 7.* A: Effects of intracellularly injected 3-Ap on VL EPSPs/ EPSCs in a regular spiking neuron. Note increases in both the amplitude and duration of the EPSP. B: Effects of intracellularly injected 3-Ap on VL EPSCs in an fPT neuron penetrated with an electrode filled with 30 mM QX-314 and 50 mM 3-Ap. Eight current responses were averaged for each trace at the different holding potentials ($V_h$) before and 10 min after injection. 3-Ap increased the amplitude of EPSCs at each holding level tested, while the I–V curve of the EPSC remained linear and the reversal potential did not change

### *Inhibitory postsynaptic responses*

Effects of 3-Ap on evoked inhibitory postsynaptic potentials (IPSPs) were analyzed by measuring their amplitude and duration (n = 16 cells, Fig. 8). IPSP amplitudes were measured 20–30 ms or 40–70 ms after stimulation. These latencies corresponded to the peak of the rapidly decaying IPSP, and the second, slowly raising and decaying IPSP [44]. To avoid the contamination of IPSPs with slow spike AHPs, cells which fired action potentials to VL or PT stimulation were excluded from these analysis. 3-Ap did not change the peak amplitude of the first IPSP, but significantly enhanced the amplitude of the second IPSP, parallel with increases in the total duration of the IPSP. All these effects developed quickly and reached maximum levels in about 4 min after injection, and than they expressed a much slower decay (Fig. 8 B). Changes in the early IPSP could be masked by potentiation of an

overlapping EPSP. However, significant changes in the early IPSP phase was not observed in those 5 cells in which 3-Ap did not produce potentiation of the EPSP. The results indicate a potentiation of the second, slow IPSP component.

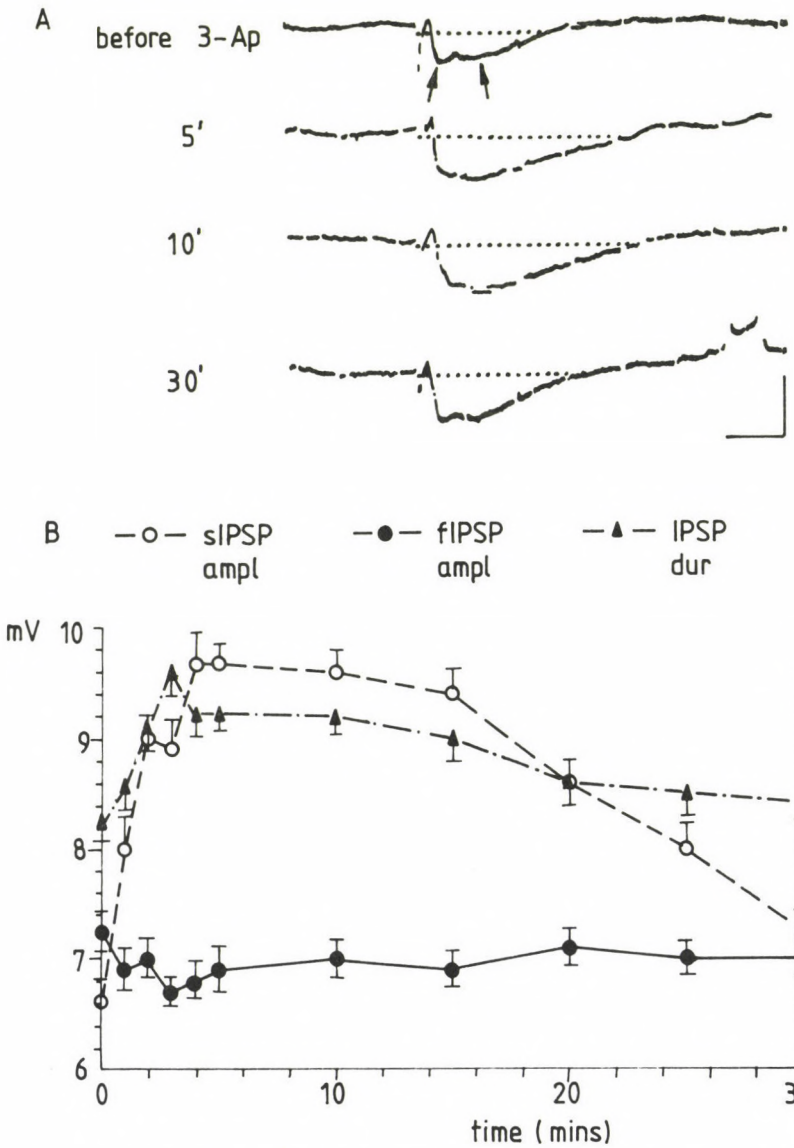


*Fig. 8.* Effects of intracellularly injected 3-Ap on the PT IPSP in an rsp/fPT cell. Arrows point to the peak of the early and the late IPSPs. A: time course of changes in the amplitudes of IPSPs measured at 20 or 50 ms after the stimulus, and the total duration of IPSPs are illustrated. Data points represent averages of 10 successive IPSPs. Calibrations: 10 mV; 50 ms

## Discussion

In this study we investigated the effects of intracellularly applied 3-Ap on the membrane and firing properties, and on the evoked synaptic responses of neurons of the motor cortex of cats. The results indicate that in addition to changes in neuronal excitability and firing properties the excitatory and inhibitory synaptic responses were also markedly altered. During 3-Ap actions no significant changes in the resting potential or input resistance occurred in the neurons studied. The prolongation of the repolarizing phase of action potentials was most characteristic in bursting cells. No consistent changes in duration of action potentials was found in fast spiking cells. Extracellular application of 4-Ap have little effects on action potential characteristics of adult myelinated axons [22] or cat spinal cord [19–20], but action potentials were broadened in unmyelinated axons [8, 9, 16, 46]. This observations can be interpreted by the variability in the quality and density of ion channels in different cell membranes. Prolongation of the repolarizing phase of action potentials can facilitate both burst generation and induction of slow spikes of higher threshold, resembling Ca-spike as it was described by others when aminopyridine was applied extracellularly [20].

Both applied 4-Ap enhanced both excitatory and inhibitory postsynaptic responses in the hippocampus [31, 32, 36]. Furthermore, both the early (mediated by $GABA_A$ receptor activation) and late phase (presumable mediated by $GABA_B$ receptor activation) of IPSPs were potentiated by 4-Ap in hippocampal CA1 and CA3 cells in vitro [32, 36]. It was concluded that potentiation of synaptic transmission produced by 4-Ap resulted primarily from presynaptic mechanisms due to facilitation of neurotransmitter release [31, 32, 39, 46, 47], or activation of recurrent excitatory collaterals [24, 27]. In the present study, on cells of the cat motor cortex intracellularly applied 3-Ap induced potentiation of EPSPs, prolonged the total duration of IPSPs, and increased the amplitude of the second, slow IPSP without much influences on the early, fast IPSP component.

The facilitatory effect of 3-Ap on excitatory postsynaptic responses was observed not only at $V_r$ but also at de- and hyperpolarized levels of membrane potential. This suggest that not only the blockage of voltage-dependent A channels are involved in the increases of EPSPs after injection of 3-Ap. One can suppose that ligand-gated A channels or other (as yet unknown) mechanisms are involved in these effects of 3-Ap. The two kinds of A channels probably have neuron- and input-specific features and they can influence EPSPs in a rather complex way, which needs further analysis.

Since 3-Ap was applied postsynaptically into the recorded cells, its maximal effects developed rapidly. In addition, 3-Ap influenced the fast and slow of IPSP components differentially. Therefore it is suggested that 3-Ap exerted its effects

mainly postsynaptically (through binding sites at the inner surface of the membrane of injected cell). Earlier studies when 4-Ap was applied extracellularly, indicated a marked pH dependence and latency of block of potassium channels which suggested that 4-Ap acted at the internal surface of the membrane [14, 17]. These suggestions have been directly confirmed by patch-clamp studies [33]. Although presynaptic effects (after leaking of 3-Ap to the extracellular space) cannot be excluded completely in our study, the differential effect of 3-Ap on the two components of IPSP is against a generalized action on synaptic transmission by presynaptic mechanisms. The effects of 3-Ap on neuronal excitability and firing properties can be explained by blockage of A channels [37] although other contributory mechanisms cannot be excluded. In hippocampal neurons very low (micromolar) concentrations of 4-Ap have been shown to block a slowly inactivating potassium current ($I_D$) [40]. Aminopyridine may have an additional action to facilitate calcium influx by means of direct action on voltage-dependent calcium channels apart from effects on potassium currents [34, 38].

At present, there is no data showing effects of aminopyridine on $Cl^-$ channels. This can explain our observations that the early $Cl^-$ mediated component of the IPSPs did not change after intracellular injection of 3-Ap. On the other hand, direct or indirect facilitation of calcium movements either through the plasma membrane or the membranes of intracellular organelles also can facilitate a potassium outflow through $Ca^{2+}$-dependent channels [34]. The late, slowly decaying component of IPSPs is generated by a $Ca^{2+}$-dependent $K^+$ conductance in neocortical cells [45]. Therefore selective increases in this late IPSP component can be interpreted as an increase of Ca-dependent $K^+$ conductance following direct or indirect facilitation of calcium movements across the cell membrane of 3-Ap injected cell.

From these results we suppose that most actions of the 3-Ap reported in this paper are derived from direct effects of 3-Ap on the postsynaptic membrane.

## REFERENCES

1. Baranyi, A., Fehér, O.: Convulsive effects of 3-aminopyridine on cortical neurons. Electroenceph. Clin. Neurophysiol. **47**, 745–751 (1979).
2. Baranyi, A., Fehér, O.: Intracellular studies on cortical synaptic plasticity: conditioning effect of antidromic activation on test-EPSPs. Exp. Brain Res. **41**, 124–134 (1981).
3. Baranyi, Szente, M. B., Woody, C. D.: Intracellular injection of phorbol ester increases the excitability of neurons of the motor cortex of awake cats. Brain Res. **424**, 396–401 (1987).
4. Baranyi, A., Szente, M. B., Woody, C. D.: Activation of protein kinase C induces long-term changes of postsynaptic currents in neocortical neurons. Brain Res. **440**, 341–347 (1988).
5. Baranyi, Szente, M. B., Woody, C. D.: Electrophysiological characterization of different types of neurons recorded in vivo in the motor cortex the cat: I. Patterns of firing activity and synaptic responses. J. Neurophysiol. in press.

6. Baranyi, Szente, M. B., Woody, C. D.: Electrophysiological characterization of different types of neurons recorded in vivo in the motor cortex of the cat: II. Membrane parameters, action potentials, current-induced voltage responses and electronic structures. J. Neurophysiol. in press.
7. Baranyi, A., Szente, M. B., Woody, C. D.: Properties of associative long-lasting potentiation induced by cellular conditioning in the motor cortex of conscious cats. Neuroscience **42**, 321–334 (1991).
8. Bostock, H., Sears, T. A., Sherrat, R. M.: The effects of 4-aminopyridine and tetraethylammonium ions on normal and demyelinated nerve fibers. J. Physiol. (London) **313**, 301–315 (1981).
9. Buckle, P. J., Haas, H. L.: Enhancement of synaptic transmission by 4-aminopyridine in hippocampal slices of the rat. J. Physiol. (London) **326**, 109–122 (1982).
10. Chesnut, T. J., Swann, J. W.: Epileptiform activity induced by 4-aminopyridine in immature hippocampus. Epilepsy Res. **2**, 187–195 (1988).
11. Constanti, A., Galvan, M.: Fast inward-rectifying current accounts for anomalous rectification in olfactory cortex neurones. J. Physiol. (London) **385**, 153–178 (1983).
12. Delgado-Escueta, A. V., Ward, A. A., Jr., Woodbury, D. M., Porter, R. J.: Advances in Neurology. New York: Raven Press, vol. **44** (1986).
13. Finkel, A. S., Redman, S. J.: Theory and operation of a single microelectrodes voltage clamp. J. Neurosci. Meth. **11**, 101–127 (1984).
14. Gillespie, J. I.: Voltage-dependent blockage of the delayed potassium current in skeletal muscle by 4-aminopyridine. J. Physiol. (London) **273**, 64–65P (1977).
15. Gustafsson, B., Galvan, M., Grafe, P., Wigstrom, H.: A transient outward current in a mammalian central neuron blocked by 4-aminopyridine. Nature **299**, 252–254 (1982).
16. Haas, H. L., Wieser, H. G., Yasargil, M. G.: 4-Aminopyridine and fiber potentials in rat and human hippocampal slices. Experientia **39**, 114–115 (1983).
17. Hermann, A., Gorman, A. L. F.: Effects of 4-aminopyridine on potassium currents in a molluscan neuron. J. Gen. Physiol. **78**, 63–86 (1981).
18. Jankowska, E., Lundberg, A., Rudomin, P., Sykova, E.: Effects of 4-aminopyridine on transmission in excitatory and inhibitory synapses in the spinal cord. Brain Res. **136**, 87–392 (1977).
19. Jankowska, E., Lundberg, A., Rudomin, P., Sykova, E.: Effects of 4-aminopyridine on Synaptic Transmission in the Cat Spinal Cord. Brain Research **240**, 117–129 (1982).
20. Kasai, H., Kameyama, M., Yamaguchi, K., Fukuda, J.: Biophys. J. **49**, 1243–1247 (1986).
21. Kita, T., Kita, H., Kitai, S. T.: Effects of 4-aminopyridine (4-Ap) on Rat Neostriatal Neurons in an In Vitro Slice Preparation. Brain Res. **361**, 10–18 (1985).
22. Kocsis, J. D., Ruiz, J. A., Waxman, S. G.: Maturation of mammalian myelinated fibers: Changes in action-potential characteristics following 4-aminopyridine application. J. Neurophysiol. **50**, 449–463 (1983).
23. Lundh, H., Thesleff, S.: The mode of action of 4-aminopyridine and guanidine on transmitter release from motor nerve terminals. Eur. J. Pharmacol. **42**, 411–412 (1977).
24. McVicar, B. A., Dudek, F. E.: Local synaptic circuits in rat hippocampus: interactions between pyramidal cells. Brain Res. **184**, 220–223 (1980).
25. Matsumoto, H., Ajmone Marsan, O.: Cortical cellular phenomena in experimental epilepsy. II. Ictal manifestations. Exp. Neurol. **9**, 305–318 (1964).
26. Mihály, A., Joó, F., Szente, M. B.: Neuropathological alterations in the neocortex of rats subjected to local aminopyridine seizures. Acta Neuropathol. **61**, 85–94 (1983).
27. Mihály, A., Tóth, G., Szente, M., Joó, F.: Neocortical cytopathology in focal aminopyridine seizures as related to the intracortical diffusion of (+H)4-aminopyridine. Acta Neuropathol. **66**, 145–154 (1985).

28. Miles, R., Wong, R. K. S.: Excitatory synaptic interactions between CA3 neurons in the guinea pig hippocampus. J. Physiol. (London) **373**, 397–418 (1986).
29. Molgo, J., Lemeignan, M., Lechat, P.: Effects of 4-aminopyridine at the frog neuromuscular junction. J. Pharmacol. Exp. Ther. **203**, 653–663 (1977).
30. Oshima, T.: Studies of pyramidal tract cells. In Basic Mechanisms of the Epilepsies (Eds Jasper, H. H., Ward, A. A. and Pope A.), Little Brown and Co., Boston, pp. 253–262 (1969).
31. Perreault, P., Avoli, M.: Effects of low concentrations aminopyridine of CA1 pyramidal cells of the hippocampus. J. Neurophysiol. **61**, 953–970 (1989b).
32. Perreault, P., Avoli, M.: Physiology and Pharmacology of Epileptiform Activity Induced by 4-aminopyridine in Rat Hippocampal Slices. J. Neurophysiol. **65**, 771–785 (1991).
33. Pettit, A., Davies, N. W., Agarwal, R., Standen, N. B.: The effect of 4-aminopyridine applied externally and internally to ATP-dependent potassium channels of frog isolated skeletal muscle. J. Physiol. **438**, 263 (1991).
34. Rogawski, M. A., Barker, J. L.: Effects of 4-aminopyridine on calcium action potentials and calcium current under voltage clamp in spinal neurons. Brain. Res. **280**, 180–185 (1983).
35. Rudy, B.: Diversity and ubiquity of K channels. Neuroscience **25**, 729–249 (1988).
36. Rutecky, P. A., Lebeda, F. J., Johnston, D.: 4-aminopyridine produces epileptiform activity in hippocampus and enhances synaptic excitation and inhibition. J. Neurophysiol. **57**, 1911–1924 (1987).
37. Segal, M., Rokarski, M. A., Barker, J. L.: A transient potassium conductance regulates the excitability of cultured hippocampal and spinal neurons. J. Neurosci. **4**, 604–609 (1984).
38. Segal, M., Barker, J. L.: Rat hippocampal neurons in culture: $Ca^{2+}$ and $Ca^{2+}$-dependent $K^+$ conductance. J. Neurophysiol. **55**, 751–770 (1986).
39. Shimara, T.: Presynaptic modulation of transmitter release by the early outward potassium current in Aplysia. Brain Res. **263**, 51–56 (1983).
40. Storm, J. F.: Temporal integration by slowly inactivating $K^+$ current in hippocampal neurons. Nature **336**, 379–381 (1988).
41. Szente, M. B., Baranyi, A.: Properties of depolarizing plateau potentials in aminopyridine-inducing ictal seizure foci of cat motor cortex. Brain Res. **495**, 261–270 (1989).
42. Szente, M. B., Baranyi, A.: Mechanism of aminopyridine-induced ictal seizure activity in the cat neocortex. Brain Res. **413**, 368–373 (1987).
43. Szente, M. B., Pongracz, F.: Aminopyridine-induced seizure activity. Electroencephalogr. Clin. Neurophysiol. **46**, 605–608 (1979).
44. Szente, M. B., Pongracz, F.: Comparative study of aminopyridine-induced seizure activities in primary and mirror foci of cat's cortex. Electroencephalogr. Clin. Neurophysiol. **52**, 353–367 (1981).
45. Szente, M. B., Baranyi, A., Woody, C. D.: Intracellular injection of apamin reduces a slow potassium current mediating afterhyperpolarizations and IPSPs in neocortical neurons of cats. Brain Res. **461**, 64–74 (1988).
46. Targ, E., Kocsis, J. D.: Action potential characteristics of demyelinated rat sciatic nerve following application of 4-aminopyridine. Brain Res. **363**, 1–9 (1986).
47. Thesleff, S.: Aminopyridines and synaptic transmission. Neuroscience **5**, 1413–1419 (1980).
48. Thompson, S.: Aminopyridine block of transient potassium current. J. Gen. Physiol. **80**, 1–18 (1982).
49. Woody, C. D., Baranyi, A., Szente, M. B., Gruen, E., Holmes, W., Nenov, V., Strecker, G. J.: An aminopyridine-sensitive, early outward current recorded in vivo in neurons of the precruciate cortex of cats using single-electrode voltage-clamp techniques. Brain Res. **480**, 72–81 (1989).

*Acta Physiologica Hungarica, Volume 81 (2), pp. 175–181 (1993)*

# MODIFICATION IN PRIMARY VISUAL CORTICAL ACTIVITY OF RAT INDUCED BY NEONATAL MONOCULAR ENUCLEATION, AN ELECRTOPHYSIOLOGICAL AND AUTORADIOGRAPHIC STUDY

J. TOLDI, I. ROJIK, O. FEHÉR

DEPARTMENT OF COMPARATIVE PHYSIOLOGY, JÓZSEF ATTILA UNIVERSITY, SZEGED, HUNGARY

Received March 10, 1992
Accepted April 29, 1992

Monocular enucleation was performed in rats at birth. The animals were raised and from the age of 3 months the evoked activity was tested in the contralateral visual cortex both by mapping of evoked potentials and autoradiography. It was found that monocular enucleation changed the distribution of evoked activity characteristically. The focus of activity shifted laterally and restricted itself to the binocular part of the primary visual cortex (Oc1B), while, in the medial part of it (Oc1M) hardly any evoked activity or labelled neurons were found.

**Keywords:** enucleation, evoked potentials, neuronal plasticity, autoradiography, visual cortex

Several studies have demonstrated that the functional and structural organization of visual system may be modified by early postnatal enucleation. After monocular enucleation the number of uncrossed optic fibers and axon terminals coming from the intact eye to the lateral geniculate body (LGB) and superior colliculus was found considerably increased [5, 11, 12]. Transneuronal effects were observed in the visual cortex: a reduction in neuropil volume and spine number of apical dendrites [2, 16]. Changes in callosal connections of the visual cortex were also observed when monocular enucleation was made early enough after birth [4, 6, 15, 17, 18]. As reported earlier, neonatal monocular enucleation induced prominent changes in the visually responsive area in both hemispheres [13]. However, contralateral to the enucleation, the highly responsive area to peripheral stimulation (area responding with the largest amplitudes and shortest latencies) was compact and

Correspondence should be addressed to
József TOLDI
Department of Comparative Physiology, József Attila University
H-6726 Szeged, Középfasor 52, Hungary

*Akadémiai Kiadó, Budapest*

restricted itself to the lateral half of the primary visual cortex while, in its medial part only responses of small amplitude were encountered. According to this finding, short latency unit activity responding to flash stimulation via the remaining eye in the medial part of the primary visual cortex proved to be strongly reduced [13].

These observations raise several questions: 1. In parallel with the lateral shift of evoked cortical activity, could any difference be detected between these two parts of the primary visual cortex with any other method? 2. If so, where is the border between them? 3. What is the explanation for this lateral shift?

To answer these questions, parallel with the electrophysiological recordings autoradiographic studies were carried out. In previous series of experiments it was proved that locally applied [$^3$H]glycine becomes incorporated into proteins of activated nerve cells [9, 10, 14]. This made possible to visualize active neurons by means of light and electronmicroscopic autoradiography. It turned out that a close correlation exists between the level of excitation and the rate of glycine incorporation into some proteins [9, 10].

## Materials and Methods

A total of 11 male and female Sprague-Dawley albino rats (200–300 g) were used in these experiments. The right eye of 7 animals was enucleated on the day of birth, under deep ether anaesthesia. Four of non-enucleated animals of the same litter served as age matched controls. Four enucleated animals were used for both electrophysiological and autoradiographic studies, three others only for autoradiaography. All these rats were sacrificed at the age of 3–4 months. They were anaesthetized with i.p. injection of Nembutal (35 mg/kg); then the left hemisphere was exposed and the dura removed. The pupil of the left eye was dilated with atropine sulphate (2%). After surgery the animals were kept at rest for 1.5–2 hours. The body temperature was maintained at 37 °C. Flashes of white light of 10 ms duration were delivered by a soundproof stroboscope to the left eye (Strobotest I. Knott Elektronik). Stimulus intensities were adjusted so as to evoke maximal responses in the occipital cortex. In non-enucleated (control) animals the right eye was covered with a plastic cup in order to restrict stimulation to the left eye, as in enucleated animals.

Evoked potentials were recorded from the cortical surface. The mapping of EPs was performed in a stereotaxic frame, using a Narishige micromanipulator, under microscopic control. 10 EPs were averaged with the aid of a MOTOROLA MC-6800 computer and the averages were drawn by an X–Y plotter. The maps were evaluated in the following manner. The amplitude of the averaged potentials at the punctum maximum was taken as 100%. All other values were expressed as percentage of it. Potentials less then 10% relative amplitude were not taken into account (Fig. 1). Other details of stimulation, recording and mapping of evoked responses have been described in detail elsewhere [15, 17].

After mapping of evoked potentials, 5 × 5 mm filter paper stripes soaked in [$^3$H]glycine solution were placed onto the surface of occipital cortex and kept there for 1 h. The specific activity of the isotope was 548 GBq/mM = 13.8 Ci/nM. Each filter paper stripe contained about 12 × $10^6$ cpm. During application of the isotope, the ipsilateral eye was stimulated with 2 Hz flashes. After 1 h stimulation, samples of the cortical areas were rapidly excised and fixed in Bouin solution. For light microscopic autoradiography, 10 μm sections were cut from paraffin-embedded blocks [8]. For this purpose, ORWO K106 stripping film was used, the exposure time was 10 weeks. Unstimulated controls were operated in

the same way, treated with glycine for 1 h and the cortical samples were dissected and processed for light microscopic autoradiography parallel with the experimental animals.

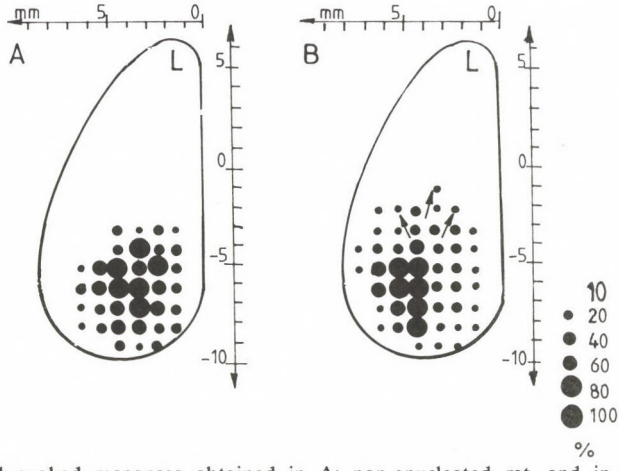


*Fig. 1.* Maps of flash-evoked responses obtained in A: non-enucleated rat, and in B: on 1st-day enucleated adult animal. Potentials were evoked by ipsilateral stimulation. Insert: the dots represent the normalized amplitudes of evoked potentials in percentages of the maximum amplitude

## Results

Since monocular enucleation on the right side induced characteristic changes in the contralateral hemisphere, we present here the results obtained in the left hemisphere. The right eye of non-enucleated animals was completely covered in order to restrict visual stimulation to the left eye (as described above). The maps of visually evoked potentials in the cortex of non-enucleated animals (Fig. 1A) was similar to the normal ones, as published previously [1, 13]. Evoked responses with largest amplitudes and shortest latencies appeared in the primary visual cortex, in the medial and lateral part of it either (area Oc1M and B). Potentials with small amplitudes and long latencies occurred in the secondary visual cortex (area Oc2M and L).

In the left hemisphere of neonatally enucleated animals on the right side, the highly excited area was small and shifted laterally. Evoked potentials with large amplitudes were recordable in the lateral part of the primary visual cortex, near to the border between Oc1B and Oc2L. In the medial part of the primary visual cortex (Oc1M) and in the surrounding secondary visual cortex (Oc2M and L) potentials only with small amplitudes were obtained. Expansion of visually responsive area (responding with small amplitudes and long latencies) into the parietal region was also observed (arrows in Fig. 1B); it is discussed in detail elsewhere [20]. Interestingly

enough, within the primary visual cortex the transition between the highly and less excited fields (areas responding with large and small amplitudes, respectively) was sharp along an antero-posterior line, 4–4.5 mm laterally from the midline (Fig. 1B).

The results of autoradiographic studies are in good accordance with the physiological observations. Coronal sections of the occipital cortices were made between 5 and 8 mm behind the bregma (Fr: −5 and −8).

In non-enucleated, non-stimulated animals the labelling of neurons in the occipital cortex was weak and uniform without any difference between the medial and lateral part. In these animals the weak spontaneous cortical activity resulted in a slight labelling ("background labelling") of neurons. No appreciable differences could be seen between samples taken from the medial and lateral part of the primary visual cortex. Only few weakly labelled pyramidal neurons were seen in layer V (Fig. 2A). Stimulation of the left eye of non-enucleated (control) rats resulted in strong labelling of cortical neurons in layer II, in the upper part of layer III in the pyramidal cells of layer V. The labelling was somewhat stronger in the lateral part of the primary visual cortex however, a good number of labelled neurons was found also in the medial part of it (Fig. 2B).

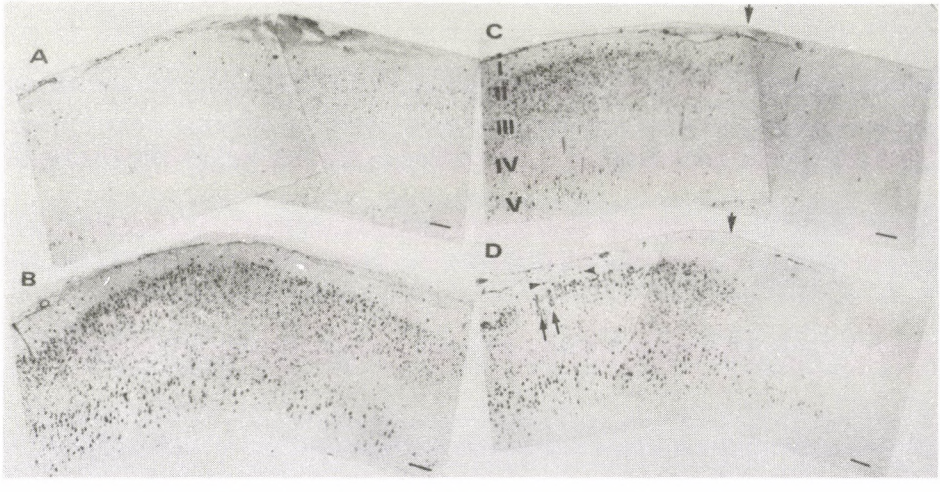


*Fig. 2.* A: Autoradiographic picture from the left occipital cortex of an unstimulated non-enucleated animal. The cortex was treated with [$^3$H]glycine for 1 h. B: The same taken from a non-enucleated animal of which left eye was stimulated. C: The same taken from an enucleated non-stimulated animal. D: The same taken from an enucleated animal stimulated through the left eye. Big arrows show the borders between the highly and much less activated cortical regions. Small arrows in D show the narrow columns of intensely labelled small pyramids and Golgi II neurons in layer II. Scale bar: 200 μm

In enucleated non-stimulated animals the high level of "background labelling" caused by the spontaneous cortical activity differed from that seen in the control ones (Fig. 2C). In the lateral part of the primary visual cortex the neurons were intensively labelled in the upper layers (II and III) and few of them in layer V, while, in the medial part of it (right to the big arrow in Fig. 2C) hardly any labelled neurons were found throughout the cortex.

The flash stimulation through the remaining eye of enucleated animals resulted in an extensive labelling of different type of neurons in the lateral half of the visual cortex. Strongly labelled neurons appeared in layers II and IV. Because of the fine labelling the apical and basal dendrites of some of the pyramidal cells in layer V could be distinguished. The pyramidal cells formed small groups consisting of 2–4 neurons, in some cases together with satellite cells.

Some regularity in the arrengement of those of few cells labelled in layer II was also recognizable: they were situated in a row parallel with the cortical surface (arrowheads in Fig. 2D). In layer II and in the upper part of layer III small pyramids and Golgi II neurons formed narrow columns oriented vertically to the surface (small arrows in Fig. 2D). Small groups of very intensely labelled cells were observable in layer II but some occurred sparsely in layer V, too.

Interestingly enough, in the lateral part of the visual cortex a good number of slightly labelled neurons could be observed in layer III (Fig. 2D).

In the medial half of the occipital cortex (right to the big arrow in Fig. 2D) hardly any labelled neurons could be seen in the upper layers. Only a few of slightly labelled pyramidal neurons were present in layer V (right to the big arrow in Fig. 2D).

## Discussion

The results presented here indicate that neonatal monocular enucleation induces characteristic changes in the functioning of the visual cortex, contralateral to the enucleated eye. Electrophysiological and autoradiographic studies showed unequivocally, that the epicenter of the evoked cortical activity became limited to the lateral part of the primary visual cortex while, in the medial part very low if any activity remained. The cortical region affected corresponds to the monocular segment of the primary visual cortex (Oc1M), receiving (dorsal lateral geniculate relayed) projections from the contralateral, but not ipsilateral retina [7].

This suggests that early enucleation of the contralateral eye eliminates all retino-geniculate and probably, most geniculo-cortical inputs to this cortical area. However, it is still puzzling, why the lateral binocular segment of the primary visual cortex shows no detectable change in level of evoked activity (e.g. there is no decrease) as shown by the results of electrophysiological and autoradiographic

studies. This was unexpected because, a previous work had demonstrated that the adult albino rat has significantly few ipsilateral projecting ganglion cells [3]. The high level of evoked activity in the lateral part of the primary visual cortex (Oc1B) of contralaterally enucleated rat is surprising even if we take into account that the number of uncrossed axons and terminals increased in the superior colliculus and dorsal lateral geniculate nucleus (dLGN) after perinatal monocular enucleation [5].

These early data and our findings presented here suggest that, as a transneuronal effect of the monocular enucleation, a mechanism like axonal sprouting either in the dorsal geniculate nucleus or in geniculocortical projections began to compensate for the loss of the normal input. However, interestingly enough, this compensating mechanism took place only in the afferent system supplying the lateral but not the medial half of the primary visual cortex (Oc1B but not Oc1M).

This idea is highly supported by the results of Robertson et al. [7]. They found that neonatal monocular enucleation resulted in a marked reduction of transient acetylcholinesterase (AChE) activity in the thalamic recipient layers of the medial part of area Oc1, contralateral to the enucleated eye, i.e. the monocular segment of the primary visual cortex (Oc1M). They suggest that transient AChE serves as a marker for the region of geniculocortical axon terminals [7]. Returning to the questions raised in the "Introduction", we can state that 1) The lateral shift of evoked activity in the primary visual cortex of neonatally monocularly enucleated animals can be observed both with electrophysiological and autoradiographic methods. 2) The border between the highly and much less responsive areas is definite and equals with the border between the monocular and binocular parts of the primary visual cortex (Oc1M and Oc1B, respectively). 3) To explain these phenomena one may suppose a rerouting of optic projections described by Lund [5]. However, further experiments are required to elucidate the detailed mechanism of these phenomena.

## Conclusion

Neonatal monocular enucleation resulted in the reduction of evoked cortical activity in the medial part of the contralateral primary visual cortex. Evoked cortical activity shifted laterally and was limited to the binocular half of the primary visual cortex. Electrophysiological and autoradiographic studies suggested that a transneuronal compensating mechanism took place in the binocular part of the primary visual cortex but not in the monocular one.

## REFERENCES


1. Ambach, G., Toldi, J., Fehér, O., Joo, F., Wolff, J. R.: Spatial correlation between sensory regions and drainage fields of pial veins in rat cerebral cortex. Exp. Brain Res. **61**, 540–548 (1986).
2. Heumann, D., Rabinowicz, T.: Postnatal development of the visual cortex of the mouse after enucleation at birth. Exp. Brain Res. **46**, 90–106 (1982).
3. Lund, R. D.: Uncrossed visual pathways of hooded and albino rats. Science **149**, 1506–1507 (1965).
4. Lund, R. D., Chang, F.-L. F., Land, P. W.: The development of callosal projections in normal and one-eyed rats. Dev. Brain Res. **14**, 139–142 (1984).
5. Lund, R. D., Cunningham, T. J., Lund, J. S.: Modified optic projections after unilateral eye removal in young rats. Brain Behav. Evol. **8**, 51–72 (1973).
6. Olavarria, J., Malack, R., Van Sluyters, R. C.: Development of visual callosal connections in neonatally enucleated rats. J. Comp. Neurol. **260**, 321–348 (1987).
7. Robertson, R. T., Fogolin, R. P., Tijerina, A. A., Yu, J.: Effects of neonatal monocular and binocular enucleation on transient acetylcholinesterase activity in developing rat visual cortex. Dev. Brain Res. **33**, 185–197 (1987).
8. Rogers, A. W.: Techniques of autoradiography. Elsevier, Amsterdam. (1967).
9. Rojik, I., Fehér, O.: Incorporation of labelled amino acids into the acoustic cortex of the cat. Acta Biol. Acad. Sci. Hung. **30**, 209–222 (1979).
10. Rojik, I., Fehér, O.: Correlations between glycine incorporation and cerebral cortical activity. Exp. Brain Res. **39**, 321–326 (1980).
11. Sakai, M., Yagi, F.: Evoked potential in the lateral geniculate body as modified by enucleation of one eye in the albino rat. Brain Res. **210**, 91–102 (1981).
12. Sakai, M., Yagi, F., Ikeda, Y.: Evoked potential in the visual cortex as modified by enucleation of one eye in the albino rat. Physiol. Psychol. **11**, 141–146 (1983).
13. Toldi, J., Joo, F., Fehér, O., Wolff, J. R.: Modified distribution patterns of responses in rat visual cortex induced by monocular enucleation. Neuroscience **24**, 59–66 (1988).
14. Toldi, J., Rojik, I., Fehér, O.: Two different polysensory systems in the suprasylvian gyrus of the cat. An electrophysiological and autoradiographic study. Neuroscience **6**, 2539–2545 (1981).
15. Toldi, J., Wolff, J. R., Wiese, U. H.: Functional consequences of modification of callosal connections by perinatal enucleation in rat visual cortex. Neuroscience **33**, 517–524 (1989).
16. Valverde, F., Esteban, M. E.: Peristriate cortex of mouse. Location and effects of enucleation on the number of dendritic spines. Brain Res. **9**, 145–147 (1968).
17. Wree, A., Angenendt, H.-W., Zilles, K.: The size of the zone of origin of callosal afferents projecting to the primary visual cortex contralateral to the remaining eye in rats monocularly enucleated at different postnatal ages. Anat. Embriol. **174**, 91–96 (1986).
18. Wree, A., Kulig, G., Gutman, P., Zilles, K.: Modification of callosal afferents of the primary visual cortex ipsilateral to the remaining eye in rats monocularly enucleated at different stages of ontogeny. Cell. Tiss. Res. **242**, 433–436 (1985).
19. Zilles, K., Wree, A., Schleicher, A., Divac, I.: Monocular and binocular subfields of the rats primary visual cortex: a quantitative morphological approach. J. Comp. Neurol. **226**, 391–402 (1984).
20. Wolff, J.-R., Toldi, J., Siklos, L., Fehér, O., Joo, F.: Neonatal enucleation induces correlated modifications in sensory areas and pial angioarchitecture of the parietal and occipital cortex of albino rats. Journal of Comp. Neurol. **317**, 187–194 (1992)

*Acta Physiologica Hungarica, Volume 81 (2), pp. 183–192 (1993)*

# BIOLOGICAL ACTIVITIES OF SOME NEW ARGININE VASOPRESSIN ANALOGUES CONTAINING UNUSUAL AMINO ACIDS

CS. VARGA, CS. SOMLAI,* L. BALÁSPIRI,* F. A. LÁSZLÓ

DEPARTMENT OF COMPARATIVE PHYSIOLOGY, JÓZSEF ATTILA UNIVERSITY OF SCIENCES, AND *DEPARTMENT OF MEDICAL CHEMISTRY, ALBERT SZENT-GYÖRGYI MEDICAL UNIVERSITY, SZEGED, HUNGARY

Received March 12, 1992
Accepted April 26, 1992

Solid-phase synthesis methods were applied to prepare some arginine vasopressin (AVP) analogues containing L- or D-pipecolic acids or α-L-homoproline in position 7, D-Cys in position 6, D-Val in position 4, O-alkylated D- or L-Tyr in position 2 and Pmp [1-(β-mercapto-β, β-cyclopentamethylidenepropionic acid)] in position 1. Antidiuretic, vasopressor, antidiuretic antagonist and vasopressor antagonist activities were measured by biological methods.

Antidiuretic effects were observed for all analogues. $Pip^7$-AVPPmp$^1$D-Tyr(Et)$^2$D-Val$^4$AVP and Mpa$^1$dGly-NH-$CH_3{}^9$ AVP had higher antidiuretic activities than that of AVP. None of the analogues exhibited an antidiuretic antagonist effect. With the exception of $Pip^7$-AVP, none of the analogues had a vasopressor effect. Small vasopressor antagonist effects were found for DPip$^7$AVP and Mpa$^1$, DPip$^7$AVP.

The pharmacological significance of these new AVP analogues and the relationship between the chemical structure and biological activity are discussed.

**Keywords**: vasopressin analogues, unusual amino acids, antidiuretic and vasopressor activities, antagonist effect, structure-biological activity relationship

We recently synthesized thirteen arginine vasopressin (AVP) analogues containing unusual amino acids, and we have now examined these analogues for antidiuretic, antidiuretic antagonist, vasopressor and vasopressor antagonist activity, and investigated the correlation between chemical structure and biological activity.

Correspondence should be addressed to
Csaba VARGA
Department of Comparative Physiology, József Attila University of Sciences
H-6726 Szeged, P. O. B. 533, Hungary

*Akadémiai Kiadó, Budapest*

## Methods

*Peptide synthesis*

The protected peptide precursors required for the syntheses were prepared by the solid-phase peptide synthesis procedure discovered by Merrifield [32] and applied for oxytocin, VP and their analogues by Manning [27]. All protected peptide amides were obtained from the acyl peptide resin by the ammonolytic cleavage. Each protected precursor was deblocked with Na in $NH_3$ with a modification of the standard work-up procedure. The blocked disulphydryl compounds were oxidatively cyclized with $K_3[Fe(CN)_6]$. The analogues were desalted and purified by gel filtration on Sephadex G-10 [33]. TLC, HPLC and amino acid analysis were applied for purity control.

The analogues listed in Table I were tested for biological activity.

**Table I**

*Chemical structures of AVP analogues*

| | 1 | 2 | 3 | 4 | 5 | 6 | 7 | 8 | 9 |
|---|---|---|---|---|---|---|---|---|---|
| AVP: | Cys- | Tyr- | Phe- | Gln- | Asn- | Cys- | Pro- | Arg- | Gly-$NH_2$ |
| VP-10: | Cys- | Tyr- | Phe- | Gln- | Asn- | Cys- | Pip- | Arg- | Gly-$NH_2$ |
| VP-11: | Cys- | Tyr- | Phe- | Gln- | Asn- | Cys- | D-Pip- | Arg- | Gly-$NH_2$ |
| VP-13: | Mpa- | Tyr- | Phe- | Gln- | Asn- | Cys- | D-Pip- | Arg- | Gly-$NH_2$ |
| VP-14: | Cys- | Tyr- | Phe- | Gln- | Asn- | Cys- | B-Homo- | Pro-Arg- | Gly-$NH_2$ |
| VP-31: | Gaba-Cys | D-Tyr(Et)- | Phe- | Val- | Asn- | Cys- | Pro- | Arg- | Gly-$NH_2$ |
| VP-35: | Pmp- | Tyr(Et)- | Phe- | Val- | Asn- | D-Cys- | Pro- | Arg- | Gly-$NH_2$ |
| VP-36: | Pmp- | D-Tyr(Et)- | Phe- | Val- | Asn- | D-Cys- | Pro- | Arg- | Gly-$NH_2$ |
| VP-37: | Pmp- | Tyr- | Phe- | D-Val- | Asn- | Cys- | Pro- | Arg- | Gly-$NH_2$ |
| VP-38: | Pmp- | Tyr(Et)- | Phe- | D-Val- | Asn- | Cys- | Pro- | Arg- | Gly-$NH_2$ |
| VP-46: | Pmp- | Phe- | Phe- | Val- | Asn- | Cys- | Pro- | Arg- | Gly-$NHCH_3$ |
| VP-47: | Mpa- | Tyr- | Phe- | Gln- | Asn- | Cys- | Pro- | Arg- | NH-$CH_3$ |
| VP-48: | Pmp- | D-Tyr(Et)- | Phe- | D-Val- | Asn- | Cys- | Pro- | Arg- | Gly-$NH_2$ |
| VP-50: | Pmp- | Tyr- | Phe- | Gln- | Asn- | Cys- | Pro- | Arg- | Gly-OH |

Pmp: 1-β-mercapto-β, β-cyclopentamethylidenepropionic acid
Mpa: Mercaptopropionic acid
Pip: Pipecolic acid

*Antidiuretic activity*

The analogues were biologically titrated according to the method of De Wied [9]. Female Wistar rats weighing 200–300 g were used for the experiments. Following deprivation of food for 12 h, the animals were hydrated with a solution containing 2 per cent ethanol and 0.2 per cent NaCl (5 per cent of body weight) via a gastric tube. One hour later, the rats were anaesthetized with 10 per cent ethanol in the same manner (5 per cent of body weight), and 2 hours after the beginning of the experiment the animals were again hydrated with the 2 per cent ethanol solution. After this pretreatment, a polyethylene cannula (diameter 1.5 mm) was inserted into the bladder and the volumes of urine excreted in intervals of 10 minutes were measured. Two per cent ethanol solution was added via the gastric tube to replace the excreted urine. The tested analogues were administered into the tail vein and the diuresis decrease

was expressed as a percentage. A 3-point assay was carried out whereby the antidiuretic activities of the analogues were determined at concentrations corresponding to between 10 and 45 micro U of the standard (AVP 400 U/mg, Organon, Oss).

*Duration of antidiuretic activity*

Brattleboro homozygous rats with diabetes insipidus were used for the experiments [5]. The urinary excretion was measured hourly. The first 2 hours was taken as the control period. The animals were then treated with 1 μg/kg b.w. of the analogue i.p. The duration of antidiuretic activity was taken as the time required for the control level to be reached. The animals received drinking water ad libitum during this period.

*Antidiuretic antagonist activity*

Exogenous AVP decreases the urinary output of alcohol-anesthetized rats in a dose-dependent manner [9]; antidiuretic antagonists block this effect [15, 23, 38]. The method described in connection with the antidiuretic activity was used to determine the antidiuretic antagonist activity. Analogues with antagonist activity were injected into the tail vein 5 min before the AVP injection. The antagonist acitivity was expressed from a comparison of two antidiuretic reactions, as the "effective dose" of the compound [28, 29, 31].

*Vasopressor activity*

The experiments were carried out on male Wistar rats weighing 250–400 g. The animals were anaesthetized with pentobarbital (Nembutal, Ceva), administered i.p. in a dose of 45 mg/kg b.w. Next, the left common carotid artery was prepared in the neck, the vagus nerve was isolated from the vessels, and 0.1 ml physiological saline containing 10% heparin was administered via a polyethylene cannula (diameter 1 mm) inserted into the carotid lumen to inhibit blood clotting. The cannula was connected to a Hellige electromanometer. Following the cervical preparation, phentolamine (Regitin, Ciba Geigy) was administered i.p. in a dose of 10 mg/kg b.w. The test compounds in logarithmically increasing doses (0.02, 0.06 and 0.18 μg/kg b.w.) were injected through a small syringe fixed into the lateral tail vein. The blood pressure increase was expressed as a percentage of the initial value. The vasopressor activities of the analogues were calculated in comparison with that of AVP (Organon, Oss).

*Vasopressor antagonist activity*

A dose of 0.18 μg/kg b.w. of AVP was administered and the BP increase was recorded. Subsequently, an AVP analogue was injected in a dose of 1 μg/kg b.w. 5 minutes before AVP administration, and the BP was measured again. The two results were compared, and the "effective dose" was calculated as the dose of the antagonist that reduces the response to the agonist to one-half of that of the same dose of agonist administered in the absence of the antagonist [28, 29, 31].

## Results

The antidiuretic activities and the duration of antidiuresis are listed in Table II.

**Table II**

*Antidiuretic activities of AVP analogues in rats*

| | Antidiuretic activity IU/mg | Time h |
|---|---|---|
| AVP | 400 ± 7.20* | 4.5 ± 0.2 |
| VP-10 | 547 ± 3.00 | 4.4 ± 0.5 |
| VP-11 | 223 ± 13.80 | 5.0 ± 0.4 |
| VP-13 | 282 ± 13.70 | 6.6 ± 1.3 |
| VP-14 | 131 ± 1.50 | 5.4 ± 0.3 |
| VP-31 | 178 ± 1.30 | 4.0 ± 0.3 |
| VP-35 | 162 ± 0.99 | 2.9 ± 0.5 |
| VP-36 | 53 ± 0.75 | 2.3 ± 0.5 |
| VP-37 | 128 ± 1.30 | 3.9 ± 0.4 |
| VP-38 | 96 ± 1.10 | 2.7 ± 0.4 |
| VP-46 | 132 ± 6.80 | 4.7 ± 0.2 |
| VP-47 | 580 ± 14.20 | 10.7 ± 0.6 |
| VP-48 | 576 ± 3.90 | 14.1 ± 0.6 |
| VP-50 | 214 ± 12.00 | 3.9 ± 0.3 |

* Mean ± SEM
n = 15

All of the AVP analogues exhibit antidiuretic effects, on the basis of which the analogues can be divided into three groups:

Group I: Antidiuretic activities higher than that of AVP:
VP-10; VP-47; VP-48.

Group II: Significant activities, but lower than that of AVP:
VP-11, VP-13; VP-50.

Group III: Antidiuretic activities minimal:
VP-14; VP-31; VP-35; VP-36; VP-37; VP-38; VP-46.

There is not a close parallel between the duration of the antidiuretic effect and the antidiuretic activity. Of the compounds with the highest antidiuretic activity (VP-10, VP-47, VP-48), VP-10 has the same duration of antidiuresis as AVP. In contrast, VP-11, VP-13, VP-14, VP-31 and VP-46 have lower antidiuretic activities, but the duration of antidiuresis is the same as or more than that AVP. No antidiuretic antagonist effect was detected for any of the analogues.

The changes in BP are outlined in Table III. It can be seen that in most cases the analogues have much lower vasopressor activities than that of AVP. Only VP-10 has a significant vasopressor potency at every dose, while VP-14 has one at the highest dose.

**Table III**

*Vasopressor effects of AVP analogues*

| | Blood pressure (percentage changes) μg/kg + : doses of VP analogues | | | |
|---|---|---|---|---|
| | I. 0.02 | II. 0.06 | III. 0.18 | IV. 1.00 |
| AVP | 24.3 ± 8.2* | 43.8 ± 1.5 | 75.0 ± 6.3 | – |
| VP-10 | 17.9 ± 1.8 | 30.1 ± 2.6 | 61.9 ± 3.9 | – |
| VP-11 | 4.8 ± 1.7 | 7.3 ± 2.7 | 7.1 ± 1.3 | – |
| VP-13 | 7.4 ± 2.4 | 4.3 ± 1.7 | 8.1 ± 1.8 | – |
| VP-14 | 3.4 ± 1.2 | 5.8 ± 0.8 | 8.6 ± 1.3 | 33.2 ± 3.8 |
| VP-31 | 7.6 ± 5.3 | 7.5 ± 3.8 | 7.0 ± 3.3 | 5.2 ± 2.4 |
| VP-35 | 3.4 ± 2.1 | 2.8 ± 1.2 | 5.0 ± 2.2 | 7.2 ± 2.2 |
| VP-36 | 3.2 ± 1.9 | 3.0 ± 2.7 | 0.8 ± 0.7 | 12.4 ± 3.4 |
| VP-37 | 2.0 ± 1.2 | 5.0 ± 0.7 | 0.8 ± 0.7 | 7.0 ± 4.0 |
| VP-38 | 5.0 ± 0.1 | 1.0 ± 0.9 | 2.5 ± 2.5 | 15.0 ± 2.8 |
| VP-46** | 7.0 ± 3.8 | 0.5 ± 0.4 | 12.5 ± 2.4 | – |
| VP-47** | 13.0 ± 0.2 | 10.0 ± 1.7 | 9.3 ± 4.6 | – |
| VP-48 | 6.8 ± 2.8 | 2.2 ± 0.6 | 3.2 ± 0.9 | 2.3 ± 1.5 |
| VP-50 | 3.0 ± 2.1 | 3.0 ± 1.6 | 5.2 ± 2.9 | – |

* Mean ± SEM
n = 10
** I: 0.0075 μg/kg
II: 0.075 μg/kg
III: 0.75 μg/kg

The vasopressor antagonist effect was studied for all analogues with the exception of VP-10 (Table IV). Two analogues (VP-11 and VP-13) showed an antagonist effect. Especially that of VP-13 is noteworthy.

**Table IV**

*Vasopressor antagonist effects of AVP analogues*

| | $V_1$ antagonist "effective dose" μg/kg |
|---|---|
| VP-11 | 1.72 ± 0.22* |
| VP-13 | 0.60 ± 0.11 |

* Mean ± SEM
n = 10

## Discussion

In the synthesis of VP analogues for the treatment of diabetes insipidus, the aim was a low vasopressor effect, together with a marked and long-lasting antidiuretic effect. The most widespread such analogue is 1-deamino-8-D-arginine vasopressin (dDAVP), synthesized by Zaoral et al. in 1967 [41]. Subsequently, many authors have studied the effect of this compound in diabetes insipidus. The antidiuretic effect of dDAVP is more pronounced and long-acting than that of the natural hormone, while at the same time its vasopressor effect is very low [8, 34, 35]. In 1973, 1-deamino-4-valine-8-D-arginine vasopressin [dVDAVP] was synthesized by Manning et al. [27]. The effect of this compound lasts four times longer than that of AVP [22]. Subsequently, more potent VP analogues have been produced, e.g. 1-deamino-6-carba-8-D-arginine vasopressin (dCDAVP) [7].

Among our test compounds, the smallest chemical modification relative to AVP was applied in the case of VP-10, with $Pip^7$ instead of $Pro^7$. This led to a higher antidiuretic activity, but the duration of antidiuresis and the vasopressor activity were approximately the same as those of AVP. The longer-lasting antidiuretic effect of dDAVP can be explained by the lack of an amino group at position 1; in its absence, the molecule is more resistant to enzymatic destruction [14, 36, 37]. VP-47 (desamination, removal of $Gly^9$ and methylation of $Arg^8$ amino group) had a higher antidiuretic activity than that of AVP. This is interesting, since desglycinamide-AVP (DG-AVP) has only low and antidiuretic vasopressor effects [10, 11].

Research lasting more than 20 years was required before the discovery of the first effective antagonist of the antidiuretic ($V_2$) response. Sawyer et al. [38] reported four $V_2$ antagonists, the most frequently used being $d(CH_2)_5Tyr(Et)^2Val^4AVP$. $V_2$ antagonists will probably be therapeutically useful drugs for treatment of the syndrome of inappropriate antidiuretic hormone secretion (SIADH), hyponatriaemia and brain oedema associated with excessive VP excretion [2, 24]. Unfortunately, our attempt to produce new $V_2$ antagonists was not successful. The insertion of $D\text{-}Cys^6$ (VP-35, VP-36) caused loss of the $V_2$ antagonist effect. From the aspect of chemical structure, VP-38 is most similar to the well-known $V_2$ antagonist $d(CH_2)_5Tyr(Et_2VAVP$, but $D\text{-}Tyr^2$ instead of $L\text{-}Tyr^2$ eliminated the antidiuretic antagonist effect. A similar phenomenon was observed with VP-48; when $L\text{-}Tyr^2$ and $L\text{-}Val^4$ were replaced by the D modifications, the strong $V_2$ antagonist effect was lost, but a highly potent and long-lasting antidiuretic response was observed.

Another important aspect to be considered in the synthetic work is the vasopressor agonist activity. Analogues with high vasopressor activity are useful in the stopping or moderation of local bleeding (gastrointestinal, surgical, gynaecological) [3]. Our study revealed that the vasopressor activity is highly responsive to chemical modification of AVP. Most of the analogues had practically

no vasopressor activity. With the minimal alteration ($Pip^7$ substitution) in VP-10, the vasopressor effect remained intact, while the antidiuretic activity significantly increased. VP-14 ($\beta$-Homo-$Pro^7$) exerted a small vasopressor effect following the administration of very large doses.

Interest in the cardiovascular effects of AVP has increased considerably over the past few years [26]. Its administration has been shown to decrease the coronary blood flow and to impair cardiac contractility [6, 13, 39]. The discovery of vasopressor ($V_1$) antagonists introduced a new perspective to the experimentation relating to the effects of the peptide on the coronary circulation. In recent studies [25, 26], the development of AVP-induced coronary vasoconstriction was completely prevented by the antagonist $d(CH_2)_5Tyr(Me)AVP$. The role of AVP in the control of the renal haemodynamics may be best elucidated through the use of $V_1$ antagonists [1, 12]. Our results suggested that the AVP antagonist prevented renal vasospasm after AVP administration to rats pretreated with oestrogen [16, 17, 21]. We concluded that VP antagonist treatment may in the future be an important means of preventing human renal cortical necrosis. The widespread applicability of $V_1$ antagonists is proved by the finding that the antagonist $d(CH_2)_5Tyr(Me)AVP$ is able to prevent the gastric haemorrhagic erosions induced by ethanol [19, 20].

A small vasopressor antagonistic effect was observed for VP-11. VP-13 (D-$Pip^7$, desamination at position 1) had a higher antagonist effect. Its pressor antagonist activity, calculated in terms of "the effective dose", appears to be one-third of that of the strongest known $V_1$ antagonist $d(CH_2)_5Tyr(Me)AVP$. $d(CH_2)_5AVP$ has a significant vasopressor antagonist effect [4, 18, 30]. In our studies, replacement of the amino group of $Gly^9$ by an OH group caused elimination of the antagonist response.

Further experiments are necessary to explain the deep relationship between chemical structure and biological activity.

**Acknowledgement**

This work was supported by the Hungarian Credit Bank, and by the Hungarian Research Foundation (OTKA, No: T 1406, I/3)

## REFERENCES

1. Aisembrey, G. A., Handelman, W. A., Arnold, P., Manning, M., Schrier, R. W.: Vascular effects of arginine vasopressin during fluid deprivation in the rat. J. Clin. Invest. **67**, 961–968 (1981).
2. Bartter, F. C., Schwartz, W. B.: The syndrome of inappropriate secretion of antidiuretic hormone. Am. J. Med. **42**, 790–806 (1967).

3. Berde, B., Boissonnas, R. A.: Basic pharmacological properties of synthetic analogues and homologues of the neurohypophysial hormones. ed. B. Berde, Springer, Berlin, In: Handbook of Experimental Pharmacology, **23**, 802–870 (1968).
4. Bicknell, R. J., Chapman, C., Leng, G.: Effects of opioid agonists and antagonists on oxytocin and vasopressin release in vivo. Neuroendocrinology **41**, 142–148 (1985).
5. Burn, J. H.: Estimation of the antidiuretic potency of pituitary (posterior lobe) extract. Q. J. Pharm. **4**, 517–529 (1931).
6. Cartheuser, C. F., Komarek, J.: Effects of vasopressin on the circulation, myocardial dynamics, and left ventricular oxygen consumption in the anaesthetized dog. Basic Res. Cardiol. **75**, 668–682 (1982).
7. Cort, J. H., Schück, O., Stribrná, J., Skopková, J., Jost, K., Mulder, J. L.: Role of the disulfide bridge and the c-terminal tripeptide in the antidiuretic action of vasopressin in man and the rat. Kidney Int. **8**, 292–302 (1975).
8. Czakó, L., Julesz, J., László, F. A.: Comparative study of the antidiuretic effects of Adiuretin-SD (DDAVP) and Pitressin Tannate in diabetes insipidus. Int. J. Clin. Pharm. **16**, 10–13 (1978).
9. De Wied, D.: A simple automatic and sensitive method for the assay of antidiuretic hormone with notes on the antidiuretic potency of plasma under different experimental conditions. Acta Physiol. Pharmacol. Neerl. **9**, 69–81 (1960).
10. De Wied, D., Greven, H. M., Lande, S., Witter, A.: Dissociation of the behavioural and endocrine effects of lysine vasopressin by tryptic digestion. Br. J. Pharmacol. **45**, 118–122 (1972).
11. De Wied, D.: Behavioral effects of intraventricularly administered vasopressin and vasopressin fragments. Life Sci. **19**, 685–690 (1976).
12. Gellai, M.: Vasopressin antagonists in studies on the role of vasopressin in renal hemodynamics. In Vasopressin, ed. R. W. Schrier, Raven Press, New York, 1985, pp. 167–170.
13. Heyndrickx, G. R., Boettcher, D. H., Vatner, S. F.: Effects of angiotensin, vasopressin and methoxamine on cardiac function and blood flow distribution in conscious dogs. Am. J. Physiol. **231**, 1579–1587 (1976).
14. Huguenin, R. L., Boissonnas, R. A.: Syntheses de la desamino-Arg$^8$-vasopressine et de la desamino$^1$-Phe$^2$-Arg$^8$-vasopressine, deux analogues possédant une activité antidiurétique plus élevée et plus selective que celle des vasopressines naturelles. Helv. Chim. Acta, **49**, 695–705 (1966).
15. Ishikava, S. E., Kim, J. K., Schrier, R. W.: Further *in vivo* evidence for antagonist to antidiuretic action of arginine vasopressin. Am. J. Physiol. **245**, R713–R717 (1983).
16. Kocsis, J., Karácsony, G., Karcsú, S., László, F. A.: Histochemical and ultrastructural study of renal cortical necrosis in rats treated with oestrone + vasopressin and its prevention with a vasopressin antagonist. Br. J. Exp. Pathol. **68**, 35–43 (1987).
17. Kocsis, J., Szabó, E., László, F. A.: Effect of a vasopressin antagonist d($CH_2$)$_5$Tyr(Me)AVP on the development of renal vasospasm induced by estrin plus vasopressin administration in rats. Invest. Radiol. **22**, 973–977 (1987).
18. Kruszynski, M., Lammek, B., Manning, M., Seto, J., Haldar, J., Sawyer, W. H.: (1-β-mercapto-β, β-cyclo-penthamethylene propionic acid, 2-O-methyl-tyrosine)-arginine vasopressin and (1-β-mercapto-β, β-cyclo-penthamethylene propionic acid) arginine vasopressin. Two highly potent antagonists of the vasopressor response to arginine vasopressin. J. Med. Chem. **23**, 364–368 (1980).
19. László, F., Karácsony, G., Náfrádi, J., Rengei, B., Vecsernyés, M., Laczi, F., Szarvas, F., Lengyel, Z., László, F. A.: A high dose of ethanol releases vasopressin and simultaneously by induces lesions in the rat stomach. – The role of vasopressin in gastric cytoprotection. *In* New Aspects of

Morphology Function and Regulation. Proc. 4th Conf. on Neurohypophysis, Coppenhagen, 1989, pp. 159–161, Oxford University Press, Oxford, England. (1989).

20. László, F., Karácsony, G., Baláspiri, L., László, F. A.: The role of vasopressin in the pathogenesis of ethanol-induced gastric hemorrhagic erosions in rats. Gastroenterology, **101**, 1242–1248 (1991).
21. László, F. A.: Renal cortical necrosis. Experimental induction by hormones. Karger, Basel, (1981).
22. László, F. A., Czakó, L.: 1-Deamino-(4-valine-8-D-arginine)-vasopressin (dVDAVP), a new synthetic vasopressin analogue for treating diabetes insipidus. Int. J. Clin. Pharmacol. **20**, 39–43 (1982).
23. László, F. A., Csáti, S., Baláspiri, L.: Effect of the vasopressin antagonist $d(CH_2)_5Tyr(Et)VAVP$ on the antidiuretic action of exogenous and endogenous vasopressin. Acta Endocrin. **106**, 52–55 (1984).
24. László, F. A., Csáti, S., Baláspiri, L.: Prevention of hyponatraemia and cerebral oedema by the vasopressin antagonist $d(CH_2)_5Tyr(Et)VAVP$ in rats treated with pitressin tannate. Acta Endocrin. **106**, 56–60 (1984).
25. László, F. A., Leprán, I., Baláspiri, L.: Cardiovascular effects of vasopressin agonist and antagonist in rats. Life Sci. Adv. (Exp. Clin. Endocr.) **7**, 91–97 (1988).
26. László, F. A., László, F., De Wied, D.: Pharmacology and Clinical Perspectives of Vasopressin Antagonists. Pharm. Rev. **43**, 73–108 (1991).
27. Manning, M., Baláspiri, L., Acosta, M., Sawyer, W. H.: Solid-phase synthesis of (1-deamino-4-valine-8-D-arginine) vasopressin (dVDAVP), a highly potent and specific antidiuretic agent possessing protracted effects. J. Med. Chem. **16**, 975–978 (1973).
28. Manning, M., Sawyer, W. H.: Invited editorial: antagonists of vasopressor and antidiuretic responses to arginine vasopressin. Ann. Intern. Med. **96**, 520–522 (1982).
29. Manning, M., Sawyer, W. H.: Design of potent and selective *in vivo* antagonists of neurohypophyseal peptides. Prog. Brain Res. **60**, 367–382 (1983).
30. Manning, M., Sawyer, W. H.: Discovery, development and some uses of vasopressin and oxytocin antagonists. J. Lab. Clin. Med. **114**, 617–632 (1989).
31. Manning, M., Lammek, B., Kolodziejczyk, A., Seto, J., Sawyer, W. H.: Synthetic antagonists of *in vivo* antidiuretic and vasopressor responses to arginine vasopressin. J. Med. Chem. **24**, 701–706 (1981).
32. Merrifield, R. B.: Solid Phase Synthesis, I. The synthesis of a tetrapeptide. J. Amer. Soc. **85**, 2149–2154 (1963).
33. Merrifield, R. B.: Solid phase peptide synthesis. Adv. Enzymol. **32**, 221–296 (1969).
34. Nemethova, V., Lichardus, B.: Clinical experience with DDAVP (1-deamino-8-D-arginine vasopressin) in the treatment of diabetes insipidus in children. Endocrinologie **63**, 137–141 (1974).
35. Robinson, A. G.: DDAVP in the treatment of central diabetes insipidus. New Eng. J. Med. **294**, 507–511 (1976).
36. Sawyer, W. H., Acosta, M., Baláspiri, L., Judd, J., Manning, M.: Structural changes in the arginine-vasopressin molecule that enhance antidiuretic activity and specificity. Endocrinology **94**, 1106–1115 (1974).
37. Sawyer, W. H., Acosta, M., Manning, M.: Structural changes in the arginine vasopressin molecule that prolong its antidiuretic action. Endocrinology **95**, 140–149 (1974).
38. Sawyer, W. H., Grzonka, Z., Manning, M.: Neurohypophyseal peptides. Design of tissue-specific agonists and antagonists. Mol. Cel. Endocrin. **22**, 117–134 (1981).
39. Sawyer, W. H., Pang, K. T., Seto, J., McEnro, M., Lammek, B., Manning, M.: Vasopressin analogs that antagonize the antidiuretic responses by rats to antidiuretic hormone. Science **212**, 49 (1981).

40. Wilson, M. F., Brackett, D. J., Archer, L. T., Hinshaw, L. B.: Mechanisms of impaired cardiac function by vasopressin. Ann. Surg. **191**, 494–500 (1980).
41. Zaoral, M., Kolc, J., Sorm, F.: Amino acids and peptides. LXXI. Synthesis of 1-deamino-8-D-gamma-aminobutirine-vasopressin. 1-deamino-8-D-lysine-vasopressin and 1-deamino-8-D-arginine-vasopressin. Coll. Czeh. Chem. Comm. **32**, 1250–1257 (1967).

*Acta Physiologica Hungarica, Volume 81 (2), pp. 193–206 (1993)*

# ULTRASTRUCTURE OF THE DEVELOPING MUSCLE AND ENTERIC NERVOUS SYSTEM IN THE SMALL INTESTINE OF HUMAN FETUS

I. BENEDECZKY, É. FEKETE, B. RESCH*

DEPARTMENT OF ZOOLOGY, JÓZSEF ATTILA UNIVERSITY, SZEGED AND *DEPARTMENT OF OBSTETRICS AND GYNECOLOGY, SZENT-GYÖRGYI ALBERT MEDICAL UNIVERSITY, SZEGED, HUNGARY

Received March 5, 1992
Accepted April 29, 1992

The ultrastructural organization and some histochemical characteristics of the enteric nervous system (ENS) were investigated in 10- and 18-week-old human fetuses. In the 10-week-old human fetus immature myoblasts, and mostly neuroblasts were found in the ganglia. Simple, undifferentiated neuropil was observed among neuronal cells. The neuropil generally did not contain synapses; however axosomatic synapse was registered rarely on the surface of certain neurons. Neuromuscular junctions were common, both axons and neurons were in close contact with the sarcolemma. In the 18-week-old human fetus the fine-structural characteristics of the intestinal smooth muscle cells were the same as in the adult. Nerve profiles were frequently found among the muscle cells. NADH-diaphorase histochemistry revealed the presence of numerous ganglia but solitary neurons still occurred. Differentiated neurons and neuroblasts could be distinguished in the myenteric ganglia. Synapses were often detected in the neuropil. Thick nerve plexuses were frequently found in the proximity of smooth muscle cells, forming "distant" and "close" myoneural contacts. Well-defined fluorescent network and several fluorescent nerve cell bodies were demonstrated by glyoxylic acid. The above organization may provide a satisfactory basis for an integrated peristaltic movement in the gut of the 18-week-old human fetus.

**Keywords**: enteric nervous system, ultrastructure, histochemistry, human fetal development

Excellent books [3, 11, 13] and hundreds of articles indicate the continuing scientific interest in the enteric nervous system (ENS). This extensive interest stems from various aspects. The gastroenterological interest arises from clinical practice: motility, gastric acid secretion, water and electrolyte transport, etc. are strongly controlled by the ENS. Neurobiological interest in the ENS is due to the fact that it is

Correspondence should be addressed to
István BENEDECZKY
Department of Zoology, József Attila University
H-6726 Szeged, Középfasor 52, Hungary

*Akadémiai Kiadó, Budapest*

nearly as complex as the central nervous system, and valuable comparisons may therefore be made. Basic structural and functional questions may be clarified in the adult animal species and in humans [2, 3, 4, 7, 9, 11, 13, 14]. Knowledge on the ontogenesis of the ENS in the chick embryo is relatively abundant [6, 8, 10, 27], however on mammals it is less complete [1, 17, 18, 19, 21], and only rather sporadic data have been published on the morphological and functional development of the gut in human fetus, because of the unavailability of tissue samples [5, 20, 25]. The main questions concerning the human fetus are the same as for other species, viz. the origin, the fate and the structural organization of enteric neurons. Neither the fine-structural characteristics of the neuromuscular junction nor the nature of the chemical substances transmitting the impulses from ENS to the target cells in the gut wall are known. The aim of the present study was to describe the fine-structural organization of the ENS in the 10- and 18-week-old human fetuses. In order to get information of the functional maturation glyoxylic acid-induced histofluorescence (GIF) [29] and the nitroblue tetrazolium/nicotinamide adenine dinucleotide (NBT/NADH) method [12] were used to follow the development of the aminergic innervation and the main morphogenetic events of enteric plexus formation.

## Material and Methods

*Electron microscopic processing:*

Human gut was obtained immediately after abortion. Fetuses were 10 and 18 weeks old. The full length of the gastrointestinal tract was immersed in an aldehyde-containing fixative: 2% paraformaldehyde, 2% glutaraldehyde, 0.5% acrolein and 0.5% dimethylsulphoxide. The pH was adjusted to 7.4 with 0.1 M cacodylate buffer. Samples were cut from duodenum, jejunum and ileum as well. Prefixation was performed overnight. After a short washing with 0.1 M cacodylate, postfixation was performed in 2% $O_SO_4$ in a refrigerator at +4 °C for 2 h. Samples were dehydrated in an ascending alcohol series and contrasted with saturated uranyl acetate in 75% alcohol for 30 min. Small samples were embedded in Durcupan ACM (Fluka). Ultrathin sections were cut on Reichert ultramicrotome and post-contrasted with lead according to Reynolds [26]. Electron micrographs were taken with TESLA BS 500 and JEM 100 B electron microscopes.

*Histofluorescence studies:*

a) For the histochemical detection of monoamines, the sucrose-phosphate glyoxylic acid (SPG) method [29] was applied to whole-mount stretch preparations of 10- and 18-week-old human fetal intestine. Immediately after abortion, the intestine was removed and exposed to the ice-cold incubation medium (6.8 g sucrose, 3.2 g $KH_2PO_4$ and 1 g glyoxylic acid in 100 ml $H_2O$). After incubation (30–60 min), the muscle layers were separated and stretched on microscope slides, dried and exposed to a temperature of 95 °C (4 min). After mounting in liquid paraffin, the preparations were viewed in a Leitz Orthoplan microscope equipped with a HBO 50 W high-pressure mercury lamp.

b) NBT/NADH method: For the NADH/diaphorase method [12], the fetal gut pieces were filled with Krebs solution, then incubated in a solution containing 5 mg NBT and 10 mg NADH in 100 ml of

0.1 M phosphate buffer. After incubation (60 min at room temperature), the tissue pieces were fixed in 10% formalin for 24 h, and whole mounts were made.

## Results

*Fine structure of muscle layer in the ileum of the 10-week-old human fetus*

The nuclei of the smooth muscle cells were elongated and often lobulated, therefore they were very similar to fibroblasts (Fig. 1). The karyoplasm often contained two nucleoli and abundant euchromatin. The cytoplasm of the muscle cell was filled with a large number of mitochondria, and abundant rough-surfaced endoplasmic reticulum and Golgi apparatus. Rich network of myofilaments were seen in the sarcoplasm but their electron density was low. Dense areas are lacking along the cell membrane, as are dense bodies, endocytotic vesicles and basal lamina. The cells are closely attached to each other, and the extracellular space is narrow.

*Neuronal cells*

The majority of the neural cells can be still regarded as neuroblasts, which form compact intramural ganglia (Fig. 2). The nuclei are rich in both hetero and euchromatin. Two nuclei can often be found in one neuronal cell. The perikaryon is usually narrow along the nucleus and contains a large number of free ribosomes, a few mitochondria and tubules of rough-surfaced endoplasmic reticulum. Many neural cells have a moderately electron-dense perikaryon, whereas the cytoplasms of the Schwann cells were electron lucent (Fig. 3). Among the neuronal cells, a simple neuropil can be found at this stage (Fig. 4). Neural processes contain well-developed system of microtubules, more or less spherical clear vesicles, and a few dense-core vesicles. A few mitochondria and free ribosomes also occur in some neural processes (Fig. 5). Synaptic contacts between neuronal elements are very rare. A few axosomatic synapses are observed (Fig. 4, insert), but the number of vesicles in the axon terminals is rather low. Neuromuscular contacts were rather frequent. Several neural processes form a plexus and the axolemma is in close contact with the sarcolemma (Figs 5 and 6). Free axon terminals among intestinal smooth muscle cells are rarely observed in the 10-week-old human fetus.

*18-week-old human fetus. Smooth muscle cells*

The fine-structural features of the intestinal smooth muscle cells are nearly the same as those in the adult (Fig. 7). The nuclei are rich in marginated heterochromatin. The extracellular spaces are wide and a continuous basal lamina

surrounds the sarcolemma. A large number of dense areas and endocytotic vesicles were observed alongside the sarcolemma, and dense bodies are also common in the sarcoplasm. The number of smooth muscle cell organelles (mitochondria, rEr, ribosomes) is strongly reduced compared to the 10-week-old developmental stage of the fetus.

*Neural elements*

Nerve profiles can frequently be found among the muscle cells (Fig. 7). Beside neuroblasts, mature ganglion cells can be seen in the myenteric plexus at this stage of the human fetus (Fig. 8). The perikaryon of the ganglion cells is wide around the nucleus and it contains a large number of cell organelles (Fig. 8). The mitochondria and tubules of rough-surfaced endoplasmic reticulum are evenly distributed in the cytoplasm. Beside these cell organelles, the most conspicuous feature is the abundance of ribosomes (mostly polysomes). Microtubules are common in every neuron, but the Golgi apparatus is still poorly developed. The lysosomes are numerous, but at the same time the transmitter containing vesicles were absent from the perikarya. Among the ganglion cells and in the plexuses (Figs 9–12) rich neuropil was found. The axon profiles contain agranular small vesicles (Fig. 9), large semiopaque neurosecretory granules (Fig. 7) and dense-core granules (Fig. 10). A mixed vesicle population, agranular vesicles and neurosecretory granules, is also observed (Fig. 11). Synapses are often detected in the neuropil (Fig. 9). Thick nerve bundles are also common in the submucosal and myenteric plexus (Figs 11–12). Both plexuses contain large numbers of axons and dendrites. Small and large dense cores may occur in the axoplasm, but most of the axons seem to be free of vesicles. Plexuses are frequently found in the proximity of the smooth muscle cells (Figs 11 and 12), forming "distant" and "close" contacts.

*Histofluorescence*

In the 18-week-old fetal intestine, fluorescence for catecholamine was detected in both the myenteric (Fig. 13) and the submucosal (Fig. 14) plexus. The fluorescence intensity is much higher in the myenteric than in the submucosal plexus. Besides the plexuses, several fluorescent nerve cell bodies are also revealed along the perivascular (Fig. 15) and submucosal (Fig. 16) plexuses. NADH-diaphorase staining reveals the most of the neurons are already ganglionated in the 18-week-old fetal intestine (Fig. 17), although small groups of solitary neuroblast-like cells are frequently found close to the mesenteric border (Fig. 18).

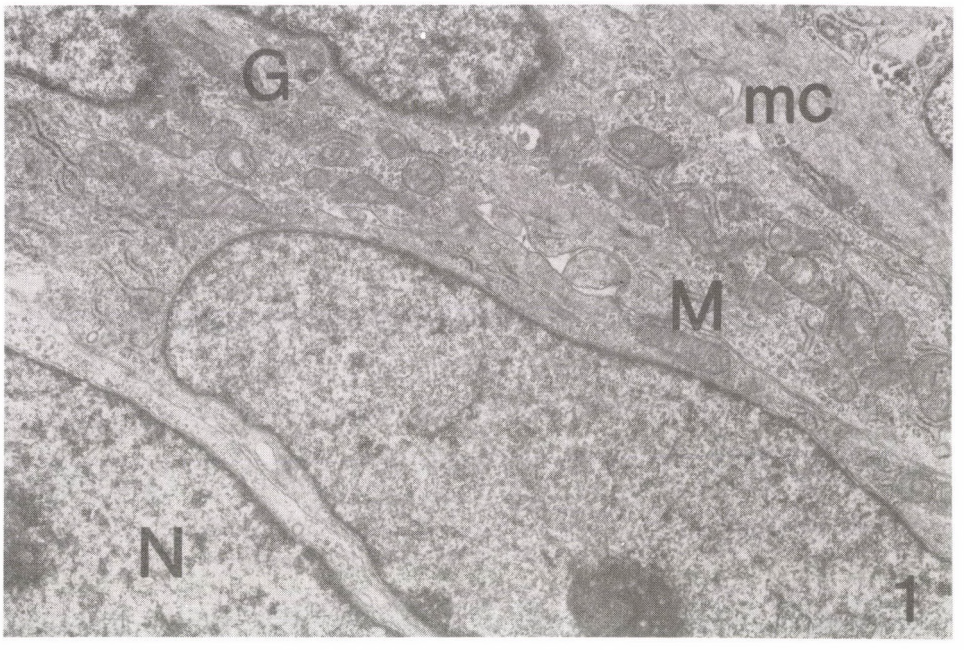


*Fig. 1.* Immature smooth muscle cells (mc) in the gut of 10-week-old human fetus. N = nucleus, M = mitochondria, G = Golgi apparatus, × 20,000

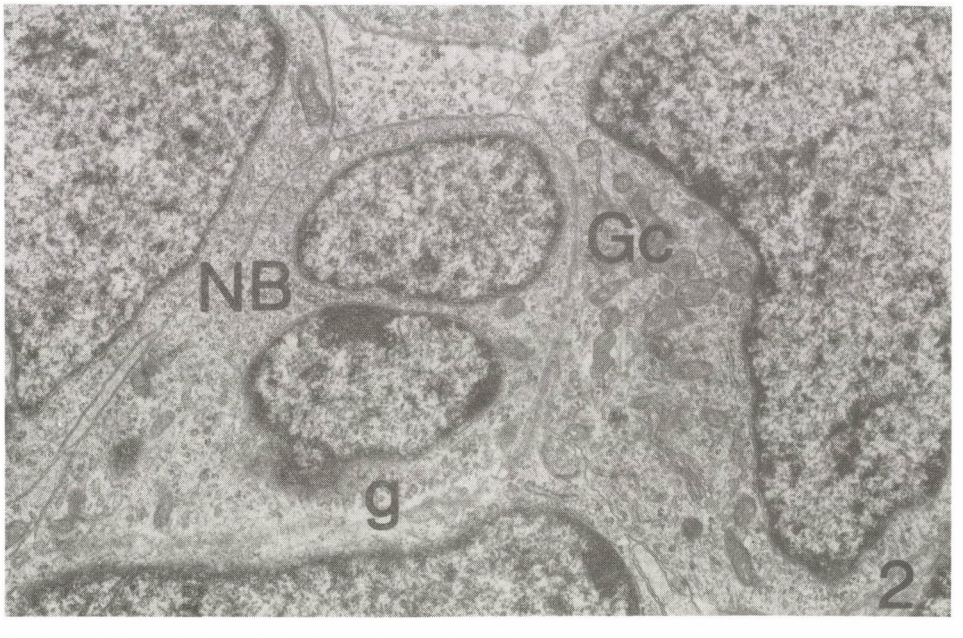


*Fig. 2.* Neuroblasts (NB) and ganglion cell (Gc) compose a loose myenteric ganglion (g) in the gut wall of 10-week-old human fetus, × 15,000

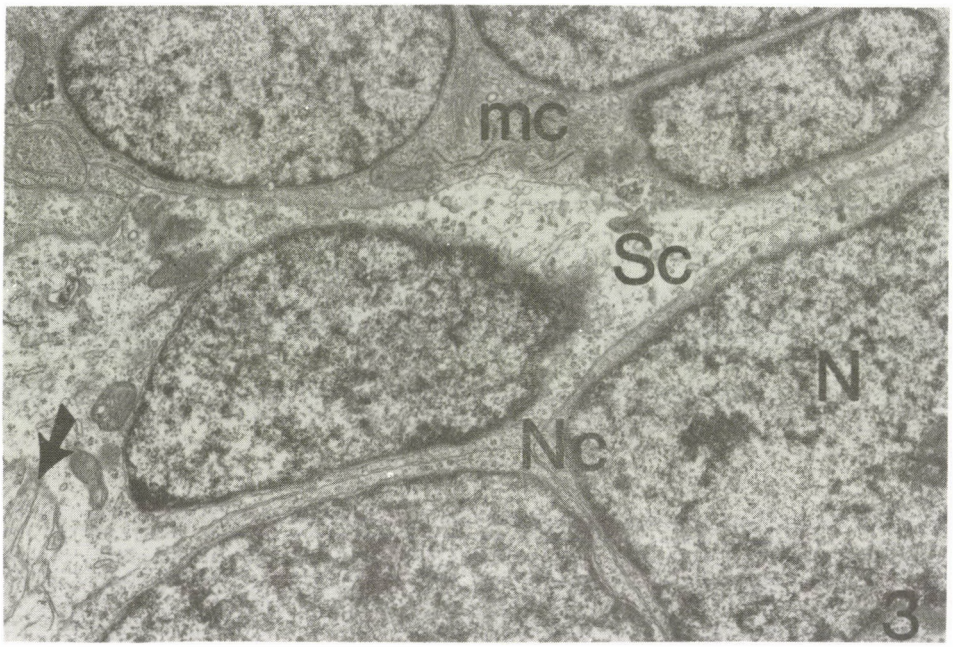


*Fig. 3.* Myocytes (mc) Schwann cell (Sc) and neuronal cells (Nc) lie side by side in the small intestine. 10-week-old human fetus. → = axon, N = nucleus, × 15,000

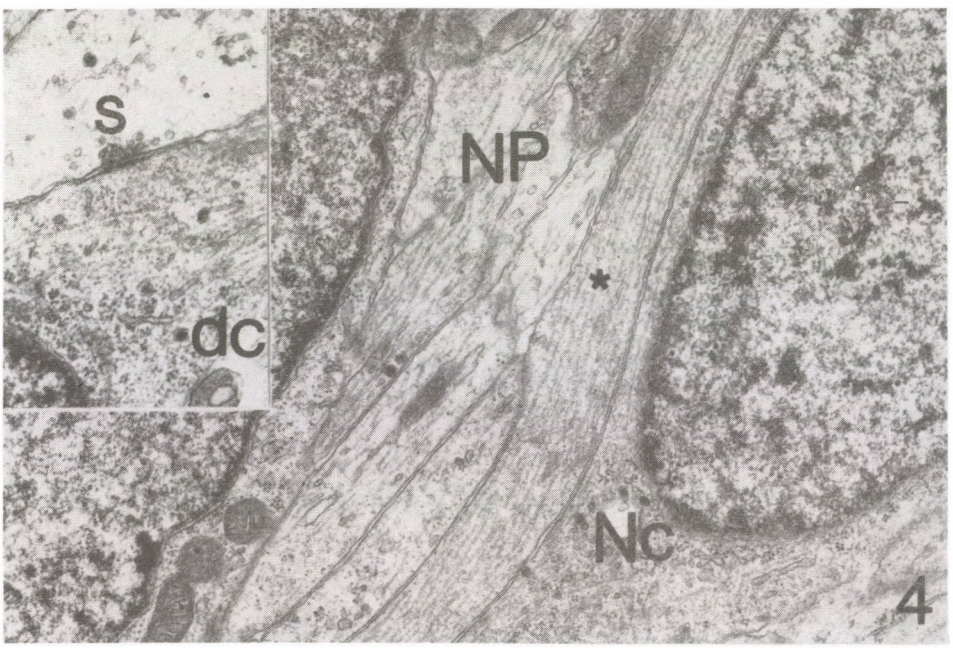


*Fig. 4.* Simple neuropil (NP) is formed among intestinal neurons in the 10-week-old fetus. Nc = nerve cell, * = microtubules, × 18,000. Insert = axosomatic synapse (s), dc = dense core vesicles in the soma, × 25,000

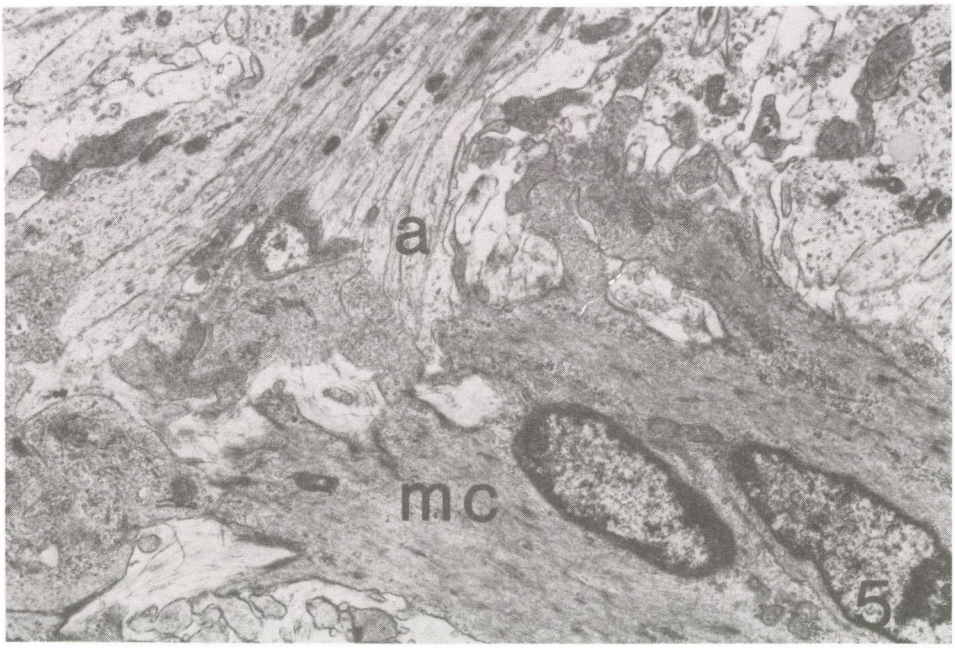


*Fig. 5.* Smooth muscle cells (mc) are often in close contact with the axons (a) in the gut wall of 10-week-old human fetus, × 15,000

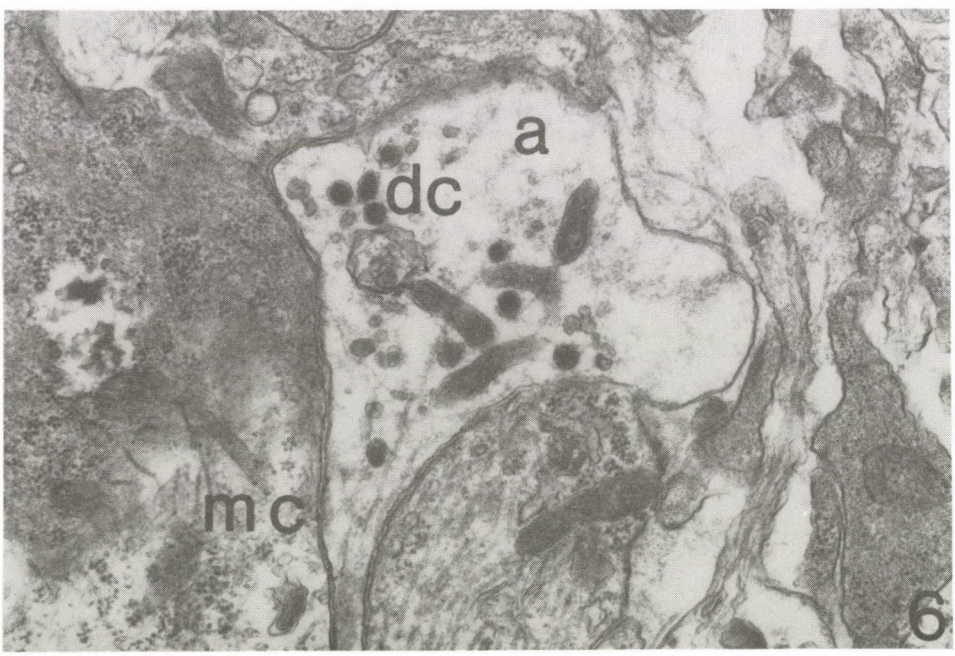


*Fig. 6.* So-called close contact, between a muscle cell (mc) and axon (a). Note large dense core granules (dc) in the axoplasm. 10-week-old human fetus, × 25,000

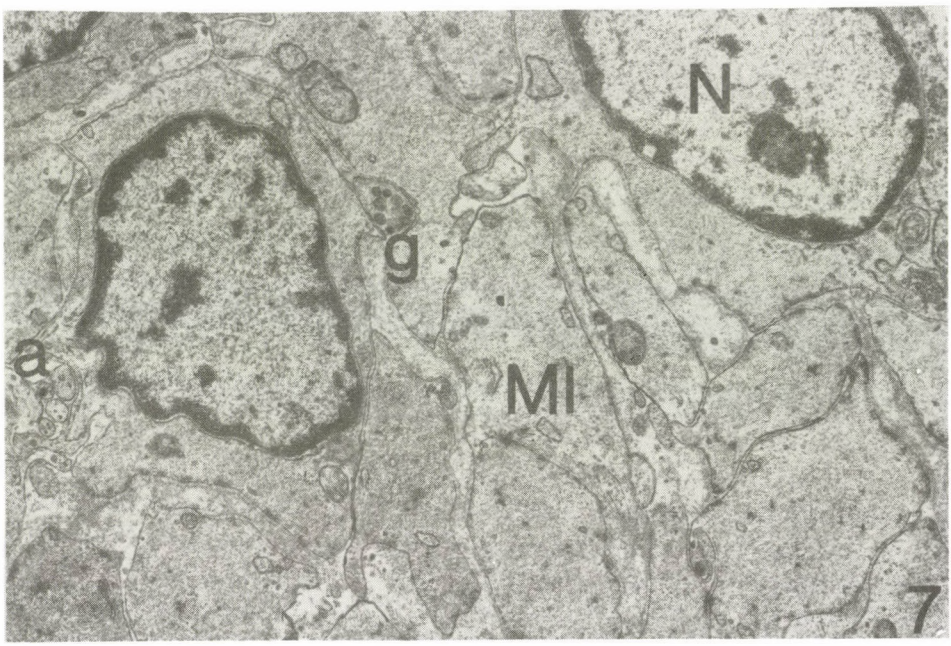


*Fig. 7.* A detail of circular smooth muscle layer (Ml) in the gut of 18-week-old human fetus. a = axon, g = granule containing axon, N = nucleus, × 15, 000

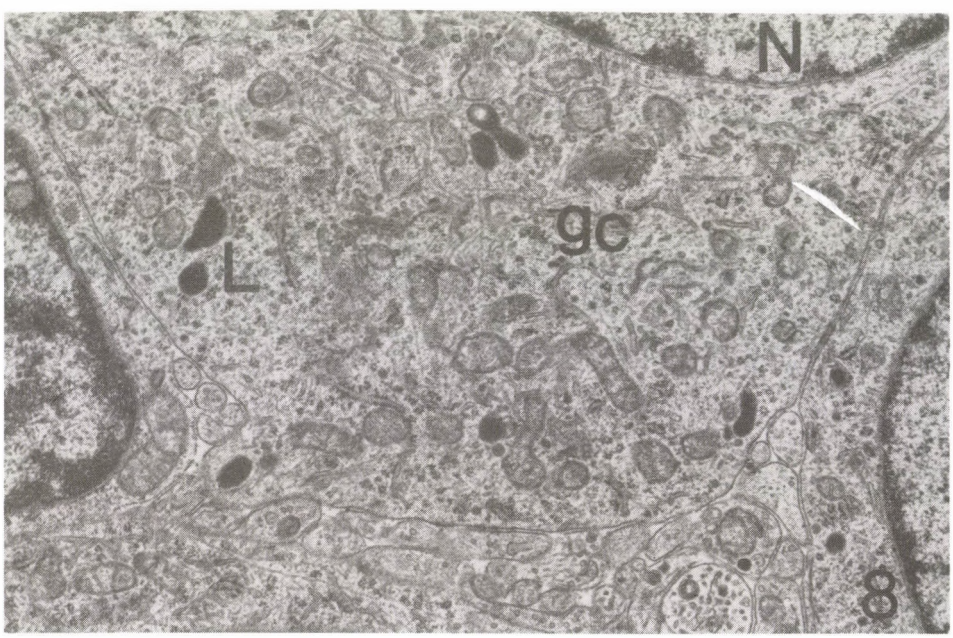


*Fig. 8.* Ganglion cells (gc) in the gut wall of 18-week-old human fetus. Perikaryon is rich in cell organelles. L-lysosomes, N = nucleus, × 20,000

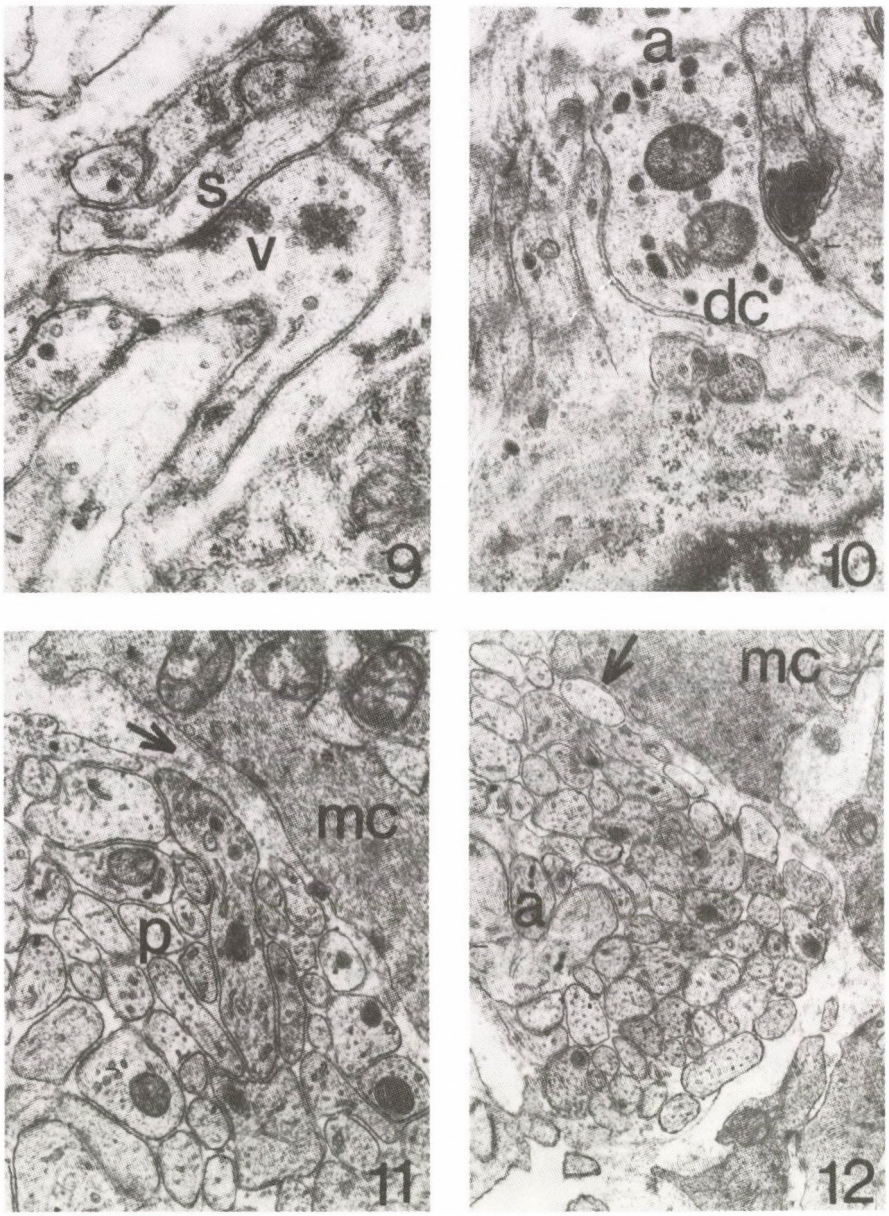


*Fig. 9.* A well-differentiated axon terminal establishes synaptic contact with undifferentiated dendrite (s). 18-week-old human fetus. Agranular vesicles (V) are accumulated at the presynaptic membrane, × 20,000

*Fig. 10.* Varicose axon (a) in the neuropil. Large and small dense core granules (dc) can be found in the axoplasm, × 25,000

*Fig. 11.* "Distant" neuromuscular contact (→) in the gut myenteric plexus (p), mc = muscle cell process, 18-week-old human fetus, × 25,000

*Fig. 12.* "Close" neuromuscular contact (→) in the jejunum of 18-week-old human fetus, a = axon, mc = muscle cell, × 25,000

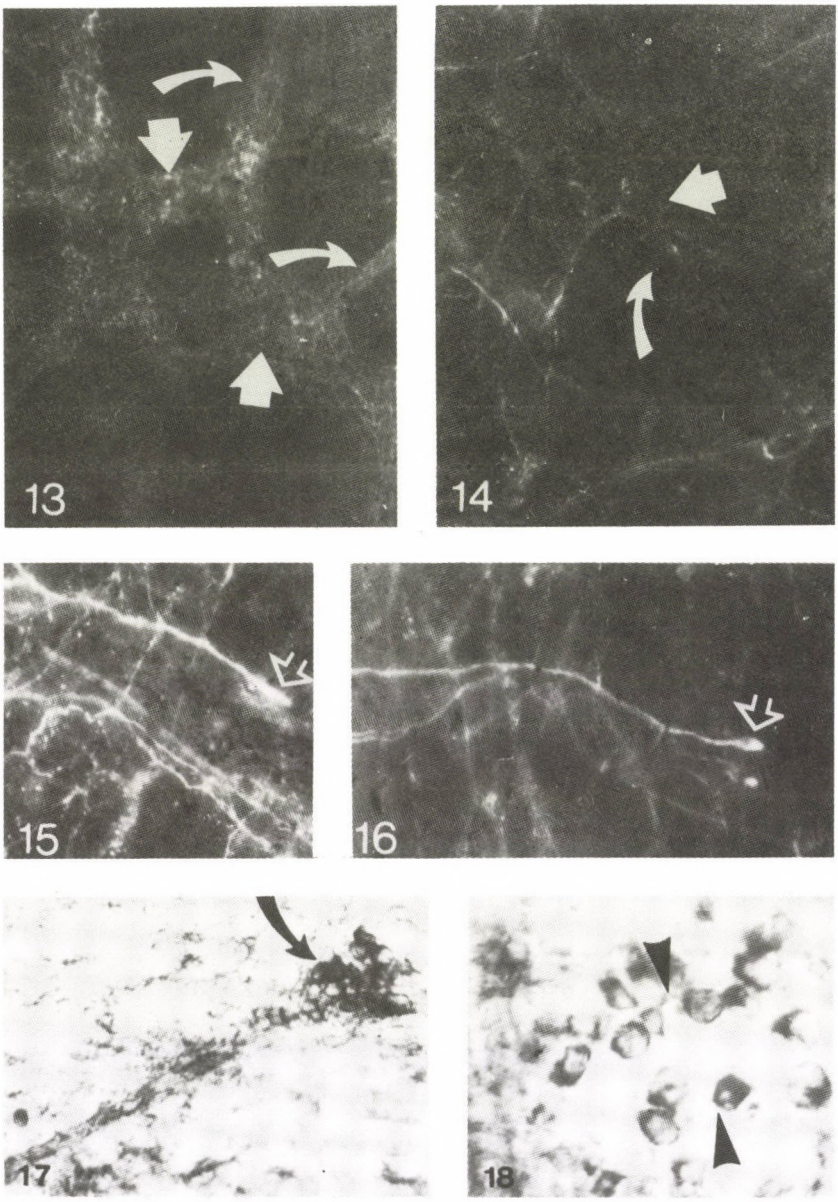


*Figs 13–16.* Whole-mount preparations from the intestine of 18-week-old human fetus after glyoxylic acid induced fluorescence. A dense fluorescent network (indicating the high catecholamine content) is present in the myenteric ganglia (Fig. 13, thick arrows) and in the internodal segments (Fig. 13, bended arrows). Several fluorescent fibres are in the submucosal ganglia (Fig. 14, arrow) and in the internodal segments (Fig. 14, bended arrows). Fluorescent cell bodies appear in the perivascular (Fig. 15, arrow) and submucosal (Fig. 16, arrow) plexuses, × 450

*Figs 17–18.* Whole-mount preparations from the intestine of an 18-week-old human fetus, after NBT/NADH reaction. Most of the cells concentrated into the ganglia (Fig. 17, arrow) × 450, although loosely arranged neurons can be seen at the mesenteric border (Fig. 18, arrowheads), × 800

## Discussion

Although human fetuses are not readily available for scientific examination, recent data suggest that various forms of digestive, absorptive and motor activity exist in the alimentary canal during fetal life [23]. The swallowing of amniotic fluid, for example, begins in week 16 of gestation and some authors consider that it may be critical for fetal gastrointestinal development [22]. Peristalsis of the small intestine has been recorded from week 12 of gestation [30], which means that intestinal transit takes place in the fetus at this age. Migration of neuroblasts in the vagal trunk begins in about week 5 and neuroblasts reach the rectum in week 12 [24]. All these facts suggest that morphological studies must be performed as early as possible. Since embryonal specimens are very fragile, several technical problems arise during preparation. For example, the gut is usually so soft that it is not suitable for whole-mount preparations (Fekete, in preparation). We achieved satisfactory ultrastructural preservation in the 10-week-old fetal intestine. The ultrastructural characteristics of the smooth muscle cells indicate that these immature myocytes are not capable of synchronized contraction. Since most of the neuronal cells are neuroblasts and the neuropil is also poorly developed, the neuronal circuits required for integrated peristalsis are lacking. This conclusion is in accordance with the observations of Daikoku et al. [5], who reported that the longitudinal muscle layer develops only in weeks 10–12, and the monodirectional (oroanal) peristalsis begins only in weeks 27–30. At the same time, it is noteworthy how common and intimate the neuromuscular junctions are in our material. Neurons, muscle cells, nerve plexuses and nerve terminals are in close contact with each other. These close contacts may provide an opportunity for nerve-muscle trophic interaction. Between weeks 10 and 18, there are no dramatic new functional changes in the alimentary canal, but a large number of enzymes (pepsin, lactase) appear together with gastric acid [23]. The smooth muscle cells lose their embryonic structural features and rather differentiated myocytes are present in both the circular and longitudinal layers. Nerve terminals among muscle cells can modify the contraction of the muscle cells, similarly as in adults. Electron microscopic studies revelaed a large number of ganglia in the myenteric plexus. The existence of these ganglia was confirmed with the NADH-diaphorase method, which is a suitable procedure for the demonstration of neurons both in ganglia and alone [12, 16]. Ultrastructurally, it is impossible to establish what kind of neurons are present in the myenteric plexuses. The number of relatively mature neurons is clearly increased but the transmitter-containing vesicles (or granules) from the perikarya are still absent, and thus the morphological data alone are not sufficient for the identification of the neurons. Our histofluorescence observations revealed well-developed plexuses in the gut wall. Since fluorescent neurons were rare, it is very probable that the observed well-developed aminergic

plexuses are extrinsic in origin. Strongly fluorescent thick plexuses have been observed in the 10-14-week-old human fetus (Fekete, in preparation), usually at the border of the gut and abdominal mesenterium. This also suggests that most of the fluorescent aminergic plexuses originate from the extrinsic sympathetic nervous system. Although more than twenty neurotransmitters may occur in the adult ENS [28], little is known about the appearance of the different transmitters during human fetal development. Substance P and metenkephalin were demonstrated by immunohistochemistry in weeks 14–16 in the human antrum [20]. In the avian gut, peptidergic neurons were also detected in the very early period of gestation, while cholinergic and serotoninergic neurons appear later [8, 27]. GABA-positive neurons can be demonstrated on day 14 of incubation [10]. These data suggest that a genetically determined chronological sequence may exist, in the appearance of the different neuronal transmitters and a knowledge of this "schedule" may be important both scientifically and clinically. Systematic immunohistochemical studies are in progress in our laboratory to identify transmitters in the human fetal ENS. Axon profiles and synaptic contacts in the 18-week-old human gut strongly suggest that not only aminergic profiles, but also cholinergic and peptidergic fibres are already present in the neuropil, and this highly organized neuronal network is effectively able to modulate the motor activity of the fetal gastrointestinal system.

## REFERENCES

1. Bailey, D. S., Cook, A., McAllister, G., Moss, M., Mian, N.: Structural and biochemical differentiation of the mammalian small intestine during fetal development. J. Cell Sci. **72**, 195–212 (1984).
2. Baumgarten, H. G., Holstein, A. F., Owmann, C.: Auerbach's plexus of mammals and man: Electron microscopic identification of three different types of neuronal processes in myenteric ganglia of the large intestine from rhesus monkey, guinea-pig and man. Z. Zellforsch. **106**, 376–397 (1970).
3. Burnstock, G.: Development of smooth muscle and its innervation. In: Smooth Muscle, eds Bulbring, E., Brading, A. F., Jones, A. W. and Tomita, T., Edward Arnold, 1981, pp. 431–459.
4. Cook, R. D., Burnstock, G.: The ultrastructure of Auerbach's plexus in the guinea pig. I. Neuronal elements. J. Neurocytol. **5**, 171–194 (1976).
5. Daikoku, S., Ikeuchi, C., Miki, S.: Electron-microscopic studies on developing intramural ganglia of the small intestine in human and rabbit fetuses. Acta Anat. **91**, 429–454 (1975).
6. Dourin, L.: The neural crest. Cambridge Univ. Press 1982.
7. Elofsson, R., Elekes, K., Myhrberg, H. E.: Catecholaminergic innervation of muscles in the hindgut of Crustaceans. Cell Tissue Res. **189**, 257–266 (1978).
8. Epstein, M. L., Sherman, D., Gershon, M. D.: Development of serotonergic neurons in the chick duodenum. Dev. Biol. 77, 22–40 (1980).

9. Feher, E., Leranth, C.: Light and electronmicroscopic immunocytochemical localization of vasoactive intestinal polypeptide, VIP-like activity in the rat small intestine. Neuroscience **10**, 97–106 (1983).
10. Fekete, E., Gabriel, R., Boros, A.: Relationship between appearance of GABA, fluorogenic monoamines and cytochrome oxidase activity during prenatal morphogenesis of chick myenteric plexus. Anat. Embryol. **184**, 489–495 (1991).
11. Furness, J. B., Costa, M.: The enteric nervous system. Churchill Livingston, Edinburgh–London–Melbourne–New York 1987.
12. Gabella, G.: Detection of nerve cells by a histochemical technique. Experienta **25**, 218–219 (1960).
13. Gabella, G.: Structure of the autonomic nervous system, John Wiley & Sons, New York 1976.
14. Gabella, G.: Innervation of the gastrointestinal tract. Int. Rev. Cytol. **59**, 129–193 (1979).
15. Gabella, G.: Structure of smooth muscles. In: Smooth Muscle. eds Bulbring, E., Brading, A. F., Jones, A. W. and Tomita, T. Edward Arnold, 1981, 1–47.
16. Gabella, G., Halasy, K.: On the nerve plexus of the chicken gizzard. Anat. Embryol. **177**, 97–103 (1987).
17. Gershon, M. D.: Properties and development of peripheral serotonergic neurons. J. Physiol. (Paris) **77**, 257–265 (1981).
18. Gershon, M. D., Thompson, E. B.: The maturation of neuromuscular function in a multiply innervated structure: development of the longitudinal muscle of the fetal mammalian gut and its cholinergic excitatory, adrenergic inhibitory and nonadrenergic inhibitory innervation. J. Physiol. (London) **234**, 257–277 (1973).
19. Gershon, M. D., Sherman, D., Gintzler, A. R.: An ultrastructural analysis of the developing enteric nervous system of the guinea pig small intestine. J. Neurocytol. **10**, 271–296 (1981).
20. Kapadia, S. E., Kapadia, R. C.: Ultrastructure and localization of substance P and met-enkephalin immunoreactivity in the human fetal gastric antrum. Cell Tissue Res. **243**, 289–297 (1986).
21. Lolova, I: Ontogenesis of the myenteric plexus in the cat gastrointestinal sphincters. III. Synaptogenesis. Z. Mikrosk. Anat. Forsch. **97**, 597–614 (1983).
22. Mulvihill, S. J., Stone, M. M., Fonkalsrud, E. W.: Trophic effect of amniotic fluid on fetal gastrointestinal development. J. Surg. Res. **40**, 291–296 (1986).
23. Neu, J.: Functional development of the fetal gastrointestinal tract. Seminars in Perinatology **13**, 224–235 (1989).
24. Okamoto, E., Ueda, T.: Embryogenesis of intramural ganglia of the gut and its relation to Hirschsprung disease. J. Pediatr. Surg. **2**, 437–443 (1967).
25. Read, J. B., Burnstock, G.: Development of the adrenergic innervation and chromaffin cells in the human fetal gut. Dev. Biol. **22**, 513–534 (1970).
26. Reynolds, E. S.: The use of lead citrate as an electron dense stain in electron microscopy. J. Cell Biol. **17**, 208–212 (1963).
27. Saffrey, M. J., Marcus, N., Jessen, K. R., Burnstock, G.: Distribution of neurons with high affinity uptake sites for GABA in the myenteric plexus of the guinea pig, rat and chicken. Cell Tissue Res. **234**, 231–235 (1983).
28. Schultzberg, M., Hokfelt, T., Nilsson, G., Terenius, L., Rehfeld, J. F., Brown, M., Elde, R., Goldstein, M., Said, S.: Distribution of peptide, and catecholamine containing neurones in the gastrointestinal tract of rat and guinea pig: immunohistochemical studies with antisera to substance P, vasoactive intestinal polypeptide, enkephalins, somatostatin, gastrin/cholecystokinin, neurotensin and dopamine beta-hydroxylase. Neuroscience **5**, 689–744 (1980).

29. De La Torre, J. C., Surgeon, J. W.: Histochemical fluorescence of tissue and brain monoamines: result in using the sucrose phosphate glyoxylic acid (SPG) method. Neuroscience **1**, 451–453 (1976).
30. Vanhoutte, J. J., Katzman, P.: Roentgenographic manifestations of immaturity of the intestinal neural plexus in premature infants. Radiology **106**, 363–367 (1973).

*Acta Physiologica Hungarica, Volume 81 (2), pp. 207–218 (1993)*

# A NEW GENERATION OF MODEL SYSTEMS TO STUDY THE BLOOD BRAIN BARRIER: THE *IN VITRO* APPROACH

F. JOÓ

LABORATORY OF MOLECULAR NEUROBIOLOGY, INSTITUTE OF BIOPHYSICS, BIOLOGICAL RESEARCH CENTER, SZEGED, HUNGARY

Received March 10, 1992
Accepted April 29, 1992

After an era of studying the unique permeability properties of cerebral endothelial cells with endogenous or exogenous tracers *in vivo*, the next generation of blood-brain barrier model systems was introduced, when the conditions for isolating the microvessels from brain tissue and culturing the endothelial cells were established. Recent advances in our knowledge of the blood-brain barrier have in part been made by studying the properties and function of cerebral endothelial cells with this *in vitro* approach. This review summarizes in brief the results obtained mainly from this rapidly growing field.

**Keywords**: blood-brain barrier, *in vitro*, cerebral endothelial cells, tissue culture, second messengers

Ever since the discovery of restricted material exchange existing between the blood and the brain [28], the ultimate goal of subsequent studies has been mainly directed towards the elucidation of relative importance of different cellular compartments in the peculiar penetration barrier constituting the structural basis of the blood-brain barrier (BBB). For many years, the decisive role of the astrocytic end feet system has prevailed in the literature [26], but – having obtained conflicting new results [10, 70] – it became generally accepted later that the *cerebral microvessels* themselves are an integral part of the BBB [7, 44, 45 68]. As the cerebral microvessels, in addition to participating in the selective material transport in an active manner, contribute to a considerable portion of the total resistance of blood flow, a better understanding of the regulation of the microvascular functions has potential implications to the delivery of nutrients and drugs across the BBB and furthermore to such clinical diseases as cerebral oedema, ischemic disorders and stroke.

Correspondence should be addressed to
Ferenc Joó
LMN, Institute of Biophysics, BRC
H-6701 Szeged, P. O. B. 521, Hungary

*Akadémiai Kiadó, Budapest*

The cerebral vasculature in general can be classified on the basis of topographical localization as extra- and intraparenchymal vessels. Much of our knowledge on brain vessels has been collected from studies on extraparenchymal vessels [21], but due to their importance in regulating the blood flow and penetration of substances circulating in the blood, it became necessary to elaborate a procedure for isolating intraparenchymal microvessels from the brain.

The aim of this review is to show the evolution of a new generation of model systems to study the physiology, biochemistry and pharmacology of cerebral endothelial cells in normal and pathological conditions.

## Remarks on methodological problems

1. *A survey and comparison of techniques used for obtaining freshly isolated intraparenchymal microvessels from brain tissue.* Though the brain, because of its extreme complexity, was thought at first not to be the best material for subcellular fractionation studies, several procedures have been successfully elaborated to isolate *synaptosomes* [19, 90] or even *perikarya of nerve* and *glial cells* [40] from other elements of it. The first description for isolation of highly purified human and bovine brain endothelial cells and nuclei was published by Siakotos et al. [78]. Special features of the *macroprocedure* were: large scale preparation, starting from 1.2–1.4 kg fresh brain, isolation by differential centrifugation and use of glass bead column filtration. Interestingly, this procedure was not employed for some reasons by others and in fact it was forgotten for a long time.

The first *micromethod* starting from 10 g of brain tissue was elaborated by us [46] without being aware of the paper of Siakotos et al. [78] using different principles: mechanical dissociation with nylon cloths of different pore sizes and density gradient centrifugation. In this procedure the animals were perfused with Krebs-Ringer solution prior to removal of the brain in order to wash out the blood constituents from the lumina of the vessels. Furthermore, slightly hypotonic (0.25 M) sucrose solution was used for homogenization, in which the glial end feet system and glial processes – known to surround the microvessels – were expected to swell to release as many capillaries as possible from the neuropil. First in the literature, the optimal sucrose concentrations (1.5, 1.3, 1.0 M) were established for separating the microvessels from the myelin, synaptosomes and dendrites, and the rate of enrichment by microvessels was expressed after alkaline phosphatase histochemistry carried out on pellets from separated fractions.

The micromethod has been adopted in many other studies [20, 34, 43, 60, 81] and modified later by several authors. Among the first, Brendel et al. [9] – by utilizing their experiences obtained on isolating the blood vessels from the retina [57] – published an other way of isolation of brain microvessels and evidenced that the vessels were metabolically active. They homogenized the cortical tissue with ten vertical strokes of a hand-held loosely fitting Teflon pestle in a smooth glass tube sieved it through a 153-μm nylon sieve for several times. In this way, a highly enriched preparation of microvessels was obtained for further studies. In the same year, Orlowski et al. [62] reported on the localization of γ-glutamyl transpeptidase in brain capillaries, in a fraction, which sedimented – by confirming our results – between 1.7 and 1.5 M sucrose. In 1975, Goldstein et al. [35] published a novel method for isolating brain capillaries from rat brain, which was based – as in the Siakotos' method – on the use of 1.2 × 1.5 cm column containing 0.25 mm glass beads. Attached capillary segments were taken off from the column and suspended in buffer with gentle agitation to release the vessels. A more simplified technique was published by Mrsulja et al. [61], in which the tissue homogenization was carried out by using a slow speed

motor driven pestle and density gradient centrifugation was performed with 1.0–1.5 M sucrose. In the same year, Sessa et al. [77] reported on the isolation from bovine brain of a fraction containing capillaries.

According to Selivonchick and Roots [76] the available techniques were not sufficient. Therefore they isolated capillary endothelia from rat brain with a new technique. This procedure is a sophisticated combination of already existing methods, including mechanical dissociation, further homogenization by loosely fitting Potter-Elvehjem Teflon homogenizer but at high speed, sucrose density gradient centrifugation and purification by passing the suspension through two glass bead column. They concluded that the capillary endothelia prepared in this way were quite pure.

As an innovation, a flotation gradient was introduced by Toews et al. [84] and Kolber et al. [52], who could show that neither trypan blue nor horseradish peroxidase entered the endothelial cells of intact isolated microvessels. On the other hand, Hwang et al. [[42] used a tight-fitting Potter-Elvehjem homogenizer with a Teflon pestle and low speed centrifugations to isolate the capillaries from the brain tissue. A comprehensive methodological study was published by Williams et al. [91], who used collagenase and glass bead filtration.

An application to physiology of microvessel preparation was developed by Morel and Godfraind [58]. The authors were interested in the possible presence of voltage-operated calcium channels with which voltage-dependent dihydropyridine receptors are associated. To accomplish the task, isolated microvessels with a length of approximately 500 μm and an external diameter of 30 to 60 μm were taken from the suspension and transferred to a thermostatically controlled organ bath. The bath consisted of a perspex block in which a 0.25 ml well had been sunk. One end of the microvessel was inserted by suction and sealed inside the tip of a 20 μm glass pipette. The other end was introduced and left free in the opening of a larger glass pipette connected to a motor driven syringe that aspirated bath solution at a constant flow rate of 0.1 ml/min. The changes in vessel diameter were measured on video recordings after different treatments.

As further applications, an isolation procedure was worked out by Joó et al. [45] for obtaining microvessels from the spinal cord by using metal sieves of 1.0 and 0.75 mm pore size. A fraction, especially enriched by *microarteries*, was used by Estrada and Krause [29] to study $^3$H-GABA binding.

Subfractionation of isolated microvessels has also been attempted. Betz et al. (1980) succeeded to identify two plasmalemmal fractions: one (the light fraction) contained alkaline phosphatase and γ-glutamyl transpeptidase, while the other (the heavier fraction) contained mostly $Na^+$, $K^+$-ATPase and 5'-nucleotidase activities. The authors concluded that the luminal and antiluminal membranes of capillaries are biochemically and functionally different. This polarity permits active solute transport across brain capillary endothelial cells. In addition, Drewes and Lidinsky [25], Lidinsky and Drewes [55] were also able to separate the endothelial cell membranes from the basement membrane and study the protein composition by SDS gel electrophoresis. They provided evidence for the different composition of luminal and antiluminal surfaces of endothelial cells. In other studies, Brendel and Meezan [8] were able to prepare isolated vascular basement membrane by treatment with detergents and DNAase. From these studies, the amino acid and carbohydrate composition of isolated basement membrane could be readily established.

However, the methods used for separating microvessels from brain and the interpretation of the subsequent investigations were not without difficulties. Experience with the preparation became wide enough to indicate that it is most useful for some purposes but inappropriate or even misleading for others. The number of different techniques used for separation of the vessels was almost as great as the investigating groups involved – a definite sign that none of the methods was ideal.

2. *The cerebral microvessels in culture.* The feature of endothelial cells in the brain microvessels to retain *in vitro* most of the fine structural features seen *in vivo* has been first noted in organotypic cultures

of nervous tissue [39, 71, 92]. With the recognition that most of the endothelial cells resisted damage during isolation, remained viable, and could be maintained in tissue culture conditions [63] a new generation of model systems has been introduced which seemed to be devoid of most of the problems experienced with the isolated cerebral microvessels.

*Procedures for long-term cultivation of cerebral microvessels and derived cells in tissue culture*

Several procedures and many modifications have been worked out for culturing *cerebral endothelial cells* (CEC) in different laboratories during the last decade. In general, all these procedures used mechanical means to disperse the brain tissue; however, a variety of techniques was employed to harvest and culture the disrupted capillaries. The most critical steps in the production of pure cerebral endothelial cell cultures are the filtration and separation of microvessels from the brain constituents. As the results showed, the CEC, like their peripheral counterparts, can resist the damage caused by the isolation and enrichment procedures. Two alternative ways have been worked out to obtain endothelial cells for culturing: (i) the use of collagenase digestion of isolated brain microvessels and (ii) the cloning of endothelial cell islands emerging from identified capillaries plated *in vitro*. Although the microvessel fraction obtained from the brain consists mainly of capillaries, the endothelial cell culture deriving from collagenase-digested microvessels is, at least to start with, a mixture of cells of capillary, arteriolar and venular origin. It has been pointed out earlier that modifications of culturing conditions could optimize a certain cell type dominance of the cultures, but so far only Goetz et al. [33] have attempted to provide preferential conditions for the growth of endothelial cells of capillary origin. On the other hand, an obvious advantage of the use of cloned endothelial cells emerging from identified capillaries is that this culture is not contaminated by endothelial cells from larger vessels. The endothelial cell culture, prepared in this way, consists almost exclusively of elongated, spindle-shaped cells, which form a non-overlapping monolayer of tightly-packed, contact inhibited cells. Since the endothelial cells of different origin have been shown to possess different biochemical and functional characteristics [93], this important methodological point should be taken into consideration, when one has to decide on the method for preparing the cultures.

For the sake of completeness, it should be mentioned that procedures for the long-term cultivation of *arterial endothelium* for middle and anterior cerebral arteries have also been reported. It was noted by Goetz et al. [33] that arterial endothelial cells did not grow as rapidly as the capillary-derived cells in RPMI 1640 with 20% fetal bovine serum The endothelial cells of arteriolar origin retained some endothelium-specific characteristics shorter than generations of capillary-derived cells. Recently, Machi et al. [56] published a procedure, by means of which the cell harvest could be increased and the reproducibility could be ensured. Taken together, these technical developments provide an opportunity to compare properties of capillary and arterial endothelium from the same tissue, and to study such processes as angiogenesis and BBB function.

It was noted by deBault et al. [14, 15] that the smaller microvessels generally gave rise to endothelial cells in culture, whereas both endothelial and smooth muscle cells were grown from the larger microvessels seeded in plastic tissue culture flasks. Endothelial cells were observed to proliferate rapidly in the 1st week of culture, forming large cobblestone colonies. On the other hand, the *smooth muscle cells* emerged rapidly from the isolated microvessels of larger diameter and, as free cells, took on fusiform or stellar shapes. With time these cells became flat and broad with a clearly visible ordered cytoskeleton. As an important development, pure cerebrovascular muscle cultures were established and characterized by Spatz et al. [81]. The method was based on the isolation of microvessels from the brain tissue by mechanical dispersion and filtration techniques, treatment with 0.01% trypsin-collagenase, and use of low (10%) concentration of fetal bovine serum, at which the growth of smooth muscle cells was

found to be preferentially facilitated during long-term cultivation. In another study, cerebral microvascular smooth muscle cultures were cloned by Moore et al. [59] from selected larger microvessels with a single-layered, smooth muscle media. In addition to characteristic structural features, the active synthesis of α-actin suggested that these cells were of smooth muscle origin. The availability of a pure cerebrovascular smooth muscle culture provides a new model system for the study of its function, as well as its interactions with endothelium and/or with glial cells, especially in relation to the regulation of cerebral blood flow and blood pressure.

A procedure for producing *in vitro* a relatively homogeneous population of *pericytes* from cerebral microvessel derived cells was reported by Carson and Haudenschild [12]. By varying several aspects of the culture conditions in the attempt to optimize a certain cell type dominance of the cultures, it was revealed that omission of all conditioned medium from the formulation resulted in the rapid domination of the culture by non-endothelial cell types and reduced endothelial cell attachment and spreading upon subculture. Moreover, pancreatin (25% in PBS)* was found to be capable of removing endothelial colonies from nearby and underlying cells, primarily pericytes. By combining these culturing conditions, pure pericyte cultures could be obtained from isolated cerebral microvessels. Increased accessibility of these important cells should facilitate to study their functional properties in normal conditions and pathological circumstances. Larson et al. [54] and Robinson et al. [73] have already utilized co-cultures of CEC** and pericytes in studying intercellular relations in the microvasculature. Finally, the results of Spatz et al. [83], and Hervonen et al. [41] should be mentioned showing that viable endothelial cells could be maintained *in vitro* in cultures of the pia-arachnoid membrane. Furthermore, a selective and dose-dependent uptake of L-DOPA was demonstrated by the endothelial cells, while the pia-arachnoid cells took up horseradish peroxidase (HRP). The absence of HRP label in the endothelial cells indicates that the pial vascular endothelium acts similarly in this respect to those in cultures from isolated brain capillary fraction or *in vitro* in the brain capillaries.

*Cerebral endothelial cells cultured on dextran microbeads*

Dextran microbeads have long been used for the isolation of endothelial cells [5, 75]. Busch et al. [11] first applied this technique to the CEC and the method has been successfully used in other studies [50, 51, 88] to evaluate some of the factors that may play a role in inducing BBB permeability changes in pathological conditions.

*Cerebral endothelial cells cultured on porous supports*

In an attempt to design a modified Ussing chamber [86] for studying the transendothelial transport, CEC were first seeded onto collagen- or fibronectin coated nylon-mesh squares and allowed to grow to confluence. They were then attached across a hole cut through a plexi-glass block to form a chamber and used to test the effect of substances on permeability of the BBB [6]. Later, Audus and Borchardt [2] applied this technique for studying drug transport and metabolism. Subsequent technical developments promoted the use of more sophisticated ways to study BBB transport *in vitro*. Thus, Audus and Borchardt [3, 4] introduced optically clear, regenerated cellulose discs for this purpose. The discs containing complete monolayers were placed in horizontal side-by-side diffusion cells for transendothelial transport studies. This method was used recently by van Bree et al. [87] to study the transport of vasopressin fragments across the BBB. In other investigations, fibronectin-coated 24-well

*PBS: Phosphate buffered saline

**CEC: Cerebral endothelial cell

multiplates [22, 23] or nitrocellulose filters [38] were used for transport studies. Recently, a full reconstitution of the endothelial-glial interface was achieved *in vitro* by culturing brain capillary endothelial cells on one side of a porous filter and astrocytes on the other [16]. Application of this technique to the CEC obtained from the human fetus has also been published [49].

Several characteristic features of the endothelial cells are retained *in vitro*. Low rate of pinocytosis and well-developed junctional complexes were observed under the electron microscope. In addition, positivity for Factor VIII-related antigen, alkaline phosphatase, γ-glutamyl transpeptidase and angiotensin-converting enzyme activities, specific binding of lectins, uptake of acetylated-LDL and prostacyclin synthesis were also detected. Recent results of Gaffney et al. [31] showed, however, that the brain capillary endothelial cells lack the receptors for modified LDL. Therefore, the use of acetylated-LDL uptake as a marker for endothelial cells of brain origin could be argued. Recently, a convenient *in situ* – in plate assay has been reported by Fukushima et al. [30] to follow quantitatively the change of BBB-associated enzymes. It should be kept in mind, however, that the presence of these markers in the cultured endothelial cells does not necessarily indicate the operation of the molecular mechanisms which restrict the free passage of macromolecules through the endothelial monolayer. Results of several studies provided evidence for the existence *in vitro* of a permeability barrier for macromolecules in the CEC. First, the free penetration of trypan blue was found to be prevented by a layer of endothelial cells grown on dextran microbeads [50, 51, 74]. In addition, HRP – an exogenous permeability marker – was also found to be unable to penetrate this *in vitro* barrier [22, 23]. The final proof on this issue was provided by Smith and Borchardt [80] showing that the permeability coefficient for albumin was almost equivalent with that observed *in vivo*. These properties of the CEC grown in culture justify their use for studying the BBB *in vitro*. Recent comparisons of drug transport [1], and transcytosis [65] between *in vitro* and *in vivo* models indicated that BBB-specific properties were better preserved *in vitro* when the endothelium was co-cultured with astrocytes [17]. The results of transendothelial electrical resistance measurements, however, point to a great variability of individual cultures.

Unfortunately, the albumin permeability and the transendothelial electrical resistance were not measured simultaneously in the same cultures. When we consider the BBB according to the classical definition to be a permeability barrier to circulating macromolecules including albumin, it would be desirable to perform direct comparisons to understand better the nature of relations.

Recently, Laabich et al. [53] reported on culturing ependymal cells on porous bottom dishes in a complete defined medium. The cells grown on the microporous membrane were oriented and formed a continuous layer of primary ependymal cells with an apical side and a basolateral side. The preparation offers a new tool for transport studies across the blood cerebrospinal barrier.

*Current understanding on transendothelial transport of macromolecules in pathological conditions*

The results of Rapoport et al. [69] indicated that when hyperosmotic solutions of urea or arabinose are infused into the carotid artery of animals or applied to the pial surface of the brain, the permeability of the microvessels to polar molecules, including HRP, is markedly enhanced. In subsequent studies, Dorovini-Zis et al. [21, 22, 23] observed a reversible separation of tight junctions with penetration of HRP across a monolayer of CEC indicating the importance of this intercellular complex in induced macromolecular transport. Other ultrastructural studies, however, suggested the significance of endothelial vesicles in the uptake and transport of certain plasma proteins across the capillary wall in vessels of peripheral origin. A transcellular diffusion across the CEC has been proposed by Rim et al. [72]. Coated or uncoated vesicles, either singly or as a part of a system of invaginations or channels, transfer proteins to lysosomes where they are degraded (endocytosis). Alternatively, protein-laden vesicles bypass the lysosomes and deliver their content to the interstitial space (transcytosis).

Endocytosis and transcytosis involve a variety of mechanisms namely high-affinity or receptor-mediated endocytosis, low-affinity adsorptive endocytosis, or bulk-flow endocytosis [79]. Although the CEC are known to be almost impermeable to circulating molecules, exposure of the endothelium to cationic ferritin resulted in [38] a significant increase in permeability of the endothelium to Evans blue dye (molecular weight 960), but not to fluorescein-dextran (molecular weight 20,000). This result indicated that ablation of endothelial surface anionic charge enhanced endothelial transport of the small, polar-charged molecule only. Since the electrical resistance of endothelial cell layer did not change after the application of cationized ferritin, a transcellular rather than a paracellular route of Evan's blue dye leakage was suggested. The characteristics of permeability and binding of bovine serum albumin (BSA) to primary cultures of bovine brain capillary endothelial cells were studied in detail by Smith and Borchardt [80] and Guillot et al. [36, 37]. Directly measuring the permeability of Lucifer Yellow, a fluid-phase endocytotic marker, and that of markers such as cationized ferritin and certain ricins (adsorptive-phase endocytic markers), a low level of uptake and adsorption of these fluid-phase markers was found by the CEC. Furthermore, it could be established that, as *in vivo*, the flux rates of cationized BSA (cBSA) and glycosylated BSA (gBSA) across the endothelial cell monolayer were seven times greater than those observed for BSA. From these results the authors concluded that the binding and transendothelial transport of cBSA and gBSA appear to proceed by adsorptive-phase endocytic mechanisms. It should be stressed, however, that studies on permeability and transport across the monolayer ought to be carried out in the future after reaching a condition existing *in vivo*, for example if the culture was found to be sufficiently tight to start with resistance $> 500\ \Omega.cm^2$.

In summary, it can be concluded that, with the use of *in vitro* approach in blood-brain barrier research, the CEC reveal in detail their chemical composition, transport processes, and complex and subtle molecular interactions, by which the nourishment of the brain is accomplished. As we have seen, the tissue culture approach has proved its viability and become a suitable model system for studying the BBB *in vitro*. In particular, it has led to a widening of our knowledge on the molecular basis of permeability regulation in the CEC. Looking at further areas of possible application, it can be predicted that, in the future, this approach will be used more frequently in drug research, with the aim of developing new means for the improvement of penetration of therapeutic substances through the cerebral endothelium.

*Isolation of microvessels from human brain*

The development of methods for the isolation of brain capillaries has promoted the accomplishment of detailed studies on human cerebral microvessels, as well. Current research is directed to study different properties of cerebral microvessels isolated either from *fresh autopsy* human brain [47, 67] or from *frozen human brain* [66, 85]. Capillaries isolated from fresh autopsy human brain were shown [64] to have high activities of BBB-specific enzymes such as γ-GTP of alkaline phosphatase, and have structurally intact insulin receptor and amino acid transport [13]. Similarly to the freshly isolated microvessels, capillaries from frozen human brain were seen to be enriched in γ-GTP, Factor VIII antigen, and a 46K protein, which is thought to be a BBB-specific protein [66].

Endothelial cell cultures have been prepared so far from the brain of human fetuses [49], from biopsy material obtained during surgery [82] or from fresh autopsy human brain [19, 24, 32].

*Further perspectives*

Apart from studying the basic molecular mechanisms underlying the regulation of transport processes in cerebral endothelial cells, the extension of studies to human brain capillary to neurologic problems such as multiple sclerosis or Alzheimer disease has paved the path for the application of the

*in vitro* approach of BBB research to human neuropathology. As examples along this line, the results of Pardridge et al. [66] should be mentioned, characterized the amino acid composition of a 4,200-Dalton peptide isolated from cortical microvessels of patients with Alzheimer disease. Furthermore, Kalaria and Harik [48] found a marked decrease in the hexose transporter of brain microvessels isolated from patients with Alzheimer disease. The low density of hexose transported at the BBB in Alzheimer disease may result consequently in a decreased cerebral oxidative metabolism that may participate in the pathogenesis of disease. No doubt that human brain banks offer an important reservoir of autopsy brain tissue of particular neurologic diseases and further research will be most likely directed towards establishing tissue cultures of cerebral endothelial cells from frozen human brain with diagnosed neurologic diseases.

## Acknowledgement

I would like to thank the valuable contribution of every coworker and collaborator who helped the accomplishment of the task at each phase of the research. I am grateful to the Hungarian Research Found (OTKA) and Scientific Research Council of the Ministry of Public Welfare for financial support.

## REFERENCES

1. Audus, K. L., Bartel, R. L., Hidalgo, I. J., Borchardt, R. T.: The use of cultured epithelial and endothelial cells for drug transport and metabolism studies. Pharm. Res. **7**, 435–451 (1990).
2. Audus, K. L., Borchardt, R. T.: Characterization of an in vitro blood-brain barrier model system for studying drug transport and metabolism. Phar. Res. **3**, 81–87 (1986a).
3. Audus, K. L., Borchardt, R. T.: Characteristics of the large neutral amino acid transport system of bovine brain microvessel endothelial cell monolayers. J. Neurochem. **47**, 484–488 (1986b).
4. Audus, K. L., Borchardt, R. T.: Bovine brain microvessel endothelial cell monolayers as a model system for the blood-brain barrier. Ann. N. Y. Acad. Sci. **507**, 9–18 (1988).
5. Boiadjieva, S., Hallberg, C., Hogstrom, M., Bush, C.: Exclusion of trypan blue from microcarriers by endothelial cells: an in vitro barrier function test. Lab. Invest. **50**, 239–246 (1984).
6. Bowman, P. D., Ennis, S. R., Rarey, K. E., Betz, A. L., Goldstein, G. W.: Brain microvessel endothelial cells in tissue culture: A model for study of blood-brain barrier permeability. Ann. Neurol. **14**, 396–402.
7. Bradbury, M.: The Concept of a Blood-Brain Barrier. Wiley, Chichester, England (1984).
8. Brendel, K., Meezan, E.: Vascular basement membranes: preparation and properties of material isolated with the use of detergents. In: The Cerebral Microvasculature. eds Eisenberg H. M. and Suddith R. L., Plenum Press, New York 1980, pp. 89–103.
9. Brendel, K., Meezan, E., Carlson, E. C.: Isolated brain microvessels: A purified, metabolically active preparation from bovine cerebral cortex. Science **185**, 953–955 (1974).
10. Brightman, M. W., Reese, T. S.: Junctions between intimately apposed cell membranes in the vertebrate brain. J. Cell. Biol. **40**, 648–677 (1969).
11. Bush, C., Cancilla, P. A., DeBault, L. E., Goldsmith, J. C., Owen, W. G.: Use of endothelium cultured on microcarriers as a model for the microcirculation. Lab. Invest. **47**, 498–504 (1982).
12. Carson, M. P., Haudenschild, C. C.: Microvascular endothelium and pericytes: high yield, low passage cultures. In Vitro Cell. Develop. Biol. **22**, 344–353 (1986).
13. Choi, T., Pardridge, W. M.: Phenylalanine transport at the human blood-brain barrier. Studies in isolated human brain capillaries. J. Biol. Chem. **261**, 6536–6541 (1986).

14. DeBault, L. E., Cancilla, P. A.: γ-glutamyl transpeptidase in isolated brain endothelial cells: Induction by glial cells in vitro. Science **207**, 653–655 (1979).
15. DeBault, L. E., Hendriquez, E., Hart, M. N., Cancilla, P. A.: Cerebral microvessels and derived cells in tissue culture: II. Establishment, identification, and preliminary characterization of an endothelial cell line. In Vitro Cell. Develop. Biol. **17**, 480–494 (1981).
16. Dehouck, M.-P., Méresse, S., Delorme, P., Fruchart, J. C., Cecchelli, R.: An easier, reproducible and mass production method to study the blood-brain barrier in vitro. J. Neurochem. **54**, 1798–1801 (1990).
17. Dehouck, M.-P., Jolliet-Riant, P., Bree, F., Fruchart, J. C., Cecchelli, R., Tillement, J. P.: Drug transfer across the blood-brain barrier: correlation between in vitro and in vivo models. J. Neurochem. 1991 (In press).
18. Cecchelli, R., Tillement, J. P.: Drug transfer across the blood-brain barrier: correlation between in vitro and in vivo models. J. Neurochem. (In press) (1991).
19. DeRobertis, E., DeIraldi, A. P., Rodriguez, G., Gomez, J.: On the isolation of nerve endings and synaptic vesicles. J. Biophys. Biochem. Cytol. **9**, 23–35 (1961).
20. Djuricic, B. M., Rogac, Lj. M., Spatz, M., Rakic, Lj. M., Mrsulja, B. B.: Brain microvessels. I. Enzymatic activities. Adv. Neurol. **20**, 197–205 (1978).
21. Dorovini-Zis, K., Bowman, P. D., Betz, A. L., Goldstein, G. W.: Hyperosmotic arabinose solutions open the tight junctions between brain capillary endothelial cells in tissue culture. Brain Res. **302**, 383–386 (1984).
22. Dorovini-Zis, K., Bowman, P. D., Betz, A. L., Goldstein, G. W.: Formation of a barrier by brain microvessel endothelial cells in culture. Fed. Proc. **46**, 2521–2522 (1987a).
23. Dorovini-Zis, K., Bowman, P. D., Betz, A. L., Goldstein, G. W.: Hyperosmotic urea reversibly opens the tight junctions between brain capillary endothelial cells in cell culture. J. Neuropathol. Exp. Neurol. **46**, 130–140 (1987b).
24. Dorovini-Zis, K., Prameya, R., Thompson, G. B.: Isolation and culture of human brain microvessel endothelial cells. Amer. Assoc. Neuropathol., 65th Annual Meeting, Dallas. (Abstract) (1989).
25. Drewes, L. D., Lidinsky, W. A.: Studies on cerebral capillary endothelial membrane. In: The Cerebral Microvasculature, eds Eisenberg, H. M. and Suddith, R. L., Plenum Press, New York 1980, pp. 17–27.
26. Edström, R.: Recent development of the blood-brain barrier concept. Int. Rev. Neurobiol. **7**, 153–190 (1964).
27. Edvinsson, L.: Sympathetic control of cerebral circulation. TINS **5**, 425–429 (1982).
28. Ehrlich, P.: Das Sauerstoff-Bedürfnis des Organismus. Eine farbenanalytische Studie. A Hirschwald, Berlin 1885.
29. Estrada, C., Krause, D. N.: Muscarinic cholinergic receptor sites in cerebral blood vessels. J. Pharmac. exp. Ther. **221**, 85–90 (1982).
30. Fukushima, H., Fujimoto, M., Ide, M.: Quantitative detection of blood-brain barrier-associated enzymes in cultured endothelial cells of porcine brain microvessels. In Vitro Cell. Develop. Biol. **26**, 612–620 (1990).
31. Gaffney, J., West, D., Arnold, A., Sattar, A., Kumar, S.: Differences in the uptake of modified low density lipoproteins by tissue cultured endothelial cells. J. Cell Sci. **79**, 317–325 (1985).
32. Gerhart, D. Z., Broderius, M. A., Drewes, L. R.: Cultured human and canine endothelial cells from brain microvessels. Brain Res. Bull. **21**, 785–793 (1988).
33. Goetz, I. E., Warren, J., Estrada, C., Roberts, E., Krause, D. N.: Long-term serial cultivation of arterial and capillary endothelium from adult bovine brain. In Vitro Cell. Develop. Biol. **21**, 172–180 (1985).
34. Goldstein, G. W., Betz, A. L., Bowman, P. D.: Use of isolated brain capillaries and cultured endothelial cells to study the blood-brain barrier. Fed. Proc. **43**, 191–195 (1984).
35. Goldstein, G., Wolinsky, J., Csejtey, J., Diamond, I.: Isolation of metabolically active capillaries from rat brain. J. Neurochem. **25**, 715–717 (1975).

36. Guillot, F. L., Audus, K. L.: Angiotensin peptide regulation of fluid-phase endocytosis in brain microvessel endothelial cell monolayer. J. Cereb. Blood Flow Metab. **10**, 827–834 (1990a).
37. Guillot, F. L., Audus, K. L., Raub, T. J.: Fluid-phase endocytosis by primary cultures of bovine brain microvessel endothelial cell monolayers. Microvasc. Res. **39**, 1–14 (1990b).
38. Hart, M. N., VanDyk, L. F., Moore, S. A., Shasby, D. M., Cancilla, P. A.: Differential opening of the brain endothelial barrier following neutralization of the endothelial luminal anionic charge in vitro. J. Neuropathol. Exp. Neurol. **46**, 141–153 (1987).
39. Hauw, J. J., Berger, B., Escourolle, R.: Ultrastructural observation on human cerebral capillaries in organ culture. Cell Tissue Res. **163**, 133–150 (1975).
40. Hemminki, K., Holmina, E.: Characterization of neuronal and glial fractions separated in sucrose and Ficoll media. Acta physiol. Scand. **82**, 135–142 (1971).
41. Hervonen, H., Spatz, M., Bembry, J., Murray, M. R.: Studies related to the blood-brain barrier to monoamines and protein in pia-arachnoid cultures. Brain Res. **210**, 449–454 (1981).
42. Hwang, S. M., Weiss, S., Segal, S.: Uptake of L-$^{35}$S-cystine by isolated rat brain capillaries. J. Neurochem. **35**, 417–424 (1980).
43. Joó, F.: The blood-brain barrier in vitro: Ten years of research on microvessels isolated from the brain. Neurochem. Int. **7**, 1–25 (1985).
44. Joó, F.: New aspects to the function of cerebral endothelium. Nature **321**, 197–198 (1986).
45. Joó, F., Dux, E., Szűcs, A.: Microvessels from the spinal cord: isolation procedure and characterization of the fraction. J. Neurochem. **39**, 263–266 (1982).
46. Joó, F., Karnushina, I.: A procedure for the isolation of capillaries from rat brain. Cytobios **8**, 41–48 (1973).
47. Kalaria, R. N., Gravina, S. A., Schmidley, J. W., Perry, G., Harik, S. I.: The glucose transporter of the human brain and blood-brain barrier. Ann. Neurol. **24**, 757–764 (1988).
48. Kalaria, R. N., Harik, S. I.: Reduced glucose transporter at the blood-brain barrier and in cerebral cortex in Alzheimer disease. J. Neurochem. **53**, 1083–1088.
49. Kása, P., Pákáski, M., Joó, F.: Endothelial cells from human fetal brain microvessels may be cholinoceptive, but do not synthesize acetylcholine. J. Neurochem. **56**, 2143–2146 (1991).
50. Kempski, O., Spatz, M.: Blood-brain barrier: in vitro studies of endothelial permeability, in Stroke and Microcirculation, eds Cervós-Navarro, J., and Ferszt, R., Raven Press, New York 1987, pp. 223–227.
51. Kempski, O., Wroblewska, B., Spatz, M.: Effects of forskolin on growth and morphology of cultured glial and cerebrovascular endothelial and smooth muscle cells. Int. J. Devl. Neurosci. **5**, 435–445 (1987).
52. Kolber, A. R., Bagnell, C. R., Krigman, M. R., Hayward, J., Morell, P.: Transport of sugars into microvessels isolated from rat brain: A model for the blood-brain barrier. J. Neurochem. **33**, 419–432 (1979).
53. Laabich, A., Sensenbrenner, M., Delaunoy, J. P.: Monolayer cultures of ependymal cells on porous bottom dishes. A tool for transport studies across the brain cerebrospinal barrier. Neurosci. Lett. **103**, 157–161 (1989).
54. Larson, D. M., Carson, M. P., Haudenschild, C. C.: Junctional transfer of small molecules in cultured bovine brain microvascular endothelial cells and pericytes. Microvasc. Res. **34**, 184–199 (1987).
55. Lidinsky, W. A., Drewes, L. R.: Composition of the blood-brain barrier: protein composition of the capillary endothelial cell membrane. J. Neurochem. **41**, 1341–1348 (1983).
56. Machi, T., Kassell, N. F., Scheld, W. M.: Isolation and characterization of endothelial cells from bovine cerebral arteries. In Vitro Cell. Develop. Biol. **26**, 291–300 (1990).
57. Meezan, E., Brendel, K., Carlson, E. C.: Isolation of a purified preparation of metabolically active retinal blood vessels. Nature **251**, 65–67 (1974).
58. Morel, N., Godfraind, T.: Pharmacological properties of voltage-dependent calcium channels in functional microvessels isolated from rat brain. Naunyn-Schmiedeberg's Arch. Pharmacol. **340**, 442–451 (1989).

59. Moore, S. A., Strauch, A. R., Yoder, E. J., Rubinstein, P. A., Hart, M. N.: Cerebral microvascular smooth muscle in tissue culture. In Vitro Cell Develop. Biol. **20**, 512–520 (1984).
60. Mrsulja, B. B., Djuricic, B. M., Mrsulja, B. J., Rogac, Lj., Spatz, M., Klatzo, I.: Brain microvessels. II. Effect of ischemia and dihydroergotoxine on enzyme activities. Adv. Neurol. **20**, 207–213 (1978).
61. Mrsulja, B. B., Mrsulja, B. J., Fujimoto, T., Klatzo, I., Spatz, M.: Isolation of brain capillaries: A simplified technique. Brain Res. **110**, 361–365 (1976).
62. Orlowski, M., Sessa, G., Green, J. P.: γ-Glutamyl transpeptidase in brain capillaries: Possible site of a blood brain barrier for aminoacids. Science **184**, 66–68 (1974).
63. Panula, P., Joó, F., Rechardt, L.: Evidence for the presence of viable endothelial cells in cultures derived from dissociated rat brain. Experientia **34**, 95–97 (1978).
64. Pardridge, W. M., Eisenberg, J., Yang, J.: Human blood brain barrier insulin receptor. J. Neurochem. **45**, 1141–1147 (1985).
65. Pardridge, W. M., Triguero, D., Yang, J., Cancilla, P. A.: Comparison of in vitro and in vivo models of drug transcytosis through the blood-brain barrier. J. Pharmacol. Exp. Therap. **253**, 884–891 (1990).
66. Pardridge, W. M., Vinters, H. V., Yang, J., Eisenberg, J., Choi, T. B., Toutellotte, W. W., Huebner, V., Shively, J. E.: Amyloid angiopathy of Alzheimer's disease: Amino acid composition and partial sequence of a 4,200-Dalton peptide isolated from cortical microvessels. J. Neurochem. **49**, 1394–1401 (1987).
67. Pardridge, W. M., Yang, J., Eisenberg, J., Tourtellotte, W. W.: Isolation of intact capillaries and capillary plasma membranes from frozen human brain. J. Neurosci. Res. **18**, 352–357 (1987).
68. Rapoport, S. I.: Blood-Brain Barrier in Physiology and Medicine. Raven Press, New York 1976.
69. Rapoport, S. I., Fredericks, W. R., Ohno, K., Pettigrew, K. D.: Quantitative aspects of reversible osmotic opening of the blood-brain barrier. Am. J. Physiol. **238**, R421–R431 (1980).
70. Reese, T. S., Karnovsky, M. J.: Fine structural localization of a blood-brain barrier to exogenous peroxidase. J. Cell. Biol. **34**, 207–217 (1967).
71. Renkawek, K., Murray, M. R., Spatz, M., Klatzo, I.: Distinctive histochemical characteristics of brain capillaries in organotypic culture. Expl. Neurol. **50**, 194–206 (1976).
72. Rim, S., Audus, K. L., Borchardt, R. T.: Relationship of octanol/buffer and octanol/water partition coefficients to transcellular diffusion across brain microvessel endothelial cell monolayers. Int. J. Pharm. **32**, 79–84 (1986).
73. Robinson, D. H., Kang, Y. H., Deschner, S. H., Nielsen, T. B.: Morphologic plasticity and periodicity: porcine cerebral microvascular cells in culture. In Vitro Cell. Develop Biol. **26**, 169–180 (1990).
74. Rutten, M. J., Hoover, R. L., Karnovsky, M. J.: Electrical resistance and macromolecular permeability of brain endothelial monolayer cultures. Brain Res. **425**, 301–310 (1987).
75. Ryan, U. S., Mortana, M., Whitaker, C.: Methods for microcarrier culture of bovine pulmonary artery endothelial cells avoiding the use of enzymes. Tissue Cell **12**, 619–635 (1980).
76. Selivonchick, D. P., Roots, B. I.: Lipid and fatty acyl composition of rat brain capillary endothelia isolated by a new technique. Lipids **12**, 165–169 (1977).
77. Sessa, G., Orlowski, M., Green, J. P.: Isolation from bovine brain of a fraction containing capillaries and a fraction containing membrane fragments of the chorioid plexus. J. Neurobiol. **57**, 51–61 (1976).
78. Siakotos, A. N., Rouser, G., Fleischer, S.: Isolation of highly purified human and bovine endothelial cells and nuclei and their phospholipid composition. Lipids **4**, 234–239 (1969).
79. Simionescu, N.: Cellular aspects of transcapillary exchange. Physiol Rev. **63**, 1536–1579 (1983).
80. Smith, K. R., Borchardt, R. T.: Permeability and mechanism of albumin and glycosylated albumin transcellular transport across monolayers of cultured bovine brain capillary endothelial cells. Pharm. Res. **6**, 466–473 (1989).
81. Spatz, M., Dodson, R. F., Bembry, J.: Cerebrovascular muscle cultures. I. Isolation, growth and morphological characterization. Brain Res. **280**, 387–391 (1983).

82. Spatz, M., Bacic, F., McCarron, R. M., Merkel, N., Uematsu, S., Long, D. M., Bembry, J.: Cholinergic and histaminergic receptors in cultured endothelium derived from human cerebral microvessels, in Neurotransmission and cerebrovascular function I. (Seylaz, J. and Mackenzie E. T., eds), Elsevier Science Publishers B. V. (Biomedical Division) 1989, pp. 105–108.
83. Spatz, M., Renkawek, K., Murray, M. R., Klatzo, I.: Uptake of radiolabeled glucose analogues by organotypic pia arachnoid cultures. Brain Res. **100**, 710–715 (1975).
84. Toews, A. D., Kolber, A., Hayward, J., Krigman, M. R., Morell, P.: Experimental lead encephalopathy in the suckling rat: concentration of lead in cellular fractions enriched in brain capillaries. Brain Res. **147**, 131–138 (1978).
85. Tsui, T., Mimori, Y., Nakamura, S., Kameyama, M.: A micromethod for the isolation of large and small microvessels from frozen autopsied human brain. J. Neurochem. **49**, 1796–1800 (1987).
86. Ussing, H. H.: A discussion on active transport of salts and water in living tissues. Introductory remarks. Philos. Trans. R. Soc. Lond. **262**, 85–90 (1971).
87. van Bree, J. M. M., de Boer, A. G., Verhoef, J. C., Danhof, M., Breimer, D. D.: Transport of vasopressin fragments across the blood-brain barrier: in vitro studies using monolayer cultures of bovine brain endothelial cells. J. Pharmacol. Exp. Therap. **249**, 901–905 (1989).
88. Villacara, A., Spatz, M., Dodson, R. F., Corn, C., Bembry, J.: Effect of arachidonic acid on cultured cerebromicrovascular endothelium: permeability, lipid peroxidation and membrane "fluidity". Acta Neuropathol. **78**, 310–316 (1989).
89. Vinters, H. V., Beck, D. W., Bready, J. V., Maxwell, K., Berliner, J. A., Hart. M. N., Cancilla, P. A.: Uptake of glucose analogues into cultured cerebral microvessel endothelium. J. Neuropathol. Exp. Neurol. **44**, 445–458 (1985).
90. Whittaker, V. P.: The isolation and characterization of acetylcholine-containing particles from brain. Biochem. J. **72**, 694–706 (1959).
91. Williams, S. K., Gillis, J. F., Matthews, M. A., Wagner, R. C., Bitensky, M. W.: Isolation and characterization of brain endothelial cells: morphology and enzyme activity. J. Neurochem. **35**, 374–381 (1980).
92. Wolff, J. R., Rajan, K. T., Noack, W.: The fate and fine structure of fragments of blood vessels in CNS tissue cultures. Cell Tissue Res. **156**, 89–102 (1974).
93. Zetter, B. R.: Endothelial heterogeneity: influence of vessel size, organ localization and species specificity on the properties of cultured endothelial cells, in Endothelial cells, vol. II, Ryan, U. ed, CRC Press Inc., Boca Raton, Florida 1988, pp. 63–79.

# INSTRUCTIONS TO AUTHORS

*Form of manuscript*

Two complete copies of the manuscript including all tables and illustrations should be submitted. Manuscripts should be typed double-spaced with margins at least 3 cm wide. Pages should be numbered consecutively.

Manuscripts should include the title, authors' names and short postal address of the institution where the work was done.

An abstract of not more than 200 words should be supplied typed before the text of the paper. The abstract should be followed by (no more than) five key-words.

*Abbreviations* should be spelled out when first used in the text. *Drugs* should be referred to by their WHO code designation (Recommended International Nonproprietary Name): the use of proprietary names is unacceptable. The *International System of Units* (SI) should be used for all measurements.

*References*

References should be numbered in alphabetical order and only the numbers should appear in the text [in brackets]. The list of references should contain the name and initials of all authors (the use of et al. instead of authors' name in the reference list is not accepted): for journal articles the title of the paper, title of the journal abbreviated according to the style used in Index Medicus, volume number, first and last page number and year of publication, for books the title followed by the publisher and place of publication.

Examples:

Székely, M., Szelényi, Z.: Endotoxin fever in the rat. Acta physiol. hung. **53,** 265–277 (1979).

Schmidt, R. F.: Fundamentals of Sensory Physiology. Springer Verlag, New York–Heidelberg–Berlin 1978.

Dettler, J. C.: Biochemical variation. In: Textbook of Human Genetics, eds Fraser, O., Mayo, O., Blackwell Scientific Publications, Oxford 1975, p. 115.

*Tables and illustrations*

Tables should be comprehensible to the reader without reference to the text. The headings should be typed above the table.

Figures should be identified by number and authors' name. The top should be indicated on the back. Their approximate place should be indicated in the text. Captions should be provided on a separate page.

*Proofs and reprints*

Reprints and proofs will be sent to the first author unless otherwise indicated. Proofs should be returned within 48 hours of receipt. Fifty reprints of each paper will be supplied free of charge.

# Acta Physiologica Hungarica

VOLUME 81, NUMBER 3, 1993



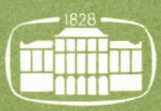


Akadémiai Kiadó, Budapest

ACTA PHYSIOL. HUNG. APHDUZ. 81(3) 219–316 (1993) HU ISSN 0231—424X

# ACTA PHYSIOLOGICA HUNGARICA

## A PERIODICAL OF THE HUNGARIAN ACADEMY OF SCIENCES

*Acta Physiologica Hungarica* publishes original reports of studies in English.
*Acta Physiologica Hungarica* is published in one volume (4 issues) per year by

AKADÉMIAI KIADÓ

Publishing House of the Hungarian Academy of Sciences

H-1117 Budapest, Prielle Kornélia u. 19—35.

Manuscripts and editorial correspondence should be addressed to

*Acta Physiologica Hungarica*

H-1445 Budapest, P.O. Box 294, Hungary

Editor: P. Bálint

Managing editor: J. Bartha

*Subscription information*

Orders should be addressed to

AKADÉMIAI KIADÓ

H-1519 Budapest, P.O. Box 245

Subscription price for Volume 81 (1993) in 4 issues US$ 92.00, including normal postage, airmail delivery US$ 20.00.

*Acta Physiologica Hungarica* is abstracted/indexed in Biological Abstracts, Chemical Abstracts, Chemie-Information, Current Contents-Life Sciences, Excerpta Medica database (EMBASE), Index Medicus, International Abstracts of Biological Sciences

CONTENTS

PHYSIOLOGY – PATHOPHYSIOLOGY

PRINTED IN HUNGARY

Akadémiai Kiadó és Nyomda Vállalat, Budapest

*Acta Physiologica Hungarica, Volume 81 (3), pp. 219–228 (1993)*

# EFFECT OF ANTIOXIDANT TREATMENT ON THE MYOCARDIUM DURING REPERFUSION IN DOGS

L. KÓNYA, Violetta KÉKESI*, S. JUHÁSZ NAGY*, J. FEHÉR

2ND DEPARTMENT OF MEDICINE AND *INSTITUTE OF VASCULAR AND HEART SURGERY, SEMMELWEIS UNIVERSITY, MEDICAL SCHOOL, BUDAPEST, HUNGARY

Received February 15, 1992
Accepted December 16, 1992

Open chest dogs undergoing 30-min occlusion of the left anterior descending coronary artery (LAD), followed by 20-min reperfusion, received silibinin (2 mg/kg body weight), allopurinol (100 mg for two days as pretreatment, 20 mg/kg body weight during ischemia and reperfusion), superoxide dismutase (SOD, 5 and 0.5 mg/kg body weight, starting from the last minute of ischemia over 6 min). Control and treated dogs were comparable with respect to myocardial regional contractile force (strain gauge), malondialdehyde (MDA) and creatin kinase (CK) levels of sinus coronarius blood samples, heart rate, and blood pressure. Allopurinol and large doses of SOD produced significant improvement in contractility and decreased MDA levels, which might suggest free radical mediated reactions during reperfusion.

**Keywords**: reperfusion, regional left ventricular function, free radical

Results of animal experiments and clinical experience show that revascularization of the ischemic myocardium by means of thrombolytic therapy, angioplasty and bypass surgery can reduce the size of infarction and improve left ventricular function as well [2, 12, 35]. However, there is increasing evidence that reperfusion has also harmful effects, e.g. damage to the vasculature, reperfusion arrhythmias, myocardial stunning, acceleration of necrosis in cells non-lethally injured by ischemia [6, 7, 9, 14, 20, 25]. A recent hypothesis links oxygen derived FRs as mediators to reperfusion damage [1, 3, 8, 10, 26]. The theory is supported mainly by experimental data, however, as to some indirect evidence (e.g. increased levels of by-products characteristic to FR-mediated reactions or the protective effect of antioxidants) could also be gathered during heart surgery in humans [13, 16, 17, 36]. At the same time contradictory observations have also been made that did not support the above hypothesis [22, 34, 37]. The importance of the question indicates the need for further investigation. In an open chest dog model we studied the

Correspondence should be addressed to
László KÓNYA
Semmelweis University Medical School, 2nd Department of Medicine
H–1088 Budapest, Szentkirályi u. 46, Hungary

*Akadémiai Kiadó, Budapest*

significance of FR reactions by evaluating the protective effect of different FR scavengers via alterations in MDA levels, which is thought to be a useful marker of FR reactions.

## Methods

Mongrel dogs of both sexes weighing 10 to 15 kg were anaesthetized with pentobarbital sodium (30 mg/kg, iv., Nambutal, Abbott, Germany). Dogs were ventilated artificially with a constant-volume respirator (RO 5, Medexport, Russia). Surgery was performed on a prewarmed operating table. After thoracotomy in the fifth intercostal space the pericardium was opened vertically and its edges were fixed to the chest wall. To allow for a transient ligation of LAD, a thread loop was placed around an arterial segment distal to the last diagonal branch. For monitoring the regional contractile force in the myocardium supplied by the LAD strain gauge clips (Walton Brodie 6) were positioned and secured in place with cardiovascular sutures. For blood sampling the coronary artery sinus was cannulated via the right auricle or the azygos vein. Another catheter was placed in the femoral vein and connected to the coronary sinus catheter to allow for blood flow after blood sampling. During the same surgical session, catheters were inserted into the femoral artery and the left atrium. These catheters served for blood pressure monitoring and administration of the tested substances. After completion of surgery time was given (10–15 min), for the stabilization of hemodynamic parameters. The dogs were then randomized into five groups.

In each group regional myocardial ischemia was produced by ligation of the LAD for 30 min. Thereafter the ligation was released for 20 min. A group of seven dogs received saline infusion for 6 min starting 1 min before reperfusion. Antioxidant treatment was administered via the left atrium as follows:

Eight dogs received 100 mg Allopurinol (Milurit, Egis, Hungary) for 2 days before the ligation and 20 mg/kg body weight of the same during ischemia and reperfusion. Six dogs were treated with Silibinin (2 mg/kg body weight, Legalon, Madeus, Germany). Five dogs received SOD (5 mg/kg body weight, Peroxinorm, Grünenthal, Germany) for 6 min starting from the last minute of ischemia. Another five dogs received 0.5 mg/kg body weight of the enzyme as above.

Regional contractile force, arterial blood pressure, heart rate, and the electrocardiogram were continuously recorded on a Hellige 64 0006 Multiscriptor (Germany). Animals that developed ventricular fibrillation were defibrillated. Blood samples for MDA and CK determination were obtained from the coronary sinus before (0 min) and during ligation (15 and 25 min) and during reperfusion (2, 7 and 20 min). Serum MDA concentrations were measured by spectrophotometry as described (30 min). Serum CK was determined by standard methods using Hitachi 717 analyser (Japan). Regional myocardial contractile force was measured by the strain gauge method of Walton Brodie. Data were analyzed for significant differences using Student file test. A p value below 0.05 was considered significant.

## Results

Due to fatal rhythm disturbances, one dog was lost in the control and silibinin groups each and three dogs in the allopurinol group. Thus the data of 26 dogs were studied.

---

| Abbreviations: | | |
|---|---|---|
| | Creatin kinase | CK |
| | free radical | FR |
| | malondialdehyde | MDA |
| | superoxide dismutase | SOD |

**Table I**

*CK content (U/L 25 C°) of coronary sinus blood during ischemia and reperfusion in control and treated dogs*

| Groups | Basal | Ischemia | | Reperfusion | | |
|---|---|---|---|---|---|---|
| | | 15' | 25' | 2' | 7' | 20' |
| Control (n=6) | 93.8±8.9 | 110.1±12.4 | 126.0±13.5 | 137.0±10.9* | 140.5±17.0* | 155.0± 17.6** |
| Allopurinol (n=5) | 159.2±43.8 | 158.0±42.6 | 177.0±47.5 | 152.0±45.5 | 218.0±59.2 | 232.0± 54.5 |
| Silibinin (n=5) | 136.0±15.5 | 145.0±19.0 | 160.0±23.0 | 169.0±22.0 | 174.0±31.3 | 168.0± 27.1 |
| Low SOD (n=5) | 220.0±37.6 | 342.0±116.2 | 357.0±126.0* | 356.0±132.0* | 368.0±133.0* | 405.0±146.0** |
| Large SOD (n=5) | 217.0±45.0 | 247.0±37.0 | 254.0±35.0 | 269.0±38.0 | 285.0±42.0 | 302.0± 51.0* |

Values are mean ± SEM

*, **, *** = $p < 0.05, 0.01, 0.001$ vs. Basal level in the same group

**Table II**

*The MDA content (μml/ml) of the coronary sinus blood during ischemia and reperfusion in control and treated dogs*

| Groups | Basal | Ischemia | | Reperfusion | | |
|---|---|---|---|---|---|---|
| | | 15' | 25' | 2' | 7' | 20' |
| Control (n=6) | 14.0±2.8 | 16.3±4.0 | 15.3±4.7 | 19.6±3.8 | 22.5±4.1* | 18.0±3.4 |
| Allopurinol (n=5) | 13.0±2.6 | 16.0±4.0 | 16.4±3.7 | 16.2±4.6 | 16.0±4.4 | 13.5±3.6 |
| Silibinin (n=5) | 8.7±1.4 | 10.5±9.6 | 9.5±1.8 | 12.5±2.4 | 18.7±7.0 | 13.7±4.3 |
| Low SOD (n=5) | 25.2±4.5 | 32.2±3.5 | 28.3±5.0 | 25.8±4.7 | 38.2±7.6 | 36.6±5.6 |
| Large SOD (n=5) | 24.1±6.5 | 22.7±5.3 | 18.2±4.2 | 19.8±5.1 | 29.1±4.8 | 23.6±8.0 |

Values are mean ± SEM

* = $p < 0.02$ v.s. Basal level in the same group

## Table III

*The heart rate (beats/min) systolic and diastolic pressure (Hgmm) during ischemia and reperfusion in control and treated dogs*

| Groups | | Basal | Ischemia | | Reperfusion | | |
|---|---|---|---|---|---|---|---|
| | | | 15' | 25' | 2' | 7' | 20' |
| Control (n=6) | a | 135.0±2.0 | 148.0±5.0* | 150.0±3.0** | 136.0±2.0 | 138.0±3.0 | 151.0±4.0** |
| | b | 132.0±8.0 | 120.0±8.0 | 118.0±8.0 | 118.0±12.0 | 109.0±8.0 | 106.0±9.0 |
| | c | 86.0±6.2 | 88.0±5.1 | 88.0±3.4 | 84.0±5.6 | 78.0±7.3 | 72.0±6.0 |
| Allopurinol (n=5) | a | 136.0±3.0 | 136.0±6.0 | 138.0±5.0 | 133.0±5.0 | 131.0±6.0 | 129.0±6.0 |
| | b | 121.0±11.0 | 111.0±11.0 | 112.0±8.0 | 108.0±8.0 | 101.0±9.0 | 103.0±8.0 |
| | c | 87.0±6.8 | 78.0±8.2 | 76.0±5.1 | 73.0±4.4 | 71.0±5.1 | 75.0±5.0 |
| Silibinin (n=5) | a | 133.0±3.0 | 136.0±2.0 | 133.0±2.0 | 129.0±3.0 | 127.0±4.0 | 124.0±5.0 |
| | b | 118.0±7.0 | 114.0±7.0 | 109.0±8.0 | 115.0±9.0 | 114.0±7.0 | 120.0±5.0 |
| | c | 78.0±5.1 | 79.0±1.0 | 73.0±3.0 | 81.0±4.0 | 79.0±3.3 | 74.0±4.0 |
| Low SOD (n=5) | a | 129.0±3.0 | 129.0±4.0 | 123.0±5.0 | 125.0±2.0 | 128.0±1.0 | 125.0±2.0 |
| | b | 114.0±7.0 | 104.0±3.0 | 99.0±3.0 | 106.0±5.0 | 108.0±5.0 | 104.0±6.0 |
| | c | 76.0±1.9 | 74.0±4.0 | 77.0±1.9 | 75.0±2.7 | 76.0±2.9 | 73.0±2.6 |
| Large SOD (n=5) | a | 126.0±4.0 | 133.0±2.0 | 128.0±5.0 | 123.0±4.0 | 124.0±2.0 | 118.0±4.0 |
| | b | 115.0±3.0 | 104.0±5.0 | 103.0±7.0 | 105.0±6.0 | 104.0±6.0 | 108.0±3.0 |
| | c | 78.0±2.0 | 78.0±3.7 | 73.0±3.0 | 77.0±2.6 | 76.0±2.4 | 79.0±2.4 |

Values are mean ±SEM

*, **, *** = $p < 0.05, 0.01, 0.001$ vs. Basal level in the same group

a = heart rate

b = systolic blood pressure

c = diastolic blood pressure

**Table IV**

*The regional myocardial force (strain gauge) during ischemia and reperfusion in control and treated dogs*

| Groups | Basal | Ischemia | | Reperfusion | | |
|---|---|---|---|---|---|---|
| | | 15' | 25' | 2' | 7' | 20' |
| Control (n=6) | 100.0±10.0 | 74.3±10.7* | 65.3±8.0*** | 69.3±12.0** | 77.3±10.7* | 76.0±10.7* |
| Allopurinol (n=5) | 100.0±9.2 | 80.1±6.3* | 80.6±5.2* | 89.5±5.8 | 86.9±5.8 | 88.0±5.8 |
| Silibinin (n=5) | 100.0±7.7 | 75.6±9.5* | 69.6±6.5** | 78.4±7.1* | 81.5±8.3 | 81.5±8.3 |
| Low SOD (n=5) | 100.0±5.5 | 74.7±7.4* | 68.5±6.8** | 74.1±8.0* | 75.9±9.3* | 74.7±8.0* |
| Large SOD (n=5) | 100.0±6.1 | 80.2±7.4 | 79.5±6.0* | 93.8±6.2 | 94.4±6.8 | 96.3±6.8 |

Values are mean ± SEM

*, **, *** = $p < 0.05, 0.01, 0.001$ vs. Basal level in the same group

Table I shows the alterations of CK. The most pronounced elevation could be observed in the control and low-dose SOD groups; both differed significantly from the last period of ischemia. Following reperfusion, MDA levels increased substantially in the control and silibinin groups, whereas a relatively minor elevation was experienced in dogs treated with allopurinol of large doses of SOD (10 and 15% elevation compared to basal level, respectively). (Table II.)

During the ischemic period tachycardia developed. The increase in heart rate was statistically significant in control animals. The most pronounced decrease of symbolic blood pressure could be observed in the same group, however, it was not statistically significant. (Table III.)

During ischemia regional contractile force of the left ventricle significantly diminished in all groups. Following the restart of circulation systolic function improved. The best improvement was observed in animals treated with allopurinol and with large doses of SOD. (Table IV.)

## Discussion

One of the most important goals of therapy during ischemia-reperfusion is to improve the contractile function of myocardium. Delayed return of contractility following ischemia is thought to be caused by free radicals [5, 8, 11, 18, 31]. The phenomenon has recently become the focus of considerable interest and therefore the effects of several antioxidant agents were studied under various circumstances (different species, various length of global and regional ischemia-reperfusion). During regional myocardial ischemia in open-chest dogs the amelioration of systolic wall motion and the global function of the left ventricle were measured by different methods (epicardial Doppler, contrast ventriculography). With the strain gauge method, which is thought to be a sensitive tool for the study of regional myocardial functions, we observed that allopurinol and large doses of SOD improved contractility of the ischemic myocardium compared to control animals. This observation underlines the role of FRs in the pathogenesis of reperfusion tissue injury. The latter is also supported by the fact that MDA, a product of free fatty acid oxidation and thus a useful marker of FR reactions [3, 21], was significantly elevated in blood samples of control animals in the early phase of reperfusion when theoretically a burst of FR generation occurs. A likely explanation for the lower MDA values in the treated groups may be that the antioxidants scavenged or inhibited the FR generation.

It is important to know whether antioxidant therapy can reduce the size of infarction. It can be demonstrated by special staining methods, which show the area at risk and the absolute size of infarction [3, 4, 29]. A direct correlation is also proven between the amount of CK released from the ischemic myocardium and the number

of injured cardiac cells [3, 22, 24]. In the present study, most expressive elevation of CK compared to basal levels was observed in the control and low-dose SOD treated groups.

## Conclusion

Indirect evidence supporting the hypothesis that FR reactions mediate (maybe in part) reperfusion tissue damage are the following:
(a) Allopurinol and large-dose SOD therapy improved the contractility of ischemic myocardium;
(b) The mildest elevation of MDA and CK, correlating with the degree of lipid peroxidation and myocyte necrosis, was observed in the above two groups. Silibinin, which is a proven effective antioxidant agent in FR-mediated liver diseases, had less favourable effects. Low-dose SOD lacked any protective effect.

## REFERENCES

1. Ambrosio, C., Becker, L. C., Hutchins, G. M., Weisman, H. F., Weisfeldt, M. L.: Reduction in experimental infarct size by recombinant human superoxide dismutase: insights into the pathophysiology of reperfusion injury. Circulation **74**, 1424–1433 (1986).
2. Anderson, J. K., Marshall, H. W., Bray, B. E., Lutz, J. R., Frederich, P. R., Yanowitz, F. G., Datz, F. I., Klausner, S. C., Nagan, A. D.: A randomized trial of intracoronary streptokinase in myocardial infarction. N. Eng. J. Med. **308**, 1312–1318 (1983).
3. Bando, K., Tago, M., Teramoto, S.: Prevention of free radical-induced myocardial injury by allopurinol. J. Thorac. Cardiovasc. Surg. **95**, 465–473 (1988).
4. Bolli, R., Patel, B. S., Zhu, W. X., O'Neill, P. G., Hartley, C. J., Charlat, M. L., Roberts, R.: The iron chelator desferrioxamine attenuates postischemic ventricular dysfunction. Am. J. Physiol. **253**, H1372–H1380 (1987).
5. Bolli, R., Zhu, W. X., Hartley, C. J., Repine, J. E., Hess, M. L., Kukreja, R. C., Roberts, R.: Attenuation of dysfunction in the postischemic "stunned" myocardium by dimethylthiourea. Circulation Vol. **76**, 458–568 (1987).
6. Braunwald, E., Kloner, R. A.: Myocardial reperfusion: a double-edged sword? J. Clin. Invest. **76**, 1713–1719 (1985).
7. Bresnahan, G. F., Robert, R., Shell, W. E., Ross, J. Jr., Sebol, B. E.: Deleterious effects due to haemorrhage after myocardial reperfusion. Am. J. Cardiol. **33**, 82–86 (1987).
8. Burton, K. P.: Superoxide dismutase enhances recovery following myocardial ischemia. Am. J. Physiol. **248**, H637–H643 (1985).
9. Capone, R. J., Most, A. S.: Myocardial haemorrhage after coronary reperfusion in pigs. Am. J. Cardiol. **41**, 259–266 (1978).
10. Chambers, D. E., Parks, D. A., Patterson, G., Roy, R., McCord, J. M., Yoshida, S., Parmley, L. F., Downey, J. M.: Xanthine oxidase as a source of free radical damage in myocardial ischemia. J. Mol. Cell. Cardiol. **17**, 145–153 (1985).
11. Charlat, M. L., O'Neill, P. G., Egan, J. M., Abernethy, D. R., Michael, H., Myers, M. L., Roberts, R., Bolli, R.: Evidence for pathogenetic role of xanthine oxidase in the "stunned myocardium". Am. J. Physiol. **252**, H566–H577 (1987).

12. DeWood, M. A., Heit, J., Spores, J., Berg, R. Jr., Selinger, S. T., et al.: Anterior transmural myocardial infarction: effects of surgical coronary reperfusion on global and regional left ventricular function. J. Am. Coll. Cardiol. **1**, 1223–1234 (1983).
13. Del Nido, P. J., Mickle, D. A. G., Wilson, G. J., Benson, L. M., Coles, J. G., Trusler, J. A., Williams, W. G.: Evidence of myocardial free radical injury during elective repair of tetralogy of Fallot. Circulation **76** (Suppl. V.), V174–V179 (1987).
14. Editorial: Reperfusion injury after thrombolytic therapy for acute myocardial infarction. Lancet II. No. **8664**, 655–657 (1989).
15. Fehér, J., Láng, I., Nékám, K., Csomós, G., Müzes, Gy., Deák, Gy.: Effect of silibinin on the activity an expression of superoxide dismutase in lymphocytes from patients with chronic alcoholic liver disease. Free Rad. Res. Comm. **3**, 373–377 (1987).
16. Ferrari, R., Alfieri, O., Curello, S., Ceconi, C., Cargnoni, A., Marzollo, P., Pardini, A., Cardonna, E., Visioli, O.: Occurrence of oxidative stress during reperfusion of the human heart. Circulation **81**, 201–211 (1990).
17. Ferreira, R., Llesuy, S., Milei, J., Scordo, D., Hourquebis, H., Molteni, L., de Palma, C., Boveris, A.: Assessment of myocardial oxidative stress in patients after myocardial revascularization. Am. Heart. J. **115**, 307–311 (1988).
18. Forman, M. B., Virmani, R., Puett, D. W.: Mechanisms and therapy of myocardial reperfusion injury. Circulation **81** (Suppl. IV), 69–78 (1990).
19. Forman, M. B., Puett, D. W., Cates, C. V., McCroskey, D. E., Beckman, J. K., Green, H. L., Virmani, R.: Glutathione redox pathway and reperfusion injury. Effect of N-acetyl-cysteine on infarct size and ventricular function. Circulation **78**, 202–213 (1988).
20. Fox, K. A. A., Bergman, R., Sobel, E. B.: Pathophysiology of myocardial reperfusion. Ann. Rev. Med. **36**, 125–144 (1985).
21. Freeman, B. A., Crapo, J. D.: Free radicals and tissue injury. Lab. Invest. **47**, 412–426 (1982).
22. Gauduel, Y., Duvelleroy, M. A.: Role of oxygen radicals in cardiac injury due to reoxygenation. J. Mol. Cell. Cardiol. **16**, 459–470 (1984).
23. Gross, G. J., Farber, N. E., Hardman, H. F., Warltier, D. C.: Beneficial actions of superoxide dismutase and catalase in stunned myocardium of dogs. Am. J. Physiol. **250**, H372–H377 (1986).
24. Guarneri, G., Ferrari, R., Visioli, O., Caldera, C. M., Nayler, W. G.: Effect of alfa tocopherol on hypoxic-perfused and reoxygenated rabbit heart muscle. J. Mol. Cell. Card. **10**, 893–906 (1978).
25. Harsányi, Á.: Heveny szívizom infarctusban végzett thrombolitikus rekanalizáció létrehozása, felismerése és jelentősége. Kandidátusi értekezés, Budapest, 73–85 (1986) (in Hungarian).
26. Hearse, D. J., Manning, A. S., Downey, J. M., Yellon, D. M.: Xanthine oxidase: a critical mediator of myocardial injury during ischemia and reperfusion? Acta Physiol. Scand. Suppl. **548**, 65–78 (1986).
27. Jurman, M. J., Schaefers, H. J., Dammenhagn, L., Haverich, A.: Oxygen-derived free radical scavengers for amelioration of reperfusion damage in heart transplantation. J. Thorac. Cardiovasc. Surg. **95**, 368–377 (1988).
28. Myers, M. L., Bolli, R., Lekcih, R. F., Hartley, C. J., Roberts, R.: Enhancement of recovery of myocardial function by oxygen free radical scavengers after reversible regional ischemia. Circulation **72**, 915–921 (1985).
29. Mitsos, S. E., Askew, T. E., Fantone, J. C., Kunkcel, S. L., Abrams, C. D., Schorch, A., Lucchesi, B.: Protective effects on N-2-mercapto-propionyl glycine against myocardial reperfusion injury after neutrophil depletion in the dog: evidence for the role of intercellular derived free radicals. Circulation **73**, 1077–1086 (1986).
30. Ottolenghi, A.: Interaction of ascorbic acid on mitochondrial lipids. Arch. Biochem. Biophys. **159**, 335–363 (1979).
31. Przyklenk, K., Kloner, R. A.: Superoxide dismutase plus catalase improve contractile function in the canine model of the "Stunned myocardium". Circ. Res. **58**, 148–156 (1986).

32. Puett, D. W., Forman, M. B., Cates, C. V., Wilson, B. H., Mande, K. R., Friesinger, G. O.: Oxypurinol limits myocardial stunning but does not reduce infarct size after reperfusion. Circulation **76**, 678–686 (1987).
33. Puri, P. S.: Contractile and biochemical effects of coronary reperfusion after extended periods of coronary occlusion. Am. J. Cardiol. **36**, 244–251 (1975).
34. Reimer, K. A., Jennings, R. B.: Failure of the xanthine oxidase inhibition by allopurinol on limit infarct size after ischemia and reperfusion in dogs. Circulation **71**, 1069–1075 (1985).
35. Sheehan, F. H., Braunwald, E., Canner, P., Dodge, H., Gore, J., Van Natta, P., Passamani, E. R., David, O., Williams, S., Zaret, B. and coinvestigators: The effect of intravenous thrombolytic therapy on left ventricular function: a report on tissue-type plasminogen activator and streptokinase from the thrombolysis in myocardial infarction (TIMI Phase I.) Trial. Circulation **75**, 817–829 (1987).
36. Török, B., Roth, E., Bar, V., Pollák, Zs.: Effects of antioxidant therapy in experimentally induced heart infarcts. Basic Res. Cardiol. **81**, 167–179 (1986).
37. Uraizee, A., Reimer, K. A., Murry, Ch. E., Jennings, P. B.: Failure of superoxide dismutase to limit size of myocardial infarction after 40 minutes of ischemia and 4 days of reperfusion in dogs. Circulation **75**, 1237–1248 (1987).

*Acta Physiologica Hungarica, Volume 81 (3), pp. 229–237 (1993)*

# AEROBIC FITNESS DOES NOT INFLUENCE *DIRECTLY* HEART RATE *REACTIVITY* TO MENTAL STRESS

A. SZABÓ[1], T. G. BROWN,[3] Lise GAUVIN,[2] P. SERAGANIAN[3]

UNIVERSITÉ DE MONTRÉAL AND CONCORDIA UNIVERSITY, MONTREAL, QUEBEC, CANADA
[1] DÉPARTEMENT D'ÉDUCATION PHYSIQUE, UNIVERSITÉ DE MONTRÉAL, C. P. 6128, SUCCURSALE A, MONTRÉAL, (QUÉBEC), CANADA, H3C 3J7
[2] DEPARTMENT OF EXERCISE SCIENCE, CONCORDIA UNIVERSITY, 7141 SHERBROOKE STREET WEST, MONTREAL, QUEBEC, CANADA, H4B 1R6
[3] DEPARTMENT OF PSYCHOLOGY, MI ANNEX, CONCORDIA UNIVERSITY, 1455 DE MAISONNEUVE BLVD. WEST, MONTREAL, QUEBEC, CANADA, H3G 1M8

Thirty-seven aerobically high and low fit male and female university students, selected on the basis of estimated aerobic capacity, completed a set of hard as well as a set of easy mental arithmetic tasks for 90 seconds in a counterbalanced order with a 10 min rest period between the tasks. Heart rate (HR) reactivity to either task was independent of aerobic fitness level. Although subjectively rated as more challenging, HR responses to the hard arithmetic task were not greater than that seen to the easy task. These results do not support the conjecture that aerobic fitness level may mediate HR response to acute mental challenge. The overall implications of these results are discussed in relation to the literature concerning aerobic fitness and mental stress.

**Keywords**: aerobic fitness, heart rate, mental arithmetic, stressor intensity, reactivity

Although aerobic fitness level has been associated with altered cardiovascular response to mental stress, the present status of this literature is controversial [14]. While some studies have found no relationship between heart rate (HR) response to mental challenge and aerobic fitness [8, 16, 19] others have related higher aerobic fitness levels to lower responses to [7, 21], or faster recovery from [6, 18] acute mental challenge.

Assuming a direct relationship between the level of difficulty (intensity) of an active mental challenge and HR reactivity, it was proposed that high intensity stressors may trigger a "ceiling" effect in HR reactivity that could mask actual differences between fitness groups [3, 18]. To test this hypothesis, it was suggested that HR reactivity should be tested in response to different intensity stressors [3]. Two studies that have examined HR responses to high and low intensity mental challenge [16, 19] did not reveal fitness related differences. However, Steptoe et al.

Correspondence should be addressed to
Attila SZABÓ, PhD
Département d'éducation physique,
Université de Montréal, C. P. 6128, Succursale A, Montréal (Québec), Canada, H3C 3J7

*Akadémiai Kiadó, Budapest*

[19] suggested that these studies may have had a relatively narrow separation between the high and low fitness groups (approximate difference between the two means (in maximal oxygen uptake capacity ($VO_2$ max): 11 ml/kg/min). A wider division between the high and low aerobic fitness groups was thought to be necessary for the detection of fitness related differences in HR reactivity to mental challenge of varying degrees of difficulty level [19].

Therefore, using a relatively broad separation between the estimated mean aerobic capacity (i.e., a $VO_2$ max difference of 18 ml/kg/min) of a high and a low aerobic fitness group (represented by both genders), the present study has reexamined the influence of aerobic fitness level on HR response to high and low intensity active laboratory mental stressors.

## Materials and methods

*Subjects*

Participants for the present study were recruited through poster and newspaper advertisements in a university milieu. Thirty-seven volunteer students (mean age 25.89 ± *SEM* = 1.05 years) participated in the study. Based on the estimated aerobic capacity, two groups were formed: 1) a high aerobic fitness group (n = 18), $VO_2$ max > 50 ml/kg/min (mean = 53.76 ± *SEM* = 1.57); (9 males, $VO_2$ max = 55.14 ± *SEM* = 2.10 / 9 females, $VO_2$ max = 52.38 ± *SEM* = 2.38 ml/kg/min), and 2) a low aerobic fitness group (n = 19), $VO_2$ max < 40 ml/kg/min (mean = 35.76 ± *SEM* = 0.89); (8 males, $VO_2$ max = 37.47 ± *SEM* = 1.64 / 11 females, $VO_2$ max = 34.5 ± *SEM* = 0.86 ml/kg/min). Aerobic fitness was estimated using the modified Astrand-Rhyming method [17].

*Mental Challenge*

Stressor intensity was delineated by task difficulty level. Two sets of mental arithmetic problems were presented via a Sony (TC-630) tape-recorder in counterbalanced order. Eight hard (e.g., $17 \times 9 - 13$) and eight easy (e.g., $2 \times 3 + 4$) problems were separated by a 10 min rest period. The presentation of each set of eight problems lasted for 90 seconds. This type of mental arithmetic has been shown to elicit HR responses that peak around 50 sec and then slowly decline [2]. Subjects were requested to provide their answer (orally) within 5 sec after the presentation of each problem. To stimulate performance, the right answer to each problem was given before the presentation of the subsequent problem.

*Heart Rate Recording*

Heart rate was continuously recorded on a second by second basis, using Ag/AgCl Medi-Trace disposable electrodes positioned on the subject in lead-1-ECG arrangement and connected to a 4-channel Beckman (Model R-511A) polygraph. The latter unit was synchronized with a Beckman (type 9857) cardiotachometer coupler interfaced for computerized data collection, that was performed continuously prior to (30 s) during (90 s) and following (30 s) each task. Recordings of the HRs on the polygraph were maintained throughout the testing session.

*Procedure*

Subjects were familiarized with the laboratory and were informed about the details of the experimental protocol both verbally and in writing. Upon obtaining consent for participation, subjects were interviewed about their medical history. Subsequently, they were introduced to the testing facility, an electrically shielded room with controlled levels of humidity and temperature. Heart rate recordings on the polygraph were started 10 min before the presentation of the first (either hard or easy) task. This interval was spent in a comfortable armchair, and it was intended for the stabilization of HR before testing. Thirty seconds prior to the presentation of both tasks, the computerized HR data collection was started and maintained throughout and up to 30 sec following each task. Following both high and low intensity problem sets, subjective perception of task difficulty was assessed in writing, by using a 10 point rating scale from one (extremely easy) to ten (extremely difficult). Upon recovery from the second mental stressor task (either the hard or the easy mathematical task), subjects were directed to an adjacent chamber where the test session was concluded by the estimation of aerobic fitness level performed on a Bodyguard (Model -990) ergometer. Since a broad separation (in aerobic capacity) between high and low aerobic fitness groups was one of the primary objectives of this study, data were retained only from students having a $VO_2$ max either below 40 (low fitness group) or above 50 ml/kg/min (high fitness group).

*Statistical Procedure*

Descriptive statistics, correlations, analysis of variance (ANOVA) and repeated measures analysis of covariance (ANCOVA), as well as the generation of the figure, were performed by using the "Systat" statistical computer software package [25]. Since HRs were recorded on a second by second basis, a large data-set was collected. To simplify the analyses, HR values were pooled into 10 sec averages that resulted in 9 reactivity and 3 recovery data points. These intervals were chosen on the basis of earlier work from our laboratory [2]. The average of the last 10 s[1] of the resting HR, prior to the mental task, was taken for baseline, as in a previous study [16].

## Results

### *Subject Characteristics*

Three subject characteristics including age, $VO_2$ max and resting (baseline) HR were analyzed using a gender by fitness ANOVA. For age, a fitness main effect was found ($F(1, 33) = 12.3$; $p < 0.001$) which revealed that subjects in the high fitness group were older (mean age = 29.2 years, $SD = 5.6$) than subjects in the low fitness group (mean age = 22.7 years, $SD = 5.5$). For $VO_2$ max, the two way ANOVA yielded a fitness main effect ($F(1, 33) = 45.8$; $p < 0.001$) which confirmed that subjects in the high aerobic fitness group (mean $VO_2$ max = 53.8 ml/kg/min, $SD = 6.7$) had a significantly greater aerobic capacity than subjects in the low aerobic fitness group (mean $VO_2$ max = 35.8 ml/kg/min, $SD = 3.9$). Furthermore, a gender

[1] Data were also analyzed by using the mean of last 30 sec resting HR as baseline which yielded identical results to the 10 sec method reported, but the latter was favoured since it allowed for comparability with at least one study in the literature that manipulated stressor intensity in high-low fit subjects, as well as because it was based on the same number of records (10) as the individual data points for the 9 stress and 3 recovery periods.

main effect ($F(1, 33) = 9.6$; $p < 0.005$) indicated that males had a higher aerobic capacity (mean $VO_2$ max = 46.8 ml/kg/min, $SD = 10.6$) than females (mean $VO_2$ max = 42.6 ml/kg/min, $SD = 10.4$). Similar to $VO_2$ max, a fitness main effect was found for resting HR ($F(1, 33) = 54.9$; $p < 0.001$) showing that subjects in the high aerobic fitness group had lower resting HR (mean = 58.5 beats per minute (bpm), $SD = 8.4$) than subjects in the low fitness group (mean = 79.3 bpm, $SD = 12.4$). A gender main effect ($F(1, 33) = 10.3$, $p < 0.005$) also indicated that males had lower resting HRs (mean = 63.2 bpm, $SD = 15.2$) than females (mean = 73.9 bpm, $SD$ = 12.2). No other effects achieved statistical significance.

*Heart Rate Reactivity*

Since aerobically fit individuals exhibited lower resting HRs than those aerobically less fit, initially it was planned that reactivity[2] data would be tested by using an analysis of covariance (ANCOVA) with resting HR as the covariate. This method filters out variability in HR reactivity due to initial differences in resting HR. (This is one method that accounts for the law of initial values [9, 24] which predicts that the limits of reactivity diminish as the initial baseline values escalate.) However, the preliminary analysis of the homogeneity of slopes assumption, using the method outlined by Wilkinson [25] (p. 536), revealed that the assumption had been violated in the data, thus the employment of an ANCOVA was inappropriate. Following the examination of the influence of the law of initial values (LIV) on the data, using the method discussed by Jamieson and Howk [9], by which a non-significant negative correlation ($r = -0.34$, in high aerobic fitness group and $r = -0.42$, in low aerobic fitness group) between resting HRs and (mean) reactivity HRs indicated negligible impact of the LIV, the method of difference scores (i.e. change from baseline) was used for the examination of the reactivity data. To account for the age differences between the two fitness groups, as well as for gender differences in $VO_2$ max, a 2 (fitness) by 2 (gender) by 2 (intensity: high and low) by 12 (9 stress and 3 recovery periods) repeated measures ANCOVA, using age as covariate[3], was used. The covariate was not significant. The analysis yielded a period by gender interaction ($F(11, 352) = 2.44$; $p < 0.01$) which did not reach significance when examined in conjunction with the Greenhouse-Geisser Epsilon probability level ($p < 0.08$). Therefore, no further analysis of the interaction was attempted. Finally, no fitness effects were observed. These results are illustrated in Fig. 1.

[2] Reactivity in the present context is defined as the change in HR from pre-task to task phase.
[3] Although the homogeneity of slopes assumption was violated when tested for resting HR, the assumption was not violated when tested for age. Thus the performance of an ANCOVA on the change scores using age as the covariate was feasible.

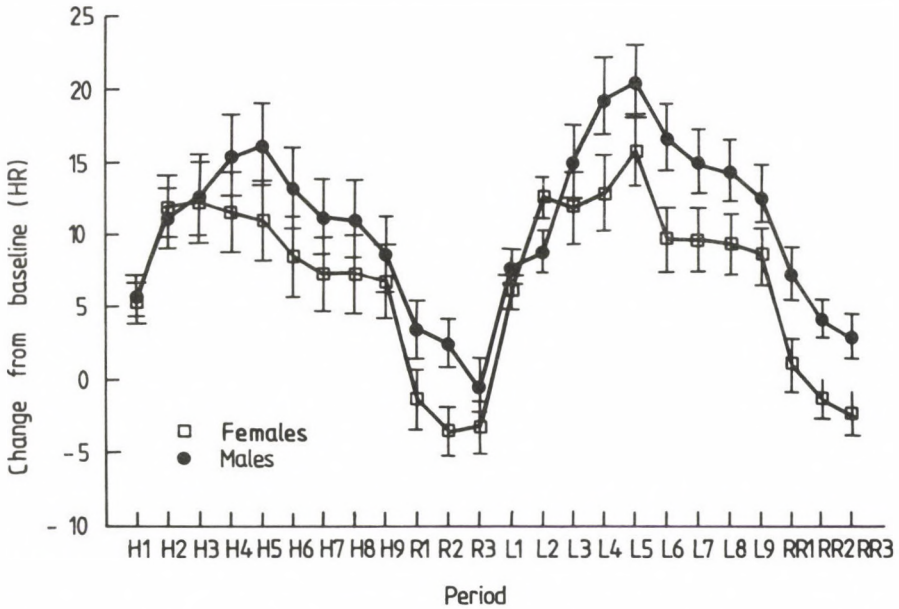


*Fig. 1.* Change in HR from baseline (represented as 0) in response to high (H1 – R3) and low (L1 – RR3) intensity mental tasks. Since no fitness effects, but a weak trend pointing toward gender effects, were observed the data are represented separately for females and for males. Each point depicts a mean HR collected over a period of 10 s. (The R and RR letters represent recovery periods)

*Subjective Measures*

A 2 (gender) × 2 (fitness) × 2 (stressor intensity rating) repeated measures ANOVA[4] yielded a stressor intensity rating main effect ($F(1, 33) = 151.1$; $p < 0.001$) with no interactions. These findings revealed that subjects perceived the hard task as more challenging (difficult) than the easy task (hard: mean = 7.32; *SD* = 1.9; easy: mean = 2.5; *SD* = 1.7). However, one subject rated the low intensity, easy task, as more challenging than the high intensity task.

## Discussion

The results of the present study do not strengthen the conjecture that aerobic fitness level mediates HR reactivity to acute mental challenge. Although some methodological drawbacks, such as the employment of mental tasks that required vocalization and the failure to record subjects' performance, were embedded in the

[4] Since age had no impact on HR reactivity and no studies present evidence for age related differences in appraisal of cognitive stressors, age was not used as a covariate.

present experiment, the two critical factors, aerobic fitness level and intensity of the mental tasks were certainly separated. Consequently, the supposition that a greater division between the aerobic fitness groups may reveal reactivity differences [19] as function of stressor intensity apparently does not hold, at least for acute active laboratory challenges.

It should be noted that while subjectively rated as more difficult, HR reactivity to the harder task was not greater than to the easy mental task. This finding illustrates that a direct relationship between HR reactivity and stressor intensity cannot be assumed. Such findings may be rationalized by the following reasoning: As Herd [5] summarized, the intensity of the effort to perform (i.e., the subjectively manifested effort to provide the best possible performance), and thus to actively cope with the stressor, is directly related to cardiovascular reactivity. The effort to perform, however, is dependent on the subjectively perceived control over the situation [13]. In the present study the harder task may have been too "potent" to provide sufficient control to the subjects, thus resulting in possibly lower effort to perform and no differences in HR reactivity in comparison to the easier task. In contrast, the easy task may have provided more control and subjects may have exerted greater effort to do well on the task and hence evinced HR responses similar to the harder task. It is unfortunate that the effort to perform was not assessed in the present experiment. Future studies in stress research should attempt to estimate the effort exerted by the subject to do well on a particular active task and should attempt to employ mental stressors that provide sufficient control to the subject. A written mental arithmetic task with subjectively controlled level of difficulty has been recently adopted in the literature [20].

The present findings seem to support the assertion that aerobic fitness may not be *directly* linked to HR *reactivity* to mental challenge [14]. Indeed, studies that report fitness effects in HR response to mental challenge may be documenting the differences in cardiovascular functions between aerobic fitness groups rather than actual differences in stress reactivity [1, 14]. Due to the emergence of numerous studies with dubious relevance in stress research (see the review by Vingerhoets and Marcelissen [23]), the examination of the possible reasons for the apparent lack of agreement in this area of research, with subsequent recommendations for future studies, appears warranted.

van Doornen, de Geus and Orlebeke [22] in their critical evaluation of the relationship between aerobic fitness level and psychological stress response stated: "... It was concluded that the two types of responses only superficially have similarity. So a simple analogy between the stress and exercise response does not allow a reliable prediction concerning the effect of fitness on the stress response." Furthermore, Péronnet and Szabo [14], in a more recent critical review and evaluation of the current status of research, elaborated on the existence of differences in control

mechanisms between responses to psychological stress and physical exercise. Briefly, the two responses have a different central origin, and while response to mental stress occurs via a direct feed-forward response to challenge – which cannot be *directly* modified by fitness –, the response to exercise is an indirect feed-back response serving to maintain the metabolic needs of the working muscle – which in turn may vary as function of fitness [14]. Accordingly, physical training and fitness may result in physiological adaptations by which greater work can be performed by the muscles at lower physiological thresholds of activation. However, changes in muscles' working capacity may not be directly related to reactivity to mental stress [14]. Therefore, it may appear idealistic to expect fitness related differences in physiological reactivity to active laboratory mental stressors.

Although the present study employs only HR as the basis of the discussion[5], changes expected and/or seen in physiological indices other than HR, in response to acute mental challenge – if they occur –, may be secondary to physiological changes emerging as a result of aerobic fitness. In fact, such secondary changes may be rationalized when examining recovery patterns from acute mental challenge.

Faster *recovery* (e.g., [6, 18]) from autonomic activation that often occurs in aerobically more fit in comparison to unfit subjects, in response to both mental challenge and exercise, may be linked to a *shared*, stronger and more adaptable cardiovascular system, that results from frequent and repeated activation of the system, as a result of exercise for example [11]. Once the influences of *different* automatic activating control mechanisms are removed, the recovery to pre-activation level is controlled by the *same* homeostatic process. Thus a so-called "carry-over"-effect from one situation to another is possible if the *same* processes are involved. Reactivity, however, may be elicited by qualitatively different stimuli [14], via *different* mechanisms and therefore the magnitude of reactivity may vary accordingly. Aerobic fitness in fact may provide grounds for higher absolute HR responses to mental challenge because the lower resting HR, associated with aerobic fitness, may allow for a greater change before reaching a "ceiling" response than a higher resting HR, as based on the LIV [24]. It is important, however, that the occurrence of such greater responses not be interpreted as changes in reactivity *per se*, but rather as changes in the physiological limits allowable for reactivity. Therefore, conceptual differentiation between response and reactivity as well as between direct and indirect influences should be observed.

[5] Some studies also measured changes in other physiological indices than HR which may have yielded different results. Current discussion, however, is restricted to HR, which although is only a crude and non-specific index of cardiovascular activity, is nevertheless a very sensitive and a commonly used measure.

The aforementioned arguments may serve as an heuristic statement concerning the lack of direct influence of aerobic fitness on HR reactivity to acute mental laboratory challenge. Outside the laboratory however, physical fitness may have an effect on psychological stress reactivity patterns, which points to new and challenging avenues of research. For example, it is well established that aerobic exercise exerts beneficial effects on such psychological variables as anxiety and affect [12, 15]. Positive changes in psychological parameters may *indirectly* affect the degree to which a situation is perceived as stressful by the individual. A sense of mastery (control) of the stressful situation can influence physiological reactivity to a large extent [13]. As such, fitness related differences in cognitive constructs, such as self-schemata for example [10], may alter one's perception of situation along with the ability to cope and therefore to respond to a given challenge. Consequently, there are new and highly promising directions for research into the relationship between mental stress and aerobic fitness. These endeavours will, however, require a multidimensional approach (instead of simple focus on a direct physiological association) and the adoption of field methodologies as opposed to laboratory inquires. In situ measurements for example, using the experience sampling method (ESM), have been already adopted in this area of research [4] and may prove to be the method of choice in future studies.

**Acknowledgements**

Gratitude is extended to the Fonds FCAR of the Province of Quebec for the financial support provided to the first author.

## REFERENCES

1. Blumenthal, J. A., Fredrikson, M., Kuhn, C. M., Ulmer, R. L., Walsh-Riddle, M., Appelbaum, M.: Aerobic exercise reduces levels of cardiovascular and sympathoadrenal responses to mental stress in subjects without prior evidence of myocardial ischemia. Am. J. Cardiol. **65**, 93–98 (1990).
2. Brown, T. G., Szabo, A., Seraganian, P.: Physical versus psychological determinants of heart rate reactivity to mental arithmetic. Psychophysiology **25**, 532–537 (1988).
3. Duda, J. L., Sedlock, D. A., Melby, C. L., Thaman, C.: The effects of physical activity level and acute exercise on heart rate and subjective response to a psychological stressor. Int. J. Sport Psychol. **19**, 119–133 (1988).
4. Gauvin, L., Szabo, A.: Application of the experience sampling method to the study of the effects of exercise withdrawal on well-being. J. Sport Exerc. Psychol. **14**, 361–347 (1992).
5. Herd, J. A.: Cardiovascular response to stress. Physiol. Rev. **71**, 305–330 (1990).
6. Hollander, B. J., Seraganian, P.: Aerobic fitness and psychophysiological reactivity. Can. J. Behav. Sci. **16**, 257–261 (1984).
7. Holmes, D. S., Roth, D. L.: Association of aerobic fitness with pulse rate and subjective responses to psychological stress. Psychophysiology **22**, 525–529 (1985).

8. Hull, E. M., Young, S. H., Ziegler, M. G.: Aerobic fitness affects cardiovascular and catecholamine responses to stressors. Psychophysiology **21**, 353–360 (1984).
9. Jamieson, J., Howk, S.: The law of initial values: A four factor theory. Int. J. Psychophysiol. **12**, 53–61 (1992).
10. Long, B.: A cognitive perspective on the stress reducing effects of physical exercise. In: Exercise Psychology: The Influence of Physical Exercise on Psychological Processes, ed. Seraganian, P., John Wiley & Sons, New York, 1993, pp. 339–357.
11. Nadel, R. E.: Physiological adaptations to aerobic training. Am. Scientist. **73**, 334–343 (1985).
12. North, T. C., McCullagh, P., Tran, W.: Effect of exercise on depression. Exerc. Sports Sci. Rev. **18**, 379–415 (1990).
13. Obrist, P. A., Gaebelein, C. J., Teller, E. S., Langer, A. W., Grignolo, A., Light, K. C., McCubbin, J. A.: The relationship among heart rate, carotid dP/dt, and blood pressure in humans as a function of the type of stress. Psychophysiology. **15**, 102–115 (1978).
14. Péronnet, F., Szabo, A.: Sympathetic response to acute psychosocial stressors in man: Linkage to physical exercise and training. In: Exercise Psychology: The Influence of Physical Exercise on Psychological Processes, ed. Seraganian, P., John Wiley & Sons, New York, 1993, pp. 172–217.
15. Petruzello, S. J., Landers, D. M., Hatfield, B. D., Kubitz, K., Salazar, W.: Effects of exercise on anxiety and mood: A meta-analysis. Sports Med. **11**, 143–182 (1991).
16. Shulhan, D., Scher, H., Furedy, J. I.: Phasic cardiac reactivity to psychological stress as a function of aerobic fitness level. Psychophysiology **23**, 562–566 (1986).
17. Siconolfi, S. F., Cullinane, E. M., Carleton, R. A., Thompson, P.: Assessing $VO_2$ max in epidemiologic studies: Modification of the Astrand-Rhyming test. Med. Sci. Sports Exerc. **14**, 335–338 (1982).
18. Sinyor, D., Golden, M., Steinert, Y., Seraganian, P.: Experimental manipulation of aerobic fitness and the response to psychosocial stress: Heart rate and self report measures. Psychosom. Med. **48**, 324–337 (1986).
19. Steptoe, A., Moses, J., Mathews, A., Edwards, S.: Aerobic fitness, physical activity, and psychophysiological reactions to mental tasks. Psychophysiology **27**, 264–274 (1990).
20. Szabo, A., Gauvin, L.: Reactivity to written mental arithmetic: Effects of exercise lay-off and habituation. Physiol. Behav. **51**, 501–506 (1992).
21. van Doornen, L. J. P., de Geus, E. J. C.: Aerobic fitness and the cardiovascular response to stress. Psychophysiology **26**, 17–27 (1989).
22. van Doornen, L. J. P., de Geus, E. J. C., Orlebeke, J. F.: Aerobic fitness and the physiological stress response: A critical evaluation. Soc. Sci. Med. **26**, 303–307 (1988).
23. Vingerhoets, A. J. J. M., Marcelissen, F. H. G.: Stress research: Its present status and issues for future developments. Soc. Sci. Med. **26**, 279–291 (1988).
24. Wilder, J.: The "law of initial values", a neglected biological law and its significance for research and practice. Translated from Zeitschrift für die gesamte Neurologie und Psychiatrie, **137**, 317–338. In: Psychophysiology, eds Porges, S. W., Coles, M. G. H., Dowden, Hutchingson & Ross, Inc., Stroudsburg, PA (1931/1976).
25. Wilkinson, L.: SYSTAT: The System for Statistics. SYSTAT, Inc., Evanston (1989).

*Acta Physiologica Hungarica, Volume 81 (3), pp. 239–251 (1993)*

# THE EFFECTS OF SIMULTANEOUS ALCOHOL AND NICKEL SULPHATE POISONING ON THE CARDIOVASCULAR SYSTEM OF RATS+

Veronika MORVAI, É. SZAKMÁRY,* GY. UNGVÁRY,* G. SZÉNÁSI

2ND DEPARTMENT OF MEDICINE, SEMMELWEIS UNIVERSITY MEDICAL SCHOOL AND *NATIONAL INSTITUTE OF OCCUPATIONAL HEALTH[X], BUDAPEST, HUNGARY

Received July 2, 1992
Accepted December 2, 1992

Two groups of male OFA rats received 10% ethanol and 5% sugar, or 5% sugar in their drinking-water. One half of each group received 5 mg/kg b.w. daily dose of nickel sulphate in 10 ml of physiological saline by gavage, for three weeks, while the other half of the groups received 10 ml physiological saline.

Morphological (light and electron microscopic) and haemodynamic (radioactive microsphere method) examinations were performed. It was found, that alcohol caused decreases of borderline significance of the arterial blood pressure and the nutritive blood flow of the heart, while nickel sulphate significantly increased the arterial blood pressure, the vascular resistance of the kidneys, liver and brain, increased TPR in a tendentious way. Following a simultaneous administration of alcohol and nickel considerably increased the arterial blood pressure (statistically interaction at a level of borderline significance) and caused the appearance of swollen mitochondria and dilated sarcoplasmatic reticulum in the ultrastructure of the heart.

It is concluded, that 1. pathomechanism of myocardium-damaging effects of nickel sulphate and alcohol is different; 2. nickel sulphate and alcohol together (at least in a certain dose range) increase the arterial blood pressure.

**Keywords**: alcohol, nickel sulphate, hypertension, rat

On our earlier studies prolonged administration of high ethanol (further alcohol) doses was found to decrease the arterial blood pressure and the nutritive blood flow of the heart in rats [15, 16, 18]. It is known that single dose of nickel decreases the contractility of the cardiac muscle [1, 7, 22, 25], while chronic nickel exposure causes degeneration of the cardiac muscle and changes of the electrocardiogram [8, 11, 23]. Alcoholism is widespread in Hungary [2]. Production

Correspondence should be addressed to
Veronika MORVAI
2nd Department of Medicine, Semmelweis University Medical School
H–1088 Budapest Szentkirályi u. 46., Hungary

+ Research supported by grant T–192/1990 from the Hungarian Ministry of Welfare

and use of nickel is growing [3], nickel pollution of foodstuff [20, 27, 28, 33], water soil and atmosphere [14, 19] is increasing. Smoking also contributes to the nickel burden of man [29, 35, 36].

For this reason we considered important to study whether cardiopathogenic effect of the two cardiotoxic substances is aggravated if administered simultaneously. Our aim was also to reveal, whether cardiovascular effects of the individual chemicals play role in the cardiopathogenic effect of nickel given alone or in that of the two substances (alcohol and nickel) given together.

## Materials and methods

Groups of male OFA rats weighing 310–350 g were made to drink water containing 10% ethanol and 5% sugar or 5% sugar only. The animals were fed by standard rat pellet ad libitum. Half of the animals in each group received daily doses of 5 mg/kg b.w. nickel sulphate in 10 ml physiological saline by gavage for three weeks, while the other half received only 10 ml of physiological saline daily for three weeks.

Routine *histological* and electron microscopic *examinations* were carried out according to the methods described in our earlier papers [17].

*Haemodynamic examinations*

After anesthesia with pentobarbital sodium (40 mg/kg body wt ip) the right femoral artery and right carotid artery were cannulated with PE–50 tubing. The femoral arterial catheter was used for the measurement of arterial blood pressure and withdrawal of the reference blood sample. While the pressure recording was continuously monitored, the right carotid arterial catheter was advanced into the left ventricle for the injection of microspheres. Carbonized microspheres (15±5 μm diameter, 3 M Company, St Paul Minn) labelled with $^{57}Co$ and $^{113}Sn$ were used in this investigation. Cardiac index, organ fractions of the cardiac output and the nutritive blood flow of the organs were measured according to McDevitt and Nies [12]; the total peripheral resistance (TPR) and vascular resistances of the individual organs were calculated.

For the statistical evaluation of the data analysis of variance and Dunett's test [5] were used. Means and standard errors are indicated on the figures and tables.

## Results

### *Morphological examinations*

On autopsy no macroscopic pathologic changes could be observed in any of the groups.

In the different organs no pathologic changes could be observed by light microscope.

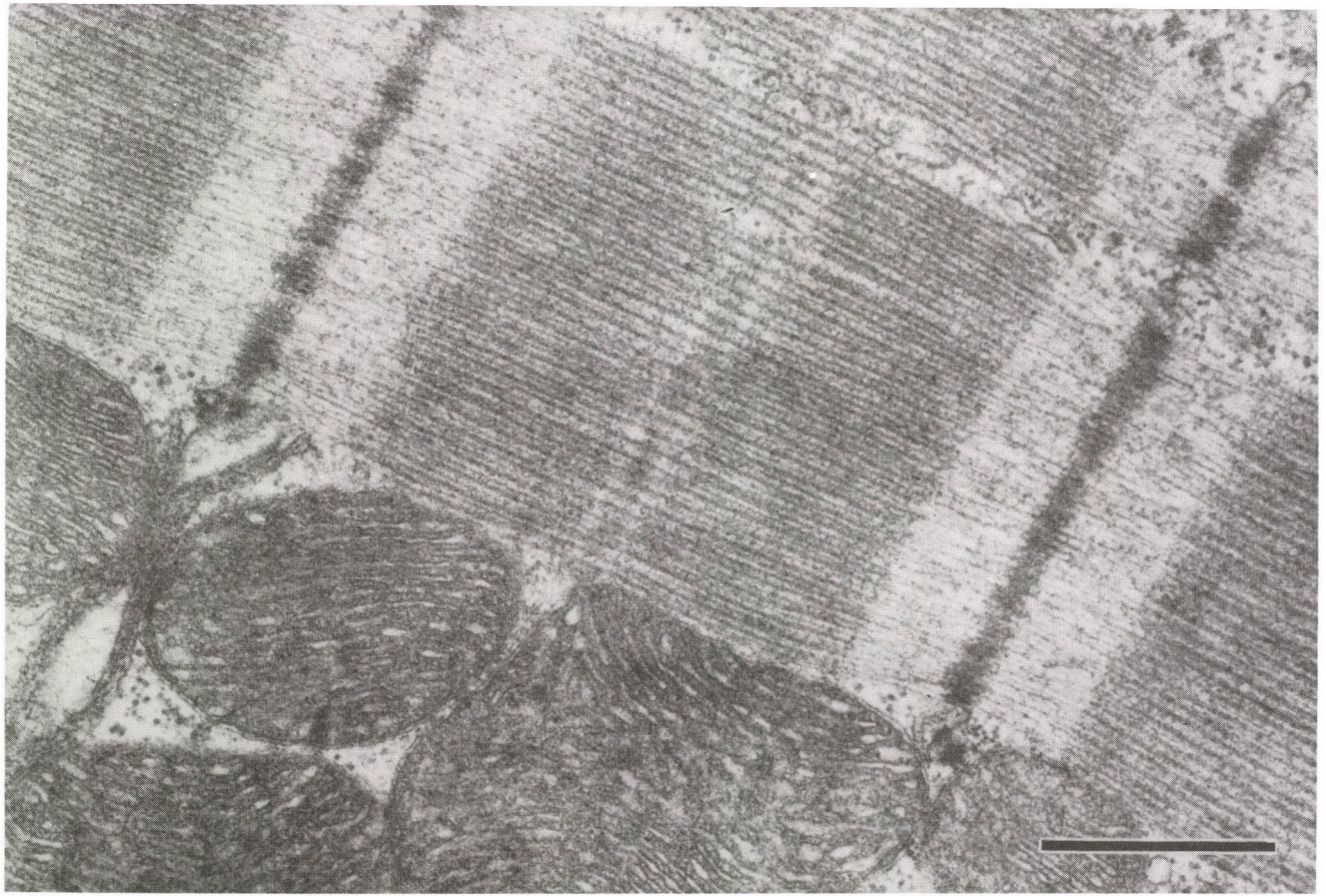

*Fig. 1.* Electronmicrograph of a part of the papillary muscle of the rat heart. Exposure: daily administration of 5 mg/kg b.w. nickel sulphate by gavage for three weeks. The bigger lower part of the picture shows a sarcomer surrounded by Z. lamellae at the left and right side. In the sarcomer the H, A and 1/2 segments, as well as the actin and myosin filaments forming them can be well identified. Also sarcoplasmatic reticulum profiles and sections of the mitochondria can be seen. No pathognostic signs can be observed as the effect of nickel exposure. Scale: 1 μm

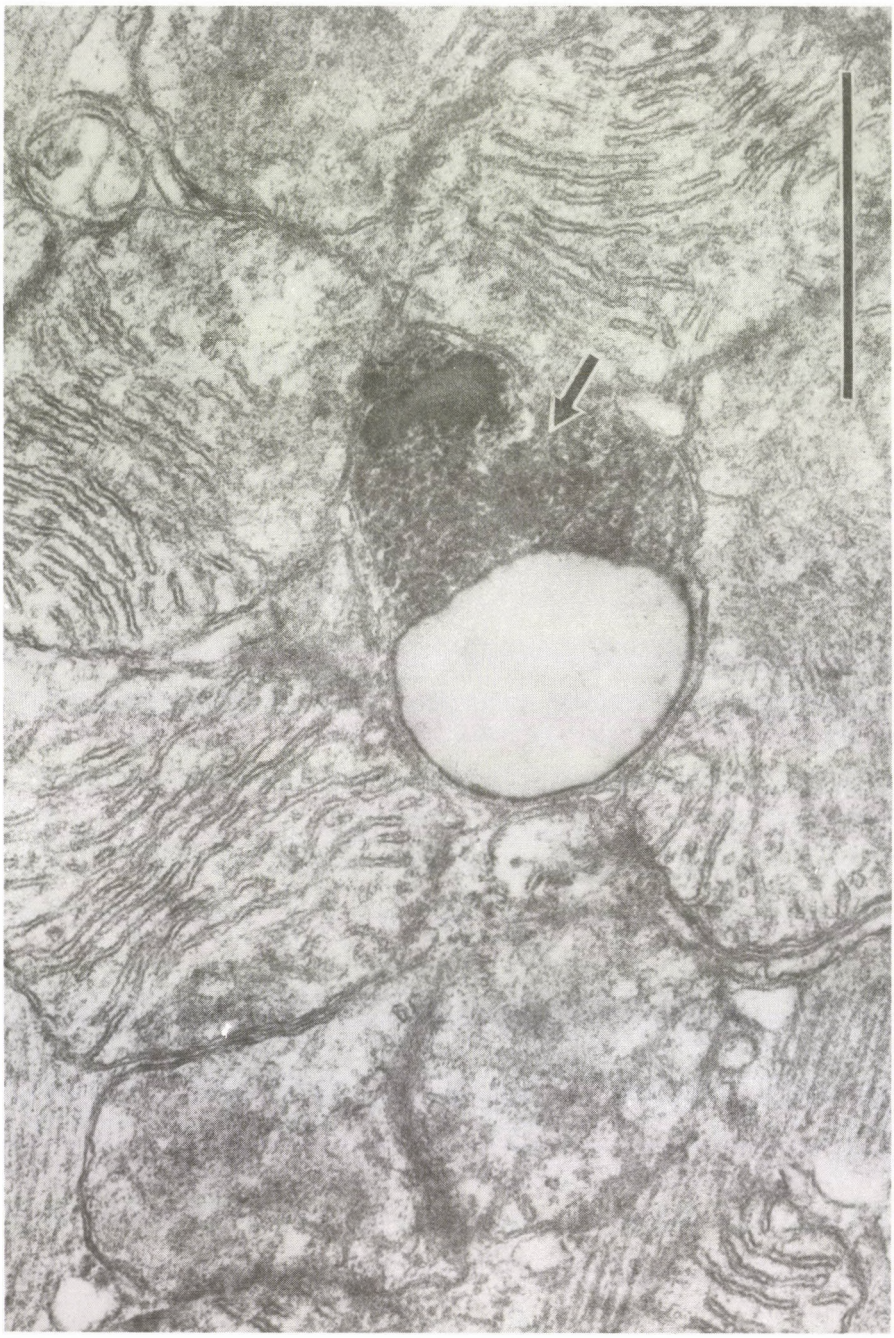

*Fig.* 2. Electronmicrograph of a part of the papillary muscle of the rat heart. Exposure: 3 weeks of drinking water containing 10% ethyl alcohol and 5% sugar. In some places the sarcoplasmatic reticulums are moderately dilated, mitochondria are swollen, electrodense granules of the mitochondria are missing, the mitochondrial matrix is clearer (electrolucent), than in normal cells. Arrow shows a lipofucsin granule. Scale: 1 μm

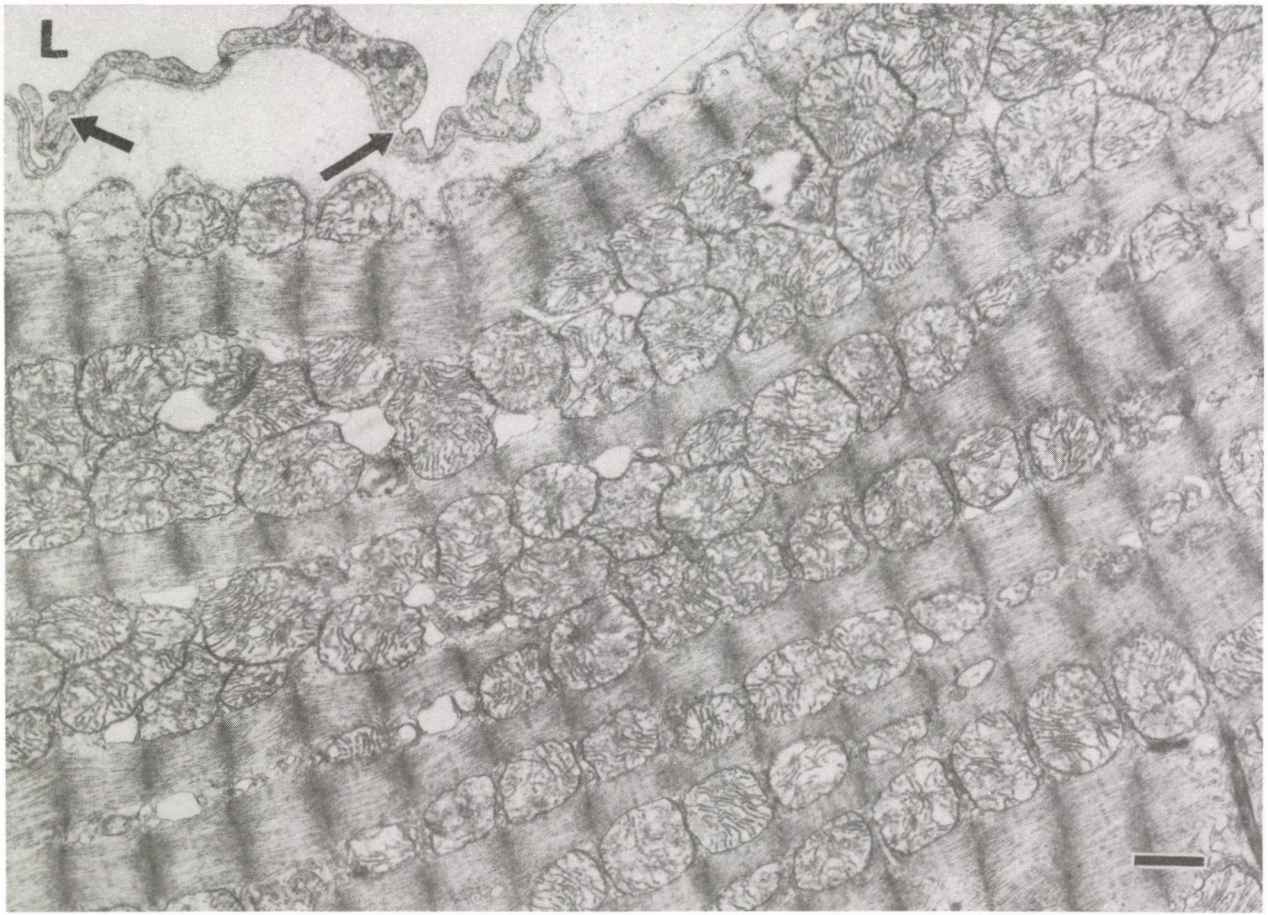


*Fig. 3.* Electromicrograph of a part of the papillary muscle of the rat heart. Exposure: 3 weeks of drinking water containing 10% ethyl alcohol and 5% sugar, and daily administration of 5 mg/kg b.w. nickel sulphate by gavage. In some places the sarcoplasmatic reticulums are moderately dilated, mitochondria are swollen, electrodense granules of the mitochondria are missing, the mitochondrial matrix is clearer (electrolucent), than in normal cells. L: capillary lumen, arrow shows an endothel cell. Scale: 1 μm

Electron microscopy revealed no significant changes caused by nickel in the ultrastructure of the heart (Fig. 1). As an effect of alcohol, swelling of mitochondria, dilation of the sarcoplasmic reticulum could be seen in some places of the myocardium; nickel increased the frequency of ultrastructural changes caused by alcohol (Figs 2, 3).

*Haemodynamic examinations*

Water containing 5% sugar. Haemodynamic parameters of the animals were similar to that measured earlier on CFY rats in our laboratory (Figs 4, 5, 6, 7, 8, Table I).

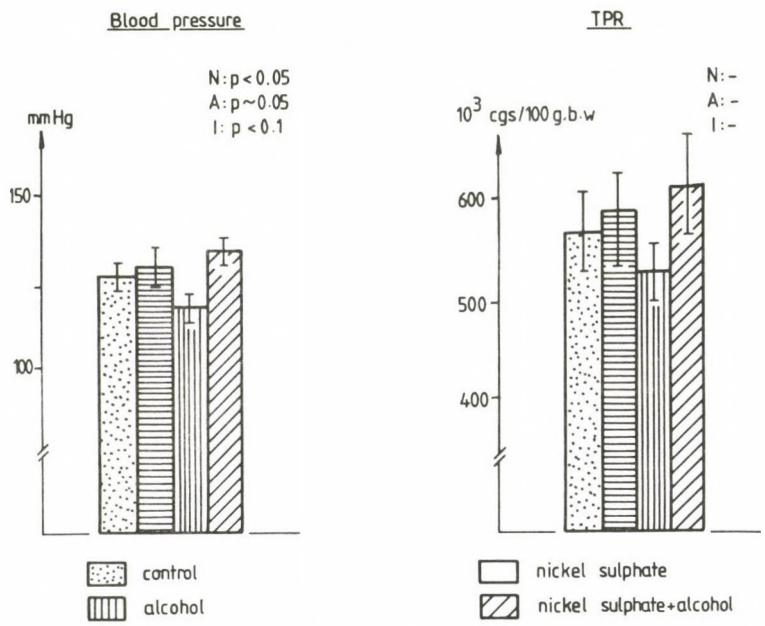


*Fig. 4.* Haemodynamic effects of alcohol and nickel sulphate in rats. Columns are mean ± SEM. n = 9 (in each group). b. w.: body weight; N: effect of nickel sulphate; A: effect of alcohol; I: interaction

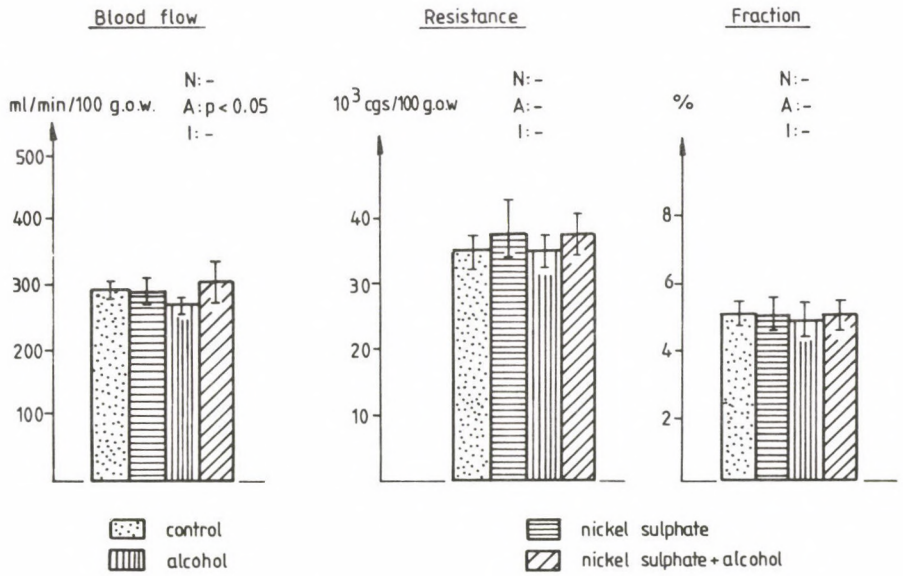


*Fig. 5.* Effects of alcohol and nickel sulphate on the circulation of myocardium in rats. Columns are mean ± SEM. n = 9 (in each group). o.w.: organ weight; N: effect of nickel sulphate; A: effect of alcohol; I: interaction

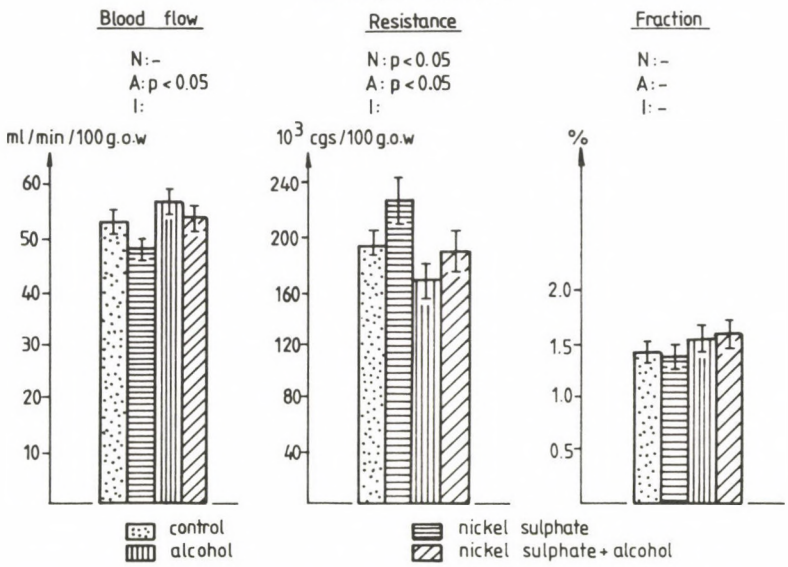


*Fig. 6.* Effects of alcohol and nickel sulphate on the circulation of brain in rats. Columns are mean ± SEM. n = 9 (in each group). o.w.: organ weight; N: effect of nickel sulphate; A: effect of alcohol; I: interaction

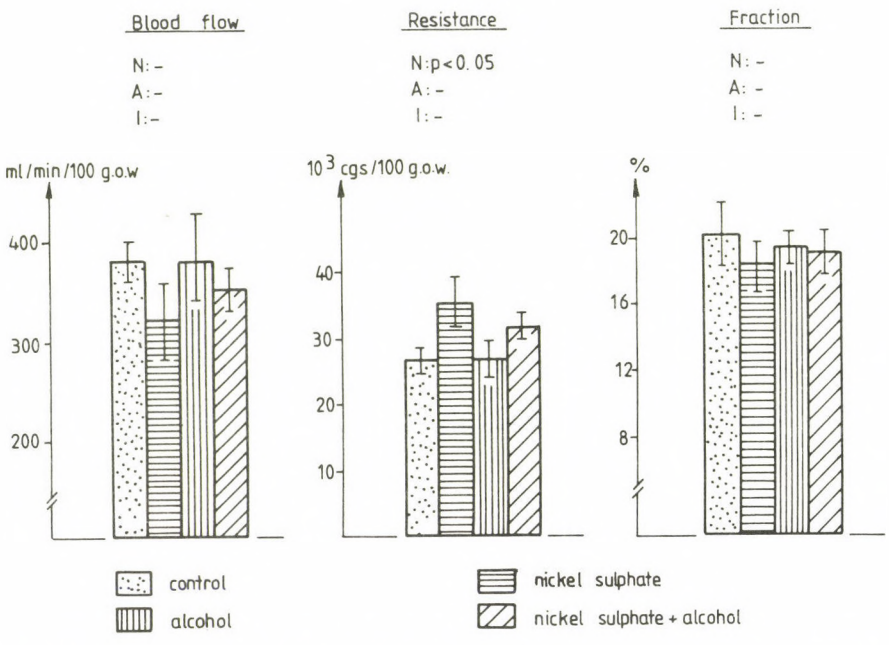


*Fig. 7.* Effects of alcohol and nickel sulphate on the circulation of kidney in rats. Columns are mean ± SEM. n = 9 (in each group). o.w.: organ weight; N: effect of nickel sulphate; A: effect of alcohol; I: interaction

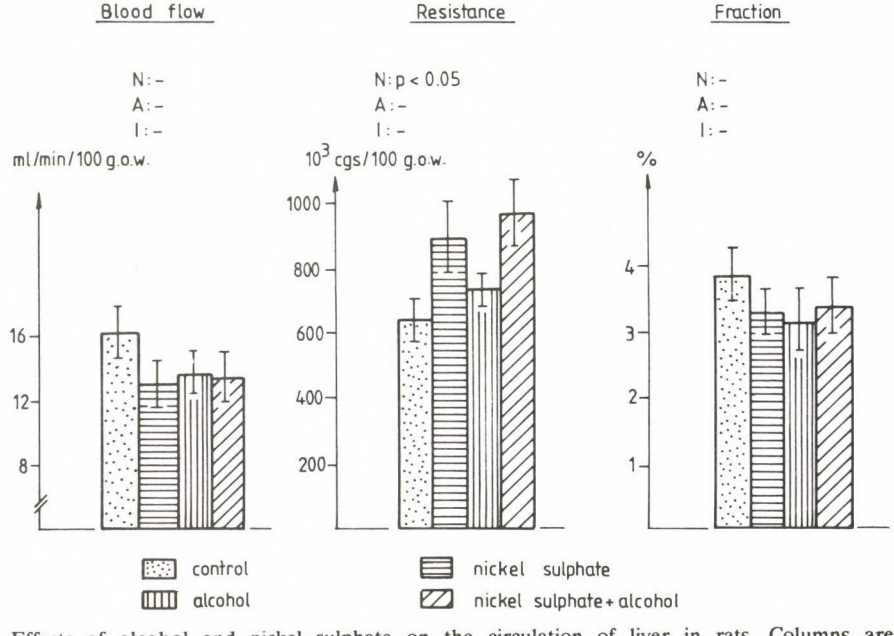


*Fig. 8.* Effects of alcohol and nickel sulphate on the circulation of liver in rats. Columns are mean ± SEM. n = 9 (in each group). o.w.: organ weight; N: effect of nickel sulphate; A: effect of alcohol; I: interaction

**Table I**

*Haemodynamic effects of alconol and nickel sulphate in rats*

| | Control n=9 | Nickel sulphate n=9 | Alcohol n=9 | Alcohol + Nickel sulphate n=9 | Values of significance p (less than) Nickel | Alcohol | Interaction |
|---|---|---|---|---|---|---|---|
| Body wt | 372.7 ±12.32 | 365.6 ±12.05 | 384.5 ±13.94 | 382.3 ±14.71 | - | - | - |
| Cardiac output | 67.85± 2.95 | 66.28± 3.49 | 71.05± 6.18 | 69.91± 5.90 | - | - | - |
| Cardiac index | 18.35± 0.92 | 18.19± 0.93 | 18.41± 1.31 | 18.54± 1.76 | - | - | - |
| *LUNG* | | | | | | | |
| Organ wt | 4.24± 0.21 | 3.69± 0.27 | 4.49± 0.29 | 4.33± 0.16 | - | $p < 0.05$ | - |
| Fraction | 2.54± 0.26 | 2.74± 0.35 | 2.94± 0.35 | 2.62± 0.46 | - | - | - |
| Blood flow | 41.66± 5.23 | 50.31± 6.96 | 45.0 ± 4.40 | 42.65± 9.83 | - | - | - |
| Resistance | 272.0 ±30.82 | 254.3 ±45.58 | 230.5 ±30.88 | 319.9 ±37.27 | - | - | - |
| *GUT* | | | | | | | |
| Organ wt | 16.08± 0.82 | 15.33± 0.79 | 17.16± 0.42 | 15.86± 0.70 | - | - | - |
| Fraction | 14.08± 1.18 | 12.95± 0.89 | 12.08± 0.70 | 13.29± 1.12 | - | - | - |
| Blood flow | 61.3 ± 6.67 | 56.42± 4.55 | 50.0 ± 4.53 | 58.73± 6.32 | - | - | - |
| Resistance | 188.1 ±27.47 | 199.4 ±22.17 | 204.4 ±23.87 | 215.9 ±35.2 | - | - | - |
| *SKIN* | | | | | | | |
| Organ wt | 63.33± 2.73 | 63.4 ± 2.79 | 67.22± 2.54 | 64.0 ± 2.40 | - | - | - |
| Fraction | 10.12± 0.55 | 9.56± 1.13 | 11.03± 0.44 | 10.56± 0.71 | - | - | - |
| Blood flow | 11.03± 0.99 | 9.83± 0.98 | 11.72± 1.0 | 11.56± 1.19 | - | - | - |
| Resistance | 990.6 ±104.3 | 1157.0 ±112.5 | 855.6 ±73.96 | 1024.0 ±101.1 | - | - | - |
| *CARCASS* | | | | | | | |
| Organ wt | 265.6 ± 8.43 | 260.0 ± 8.60 | 271.3 ±10.22 | 274.5 ± 11.19 | - | - | - |
| Fraction | 42.24± 1.39 | 46.4 ± 2.60 | 44.57± 1.93 | 44.3 ± 2.63 | - | - | - |
| Blood flow | 10.81± 0.54 | 12.1 ± 1.24 | 11.7 ± 1.07 | 11.88± 1.88 | - | - | - |
| Resistance | 976.2 ±86.68 | 945.8 ±101.4 | 853.4 ±64.2 | 1062.0 ±116.0 | - | - | - |

Values are means ± SEM. Body weight, g; cardiac output, ml/min; cardiac index, ml/min/100 g b.w.; organ weight (o.w.), g; fraction = organ blood supply expressed in percent of cardiac output; blood flow, ml/min per 100 g o.w.; resistance, $10^3$ cgs/100 g o.w.

*Alcohol*

A decrease of borderline significance of the arterial blood pressure and myocardial blood flow was observed. Vascular resistance of the brain decreased significantly, while cerebral blood flow increased (Figs 4, 5, 6).

*Nickel*

It increased the arterial blood pressure, the vascular resistance of the kidneys, the brain and the hepatic artery. It increased the TPR in a tendentious way and decreased the blood flow of the kidneys (Figs 4, 6, 7, 8).

Following a simultaneous administration of alcohol and nickel the arterial blood pressure increased further compared to the group treated only with nickel – nickel inhibited the hypotensive effect of alcohol (Fig. 4).

## Discussion

In our present study ethanol was administered as "drinking water" in a concentration of 10% in water containing 5% sugar. The alcohol dose this way amounts 7–9 g/kg/day, which is less than the dose that can be given rats using the Lieber's liquide diet modified by our team (11.5–12.5 g/kg/day) [4, 15, 31, 32]. Despite of this, alcohol caused a decrease of borderline significance of the arterial blood pressure and of the nutritive blood flow of the heart, besides the insignificant ultrastructural changes of the myocardium – this supporting our earlier results [15, 16, 17, 18].

Nickel is an essential substance in many mammals [21] and in human beings [10]. It is known, however, that nickel causes focal myocardial necrosis [11] furthermore, that serum nickel concentration increases in myocardial infarction and in other ischemic heart diseases such as unstable angina [8, 13, 30], the origin and reason of which are not known. These observations are in agreement – at least partly – with the results of our present study, as nickel significantly increased the arterial blood pressure, the vascular resistance of some organs, such as kidneys, brain, liver, and there was a tendency to increase TRP. Hypertension is known as one of the most important risk factors of ischemic heart disease [6].

As environmental nickel pollution is growing year by year [21] nickel deserves the special attention of social medicine not only because it is a human carcinogen [34, 35] but also because of its anticipated cardiovascular effect. Therefore preventive measures should be taken to decrease occupational and environmental exposure by keeping the level of nickel contamination as low as possible.

Cardiovascular effects of alcohol and nickel observed in our study differed from each other in many respect. This manifested itself especially in their opposite effects on blood pressure. In case of dual exposure – simultaneous administration of alcohol and nickel – nickel not only inhibited the moderate hypotensive effect of alcohol but under the joint effect of the two substances the arterial blood pressure increased more than under the effect of nickel alone. That is, such an interaction appeared between the effects of a low dose of alcohol and a medium dose of nickel (1/100 of $LD_{50}$), which caused significant increase of the arterial blood pressure in the animals. We have concluded, that – at least in a certain dose range – joint exposure to alcohol and nickel may increase the risk of ischemic heart disease. In the pathomechanism of this phenomenon the vascular-resistance-increasing effect of nickel may play a major role. In this respect it is the increased vascular resistance of the kidney that deserves attention first of all.

As for the interaction between the myocardium-damaging-effects of alcohol and nickel, our results did not supply enough information to draw acceptable conclusions. Rubányi et al. [26], as well as Leach and Sunderman Jr. [9] observed the vascoconstrictive effect of nickel on the coronaries in their *in vitro* and *in vivo* investigations. Mather [11] found myocardial necrosis in rats after the administration of 3 mg/kg daily doses of nickel-sulphate for 60 days. Electron microscopic examinations of the myocardium of chamber – exposed rats revealed evidence of muscle fibre lesions at sites of intercalary discs and changes in mitochondrial structure as a result of accumulated nickel [24]. In our study we have observed neither myocardial necrosis nor the increase of the vascular resistance of the coronaries in animals exposed to nickel (5 mg/kg daily doses for three weeks). Despite of this, our results can be fitted to the data of others [11, 23, 24]. Our ultrastructural findings showed an increased number of swollen mitrochondria and dilated profiles of sarcoplasmic profiles of sarcoplasmic reticulum. These signs are mostly of hypoxic or toxic origin and may indicate the early stage of the later myocytolysis (focal necrosis). As for the time being in our study no influence on the coronaries has been detected, we cannot answer the question whether there is a causal relationship between the increased blood pressure, which is one of the most important risk factors of ischemic heart disease, and the myocardial alterations (e.g. temporary coronary spasms).

## Acknowledgements

We thank to Ms. Karola Albert, Ms. Magdolna Bajusz, Mrs. Katalin Békés, and Mr. Imre Szarvassy for their high-level technical assisstance.

## REFERENCES


1. Babskii, E. B., Donskih, E. A.: The effects produced by $NiCl_2$ on the electrical and mechanical activity of the frog myocardium. DOKL. Akad. Nauk. SSSR. **163**, 1197–1200 (1965).
2. Boór, K., Nagy, Gy.: Az alkoholfogyasztás és az alkoholizmus közgazdasági és társadalmi problémái. Alkohológia **8**, 87–93 (1977). (in Hungarian)
3. Corrick, K. D.: In: Bureau of Mines Minerals Yearbook. U.S. Department of the Interior, Washington D. C. 1973
4. DeCarli, L.M., Lieber, C.S.: Fatty liver in the rat after prolonged intake of ethanol with a nutritionally adequate new liquid diet. J. Nutr. **91**, 331–336 (1967).
5. Dunett, C. W.: A multiple comparison procedure for comparing several treatments with control. J. Amer. Statist. Assoc. **50**, 1096–1121 (1955).
6. Kannel, W. B.: Role of blood pressure in cardiovascular disease: The Framingham Study. Angiology **26**, 1–12 (1975).
7. Kaufmann, R., Fleckenstein, A.: Ca-kompetitive elektromechanische Entkoppelung durch Ni- und Ca Ionen am Warmblüter Myokard. Arch. ges. Physiol. **282**, 290–297 (1965).
8. Leach, C. N. Jr., Linden, J. V., Hopfer, S. M., Crisostomo, M. C., Sunderman, F. W. Jr.: Nickel concentrations in serum of patients with acute myocardial infarction or unstable angina pectoris. Clin. Chem. **31**, 556–560 (1985).
9. Leach, C. A. Jr., Sunderman, F. W. Jr.: Hypernickelaemia following coronary arteriography, caused by nickel in the radiographic contrast medium. Ann. Clin. Labor. Sci. **17**, 137–144 (1987).
10. Mancinella, A.: Nickel, an essential trace element. Metabolic, clinical and therapeutic considerations. Clin. Ther. **138(3–4)**, 159–65 (1991).
11. Mather, A. K.: Arch. Toxicol. **37**: 159, 1977. cit.: Patty's Industrial Hygiene and Toxicology. Clayton F. D., Clayton F. E. eds. Wiley-Interscience Publ. New York. Chichester. Brisbane. 1981. p. 1827.
12. McDevitt, D. G., Nies, A. S.: Simultaneous measurements of cardiac output and its distribution with microspheres in the rat. Cardiovasc. Res. **10**, 494–498 (1976).
13. McNeely, A., Sundermann, F. W. Jr.: Abnormal concentrations of nickel in serum in cases of myocardial infarction, stroke, burus hepatic cirrhosis and uremia. Clin. Chem. **17**, 1123–1128 (1971).
14. McNeely, M. D., Nechay, M. W., Sunderman, F. W. Jr.: Measurements of nickel in serum and urine as indices of environmental exposure to nickel. Clin. Chem. **18**, 992–995 (1972).
15. Morvai, V., Ungváry, Gy.: Effects of simultaneous alcohol and toluene poisoning on cardiovascular system of rats. Toxicol. Appl. Pharmacol. **50**, 381–389 (1979a).
16. Morvai, V., Ungváry, Gy.: Effect of chronic exposure to alcohol on the circulation of rats of different ages. Acta Physiol. Acad. Sci. Hung. **53**, 433–441 (1979b).
17. Morvai, V., Ungváry, Gy.: Morphological alterations due to long term alcohol intake in rats. Exp. Pathol. **31**, 153–160 (1987).
18. Morvai, V., Ungváry, Gy., Carga, K., Albert, K., Folly, G.: Effects of long-term alcohol intake on the cardiovascular system of the rat. Acta Physiol. Acad. Sci. Hung. **37**, 229–237 (1979).
19. NAS. Nickel. National Research Council, National Academy of Sciences, Washington D. C. 1975.
20. Nodiya, P. I.: Study of cobalt and nickel balance in the organism of students of industrial technical schools. Gig. Sanit. **37**, 108–109 (1972). (In Russian)
21. Norseth, T.: Nickel. In: Handbook on the Toxicology of Metals, Friberg L., Nordberg G. F. and Vouk V., eds, Elsevier Science Publishers, B. V., 1986, Chapter **18**, pp. 462–481.
22. Ong, S. D., Bailey, L. E.: Uncoupling of excitation from contraction by nickel in cardiac muscle. Am. J. Physiol. **224**, 1092–1098 (1973).
23. Patai, K., Balogh, I.: Nickel- and cadmium-induced fetal myocardial changes in the mouse: the hazards of cigarette smoke in pregnancy. Acta Chir. Hung. **29**, 315–321 (1988).

24. Reichrtova, E., Sulicova, L., Vesela, A., Bencko, V.: Bio-accumulation of metals from nickel smelter waste in P and $F_1$ generation of exposed animals. J. Hyg. Epidemiol. Microbiol. Immunol. **34**, 337–341 (1990).
25. Rubányi, G., Kovách, A. G. B.: Cardiovascular actions of nickel ions. Acta Physiol. Acad. Sci. Hung. **55**, 345–353 (1980).
26. Rubányi, G., Kalabay, L., Pataki, T., Hajdú, K.: Nickel induces vasoconstriction in the isolated canine coronary artery by a tonic $Ca^{2+}$-activation mechanism. Acta Physiol. Acad. Sci. Hung. **59**, 155–159 (1982).
27. Schlettwein-Gsell D., Mommsen-Straub, S.: Int. Z. Vitam. Ernaehrungsforsch. **41**, 429–437 (1971). Cit.: Norseth, T.: Nickel. In: Handbook on the Toxicology of Metals, Friberg L., Nordberg G. F. and Vouk V., eds, Elsevier Science Publishers, 1986 Chapter **18**. pp. 462–481.
28. Schroeder, H. A., Balassa, J. J., Tiptin, I. H.: Abnormal trace metals in man – nickel. J. Chronic Dis. **15**, 51–65 (1962).
29. Sunderman, F. W., Sunderman, F. W. Jr.: Nickel poisoning. XI. Implication of nickel as a pulmonary carcinogen in tobacco smoke. Am. J. Clin. Pathol. **35**, 203–209 (1961).
30. Sunderman, F. W. Jr., Nomoto, S., Pradhan, A. M., Levine, H., Bernstein, S. H., Hirsch, R.: Increased concentrations of serum nickel following acute myocardial infarction. N. Engl. J. Med. **283**, 896–899 (1970).
31. Ungváry, Gy., Hudák, A.: Hosszan tartó, nagy dózisú orális alkohol kezelés módjai és ezek gyomorbél tractusra és a májra kifejtett hatásának összehasonlítása CFY patkányokban. Kísérl. Orvostud. **29**, 86–93 (1977). (In Hungarian)
32. Ungváry, Gy., Tátrai, E., Szeberényi, Sz. Barcza, Gy., Morvai, V., Lada, Gy.: Hogyan vizsgálható az alkohol embriotoxikus-teratogén hatása? Alkohol hatás-e a magzati alkohol szindróma? Modell kísérletek CFY patkányokban. Egészségtudomány **29**, 151–158 (1985). (In Hungarian)
33. Vanselow, A. P.: In: Diagnostic Criteria for Soils and Plants, pp. 302–309, Chapman, H. D. (Ed.). University of California. Riverside. 1966.
34. WHO-IARC Monographs on the Carcinogenetic Risk of Chemicals to Humans. Some inorganic and organo-metallic compounds. WHO-IARC. Lyon. Vol. 2. 1973.
35. WHO-IARC. Monographs on the Carcinogenic Risk of Chemicals to Humans. Tobacco smoking. WHO-IARC. Lyon. Vol. 39. 1986.
36. WHO-IARC. Tobacco. A major international health hazard. Eds Zaridze, D., Peto, R. In: IARC Scientific publications, No. 74, WHO-IARC Lyon. 1986.

*Acta Physiologica Hungarica, Volume 81 (3), pp. 253–261 (1993)*

# THE EFFECTS OF SIMULTANEOUS ALCOHOL AND COBALT CHLORIDE ADMINISTRATION ON THE CARDIOVASCULAR SYSTEM OF RATS+

Veronika MORVAI, É. SZAKMÁRY,* Erzsébet TÁTRAI,* GY. UNGVÁRY,* G. FOLLY**

SEMMELWEIS MEDICAL UNIVERSITY, 2ND DEPARTMENT OF MEDICINE, *NATIONAL INSTITUTE OF OCCUPATIONAL HEALTH, AND **INSTITUTE OF EXPERIMENTAL MEDICINE OF THE HUNGARIAN ACADEMY OF SCIENCES, BUDAPEST, HUNGARY

Received July 4, 1992
Accepted September 4, 1992

CFY male rats received drinking water which contained 10% ethyl alcohol and 5% sugar and were treated with 50 mg/kg daily doses of cobalt chloride for three weeks by gavage. Haemodynamic examinations were carried out using radioactive microspheres.

Alcohol caused no significant injury of the structure of the myocardium, while cobalt chloride caused incipient multifocal myocytolysis. Blood pressure and nutritive blood flow of the heart were decreased slightly by alcohol and significantly by cobalt chloride. Alcohol additively increased the effect of cobalt chloride decreasing the nutritive blood flow of the heart. It is suggested, that hypoxia increased by dual exposure is responsible for the aggravating effect of alcohol on the myocardial injury caused by the cobalt salt.

**Keywords**: alcohol, cobalt chloride, myocardium blood flow, rat

The compositions of alcoholic beverages is rather variable basically depending on raw materials (fruit, corn, etc.), on ingredients of the soil at the site of production (natural ingredients, pollutants – fertilizers, heavy metal content of ameliorators), and on the technology of production (e.g. type of fermentation).

Although the main ingredients are ethyl alcohol, water and sugar, the accompanying long-chain alcohols (amyl, isoamyl, propyl, isopropyl, butyl, isobutyl and phenyl alcohols), methanol, aldehydes, ketones, esters, amino acides, peptides, other acids, tannins, metal salts, pesticide residues, fungal contamination (e.g. aflatoxin – found mainly in home made drinks) may significantly modify the effects of alcoholic beverages on the organism [10]. This finding has been supported by a number of epidemiological, clinical, analytical chemical and experimental studies [4,

Correspondence should be addressed to
Veronika MORVAI
2nd Department of Medicine, Semmelweis University Medical School
1088 Budapest Szentkirályi u. 46., Hungary

+Research supported by grant T–192/1990 from the Hungarian Ministry of Welfare

6, 7, 11, 12, 19, 24, 25, 29]. It has been known for a long time, that cobalt salts cause the injury of the myocardium – cardiomyopathy [21]. In employees working in cobalt exposure the cardiomyopathy was established [4, 14, 30].

The cardiomyopathy inducing effect of alcohol – as one of the fatal outcome of chronic alcoholism – is also well known [8, 26, 28]. Long-term, high-dose alcohol administration decreased the arterial blood pressure and the nutritive blood flow of the heart in rats [23].

On the basis of the literary data available to date we have supposed that there is a cardiotoxic interaction between alcohol and cobalt, also when the alcoholic drink is cobalt-free, but cobalt gets into the organism for example, via occupational cobalt exposure.

Furthermore we have supposed, that the cardiomyopathy-inducing effect of the two substances – ethanol and cobalt – manifests itself through the alteration of the nutritive blood flow of the heart and other haemodynamic parameters.

The present study aimes at proving these two hypotheses.

## Materials and methods

Two groups of CFY male rats (LATI, Gödöllő) weighing 340–390 g, were made to drink water containing 5% sugar and 10% ethyl alcohol or water containing 5% sugar only. (The animals were fed on standard LATI pellets ad libitum.) One half of each group received 50 mg/kg cobalt chloride dissolved in physiological saline, while the other half received 10 mg/kg physiological saline by gavage for three weeks.

*Routine histology*

Specimens of the internal organs of 5 animals in each group were fixed in 8% formaldehyde, embedded in paraffin using a Shandon embedding processor. Sections of 6 μm thickness were stained with haematoxyline-eosine (HE).

*Fine structural studies*

Hearts of three living, narcotized animals in each group were perfused by glutaraldehyde-paraformaldehyde solution of pH 7.2 according to Karnovsky [13], through a cannula in the thoracic aorta (retrograde). Samples (papillar muscle) of the perfused hearts were fixed in fixative similar to the perfusing solution and in 2% solution of osmium tetroxide for 2–4 and 1 hour, respectively. After fixation the specimens were dehydrated in ascending alcohol series and propylene oxide, then embedded in to Durcupan ACM (Fluka). Semithick and ultrathin sections were made by Reichert OMU III ultramicrotome, contrasted by uranyl acetate and lead citrate. The sections were studied by JEOL-JEM 100 c electronmicroscope.

*Haemodynamic examinations (8 animals in each group)*

The arterial blood pressure was continuously measured and recorded in the right femoral artery and the cardiac output, organ fractions of the cardiac output, the nutritive blood flow of the organs were determined according to McDevitt and Nies [18], using $^{57}Co$ and $^{113}Sn$ microphores (of 15 ± 5 μm

diameter, 3 M Company, St Paul, Minn); the total peripheral resistance and the vascular resistance of the individual organs were calculated.

For statistical analysis of the data analysis of variance and Dunett's test [9] were used. Means and standard errors are given on the figures and in the tables.

## Results

### *Morphological observations*

Alcohol had no influence on the structure of myocardium studied by light microscope. Cobalt chloride caused incipient, multifocal myocytolysis. Alcohol increased the myocardium damaging effect of the cobalt salt. By electronmicroscope also some non-specific, toxic alterations attributed to alcohol were observed as the effect of alcohol, such as the scattered dilation of the sarcoplasmic reticulum, and swollen mitochondria. The number of changes, however was not significant. Cobalt, or cobalt and alcohol together, exerted injury of the contractile elements – myocytolysis, degeneration of myofibrilles. Swollen mitochondria could be seen more frequently. There were no changes in the coronary arteries and veins.

### *Haemodynamic observations*

Alcohol decreased the arterial blood pressure slightly and the nutritive blood flow of the heart significantly (Figs 2 and 3).

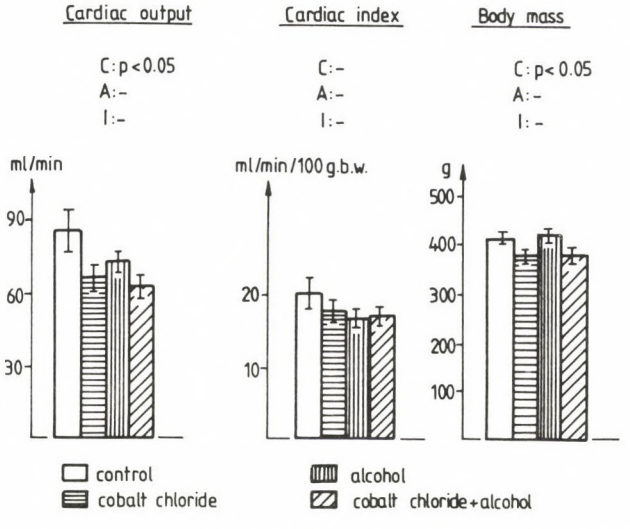


*Fig. 1.* Haemodynamic effects of alcohol and cobalt chloride in rats. Columns are mean ± SEM. n = 8 (in each group). b.w.: body weight. C: effect of cobalt chloride; A: effect of alcohol; I: interaction

**Table I**

*The effect of alcohol and cobalt chloride on blood circulation of rats*

| | Control n=8 | $CoCl_2$ n=8 | Alcohol n=8 | Alcohol $+CoCl_2$ n=8 | Significanc of the effect $CoCl_2$ | Alcohol | Inter-action |
|---|---|---|---|---|---|---|---|
| **Brain** | | | | | | | |
| organ weight | 1.91±0.04 | 1.83±0.04 | 1.87±0.04 | 1.84±0.02 | - | - | - |
| fraction | 1.37±0.12 | 1.37±0.24 | 1.55±1.15í | 1.35±0.04 | - | - | - |
| blood flow | 58.24±3.18 | 52.55±8.53 | 58.31±2.52 | 46.38±3.29 | $p<0.1$ | - | - |
| resistance | 197.42±12.72 | 219.51±40.05 | 172.38±10.78 | 199.30±8.05 | - | - | - |
| **Lung** | | | | | | | |
| organ weight | 3.99±0.26 | 4.20±0.23 | 4.46±0.23 | 3.31±0.25 | - | - | - |
| fraction | 2.73±0.65 | 2.83±0.75 | 2.30±0.47 | 3.24±0.93 | - | - | - |
| blood flow | 62.40±18.78 | 43.24±10.98 | 37.81±7.27 | 66.33±20.81 | - | - | - |
| resistance | 269.07±51.29 | 321.95±68.83 | 333.69±57.94 | 262.00±67.79 | - | - | - |
| **Liver** | | | | | | | |
| organ weight | 21.58±0.82 | 19.95±0.71 | 21.67±0.83 | 18.43±0.07 | $p<0.01$ | - | - |
| fraction | 3.08±0.54 | 3.69±0.57 | 3.44±0.48 | 3.57±0.59 | - | - | - |
| blood flow | 11.66±2.02 | 12.28±2.07 | 11.13±1.01 | 11.83±1.75 | - | - | - |
| resistance | 1144.83±161.51 | 896.25±126.50 | 942.02±88.16 | 903.73±143.89 | - | - | - |
| **Intestine** | | | | | | | |
| organ weight | 19.85±0.86 | 18.06±0.89 | 19.39±0.89 | 18.78±0.75 | - | - | - |
| fraction | 15.62±2.02 | 20.62±2.22 | 17.94±1.44 | 20.60±1.40 | $p<0.05$ | - | - |
| blood flow | 68.14±10.23 | 75.96±9.10 | 68.46±7.53 | 69.90±7.35 | - | - | - |
| resistance | 249.41±89.30 | 134.08±15.26 | 158.15±19.41 | 135.62±7.82 | - | - | - |

| | Control n=8 | $CoCl_2$ n=8 | Alcohol n=8 | Alcohol $+CoCl_2$ n=8 | Significanc of the effect $CoCl_2$ | Alcohol | Inter-action |
|---|---|---|---|---|---|---|---|
| **Kidney** | | | | | | | |
| organ weight | 3.90±0.08 | 3.59±0.11 | 3.67±0.17 | 3.42±0.11 | $p<0.05$ | - | - |
| fraction | 17.58±1.64 | 20.15±1.15 | 18.73±1.01 | 21.46±1.01 | $p<0.05$ | - | - |
| blood flow | 367.31±26.73 | 380.98±44.27 | 383.14±30.36 | 392.47±24.41 | - | - | - |
| resistance | 32.84±4.32 | 26.43±2.57 | 27.81±3.92 | 23.63±1.51 | - | - | - |
| **Skin** | | | | | | | |
| organ weight | 70.0±2.0 | 62.75±3.02 | 70.38±2.18 | 61.88±2.18 | $p<0.01$ | - | - |
| fraction | 8.42±0.87 | 6.48±0.51 | 8.09±0.95 | 7.03±0.86 | $p<0.1$ | - | - |
| blood flow | 10.20±1.43 | 6.88±0.69 | 8.44±1.07 | 7.77±1.13 | $p<0.1$ | - | - |
| resistance | 1314.5±227.1 | 1520.11±201.64 | 1199.65±245.88 | 1346.86±203.86 | - | - | - |
| **Carcass** | | | | | | | |
| organ weight | 295.22±7.62 | 273.43±12.14 | 298.50±9.72 | 272.63±9.44 | $p<0.05$ | - | - |
| fraction | 44.83±2.44 | 38.46±2.58 | 41.53±1.94 | 37.37±1.82 | $p<0.05$ | - | - |
| blood flow | 13.14±11.17 | 9.58±1.11 | 10.30±1.25 | 8.90±0.95 | $p<0.05$ | - | - |
| resistance | 971.64±132.11 | 1082.34±145.61 | 939.24±89.91 | 1088.11±91.28 | - | - | - |

Arithmetic means and ± SE are indicated for each parameter. Organ weight is given in gs, organ fractions of cardiac output in %, organ blood flow in ml/min 100 g organ weight, resistance in $10^3$ cgs/100 g organ weight.

It had practically no influence on any other haemodynamic parameters (Fig. 1 and Table I).

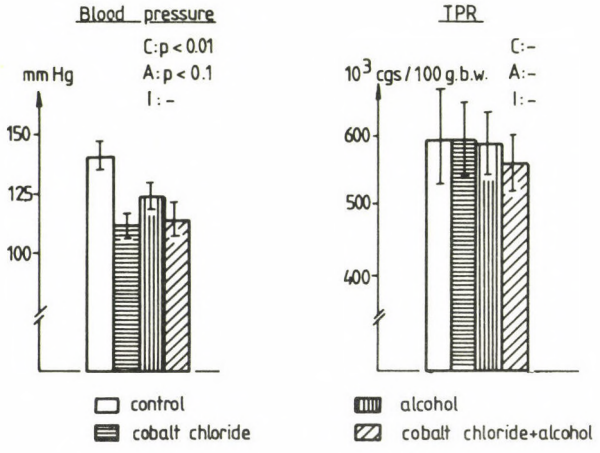


*Fig. 2.* Haemodynamic effects of alcohol and cobalt chloride in rats. Columns are mean + SEM. n = 8 (in each group). TPR: total peripheral resistance, b.w.: body weight. C: effect of cobalt chloride; A: effect of alcohol; I: interaction

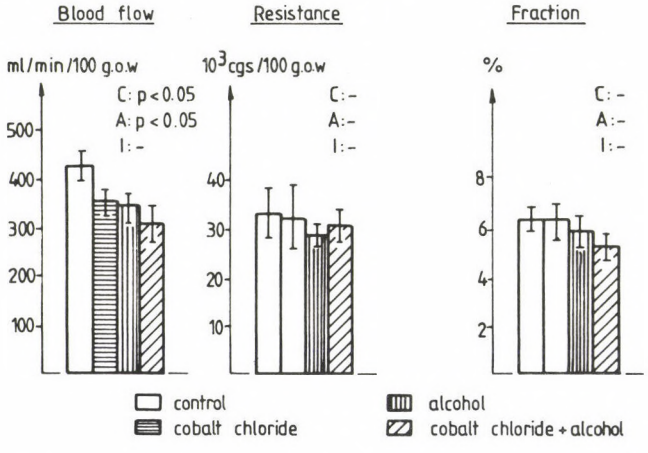


*Fig. 3.* Effects of alcohol and cobalt chloride on the circulation of myocardium. Columns are mean ± SEM. n = 8 (in each group). o.w.: organ weight. C: effect of cobalt chloride; A: effect of alcohol; I: interaction

Cobalt chloride decreased the arterial blood pressure, the cardiac output, the blood flow of the heart and the carcass. It also decreased the blood flow of the brain and skin slightly (Figs 1, 2 and 3, Table I). Furthermore it decreased the body weight of the animals, the kidney, skin and carcass fractions of the cardiac output (Fig. 1 and Table I).

Following simultaneous administration of alcohol and cobalt chloride the effects described at the individual substances appeared independently of each other or summarized (addition). Addition could be observed in the decreases of the nutritive blood flow of the heart (Figs 1, 2, 3 and Table I).

## Discussion

In the present work cobalt salt administered intragastrially caused multifocal myocytolysis in the heart of rats. Repeated parenteral and oral cobalt exposures cause the degeneration of the myocardium accompanied by ECG changes in experimental animals [16].

In our study alcohol caused no pathogenic alterations in the myocardium observable by light microscope, but given simultaneously with cobalt, it increased the myocytolyzing effect of the latter – more myocardial cells were affected, than in the groups treated only with cobalt. This is in good agreement with the observation, that those beers, which are contaminated significantly with cobalt, cause cardiomyopathy more frequently than other drinks [2, 20, 21].

Histological examination of the dead revealed the degeneration of the myocardial cells [5]. The heavy beer drinkers consume daily some 10 l beer and 10 mg cobalt in it. This dose may seem relatively high, although even higher cobalt doses are used in the treatment of anaemias. Thus the disease seems to be of multifactorial origin and besides cobalt, not only the extreme alcohol consumption, but malnutrition associated with it, play role in the myocardial injury [3, 16]. The results of our present study indicate, that alcohol potentiates the myocardium damaging effect of cobalt, without the obvious signs of malnutrition. Direct myocardium damaging effect of alcohol has been proven both in animal experiments [15, 17, 27] and in human clinical investigations [1, 8, 15, 27]. Alcohol dose used in our experiments did not cause myocardial degeneration, however, – similarly to our earlier experiments – alcohol decreased the nutritive blood flow of the myocardium [23].

Cobalt exposure also decreased the nutritive blood flow of the myocardium. In case of dual exposure the two blood flow decreasing effects were additive. For this reason, the summarized hypoxia may be responsible for the effect of alcohol increasing the myocardium damaging effect of cobalt. This is supported by our histological results. Swelling of mitochondria, dilation of the sarcoplasmic reticulum

caused by alcohol are of hypoxic origin, while injury of the contractile elements (myocytolysis and degeneration of myofilaments) is in connection with the direct cytotoxic effect of cobalt and hypoxia. – Hypoxia alone is also capable to induce similar damages.

Our results also call attention to the fact, that in case of simultaneous exposure to alcohol and cobalt, damage to the myocardium may occur even when the doses of neither substances reach the health damaging level. This possibility endangers mainly those working in cobalt exposure.

**Acknowledgements**

We thank for the high level technical assistance of Ms Karola Albert, Ms Magdolna Bajusz, Mrs Katalin Békés, Mrs Magdolna Horváth and Mr Imre Szarvassy.

## REFERENCES

1. Alexander, C. S.: Idiopathic heart disease. II. Electron microscopic examination of myocardial biopsy specimens in alcoholic heart disease. Am. J. Med. **41**, 229–234 (1966).
2. Alexander, C. S.: Cobalt-beer cardiomyopathy. A clinical and pathological study of twenty-eight cases. Am. J. Med. **53**, 395–416 (1972).
3. Balazs, T., Herman, E. H.: Toxic cardiomyopathies. Ann. Clin. Lab. Sci. **6**, 467–476 (1976).
4. Barborik, M., Dusek, J.: Cardiomyopathy accompanying industrial cobalt exposure. Br. Heart J. **34**, 113–116 (1972).
5. Bonenfant, J.-L., Auger, C., Miller, G., Chenard, J., Roy, P. E.: Quebec beer drinkers, myocardosis. Pathological aspects. Ann. N. Y. Acad. Sci. **156**, 577–582 (1969).
6. Burch, G. E., Harb, J. M., Colcolough, H., Tsui, C. Y.: The effect of prolonged consumption of beer, wine and ethanol on the myocardium of the mouse. Hopkins Med. J. **129**, 130–148 (1971).
7. Coudray, C., Boucher, F., Richard, M. J., Arnaud, J., De Leiris, J., Favier, A.: Zinc deficiency, ethanol, and myocardial ischemia affect lipoperoxidation in rats. Biol. Trace Elem. Res. **30**, 103–118 (1991).
8. Demakis, J. G., Prostkzey, A., Rahimtoola, S. H., Jamil, M., Sutton, G. C., Rosen, K. M., Gunnar, R. M., Tobin, R. J.: The natural course of alcoholic cardiomyopathy. Ann. Int. Med. **80**, 293–297 (1974).
9. Dunett, C. W.: A multiple comparison procedure for comparing several treatments with control. J. Amer. Statist. Assoc. **50**, 1096–1121 (1955).
10. Feinman, L., Lieber, C. S.: Toxicity of ethanol and other components of alcoholism: Clin. Exper. Res. **12**, 2–6 (1988).
11. Gerhard, R. E., Crecelius, E. A., Hudson, J. B.: Moonshine-related arsenic poisoning. Arch. Intern. Med. **140**, 211–213 (1980).
12. Hennekens, C. H., Willett, W., Rosner, B., Cole, D. S., Mayrent, S. L.: Effects of beer, wine, and liquor in coronary death. JAMA **242**, 1973–1974 (1979).
13. Karnovsky, M. J.: A formaldehyde-glutaraldehyde fixative of high osmolality for use in electron microscopy. J. Cell Biol. **27**, 137A (1965).
14. Kennedy, A., Dornan, J. D., King, R.: Fatal myocardial disease associated with industrial exposure to cobalt. Lancet **1**, 412–414 (1981).
15. Khetarpal, V. K., Volicer, L.: Alcohol and cardiovascular disorders. Drug Alcohol Depend. **7**, 1–30 (1981).

16. Linder, C. G., Friberg, L.: Handbook on the Toxicology of Metals. 2nd edition Friberg L., Nordberg G. F. and Vouk V, eds Elsevier Science Publishers. B., V., 1986, Chapter 9. pp. 211.
17. Maines, J. E., Aldinger, E. E.: Myocardial depression accompanying chronic consumption of alcohol. Am. Heart J. **73**, 55–63 (1967).
18. McDevitt, D. G., Nies, A. S.: Simultaneous measurement of cardiac output and its distribution with microspheres in the rat. Cardiovasc. Res. **10**, 494–498 (1976).
19. McDonald, J. T., Margen, S.: Wine versus ethanol in human nutrition. II. Fluid, sodium, and potassium balance. Am. J. Clin. Ntr. **32**, 817–822 (1979).
20. Mercier, G., Patry, G.: Quebec beer-drinkers' cardiomyopathy. Clinical signs and symptoms. Canad. Med. Ass. J. **97**, 884–888 (1967).
21. Morin, Y. L., Foley, A. R., Martineau, G., Roussel, J.: Quebec beer-drinkers' cardiomyopathy: forty-eight cases. Canad. Med. Ass. J. **97**, 881–883 (1967).
22. Morvai, V., Folly, G., Kardos, Gy.: Changes in cardiac function in the "preclinical" stage of alcoholic heart disease. Acta Med. Acad. Sci. Hung. **37**, 229–237 (1980).
23. Morvai, V., Ungváry, Gy., Varga, K., Albert, K., Folly, G.: Effect of long-term alcohol intake on the cardiovascular system of the rat. Acta Physiol. Acad. Sci. Hung. **54**, 369–379 (1979).
24. Murphree, H. B., Greenberg, L. A., Carroll, R. B.: Neuropharmacological effects of substances other than ethanol in alcoholic beverages. Fed. Proc. **26**, 1468–1473 (1967).
25. Potter, J. D., McMichael, A. J., Hartshorene, J. M.: Alcohol and beer consumption in relation to cancers of bowel and lung: an extended correlation analysis. J. Chronic Dis. **35**, 833–842 (1982).
26. Regan, T. J., Haider, B., Ahmed, S. S., Lyons, M. M., Oldewurtel, H. A., Ettinger, P. O.: Whiskey and the heart. Cardiovasc. Res. **2**, 165–176 (1977).
27. Regan, T. J., Khan, M. I., Ettinger, P. O., Haider, B., Lyons, M. M., Oldewurtel, H. A.: Myocardial function and lipid metabolism in the chronic alcoholic animal. J. Clin. Invest. **54**, 740–752 (1974).
28. Rubin, E.: Alcoholic myopathy in heart and skeletal muscle. N. Engl. J. Med. **301**, 28–33 (1979).
29. Singer, M. V., Eysselein, V., Goebel, H.: Beer and wine but nor whisky and pure ethanol do stimulate release of gastrin in humans. Digestion **26**, 73–79 (1983).
30. Vermel, A. E., Nikita, L. S., Barabanov, A. A., Druzhinin, V. I., Ivanova, L. A., Shatskaia, N. N.: Cobalt-induced cardiomyopathy in workers engaged in the manufacture of hard alloys. Ter. Arkh. **63**, 101–104 (1991) (in Russian).

*Acta Physiologica Hungarica, Volume 81 (3), pp. 263–267 (1993)*

# PHOSPHOLIPIDS OF HUMAN THYROID GLAND

H. STELMACH, P. MOŚKO, L. JAROSZEWICZ, Z. PIOTROWSKI,* Z. PUCHALSKI*

DEPARTMENT OF PHYSICAL CHEMISTRY AND SURGERY*, MEDICAL ACADEMY, BIALYSTOK, POLAND

Received August 10, 1992
Accepted December 16, 1992

The phospholipids from human thyroid have been identified and determined by two-dimensional chromatography.

The total amount of lipid phosphorus was higher in pathological thyroids (especially in thyroid with Graves' disease) as compared to postmortem tissue. Insignificant differences in percentage distribution of phospholipids between normal tissue and from patients with Graves' disease and nodular goiter were noted. An increase of phosphatidylcholine and a decrease of phosphatidylinositol and sphingomyelin in pathological thyroids were observed. Physiological role of phospholipids in thyroid gland is discussed.

**Keywords**: phospholipids, thyroid gland

Lipid compositional changes are known to regulate cellular metabolism, since altered phospholipid patterns exert a variety of effects on the membrane bound enzymes and membrane associated processes [11]. The phospholipid composition of mammalian tissues can be modified by the action of hormones and other agents as well as by metabolic disturbances [1, 10]. Thyrotropin stimulates both adenyl cyclase and inositol lipid signalling system in the thyroid [7, 12, 14]. Changes in cellular lipid metabolism initiated by receptor mediated activation of various phospholipases could play an important role both in normal and pathological thyroid gland. Studies on phospholipid composition was performed mostly in animal thyroid glands [8, 12]. Information regarding the phospholipids of human thyroid is still largely lacking. It was therefore of interest to investigate the phospholipid composition of normal human thyroid and the possible alterations of phospholipids in thyroid obtained from patients with nodular goiter and Graves' disease.

Correspondence should be addressed to
Leokadia JAROSZEWICZ
Medical Academy, Department of Physical Chemistry
15 230 Bialystok 8, ul. Mickiewicza 2A, Poland

*Akadémiai Kiadó, Budapest*

## Materials and methods

Human thyroid tissue was obtained from surgically treated patients aged of 31–53 years with nodular goiter and Graves' disease. Thyroid tissue was also obtained from postmortem individuals not suffering from any thyroid disease, within less than 10 hours after death. The present study was done with thyroid tissue obtained from female subjects only. The material was immediately frozen and stored at −20 °C until the time of assay.

Extraction and isolation of phospholipids.

Thyroids (1 g) were sliced and extracted in Potter homogenizer with 15 ml of cold chloroform-methanol (1:2, v/v), next 3 ml of 1N HCl were added and extraction was continuing for 10 min. Addition of HCl is necessary for a more complete extraction of the acidic phospholipids especially the polyphosphoinositides. The mixture was transferred to the stoppered tubes. 5 ml of chloroform to wash homogenizer and 4 ml of 2M KCl were added. Then the mixture was thoroughly shaken and centrifuged to separate two phases. The lower, chloroform phase was transferred to a test tube and the aqueous phase was washed once with 5 ml of chloroform and centrifuged. Chloroform lower phases were collected, mixed with equal volume of 0.1 N HCl, shaken briefly and centrifuged. After centrifugation chloroform phase was neutralized with $NH_3$ steam and evaporated in rotary vacuum evaporator to dryness. The dried residue was dissolved in 500 μl of benzene-ethanol mixture (4:1, v/v) and stored at −20 °C until use.

Individual phospholipids classes were separated by thin-layer chromatography (TLC). Lipid extracts were quantitatively applied onto 1% potassium oxalate impregnated silica gel 60 TLC plates (MERCK), activated for 90 min at 110–130 °C. Phospholipids were separated using the system chloroform : methanol: $NH_4OH$ : water (98 : 80 : 12.5 : 9 by vol.) in the first direction and chloroform : methanol : acetic acid : water (98 : 13 : 50 : 10 by vol.) in the second direction. Spots were coloured with iodine vapours. Phospholipids were identified on TLC plates by comparison with standards. Spots of phospholipids were scraped from plates into test tubes. Lipid phosphorus was estimated according to Bartlett [2] after digestion with 72% perchloric acid for 1.5 h at 165 °C.

Statistical analyses were performed using Student's *t*-test.

## Results and discussion

The phospholipids from human thyroids were obtained by acidulated extraction method and separated by two-dimensional thin-layer chromatography. A typical thin-layer chromatogram of human thyroid phospholipids is shown in Fig. 1. Twelve components are visible: spingomyelin (SPH), phosphatidylinositol (PI), phosphatidylcholine (PC), phosphatidylethanolamine (PE), phosphatic acid (PA), lysophosphatidylcholine (LPC), phosphatidylinositol-4-phosphate (PIP), non-polar lipids (NP) and three non identified components.

The quantitative composition of phospholipids presented in Table I shows differences in particular phospholipids levels between postmortem thyroids and from patients with nodular goiter and Graves' disease. The total lipid phosphorus in pathological thyroids (especially from patients with Graves' disease) is higher when compared to postmortem tissue.

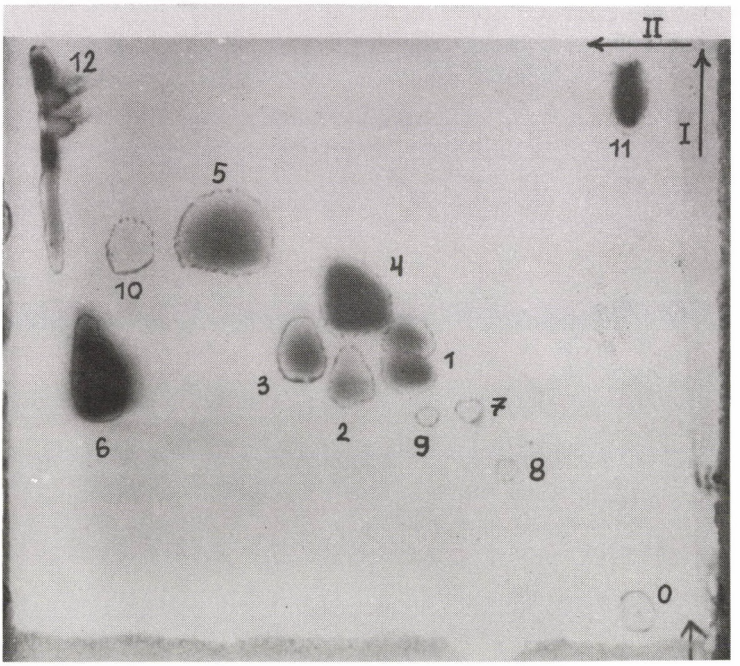


*Fig. 1.* Thin layer chromatogram of human thyroid lipid extract Spots were coloured with iodine vapour. o – origin, 1 – sphingomyelin, 2 – phosphatidylinositol, 3 – phosphatidylserine, 4 – phosphatidylcholine, 5 – phosphatidylethanolamine, 6 – phosphatic acid + hematin, 7 – lysophosphatidylcholine, 8 – phosphatidylinositol-4-phosphate, 9, 10, 11 – unidentified components, 12 – non-polar lipids

**Table I**

*Phospholipid composition of human thyroid*

| Phospholipid | Nodular goiter (n = 10) | Graves' disease (n = 7) | Postmortem (n = 5) |
|---|---|---|---|
| Sphingomyelin | 10.7 ± 3.6 | 10.9 ± 5.9 | 14.1 ± 2.0 |
| Phosphatidylcholine | 48.3 ± 6.0 | 45.7 ± 9.4 | 42.3 ± 4.8 |
| Phosphatidylserine | 8.1 ± 2.3 | 6.8 ± 3.4 | 10.8 ± 2.8 |
| Phosphatidylethanolamine | 19.5 ± 2.8 | 22.9 ± 8.9 | 21.7 ± 2.3 |
| Phosphatidylinositol | 5.9 ± 1.4 | 5.2 ± 3.3 | 6.2 ± 1.1 |
| Phosphatidylinositol-4-phosphate | 0.2 ± 0.1 | 0.2 ± 0.2 | 0.1 ± 0.1 |
| Phosphatic acid | 1.5 ± 1.0 | 1.5 ± 0.2 | 1.2 ± 0.5 |
| Lysophosphatidylcholine | 0.7 ± 0.5 | 0.8 ± 0.6 | 1.2 ± 0.5 |
| Other | 5.1 ± 1.8 | 6.0 ± 2.3 | 2.4 ± 1.0 |
| Total lipid phosphorus µg/1 g of tissue | 234.0 ± 40.0 | 316.0 ± 42.0* | 218.5 ± 29.5 |

*$p < 0.002$ vs postmortem

Value represent means ± S. E. and are expressed in mol per 100 mol of phosphorus recovered

The most abundant phospholipids in all human thyroids are PC and PE. The average of PC is higher in thyroids from patients with nodular goiter and Graves' disease, whereas PI, PS and SPH are lower. Considerable variations in the amount of particular phospholipids in thyroid from patients with Graves' disease were noted.

It is well documented that phospholipid metabolism in the thyroid is affected by TSH [8, 12, 13]. In rat thyroid cell line FRTL-5, TSH causes changes in membrane fluidity associated with a variation of the relative proportions of the major phospholipids [3]. Withdrawal of TSH from the medium of FRTL-5 cells caused a decrease in membrane fluidity, modest increase of total lipid-bound phosphorus, an increase of PC and decrease of PE and PI. The results of present study show that the changes in total lipid phosphorus and major phospholipid composition in pathological thyroids compared to postmortem tissue are similar to observed in experiments with FRTL-5 cells starved in TSH. An increase of total lipid phosphorus and PC and a decrease of PI in pathological thyroids were evident. The amount of PE was slightly lower only in thyroid from patients with nodular goiter. In the thyroids from patients with Graves' disease the average amount of PS was the lowest. It is known that PS by decarboxylation can give rise to PE, which next by methylation can be converted to PC. The interrelationship of these pathways in thyroid gland is unknown. The enzymes metabolizing these particular phospholipids may be involved in the response of cell to TSH. PS or other negatively charged phospholipids are in general essential for $(Na^+ + K^+)$-ATP-ase activity [11]. The decrease of PS in thyroid with Graves' disease may exert a considerable effect on the ATP-ase activity.

Recent investigations showed that certain hormones can stimulate PC synthesis and hydrolysis [6]. In our laboratory a decrease of thyroidal PC and simultaneously an increase of LPC in the presence of TSH were observed. This TSH-effect suggests the stimulation of phospholipase $A_2$ activity (unpublished data).

Sphingomyelin constituted about 14% of all phospholipids in postmortem thyroid and was lower in pathological thyroids. It was suggested that SPH plays stabilizing role in the maintenance of membrane structure and hence in the modulation of phospholipase activity [5]. A decrease of SPH level in pathological thyroids may also caused some effects on phospholipase activity.

Phosphatidylinositol represents above 6% of the lipid phosphorus in postmortem thyroids. No statistical differences in PI content in particular groups of patients were found, although average amount of PI was the lowest in thyroid from patients with Graves' disease. The most interesting feature of phosphatidylinositol metabolism is its special response in mammalian cells to wide variety of stimuli [3, 4]. Although most of the effects of TSH on thyroid gland are mediated via activation of adenyl cyclase – cyclic AMP system, existence of another signalling system involved inositol phospholipids with generation inositol phosphates and diacyloglycerol was

demonstrated [7, 8, 16]. Studies in our laboratory with [$^3$H]-inositol showed that TSH stimulated inositol phosphate formation in thyroid slices from patients with nodular goiter and Graves' disease [9]. It suggests that inositol phospholipids are also involved in the signalling system regulated by TSH in human thyroids.

Occasionally, the occurrence small additional spots of phospholipids on the chromatogram especially in thyroid extracts from patients with Graves' disease were observed. The identification of additional spots needs further investigations.

Insignificant changes in phospholipid composition may have an important role on the maintenance of thyroid gland in full functional activity.

## REFERENCES


1. Ansell, G. B., Spanner, S.: Phosphatidylserine, phosphatidylethanolamine and phosphatidylcholine. The effect of drug and other agents on metabolism. In Phospholipids (Editors J. W. Hawthorne and G. B. Ansell), pp. 33–41, Elsevier Biomedical Press Amsterdam; New York, Oxford, 1972.
2. Bartlett, G. R.: Phosphorus assay in column chromatography. J. Biol. Chem. **234**, 466–468 (1959).
3. Beguinot, F., Beguinot, L., Tramontano, D., Duilio, C., Formisano, S., Bifulco, M., Ambesi-Impiombato, F. S., Aloj, S. M.: Thyrotropin regulation of membrane lipid fluidity in the FRTL–5 thyroid line. J. Biol. Chem. **262**, 1575–1582 (1987).
4. Berridge, M. J.: Inositol trisphosphate and diacylglycerol as second messengers. Biochem. J. **220**, 345–369 (1984).
5. Dawson, R. M. C., Hemington, N., Irvine, R. F.: The inhibition of diacylglycerol-stimulated intracellular phospholipases by phospholipids with a phosphocholine-containing polar group. A possible physiological role for sphingomyelin. Biochem. J. **230**, 61–68 (1985).
6. Exton, J. H.: Signaling through phosphatidylcholine breakdown. J. Biol. Chem. **265**, 1–4 (1990).
7. Field, J. B., Ealey, P. A., Marshall, N. J., Cockcroft, S.: Thyroid-stimulating Hormone stimulates increase in inositol phosphates as well as cyclic AMP in the FRTL–5 thyroid cell line. Biochem. J. **247**, 519–524 (1987).
8. Igarashi, Y., Kondo, Y.: Acute effect of thyrotropin on phosphatidylinositol degradation and transient accumulation of diacylglycerol in isolated thyroid follicles. Biochim. Biophys. Res. Commun. **97**, 759–765 (1980).
9. Jaroszewicz, L., Zarzycki, W., Kinalska, I., Mośko, P., Świetochowska, K., Piotrowski, Z.: Effect of thyrotropin on inositol phospholipids hydrolysis in human thyroid. An International Symposium "Genomic and non-genomic actions of hormones in reproduction" Mragowo, Poland, 1991.
10. Kuo, J. F.: Phospholipids and cellular regulation. (1985) vols 1 & 2, CRP Press, Boca Raton.
11. Sanderman, H.: Regulation of membrane enzymes by lipids. Biochim. Biophys. Acta, **515**, 209–237 (1978).
12. Scott, T. W., Freinkel, N., Klein, J., Nitzan, M.: Metabolism of phospholipids, neutral lipids and carbohydrates in dispersed porcine thyroid cells: comparative effect of pituitary thyrotropin and dibutynyl-3'-S'-adenosine monophosphate on the turnover of individual phospholipids in isolated cells and slices from pig thyroid. Endocrinology **87**, 854–863 (1970).
13. Scott, T. W., Mills, S. C., Freinkel, N.: The mechanism of thyrotropin action in reaction to lipid metabolism in thyroid tissue. Biochem. J. **109**, 328–332 (1968).
14. Taguchi, M., Field, J. B.: Effects of thyroid-stimulating hormone, carbachol, norepinephrine and adenosine 3'5'-monophosphate on polyphosphatidylinositol phosphate hydrolysis in dog thyroid slices. Endocrinology **123**, 2019–2026 (1988).

*Acta Physiologica Hungarica, Volume 81 (3), pp. 269–275 (1993)*

# RESPONSE OF SERUM CALCIUM TO ADMINISTRATION OF 1,25-DIHYDROXYVITAMIN $D_3$ IN THE FRESHWATER CARP *CYPRINUS CARPIO* MAINTAINED EITHER IN ARTIFICIAL FRESHWATER, CALCIUM-RICH FRESHWATER OR CALCIUM-DEFICIENT FRESHWATER

S. K. SRIVASTAV, R. JAISWAL, A. K. SRIVASTAV

DEPARTMENT OF ZOOLOGY, UNIVERSITY OF GORAKHPUR, GORAKHPUR, INDIA

Received September 15, 1992
Accepted November 9, 1992

Freshwater carps (*Cyprinus carpio*) were injected daily intraperitoneally either with vehicle (0.1 ml 95% ethanol/100 gm body wt), or $1,25(OH)_2D_3$ (5 IU/100 gm body wt) and maintained either in artificial-freshwater, calcium-rich freshwater or calcium-deficient freshwater for 15 days. The specimens were sacrificed on day 1, 3, 5, 10 and 15 after initiation of the experiment and serum calcium levels were analysed.

(i) Artificial freshwater: Serum calcium level of $1,25(OH)_2D_3$ treated specimens increases progressively from day 3 to day 5. Thereafter, on day 10 and day 15 the level becomes normocalcemic.

(ii) Calcium-rich freshwater: In vehicle-injected fish the serum calcium level increases progressively from day 3 to day 10. On day 15 the level becomes normocalcemic.
In $1,25(OH)_2D_3$-treated animals the serum calcium levels increase significantly from day 3 to day 5. The serum calcium level exhibits a slight fall on day 10 and day 15 although the value is still hypercalcemic.

(iii) Calcium-deficient freshwater: In vehicle-injected specimens the serum calcium level shows a progressive hypocalcemia from day 3 to day 5. Thereafter the level increases thus resulting in hypercalcemia on day 15.
In the $1,25(OH)_2D_3$ treated specimens there is a significant increase in the serum calcium level from day 3 to day 10. On day 15 the level depicts a slight decrease.

**Keywords**: calcium, 1,25-Dihydroxyvitamin $D_3$, calcium-rich freshwater, calcium-deficient freshwater

Few studies have been performed to demonstrate the physiological action of $1,25(OH)_2D_3$ in teleosts. These reports clearly show that 1,25 dihydroxyvitamin $D_3$ ($1,25(OH)_2D_3$) administration causes – (i) hypercalcemia [5, 14, 17] and (ii) increased intestinal uptake [3, 7, 16].

Correspondence should be addressed to
Ajai K. SRIVASTAV
Department of Zoology, University of Gorakhpur
Gorakhpur – 273 009, India

*Akadémiai Kiadó, Budapest*

It has been suggested that direct absorption of $Ca^{++}$ from the water by the gills is the predominant route for $Ca^{++}$ uptake in freshwater fish [1, 2, 10]. Formerly, acellular bone has been considered to be the metabolically inert, thus unable to contribute to the calcium homeostasis in fish. Observations of Fleming [6], Yamane et al. [24] and Takagi et al. [19] reveal that fish can mobilize calcium from internal sources such as bones, scales or soft tissues. Pang and Pang [12] believed that it is possible that the environmental calcium provides a continuous source for normal maintenance of internal homeostasis and that bone serves as a source when excessive demand is experienced.

Thus, it can be concluded that fish can obtain calcium either from external (food and aquatic environment) or internal (bones, scales and soft tissues) sources. The aim of the present study was to evaluate whether $1,25(OH)_2D_3$ can elevate the serum calcium levels of the freshwater carp *Cyprinus carpio* when this ion is not available to the fish from the external source (food and environment). To deprive the fish the availability of calcium from external sources we have not fed the fish and maintained them in calcium-deficient freshwater.

## Materials and methods

Adult specimens (both sexes) of *Cyprinus carpio* (body wt 100–125 g) were procured and acclimatized to the laboratory conditions for one week prior to use. An initial sampling of blood (from six specimens) was taken prior to the start of the experiment (zero hour). The fish were injected daily for 15 days intraperitoneally with 5 IU of $1,25(OH)_2D_3$ and were maintained in three artificial media i.e. artificial freshwater, calcium-rich freshwater and calcium-deficient freshwater. Simultaneously, a control group was injected daily with vehicle (.1 ml/100 gm body wt) and maintained in these three artificial media.

$1,25(OH)_2D_3$ used was dissolved in 95% ethanol. Three different artificial media i.e. artificial freshwater, calcium-rich freshwater and calcium-deficient freshwater were prepared as follows:

(i) Artificial freshwater: Distilled water containing (in m mol/litre): NaCl 2.10; $Na_2SO_4$ 0.45; KCl 0.06; $CaCl_2$ 0.8; $MgCl_2$ 0.20. pH of the solution was adjusted to 7.6 with $NaHCO_3$.
(ii) Calcium-deficient freshwater: Same as above without $CaCl_2$.
(iii) Calcium-rich freshwater: 13.4 m mol $CaCl_2$/litre is added to the artificial freshwater.

Six fish from each group were anaesthetized with MS 222 and blood samples were taken 4 h after the last injection by sectioning the caudal peduncle on day 1, 3, 5, 10 and 15 following the treatment. The sera were separated and analyzed for calcium according to Trinder [20] method.

Fish were not fed during the experiment. Student's *t*-test was used to determine statistical significance. In all studies, the experimental group was compared to its specific time control group.

## Results

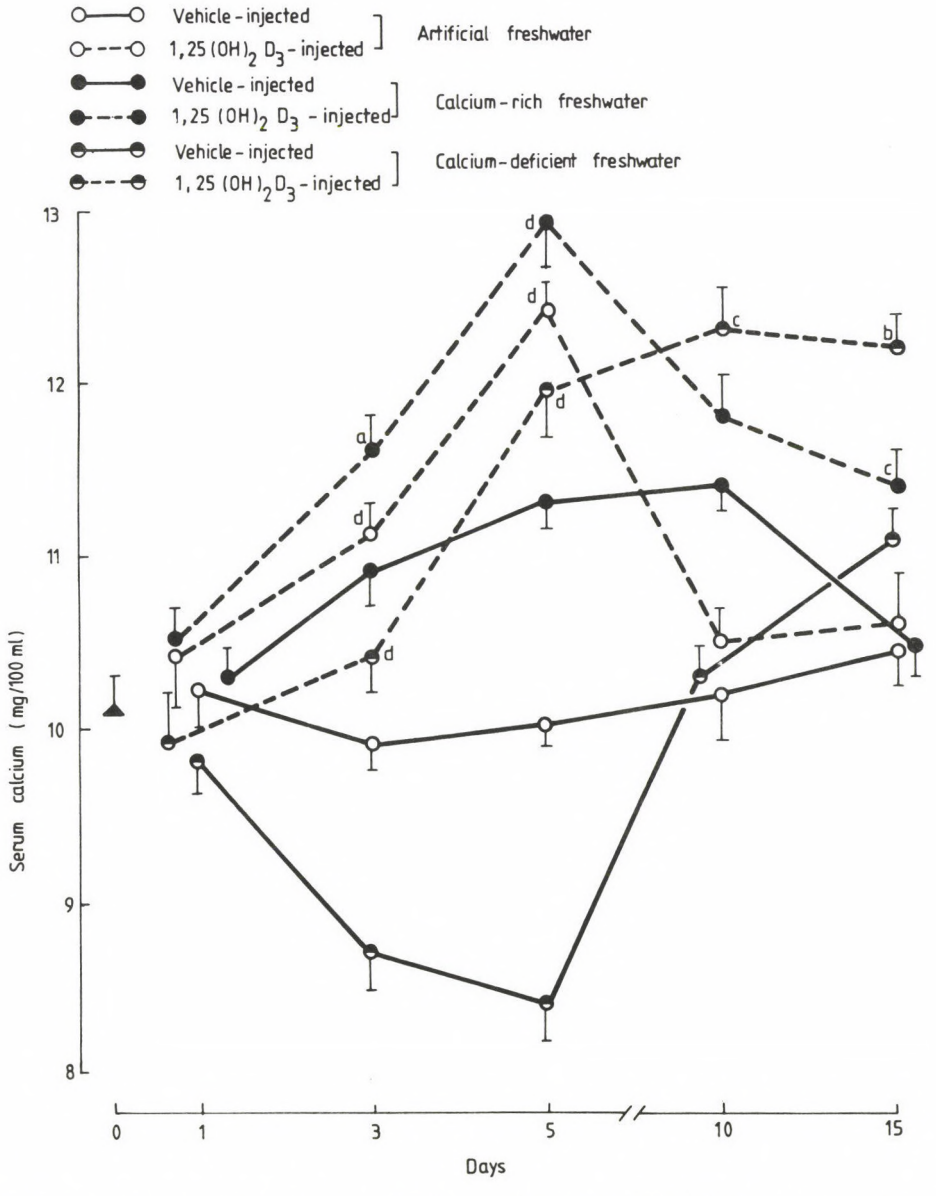


*Fig. 1.* Changes in the serum calcium levels of *Cyprinus carpio* kept either in artificial freshwater, calcium-rich freshwater or calcium-deficient freshwater and treated with vehicle or 1,25 $(OH)_2D_3$. Each value represents mean ± SE of six specimens. a, b, c, and d indicate significant differences from the vehicle injected group: $P < 0.025$, $P < 0.01$, $P < 0.005$ and $P < 0.001$, respectively

(i) Artificial freshwater:

The serum calcium level of vehicle-injected fish exhibits almost no change throughout the experiment (Fig. 1).

The serum calcium level remains unaffected on day 1 following $1,25(OH)_2D_3$ treatment. Thereafter it increases progressively from day 3 to 5. The value becomes normocalcemic after day 10 and 15.

(ii) Calcium-rich freshwater:

In vehicle-injected fish the serum calcium level is elevated on days 3, 5 and 10. At day 15 the value tends to become normal.

Following $1,25(OH)_2D_3$ treatment there is almost no change in the serum calcium level on day 1. The value increases progressively from day 3 to day 5, thereafter it declines on day 10 and 15, but the value is still hypercalcemic (Fig. 1).

(iii) Calcium-deficient freshwater:

The serum calcium level of vehicle-injected specimens exhibit a progressive decrease from day 3 to day 5. Thereafter, the serum calcium level exhibits an increase thus resulting into hypercalcemia on day 15.

Serum calcium levels of $1,25(OH)_2D_3$ treated specimens remain unaffected on day 1. The value exhibit a progressive increase from day 3 to day 10. Thereafter, the level exhibits a slight fall on day 15 although it is still hypercalcemic (Fig. 1).

## Discussion

Administration of $1,25(OH)_2D_3$ induced a significant hypercalcemia in *Cyprinus carpio* which were maintained in artificial freshwater. The hormone causes a greater effect when the fish were maintained in calcium-rich freshwater. This response of $1,25(OH)_2D_3$ in *Cyprinus carpio* derives support from the earlier studies of Swarup and Srivastav [18] (*Clarias batrachus*), Srivastav [13] (*Amphipnous cuchia*), Swarup et al. [17] (*Clarias batrachus*), Fenwick et al. [5] (*Anguilla rostrata*), Srivastav and Srivastav [14] (*Clarias batrachus*), Srivastav and Singh [15] (*Heteropneustes fossilis*), who have observed a similar response of serum calcium in certain fishes after administration of vitamin D and its metabolites and/or maintenance in calcium-rich environment. Moreover, injection of 0.68 M $CaCl_2$ solution (10 μl/100 gm fish/day) is effective in increasing the plasma calcium levels of trout and eel (Lafeber et al. [11]). Keeping in view the negative effects of administration of vitamin D or its metabolites on plasma calcium levels of marine fishes, Sundell and Bjornsson [16] have questioned the necessity of an endocrine system to increase the $Ca^{++}$ uptake in marine teleost since they are exposed to large concentration gradient directed inward.

In the foregoing study we have observed hypercalcemia in the fish injected with $1,25(OH)_2D_3$ and maintained in calcium-deficient freshwater. There exists a single report which describes that vitamin $D_3$ induces hypercalcemia in the fish *Heteropneustes fossilis* kept in calcium-deficient media [15]. The hypercalcemia observed in *Cyprinus carpio* could not be linked to the calcium absorption at the intestinal mucosa as the fish were unfed and calcium was not available in the medium.

The observed hypercalcemia in *Cyprinus carpio* after $1,25(OH)_2D_3$ administration may be due to the increased resorption of bone and/or mobilization of calcium from scales or soft tissues.

The serum calcium level exhibits a decline from day 3 to day 5 in *Cyprinus carpio* injected with vehicle and kept in calcium-deficient freshwater. Wendelaar, Bonga et al. [21] have also reported a significant hypocalcemia in tilapia after 5 days of its transference to low ambient calcium. This response may be due to the increased efflux of $Ca^{++}$ through the gill. It has been suggested that low calcium concentration in the ambient water of tilapia would allow intercellular $Ca^{++}$ to diffuse out of the animal [8]. These authors have further explained that branchial efflux routes of calcium following paracellular routes could be increased as a result of lower ambient $Ca^{++}$. The observed hypocalcemia in *Cyprinus carpio* maintained in calcium-deficient water also derives support from the studies of Wendelaar Bonga and Van der Meij [23], who have noticed increased integumental water permeability at low ambient calcium. This increased water uptake at low ambient calcium may increase urine production which leads to extra $Ca^{++}$ loss from the body [4].

In calcium-deficient freshwater the serum calcium levels of vehicle injected *Cyprinus carpio* were restored on day 10 and elevated after day 15. An elevation of plasma calcium level after acclimation of the fish to low ambient calcium has been reported by Wendelaar Bonga et al. [22] and Flik et al. [8]. According to Wendelaar Bonga et al. (1984) this restoration of plasma calcium levels is most probably mediated by an increased production of prolactin. Prolactin has been reported to stimulate uptake of $Ca^{++}$ from the water in intact tilapia [9]. In this study $Ca^{++}$ was not available in the medium therefore the restoration of calcium can possibly be due to bone demineralization and/or increased mobilization from the scales and soft tissues. As our study lacks determination of bone and scale calcium it is not possible at present for us to emphasize that bone/scale demineralization occurred in *Cyprinus carpio*.

## Acknowledgements

CSIR, New Delhi is acknowledged for financial assistance for providing Research Associateship to the first author (SKS).

## REFERENCES


1. Berg, A.: Studies on the metabolism of calcium and strontium in fresh-water fish. I. Relative contribution of direct and intestinal absorption. Mem. Ist. Ital. Idrobiol. **23**, 161–196 (1968).
2. Berg, A.: Studies on the metabolism of calcium and strontium in freshwater fish. II. Relative contribution of direct and intestinal absorption in growth conditions. Mem. Ist. Ital. Idrobiol. **26**, 241–255 (1970).
3. Chartier, M. M., Milet, C., Martelly, E., Lopez, E., Warrot, S.: Stimulation per la vitamine $D_3$ et le 1,25-hydroxyvitamine $D_3$ de l'absorption intestinale du calcium chez l'anguille (*Anguilla anguilla* L.). J. Physiol. (Paris). **75**, 275–282 (1979).
4. Fenwick, J. C.: The renal handling of calcium and renal $Ca^{2+}$ ($Mg^{2+}$) – activated adenosinetriphosphatase activity in freshwater and seawater – acclimated North American eels (*Anguilla rostrata* Le sueue). Can. J. Zool. **59**, 478–485 (1981).
5. Fenwick, J. C., Smith, K., Smith, J., Flik, G.: Effect of various vitamin – D analogs on plasma calcium and phosphorus and intestinal calcium absorption in fed and unfed American eels, *Anguilla rostrata*. Gen. Comp. Endocrinol. **55**, 398–404 (1984).
6. Fleming, W. R.: Calcium metabolism of teleost. Amer. Zool. 7, 835–842 (1967).
7. Flik, G., Reijntjens, F. M. J., Stikklebroeck, J., Fenwick, J. C.: 1,25-vitamin $D_3$ and calcium transport in the gut of tilapia (*Sarotherodon mossambicus*). J. Endocrinol. **94**, 40 (1982).
8. Flik, G., Fenwick, J. C., Kolar, Z., Mayer-Gostan, N., Wendelaar, Bonga, S. E.: Effects of low ambient calcium levels on whole body $Ca^{2+}$ flux rates and internal calcium pools in the freshwater cichlid teleost, *Oreochromis mossambicus*. J. Exp. Biol. **120**, 249–264 (1986a).
9. Flik, G., Fenwick, J. C., Kolar, Z., Mayer-Gostan, N., Wendelaar Bonga, S. E.: Effects of ovine prolactin on calcium uptake and distribution in the freshwater cichlid teleost fish, *Oreochromis mossambicus*. Am. J. Physiol. **250**, 161–166 (1986b).
10. Hughes, G. M.: Morphometric of fish grills. Respir. Physiol. **14**, 1–25 (1972).
11. Lafeber, F. P. J. G., Hanssen, R. G. J. M., Choy, Y. M., Flik, G., Herrmann-Erlee, M. P. M., Pang, P. K. T., Wendelaar Bonga S. E.: Identification of hypocalcin (teleocalcin) isolated from trout Stannius corpuscles. Gen. Comp. Endocrinol. **69**, 19–30 (1988).
12. Pang, P. K. T., Pang, R. K.: Hormones and calcium regulation in *Fundulus heteroclitus*. Amer. Zool. **26**, 225–234 (1986).
13. Srivastav Ajai K.: Calcemic responses in the freshwater mud eel, *Amphipnous cuchia*, to vitamin $D_3$ administration. J. Fish Biol. **23**, 301–303 (1983).
14. Srivastav Ajai K., Srivastav S. P.: Corpuscles of Stannius of *Clarias batrachus* in response to 1,25 dihydroxyvitamin $D_3$ administration. Zool. Sci. 5, 197–200 (1988).
15. Srivastav, A. K., Singh, S.: Effect of vitamin $D_3$ administration on the serum calcium and inorganic phosphate levels of the freshwater catfish, *Heteropneustes fossilis* maintained in artificial freshwater, calcium-rich freshwater and calcium-deficient freshwater. Gen. Comp. Endocrinol. In press (1992).
16. Sundell, K., Bjornsson, B.: Th. Effects of vitamin $D_3$, 25(OH) vitamin $D_3$, 24 25$(OH)_2$ vitamin $D_3$ and 1,25$(OH)_2$ vitamin $D_3$ on the *in vitro* intestinal calcium absorption in the marine teleost, Atlantic cod (*Gadus morhua*). Gen. Comp. Endocrinol. **78**, 74–79 (1990).
17. Swarup, K., Norman, A. W., Srivastav, A. K., Srivastav, S. P.: Dose dependent vitamin $D_3$ and 1,25 dihydroxycholecalciferol induced hypercalcemia and hyperphosphatemia in male catfish *Clarias batrachus*. Comp. Biochem. Physiol. **78**, 553–555 (1984).
18. Swarup, K., Srivastav, S. P.: Vitamin $D_3$ induced hypercalcemia in male catfish, *Clarias batrachus*. Gen. Comp. Endocrinol. **46**, 271–274 (1982).
19. Takagi, Y., Hirano, T., Yamada, J.: *In vitro* measurements of calcium influx into isolated goldfish scales in reference to the effects of putative fish calcemic hormone. Zool. Sci. **6**, 83–89 (1989).
20. Trinder, P.: Colorimetric microdetermination of calcium in serum. Analyst **85**, 889–894 (1960).

21. Wendelaar-Bonga, S. E., Flik, G., Fenwick, J. C.: Prolactin and calcium metabolism in fish: effects on plasma calcium and high-affinity $Ca^{2+}$-ATPase in gills. In "Endocrine Control of Bone and Calcium Metabolism". (D. V. Cohn, J. T. Potts Jr. and T. Fujita, Eds.), pp. 188–190, Elsevier Science Publishers B. V.
22. Wendelaar, Bonga, S. E., Flik, G., Lowik, C. W., Van Eys C. J.: Environmental control of prolactin secretion in the teleost fish *Oreochromis* (formerly *Sarotherodon*) *mossambicus*. Gen. Comp. Endocrinol. **57**, 352–359 (1985).
23. Wendelaar, Bonga, S. E., Van der Meij J. C. A.: Effect of ambient osmolarity and calcium on prolactin cell activity and osmotic water permeability of the gills in the teleost *Sarotherodon mossambicus*. Gen. Comp. Endocrinol. **43**, 432–442 (1981).
24. Yamane, S., Iguchi, M., Ogasawara, T., Nakamura, Y.: Effects of blockage of exogenous calcium and phosphorus on the calcium regulatory systems in goldfish. Comp. Biochem. Physiol. **A 72**, 709–713 (1982).

*Acta Physiologica Hungarica, Volume 81 (3), pp. 277–288 (1993)*

# DETECTION OF EARLY MEMBRANE AND NUCLEAR ALTERATIONS OF THYMOCYTES UPON *IN VITRO* IONIZING IRRADIATION

Tamara KUBASOVA, A. B. CHUKHLOVIN,* Z. SOMOSY, S. D. IVANOV,*
G. J. KÖTELES, E. A. ZHERBIN,* K. P. HANSON*

"FRÉDÉRIC JOLIOT-CURIE" NATIONAL RESEARCH INSTITUTE FOR RADIOBIOLOGY AND RADIOHYGIENE, BUDAPEST, HUNGARY AND
* CENTRAL RESEARCH INSTITUTE OF ROENTGENOLOGY AND RADIOLOGY, ST. PETERSBURG, RUSSIA

Received October 1, 1992
Accepted November 18, 1992

Some membrane and nuclear parameters of rat thymocytes were studied after *in vitro* X- or gamma-irradiation with doses of 0.5, 1, 2 and 4 Gy followed by incubation for 0.5 to 4 hours at 21–22 °C.

Early (within the first 2 hours) distinct functional changes of plasma membranes, i.e. increase in Con A binding, autologous rosette-forming capacity, Alcian Blue-induced agglutination, and a decrease in amount of surface negative charges were observed. Meanwhile, the doses applied did not influence the DNA content, and the proportion of pyknotic nuclei did not grossly differ from that of the time-matched controls. However, an increase in AT-rich DNA component was noted.

The radiation-induced changes proved to be transient and dose-dependent. In the whole cell populations no irreversible, death-associated events could be detected under the given experimental conditions.

**Keywords**: thymocytes, ionizing radiation, cell membrane surface charges, nuclear parameter, DNA

High sensitivity of lymphoid cells to various stress-factors of organism and environment is a well-known phenomenon. In particular, accelerated interphase death of thymic lymphoid cells is a suitable experimental model for studies of radiation effects as well as immunotoxicity of certain steroid hormones and various lympholytic agents [1, 8, 9]. Along with evidence of nuclear pathology some early

Correspondence should be addressed to
Tamara KUBASOVA
"Frédéric Joliot-Curie" National Research Institute for Radiobiology and Radiohygiene
1775 Budafok 1, P.O. Box 101, Anna u. 5., Hungary

*Akadémiai Kiadó, Budapest*

irreversible losses of specific membrane receptors from the surface of irradiated lymphocytes were observed [13].

Some transient changes of cell surfaces after irradiation deserve special interest because they proved to be characteristic to both radiosensitive and resistant cell species. For instance, similar alterations of Concanavalin A (Con A)-binding sites have been revealed for blood lymphocytes, erythrocytes and platelets after *in vitro* or *in vivo* radiation treatment [14, 15]. Therefore, additional studies with lymphoid cells were carried out to reveal other reversible features of membrane damage shortly after irradiation. Because of rapid development of lethal events in thymic populations, such observations were more likely to be performed at 'suboptimal' regime of incubation (i.e. at decreased temperature) leading to retardation of death-associated pathology.

The aim of present work was a complex study of cell surface and DNA changes of *in vitro* irradiated rat thymocytes to provide data on an apparent reversibility of several radiation-induced alterations at the levels of membrane and nuclear structures.

## Materials and methods

*Cell preparation and irradiations*

Wistar male rats of 130–150 g were used. For autologous rosetting, whole blood was collected into glass tubes with heparin. Preparation of thymic lymphocytes and purification of red blood cells were performed as previously described [21]. Thymocytes were adjusted to a final concentration of $5 \times 10^6$ cells per ml in Parker medium.

Gamma-irradiation of cell suspensions was performed in glass tubes, with $^{60}Co$ source at a dose-rate of 0.52 Gy per min. For treatment with X-rays, the samples were placed into Teflon tubes. Irradiation was carried out with a THX-250 machine (Medicor, Hungary) at a dose-rate of 0.287 Gy per min, 200 kV, 1 mm Cu, SSD (subject-source distance) 60 cm. The exposures were measured by a calibrated ionization chamber (Farmer dose meter Type 2502/3, 0.6 $cm^3$ ionization chamber). For calculation of the absorbed doses in water, conversion factors and the values of HVL (half value layer) were used. RBE (relative biological effect) for gamma-rays was assumed as 0.92, based on the criteria of radiation-induced nuclear pyknosis. In the experiments, the effects of 0.5, 1, 2 and 4 Gy were studied.

Incubation of irradiated cell suspensions proceeded at 21–22 °C, or in some cases, at 37 °C. The separate samples were taken for analysis at various time-points of 0.5 to 4.0 hours after radiation treatment.

*Chemicals*

Acridine Orange was obtained from Reachim, Moscow, Alcian Blue (AB) was obtained from Loba Chemie, Austria. Triciated concanavalin A (3H-ConA) was purchased from New England Nuclear, Boston. Cationized ferritin (CF) originated from Sigma. Glutaraldehyde (Merck, Germany) was obtained as 25 per cent solution; 4'6-diamidino-2-phenylindole and ethidium bromide were obtained from Serva, Germany.

*Cell viability assays*

Supravital staining of cells was performed by Trypan Blue at 0.3 per cent final concentration of the dye. The incidence of pyknotic nuclei was revealed by the luminescence method using Acridine Orange staining [21].

*$^3$H-Con A binding to the thymocyte surfaces*

The lectin-binding procedure was performed in glass tubes at room temperature for 10 minutes. The binding system of 0.2 ml volume consisted of 0.1 ml of thymocyte suspension ($1.10^6$ cells) and 0.1 ml of $^3$H-ConA solution (1 μCi/ml). At the end of incubation, the unbound ligand was diluted and washed out with physiological saline at 4 °C by centrifugation repeated 3 times.

*Autologous rosetting and Alcian Blue-induced agglutination*

Estimation of autologous rosette-forming cells (ARFC) was performed, as described earlier [21]. Close contact of thymocytes with two or more red blood cells (RBC) was registered as ARFC.

Alcian Blue (AB)-induced agglutination of thymocytes was carried out according to method already described [10]. At the endpoint of incubation, 0.2 ml of isotonic AB solution (0.1 per cent) was added to 0.8 ml samples of thymic suspensions ($5.10^6$ cells). The probes were rapidly spun down at 180 g for 5 min. After vigorous resuspension, the non-agglutinated ('free') cells were counted in Bürker chamber. The data were expressed as cell counts per chamber. Specificity of the assay was checked with heparin (20–40 IU/ml) which inhibited AB-agglutination by approximately 90 per cent.

*Binding of cationized ferritin (CF)*

The cell membrane conditions of unirradiated thymocytes and after irradiation with various doses were studied with CF. Thymocytes were stabilized by glutaraldehyde at 15 and 60 minutes of the post-irradiation period. The final concentration of glutaraldehyde was 0.025 percent, and the fixation time lasted for 30 minutes. This procedure was followed by the centrifugation of cells, then thymocyte smears were prepared on glass surfaces and fixed by 2.5 per cent glutaraldehyde. For visualization of the negative charges on the cell surfaces, the smears were treated by 0.3 mg/ml of CF in phosphate-buffered saline (PBS) at room temperature for 5 minutes, then washed in PBS and embedded. Transmission electron microscopic (TEM) procedure was performed as earlier described [19].

*Determination of DNA parameters*

Cell suspensions of 0.02 ml volumes were treated with 0.2 ml of lysing solution [6]. Total amount of DNA in resulting nucleoids was determined with ethidium bromide (3 μg/ml) using Hitachi spectrofluorimeter (model 650–40). The wavelengths for excitation and emission were 510 and 590 nm, respectively. The contents of AT-rich DNA regions were evaluated with 4'6-diamidino-2-phenylindole (DAPI). This compound sufficiently increases its fluorescence upon interactions with 3–4 AT-pairs of DNA, thus allowing to apply DAPI as a specific label for quantitative assays of these regions in the genome [7, 16, 17]. The procedure already published was used in the present work [12]. Excitation and emission wavelengths were 350 and 450 nm, respectively [4]. Cold phenol-extracted, sonicated DNA samples from rat thymus were tested as a standard. All measurements were made, at least, in duplicate. The data were statistically evaluated by Student's test [2].

## Results

*Cell parameters in the unirradiated controls*

As shown in the Table I, incubation of thymocytes at 21 – 22 °C for 4 hours lead to alteration of some cellular indices, while others remained unchanged. Thus, the proportion of viable (Trypan Blue-excluding) cells was found to be 81 to 85 per cent. At the same time, the unirradiated populations exhibited slight but significant increase in the numbers of pyknotic nuclei, gradual enhancement of autologous rosetting, along with increased AB-agglutinability. As for $^3$H-ConA binding, a slight tendency of increased binding of this lectin to cell surface (about 13 per cent) was observed within 4 hours of incubation.

**Table I**

*Time-dependent changes in the unirradiation thymic cell suspensions*

| Parameters assayed | Time of incubation (hours) | | | | |
|---|---|---|---|---|---|
| | 0.5 | 1.0 | 2.0 | 4.0 | |
| Incubation t °C | 21 – 22 | 21 – 22 | 21 – 22 | 21 – 22 | 37 |
| Viable cells (per cent) | 81.0 ± 3.8 | 83.0 ± 5.0 | 85.0 ± 6.3 | 81.4 ± 6.8 | 81.6 ± 1.3 |
| Pyknotic cells (per cent) | 1.2 ± 0.3 | 1.3 ± 0.4 | 1.7 ± 0.2 | 4.1 ± 0.4* | 23.5 ± 1.9** |
| ARFC (per cent) | 24.0 ± 3.1 | 27.2 ± 4.4 | 37.9 ± 4.6* | 34.0 ± 3.8* | 12.8 ± 2.6** |
| Alcian Blue-non-agglutinable cells (abs. number per chamber) | 1680 ± 45 | 1755 ± 66 | 1515 ± 99* | 1365 ± 35* | 1210 ± 124** |
| $^3$H-ConA binding (dmp per $10^6$ cells) | 7940 ± 508*** | ND | MD | 9113 ± 642*** | ND |
| Total DNA content (arb. units) | 33.4 ± 2.1 | 33.1 ± 2.5 | 35.2 ± 1.3 | 36.8 ± 3.8 | 36.9 ± 11.3 |
| AT-rich (DAPI-binding) DNA content (arb. units) | 36.1 ± 3.4 | 44.0 ± 6.9 | 46.4 ± 2.6 | 41.0 ± 4.7 | 42.2 ± 11.0 |

* The difference from the '0.5 h' point is significant by $p < 0.05$;

** The difference from the '4.0 h, 21 °C' point is significant by $p < 0.01$.

*** Mean values ± SE of 5 separate experiments, with 4 parallels each; ND – not done

Practically, no changes in total DNA contents were observed. A marginal increase of AT-rich fraction of DNA was not statistically significant, confirming the absence of gross changes in the whole thymic population at suboptimal temperature regime.

Meanwhile, the incubation of thymocytes at physiological temperature (37 °C) for 4 hours revealed more pronounced alterations concerning decreased spontaneous

survival of cells. Percentage of pyknotic nuclei at this time became rather high, along with sufficient decrease in autologous rosetting (see the right graph of Table I). However, other markers of cellular state did not differ significantly from the values obtained at 21–22 °C after 4 hours of incubation. Hence, a conclusion might be drawn that suboptimal temperature of incubation is an important factor which inhibits and/or retards some basic features of interphase death of thymocytes (i.e. nuclear pyknosis). Therefore, such experimental regime permits to detect the very early cellular changes induced by external influence.

*Surface changes of irradiated thymocytes*

1. *$^3$H-ConA binding*

Upon the effect of X-irradiation, the amount of lectin bound to the thymocyte plasma membranes changed depending on doses and post-irradiation time (Fig. 1). All doses applied caused an early increase in lectin binding within the first 2 hours, while later (at 4 hours) the values returned to the control level. The most pronounced effect was observed with 1 Gy dose.

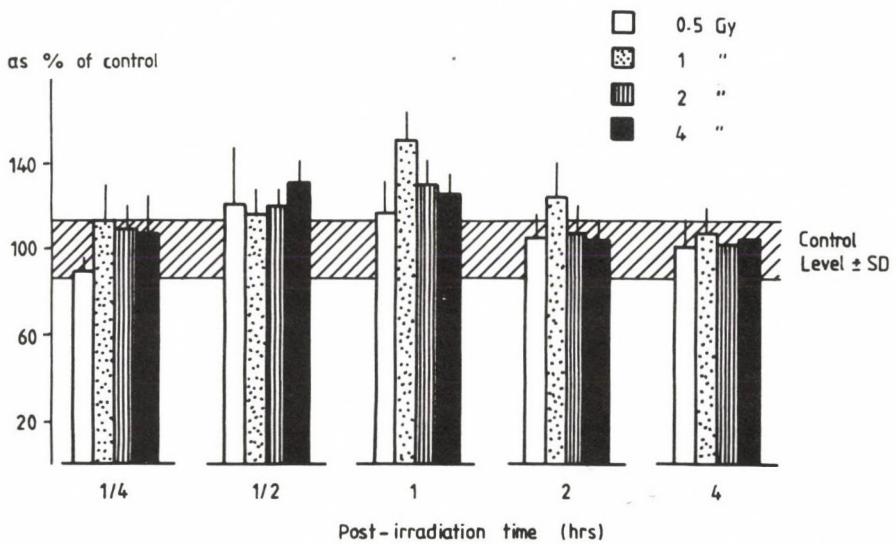


*Fig. 1.* $^3$H-ConA binding to the plasma membranes or rat thymocytes at various time-points after the effect of X-irradiation expressed as percentage of the control (average values ± SD)

2. *Alcian Blue-induced agglutination*

The proportion of AB-agglutinable cells in the control thymic suspensions was rather high (from 62 to 68 per cent). Therefore, we studied the post-irradiation changes in the 'free' cell counts because this population diminished during incubations. The number of AB-non-agglutinable thymocytes tended to drop below the control time-matched values at 1 and 2 hours following irradiation (Fig. 2). The most pronounced decrease was found with doses of 2 and 4 Gy. At the end of incubation, this parameter returned to the control.

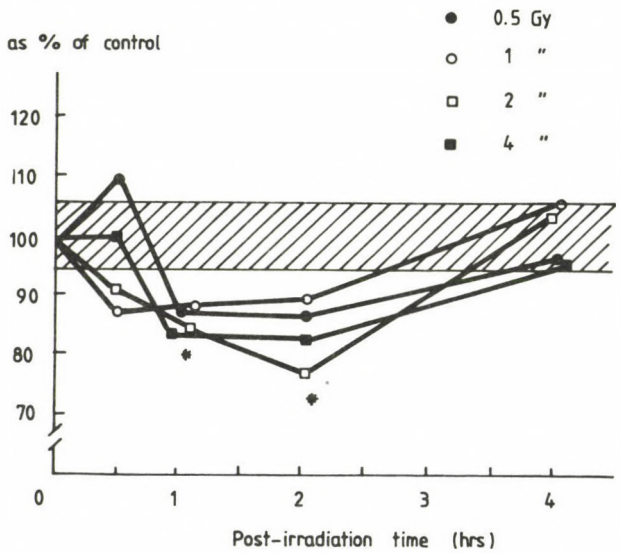


*Fig. 2.* Changes in Alcian Blue-induced agglutination of rat thymocytes at various time-points after gamma-irradiation. Abscisse: time of incubation, hrs. Ordinate: numer of 'free' (non-agglutinated) cells, per cent of time-matched controls. Horizontal bars indicate the scattering interval in controls, asterisks represent statistical significance at level of $p < 0.05$

3. *Autologous erythrocyte rosetting*

The numbers of ARFC changed significantly in the course of time following irradiation. Rosette-forming ability increased at 1 hour of incubation, after gamma-irradiation of 1 or 2 Gy (Fig. 3). It was followed by decrease of ARFC contents at 2 hours post-irradiation with doses of 2 and 4 Gy. To 4 hours of observation, the number of ARFC was similar again to that in the control.

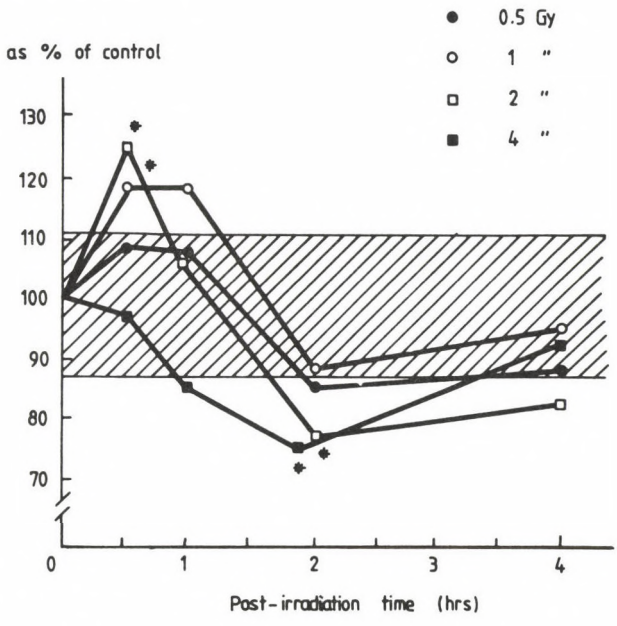


*Fig. 3.* Alterations in ARFC contents at different time-point following gamma-irradiation of rat thymocytes expressed as percentage of time-matched controls. Horizontal bars indicate the scattering interval in controls, asterisks represent statistical significance at level of $p < 0.05$

4. *Cationized ferritin binding*

The binding of CF to the negatively charged sites on thymocyte surfaces was altered by X-irradiation (Fig. 4). It decreased already at 15 minutes after treatment. This phenomenon was most pronounced at 1 hour of post-irradiation time (Fig. 4B) as compared to the unirradiated control (Fig. 4A). The changes seemed to be transient as the mentioned conditions of cell surfaces were restored by 4 hours (non-shown).

5. *DNA parameters of irradiated cells*

The percentage of pyknotic nuclei and total amounts of DNA in the samples of thymic cells did not alter significantly following irradiation at either doses tested (data not shown). Determination of AT-rich component of cell nucleoids revealed, however, some transient changes in the structure of genetic material (Fig. 5). Thus, 30 minutes after 4 Gy of gamma-rays, a significant increase in this parameter occurred, whereas 2 hours following treatment with low doses (0.5 or 1.0 Gy), a transient decrease in DAPI binding was observed. At 4 hours after irradiation an increase of this parameter was noted in the samples irradiated with 0.5 Gy.

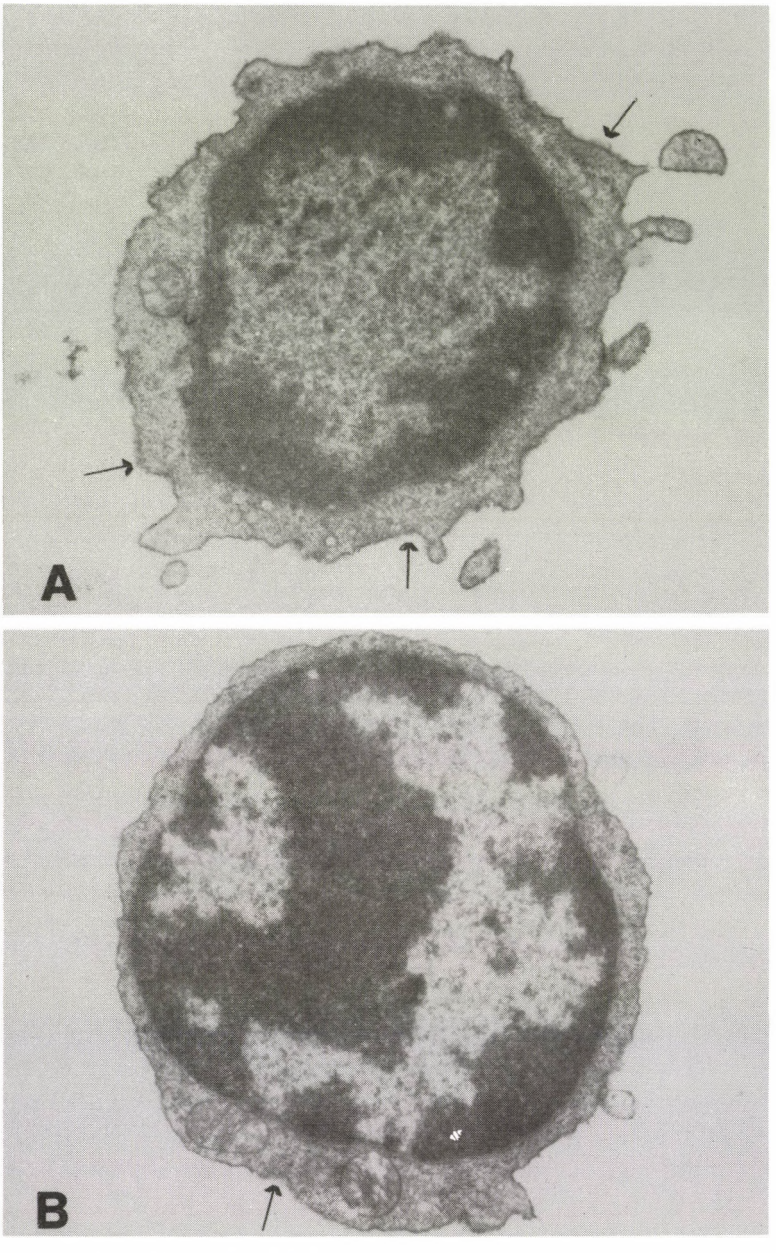


*Fig. 4.* Loss of ferritin-binding sites from the surface of rat thymocytes at 1 hour after the radiation effect. On the surface of unirradiated cell (A), the ligand occurs evently (→). After X-irradiation (B) CF binds in separate groups (→). Magnification: 21 000 x

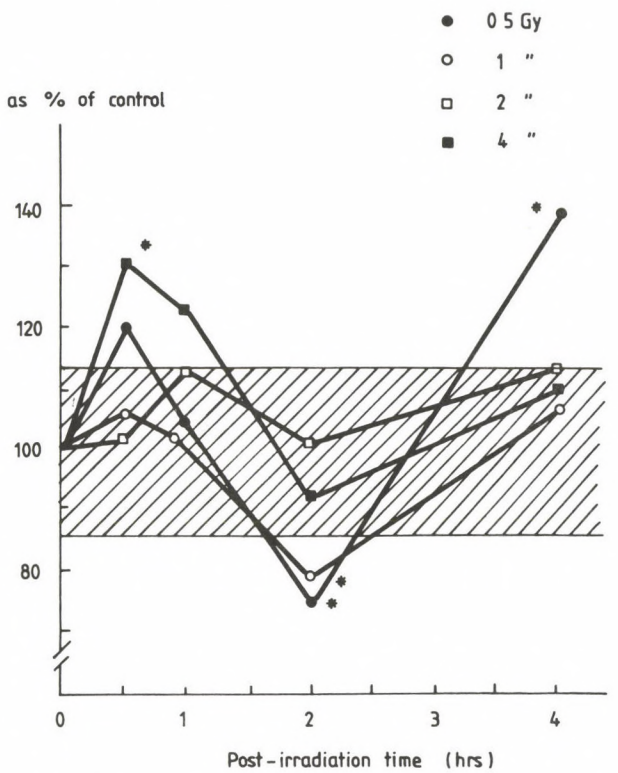


*Fig. 5.* Contents of nucleoid AT-rich DNA in the rat thymocytes after gamma-irradiation expressed as percentage of time-matched controls. Horizontal bars indicate the scattering interval in controls, asterisks represent statistical significance at level of $p < 0.05$

## Discussion

In order to reveal the time-dependent alterations of thymocytes *in vitro*, their parameters were assayed in the untreated population following incubation at 21–22 °C, or at 37 °C (at the endpoint of study). Some conventional markers of cellular death including nuclear pyknosis and Trypan Blue exclusion were also tested. The results have shown that incubation at physiological temperature is accompanied by accelerated death of significant subpopulation which is confirmed by nuclear pyknosis, whereas data obtained at 21–22 °C have exhibited far less pronounced changes of nuclear and membranes features. Our previous findings support the suggestion on low *in vitro* viability of the major population of thymocytes that is easily revealed during 1 to 4 hours under "physiological" conditions [21].

Thus, studying the post-irradiation changes of thymocytes at suboptimal temperature seems to be rather suitable for detection of early reversible alterations of membrane and nuclei. In this respect, such approach may be superior to the usage of various inhibitors of interphase death [11]. For example, suppression of thymocytes' death with $Cd^{2+}$ ions prevents the whole complex of lethal events including the very early changes of cellular structures [22].

The surface markers investigated in the present work have characterized certain molecular structures of the thymic cell membranes. For example, through the ConA binding, the presence of available glucose- and mannose-containing glycoproteins on cell surfaces can be detected [13]. The early post-irradiation increase in the amount of bound lectin took place as a consequence of radiation-provoked membrane perturbation. Radiation treatment affected both the number of binding sites and their affinities (unpublished data). In the course of post-irradiation period, the phenomenon fades away reflecting the 'normalization' of functional condition of plasma membrane.

Autologous rosetting at 21–22 °C also expressed reversible changes following irradiation, unlike the dramatic loss of this ability under 'physiological' regime [21]. Increase in ARFC numbers may be regarded as very early radiation-induced alteration, along with enhanced ConA binding and decreased avidity for cationized ferritin at these terms of observation. The later decrease of ARFC content after 2–4 Gy should be considered as a prelethal event which, however, is transient, due to suboptimal experimental conditions. *In vivo* such loss in rosette-forming ability reached its full development within 4 hours after irradiation, and it was followed by massive nuclear pyknosis [3].

To the contrary, AB-agglutinability of cells may reflect their net negative charge, determined by the total surface sialic acids [10]. Post-irradiation increase in AB-agglutination of thymocytes also suggested the transient membrane rearrangements. This observation is in good agreement with the TEM findings demonstrating a decrease of cationized ferritin-binding sites on the surface of irradiated thymocytes.

Along with marked surface changes, some radiation-induced alterations of DNA properties occurred under these experimental conditions. It is of importance that the enhancement of ConA binding up to 1 hour after irradiation at low doses (1.0–2.0 Gy) was not accompanied by the changes in DNA structure. This surface event may, thus, be caused by specific response of membranes, without direct connection with subsequent reaction of nuclear substance. At the higher dose of 4 Gy, the more complex response of cells with simultaneously enhanced ConA binding and increased DNA-DAPI interaction was observed. This coincidence supposes a probable connection between the early post-irradiation enhancement in the number of membrane binding sites for ConA or autologous erythrocytes, and some changes

of genome structure (probably with its decondensation due to DNA repair). It is known that those flank regions of eukaryotic genes which play the initiating role for RNA transcription, are AT-rich [18]. Another argument for relative specificity of DAPI as a suitable tool for such studies is depression of DNA template activity upon interaction with this compound [5]. Meanwhile, increase of available AT-rich DNA regions after irradiation with 0.5 Gy at 4 hours of incubation may be explained by repair of chromatin template ability after low-dose irradiation. To the contrary, the decrease in DAPI binding to cell nucleoid at 2 hours after treatment with low doses would be a feature of genome suppression [20].

The regeneration of thymocyte membranes after low-dose exposures as shown in these experiments are in good agreement with our previous *in vitro* and *in vivo* observations on the lectin bindings of peripheral lymphocytes as well as on the CF binding of human fibroblasts [14, 19].

Thus, nearly all radiation-induced membrane changes and DNA alterations observed at 21–22 °C proved to be transient. Therefore, it may be presumed that the proposed experimental model permitted to reveal especially the early reversible changes in the plasma membrane and nuclei of irradiated thymic lymphoid cells, without whole-scale development of cellular lethal process. This important type of prelethal phase alterations of cell surface is worth of further studies with cells and tissues of different radiosensitivity.

## Acknowledgements

The authors wish to express their appreciation to Professor Dr. L. B. Sztanyik, Director-General of the Institute in Budapest for his interest and support, to Mrs. Ella Hrisztodulakisz for her excellent technical assistance.

## REFERENCES

1. Anderson, R. E., Standefer, J. C.: Radiation injury in the immune system. In: Cytotoxic insult of tissue. Effects on cell lineages, eds C. S. Potten, J. H. Hendry, Edinburgh pp. 67–104, 1983.
2. Bailey, N. T. J.: Statistical methods in biology. ed.: English University Press, Oxford, 200 pages 1959.
3. Borisova, E. A., Chukhlovin, A. B., Siliev, A. A., Zherbin, E. A., Zhivotovsky, B. D., Hanson, K. P.: Degree of chromatin fragmentation and frequency of nuclear pyknosis in Percoll-fractionated thymocytes of irradiated rats. Int. J. Radiat. Biol. **51**, 421–428 (1987).
4. Brunk, D. F., Jones, K. C., James, Th. W.: Assay for nanogram quantities of DNA in cellular homogenates. Analyt. Biochem. **92**, 497–500 (1979).
5. Chandra, P., Mildner, B., Dann, O., Metz, A.: Influence of 4'-6-diamidino-2-phenylindole on the secondary structure and template activities of DNA and polydeoxynucleotides. Mol. Cell. Biochem. **18**, 81–86 (1977).
6. Cook, P. R., Brazell, J. A.: Spectrofluorimetric measurement of the binding of ethidium to super-helical DNA from cell nuclei. Eur. J. Biochem. **84**, 465–477 (1978).

7. Daxhelet, G. A., Coene, M. M., Hoet, P. P., Cocito, C. G.: Spectrofluorimetry of dyes with DNAs of different base composition and conformation. Analyt. Biochem. **179**, 401–403 (1989).
8. Descotes, J.: Immunotoxicology of drugs and chemicals. Amsterdam, Elsevier Publ. (1986).
9. Fawthrop, D. J., Boobis, A. R., Davies, D. S.: Mechanisms of cell death. Arch. Toxicol. **65**, 437–444 (1991).
10. Halbhuber, K. J., Geyer, G., Feuerstein, H.: Agglutinationsverhalten roter Blutzellen nach experimenteller Glykokalyxalteration. Fol. Haematol. **104**, 85–97 (1977).
11. Hanson, K. P., Komar, V. E.: Molecular mechanisms of radiation cell death. ed.: Energoatomizdat, Moscow (in Russian), 250 pages 1985.
12. Kapuscinski, J., Szer, W.: Interaction of 4'-6-diamidine-2-phenylindole with synthetic polynucleotides. Nucl. Acid Res. **6**, 3519–3534 (1979).
13. Köteles, G. J.: Cell membranes in radiation injury. Isotopenpraxis **10**, 361–368 (1986).
14. Kubasova, T., Köteles, G. J., Varga, L. P.: Surface alteration of mammalian cells upon ionizing radiation as detected by lectin-binding techniques. I. Binding of concanavalin A by blood cells of X-irradiated mice. II. Binding of concanavalin A by human blood cells X-irradiated in vitro. Int. J. Radiat. Biol. **40**, 175–194 (1981).
15. Kubasova, T., Köteles, G. J., Simbirtzeva, L. P. Mus, V. F., Zherbin, E. A., Hanson, K. P., Sinkovics, I., Karika, Zs.: Use of lectin-binding technique as a tool to assess the radiation dose. Measurement on blood cells of radiotherapy patients. Radiobiol. Radiother. **27**, 783–791 (1986).
16. Lin, M. S., Comings, D. E., Alfi, O. S.: Optical studies of the interaction of 4'-6-diamidino-2-phenylindole with DNA and methaphase chromosomes. Chromosoma **60**, 1, 15–25 (1977).
17. Manzini, G., Barcellona, M. L., Avitabile, M., Quadrifoglio, F.: Interaction of diamidino-2-phenylindole (DAPI) with natural and synthetic nucleic acids. Nucl. Acid Res. **11**, 8861–8876 (1983).
18. Scherrer, K., Moreau, J.: Significance of AT-rich DNA segments in organization and function of eukaryotic genomes. In: Proceedings of 16th FEBS Congress, Moscow, Nauka Publ., Vol. **1**, 305–315 (1987).
19. Somosy, Z., Kubasova, T., Ecsedi, G. S., Köteles, G. J.: Radiation-induced changes of negative charge on the cell surface of primary human fibroblasts. Int. J. Radiat. Biol. **49**, 969–978 (1986).
20. Valkovich, A. A., Hanson, K. P.: Correlation between the structural state of chromatin and biosynthesis of the rapidly labeling nuclear RNA in the thymus of rats subjected to total body X-irradiation. Vopr. Med. Chimii **22**, 643–648 (1976).
21. Zherbin, E. A., Chukhlovin, A. B.: Possible association of membrane and nuclear changes in gamma-irradiated rat thymocytes. Int. J. Radiat. Biol. **45**, 179–183 (1984).
22. Zherbin, E. A., Chukhlovin, A. B., Köteles, G. J., Kubasova, T. A., Vashchenko, V. I., Hanson, K. P.: Effects of in vitro cadmium ions on some membrane and nuclear parameters of normal and irradiated thymic lymphoid cells. Arch. Toxicol. **59**, 21–25 (1986).

*Acta Physiologica Hungarica, Volume 81 (3), pp. 289–299 (1993)*

# THE COMPARATIVE ANTIARRHYTHMIC AND PROARRHYTHMIC ACTIVITY OF A 3,7-DIHETERO-BICYCLO[3.3.1]NONANE, BRB–I–28, AND LIDOCAINE IN THE 1–4-DAY-OLD INFARCTED DOG HEART

T. FAZEKAS, B. J. SCHERLAG, P. MABO, K. D. BERLIN,* G. L. GARRISON,* C. L. CHEN,** S. SANGIAH,** E. PATTERSON, R. LAZZARA

DEPARTMENT OF MEDICINE, CARDIOVASCULAR SECTION,
OKLAHOMA UNIVERSITY HEALTH SCIENCES CENTER, OKLAHOMA CITY;
* DEPARTMENT OF CHEMISTRY, ** DEPARTMENT OF PHYSIOLOGICAL SCIENCES,
OKLAHOMA STATE UNIVERSITY, STILLWATER; OKLAHOMA, USA

Received October 15, 1992
Accepted December 16, 1992

We compared the electrophysiological effects and quantified the antiarrhythmic/proarrhythmic potential of the 3,7-diheterobicyclo[3.3.1]nonane-derivative, BRB–I–28 and lidocaine in 15 consecutive postinfarction dogs. Electrophysiologic studies were performed in anesthetized animals, 1–4 days (mean ± SE = 2.47 ± 0.36) after the two-stage ligation of the left anterior descending coronary artery. Inducibility of sustained monomorphic ventricular tachycardia (SMVT) was compared in the pre-drug state, and after i.v. lidocaine (3 and 6 mg/kg) and BRB–I–28 (3 and 6 mg/kg) administration. During the control state, SMVT was inducible in 6/15 dogs (40%). After the administration of lidocaine, the rate of the inducible SMVT slowed (353 ± 91 to 272 ± 96 beat/min; $p < 0.01$), but due to the proarrhythmic action of the drug, SMVT became inducible in 13/15 dogs (87%). Sustained reentry was induced after 3 mg/kg lidocaine in 3 dogs and after 6 mg/kg in 4. The mean aortic blood pressure in these SMVTs was 36 ± 8 mm Hg. After administration of BRB–I–28 (6 mg/kg) SMVT was not inducible in 2/6 and in 4 the SMVT rate was slowed (380 ± 104 to 208 ± 105 beat/min; $p < 0.005$) before termination in 3. In 2 dogs SMVT was induced after BRB–I–28 was given whereas they were non-inducible in the control state (proarrhythmic effect: 13%). Furthermore the hemodynamic state during the SMVTs was more stable after BRB–I–28 (mean aortic blood pressure = 65 ± 7 mm Hg; post–BRB–I–28 vs post-lidocaine, $p < 0.001$). During sinus rhythm, lidocaine caused a transient lowering of the MBP (105 ± 17 to 84 ± 18 mm Hg; $p < 0.001$), whereas, BRB–I–28, induced a consistent but short-lasting pressor response (98 ± 18 to 120 ± 29 mm Hg; $p < 0.001$) after its bolus injection. The low proarrhythmic activity and the lack of a cardiodepressant action makes this new chemical class of antiarrhythmics worthy of further development.

**Keywords**: BRB–I–28, lidocaine, electrophysiology, myocardial infarction, dog

Correspondence should be addressed to
Tamás FAZEKAS,
First Department of Medicine, Szent-Györgyi Albert University Medical School,
H–6701, Szeged, Korányi fasor 10, P.O. Box 469, Hungary

*Akadémiai Kiadó, Budapest*

The Cardiac Arrhythmia Suppression Trial (CAST) underscored the clinical relevance of the proarrhythmic effect of antiarrhythmic drugs particularly in regard to inducing sudden arrhythmic cardiac death [11, 19, 31]. The high incidence (10–15%) and potential life-threatening nature of proarrhythmic response during antiarrhythmic pharmacotherapy [19] has prompted a new way of thinking among investigators who are dealing with the design, pharmacology and clinical evaluation of antiarrhythmic compounds [7, 28]. One possible approach in post-CAST era is the development of those kinds of antiarrhythmics, which do not depress the mechanical or electrical activity of normal myocardium but act specifically on the ischemically-damaged substrate and thereby inhibit or suppress the reentrant mechanism responsible for the malignant cardiac arrhythmia.

A new class of agents, the 3,7-diheterobicyclo[3.3.1]nonanes (BRB–I–28, GLG–IV–78, GLG–V–13, GLG–IV–57) have *in vivo* antiarrhythmic activity [1, 2, 20, 25, 27, 29, 34, 35]. The study of this group of compounds is promising because of the fact that their efficacy may be better and the cardiodepressant action seems to be lacking or more moderate in comparison with presently approved antiarrhythmic drugs [8].

The goal of the present study was to confirm and further evaluate the electrophysiological and hemodynamic effects of the prototypical agent of the 3,7-diheterobicyclo[3.3.1]nonanes (DHBCNs), BRB–I–28 (7-benzyl-7-aza-3-thiabicyclo[3.3.1]nonane $HClO_4$). We compared the antiarrhythmic and proarrhythmic potential of BRB–I–28 with that of lidocaine. Lidocaine was selected as a prototypic class I agent based upon its moderate cardiodepressant effects and its reported low incidence of proarrhythmia compared to other class I antiarrhythmic drugs.

## Methods

Fifteen mongrel dogs were anesthetized with sodium pentobarbital (30 mg/kg i.v.). Using aseptic technique after left thoracotomy, the left anterior descending coronary artery (LAD) was dissected free and the two-stage ligation was performed [12]. The dogs received antibiotic and analgesic therapy post-operatively.

Electrophysiological study was performed 24–96 hours (mean ± SEM = 2.47 ± 0.36 day) after the occlusion of the LAD. Anesthesia was reinduced and a 12-lead ECG was recorded to ascertain the presence and extent of myocardial infarction (MI). Specifically we looked for QS-complexes across the anterior chest leads. During the experiment, limb lead II and aVR were registered continuously. An electrode catheter was introduced into the proximal aortic root through the common carotid artery for registering the His-bundle electrogram ($Hb_{eg}$) [22]. The mean aortic blood pressure (MBP) was measured by means of a Statham P–24D transducer. Lidocaine and BRB–I–28 were administered in cumulative doses of 3 and 6 mg/kg i.v., each over a period of 1 minute. The latter drug was injected 1 hour after lidocaine, when the electrophysiological effects of the former had completely dissipated [2, 16, 25]. This was determined by the electrophysiological evaluation of the ventricular effective refractory

period (VERP). In order to record the activation of the subepicardial myocardium overlying the MI [13], composite electrodes were placed onto the infarcted anteroapical ($IZ_{epi}$) epicardium and on the non-infarcted posterior wall of the left ventricle ($NZ_{epi}$) for comparative purposes [26]. In six animals, another electrode catheter passed through the other carotid artery was positioned by ECG monitoring onto the endocardial surface subjacent to the infarct zone ($IZ_{endo}$) [23]. The ECG and the electrograms were registered continuously on an oscilloscope (Electronics for Medicine VR-12; Pleasantville, NY, USA) and recordings made at paper speeds of 50-250 mm/sec on a Gould (ES 1000) paper drive (Gould Electronics; Valley View, OH, USA) interfaced with the Electronics for Medicine recorder. The heart was electrically stimulated from the right ventricular outflow tract to induce sustained monomorphic ventricular tachycardia (SMVT = ventricular tachycardia of uniform QRS morphology lasting > 30 sec at the rate of > 250 min; 24). The cycle length of the SMVT was measured as an average of 10 consecutive complexes. Two kinds of stimulation protocols were used: the traditional programmed extrastimulus technique and the rapid (240-420/min) asynchronous burst pacing protocol [3, 10, 17]. The previous was delivered by a Medtronic 5328 stimulator, the latter with an S-88 Grass equipment. During the programmed electrical stimulation (PES) using a baseline cycle length of 300 msec, 1, 2 or 3 premature stimuli were delivered. The duration of the stimuli was 2 msec at twice the diastolic threshold level. VERP was measured by the $S_1S_2$ technique. A sensitive reversed-phase high-performance liquid chromatographic (HPLC) technique with UV detection has been developed to determine the concentration of BRB-I-28 in dog plasma [5]. A previous study has shown that the electrophysiological duration of action of BRB-I-28 is about 40 min [2]. Therefore, blood samples were taken, 5, 15 and 30 minutes after the injection of 6 (n = 4) or 3 (n = 1) mg/kg BRB-I-28. Data are expressed as the mean ± the standard error of the mean. Statistical evaluation of the results was done by the paired and unpaired *t* test. An analysis of variance (ANOVA) was used to evaluate for differences within or between groups. Fisher's exact test was used to evaluate for differences between treatment groups for the incidence of SMVT.

## Results

Compared to the baseline (152 ± 25/min), neither lidocaine (151 ± 26/min) nor BRB-I-28 (145 ± 28/min) influenced heart rate. After the bolus of lidocaine there was a short lasting (1-1.5 min), but consistent, decrease of MBP (105 ± 17 to 84 ± 18 mm Hg; $p < 0.001$). After the administration of BRB-I-28 there was a (1-1.5 min) pressor response (98 ± 18 to 120 ± 29 mm Hg; $p < 0.001$). Neither lidocaine nor BRB-I-28 prolonged AH interval (baseline 57 ± 8 msec, after lidocaine 57 ± 7 msec, after BRB-I-28 60 ± 7 msec; NS). Lidocaine did not induce HV interval prolongation (33 ± 2 msec), compared to the control (30 ± 3 msec). BRB-I-28, however, provoked a biologically moderate, but statistically significant HV prolongation (40 ± 6 msec; $p < 0.001$), however, no instance of infranodal block was observed even at high pacing rates. VERP (baseline 142 ± 14 msec) was prolonged both by lidocaine (167 ± 24 msec; $p < 0.01$) and BRB-I-28 (163 ± 10 msec; $p < 0.001$). There was no statistically significant QT interval (baseline: 199 ± 28 msec) prolongation neither by lidocaine (200 ± 30 msec; NS) nor by BRB-I-28 (205 ± 34 msec; NS).

In regard to the inducibility of SMVT, in 15 animals in the drug-free state, we could induce SMVT 6/15 by one or both stimulation protocols. As published previously [9, 14, 18, 24], lidocaine pretreatment highly facilitates the induction of SMVT in this particular dog model: after its injection, 7 additional dogs became inducible compared to the baseline (13/15; post-lidocaine vs. pre-lidocaine $p < 0.02$). Sustained reentry was induced after 3 mg/kg lidocaine in 4 animals and by 6 mg/kg in an additional 3. After the administration of BRB-I-28, SMVT was inducible in 6 dogs (6/15) of which 4 were inducible in the control state and 2 which were then due to proarrhythmia (control vs. post-BRB-I-28 NS). A higher incidence of pacing-induced SMVT with lidocaine versus BRB-I-28 was found ($p < 0.057$). In the 4 dogs both inducible in the control state and after 3 and 6 mg/kg BRB-I-28, the DHBCN derivative caused a marked slowing of SMVT (380 ± 104/min to 280 ± 105; $p < 0.005$) and the tachycardia spontaneously terminated in 3. During the slowed tachycardia a higher MBP (65 ± 7 mm Hg) was observed than that seen during SMVT in the control state (51 ± 24 mm Hg) or after lidocaine administration (36 ± 8 mm Hg; post-lidocaine vs. post-BRB-I-28, $p < 0.001$), and this may have contributed to the spontaneous restoration of sinus rhythm. An example of an SMVT induced in the control state is shown in Figure 1. After 90 sec at 30 mm Hg MBP, the rhythm degenerated into ventricular fibrillation. In Figure 2 the same induced SMVT, but at a slower rate and higher MBP (65 mm Hg) spontaneously terminated after BRB-I-28, 6 mg/kg was administered. After the administration of the DHBCN derivative, we frequently observed the local use-dependent subepicardial ($IZ_{epi}$) block of electrophysiological response to successive stimuli. The propagating impulse was not altered in the normal myocardium nor in the moderately damaged endocardial zone ($IZ_{endo}$) (Figs 3a-3b).

The plasma concentrations after the injection of 6 mg/kg BRB-I-28 were: at 15 min 2.44 ± 0.28; at 15 min 1.91 ± 0.27; and at 30 min 1.25 ± 0.35 mg/l (Fig. 4). After 3 mg/kg the plasma levels were somewhat lower: at 5 min 1.49; at 15 min 1.03; and at 30 min 0.76 mg/l. Thus, following intravenous administration of BRB-I-28 at 6 and 3 mg/kg, there was a rapid decline in the plasma concentration. This suggests that BRB-I-28's short duration of electrophysiologic action (30-40 min) could be due to its rapid metabolism and elimination from the body.

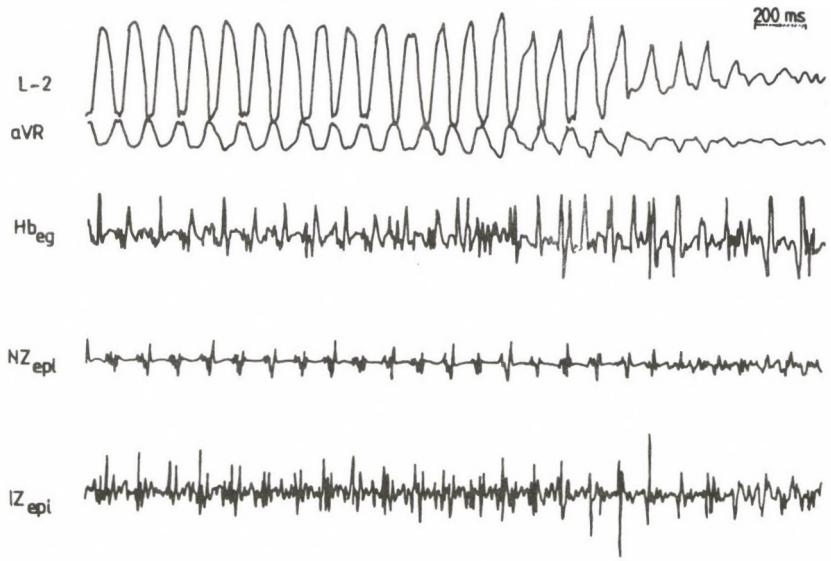


*Fig. 1.* After BRB-I-28 (6 mg/kg), the same induced SMVT (shown in Fig. 1) has a slower rate (400 beat/min) and higher MBP (65 mm Hg) and spontaneously terminates after 50 sec

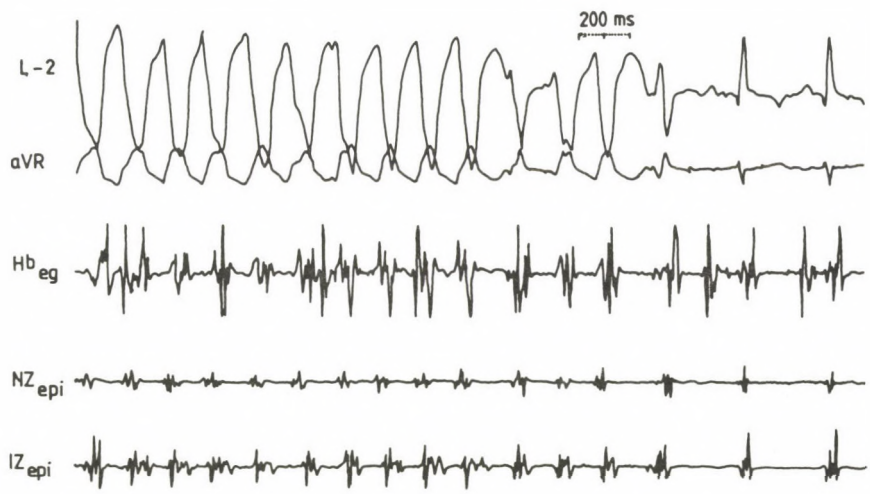


*Fig. 2.* Sustained monomorphic ventricular tachycardia (SMVT, 480 beat/min) induced by programmed electrical stimulation in the drug-free state. $IZ_{epi}$ shows continuous electrical activity, the MBP during the tachycardia is 30-35 mm Hg. After 1.5 min SMVT degenerates into ventricular fibrillation

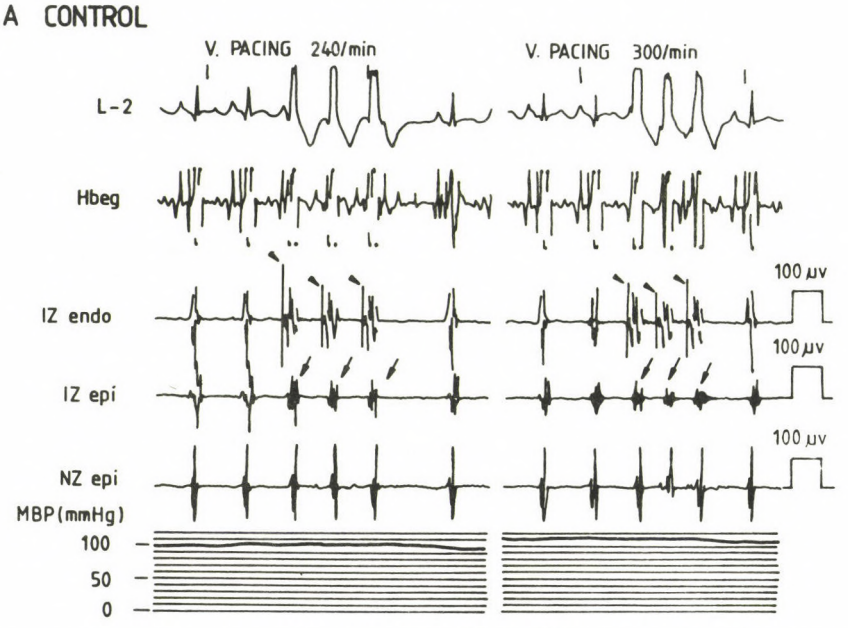


*Fig. 3a.* In the drug-free state, ventricular burst pacing (240/min, 300/min) induces impulses propagating in both $IZ_{endo}$ (arrowheads) and $IZ_{epi}$ (arrows)

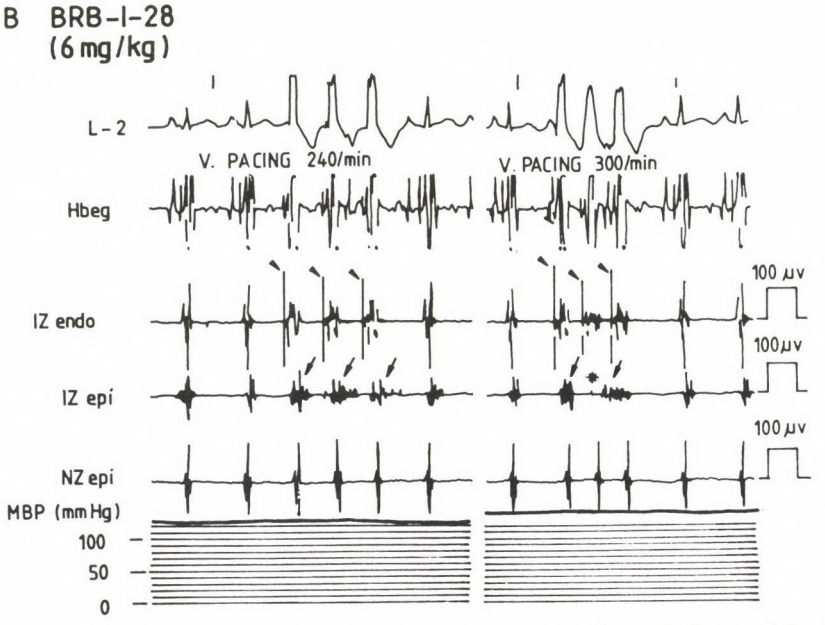


*Fig. 3b.* BRB-I-28 (6 mg/kg) prolongs refractoriness primarily in the ischemically more injured $IZ_{epi}$ resulting in a local rate-dependent subepicardial block of the 2nd stimulus artifact at the higher pacing rate (300 beat/min; asterisk)

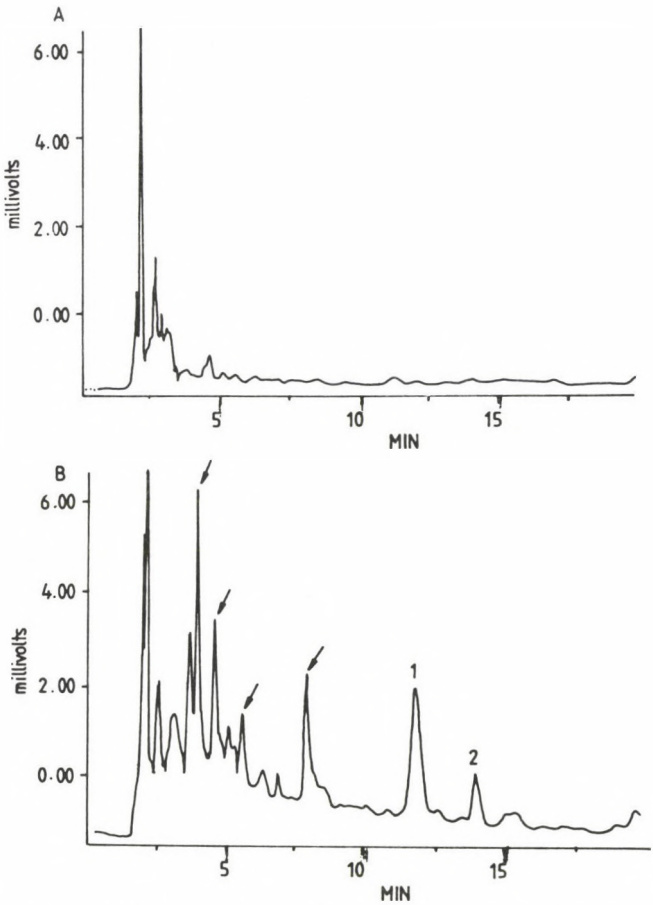


*Fig. 4.* High-performance liquid chromatographic (HPLC) profile of control plasma (A) and a plasma sample 5 min after i.v. dose of 6 mg/kg of BRB-I-28 (B). Peaks: 1 = SAZ-VII-23, internal standard 2 = BRB-I-28. Arrows show possible metabolites

## Discussion

BRB-I-28 is a new antiarrhythmic compound belonging to the DHBCN group [1, 2, 15]. Previously we have shown that the agent is able to prevent or slow the electrically-induced SMVT provoked in the 1-4-day-old infarcted canine heart [25]. In a series of *in vivo* studies we found that BRB-I-28 does not alter the rate of the sinus or underlying ventricular automaticity in the normal or infarcted dog heart [25]. *In vitro*, the automatic firing of spontaneously active canine Purkinje fibers was unaffected by the drug across a large dose range (0.1, 0.32, 1.0 and 3.2 mg/l)

comparable with the canine-effective plasma level (1–3 mg/l) of BRB–I–28 measured *in vivo* [5, 15]. The electropathological basis of SMVT induced by electrical stimulation is ventricular reentry [23]. Thus the striking antiarrhythmic action of BRB–I–28 on induced SMVT indicates that we are dealing with an arrhythmia-specific suppressive agent since it acts selectively on reentrant tachycardias and does not alter cardiac automaticity.

Electrophysiological studies performed on normal canine Purkinje fibers and epicardial and endocardial ventricular muscle preparations have shown that BRB–I–28 (1.0 and 3.2 mg/l) decreases the velocity of the rapid upstroke phase ($V_{max}$) and amplitude of the cardiac action potential, without influencing the action potential duration (ADP) [15]. BRB–I–28 decreases conduction velocity in the normal myocardium only at fast ( > 210/min) pacing rates. The $V_{max}$ recovery time ($T_{1/2}$) in the presence of BRB–I–28 is short (160 ± 26 msec) which is consistent with the lipophilic nature and low molecular weight (233.1 dalton) of the compound [15]. The short $V_{max}$ recovery time is similar to that of lidocaine (100–230 msec), mexiletine (208–440 msec) and tocainide (270–390 msec) [32]. The rate-dependent slowing of conduction during fast pacing and the lack of effect on the APD indicates that BRB–I–28 belongs to the subgroup Ib of $Na^+$ channel blocking antiarrhythmics [15]. Electrophysiological studies carried out on ventricular epicardial and endocardial muscle preparations isolated from the infarcted dog heart revealed that BRB–I–28 prolongs ventricular refractoriness primarily in the ischemically-damaged myocardium, its action on the normal cardiac muscle is rather weak [16]. Proarrhythmia has been suggested to be caused by depressed conduction in moderately damaged tissue which brings its slowed conduction into the reentry zone [7, 25]. The other advantages that characterize this new compound is that both *in vivo* and *in vitro*, the conduction delay in moderately sick tissues and normal zones is minimal compared to another commonly used Ib agent, lidocaine. This could explain BRB–I–28's lower proarrhythmic potential [8, 9, 18, 25]. BRB–I–28 seems to be more selective than lidocaine on the more injured myocardium and more depressive on the more ischemically damaged tissue. Conversely it is less depressive on moderately damaged cardiac areas [16]. However, at pacing rates higher than 180/min BRB–I–28 also slows intraventricular conduction even in normal tissue, which shows that at higher heart rates this compound could induce a greater amount of conduction delay in moderately sick cardiac tissue which may generate reentry and manifest clinically as proarrhythmic tachycardia [16].

The mechanism of the transient increase of the MBP induced by BRB–I–28 is still unknown. We don't know whether the basis of this observation is a direct positive inotropic action or an indirect, peripheral vascular one or both. The lack of hypotension after i.v. administration and the slowing of the rate of SMVTs after BRB–I–28 combines to provide more opportunity for the restoration of the sinus

rhythm (see Fig. 2). It seems to be relevant, as well, that BRB-I-28 and its derivatives (SAZ-VII-22, SAZ-VII-23; 5) inhibit microsomal $Na^+$, $K^+$-ATPase prepared from guinea pig heart [6]. It is quite possible that the increase in MBP during sinus rhythm could be mediated by the inhibitory effect of BRB-I-28 on cardiac $Na^+$, $K^+$-ATPase activity and increase Na/Ca exchange, which is similar to ouabain's effect on this enzyme [6]. As a matter of course the enzyme inhibiting action of DHBCNs is much weaker than that of ouabain. However this observation may suggest that the common feature of these compounds is that they have some positive inotropic action [6].

Summarizing, we can conclude that BRB-I-28, the prototypical Ib DHBCN derivative, is an effective antiarrhythmic agent with low proarrhythmic activity. Further work on other analogues in this new chemical class has shown additional Vaughan Williams class III and possible class II electrophysiological properties [8]. The lack of considerable cardiodepressant action and the strong antiarrhythmic and heart rate lowering effects of some new DHBCNs (GLG-V-13, GLG-IV-57) make these antiarrhythmics worthy of further development.

## REFERENCES


1. Alavi, F. K., Clarke, C. R., Sangiah, S., Berlin, K. D., Zisman, S. A., Chen, C. L., Garrison, G. L., Scherlag, B. J., Lazzara, R.: Disposition of BRB-I-28 (7-benzyl-7-aza-3-thiabicyclo[3.3.1]nonane hydroperchlorate), a novel antiarrhythmic agent. Drug Invest. **3**, 317-323 (1991).
2. Bailey, B. R., Berlin, K. D., Holt, E. M., Scherlag, B. J., Lazzara, R., Brachmann, J., van der Helm, D., Powell, D. R., Pantaleo, N. S., Ruenitz, P. C.: Synthesis, conformational analysis, and antiarrhythmic properties of 7-benzyl-3-thia-7-azabicyclo[3.3.1]nonan-9-one, 7-benzyl-3-thia-7-azabicyclo[3.3.1]nonane hydroperchlorate and 7-benzyl-9-phenyl-3-thia-7-azabicyclo[3.3.1]nonan-9-ol hydroperchlorate, and derivatives: single-crystal X-ray diffraction analysis and evidence for chair-chair and chair-boat conformers in the solid state. J. Med. Chemistry **27**, 758-767 (1984).
3. Bhandari, A. K., Widerhorn, J., Sager, Ph. T., Leon, C., Hong, R., Kotlewski, A., Hackett, J., Rahimtoola, S. H.: Prognostic significance of programmed ventricular stimulation in patients surviving complicated acute myocardial information: a prospective study. Am. Heart J. **124**, 87-96 (1992).
4. Brachmann, J., Kabell, G., Scherlag, B. J., Harrison, L., Lazzara, R.: Analysis of the interectopic activation patterns during sustained ventricular tachycardia. Circulation **67**, 449-456 (1983).
5. Chen, C. L., Lessley, B. A., Clarke, C. R., Roder, J. D., Sangiah, S., Berlin, K. D., Garrison, G. L., Scherlag, B. J., Lazzara, R., Patterson, E.: High-performance liquid chromatographic determination of BRB-I-28, a novel antiarrhythmic agent, in dog plasma and urine. J. Chromatography - Biomedical Applications, accepted for publication.
6. Chen, C. L., Sangiah, S., Patterson, E., Berlin, K. D., Garrison, G. L., Dunn, W., Nan, Y., Scherlag, B. J., Lazzara, R.: Effects of BRB-I-28, a novel antiarrhythmic agent, and its derivatives on cardiac $Na^+$, $K^+$-ATPase, $Mg^{2+}$-ATPase activities and contractile force. Res. Comm. Chem. Pathol. Pharmacol., accepted for publication.

7. El-Sherif, N.: Experimental models of reentry, antiarrhythmic, and proarrhythmic actions of drugs. Complexities galore! Circulation **84**, 1871–1875 (1991).
8. Fazekas, T., Mabo, P., Berlin, K. D., Scherlag, B. J., Lazzara R.: Comparative electrophysiological effects of a new chemical class of anti-arrhythmic agents, 3,7-diheterobicyclononanes, in the 1–4-day-old infarcted dog heart. The Physiologist **35**, 221 (1992).
9. Fazekas, T., Mabo, P., Scherlag, B. J., Lazzara, R.: Unmasking the reentrant susbstrate by lidocaine in the 1–4-day infarcted dog heart. 65th Scientific Session of the American Heart Association, 16–19 November, New Orleans, Oral presentation (1992).
10. Garan, H., Ruskin, J. N. McGovern, B., Grant, G.: Serial analysis of electrically induced ventricular arrhythmias in a canine model of myocardial infarction. J. Am. Coll. Cardiol. **5**, 1096–1106 (1985).
11. Greene, H. L., Roden, D. M., Katz, R. J., Wossley, R. L., Salerno, D. M., Henthorn, R. W. and the CAST Investigators: The Cardiac Arrhythmia Suppression Trial: first CAST...Then CAST–II. J. Am. Coll. Cardiol. **19**, 894–898 (1992).
12. Harris, A. S.: Delayed development of ventricular ectopic rhythms following experimental coronary occlusion. Circulation **1**, 1318–1328 (1950).
13. Littmann, L., Svenson, R. H., Gallagher, J. J., Selle, J. G., Zimmern, S. H., Fedor, J. M., Colavita, P. G.: Functional role of the epicardium in postinfarction ventricular tachycardia. Circulation **83**, 1577–1591 (1991).
14. Patterson, E., Gibson, J. K., Lucchesi, B. R.: Electrophysiologic actions of lidocaine in a canine model of chronic myocardial ischemic damage – arrhythmogenic actions of lidocaine. J. Cardiovasc. Pharmacol. **4**, 925–934 (1982).
15. Patterson, E., Scherlag, B. J., Berlin, K. D., Lazzara, R.: Electrophysiological actions of BRB–I–28 in canine myocardial tissues. J. Pharmac. Exp. Therap. **259**, 558–565 (1991).
16. Patterson, E., Scherlag, B. J., Berlin, K. D., Lazzara, R.: Electrophysiologic actions of BRB–I–28 in ischemically-injured canine myocardium. J. Cardiovasc. Pharmacol., in press.
17. Patterson, E., Scherlag, B. J., Lazzara, R.: Mechanism of prevention of sudden death by nadolol: differential actions on arrhythmia triggers and substrate after myocardial infarction in the dog. J. Am. Coll. Cardiol. **8**, 1365–1372 (1986).
18. Patterson, E., Scherlag, B. J., Lazzara, R.: Electrophysiologic actions of clofilium and lidocaine in ischemically-injured canine epicardium. J. Pharmac. Exp. Therap. **262**, 375–382 (1992).
19. Podrid, P. J., Fogel, R. I.: Aggravation of arrhythmia by antiarrhythmic drugs, and the important role of underlying ischemia. Am. J. Cardiol. **70**, 100–102 (1992).
20. Pusley, M. K., Walker, M. J. A., Garrison, G. L., Howard, P. G., Lazzara, R., Patterson, E., Penz, W. P., Scherlag, B. J., Berlin, K. D.: The cardiovascular and antiarrhythmic properties of a series of novel sparteine analogs. Proc. West. Pharmacol. Soc. **35**, 87–91 (1992).
21. Sager, P. T., Perlmutter, R. A., Rosenfeld, L. E., Batsford, W. P.: Antiarrhythmic drug exacerbation of ventricular tachycardia inducibility during electrophysiologic study. Am. Heart J. **123**, 926–933 (1992).
22. Scherlag, B. J., Abelleira, J. L., Samet, P.: Electrode catheter recordings from the His bundle and left bundle in the intact dog. In: Research in Physiology. Kao, F. F., Koizumi, K., Vassale, M. (eds), Aulo Gaggi Publisher, Bologna, 223–238, 1971.
23. Scherlag, B. J., Kabell, G., Brachmann, J., Harrison, L., Lazzara, R.: Mechanisms of spontaneous and induced ventricular arrhythmias in the 24-hour infarcted dog heart. Am. J. Cardiol. **51**, 207–213 (1983).

24. Scherlag, B. J., Patterson, E., Lazzara, R.: Mechanisms of ventricular tachycardias in the experimental models of ischemic heart disease. In: Ventricular Tachycardias. From Mechanism to Therapy. Aliot, E., Lazzara, R. eds. Martinus Nijhoff Publishers, Dordrecht/Boston/Lancaster, 1987, pp. 26–41.
25. Scherlag, B. J., Patterson, E., Lazzara, R., Bailey, B. R., Thomson, M. D., Berlin, K. D.: Comparative electrophysiological and hemodynamic actions of BRB-I-28 and lidocaine in the normal and infarcted dog heart. J. Electrophysiol. **2**, 461–477 (1988).
26. Scherlag, B. J. Patterson, E., Berbari, E. J., Lazzara, R.: Slow conduction in experimental arrhythmias: mechanisms and role in reentry. In: Cardiac Electrophysiology and Arrhythmias. Fisch, C., Surawicz, B., Elsevier, New York/Amsterdam/London/Tokyo, 1991, pp. 96–107.
27. Smith, G. S., Thomson, M. D., Berlin, K. D., Holt, E. M., Scherlag, B. J., Patterson, E., Lazzara, R.: A study of the synthesis and antiarrhythmic properties of selected 3,7-diheterabicyclo[3.3.1]nonanes with substituents at the 2,4-positions and at the 9-position. Eur. J. Med. Chem. **25**, 1–8 (1990).
28. The Task Force of the Working Group on Arrhythmias of the European Society of Cardiology: The 'Sicilian Gambit'. A new approach to the classification of antiarrhythmic drugs based on their actions on arrhythmogenic mechanisms. Eur. Heart J. **12**, 1112–1131 (1991).
29. Thomson, M. D., Smith, G. S., Berlin, K. D., Holt, E. M., Scherlag, B. J., van der Helm, D., Muchmore, S. W., Fidelis, K. A.: Synthesis and antiarrhythmic properties of novel 3-selena-7-azabicyclo[3.3.1]nonanes and derivatives. Single-crystal X-ray diffraction analysis of 7-benzyl-3-selena-7-azabicyclo[3.3.1]nonan-9-one and 7-benzyl-3-selena-7-azabicyclo[3.3.1]nonane hydroperchlorate. J. Med. Chemist. **30**, 780–788 (1987).
30. Varró, A., Surawicz, B.: Effect of antiarrhythmic drugs on membrane channels in cardiac muscle. In: Cardiac Electrophysiology and Arrhythmias. Fisch, C., Surawicz, B. (eds) Elsevier, New York/Amsterdam/London/Tokyo, 1991, pp. 277–296.
31. Vaughan Williams, E. M.: Significance of classifying antiarrhythmic actions since the Cardiac Arrhythmia Suppression Trial. J. Clin. Pharmacol. **31**, 123–135 (1991).
32. Weirich, J., Antoni, H.: Differential analysis of the frequency-dependent effects of class 1 antiarrhythmic drugs according to periodical ligand binding: implications for antiarrhythmic and proarrhythmic efficacy. J. Cardiovasc. Pharmacol. **15**, 998–1009 (1990).
33. Zefirov, N. S., Palyulin, V. A.: Conformational analysis of bicyclo[3.3.1]nonanes and their hetero analogs. In: Topics in Stereochemistry. Eliel, E. L., Wilen, S. H. eds., John Wiley & Sons, Inc., New York/Chichester/Brisbane/Toronto/Singapore, 1991, **20**, pp. 171–230.
34. Zisman, S. A., Berlin, K. D., Alavi, F. K., Sangiah, S., Clarke, C. R., Scherlag, B. J.: Synthesis of 7-benzyl-7-aza-3-thiabicyclo[3.3.1]nonane hydroperchlorate-6,8,10-$^{14}C_3$. J. Lab. Compounds Radiopharm. **27**, 885–888 (1989).
35. Zisman, S. A., Berlin, K. D., Scherlag, B. J.: The preparation of amide derivatives of 3-azabicyclo[3.3.1]nonanes as new potential antiarrhythmic agents. Org. Preparations Procedures Int. **22**, 255–264 (1990).

*Acta Physiologica Hungarica, Volume 81 (3), pp. 301–307 (1993)*

# MECHANICAL RESPONSE OF LIZARD SKELETAL MUSCLES TO DISUSE:
## I. EFFECT OF SHORT-TERM TENOTOMIZATION

S. ARIFA, M. ABDUL AZEEM, S. SHAHINA, Khairunnisa SHAIKH*, Hilal A. SHAIKH

NEUROMUSCULAR PHYSIOLOGY UNIT, DEPARTMENT OF PHYSIOLOGY,
*DEPARTMENT OF PHARMACOLOGY, FACULTY OF PHARMACY, UNIVERSITY OF KARACHI, KARACHI, PAKISTAN

Received August 19, 1992
Accepted December 2, 1992

The gastrocnemius muscles of the reptile, *Uromastix hardwickii* were tenotomized for seven days according to the method described earlier [7] and their mechanical responses were recorded to study the effect of cessation of proprioceptive impulses on the functioning of these muscles. The parameters measured were isometric twitch and tetanic tensions, time dependent tension parameters and other time dependent parameters of twitch and tetanus records. The isometric twitch and tetanic tensions, their ratios and the rate of rise in twitch and tetanus along with P/ms were found significantly lesser in the tenotomized muscles. The other time dependent tension parameters, i.e. twitch contraction and tetanus half relaxation times and their ratios were however, unaffected as compared to their controls. The duration of active state on the contrary, was significantly reduced in the tenotomized muscles. The tenotomization effects observed on the mechanical parameters are discussed in terms of muscle fiber architecture and the degree/rate of cross bridge interaction in these muscles.

**Keywords**: tenotomization, gastrocnemius muscle, tension parameters, duration of active state

Tenotomization is a procedure in which the distal tendon of a muscle is sectioned to produce flaccidity and disuse in the muscle. Physiologically, tenotomization generally interrupts the influence of incoming proprioceptive impulses on the muscle alongwith a reduction in passive stretching and hence the muscle would no longer be able to exert effective tensions [5].

Correspondence should be addressed to
M. Abdul AZEEM,
Neuromuscular Physiology Unit,
Department of Physiology,
University of Karachi,
Karachi – 75270, Pakistan

*Akadémiai Kiadó, Budapest*

The contractile activity of tenotomized muscles is being studied since the time Eccles [9] found that the mammalian muscles produced lesser isometric twitch and tetanic tensions after tenotomization. Later, 66% lesser tetanic tensions have also been reported in the tenotomized rat muscles [21]. In addition, other investigators [7, 3] have also observed that a decrease in tension in the tenotomized rabbit muscles was accompanied by a slight shortening in the contraction time but a larger reduction in the half relaxation time. The above authors have thus suggested that such changes were due to the rapid atrophy of the slow contracting fibers rather than the changes occuring in the speed of the contractile elements themselves. This view has also been supported by in rabbit [12] and in guinea pig muscles [20].

In addition, some investigators [6] have observed that tenotomy was uneffective in modifying the dynamic properties of the tenotomized denervated rat soleus muscles and thus suggested that, by changing the pattern of fibrillation, tenotomization had modified the effects of denervation. Similarly, it has also been demonstrated [8] that denervation and denervation combined with tenotomy both decreased the time characteristics of soleus and plantaris muscles of rat and that there were no differences in the time characteristics between the denervated and denervated-tenotomized muscles after three weeks of operation, suggesting that any mechanical change that might have occurred following tenotomy, actually required the presence of an intact innervation and that the shortened condition of the muscle or inhibition of stretch reflex would not alter the mechanical activity. They have further elaborated that a slight increase in muscle speed was due to the severance of the muscle tendon and this was possibly related to an alteration in the muscle spindle activity that occurred after tenotomy. They have thus, concluded that tenotomy was probably responsible for a transformation of slow contracting fibers into fast contracting ones.

The above studies have demonstrated clearly that most of the work on tenotomy was carried out on mammalian muscles. The muscles of other animals and particularly the reptilian ones have totally been ignored. In addition, the reported results have also demonstrated a large variety of variations and contradictions. Since it has been demonstrated earlier [1] that there are differences in the contractile behavior of reptilian skeletal muscles from those of other animals, the present study was carried out to determine the effects of tenotomy on the skeletal muscle of uromastix.

## Materials and methods

Both the sexes of the reptile, *Uromastix hardwickii* were obtained from the desert area in the interior of Sind, Pakistan. The experiments were performed on the gastrocnemius muscles of both the hind limbs and isometric tensions were recorded on Universal Oscillograph from Harvard Appartus Ltd., (UK). Generally, the left gastrocnemius muscles were tenotomized for 7 days while the right ones were treated as controls.

*1. Tenotomization*

For this purpose, the animals were anaesthetized by injecting 1 ml of 2% xylocaine below the sacral region of spinal cord, in the gluteal muscle. This procedure kept the animals calm during tenotomization. The anaesthetized animal was fixed on the dissection table with its hind limbs in the stretched position. A small incision was then made in the skin just above the Achilles tendon at the lateral side of the limb and the achilles tendon was exposed. A watch makers forcep was then inserted beneath the tendon in order to separate it from the connective tissues. A piece of almost 0.5 to 1 cm of the tendon was then cut off an the wound was cleaned with ethyl alcohol which was later sprinkled with cicatrin powder. The exposed skin was then stitched and furacin cream was occasionally applied to avoid infections during the healing process.

At the end of 7 days, the animals were decapitated and the method of decapitation and dissection for isolating the muscle was the same as reported earlier [1]. The bathing medium used during experimentation was the reptilian buffer solution described elswhere [11].

*2. Tension Recordings*

The isometric twitch and tetanus were recorded and used to measure the various parameters, according to the method described previously [15, 1, 2].

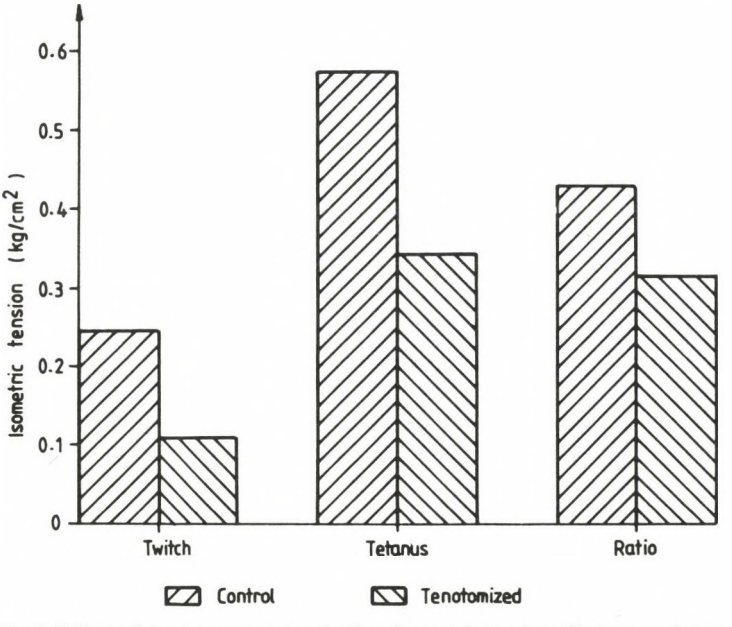


*Fig. 1.* Effect of short-term tenotomization. Isometric tension. Gastrocnemius muscle.

## Results

The results regarding the tension parameters demonstrated that the twitch and tetanic tensions and twitch/tetanus ratios obtained from seven days tenotomized muscles were 55%, 40% and 26% lesser respectively when compared with their respective controls (Fig. 1). Statistically, these differences between the control and tenotomized muscles were significant.

Similarly, the results of the time dependent tension parameters, i.e. rate of rise in twitch and tetanus and % of maximum tetanic tension (Po/mS), obtained from the tenotomized muscles were found to be 59% lesser in twitch, 50% lesser in tetanus and 27% lesser in Po/mS as compared to their respective controls (Fig. 2). These difference were also statistically significant ($p < 0.005$).

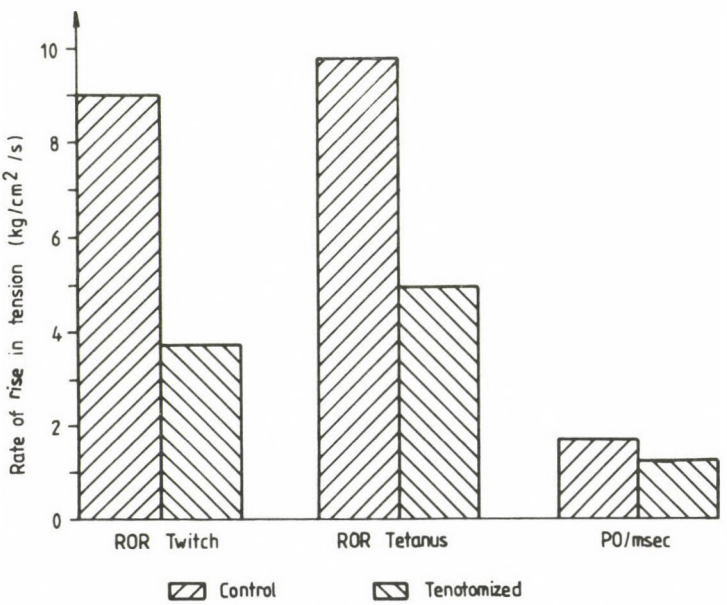


*Fig. 2.* Effect of short-term tenotomization. Rate of rise in tension. Gastrocnemius muscle

On the contrary, most of the time dependent parameters, i.e. twitch contraction and twitch & tetanus half relaxation times, and twitch/tetanus half relaxation time ratios and the peak duration in twitch were slightly lesser in tenotomized muscles and non-significant (Table I). However, the duration of active state in twitch had decreased by about 21% in the tenotomized muscles and this decrease was significant ($p < 0.05$).

**Table I**

*A comparison of time dependent parameters measured from twitch and tetanus records obtained from 7 days tenotomized and their control gastrocnemius muscles of uromastix*

| Parameters | Time periods (Mean ± S. E.) | | p |
|---|---|---|---|
| | Control | Tenotomization | |
| I. Time dependent parameters (s), | | | |
| Twitch contraction time | 0.065 ± 0.002 (7) | 0.060 ± 0.003 (8) | ($p > 0.05$) |
| Twitch half relaxation time | 0.042 ± 0.003 (5) | 0.036 ± 0.003 (6) | ($p > 0.05$) |
| Tetanus half relaxation time | 0.081 ± 0.005 (6) | 0.076 ± 0.004 (8) | ($p > 0.05$) |
| Twitch tetanus half relaxation ratio | 0.620 ± 0.115 (7) | 0.565 ± 0.050 (8) | ($p > 0.05$) |
| II. Durations in twitch (ms), | | | |
| Twitch peak duration | 18.00 ± 4.550 (7) | 24.000 ± 5.150 (8) | ($p > 0.05$) |
| Duration of active state | 22.71 ± 1.924 (7) | 17.900 ± 2.280 (8) | ($p < 0.05$) |

## Discussion

The results obtained during the present investigation demonstrated clearly that the contractile activity, i.e. isometric twitch and tetanic tensions of the gastrocnemius muscles had decreased significantly when the muscles were tenotomized or deprived of their tendon of insertion. These findings in uromastix were similar to those reported for the cat muscles [9], for the rats [21] and also for rabbits [7, 3]. Similar results were also obtained in uromastix during isotonic studies [13]. It has previously been suggested that, in addition to the deprived influence of the golgi tendon organ, tenotomization also effected the muscle fiber architecture, specially the composition of contractile components and a dispersion of the sarcomeres [18]. In addition, an alteration in the plasma membrane has also been reported following tenotomization [4]. Our results of twitch/tetanus ratio moreover, showed significantly lesser values in the tenotomized muscles, representing that the elasticity of the gastrocnemius muscle was also affected by tenotomization. This view is based upon the earlier observation that twitch/tetanus ratio is a valid measure of muscle elasticity [10]. It means that not only the contractile but non contractile elements were also effected after 7 days of tenotomization. It is therefore, suggested that the tenotomized gastrocnemius muscles of uromastix used during the present investigation might have undergone some morphological changes, probably in their contractile as well as non contractile components. This opinion has further been strengthened by our observations of the duration of active state which showed a 21% decrease in the tenotomized muscles. Since the duration of active state has been suggested to be directly associated with

the availability of free ionic calcium [14, 16, 17], we conclude that the myofibrils in the tenotomized muscles, were probably unable to get the sufficient quantity of sarcoplasmic $Ca^{++}$ for the contractile process. However, the suspected morphological changes and the non availability of sufficient quantities of calcium have yet to be confirmed in tenotomized muscles of uromastix.

The results of the rate of rise of tension in twitch, tetanus and Po/mS represented significantly lesser values in the tenotomized muscles (Fig. 2). Other investigators [7], in their experiments on the tenotomized muscles of rabbit, have also reported a similar decrease in maximum rate of rise in tetanic tension. However, contradictory to these investigators [7], Noreldeen [13] observed no change in the rate of rise in isotonic tensions produced by the tenotomized gastrocnemius muscles of uromastix. In addition to these two contradictory results, others [19] have shown a decrease in $Ca^{++}$ activated myofibriliar ATPase activity and a decrease in the succinate dehydrogenase enzyme after tenotomization in the rat soleus muscles. We have thus, no doubt in saying that tenotomization of the gastrocnemius muscles of uromastix produced more or less similar effects on the isometric contraction behaviour as was observed in other animals. However, our suggestion is that tenotomization probably produced its effect indirectly on the degree of cross bridge interaction and the rate at which the cross bridges interacted in the presence of $Ca^{++}$ ions. In addition, there could have also been an involvement of the presence of a low titre of myofibrillar ATPase enzyme. In our opinion, a 33% prolongation in twitch peak duration in our tenotomized muscles, alongwith a lesser rate of rise, indicated that although $Ca^{++}$ was being released slowly from the sarcoplasmic reticulum, this calcium was not being resequestered back rapidly.

A non-significant decrease in twitch contraction and half relaxation time values in our tenotomized gastrocnemius muscles were however, analogous to the results of some workers [8]. They have also reported no change in the time dependent parameters of tenotomized plantaris muscles of rat although they observed significant changes in these parameters in soleus muscles of the same animal. Similarly, it has also been reported [6] that tenotomization was uneffective in modifying the dynamic properties of the tenotomized-denervated rat soleus muscles.

In view of these findings, we suggest that the observed differences in the effects of tenotomization on the time dependent parameters in various animals either represent procedural differences on the differences in the response on different muscles to tenotomization.

## REFERENCES


1. Azeem, M. A., Shaikh, H. A.: Correlation between the anatomical and mechanical characteristics of gastrocnemius and sartorius muscles of *Uromastix hardwickii*. Acta Biol. Caraco. Zool. **29**, 105–114 (1987).
2. Azeem, M. A., Shaikh, H. A.: Seasonal variations in the contractile behaviour of gastrocnemius muscles of *Uromastix hardwickii*. Acta Physiologica Hungarica 77 (2), 159–168 (1991).
3. Bagust, J.: The effect of tenotomy upon the contraction characteristics of motor units in rabbit soleus muscles. J. Physiol. **290**, 1–10 (1979).
4. Baker, J. H., Baldwin, K. M.: Changes in membrane structure following tenotomy of the rat soleus muscle. Muscle and Nerve **5**, 222–225 (1982).
5. Beranek, R., Hnik, P.: Long term effect of tenotomy on spinal monosynaptic response in the cat. Science, **130**, 547–573 (1959a).
6. Betto, D. D., Midrio, M.: Combined effect of tenotomy and denervation on the dynamic properties of soleus muscle of the rat. Arch. Sci. Biol. **62** (1–4), 31–40 (1978).
7. Buller, A. J., Lewis, D. M.: Some observations on the effect of tenotomy in the rabbits. J. Physiol. **178**, 326–342 (1965).
8. Dasse, K. A., Chase, D., Burke, D., Ullrick, W. C.: Mechanical properties of tenotomized and denervated tenotomized muscle. Amer. J. Physiol. **241** (Cell Physiol. 10), C150–C153 (1981).
9. Eccles, J. C.: Investigation on muscle atrophies arising from disuse and tenotomy. J. Physiol. **103**, 253–266 (1944).
10. Huddart, H.: The Comparative Structure and Function of Muscle. First Ed. Pergamon Press, Oxford (1975).
11. Khalil, F., Messeih, A.: Water content of desert adapted reptile and mammals. J. Exp. Zool. **125**, 407–417 (1954).
12. McMinn, R. M. H., Vrbova, G.: Morphological changes in red and pale muscles following tenotomy. Nature **159**, 509 (1962).
13. Noreldeen, A. S. S.: Effect of tenotomy on the mechanical contraction properties of uromastix gastrocnemius muscles. Unpublished results (1992).
14. Shaikh, H. A., Saify, Z. S., Padsha, S. M.: The denervated muscles: A Review. J. Sci. Kar. Univ. **3 (1 & 2)**, 1–22 (1974a).
15. Shaikh, K. N., Shaikh, H. A., Siddiqui, P. Q. R., Padsha, S. M.: The temperature dependent contractile properties of normal and denervated skeletal muscle. Nat. Sci. **1**, 16–32 (1979a).
16. Shaikh, K. N., Shaikh, H. A., Siddiqui, P. Q. R., Padsha, S. M.: Effect of temperature on the duration of active state in normal and denervated skeletal muscles. Nat. Sci. **1**, 33–40 (1979b).
17. Shaikh, H. A.: Changes in some of the properties of muscle membrane produced by chronic denervation in rat diaphragm. (Unpublished Results).
18. Sjozsa, L., Balint, B. J., Vandor, E.: Changes in the contractile material of human skeletal muscle following tendinous injury. Acta. Physiol. Acad. Sci. Hung. **53** (3), 299–310 (1979).
19. Talesara, C. L., Jasra, P. K.: Response of rat soleus muscle to tenotomy: A correlative histochemical and biochemical study. Indian J. Exp. Biol. **22** (9), 467–470 (1984).
20. Tomanek, R. J., Cooper, R. R.: Ultrastructural changes in tenotomized fast and slow-twitch muscle fibers. J. Anat. **113**, 409–424 (1972).
21. Walker, S. M., Schrodt, G. R., Truong, X. Y. T., Wall, E. J.: Electron microscope study of sarcoplasmic reticulum and myofilaments of tenotomized rat muscle. Amer. J. Physiol. Med. **4** 176–192 (1965).

*Acta Physiologica Hungarica, Volume 81 (3), pp. 309–316 (1993)*

# MECHANICAL RESPONSE OF LIZARD SKELETAL MUSCLES TO DISUSE:
## II. EFFECT OF SHORT-TERM DENERVATION

N. SHAHINA, M. ABDUL AZEEM, S. ARIFA, Khairunnisa SHAIKH*, Hilal A. SHAIKH

NEUROMUSCULAR PHYSIOLOGY UNIT, DEPARTMENT OF PHYSIOLOGY, AND
*DEPARTMENT OF PHARMACOLOGY, FACULTY OF PHARMACY, UNIVERSITY OF KARACHI, KARACHI, PAKISTAN

Received August 19, 1992
Accepted December 2, 1992

The gastrocnemius muscles of Uromastix hardwickii were used to determine the effects of the absence of neural influence on them. For this purpose, the muscles were denervated for 7 days and were used to record isometric twitch and tetanus. The contraction parameters thus obtained from the denervated muscles were then compared with their own controls. The isometric tensions and time dependent tension parameters were significantly lower in the denervated muscles. The time dependent parameters, peak duration in twitch and duration of active state in twitch were however, found to be unaffected by short-term denervation with the exception of twitch/tetanus half relaxation time ratio, which was significantly higher in the denervated muscles. The denervation effects observed on the mechanical contraction behaviour of the gastrocnemius muscle have been discussed in terms of electrical excitation, excitation – contraction coupling and cross bridge interaction.

**Keywords**: disuse, denervation, isometric tensions, time dependent parameters

Mechanical contraction behaviour of denervated muscles have been studied by a number of workers to demonstrate the effect of disuse on the contractile apparatus of these muscles. For this purpose, the skeletal muscles of different animals have been denervated for different time periods [9, 12, 14, 15, 16, 17, 18, 19, 20 and 21]. In this connection, the mechanical contraction parameters of the denervated muscles have always been compared with their own controls to evaluate the changes occurring due to the cessation of nerve impulses. By examining these changes, the role of the so-called 'trophic influence' has been usually ascertained.

Correspondence should be addressed to
M. Abdul AZEEM,
Neuromuscular Physiology Unit,
Department of Physiology,
University of Karachi,
Karachi – 75270, Pakistan

*Akadémiai Kiadó, Budapest*

In various studies, different magnitudes of denervation effects have been associated with the denervation periods, i.e. the 7 days denervated rat diaphragms have been shown to exhibit lesser mechanical activity in comparison with their controls [19]. Similarly, Mothers [12] have also shown lesser tensions in the denervated rat diaphragms. However, contradictory results have also been reported [5], demonstrating a faster speed of shortening and rate of rise in tension along with a decrease in contraction time and twitch/tetanus ratio in 7 to 8 months denervated soleus muscles of rat. Other studies [11] have also demonstrated a decrease in contraction and relaxation times and in the rate of isometric tension development of denervated muscles. Similarly, a prolongation of time dependent parameters has been reported in denervated external digitorum longus (EDL) and soleus (SOL) muscles of rat [7] and in the denervated EDL and SOL muscles of the guinea pigs [6]. In amphibians, toad sartorius muscles were used for long-term denervation [10] and no change has been reported in the time dependent parameters along with lesser tensions after denervation of these muscles. Similarly, no change has been reported [13] in the time dependent parameters of denervated soleus muscles of rat. These conflicting results regarding the denervation effects in various animals compelled us to study the mechanical contraction properties of denervated gastrocnemius muscles of the lizards, Uromastix *hardwickii*.

## Materials and methods

### *Animal*

The Uromastix *hardwickii* is a cold blooded lizard which is mostly found in the hot desert areas of tropical regions. Both the sexes of this animal, weighing from 195–500 gms, were used. It possesses scales on the surface of its skin which provide protection against water evaporation.

### *Denervation Procedure*

Prior to denervation, the animal length and weight was recorded and then it was anaesthetized by injecting 1 ml of 2% xylocaine according to the method described earlier [1]. All the surgical instruments were sterilized by boiling. Later, the gastrocnemius muscle of right hind limb was denervated by making a small incision on the groove between upper adductor longus and lower gracialis muscles. Skin was then removed carefully to prevent any damage to the muscle and the peripheral blood vessels. The sciatic nerve was then exposed by lifting the upper adductor longus and lower gracialis muscles. Fine tipped forceps were then inserted beneath the sciatic nerve to get some space to section a piece of about 1.5 cm of the nerve. The wound was cleaned with cotton, soaked in ethylalcohol and cicatrin powder was sprinkled over it. After stitching the incised skin, furacin cream was applied over it to avoid infection. The animals were then kept in cages till they were used for experimentation. At the end of required denervation period, the animals were weighed and later decapitated to dissect out both the control and denervated muscles by following the method described earlier [2].

Recording of mechanical contractions, method of measurements used and the calculation procedures were exactly the same as reported previously by [17, 18]. The buffer solution used during the recording of mechanical activity was the same buffer solution as described for the reptilian tissues [8].

## Results

### *Isometric Tension Parameters*

The isometric twitch and tetanic tensions and twitch/tetanus ratios obtained from the denervated gastrocnemius muscles showed lesser values in comparison to their controls. This difference between the denervated muscles and their controls was about 32% in twitch, 23% in tetanus and 26% in the twitch/tetanus ratio and significant statistically (Fig. 1).

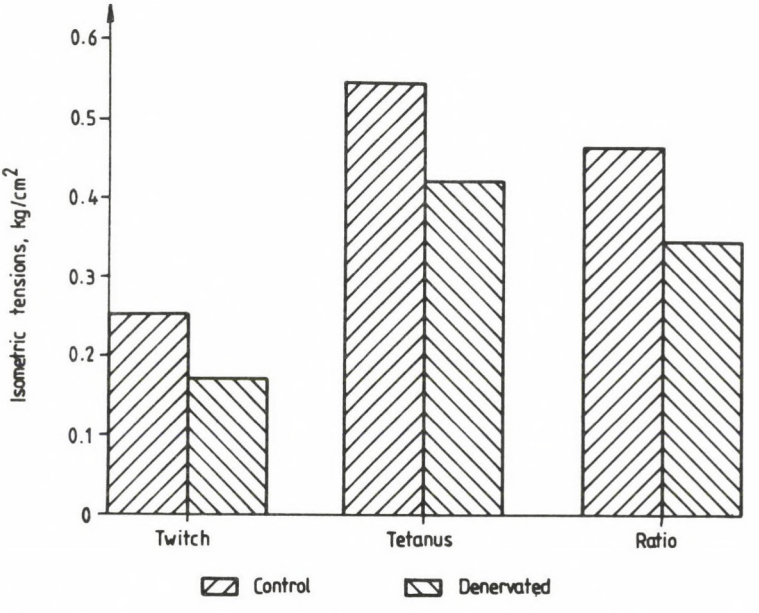


*Fig. 1.* Effect of 7-day denervation. Isometric tension. Gastrocnemius muscle

### *Time Dependent Tension Parameters*

The isometric twitch and tetanus records were also used for the measurements of the time dependent tension parameters. The maximum rate of rise in twitch and tetanic tensions and the rate of rise in tetanus as percent of the maximum tetanic tension (Po/mS) were also found to be significantly lesser in the denervation muscles, being 26%, 34%, and 25% smaller than their respective controls (Fig. 2).

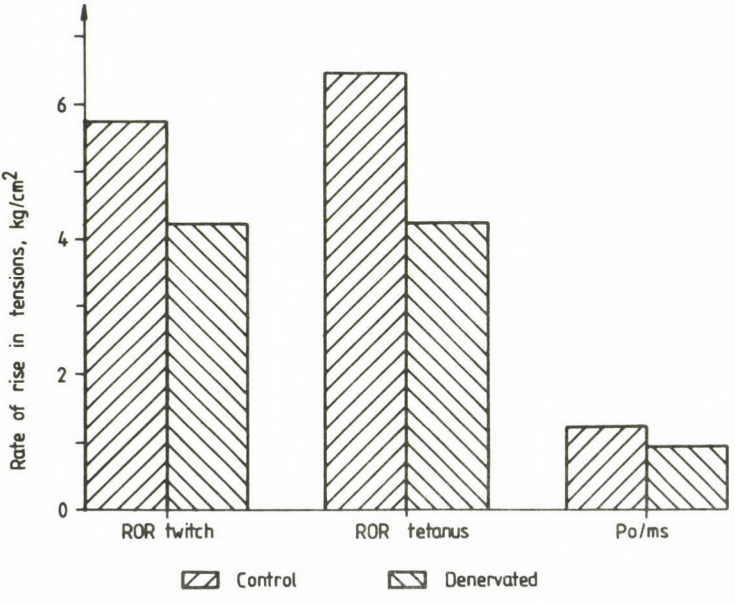


*Fig. 2.* Effect of 7-day denervation. Rate of rise in tension. Gastrocnemius muscle

*Time Dependent Parameters*

The time dependent parameters namely the twitch contraction times and twitch and tetanus half relaxation times were found to be non-significantly changed in the denervated muscles when compared with their own controls (Table I). On the contrary, the twitch/tetanus half relaxation time ratios were found to be 54% higher in the denervated muscles, being significant statistically ($p < 0.025$). However, the twitch peak durations and the duration of active state in twitch showed non-significant changes in the denervated muscles.

**Table I**

*A comparison of time dependent parameters measured from isometric twitch and tetanus records. These records were obtained from 7-day-denervated gastrocnemius muscles of uromastix*

| Parameters measured | Time periods (Mean ± S. E.) | | |
|---|---|---|---|
| | Control | Denervated | p |
| I. Time dependent parameters, (s) | | | |
| Twitch contraction time | 0.066 ± 0.002 (10) | 0.064 ± 0.002 (11) | ($p > 0.05$) |
| Twitch half relaxation time | 0.048 ± 0.002 (10) | 0.050 ± 0.004 (10) | ($p > 0.05$) |
| Tetanus half relaxation time | 0.074 ± 0.006 (8) | 0.066 ± 0.011 (6) | ($p > 0.05$) |
| Twitch/tetanus half relaxation ratio | 0.714 ± 0.057 (6) | 1.099 ± 0.148 (5) | ($p < 0.025$) |
| II. Duration in twitch, (ms) | | | |
| Peak duration in twitch | 18.00 ± 0.20 (12) | 18.00 ± 2.00 (12) | ($p > 0.05$) |
| Active state in twitch | 20.00 ± 1.39 (6) | 21.17 ± 0.95 (6) | ($p > 0.05$) |

## Discussion

The purpose of this study was to observe the effects of short-term denervation (7 days) on the contractile properties of the gastrocnemius muscles of uromastix. Our results of maximum isometric twitch and tetanic tensions and twitch/tetanus ratios obtained from 7 days denervated muscles showed significantly lesser values in comparison with their own controls. These findings in uromastix are similar to those observed in the rat diaphragm [19, 12]. The results of twitch/tetanus ratios have indicated that, unlike control muscles, the tetanic tension development in the denervated muscles were greater in proportion than the twitch tensions. It means that in the control muscles, maximum possible number of muscle fibers were stimulated during single twitch elicitation. On the contrary, in the denervated muscles, this single twitch elicitation had either stimulated only a few muscle fibers, or the tetanic current provided to the denervated muscles was unable to fully stimulate the partially degenerating muscle fibers, resulting in a greater twitch/tetanus ratio in the denervated muscles.

The results of the maximum rate of rise in tension obtained from denervated muscles showed 26%, 34% and 25% lesser values for the rate of rise in twitch, tetanus and $P_o$/mS, respectively. Our results of the rate of rise in tension were analogous to the previous findings [11] reported for mammalian muscles. However, the decreases in the rate of rise of tensions and % $P_o$/mSec in the denervated muscles was most probably due to a change in the excitation contraction coupling

mechanism as has also been suggested by [4] for the denervated rat extensor digitorium longus and soleus muscles. It is probable that the influences of motor nerve usually excercized on various aspects of excitation contraction coupling as suggested for the mammalian muscles [4], have also been changed by denervation in uromastix muscles. Obviously, a possibly slow propagation of action potentials through sarcolemma and sarcoplasmic tubules to the interior of the fiber along with a slow release of free ionic calcium might have decreased the rate of rise in tensions in the denervated muscles of this animal. Since the rate of rise in tension is a valid measure of muscle speed [3], this factor, alongwith other possible changes that short-term denervation might have produced in the gastrocnemius muscles of uromastix, were responsible for the observed decrease in the speed of tension generation in these muscles.

The time-dependent parameters in the denervated muscles were not affected significantly. These results suggested the period of interaction between the cross bridges and their detachment during relaxation were similar in both the denervated muscles and their controls. These results were similar to those reported earlier [10] where no changes were shown to occur in the isometric twitch time to peak, half relaxation times and twitch/tetanus ratio in the long term denervated toad sartorius muscles. However, the above authors have related these results to their previous findings where they observed no change in the action potentials of the amphibian denervated muscles. In our experiments however, we are unable to accept lack of change in the action potentials since we have obtained significant fall in the rate of rise of tension in the denervated muscles, which was unable to raise the contraction time in them. We suggest that short-term denervation has probably affected both the immediate availability of calcium for contraction and the availability of cross bridges for a prolonged interaction to produce greater force during contraction. However, a non-significant denervation change in the duration of active state and peak twitch duration can not be explained presently. It may however, be proposed that although, the short-term denervation in our gastrocnemius muscles might have reduced the magnitude of mechanical act, it was unable to reduce the durations for which the mechanical acts were excercized during muscle contraction. Our results of twitch/tetanus half relaxation time ratios represented 54% significantly higher values for the denervated muscles. We attribute this difference to the rapid relaxation during tetanus as compared to the slow relaxation when twitch was elicited. These results have suggested that denervation had not influenced relaxation of the muscles after tetanization.

## REFERENCES


1. Arifa, S., Azeem, M. A., Shahina, N., Shaikh, K. N., Shaikh, H. A.: Mechanical response of lizard skeletal muscle to disuse: II. Effect of short term tenotomization. Acta Physiol. Hungarica. **81**, 309–315 (1993).
2. Azeem, M. A., Shaikh, H. A.: Correlation between the anatomical and mechanical characteristics of gastrocnemius and sartorius muscles of Uromastix hardwickii. Acta Biol. Coraco. Zool. **29**, 105–113 (1987).
3. Buller, A. J., Lewis, D. M.: Some observations on the effect of tenotomy in the rabbit. J. Physiol. **178**, 326–342 (1965).
4. Dulhunty, A. F.: Excitation-contraction coupling and contractile properties in denervated rat extensor digitorum longus and soleus muscles. J. Muscle Res. Cell. Mot. **6 (2)**, 207–226 (1985).
5. Guth, L.: Physiological and histochemical properties of the soleus muscle after denervation and its antagonists. Expt. Neurol. **36**, 463–471 (1972).
6. Gutmann, E., Melichna, J. A.: Contractile and histochemical properties of denervated and reinnervated fast and slow muscles of newborn and adult guinea pigs. Physiol. Bohemoslov. **28 (1)**, 35–42 (1979).
7. Gutmann, H., Hanzlikova, M.: Compensatory hypertrophy of denervated muscle. Cesk. Physiol. **21**, 9–12 (1972).
8. Khalil, F., Messeih, A.: Tissue constituent of reptiles in relation to their mode of life: Lipid content. Comp. Biochem. Physiol. **6**, 171–174 (1962).
9. Lahrtz, H., Lullman, H., Reis, H. B.: Über den Einfluss von Kalium und Carbachol auf die Calcium-Abgabe normaler und chronisch denervierter Ratten. Pflüg. Arch. **297**, 10–18 (1967).
10. Mcdonagh, M. J. N., Lewis, D. M., Moller, S. W.: Mechanical properties of denervated amphibian muscles. Comp. Biochem. Physiol. A Comp. Physiol. **84 (1)**, 123–126 (1968).
11. Melichna, J., Gutmann, E.: Stimulation and immobilization effect on contractile and histochemical properties of denervated muscle. Pflügers Arch. Eur. J. Physiol. **352 (2)**, 165–178 (1974).
12. Miledi, R., Slater, C. R.: Electron microscopic structure of denervated skeletal muscle. Proc. Soc. London. Ser. L. **174**, 253–269 (1969).
13. Narusawa, M.: Change in fiber type in partially denervated soleus muscle of the rat. Tokai. J. Exp. Clin. Med. **10**, (5), 508 (1985).
14. Ranatunga, K. W.: Changes produced by chronic denervation in the temperature-dependent isometric contractile characteristics of rat fast and slow twitch skeletal muscle. J. Physiol. **273**, 255–262 (1977).
15. Shaikh, H. A., Padsha, S. M.: Studies on calcium fluxes in denervated muscles: Effect of fiber damage and poisoning on mitochondrial uptake and release. J. Sci. Univ. Kar. **2 (2)**, 181–194 (1973).
16. Shaikh, H. A., Saify, Z. S., Padsha, S. M.: The denervated muscle: A Review. J. Sci. Univ. Kar. **3 (1 & 2)**, 1–22 (1974).
17. Shaikh, K. N., Shaikh, H. A., Siddiqui, P. Q. R., Padsha, S. M.: The temperature dependent contractile properties of normal and denervated skeletal muscle. Nat. Sci. **1**, 16–32 (1979a).
18. Shaikh, K. N., Shaikh, H. A., Siddiqui, P. Q. R., Padsha, S. M.: Effect of temperature on the duration of active state in normal and denervated skeletal muscles. Nat. Sci. **1**, 33–40 (1979b).

19. Shaikh, K. N., Shaikh, H. A.: Effect of denervation period on various mechanical parameters of twitch and tetanus in rat diaphragm. J. Pharm. Univ. Kar. **5**, 113–127 (1987).
20. Sola, O. M., Martin, A. W.: Denervation hypertrophy and atrophy of the hemidiaphragm of the rat. Amer. J. Physiol. **172**, 324–332 (1953).
21. Stewart, D. M.: Changes in the protein composition of muscles of the rat in hypertrophy and atrophy. Biochem. J. **59**, 553–558 (1955).

# INSTRUCTIONS TO AUTHORS

*Form of manuscript*

Two complete copies of the manuscript including all tables and illustrations should be submitted. Manuscripts should be typed double-spaced with margins at least 3 cm wide. Pages should be numbered consecutively.

Manuscripts should include the title, authors' names and short postal address of the institution where the work was done.

An abstract of not more than 200 words should be supplied typed before the text of the paper. The abstract should be followed by (no more than) five key-words.

*Abbreviations* should be spelled out when first used in the text. *Drugs* should be referred to by their WHO code designation (Recommended International Nonproprietary Name): the use of proprietary names is unacceptable. The *International System of Units* (SI) should be used for all measurements.

*References*

References should be numbered in alphabetical order and only the numbers should appear in the text [in brackets]. The list of references should contain the name and initials of all authors (the use of et al. instead of authors' name in the reference list is not accepted): for journal articles the title of the paper, title of the journal abbreviated according to the style used in Index Medicus, volume number, first and last page number and year of publication, for books the title followed by the publisher and place of publication.

Examples:

Székely, M., Szelényi, Z.: Endotoxin fever in the rat. Acta physiol. hung. **53,** 265–277 (1979).

Schmidt, R. F.: Fundamentals of Sensory Physiology. Springer Verlag, New York–Heidelberg–Berlin 1978.

Dettler, J. C.: Biochemical variation. In: Textbook of Human Genetics, eds Fraser, O., Mayo, O., Blackwell Scientific Publications, Oxford 1975, p. 115.

*Tables and illustrations*

Tables should be comprehensible to the reader without reference to the text. The headings should be typed above the table.

Figures should be identified by number and authors' name. The top should be indicated on the back. Their approximate place should be indicated in the text. Captions should be provided on a separate page.

*Proofs and reprints*

Reprints and proofs will be sent to the first author unless otherwise indicated. Proofs should be returned within 48 hours of receipt. Fifty reprints of each paper will be supplied free of charge.

# Acta Physiologica Hungarica

VOLUME 81, NUMBER 4, 1993




Akadémiai Kiadó, Budapest

ACTA PHYSIOL. HUNG. APHDUZ, 81(4) 317–424 (1993) HU ISSN 0231—424X

# ACTA PHYSIOLOGICA HUNGARICA

## A PERIODICAL OF THE HUNGARIAN ACADEMY OF SCIENCES

*Acta Physiologica Hungarica* publishes original reports of studies in English.
*Acta Physiologica Hungarica* is published in one volume (4 issues) per year by

AKADÉMIAI KIADÓ

Publishing House of the Hungarian Academy of Sciences

H-1117 Budapest, Prielle Kornélia u. 19—35.

Manuscripts and editorial correspondence should be addressed to

*Acta Physiologica Hungarica*

H-1445 Budapest, P.O. Box 294, Hungary

Editor: P. Bálint

Managing editor: J. Bartha

*Subscription information*

Orders should be addressed to

AKADÉMIAI KIADÓ

H-1519 Budapest, P.O. Box 245

Subscription price for Volume 81 (1993) in 4 issues US$ 92.00, including normal postage, airmail delivery US$ 20.00.

*Acta Physiologica Hungarica* is abstracted/indexed in Biological Abstracts, Chemical Abstracts, Chemie-Information, Current Contents-Life Sciences, Excerpta Medica database (EMBASE), Index Medicus, International Abstracts of Biological Sciences

CONTENTS

PHYSIOLOGY – PATHOPHYSIOLOGY

PRINTED IN HUNGARY

Akadémiai Kiadó és Nyomda Vállalat, Budapest

*Acta Physiologica Hungarica, Volume 81 (4), pp. 317–326 (1993)*

# CHANGES OF LIPID PEROXIDATION PARAMETERS IN DOGS WITH ALLOXAN DIABETES

P. VAJDOVICH, T. GAÁL, A. SZILÁGYI

DEPARTMENT AND CLINIC OF INTERNAL MEDICINE,
UNIVERSITY OF VETERINARY SCIENCE, BUDAPEST, HUNGARY

Received August 25, 1992
Accepted September 13, 1992

Diabetic human patients and laboratory animals show abnormities which can be observed also in enhanced lipid peroxidation (LPO) induced *in vitro*. It seemed to be necessary to demonstrate the presence of these processes also in dogs with experimentally induced alloxan diabetes.

In a 5-day experiment, five 1 to 5-year-old dogs of mixed sex were examined. Blood samples were taken before the intravenous administration of 60 mg alloxan/kg body mass and then daily for a period of 5 days. After the administration of alloxan, the dogs became depressed and lost their appetite. Their urine contained varying concentrations of glucose detectable with a test strip. As compared to the physiological values, *blood glucose* concentration increased considerably throughout. *Alanine aminotransferase* (*ALT*) *enzyme activity* underwent an 8-fold increase by the 24th hour; subsequently, it remained practically unaltered. The *malonyldialdehyde* (*MDA*) concentration of red blood cell (RBC) haemolysate also rose with respect to the basal values. *Glutathione-peroxidase* (*GSH–Px*) activity increased only transiently, up to the second day of the experiment; subsequently, its activity dropped below the basal values. Similar changes were found in *catalase* activity, while the activity changes of *superoxide dismutase* (*SOD*) were identical in tendency to the above ones; in fact, it hardly showed any alterations.

Besides the severe pancreatic and liver damage caused by alloxan, increased MDA production in the RBC haemolysate indicated enhanced peroxidation of polyunsaturated fatty acids, i.e. intensification of the LPO processes. The increase of GSH–Px and catalase activity, followed by their decrease was suggestive of changes in the enzymatic defence mechanism acting against free radicals.

**Keywords:** diabetes mellitus, dog, alloxan, lipid peroxidation parameters, blood

Correspondence should be addressed to
Tibor GAÁL
Clinic of Internal Medicine, University of Veterinary Sciences
H–1078 Budapest, István u. 2, Hungary

*Akadémiai Kiadó, Budapest*

Numerous studies have demonstrated that in certain organs and cells of diabetic humans abnormities occur which can be observed also in enhanced lipid peroxidation (LPO) induced *in vitro* [5, 10, 14].

Red blood cell (RBC) life span has been found to be shorter [19, 23], erythrocyte aggregation enhanced [29, 30], the organisation of red cell membrane phospholipids altered [32], and erythrocyte adherence to endothelial cells increased [32] in patients suffering from diabetes mellitus. *In vitro* experiments with human RBC and *in vivo* studies using rat and rabbit RBC have shown that similar changes occur in connection with increased membrane lipid peroxidation [12, 13, 15, 16, 33].

Activity and concentration changes of some enzymes (e.g. glutathione-peroxidase, GSH-Px; superoxide dismutase, SOD; catalase) and some substrates (e.g. hydrogen peroxide, certain peroxi-fatty acids, malonyldialdehyde and glutathione) indicate the presence of LPO processes in the organism [4]. These enzymes and substrates have been shown to change also in diabetes mellitus, proving that free radicals exert their effect in the organism in this disease [5, 14, 22]. E.g., RBC from 25 to 35-year-old human diabetics have been shown to possess significantly enhanced GSH-Px and reduced SOD activity [22]. Other investigations have indicated that the concentration of MDA, one of the end-products of LPO processes, is significantly elevated in the erythrocyte membrane of diabetics [14].

Most of the investigations mentioned above have been carried out using human, rat and rabbit RBC. Few data are available, however, on the LPO parameters of diabetic dogs, though this is the species in which spontaneous diabetes mellitus occurs most frequently of all animals.

Before investigating spontaneous diabetes mellitus of dogs in this respect, we wished to study different parameters of the LPO processes in diabetes induced with alloxan. The diabetogenic action of alloxan is thought to involve redox cycling between alloxan and its reduced form, dialuric acid, generating – under aerobic conditions – oxygen free radicals which damage, among others, the insulin-producing beta cells of the pancreas [8]. Damage of the beta cells leads to reduced insulin secretion, secondary hyperglycaemia and further free radical generation [7, 10, 21, 34]. Although alloxan is *ab ovo* a free radical forming compound, the LPO processes induced by it can only partly be considered as its direct consequence. This is proved by the similar enzyme activities measured in the blood and organ homogenates of rats with alloxan diabetes and in the cells and organ samples of human patients with genuine diabetes mellitus. Thus, oxidative stress occurs in alloxan diabetes in the same way as in genuine diabetes [22].

Diabetes was induced in dogs and its effect on blood LPO parameters was studied in order to demonstrate that LPO changes occur in dogs similarly as in human diabetics, rats and rabbits.

## Materials and methods

*Experimental animals. Application of alloxan*

Five 1 to 5-year-old dogs of mixed sex (body mass: 9.0–29.5 kg) were selected for the 5-day experiment. Alloxan (alloxan monohydrate 98%, Aldrich Cat. No. 23.437–0; Merck Index: 11.281) was administered at a 200 g/l concentration (expressed for pure active ingredient), in a distilled water solution, in a single intravenous dose of 60 mg/kg body mass. This mode of application is similar to that used by others in dogs and in other species [6, 11, 28].

*Sampling*

The first blood samples (base values) were taken immediately before alloxan administration. Subsequently, further blood samples were collected from the *v. cephalica antebrachii* into heparinized blood sampling tubes. First, 1 ml blood was separated for SOD determination, diluted tenfold and haemolysed with distilled water. The remaining part of the blood samples was centrifuged at 2000 rpm for 10 min, then the blood elements were separated from the plasma. The RBC were washed with saline three times, then the washed RBC suspension was diluted tenfold and haemolysed with distilled water.

*Methods*

Glucose concentration was determined from the plasma by Trinder's enzymatic colorimetric method [31]. The activity of alanine aminotransferase (ALT, EC 2.6.1.2.) enzyme was also determined from the blood plasma, by a colorimetric method [27]. Of the LPO parameters, one of the end-products of polyunsaturated fatty acid peroxidation, malonyldialdehyde (MDA) reacting with thiobarbituric acid (TBA) was determined from RBC haemolysate by Placer's method [24]. The determination of glutathione peroxidase (GSH–Px, EC 1.11.1.9) was done from RBC haemolysate using glutathione, cumene hydroperoxide and Ellman's reagent, as described by Lawrence and Burk [19]. Catalase (Cat, EC 1.11.1.6) activity was also measured in the RBC haemolysate, by determination of hydrogen peroxide concentration by a direct UV technique [1]. Superoxide dismutase (SOD, EC 1.15.1.1) was determined from whole blood haemolysate by formazan-forming reaction in which the superoxide ion enters into reaction with nitrotetrazolium blue and forms a coloured end-product, formazan, which can be measured photometrically [20]. Glucose content of the urine was checked using a Bili-Labstix reagent strip (Ames).

The means and standard deviations (SD) of the obtained results were used for biometric calculations by analysis of variance, with the help of a SAS/SAT computer programme. The results are illustrated graphically, indicating the means and SD. The figures beside the columns are numerical values of the means. Columns found significantly ($P < 0.05$) different by analysis of variance are marked with different letters.

## Results

In the days following the administration of alloxan, the dogs became depressed lost their appetite, and varying amounts of glucose detectable with the test strip appeared in their urine.

*Blood glucose* concentration markedly increased from day to day, as compared to the physiological values (Fig. 1).

*ALT activity* had undergone an 8-fold increase already by the 24th hour (Fig. 2); then it did not change further during the subsequent three days.

*MDA concentration* of the blood haemolysate, indicative of the presence of TBA-reactive substances, significantly rose with respect to the base values (Fig. 3).

*GSH–Px activity* increased only transiently, up to the second day of the experiment. Subsequently, on days 3 and 4 it dropped below the basal values (Fig. 4).

Similar changes were found for *catalase activity*; however, though the mean values showed marked changes, the differences were not significant (Fig. 5).

*SOD activity* did not show significant differences either during the experiment (Fig. 6). Although its values tended to increase up to the 48th hour, from the third day they started to decrease.

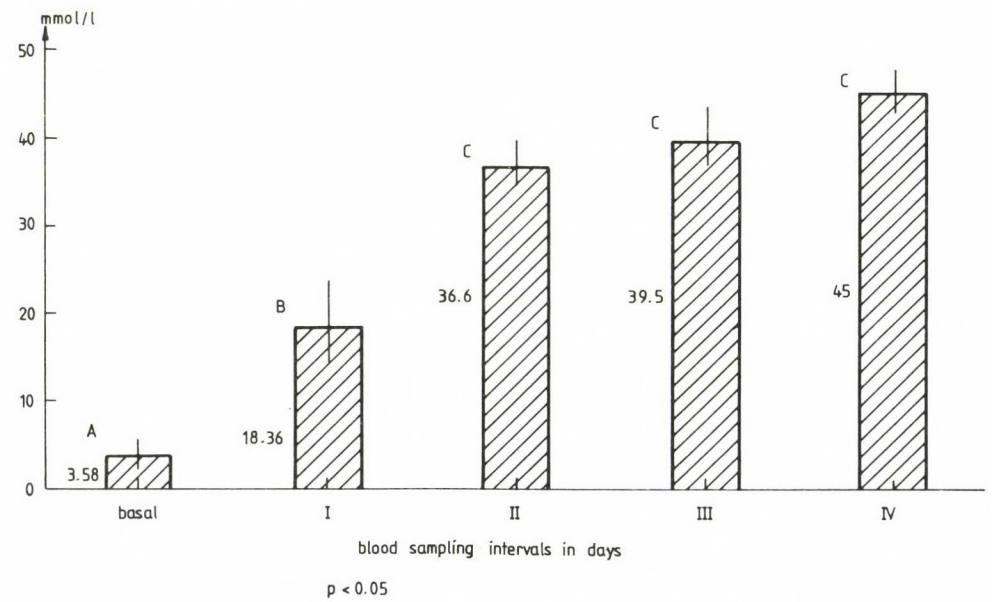


*Fig. 1.* Changes in blood glucose concentration of dogs following alloxan administration

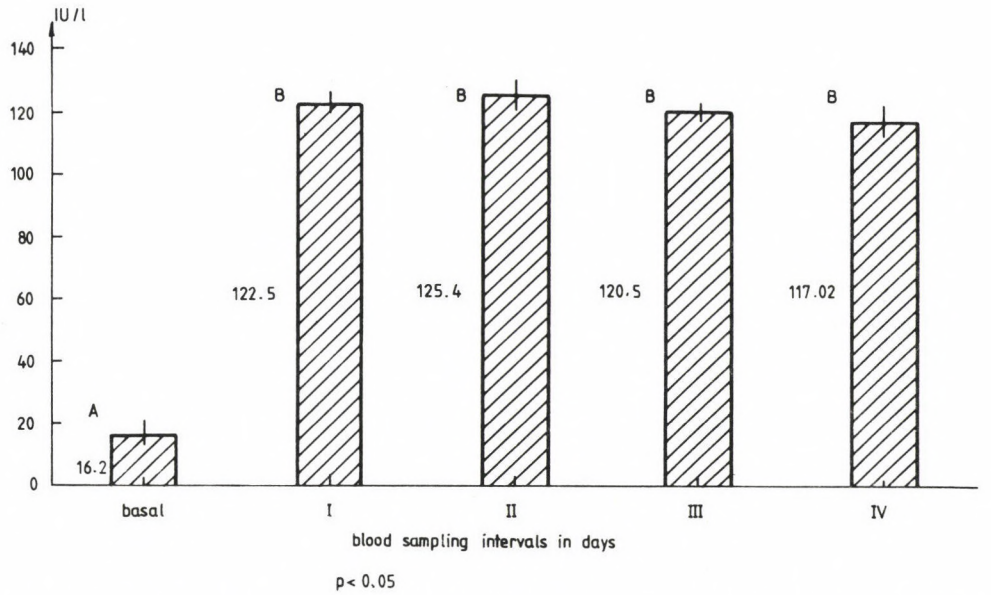


*Fig. 2.* Alanine aminotransferase (ALT) activity of the blood plasma in dogs following alloxan administration

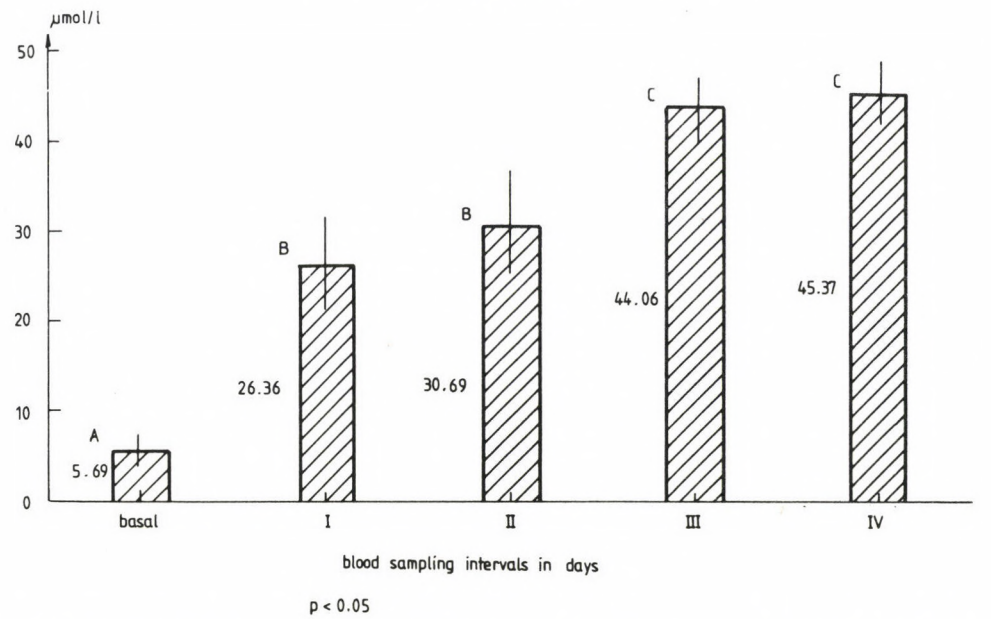


*Fig. 3.* Malonyldialdehyde (MDA) concentration of the red blood cell haemolysate in dogs following alloxan administration

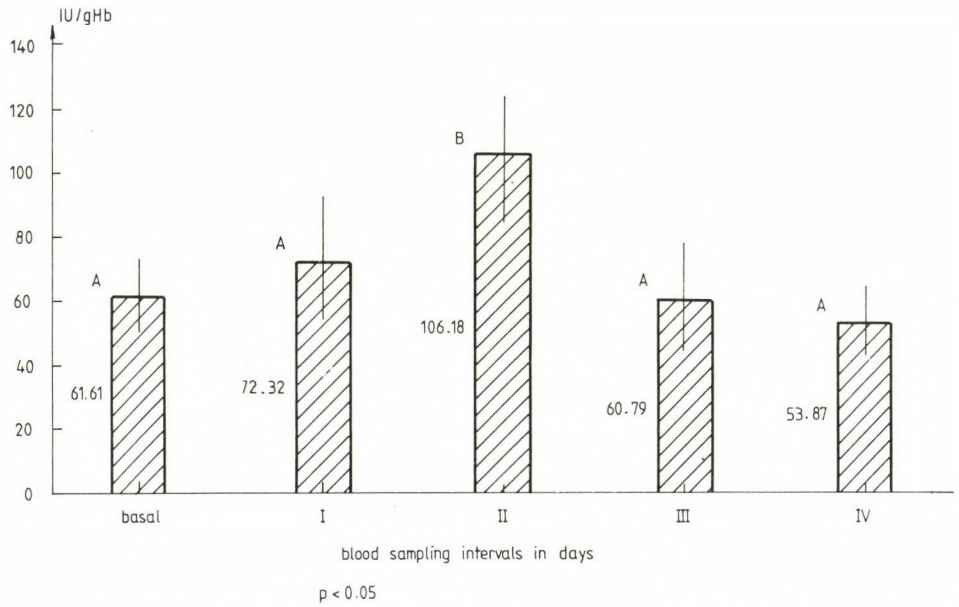


*Fig. 4.* Glutathione-peroxidase (GSH – Px) activity of the red blood cell haemolysate in dogs following alloxan administration

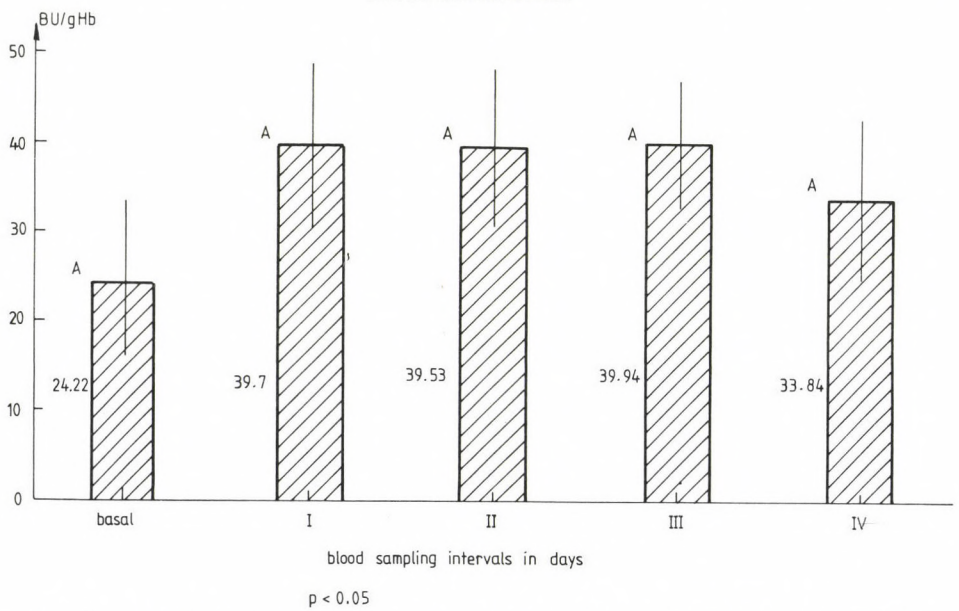


*Fig. 5.* Catalase activity of the red blood cell haemolysate in dogs following alloxan administration

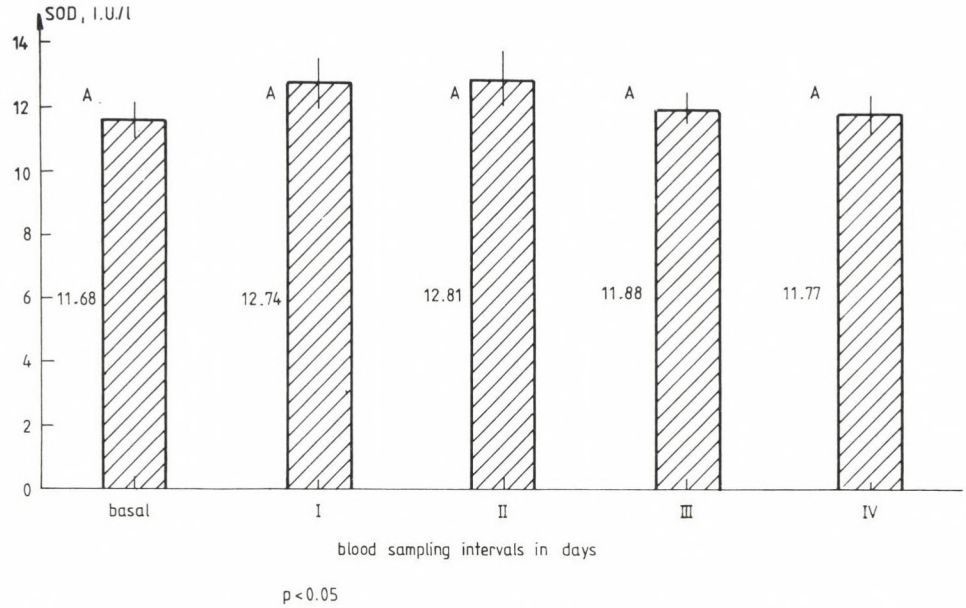


*Fig. 6.* Superoxide dismutase (SOD) activity of the whole blood haemolysate in dogs following alloxan administration

## Discussion

Elevated blood glucose concentration caused by the destruction of the insulin-producing beta cells of the pancreas and the increased activity of ALT, an enzyme considered to be liver-specific in dogs, proved the severe pancreato- and hepatotoxic effect of alloxan in the dogs used in this experiment. Regarding to the studies performed on diabetic humans, rats and rabbits [5, 13, 14, 17, 22], we think that the process causing changes in different LPO parameters in dogs was similar to the previously examined species. The elevated concentration of MDA, a marker of TBA-reactive compounds, in the RBC haemolysate indicated enhanced peroxidation of the polyunsaturated fatty acids. In addition to its elevated mean value, the high standard deviation of MDA observed 24–48 hours after alloxan administration indicated differences in the dogs, reaction to alloxan. The individual differences observed between dogs at that time became indistinct later, and the SD values again became similar to those of the base values.

The activity of GSH–Px, catalase and SOD tended to increase in the first two days of the experiment (however changes of SOD and catalase activity were not significantly different), suggesting enhanced activity of the enzymatic defence mechanism acting against free radicals, as it has been interpreted also by others [5,

22]. In the subsequent days, the activity of these enzymes decreased. This may be attributed to the fact that with the progression of alloxan toxicosis the free radicals ($O_2^-$, $H_2O_2$, etc.) generated by a chain reaction may have exhausted the defence mechanism, destroyed the enzymes and, in the case of GSH-Px, may have entered into direct reaction with reduced glutathione (GSH). As in the latter case GSH concentration may drop drastically, the oxidizing activity of GSH-Px may also have decreased. The reduction in enzyme activity may also have been caused by the fact that from the second day of the experiment the severely affected dogs hardly ate anything; the resulting nutrient deficiency may have hampered the generation of enzymes of protein nature.

Several studies have confirmed the role of free radicals and lipid peroxidation in genuine diabetes mellitus [5, 11, 17, 22]. The mechanism by which elevated blood glucose level induces enhanced LPO of erythrocyte membranes is not known in every detail yet. At the same time, recent *in vitro* studies have proved that glucose is able to enolize and, thus, reduce molecular oxygen also under physiological conditions; as a result, alpha-keto-aldehydes, hydrogen peroxide and free radicals arise as intermediary products [21, 34]. During that mechanism, oxygen free radicals are generated in excess of the antioxidant capacity of RBCs and damage RBC membrane phospholipids by peroxidation, induce MDA accumulation in the cells, and enhance the activity of the enzymes of the defence mechanism [2, 3, 7].

Recognition of the role of LPO processes in the pathogenesis of diabetes mellitus may offer new possibilities in the therapy of insulin dependent diabetes mellitus of dogs. Besides the classical antidiabetic intervention (the administration of insulin), antioxidants, e.g. butylated hydroxytoluene (BHT) as synthetic [11, 14] and *Bryonia alba* root extract as natural antioxidant [17], can be used as adjuvant therapy. SOD enzyme can also be used as part of the therapy against free radicals [9].

To confirm the above assumption, however, LPO processes and enzyme activities should be studied also in natural cases of diabetes mellitus in dogs similarly as described in this paper.

## REFERENCES

1. Beers, R. F., Sizer, I. W.: Spectrophotometric method for measuring the breakdown of hydrogen peroxide by catalase. J. Biol. Chem. **195**, 133-140 (1952).
2. Carrel, R. W., Winterbourn, C. C., Rachmilewitz, E. A.: Activated oxygen and haemolysis. Br. J. Haematol. **30**, 259-264 (1975).
3. Clark, I. A., Cowden, W. B., Hunt, N. H.: Free radical-induced pathology. Med. Res. Rev. **5**, 297-352 (1985).
4. Fehér, J., Vereckei, A.: Significance of free radical reactions in medicine (in Hungarian). Biogal Gyógyszergyár, Budapest, 1985.

5. Gandy, S. E., Buse, M. G., Crouch, R. K.: Protective role of superoxide dismutase against diabetogenic drugs. J. Clin. Invest **70**, September 650–658 (1982).
6. Godin, D. V., Wohaieb, S. A., Garnett, M. E., Goumeniouk, A. D.: Antioxidant enzyme alterations in experimental and clinical diabetes. Mol. Cell. Biochem. **84**, 223–231 (1988).
7. Goldner, M. G., Gömöri, G.: Studies on the mechanism of Alloxan diabetes. Endocrinology **35**, 241 (1944).
8. Halliwell, B., Gutteridge, M. C.: Oxygen toxicity, oxygen radicals, transition metals and disease. Biochem. J. **219**, 1–14 (1984).
9. Heikkila, R. A., Winston, B., Cohen, G., Barden, H.: Alloxan-induced diabetes – evidence for hydroxyl-radical as a cytotoxic intermediate. Biochem. Pharmacol. **25**, 1085–1092 (1976).
10. Holcenber, J. S., Roberts, J.: Enzymes as drugs. J. Wiley and Sons, New York, 1981.
11. Hunt, J. V., Dean, R. T., Wolff, S. P.: Hydroxyl radical production and autoxidative glycosylation: glucose autoxidation as the cause of protein damage in the experimental glycation as a model of diabetes mellitus and aging. Biochem. J. **256**, 205–212 (1988).
12. Ivanov, V. V., Vaseneva, I. V., Udintsev, N. A.: Lipid peroxidation in the liver of rats with alloxan diabetes (in Russian). Probl. Endorkrinol. (Moscow) **30**, 70–73 (1984).
13. Jain, S. K.: The accumulation of malonyldialdehyde, an end product of fatty acid peroxidation, can disturb aminophospholipid organization in the membrane bilayer of human erythrocytes. J. Biol. Chem. **259**, 3391–3394 (1984).
14. Jain, S. K.: In vivo externalization of phosphatidylserine and phosphatidylethanolamine in the membrane bilayer and hypercoagulability by the lipid peroxidation of erythrocytes in rats. J. Clin. Invest. **76**, 281–286 (1985).
15. Jain, S. K., McVie, R., Duett, J., Herbst, J. J.: Erythrocyte membrane lipid peroxidation and glycosylated hemoglobin in diabetes. Diabetes **38**, 1539–1543 (1989).
16. Jain, S. K., Mohandas, N., Clark, M., Shohet, S. B.: The effect of malonyldialdehyde, a product of lipid peroxidation, on the deformability, dehydration, and 51-Cr-survival of erythrocytes. Br. J. Haematol. **53**, 247–255 (1983).
17. Jones, R. L., Peterson, C. M.: Hematologic alteration in diabetes mellitus. Am. J. Med. **70**, 339–352 (1981)
18. Karagezian, K. G., Vartanian, G. S., Panosian, A. G.: Effect of an extract from the roots of bryony (Bryonia alba) on lipid peroxidation in the liver of rats with alloxan diabetes (in Russian). Bull. Eksp. Biol. Med. **92**, 35–37 (1981).
19. Lawrence, R. A., Burk, R. F.: Glutathione peroxidase activity in selenium-deficient rat liver. Biochem. Biophys. Res. Comm. **71**, 952–958 (1976).
20. Lehrman, M. L.: Reversible hematologic sequelae of diabetes mellitus. Ann. Intern. Med. **86**, 425–429.
21. Nishikimi, M., Rao, N. A., Yagi, K.: The occurrence of superoxide in the reaction of reduced phenazine methosulfate and molecular oxygen. Biochem. Biophys. Res. Comm. **46**, 849 (1972).
22. Mashino, T., Fridovich, I.: Mechanism of the cyanide-catalysed oxidation of alpha-ketoalcohols. Arch. Biochem. Biophys. **252**, 163–170 (1987).
23. Matkovics, B., Varga, S. I., Szabo, L., Witas, H.: The effect of diabetes on the activities of the peroxide metabolism enzymes. Horm. Metab. Res. **14**, 77–79 (1982).
24. Pescarmona, G. P., Bosia, A., Chigo, D.: Shortened red cell life span in diabetes: mechanism of hemolysis. In: Weatherall, D. J., Fiorelli, G., Gorini, S. (eds): Advances in Red Cell Biology. Raven Press, New York, 1982, pp. 391–397.
25. Placer, Y. A., Cushman, L., Johnson, B. C.: Estimation of product of lipid peroxidation (malonyldialdehyde) in biochemical systems. Anal. Biochem. **16**, 359–364 (1966).

26. Pryor, W. A.: Free Radicals in Biology. Vol. V. Academic Press, New York, 1982.
27. Reif, D. W., Samokyszyn, V. M., Miller, D. M., Aust, S. D.: Alloxan- and glutathione-dependent ferritin iron release and lipid peroxidation. Arch. Biochem. Biophys. **269**, 407–414 (1989).
28. Reitman, S., Frankel, S.: A colorimetric method for the determination of serum glutamic oxalacetic and glutamic pyruvic transaminases. Am. J. Clin. Path. **28**, 56–63 (1957).
29. Sano, H., Takahashi, K., Ambo, K., Tsuda, T.: Rates of blood glucose appearance and disappearance during hyperglycaemia induced by alloxan in sheep. Tohoku Journal of Agricultural Research **36**, 9–15 (1985).
30. Satoh, M., Imazumi, K., Bessho, T., Shiga, T.: Increased erythrocyte aggregation in diabetes mellitus and its relationship to glycosylated haemoglobin and retinopathy. Diabetologia **27**, 517–521 (1984).
31. Schmid-Schönbein, H., Volger. E.: Red-cell aggregation and red-cell deformability in diabetes. Diabetes **25**, (Suppl. 2), 897–902 (1976).
32. Trinder, P.: Determination of blood glucose using 4-amino phenazone as oxygen acceptor. Ann. Clin. Biochem. **6**, 24–26 (1969).
33. Wali, R. K., Jafe, S., Kumar, D., Kalra, V. K.: Alterations in organisation of phospholipids in erithrocytes as factor in adherence to endothelial cells in diabetes mellitus. Diabetes **37**, 104–111 (1988).
34. Wali, R. K., Jafe, S., Kumar, D., Sorgenete, N., Kalra, V. K.: Increased adherence of oxidant-treated human and bovine erythrocytes to culture endothelial cells. J. Cell Physiol. **113**, 25–36 (1987).
35. Wolff, S. P., Dean, R. T.: Glucose autoxidation and protein modification: the potential role of autoxidative glycosylation in diabetes. Biochem. J. **245**, 243–250 (1987).

*Acta Physiologica Hungarica, Volume 81 (4), pp. 327–339 (1993)*

# IN VITRO EFFECT OF LEUCINE-O-METHYLESTER ON POLYMORPHONUCLEAR AND MONONUCLEAR CELLS

Magda SOLYMOSSY, Ildikó CSUKA, F. ANTONI, Ágnes TEMESI

FIRST INSTITUTE OF BIOCHEMISTRY, SEMMELWEIS UNIVERSITY MEDICAL SCHOOL BUDAPEST, HUNGARY

Received November 4, 1992
Accepted January 27, 1993

The uptake of Leu-OMe and Leu-Leu-OMe was studied in vitro in porcine PMN cells. Both methylesters are metabolized leading to the intracellular accumulation of leucine. Part of the hydrolyzed leucine gradually filtrates back into the culture medium in a time-, temperature- and methylester substrate concentration-dependent manner. Another portion of Leu-OMe is converted to Leu-Leu dipeptide. With respect to the cellular effects of Leu-OMe treatment ultrastructural studies showed the presence of large vacuoles without significant alteration of cell viability. Increased exocytosis of lysosomal enzymes did not lead to lytic events. Changes in the plasma membrane are indicated by the observation that Leu-OMe treatment causes the loss of the chemotactic activity to formyl-Met-Leu-Phe.

**Keywords:** polymorphonuclear, mononuclear cells, Leucin-O-Methylester, metabolism, dipeptide

**Abbreviations:** PMN, polymorphonuclear neutrophil; L-Leu, L-Leucine; L-Leu-OMe, L-Leucine-methylester; L-Leu-Leu-OMe, L-Leucyl-leucine-methylester; LDH, lactate dehydrogenase; Gey's solution, incubation buffer (pH 7.4); PBS, phosphate buffered saline; fMLP, N-formyl-L-Methionyl-L-Leucyl-L-Phenylalanine

The recent upsurge of amino acid metabolism is mainly due to the post-transcriptional modification (phosphorylation, methylation, acetylation) of proteins due to an alternative pathway to the extraribosomal peptide formation of amino acid metabolism driven by enzymatic reactions. Formyl-Met-Leu-Phe as a chemotactic agent and soluble mediator of the immune response exemplifies the chemotactic importance of the formyl group which plays also an initiative role in protein biosynthesis [4].

Correspondence should be addressed to
Magda SOLYMOSSY
First Institute of Biochemistry, Semmelweis University Medical School
H – 1444 Budapest, P.O. Box 260, Puskin u. 9, Hungary

*Akadémiai Kiadó, Budapest*

Methylesters of L-amino acids are known to diffuse readily into certain cells such as hepatocytes and monocytes, penetrating into lysosomes. Among the derivatives L-Leucine methylester (Leu-OMe), L-Leucyl-Leucine-methylester (L-Leu-Leu-OMe) and a variety of methylesters of other amino acids were found to be effective lysosomotropic agents [17]. L-amino acid methylesters taken up by the cells are rapidly hydrolyzed in lysosomes to free amino acids, to which lysosomal membranes are generally less permeable. The result is the lysosomal accumulation of amino acids which as an efficient osmolyte causes the swelling and eventually the disruption of the lysosomes [16, 18, 19]. As a further effect, the depletion of cells by Leu-OMe and Leu-Leu-OMe leads to the activation of antigen specific B cells and to the production of monoclonal antibodies [5, 6, 25–28].

We have found that in murine peritoneal macrophages treated with Leu-OMe in vitro the incorporation of amino acids is prevented and vacuolization in the cytoplasm may lead to the leakage of cells [1, 2, 10, 11]. In this paper we describe the effect of Leu-OMe or Leu-Leu-OMe treatment of PMN cells isolated from porcine blood and the metabolism of these compounds.

## Materials and methods

*PMN preparation*

Granulocytes were obtained from sodium citrate-anticoagulated porcine blood by Lymphoprep (Nyegaard and Co-AS-Oslo) centrifugation followed by hypotonic lysis of erythrocytes. After centrifugation (400 × g, 20 min) granulocytes from the pellet were washed three times with Gey's, pH 7.4 [14]. Centrifugation was repeated (200 × g, 10 min) and the cells were suspended in Gey's at a concentration of $5 \times 10^6$/ml. The purity was above 96–98% granulocytes. The viability of the freshly prepared cell suspension tested by the trypan blue exclusion method, was about 96–98%.

*PMN chemotaxis*

Isolated intact or 5.0 mM Leu-OMe treated neutrophils were suspended in Gey's solution (pH 7.4) suspended with 1.0% bovine serum albumin at $1 \times 10^6$ cells/ml in the upper compartment of the modified Boyden chambers, 3 μm pore size, 13 mm diameter cellulose nitrate filter (Sartorius Test) substances, including various concentration of fMLP or Control medium (Gey, pH 7.4) were placed in the lower compartment. After 45 min at 37 °C the chambers were disassembled and the filters were cleared with methanol and stained with hematoxylin. All assays were performed in triplicate. Five high power (× 400) fields were counted per filter using the leading from technique [14].

*Treatment of cells with methylesters*

L-Leu and L-Leucine-O-methylesters were purchased from Sigma Chemical Company. $5 \times 10^7$ PMN/ml in Gey, ph 7.4, was treated with L-Leu-OMe (1.5–5.0 mM) or L-Leu-Leu-OMe (1.5–5.0 mM) for max 120 minutes at 37 °C or 4 °C. Cells were centrifuged (200 × g, 10 min, 4 °C) washed cells were suspended in Gey's buffer in a concentration of $5 \times 10^7$ cell/ml (cell 0 min) and incubated at 37 °C for

30 min. After incubation we measured the quantity of compounds with HPLC from the acetone extract of washed and centrifuged cells (Cells 30 min) and their medium (Medium 30 min) and performed the determination of compounds by TLC, too.

*High performance liquid chromatography (HPLC)*

Samples were analyzed by a Hewlet-Packard Inst. HP 1090 Aminoquant, $C_{18}$RP column. (Pre column OPA derivatization was used.)

*Thin layer chromatography (TLC)*

DX-Alufolien Kieselgel 60 (Merck, without fluorescent indicator) was used. One-dimension chromatography was performed in butanol: pyridine: acetic acid: water (60:20:6:11 v/v). Chromatograms were developed with ninhidrin reagent. Chromatography was carried out under identical conditions with "marker" compounds. The determination of amino acids and their methylesters took place after TLC chromatography by scarping off the ninhydrin spots dissolving in 0.5 ml ethanol and measuring their absorbance at 570 nm.

*Exocytosis*

PMN cells ($5 \times 10^6$/ml) were pretreated depending on the purpose either with L-Leu (1.0 mM) or NaF (20 mM), or untreated isolated cells were treated with Leu-OMe (0.5–5.0 mM at 4 °C and 37 °C). If needed the chemoattractant (formyl-Met-Leu-PHe, $10^{-7}$ M) was used. Samples were taken at different time intervals and the cells were separated (200 × g, 10 min, 4 °C) from the medium. Enzyme activities (lysozyme, protease, lactate dehydrogenase) were determined in both systems.

*Lactate dehydrogenase (LDH) assay*

Release of the cytoplasmic enzyme (LDH) was analyzed by the method of Schwert [20].

*Protease assay*

Non-specific neutral protease was analyzed by the method of Charney and Tomarelli [9]. Azocasein (Serva, Feinbiochemic Heidelberg) served as substrate (10 mg/ml). Protease activities of the intact and treated PMN suspensions, the lysatum of harvested cells and cell free medium were measured at 37 °C after 30 min incubation.

## Results

Porcine PMNs were incubated at 37 °C with either L-Leu-OMe (1.5 mM), or L-Leu (1 mM) plus L-Leu-OMe (1.5 mM) or L-Leu-Leu-OMe (1.5 mM) and samples were taken at different intervals for their acetonic extraction and HPLC (Fig. 1). Untreated cells which were not incubated or incubated for 120 min do not contain appreciable amounts of Leu or Leu-OMe. In the presence of L-Leu-OMe cells take up the drug and convert it immediately to Leu and Leu-Leu-OMe (Fig. 1A, 5 min). However, the Leu-Leu-OMe formed is rapidly hydrolyzed (Fig. 1A, 40 min).

Finally Leu-OMe disappears and only Leu is left in the cell extract (Fig. 1A, 120 min). Cells treated with Leu-Leu-OMe contain relatively low amount of dipeptide which is obviously hydrolyzed to Leu-OMe and Leu (Fig. 1B, 40 min). The treatment of cells both with Leu-OMe and L-Leu did not result in the formation of the dipeptide Leu-Leu-OMe (Fig. 1C, 40 min).

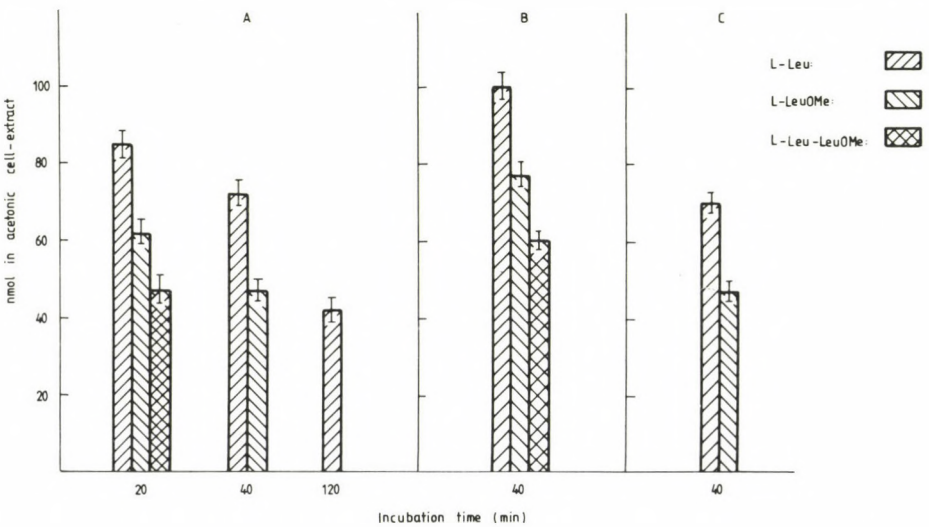


*Fig. 1.* Relative amount of leucine and leucine-O-methylesters in acetone cell-extract
A: acetone cell-extract from L-Leu-OMe (1.5 mM) treated cell, at 20, 40, 120 minutes incubation time.
B: acetone cell-extract from L-Leu-Leu-OMe (1.5 mM) treated cell, at 40 minutes incubation time.
C: acetone cell-extract from L-Leu-OMe (1.5 mM) plus L-Leu (1 mM) treated cell, at 40 minutes incubation time

The effect of temperature on the uptake of Leu-OMe and Leu-Leu-OMe was also measured. The uptake of both Leu-OMe and Leu-Leu-OMe depends primarily on the concentration of leucine-methylesters and to a lesser extent on the temperature used for the treatment. It is noteworthy to mention the rapid conversion of both methylesters to Leu which is influenced not only by the concentration of the substrate but also by the temperature (data are not presented).

The rapid accumulation of leucine in cell extracts raised the question whether the leucine formed could have traversed the cell membrane and flowed back into the medium. The physiological level of leucine concentration gradually drops when cells are incubated in Gey's solution supporting the notion that part of the leucine

migrates into the medium. This tendency was observed when cells were loaded with L-Leu or when leucine accumulated inside the cells as a consequence of the treatment and the hydrolysis of L-Leu-OMe. The physiological concentration of Leu was traced in cells with the sensitive HPLC separation technique (Fig. 2). Untreated cells (Fig. 2a, cells 0 min) were incubated with Gey's solution for 30 min. Some of the Leu (30%) migrated into the incubation medium (Fig. 2a, medium 30 min). The loading of cells with 5 mM L-Leu increased the intracellular Leu concentration to 4–6 fold (Fig. 2b, cells 0 min). Further incubation in Gey's for 30 min decreased cellular Leu concentration by 30% which could be traced in the extracellular medium (Fig. 2b, medium 30 min). After treatment with L-Leu-OMe which was rapidly converted to Leu cells accumulated 96–100-times more Leu (Fig. 2c, cells 0 min) than that of the physiological concentration (Fig. 2a, cells 0 min). Incubation in fresh medium caused the loss of about 20% Leu which could be quantitatively measured in the incubation medium (Fig. 2c, medium 30 min).

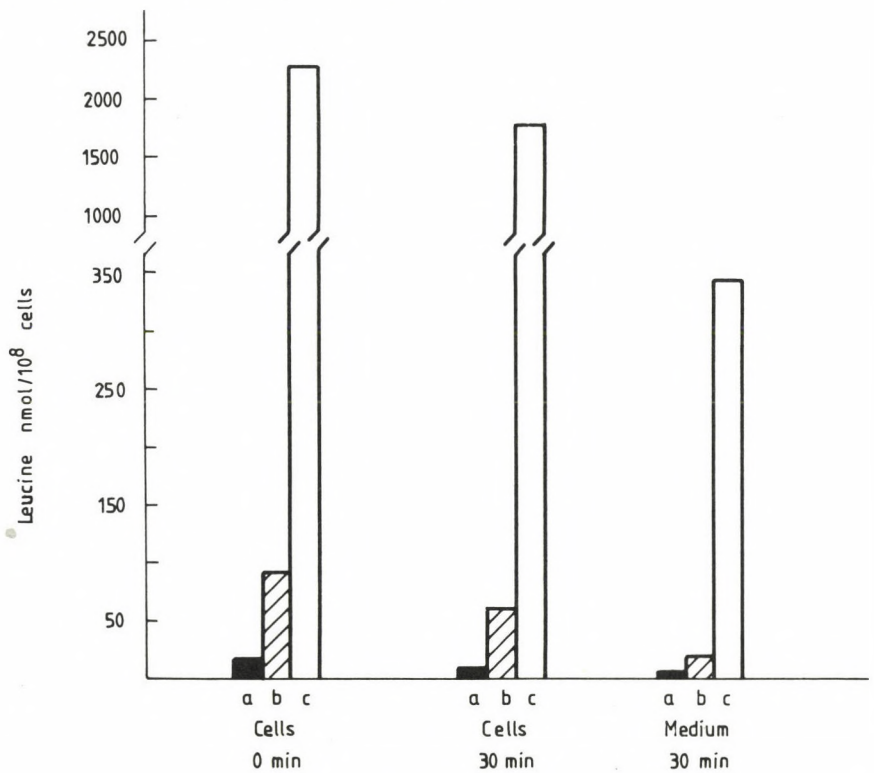


*Fig. 2.* Leucine accumulation in cells
Leucine content of control cell, at 0 min and 30 min after incubation in cells and in medium: ■ ; cells pretreated with 5.0 mM L-Leu: ▨ ; and pretreated with 5.0 mM L-Leu-OMe: □

Above experiments have raised another question, namely whether cellular functions including chemotaxis are influenced when cells treated with Leu-OMe. To answer this question Leu-OMe pretreated cells were incubated in the presence of the chemoattractant N-formyl-Met-Leu-Phe. It was found that the concentration-dependent chemotaxis was completely inhibited by Leu-OMe treatment as it is documented in Fig. 3. When Leu-OMe and the chemoattractant were used at the same time, the chemotaxis was equally blocked (results are not shown).

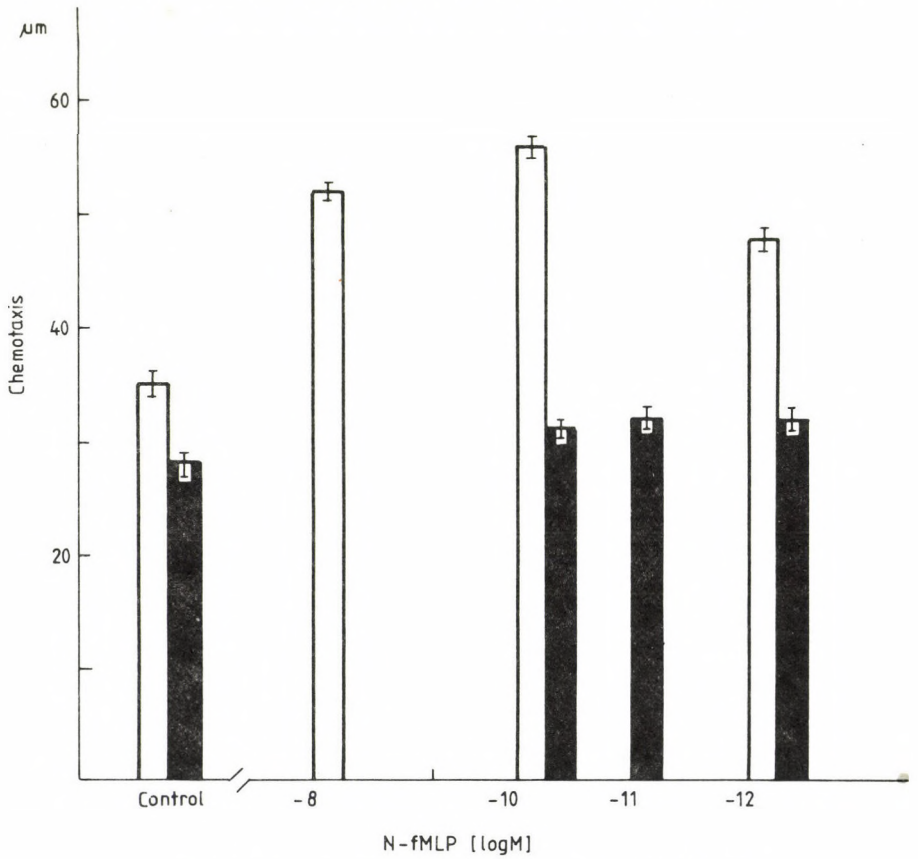


*Fig. 3.* Chemotaxis of Leu-OMe (5.0 mM)-pretreated PMN cells
Control: □ ;
Pretreated cells: ■ .
The values (leading front: μm) given are the means of four experiments ± SD

An increase in exocytosis of PMN cells was observed after in vitro Leu-OMe treatment. This was detected by the release of lysozyme (A) and neutral protease (B) activities in a concentration- and temperature-dependent manner (Fig. 4).

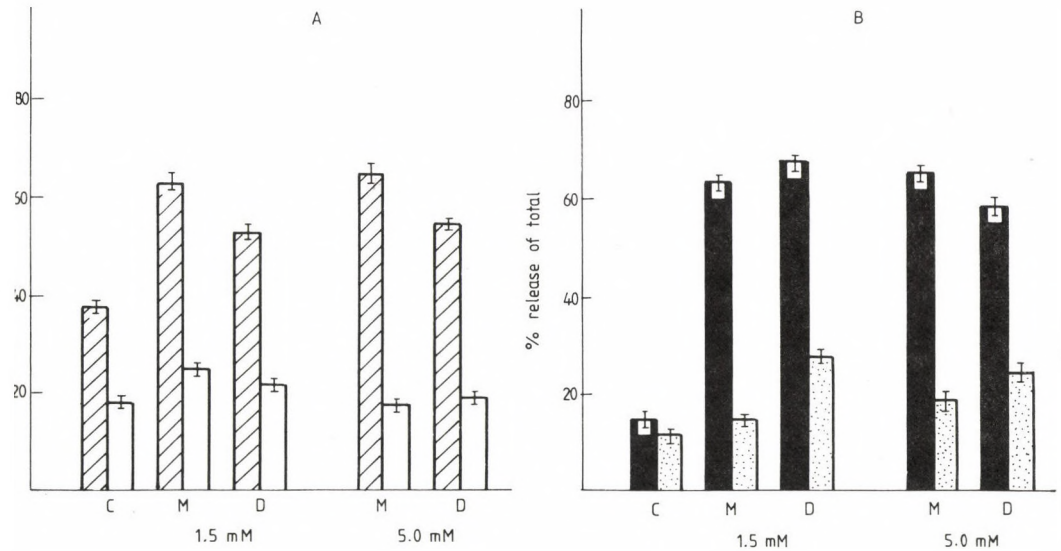


*Fig. 4.* Lysosyme (A) and neutral protease (B) release induced in porcine PMNs by different concentrations of Leu-OMe and Leu-Leu-OMe at 37 °C and 4 °C. After incubation for 40 min, the experiment was terminated and lysozyme and neutral protease release was determined as described in the methods. The values given are the means of four experiments ± SD.
Lysozyme release: treatment, at 4 °C, □ ; Treatment at 37 °C ▨ .
Neutral protease release: treatment, at 4 °C, ⊠ ; treatment at 37 °C ■

Maximal release of these two marker enzymes was measured at 1.5 mM Leu-OMe at 37 °C. Elevation of the methylester (M) or dipeptide methylester (D) load did not increase the release of lysozyme significantly (A). When dipeptide methylester was used as an inductor of the exocytosis similar changes occurred with respect to the lysozyme (A) and neutral protease activities (B). We have also examined how the energy status of the cells influences the release of enzyme in Leu-OMe treated PMN cells [15]. NaF treatment of PMN cells was used to measure the energy dependence of exocytosis (Table I).

Although, NaF did rapidly deplete ATP stores in PMN, the level of ATP seems to be unassociated with Leu-OMe treatment. This probably means that the exocytosis brought about by L-Leu-OMe treatment is an energy independent process.

Although, Table I does not show the values of trypan blue dye exclusion which were measured simultaneously, these values ranged between 82 and 96% indicating that the viability of cells after different treatments did not change and no serious cellular damage occurred.

Morphological studies revealed the presence of vacuoles in Leu-OMe treated cells (Fig. 5) which, however, did not influence the viability of cells.

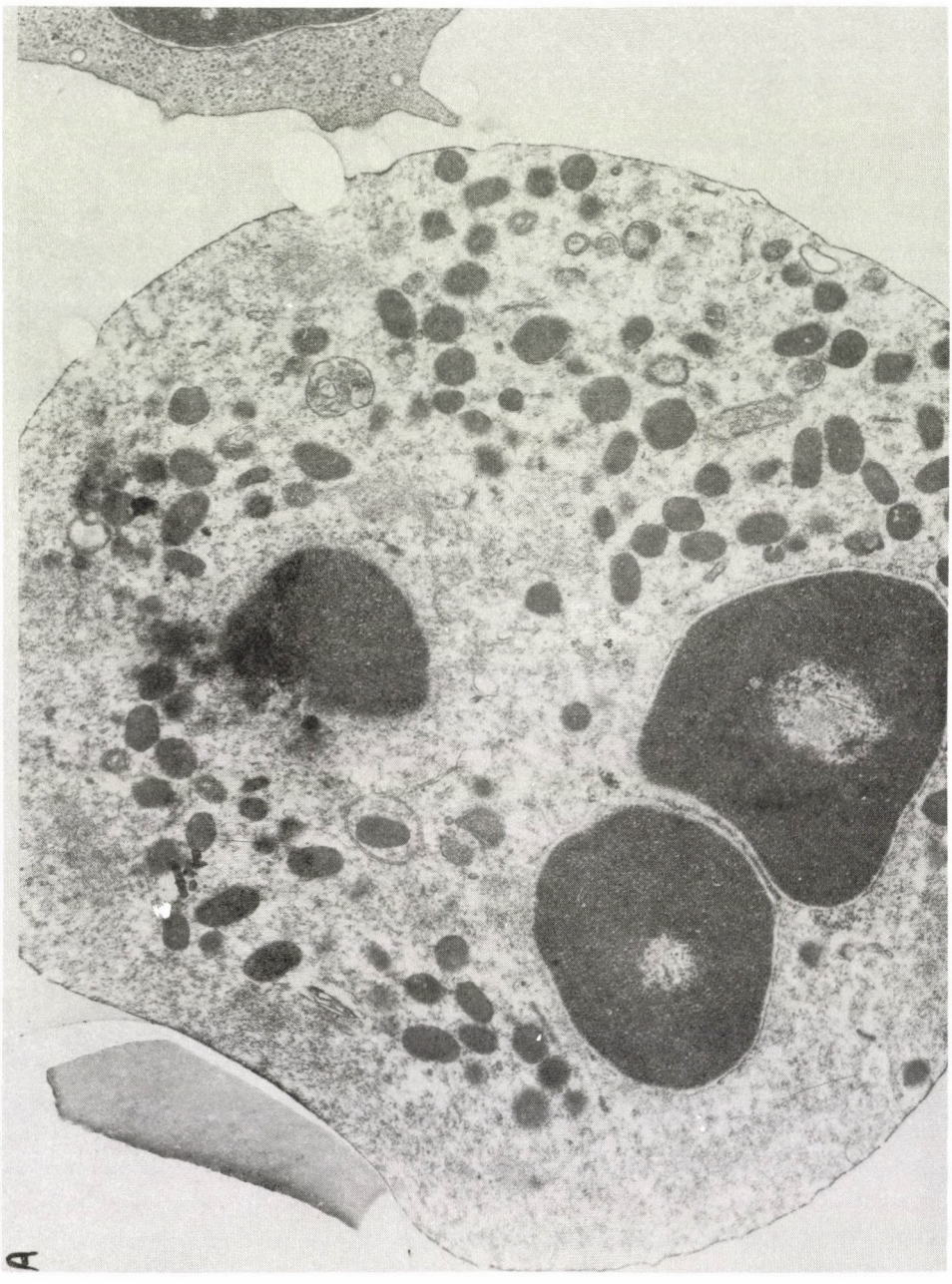


*Fig. 5.* Intracellular changes following treatment with Leu-OMe (1.5 mM; 37 °C; 40 min) A: Control 19 800 × magnification

B: Treated cells with Leu-OMe (1.5 mM; 37 °C; 40 min) 13 200 × magnification

**Table I**

*Energy-independence of the exocytosis*

| Pretreatment | Addition | Enzyme release % | |
|---|---|---|---|
| | | LDH | Lysozyme |
| None | – | 1±2 | 27±2 |
| None | + 1.5 mM Leu-OMe | 5±1.5 | 68±3 |
| None | + 0.5 mM I-acetate | 2±2 | 34±2 |
| None | + 0.5 mM I-acetate + 1.5 mM Leu-OMe | 8±2 | 61±3 |
| None | + 5.5 mM glucose + 10 mM 2-deoxiglucose | 5±2 | 36±2 |
| None | + 5.5 mM glucose + 10 mM 2-deoxiglucose + + 1.5 mM Leu-OMe | 8±2 | 64±4 |
| 20 mM NaF – glucose | | 4±2 | 42±2 |
| 21 mM NaF – glucose + 3 mM $Ca^{2+}$ | | 5±2 | 43±3 |
| 20 mM NaF – glucose | + 1.5 mM Leu-OMe | 8±2 | 82±4 |
| 20 mM NaF – glucose + 3 mM $Ca^{2+}$ | + 1.5 mM Leu-OMe | 8±3 | 82±3 |
| 1 mM Leu | – | | 32±2 |
| 1 mM Leu | + 1.5 mM Leu-OMe | | 69±5 |

L-Leu-OMe (1.5 mM, 37 °C, 40 min) induced LDH and lysozyme release
Total = 100% (enzyme activities in cells homogenate = enzyme activities in medium + remained enzyme activities in cells)

## Discussion

Neutrophils of the peripheral blood play a decisive role in the early phase of immune defense against foreign substances and produce several soluble factors influencing the immune system. The role of neutrophils is also known in the effector system, characterized by these participants of the immune response. Phagocytosis and exocytosis are among the important functions accomplished by neutrophils. Cells discharge their granular contents in response to various stimuli such as the chemoattractant peptide f-Met-Leu-Phe. As a result of degranulation the lysosomal content is discharged into phagocytic vacuoles or into the environment. Azurophil and specific granules such as lysosomes may join a newly formed vacuole at its internal border and unite their contents. Azurophil granules contain microbicidal enzymes such as neutral proteinases, myeloperoxidase, lysozyme and acid hydrolases. Specific granules contain lysozyme and other enzymes. These enzymes can attack host tissues as well [3, 13, 21, 29]. Foreign substances are attacked by these enzymes inside the vacuoles which are closed entities preventing leakage. Overloading of vacuoles may cause the escape of enzymes from cells. We have attempted to load

porcine neutrophils with leucine by treating PMN cells with Leu-OMe. Leucine-methylester has been reported as a lysosomotropic agent [17]. Lysosomes are swelling in its presence resulting in the disruption of these organelles. Lysosomal enzymes flow into the cytoplasm causing the formation of vacuoles and damages to other organelles manifested in the morphological picture.

As a consequence of Leu-OMe treatment the accumulation of free Leu increases the amino acid pool of cells. Another part diffuse back into the incubation medium or else it can be traced as Leu-Leu dipeptide or Leu-Leu-OMe in cells. The dipeptide formation is likely to compensate the intracellular accumulation of free Leu. It is also expected that much more dipeptides are formed but due to the concomitant peptidase activity only the remaining equilibrium level of dipeptide formation could be seen. The dipeptide formation will be discussed in the accompanied paper. With respect to the methyl-group of Leu-OMe it is expected to be demethylated and in the esterolysis probably methanol is formed which is oxidized to formaldehyde. Alternatively, other types of methylations of intracellular compounds expected are logical to assume.

We have demonstrated earlier that Leu-OMe inhibits protein synthesis in cells isolated from murine peritoneal exudates. Similarly, the final stage of fagocytosis the so-called engulfing was prevented in cells from these peritoneal exudates [1, 2, 10, 11, 12, 24].

Borrenbaeck et al. [5, 6, 7, 8] described that the Leu-OMe can be used selectively for the in vitro elimination of monocytes and that treatment is needed for the production of monoclonal antibodies. Although, the treatment of neutrophils with Leu-OMe led to several cellular damages, viability of cells was not affected as demonstrated by the trypan blue exclusion test. This probably means that the integrity of the plasma membrane was not endangered, although other membrane functions such as the affinity of cells to chemotactic peptides (formyl-Met-Leu-Phe) have been lost.

The lysosomal system suffers serious damages after Leu-OMe treatment. It was evidenced by the increase of excretion of lysosomal enzymes including lysozyme and neutral proteases. The most likely cause of excretion of lysosomal enzymes is exocytosis [3, 13, 21–23, 29].

Our results also indicate that Leu-OMe and Leu-Leu-OMe cause cellular damages of the neutrophils themselves, first of all their transport and other functions related to their effector function are influenced. The temperature- and concentration-dependent dipeptide synthesis points to the enzymatic nature of the dipeptide formation excluding the possibility of a spontaneous chemical process. On the other hand the exocytosis which is elevated seems to be a process being independent of extra energy.

## Acknowledgements

The authors express their gratitude to Prof. Károly Lapis for the ultrastructural studies. The authors wish to express their thanks to Mrs. Teodora Kajtor and Mrs. Ilona Mongyi for the skillful technical assistance and to Mrs. Irén Oláh Sipka for the typing of the manuscript. This work was supported by the grant No 2612 "B".

## REFERENCES

1. Antoni, F., Csuka, I., Hrabák, A., Temesi, Á., Szende, B., Lapis, K.: The effect of L-leucine methyl ester on the phagocytosis and amino-acid incorporation of murine peritoneal cells. Acta Biochim. Biophys. Acad. Sci. Hung. **24**, 299–311 (1989).
2. Antoni, F., Szende, B., Lapis, K., Csuka, I.: Various sensitivity of macrophage enzymes for endogenous proteases. Acta Paediat. Hung. **29**, 41–42 (1989).
3. Barrowman, M. M., Cockroft, S., Comperts, B. D.: Differential control of azurophilic and specific granule exocytosis in sendai-virus permeabilized rabbit neutrophils. J. Physiol. **383**, 115–124 (1987).
4. Bennett, J. P., Hirth, K. P., Fuchs, E., Sarvas, M., Warren, G. B.: The bacterial factors which stimulate neutrophils may be derived from prokaryote signal peptide. FEBS Letters **116**, 57–61 (1980).
5. Borrenbaeck, C. A. K.: Human monoclonal antibodies produced from primary in vitro immunized leucine methyl ester-treated peripheral blood lymphocytes. Progr. Biotechnology **5**, 209–229 (1988).
6. Borrenbaeck, C. A. K.: Human mABs produces by primary in vitro immunization. Immunol. Today **9**, 355–359 (1988).
7. Borrenbaeck, C. A. K., Danielsson, L., Möller, S. A.: Human monoclonal antibodies produced by primary in vitro immunization of peritoneal blood lymphocytes. Proc. Natl. Acad. Sci. **85**, 3995–3999 (1988).
8. Borrenbaeck, C. A. K.: Strategy for the production of human monoclonal antibodies using in vitro activated B cells. J. Immunol. Methods **123**, 157–165 (1989).
9. Charney, J., Tomarelli, R. M.: A colorimetric method for the determination of the proteolytic activity of pancreatic juice. J. Biol. Chem. **171**, 501–508 (1947).
10. Csuka, I., Szende, B., Antoni, F., Lapis, K.: Specific effect of leucine-O-methylester on macrophages. Acta Paediat. Hung. **29**, 43 (1980).
11. Csuka, I., Szende, B., Antoni, F., Lapis, K.: Effect of O-methylesters of amino acids on macrophages. Hung. Biochem. Soc. SOTE Press (1987).
12. Csuka, I., Antoni, F.: Selective cytotoxic effect of L-Leu-OMe on mice PEC. Cell to Cell Interaction, Int. Symp. ed Karger, S. Basel 1990. p. 71.
13. Henson, P. M.: The immunologic release of constituents from neutrophil leukocytes. J. Immunol **107**, 1535–1546 (1971).
14. Keller, H., Wissler, J. H., Damerau, B., Hess, M. W., Cottier, H.: The filter technique for measuring leukocyte locomotion in vitro. Composition of three modifications. J. Immunol. Meth. **36**, 41–53 (1980).

15. Okada, K., Brown, E. J.: Sodium fluoride reveals multiple pathways for regulation of surface expression of the C3b/C4b receptor (CR1) on human polymorphonuclear leukocytes. J. Immunol. **140**, 878–881 (1988).
16. Poole, B., Okkuma, S.: Effect of weak bases on the intalysosomal pH in mouse peritoneal macrophages. J. Cell Biology **90**, 665–669 (1981).
17. Ransom, J., Reeves, J. P.: Accumulation of amino acids within intracellular lysosomes of rat polymorphonuclear leukocytes incubated with amino acid methyl esters. J. Biol. Chem. **258**, 9270–9275 (1983).
18. Reeves, J. P.: Accumulation of amino acids by lysosomes incubated with amino acid methyl esters. J. Biol. Chem. **254**, 8914–8921 (1979).
19. Reeves, J. P., Decker, R. S., Crie, J. S., Widdenthal, K.: Intracellular disruption of rat heart lysosomes by leucine methylester: effects on protein degradation. Proc. Natl. Acad. Sci. USA **78**, 4426–4429 (1981).
20. Schwert, G. W., Wiener, A. D.: Lactate Dehydrogenase Enzymes. Academic Press. New York – London, 1963. vol. 7. (1969) p. 127.
21. Smolen, J. E., Korchak, H. M., Weismann, G.: Initial kinetics of lysosomal enzyme secretion and superoxide anion generation by human PMN. Inflammation **4**, 145–163 (1980).
22. Solymossy, M., Csuka, I., Antoni, F., Temesi, Á.: In vitro effect of Leu-OMe on polymorphonuclear and mononuclear cells. Amino Acids **1**, 174 (1991).
23. Solymossy, M., Csuka, I., Antoni, F., Szende, B., Lapis, K.: The effect of Leucine-Methylesters on the granulocyte. Third European Congress on Cell Biology, Firenze, Italy, Cell Biology International Reports **14**, 158 (1990).
24. Szende, B., Lapis, K., Tímár, J., Antoni, F., Csuka, I.: Morphological studies on the effect of L-leucine methyl ester on mouse peritoneal macrophages in vitro. J. Exp. Pathology **42**, 121–127 (1991).
25. Thiele, D. L., Lipsky, P. E.: Modulation of human natural killer cell function by L-leucine methyl ester: monocyte-dependent depletion from human peripheral blood mononuclear cells. J. Immunol. **134**, 786–793 (1985).
26. Thiele, D. L., Lipsly, P. E.: The immunosuppressive activity of L-leucyl-leucine methyl ester: selective ablation of cytotoxic lymphocytes and monocytes. J. Immunol. **136/3**, 1038–1048 (1986).
27. Thiele, D. L., Lipsky, P. E.: Regulation of cellular function by products of lysosomal enzyme activity: Elimination of human natural killer cells by a dipeptide methyl ester generated from L-leucine methyl ester by monocytes or polymorphonuclear leukocytes. Proc. Natl. Acad. Sci. **82**, 2468–2472 (1985).
28. Thiele, D. L., Lipsky, P. E.: Modulation of the cytotoxic function of human peripheral blood mononuclear cells (PBM) by L-Leucine Methyl Ester (LMe). Ablation by a monocyte-granulocyte derived product. Fed. Proc. **43**, 1907 (1984).
29. Zurier, R. B., Hoffstein, S., Weissmann, G.: Mechanism of lysosomal enzyme release from human leukocytes. J. Cell Biol. **58**, 27–41 (1973).

*Acta Physiologica Hungarica, Volume 81 (4), pp. 341–354 (1993)*

# PHOSPHOCHOLINE TRANSFERASE IS MORE EFFICIENT THAN DIACYLGLYCEROL KINASE AS POSSIBLE ATTENUATOR OF DIACYLGLYCEROL SIGNALS IN PRIMORDIAL HUMAN PLACENTA

M. TÓTH, G. GIMES*

1ST INSTITUTE OF BIOCHEMISTRY AND
*2ND DEPARTMENT OF OBSTETRICS AND GYNECOLOGY, SEMMELWEIS MEDICAL UNIVERSITY, BUDAPEST, HUNGARY

Received January 13, 1993
Accepted March 31, 1993

Diacylglycerols (DAG) are assumed to play intracellular signal roles in rapidly growing tissues like those present in the primordial human placenta. The aim of the present study was to gain information on the capacity of DAG-kinase and CDP-choline: DAG phosphocholine transferase enzymes to eliminate DAG and behave as possible signal attenuators in these tissues. Previous and present results has provided evidence that Triton X-100 (0.05%, v/v), when incubated with placenta mince, (I) causes the accumulation of DAG by inhibiting DAG-acyltransferase and by a suggested acceleration of phosphatidylcholine (PC) decomposition, (II) inhibits the synthesis of PC and (III) increases the formation of phosphatidic acid (PA) without decreasing the conversion of PA into acylglycerols. Inhibition by the synthetic DAG: dioctanoylglycerol (DOCG) and by the DAG-analog: dioctanoylethyleneglycol (DOEG), of the Triton-induced ($^{3}$H)PA-accumulation from ($^{3}$H)glucose and of the increased labeling of PA with ($^{32}$P)phosphate indicated some DAG-attenuating roles of DAG-kinase, but this mechanism appeared not to be very efficient. The low rate of conversion of DOCG into ($^{32}$P)$PA_{DOCG}$ species in incubations with ($^{32}$P)phosphate confirmed this view. Compared to the rate of formation of $PA_{DOCG}$, DOCG was eliminated in the form of $PC_{DOCG}$ more than one order of magnitude faster. In addition, DOCG stimulated, whereas DOEG inhibited the formation of endogenous PC. These findings suggest that in the primordial human placenta transformation of DAG into PC by phosphocholine transferase and an attending stimulation of PC synthesis represent a more effective attenuator mechanism than the conversion of DAG into PA by DAG-kinase.

**Keywords:** diacylglycerol, diacylglycerol kinase, phosphocholine transferase, signal attenuation, primordial placenta (human)

Correspondence should be addressed to
Miklós TÓTH
1st Institute of Biochemistry, Semmelweis Medical University
H–1444 Budapest 8, P.O. Box 260, Puskin u. 9, Hungary

*Akadémiai Kiadó, Budapest*

Accumulating experimental evidence supports the view that diacylglycerols (DAG) represent a class of intracellular signal molecules mediating at least some of the effects of various hormones, growth factors, autocoids, tumor promoters and certain oncogene products [1, 4, 13, 18, 19]. Turning off or attenuation of the DAG signal may be a crucial step in the regulatory process and may represent one of the targets where the efficiency of signal transduction and amplification can be influenced.

In previous studies we have found a 4–6-fold increase of ($^{32}$P)phosphatidic acid and a simultaneous inhibition of the formation of ($^{32}$P)phosphatidylcholine induced by low micellar concentration of Triton X-100, a non-ionic detergent, in minced primordial human placenta incubated with ($^{32}$P)phosphate [28]. Furthermore we have observed that Triton treatment leads to an about 5-fold elevation of ($^{3}$H)DAG and an attending 3-fold rise in ($^{3}$H)phosphatidic acid in incubations where ($^{3}$H)glucose serves as labeled precursor [14]. Since our experiments indicated the lack of inhibitory effect of Triton on phosphatidate phosphohydrolase, the increased production of phosphatidic acid was attributed to the action of DAG-kinase [14]. The primordial placenta is composed of rapidly proliferating tissues, therefore the implication of DAG acting as signal for cellular growth in these tissues is a reasonable suggestion [26].

It is assumed that the metabolic clearance of cellular diacylglycerols occurs by the catalytic action of DAG-lipase [8, 21, 24] and/or DAG-kinase [3–5, 21, 24] enzymes in the following reactions:

$$\text{DAG} + \text{H}_2\text{O} \xrightarrow{\text{DAG lipase}} \text{2-monoacylglycerol} + \text{fatty acid}$$

$$\text{DAG} + \text{ATP} \xrightarrow{\text{DAG-kinase}} \text{phosphatidic acid} + \text{ADP}$$

Another reaction, which has been ignored so far in DAG attenuation is the conversion of DAG into phosphatidylcholine (PC):

$$\text{CDP-choline} + \text{DAG} \xrightarrow[\text{phosphocholine transferase}]{\text{CDP-choline: DAG}} \text{PC} + \text{CMP}$$

In the present study the DAG-kinase inhibitor: dioctanoylethyleneglycol (DOEG) [5] and the synthetic, metabolizable DAG-analog: dioctanoylglycerol (DOCG) [3] were used as competitive agents to estimate the contribution of DAG-kinase to the elimination of endogenous DAG accumulating in the presence of Triton [14]. In addition, to compare the capacities of DAG-kinase and phosphocholine transferase in DAG-elimination, the rate of conversion of DOCG into phosphatidic acid and PC was also determined.

## Materials and methods

*Radioactive isotopes*

(2-$^3$H)glucose (20 Ci/mmole) and ($^3$H-met)choline (15 Ci/mmole) were the products of Amersham International (England). Carrier-free ($^{32}$P)phosphate was obtained from IZINTA (Hungary).

*Chemicals*

1,2 (sn)dioctanoylglycerol (DOCG), dioctanoylethyleneglycol (DOEG) and various neutral and phospholipids were purchased from Sigma Chemical Co. (USA), Silicagel H was from Merck (Germany). ($^3$H)$PC_{DOCG}$ and ($^{32}$P)$PA_{DOCG}$ markers were prepared by incubating placenta tissue with DOCG and ($^3$H)choline or ($^{32}$P)phosphate followed by lipid extraction and TLC separation of lipids [3].

*Tissue*

Primordial placenta fragments were collected during legal instrumental interruption of normal, 8-10 week old pregnancies at the 2nd Department of ObGyn, Semmelweis University of Medicine, Budapest. The tissue was rinsed with and then suspended in ice-cold 0.9% NaCl, 40 mM Hepes-Na (pH 7.4), 1 mg/ml glucose solution and transported immediately to the biochemical laboratory.

*Incubation and lipid extraction*

Details are described in a previous paper [14]. Briefly, mince of primordial placenta was incubated in 2 ml Hanks medium buffered with 40 mM Hepes-Na (pH 7.4), in open vials shaken continuously in a 37 °C water bath for 60 min. When indicated, DOCG or DOEG was added at 20 min, in 0.25 mM and 1.0 mM final conc., respectively, whereas Triton X-100 was added at 30 min in 0.05% final conc. At the same time control incubates were given only the solvent (DMSO or 0.9% NaCl). The concentrations of DAG analogs were selected on the basis of preliminary and previous [28] experiments. Lipids were extracted using a modified method [28] of Bligh and Dyer [2].

*Radio TLC of neutral and phospholipids*

The solvent systems used have been described [14]. Separate solvent systems were used for the separation of (I) neutral lipids (including monoacylglycerols, 1,2-diacylglycerols, 1,3-diacylglycerols, fatty acids and triacylglycerols), (II) phosphatidic acid, the DOCG species of phosphatidic acid and acylglycerols and (III) lysophosphatidylcholine, phosphatidylcholine, phosphatidylinositol, and the DOCG species of phosphatidylcholine. Lipids, carrier and marker compounds were visualized by iodine vapor. Gel portions were scraped off into counting "mini" vials and after adding 2 ml scintillation solution [28], radioactivity was counted using a Beckman LS 7800 liquid scintillation spectrometer.

*Calculation of results*

Results were calculated in cpm/500 mg tissue as described previously [14, 28]. Statistical evaluation was done using Student's "t" test. A difference was regarded statistically significant when p was less than 0.05.

## Results

When the minced tissue was incubated with ($^3$H) glucose a low micellar concentration of Triton X-100 enhanced severalfold the labeling of DAG and phosphatidic acid (Fig. 1). When added alone, DOCG or DOEG did not influence appreciably the labeling of these lipids but both of them proved to be inhibitory on the stimulating effect of the detergent. The percentage inhibition of the labeling of phosphatidic acid was about 2 times higher (40%) than that of the DAG (20%). Consistent with our previous report [14] Triton did not have any effect on the labeling of acylglycerols (including the sum of mono, di-, and triacylglycerols) and phospholipids, whereas the labeling of triacylglycerols was markedly inhibited (Table I). On the other hand, both DOCG and DOEG had some inhibitory effect on the synthesis of acylglycerols, first of all on the formation of triacylglycerols. However, they do not have measurable effects on the formation of phospholipids (Table I). The inhibitory effect of these lipid analogs on the synthesis of acylglycerols was slightly relieved by Triton while the inhibitory effect on the rate of formation of triacylglycerols was enhanced further by the detergent.

**Table I**

*Effects of dioctanoylglycerol (DOCG) and dioctanoylethyleneglycol (DOEG) on the rate of conversion of ($^3$H)glucose into triacylglycerols (TG), acylglycerols (AG) and total phospholipids (PL) in the presence or absence of Triton X-100 (T)*

| Compounds tested | cpm/500 mg tissue TG | AG | PL |
|---|---|---|---|
| control | 12895 ± 903 (1.00) | 14486 ± 869 (1.00) | 2999 ± 210 (1.00) |
| T | 7608 ± 258 (0.59)[1] | 14631 ± 579 (1.01) | 3000 ± 150 (1.00) |
| DOCG | 8382 ± 516 (0.65)[1] | 9995 ± 579 (0.69)[1] | 2820 ± 90 (0.94) |
| DOCG+T | 6061 ± 258 (0.47)[2] | 11589 ± 290 (0.80) | 2821 ± 91 (0.94) |
| DOEG | 9929 ± 516 (0.77) | 11444 ± 579 (0.79) | 2819 ± 89 (0.94) |
| DOEG+T | 6190 ± 387 (0.48)[2] | 12023 ± 435 (0.83) | 3060 ± 214 (1.02) |

Data are from the experiments described in the legend to Fig. 1. Mean values ± SE are given from 3 experiments with triplicate incubations each. Relative changes are indicated by figures shown in parentheses. 1: significant difference ($p < 0.05$) relative to control, 2: significant difference relative to incubations containing the same DAG analog but no Triton.

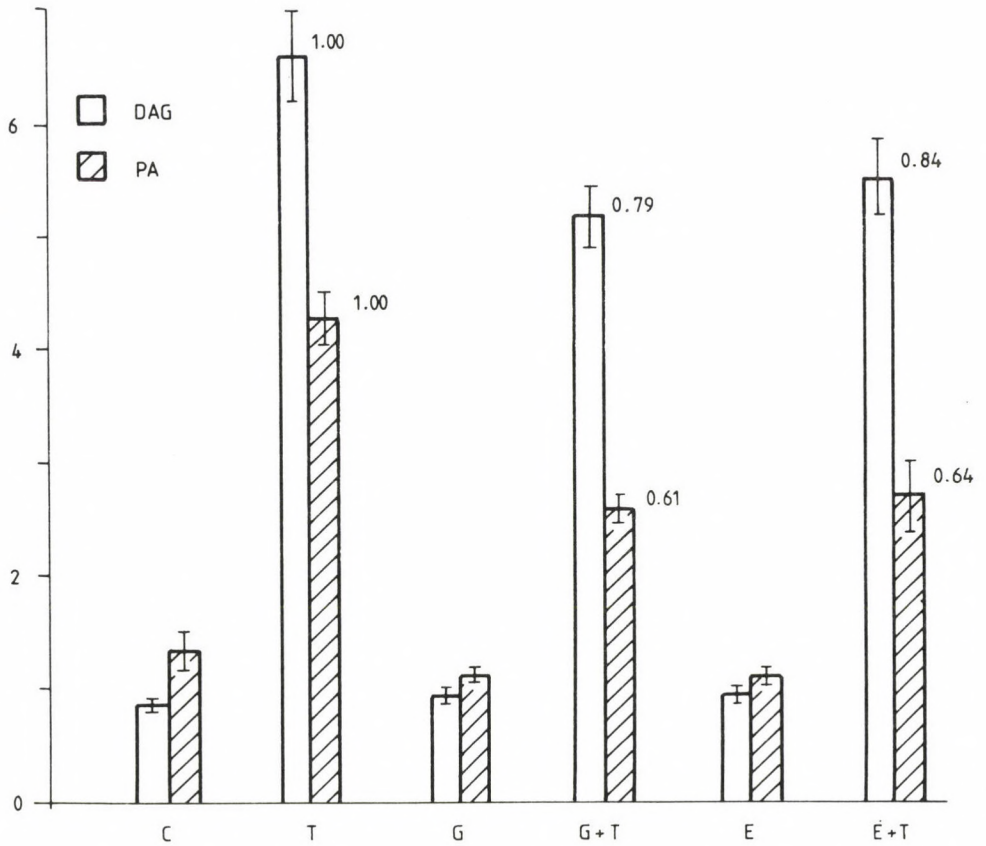


*Fig. 1.* Effects of dioctanoylglycerol (G) and dioctanoylethyleneglycol (E) on the rate of conversion of ($^3$H)glucose into 1,2-diacylglycerols (open bars) and phosphatidic acid (hatched bars) in the presence or absence of Triton X-100 (T).

Minced tissue (500 mg) of primordial placenta was incubated in buffered Hanks medium (prepared without glucose) with 10 μCi ($^3$H)glucose at 37 °C for 60 min in open vials shaken continuously. G (an abbreviation for DOCG) or E (an abbreviation for DOEG) were added in 0.25 mM and 1 mM final conc., resp., after 20 min, whereas Triton X-100 (0.05%, final conc.) was added after 30 min preincubation. Control incubates were given the respective solvent (DMSO or 0.9% NaCl). Mean values ±SE (shown by brackets) are presented from 3 experiments with triplicate incubations each. Relative changes are indicated by numbers on top of the bars

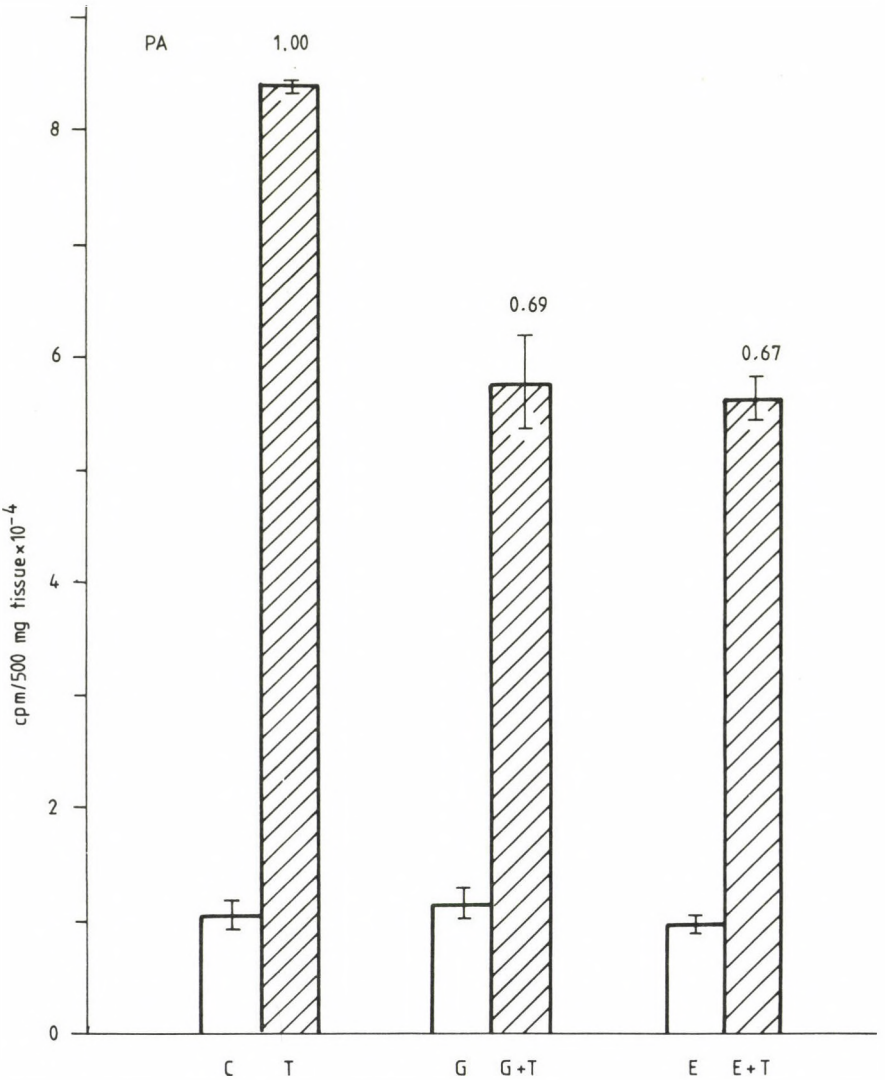


*Fig. 2.* Effects of dioctanoylglycerol (G) and dioctanoylethyleneglycol (E) on the rate of incorporation of ($^{32}$P)phosphate into phosphatidic acid in the presence (hatched bars) or absence (open bars) of Triton X-100 (T).

Minced tissue (500 mg) of primordial placenta was incubated in 2.0 ml buffered Hanks solution (prepared without phosphate) with 25 μCi ($^{32}$P)phosphate at 37 °C for 60 min in open vials shaken continuously. DOCG (G) or DOEG (E) were added in 0.25 mM and 1 mM final concentrations, resp., after 20 min, whereas Triton X-100 (0.05%, final conc.) was added after 30 min preincubation. Parallel incubates were given the appropriate solvent (DMSO or 0.9% NaCl). Mean values ±SE (shown by brackets) are presented from 3 experiments with duplicate incubations each. Relative changes are indicated by numbers on top of the bars

Data in Fig. 2 demonstrates, that using ($^{32}$P)phosphate as labeled precursor, DOCG and DOEG inhibited the stimulatory effect of Triton on the labeling of phosphatidic acid similarly to that obtained with ($^{3}$H)glucose as radiolabeled precursor (Fig. 1). Again, in the absence of Triton, no effect was found on the incorporation of ($^{32}$P)phosphate into phosphatidic acid. With the exception of the finding that DOEG increased the marginal effect of Triton on the labeling of phosphatidylinositol with ($^{32}$P)phosphate (Table II), the DAG analogs: DOCG and DOEG had little influence on the phosphatidylinositol metabolism.

**Table II**

*Effects of dioctanoylglycerol (DOCG) and dioctanoylethyleneglycol (DOEG) on the rate of incorporation of ($^{32}$P)phosphate into phosphatidylinositol (PI) and phosphatidylcholine (PC) in the presence or absence of Triton X-100*

| Compounds tested | cpm/500 mg tissue PI | PC |
|---|---|---|
| control | 13664 ± 956 (1.00) | 96487 ± 6754 (1.00) |
| T | 18310 ± 1831 (1.34) | 41489 ± 622 (0.43) |
| DOCG | 11614 ± 697 (0.85) | 123503 ± 4940 (1.28) |
| DOCG+T | 14211 ± 1847 (1.04) | 34735 ± 1042 (0.36) |
| DOEG | 11204 ± 448 (0.81) | 78154 ± 3126 (0.81) |
| DOEG+T | 24459 ± 734 (1.79) | 35700 ± 1071 (0.37) |

Data are from the experiments described in the legend to Fig. 2. Mean values ± SEM are given from 3 experiments with duplicate incubations each. Changes relative to control (= 1.00) are indicated by figures shown in parentheses. Effects of DOCG and DOEG on PC synthesis were statistically significant relative to control ($p < 0.05$).

In view of our previous findings [28], the dramatic inhibition by Triton of the incorporation of ($^{32}$P)phosphate into PC is not a surprise (Table II). On the other hand attention should be paid to the observation that DOCG promoted significantly ($p < 0.05$) the labeling of PC with ($^{32}$P)phosphate. In contrast with this, DOEG showed a definite inhibitory effect (Table II).

The results of the experiments done with ($^{3}$H)glucose and ($^{32}$P)phosphate allowed us to compare the rate of incorporation of ($^{32}$P)phosphate into phosphatidic acid with the labeling rate both of DAG and phosphatidic acid synthesized from ($^{3}$H)glucose (Table III). Either in the presence or absence of Triton and irrespective of the presence of a DAG-kinase inhibitor (DOCG or DOEG), the extent of formation of ($^{32}$P)phosphatidic acid showed a fairly close correlation with the accumulation of ($^{3}$H)DAG, whereas no such correlation was found when the ($^{32}$P)phosphate incorporated into phosphatidic acid was compared to tritium that

appeared in phosphatidic acid in incubations with ($^3$H)glucose. These ratios suggest that DAG accumulating due to the inhibition of DAG acyltransferase by Triton is not the major percursor for formation of ($^{32}$P)phosphatidic acid.

**Table III**

*Rate of labeling of phosphatidic acid (PA) with ($^{32}$P)phosphate as related to the rate of conversion of ($^3$H)glucose into diacylglycerols (DAG) and phosphatidic acid (PA), respectively*

| Compounds tested | Ratios of cpm/500 mg tissue values | |
|---|---|---|
| | $\frac{(^{32}P)PA}{(^3H)DAG}$ | $\frac{(^{32}P)PA}{(^3H)PA}$ |
| control | 12.21 | 7.91 |
| Triton X-100 (T) | 12.71 | 19.60 |
| DOCG | 12.32 | 10.33 |
| DOCG+T | 11.12 | 22.15 |
| DOEG | 10.36 | 8.84 |
| DOEG+T | 10.19 | 20.72 |

Values were calculated from data presented in Figs 1 and 2.

DOCG was used not only to inhibit DAG-kinase activity but to gain information on the capacity of DAG-kinase and phosphocholine transferase for the elimination of excess DAG. A summary of data (Table IV) indicated that at 0.25 mM final concentration of DOCG about 800 cpm ($^{32}$P)phosphate was incorporated into $PA_{DOCG}$ while 26 000 cpm was found in $PC_{DOCG}$ illustrating that phosphocholine transferase was about 30-fold more efficient than DAG-kinase in removing the DAG-analog. In addition to this, endogenous PC was synthesized faster in the presence of DOCG (Table II) contributing to the elimination of a further amount of DAG (equivalent approximately to 28 000 cpm). Furthermore, results presented in Table IV demonstrate that Triton had no influence on the activity of DAG-kinase but it abolished completely the synthesis of PC from DOCG.

Using ($^3$H)choline as labeled precursor (Fig. 3) we confirmed the metabolic clearance of DOCG in the form of $PC_{DOCG}$ with a concomitant DOCG-stimulated conversion of endogenous DAG into PC.

**Table IV**

*Labeling of the dioctanoylglycerol species of phosphatidic acid ($PA_{DOCG}$) and phosphatidylcholine ($PC_{DOCG}$) with ($^{32}P$)phosphate in the primordial placenta in the presence and absence of Triton X-100 (T)*

| Additions | cpm/500 mg tissue | |
|---|---|---|
| | $PA_{DOCG}$ | $PC_{DOCG}$ |
| DOCG | 797 ± 59 | 26236 ± 1407 |
| DOCG+T | 1210 ± 443 | −704 ± 452 |

Data are from the experiments described in Fig. 2 and Table 2. DOCG was added in 0.25 mM final concentration at 20 min, Triton X-100 was added in 0.05% (v/v) final concentration at 30 min of incubation. The duration of incubation was 60 min. Cpm values measured in the $PA_{DOCG}$ and $PC_{DOCG}$ spots of radio TLC chromatograms were corrected for "background" cpm values found in the respective spots of these phospholipids in control chromatograms (1475 ± 103 and 5026 ± 503 cpm/500 mg tissue, for $PA_{DOCG}$ and $PC_{DOCG}$, respectively). Mean values ± SEM (n = 3) are presented.

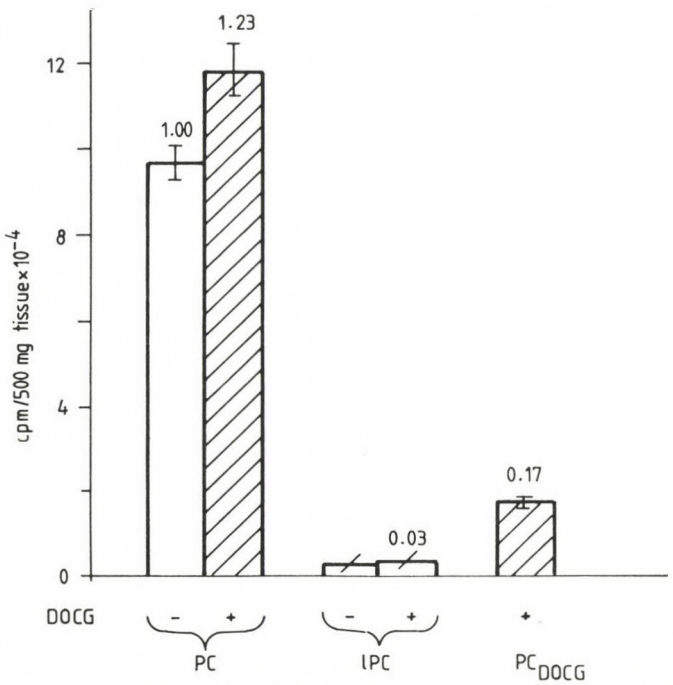


*Fig. 3.* Rate of labeling of phosphatydylcholine (PC), lyso-PC (1-PC) and the dioctanoyl species of PC ($PC_{DOCG}$) with ($^3H$)choline in the primordial placenta.

Triplicate samples of tissue mince was incubated with 5 μCi ($^3H$)choline under the standard conditions for 60 min. DOCG was added in 0.25 mM final concentration at 20 min, whereas control incubates received the solvent (DMSO) only. $PC_{DOCG}$ values have been corrected for "background" cpm (624 ± 336) found in the $PC_{DOCG}$ site on control chromatograms. Bars represent mean values ± SD (n = 3). Numbers above the bars are comparisons with the labeling of PC in control incubates

## Discussion

Our previous finding [14] showing that a low micellar concentration of Triton X-100 inhibits efficiently the conversion of DAG into triacylglycerols in the primordial human placenta has offered the possibility of studying the mechanisms whereby accumulating DAG is removed (DAG-attenuation). The previous [14] and present results, that in the presence of Triton there is a marked accumulation of DAG synthesized from ($^3$H)glucose and accumulation of ($^3$H)phosphatidic acid remains well behind to that of ($^3$H)DAG indicate that DAG-lipase and DAG-kinase activities are not very efficient attenuators in this tissue. It is important to note, that Triton X-100 inhibits the formation of PC, the primary cause of which seems to be the dissociation of CTP: phosphocholine cytidylyl transferase, the rate-limiting enzyme in PC synthesis, from the cellular membranes with a consequent decrease of its activity [9, 10]. This marked inhibitory action of Triton has been demonstrated in our previous [28] as well as present experiments, and the complete abolishment of the formation of the DOCG species of PC in the presence of Triton (Table III) is a supportive evidence in favor of such an effect in the primordial placenta. Since in the presence of Triton X-100 PC-production is blocked and DAG elimination by DAG-kinase is slow, in the absence of Triton a rapid DAG-removal by PC-synthesis remains a possibility.

Collectively, several findings (such as, the low degree of inhibition of Triton-induced formation of phosphatidic acid from DAG by 1 mM DOEG or 0.25 mM DOCG, and the low rate of conversion of DOCG into $PA_{DOCG}$ at 0.25 mM DOCG concentration) suggest that relatively large amounts of DAG accumulate in the placenta tissue in response to the detergent treatment. Although the possibility that during Triton treatment some of the phosphatidic acid is not produced by DAG-kinase cannot be ruled out, our present and previous results are more compatible with a reaction catalyzed by DAG-kinase and utilizing various Triton-activatable sources of DAG in this tissue. Thus phosphatidic acid was found to be labeled in response to Triton, with ($^{32}$P)phosphate to a higher extent than from ($^3$H)glucose and the ratio of ($^{32}$P)phosphatidic acid to ($^3$H)DAG was not found to change significantly in the presence of DAG analogs (Table III). Recently, it has been reported that low micellar concentration of Triton activates PC-specific phospholipase D in canine kidney [15]. One of the products of this reaction is phosphatidic acid which can be converted further into DAG by a phosphatidate phosphohydrolase residing in plasma membrane [16]. Interestingly, $\tau_1$ isozyme of $PIP_2$-specific phospholipase C is inhibited by this detergent [20].

A scheme presented in Fig. 4 summarizes the proposed effects of Triton in human primordial placenta. These effects lead to a marked increase in DAG content, the conversion of some of the DAG into phosphatidic acid and the blockade of DAG-attenuating PC synthesis. This scheme is compatible with our present and previous findings [14, 28].

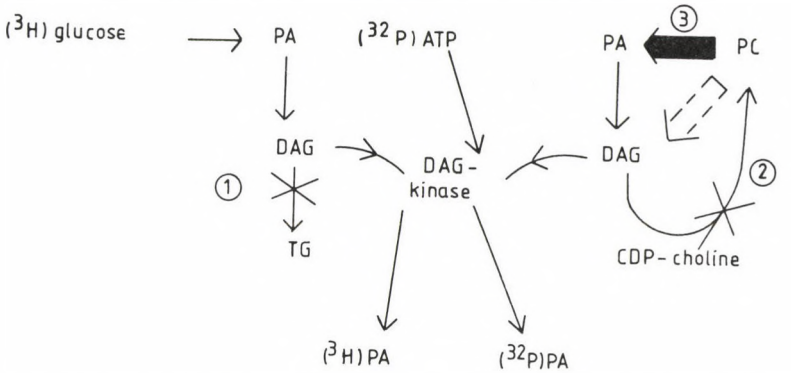


*Fig. 4.* Scheme to illustrate the effect of Triton on the formation of labelled PA via the action of DAG-kinase in incubations with ($^3$H)glucose or ($^{32}$P)phosphate.

1 = DAG-acyltransferase
2 = phosphocholine transferase
3 = PC-specific phospholipase D (open arrow: phospholipase C)
X = inhibition by Triton X-100
solid arrow = stimulation by Triton X-100
PA = phosphatidic acid, PC = phosphatidylcholine, DAG = 1,2-diacylglycerol, TG = triacylglycerol

Both DOCG and DOEG decreased the formation of acylglycerols from ($^3$H)glucose without a simultaneous elevation of ($^3$H)phosphatidic acid (Fig. 1 and Table I), suggesting their interference with the de novo synthesis of phosphatidic acid from glycolytic intermediates rather than an inhibition of the activity of phosphatidate phosphohydrolase. At the same time, Triton, when added together with DOCG or DOEG, tended to increase the rate of acylglycerol formation (Table I), ruling out an inhibition of phosphatidate phosphohydrolase in this situation. On the other hand, DOCG or DOEG potentiated the inhibitory effect of Triton on DAG-acyltransferase, resulting theoretically expectable maximum inhibition (50%) of the conversion of DAG into triacylglycerols (Table I). Whether DOCG is a substrate for DAG-acyltransferase in the primordial placenta remains to be elucidated.

Testing of the metabolic clearance of DOCG provided evidence of phosphocholine transferase being a much more efficient attenuator than DAG-kinase. This evidence comprises three experimental results (Tables II and IV, Fig. 2): (1) DOCG is converted into $PC_{DOCG}$ much more extensively than into $PA_{DOCG}$, (2) labeling of endogenous PC is inhibited by DOEG without any change in that of phosphatidic acid, and (3) labeling of endogenous PC is stimulated by DOCG without any influence on the labeling of endogenous phosphatidic acid by this synthetic DAG analog.

With regard to the above results it should be pointed out that the labeling of $PA_{DOCG}$ and $PC_{DOCG}$ species with ($^{32}$P)phosphate occur at the expense of the same

ATP pool via reactions catalyzed by DAG-kinase and choline-kinase, respectively [27]. Therefore the comparison made on the basis of labeling with ($^{32}$P)phosphate may be considered as the true reflection of the difference in synthetic rates. While DOEG is to be viewed as a competitive antagonist of DAG for phosphocholine transferase, DOCG is not only a substrate for phosphocholine transferase but also a known activator of phosphocholine: CTP cytidylyl transferase [17, 25], the enzyme that is responsible for the formation of CDP-choline [27]. In addition, DOCG may activate protein kinase [23], with subsequent stimulation of the activity of cytidylyl transferase [27] and PC-specific phospholipase D [6, 7, 13, 18, 19] and the rate of the phosphatidylcholine cycle [11, 12, 22]. In fact, the abundance of PC in cell membranes makes it possible for certain membrane regions to be involved in the generation of DAG signal while other regions may play an attenuating role for this signal.

Apparently, DOCG does not compete with endogenous DAG in PC formation since the labeling both of $PC_{DOCG}$ and endogenous PC increased, either ($^{32}$P)phosphate of ($^{3}$H)choline was used as labeled precursor. Thus an important characteristic of the removal of DAG in the form of PC is the ability of DAG to enhance the capacity of PC synthesis and to adjust it to the DAG concentration present in the cell.

On the basis of the present findings we propose that conversion of DAG into PC could be an important attenuating mechanism of DAG-signal. A major advantage of this pathway would be the production of a molecule having no signal activity. Considering that phosphatidic acid produced by DAG-kinase [18] and arachidonate produced by the sequential action of DAG-lipase and monoacylglycerol-lipase [21, 24] can themselves be signal molecules, we propose that channelling of DAG into PC may represent a true signal-termination episode in the primordial human placenta.

## REFERENCES

1. Besterman, J. M., Duronio, V., Cuatrecasas, P.: Rapid formation of diacylglycerol from phosphatidylcholine: a pathway for generation of a second messenger. Proc. Natl. Acad. Sci. USA **83**, 6785–6789 (1986).
2. Bligh, E. G., Dyer, W. J.: A rapid method of total lipid extraction and purification. Can. J. Biochem. Physiol. **37**, 911–917 (1959).
3. Bishop, W. R., Bell, R. M.: Attenuation of sn-1,2-diacylglycerol second messengers: metabolism of exogenous diacylglycerols by human platelets. J. Biol. Chem. **261**, 12513–12519 (1986).
4. Bishop, W. R., Bell, R. M.: Functions of diacylglycerol in glycerolipid metabolism, signal transduction and cellular transformation. Oncogene Res. **2**, 205–218 (1988).

5. Bishop, W. R., Ganong, B. R., Bell, R. M.: Attenuation of s,n-1,2-diacylglycerol second messengers by diacylglycerol kinase: inhibition by diacylglycerol analogs in vitro and in human platelets. J. Biol. Chem. **261**, 6993–7000 (1986).
6. van Blitterswijk, W. J., Hilkmann, H., de Widt, J., van der Bend, R. L.: Phospholipid metabolism in bradykinin-stimulated human fibroblasts. I. Biphasic formation of diacylglycerol from phosphatidylinositol and phosphatidylcholine, controlled by protein kinase C. J. Biol. Chem. **266**, 10337–10343 (1991).
7. van Blitterswijk, W. J., Hilkmann, H., de Widt, J., van der Bend, R. L.: Phospholipid metabolism in bradykinin-stimulated human fibroblasts. II. Phosphatidylcholine breakdown by phospholipases C and D; involvement of protein kinase C. J. Biol. Chem. **266**, 10344–10350 (1991).
8. Chan, L. Y., Tai, H. H.: Monoglyceride and diglyceride lipases from human platelet microsomes. Biochim. Biophys. Acta **963**, 436–444 (1988).
9. Cornell, R., Vance, D. E.: Translocation of CTP: phosphocholine cytidylyltransferase from cytosol to membranes in Hela cells: stimulation by fatty acid, fatty alcohol, mono- and diacylglycerol. Biochim. Biophys. Acta **919**, 26–36 (1987).
10. Cornell, R., Vance, D. E.: Binding of CTP: phosphocholine cytidylyltransferase to large unilamellar vesicles. Biochim. Biophys. Acta **919**, 37–48 (1987).
11. Daniel, L. W., Waite, M., Wykle, R. L.: A novel mechanism of diglyceride formation. J. Biol. Chem. **261**, 9128–9132 (1986).
12. Dennis, E. A., Rhee, S. G., Billah, M. M., Hannun, Y. A.: Role of phospholipases in generating lipid second messengers in signal transduction. FASEB J. **5**, 2068–2077 (1991).
13. Exton, J. H.: Signaling through phosphatidylcholine breakdown. J. Biol. Chem. **265**, 1–4 (1990).
14. Gimes, G., Tóth, M.: Low concentration of Triton X–100 inhibits diacylglycerol acyltransferase without measurable effect on phosphatidate phosphohydrolase in the human primordial placenta. Acta Physiol. Hung. **81**, 101–108 (1993).
15. Huang, C., Wykle, R. L., Daniel, L. W., Cabot, M. C.: Identification of phosphatidylcholine-selective and phosphatidylinositol-selective phospholipases D in Madin-Darby canine kidney cells. J. Biol. Chem. **267**, 16859–16865 (1992).
16. Jamal, Z., Martin, A., Gomez-Munoz, A., Brindley, D. N.: Plasma membrane fractions from rat liver contain a phosphatidate phosphohydrolase distinct from that in the endoplasmic reticulum and cytosol. J. Biol. Chem. **266**, 2988–2996 (1991).
17. Kolesnick, R. N., Paley, A. E.: 1,2-diacylglycerols and phorbol esters stimulate phosphatidylcholine metabolism in $GH_3$ pituitary cells. J. Biol. Chem. **262**, 9204–9210 (1987).
18. Liscovitch, M.: Crosstalk among multiple signal-activated phospholipases. Trends in Biochem. Sci. **17**, 393–399 (1992).
19. Löfflerholz, K.: Receptor regulation of choline phospholipid hydrolysis. A novel source of diacylglycerol and phosphatidic acid. Biochem. Pharmacol. **38**, 1543–1549 (1989).
20. Nishibe, S., Wahl, M. I., Hernandez-Sotomayor, S. M. T., Tonks, N. K., Rhee, S. G., Carpenter, G.: Increase of the catalytic activity of phospholipase C–$\tau_1$ by tyrosine phosphorylation. Science **250**, 1253–1256 (1990).
21. Okazaki, T., Sagawa, N., Okita, J. R., Bleasdale, J. E., McDonald, P. C., Johnston, J. M.: Diacylglycerol metabolism and arachidonic acid release in human fetal membranes and decidua vera. J. Biol. Chem. **256**, 7316–7321 (1981).
22. Pelech, S. L., Vance, D. E.: Signal transduction via phosphatidylcholine cycles. Trends in Biochem. Sci. **14**, 28–30 (1989).
23. Rando, R. R.: Regulation of protein kinase C activity by lipids FASEB J. **2**, 2348–2355 (1988).

24. Sagawa, N., Okazaki, T., McDonald, P. C., Johnston, J. M.: Regulation of diacylgycerol metabolism and arachidonic acid release in human amniotic tissue. J. Biol. Chem. **257**, 8158–8162 (1982).
25. Slack, B. E., Breu, J., Wurtman, R. J.: Production of diacylglycerol by exogenous phospholipase C stimulates CTP: phosphocholine cytidylyltransferase activity and phosphatidylcholine synthesis in human neuroblastoma cells. J. Biol. Chem. **266**, 24503–24508 (1991).
26. Suzuki-Sekimori, R., Matuoka, K., Nagai, Y., Takenawa, T.: Diacylglycerol, but not inositol 1,4,5-trisphosphate, accounts for platelet-derived growth factor-stimulated proliferation of BALB 3T3 cells. J. Cellular Physiol. **140**, 432–438 (1989).
27. Tijburg, L. B. M., Geelen, M. J. H., van Golde, L. M. G.: Regulation of the biosynthesis of triacylglycerol, phosphatidylcholine and phosphatidylethanolamine in the liver. Biochim. Biophys. Acta **1004**, 1–19 (1989).
28. Tóth, M., Gimes, G., Hertelendy, F.: Triton X–100 promotes the accumulation of phosphatidic acid and inhibits the synthesis of phosphatidylcholine in human decidua and chorion frondosum tissues. Biochim. Biophys. Acta **921**, 417–425 (1987).

*Acta Physiologica Hungarica, Volume 81 (4), pp. 355–361 (1993)*

# EFFECTS OF HIGH SALT CONCENTRATION ON THE OPEN PROBABILITY OF THE BACKGROUND CHLORIDE CHANNEL

C. TREQUATTRINI, ANNA PETRIS, F. FRANCIOLINI

ISTITUTO BIOLOGIA CELLULARE, UNIVERSITA DI PERUGIA, PERUGIA, ITALY

Received January 31, 1993
Accepted March 17, 1993

We report here single channel data showing that high concentration of NaCl or CsCl at the cytoplasmic side of the membrane increases the open probability of the background Cl channel from hippocampal neurons. The open probability vs. voltage curve was shifted by 36 mV towards more negative voltages, when salt concentration was raised from 300 to 1000 mM. The steepness of the curve remained unchanged. Possible explanations for this effect are discussed.

**Keywords**: chloride channel, hippocampal neurons, cytoplasmic side of the cell membrane

In voltage-dependent channels, transitions between the closed and open states are driven by voltage changes across the membrane. Although voltage is the primary factor in gating this type of channel, several elements can concur in modulating the gating mechanism. A number of toxins, enzymes, low-weight chemical compounds have been reported to variously interact with ionic channels, and modify gating (i.e., channel activation, deactivation, inactivation parameters: cf. [8]). In this paper we report a study on the effect of ionic strength, a particular type of gating modulator, on the open probability of the background Cl channels from rat hippocampal neurons [4], and discuss the two most likely explanations. 1) The surface charge effect, i.e., the decrease of the negative surface potential at the cytoplasmic side of the membrane, due to the screening effect exerted by the excess positive ions. 2) The "foot in the door" effect, the effect exerted by permeant ions which prevent the closing of the channels while bound to the channel site, and as a result the channel open probability increases.

Correspondence should be addressed to
F. FRANCIOLINI
Istituto Biologia Cellulare Universita di Perugia
via Pascoli 1, I–06100 Perugia, Italy

*Akadémiai Kiadó, Budapest*

## Methods

Experiments were carried out on hippocampal neurons dissected from 18-d-old rat embryos, and plated on collagen/polylysine-coated culture dishes containing basic tissue culture medium (N5) supplemented with a fraction of horse serum. Neurons were kept in culture for 2–4 weeks before the experiment.

The patch clamp method [6] was used to record single-channel currents in the inside-out configuration. The cell membrane was voltage-clamped and current was recorded with a List EPC-7 patch clamp amplifier. The pClamp-5 (Axon-Instrument, USA) package of hardware and software was routinely used during experiments for stimulating, recording the currents, and analyzing the data. Single channel currents were filtered at 1.0 kHz (−3 dB) and digitized at 2.5 kHz. Single-channel records were recorded in steady-state conditions attained by stepping the membrane voltage to the desired level, and maintaining that value for tens of seconds to minutes. Recording began several seconds after the step potential, to allow relaxation processes subsequent to the voltage step to reach completion. Current amplitude histograms were constructed from 10–25 s stretches of current records, and used to measure single-channel current and channel open probability. Single-channel current was measured as interpeak distance and channel open probability was calculated from the integral areas of the amplitude histogram peaks.

Solutions contained either 300 or 1 000 mM NaCl or CsCl, 2 mM morpholinopropanesulphonic acid (MOPS), and 1 mM EGTA. The solutions were adjusted to pH 7.3. These solutions will be referred to by specifying the concentration (mM) of the main ions, e.g. 300 NaCl//300 NaCl for intracellular//extracellular concentrations. Effective change of test solutions at the cytoplasmic surface of the patch in the inside-out configuration was obtained by placing the membrane patch into the mouth of a perfusion pipette containing the desired solution. Experiments were carried out at 22–25 °C.

## Results

Figure 1 shows single channel recordings at different voltages, and corresponding amplitude histograms and I/V plots from a background Cl channel in symmetrical 300//300 (A) and 1,000//300 mM NaCl (B), respectively. The identification of this channel as a background Cl channel was based on conductance measurement, and on the significant cation permeability, evidenced here by the discrepancy between the actual reversal potential of +19 mV in 1,000//300 mM NaCl (Fig. 1B, right side panel) and the reversal potential of +31 mV expected for a perfectly selective Cl channel at this salt gradient condition.

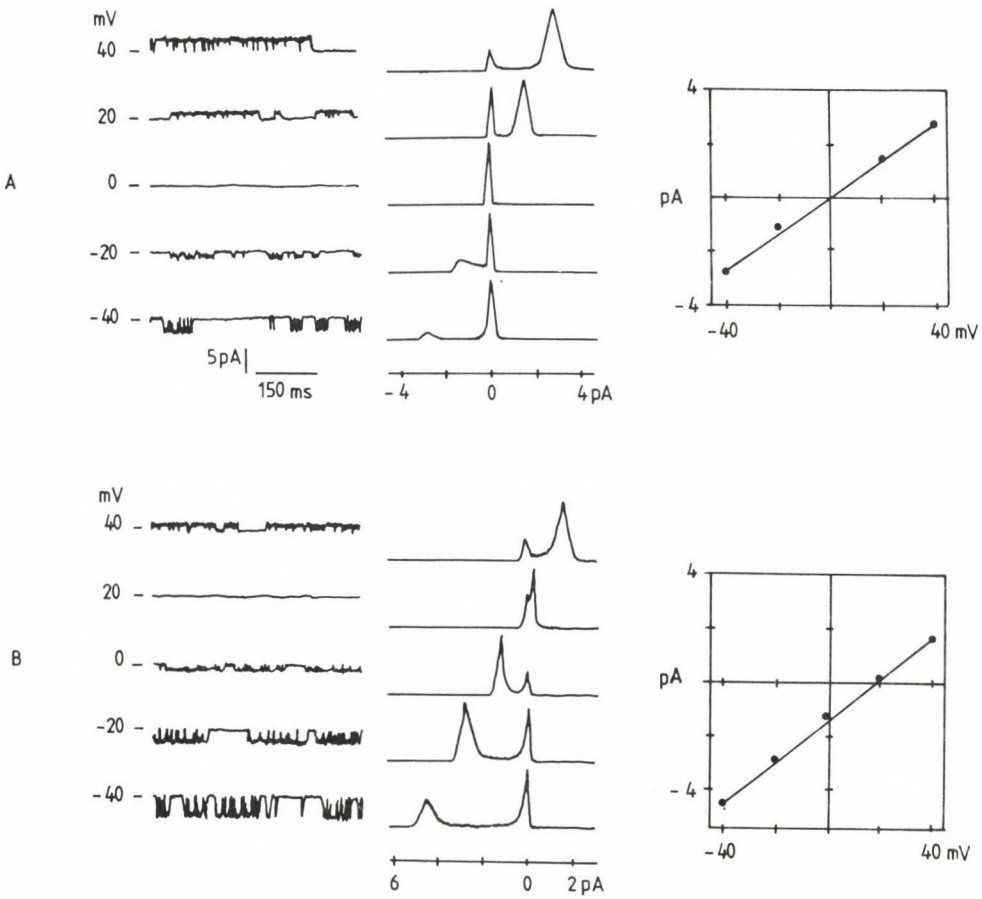


*Fig. 1.* Effect of ionic concentration on the open probability of the background Cl channel of rat hippocampal neurons. Single channel currents at different voltages and perfusing conditions are shown, together with relative amplitude histograms and current voltage plots. Pipette solution is 300 mM NaCl. Amplitude histograms are derived from 10–25 s stretches of single channel activity. The corresponding segments shown in the figure contributed, in part, to the histograms. The measured currents, sampled every 400 μs, were binned at 0.04 pA resolution, and the number of observations in each bin plotted against the current range for each bin. Note that the channel is active at negative voltages at both ionic concentrations, displaying short open times and marked flickering. Current records are not indicative of channel activity as they were selected to show the most openings at each voltage. (A) Perfusion conditions of 300//300 mM NaCl. The current reverses at 0 mV, as expected for the symmetrical ionic conditions. Single channel conductance is 65 pS. (B) Salt gradient condition of 1,000//300 mM NaCl. The reversal potential is 19 mV. This value, considerably lower than the value (31 mV) expected for a perfectly selective Cl channel at the above gradient conditions, can be accounted for by the Goldman-Hodgkin-Katz voltage equation $E_{rev} = RT/F \ln[P_{Na,o} + P_{Cl,i}]/[P_{Na,i} + P_{Cl,o}]$ assuming a permeability ratio of Na relative to Cl ($P_{Na}/P_{Cl}$) of 0.25

The relevant point of this figure is that at any given voltage the channel open probability is markedly higher when the patch is perfused with 1,000 mM NaCl, as compared to 300 mM NaCl. This effect is not clearly evident by looking at the single channel recordings, since they have been selected to show high activity at both conditions, thus they do not necessarily reflect the gating behavior of the channel. Rather, the effect is fully evident when the amplitude histograms, taken at different ionic concentrations and at the same voltage, are compared. Amplitude histograms are the reliable indicator of the channel gating behavior, since they are constructed from long stretches (10–25 sec) of single channel recordings. The dependence of channel open probability on ion concentration is clearly shown at negative voltages, where the open-state probability of the channel is low. At −40mY the open-state peak in 300 mM NaCl is barely visible (representing only 12% of total peak area), whereas it represents more than half of the total peak area in 1,000 mM NaCl. This effect is still very pronounced at −20 mV where the open-state peaks are 33% and 68% of total peak area, respectively. It is not possible to make the comparison, at zero and +20 mV since the patch is at, or very close to, the equilibrium potential for Cl; the open-state peaks are absent in the first case and poorly resolved in the second. At more positive voltages, +40 mV, when the open probability is already high even with 300 mM NaCl ($P_o > 0.8$), increases brought about by ionic concentration are barely noticeable. Similar results were obtained when Cs replaced Na as the main cation.

A quantitative analysis of the effect of ionic concentration on channel gating is illustrated in Fig. 2, where the channel open probability is plotted as a function of membrane potential at the two ionic concentrations. The two sets of data are both fitted with Boltzmann isotherms. The main point here is that while the parameter $z$ remains essentially the same in the two cases ($z_1 = 1.67$; $z_2 = 1.41$), $V_{1/2}$, the voltage at which $P_o = 0.5$, is shifted to more negative voltages by 35 mV. Since $z$ represents the equivalent number of charges in the voltage sensor of voltage-gated channels, the constancy of this parameter would suggest that ionic concentration does not interfere with the translocation of charges, i.e., with the opening rate of the channel. On the contrary, the marked shift on the curve at high ionic concentration to more negative voltages, which indicates a higher open channel probability, is evidence of an effect of ionic concentration on the stability of the (open and closed) conformational states of the channel.

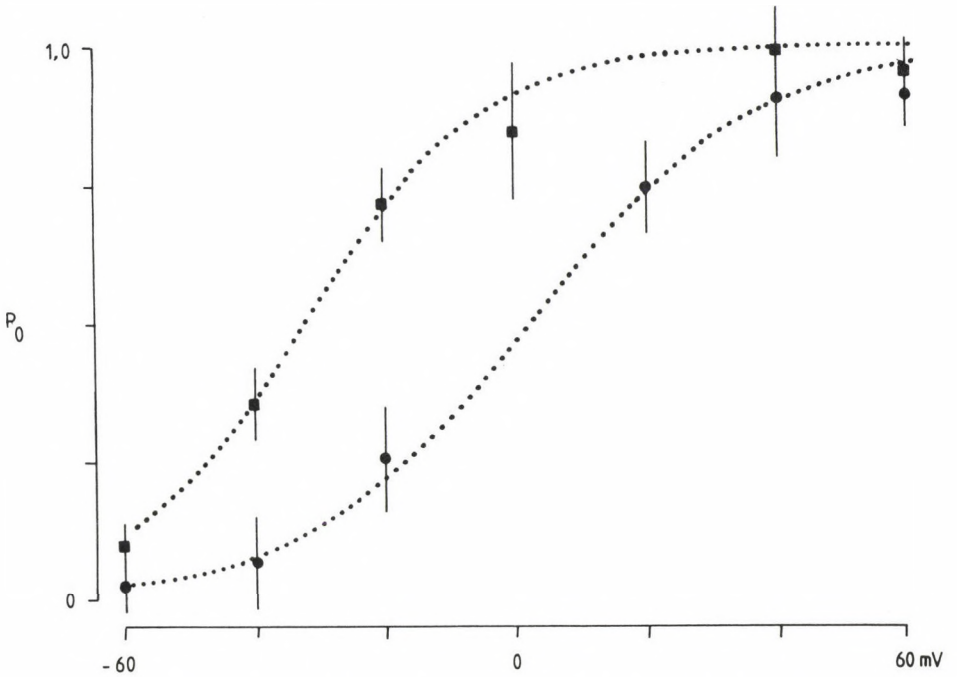


*Fig. 2.* Quantitative analysis of the effect of ionic concentration on the open probability vs. voltage relation of the background Cl channel. Plot of the channel open probability, $P_o$, as function of voltage in symmetrical 300//300 mM NaCl (circles, 3 patches, mean ± SD) and in 1,000//300 mM NaCl (squares, 4 patches, mean ± SD). The dotted curves are fits for the experimental points according to the eqn. $P_o = 1/\{1 + \exp[-zF(V-V_o)/RT]\}$, where V is membrane voltage and $V_o$ the voltage at which $P_o = 0.5$. The fitted curves in the two different ionic conditions have nearly the same z ($z_1 = 1.67$; $z_2 = 1.41$), but the midpoints, $V_o$, are about 35 mV apart

## Discussion

We have presented single channel data on the effect of ion concentration on the gating of the background Cl channel from rat hippocampal neurons. In particular, we have shown that increasing the ion concentration at the cytoplasmic side of the membrane increases the open probability of the channel, which results in a shift of the open probability vs. voltage curve towards more negative voltages.

Shifts of the activation curve upon changes of ion concentration have been described for several ionic channels [2, 3, 7, 10]. In general, an increase of ion concentration on the external side of the membrane results in a shift of the activation curve towards more positive voltages, whereas a concentration increase on the intracellular side of the membrane produces an opposite effect it widely accepted explanation of these effects is that positive ions neutralize the excess of negative

charge present on the membrane surface [3]. This results in a modification of the local electric field across the membrane, which is sensed by the channel voltage sensor. A number of observations, however, do not fit with this view. For instance, although the change in the electric field brought about by the screening of charge is homogeneously distributed over the membrane, not all channels are affected to the same extent. Increasing the [Ca] outside the squid axon produces a shift of Na channel activation significantly higher than for K channels [5]. Similar observations were reported on frog node by Hille [7]. In addition, it was found that the different gating parameters within a given channel were also modified to a different extent. For example, following a [Ca] increase, Na channel activation is shifted considerably more than inactivation [5]. Only to a certain extent, these observations can be accounted for by the fact that the different gating systems in different channels, as well as the two gating systems (activation and inactivation) of Na channels may depend (and in fact this is our present view) on different gating structures which could be sensing a significantly different electric field.

An alternative interpretation of these effects, initially proposed to explain how certain permeant ions increased the channel open time of the Ach receptors of *Aplysia* [1], suggests that permeant ions stabilize the channel in the open conformation by preventing the channel from closing while the ion is bound within the channel pore. As channel occupancy is a direct function of ion concentration, an increase of the latter parameter would increase the channel open probability.

A specific test of this hypothesis was made by Marchais and Marty [11] by carrying out relaxation experiments at different ionic concentration to see whether an increase of ionic concentration (thus higher binding site occupancy) would increase the relaxation time constant, i.e., the mean open time. Their results showed that the relaxation time constant was a direct function of ionic concentration, thus reinforcing the view that the channel closes less easily if an ion is bound to the site. Indeed, these authors presented a model based on the assumption that the open channel cannot close when an ion is in the pore, and quantitatively showed that the model is fully consistent with the experimental data.

Results consistent with this view were obtained on the K channel of squid axon by Swenson and Armstrong [12] who found that the closing rate of the K channel depends on the type of ion present in the surroundings. On observing that Rb was more effective than K in slowing the closing of the channel, and relating this effect to the longer dwell-time in the channel site that Rb has as compared to K, these authors reached the same conclusion that ion-occupied channels cannot close. This effect of ions preventing the closing of the channel is termed "foot in the door" where the foot is played by the ion.

This model implies that: 1) The channel has (at least) two open states, one with the site empty, and one with the site occupied from which it cannot close; 2) since a

channel in the open-occupied state cannot close, the mean overall open time of the channel increases with the probability that the channel is occupied by an ion; 3) since an occupied channel cannot close, a closed channel cannot exist with an ion trapped in the site, thus there can only be one transition rate to the open state.

Single channel recording is the ideal method to test the two hypotheses, since it allows accurate measurements of open and closed dwell times from which the number of open and closed states, as well as their transition rate values can be determined. In this work requirement 2) of the model has been verified. We are presently testing the other two implications of the model to see which of the two hypotheses illustrated above more adequately account for our data.

## Acknowledgements

The authors thank Massimo Baldracchini for technical assistance. This work was supported by grant Progetto Bilaterale No. 910040104/11521 from the Italian Consiglio Nazionale Ricerche.

## REFERENCES

1. Ascher, P., Marty, A., Neild, T. O.: Lifetime and elementary conductance of the channels mediating the excitatory effects of acetylcholine in *Aplysia* neurones. J. Physiol. (Lond.) **278**, 177–206 (1978).
2. Campbell, D. T., Hille, B.: Kinetic and pharmacological properties of the sodium channel of frog skeletal muscle. J. Gen. Physiol. **67**, 309–323 (1976).
3. Chandler, W. K., Hodgkin, A. L., Meves, H.: The effects of changing the internal solution on sodium inactivation and related phenomena in giant axons. J. Physiol. (Lond.) **180**, 821–836 (1965).
4. Franciolini, F., Nonner, W.: Anion and cation permeability of a chloride channel in rat hippocampal neurons. J. Gen. Physiol. **90**, 453–478 (1987).
5. Frankenhaeuser, B., Hodgkin, A. L.: The action of calcium on the electrical properties of squid axons. J. Physiol. (Lond.) **137**, 218–244 (1957).
6. Hamill, O. P., Marty, A., Neher, E., Sakmann, B., Sigworth, F. J.: Improved patch-clamp techniques for high resolution current recording from cells and cell free membrane patches. Pfluegers Arch. **391**, 85–100 (1981).
7. Hille, B.: Charges and potentials at the nerve surface: Divalent ions and pH. J. Gen. Physiol. **51**, 221–236 (1968).
8. Hille, B.: Ionic channels of excitable membranes. Sinauer Associates Inc. Sunderland, Massachusetts. p: 607 (1992).
9. Hille, B., Woodhull, A. M., Shapiro, B. I.: Negative surface charge near sodium channels of nerve: Divalent ions, monovalent ions, and pH. Phil. Trans. R. Soc. Lond. B **270**, 301–318 (1975).
10. Kostyuk, P. G., Mironov, S. L., Doroshenko, P. A., Ponomarev, V. N.: Surface charges on the outer side of mollusc neuron membrane. J. Physiol. (Lond.) **70**, 171–179 (1982).
11. Marchais, D., Marty, A.: Interaction of permeant ions with channels activated by acetylcholine in Aplysia neurones. J. Physiol. (Lond.) **297**, 9–45 (1979).
12. Swenson, R. P. Jr., Armstrong, C. M.: $K^+$ channels close more slowly in the presence of external $K^+$ and $Rb^+$. Nature **291**, 427–429 (1981)

*Acta Physiologica Hungarica, Volume 81 (4), pp. 363–370 (1993)*

# ENDOTHELIAL CHANGES FOLLOWING REPEATED EFFECT OF VASOCONSTRICTIVE SUBSTANCES IN VITRO

VIERA KRISTOVÁ, M. KRIŠKA, R. CAŇOVÁ, E. HEJDOVÁ, D. KOBZOVÁ*, P. DOBROCKÝ

DEPARTMENT OF PHARMACOLOGY AND *DEPARTMENT OF PATHOLOGY, FACULTY OF MEDICINE, COMENIUS UNIVERSITY, BRATISLAVA, SLOVAK REPUBLIC

Received February 23, 1993
Accepted May 12, 1993

Using perfusion method the reactivity of rabbit femoral and ear arteries was investigated following the administration of rising noradrenaline doses in four consecutive intervals. Progressive increase of vasoconstrictive activity of vessel segments was found. Results of histological examination showed a progressive deendothelization of perfused vessels. The loss of endothelium increased depending on time of action and on intensity of vasoconstrictive stimuli.

**Keywords**: vessel perfusion, increase of contractivity, endothelium loss

The endothelial cells modulate the reactivity of vessels to various stimuli secreting relaxing factors ($EDRF_1$, $EDRF_2$, $PGI_2$) and constrictive factors (endothelin, prostaglandins). The endothelium damage can considerably influence the vessel reactivity interfering in the production of endothelial secretory substances. Thus, the study of endothelium-dependent responses can contribute to the clarification of the endothelium role in the vessel reactivity to various vasoconstrictive and vasodilating substances. In accord with recent data about the role of endothelium in regulation of vessel tonus our aim was to study the endothelial changes in isolated vessels during the use of perfusion method. In our previous experiments with fetal vessels (pulmonary artery, ductus arteriosus) characterized by higher fragility, an endothelium loss following repeated vasoconstrictive stimuli has been found [2]. In series of experiments with long-term administration of vasoconstrictive substance, the constrictive activity of vessels increased progressively. The aim of our study has been to investigate whether this finding is in connection with the state of endothelial lining.

Correspondence should be addressed to:
Viera KRISTOVÁ
Department of Pharmacology, Faculty of Medicine, Comenius University
Sasinkova 4, 811 00 Bratislava, Slovak Republic

*Akadémiai Kiadó, Budapest*

Therefore the reactivity of rabbit isolated femoral and ear arteries was evaluated following rising noradrenaline doses in four intervals and the state of endothelium of perfused vessels was histologically examined.

## Materials and methods

Rabbit vessels (Cincilla, male, 6 to 12 months old, of body weight 2 to 2.5 kg) were used in experiments. The animals were sacrificed by cervical dislocation. The preparation of vessels was as follows.

*Femoral artery*

Femoral artery was prepared together with the iliac artery from the inguinal channel and cut up in the knee joint. The vessels were placed into Tyrode's solution (composition in mmol × $l^{-1}$ was: NaCl 137, KCl 2.7, $MgCl_2$ 1.1, $NaH_2PO_4$ 0.32, $CaCl_2$ 0.9, $NaHCO_3$ 11.9, glucose 5.5). The removing of the surrounding tissue and the canulation of femoral artery were performed during permanent moistening with Tyrode's solution. In all perfusion experiments the same segment was used. The canula was inserted into the femoral artery through the iliac artery. This procedure enables the insertion of a canula larger in inner diameter, keeping the wessel minimally demaged. The vessel was fixed to the canula by cotton thread and the distal segment was cut up to a constant length of 5 mm. The free segment of femoral artery represents the functional part of the vessel and was used after finishing the experiment for histological examination.

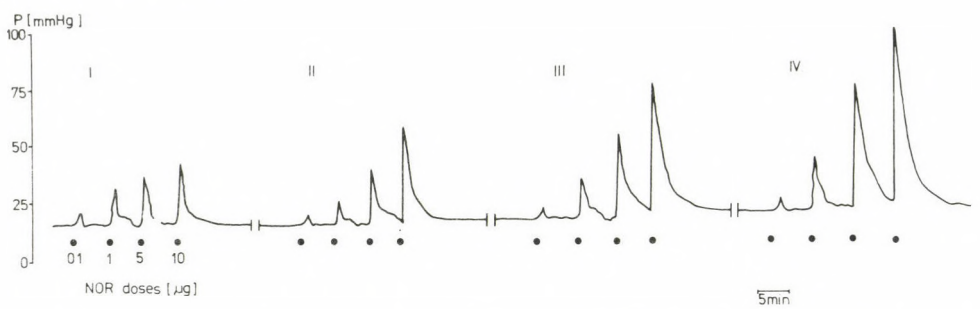


*Fig. 1.* Method of evaluation of isolated rabbit femoral artery reactivity to noradrenaline administered in 4 time intervals (I – IV) – record from an experiment. P – perfusion pressure, NOR – noradrenaline

Isolated femoral artery was placed into an organ chamber filled with Tyrode's solution, saturated by atmospheric oxygen and maintained at constant temperature 37 °C. The vessel segment was perfused by constant flow and recording of the perfusion pressure changes was performed by means of tensometric transducer (LPD 102 Tesla) and recorder (TZ 4200 Tesla). The equilibration of the vessel lasted 30 minutes. Following the equilibration the flow through the vessel was 25 ml/min and the basal perfusion pressure was about 18 to 20 mmHg. Noradrenaline was added in four increasing single doses (100 ng, 1, 5 and 10 μg) in 0.1 ml volume directly into the canula, the outflow of perfused liquid from the vessel into the stock solution being meanwhile interrupted. The procedure used for estimation of the femoral artery reactivity following repeated noradrenaline administrations is shown in Fig. 1. Four

noradrenaline doses were added following the equilibration with a subsequent interval interruption of 10 min (the duration of one series of noradrenaline administration was about 30 min). Three further series of noradrenaline additions in equal doses followed thereafter. The vessel samples for histological examination were taken after the first, third and fourth series of noradrenaline additions, it means in three sets of preparations. The samples cannot be taken continuously because the functional segment of the vessel could become contracted.

*Ear artery*

Isolation of central ear artery was performed after the auricula being amputated. The canula was inserted into the vessel and fixed by cotton thread. The length of the free segment was 5 mm. Equilibration lasted 30 min, the flow was 3 ml/min and the basal perfusion pressure was about 30 mmHg. Noradrenaline was added in three doses (10, 50, 100 ng) and as in the femoral artery four series of noradrenaline applications followed in 30-min intervals. At the end of the experiment the functional state of the endothelium was tested using the acetylcholine test – in noradrenaline preconstricted vessel in a concentration of $3 \times 10^{-6}$ mol. $l^{-1}$, response to acetylcholine in 10 μg dose was evaluated. The state of endothelium was histologically investigated after the experiment had been finished.

*Histological preparations*

At the end of the experiment vessels were filled with Bacto-agar (Difco Laboratories, USA) to preserve the endothelium in situ. After fixation in 10% formaldehyde solution (2 hours) the vessels were processed by routine paraffin method. Vertical slices were stained with hematoxilin and eosin.

*Evaluation of results*

Results are given as mean response values and S.E.M. Statistical analysis was performed using Student's t-test.

*Substances used*

Noradrenalin inj. (Spofa), Acetylchloline subst. (Dispersa AG). All solutions were prepared freshly before each experiment. The substances were dissolved in physiological saline solution. For dilution of drugs Thyrode's solution was used.

## Results

The reactivity of isolated rabbit femoral and ear arteries to rising noradrenaline doses, given in four series was evaluated. The comparison of the femoral artery dose-dependent responses (Fig. 2) shows apparently that the intensity of vasoconstrictive responses following the I and II noradrenaline application series was not changed. An important increase of vasoconstrictive activity occurs following the III noradrenaline treatment series, but in comparison to the IV series no significant differences were observed.

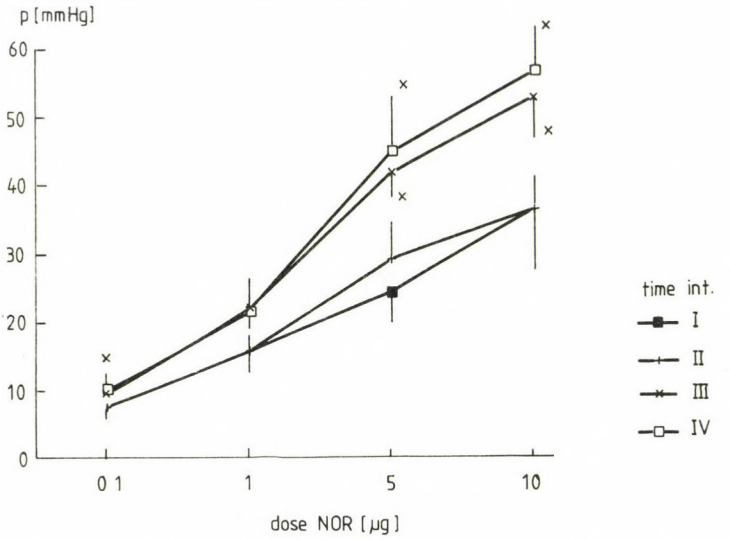


*Fig. 2.* Dose-response curves of rabbit femoral artery to noradrenaline in 4 time intervals. Each value represents mean ± S.E.M. (n = 6), *$p < 0.05$, significant differences between I–III and I–IV intervals

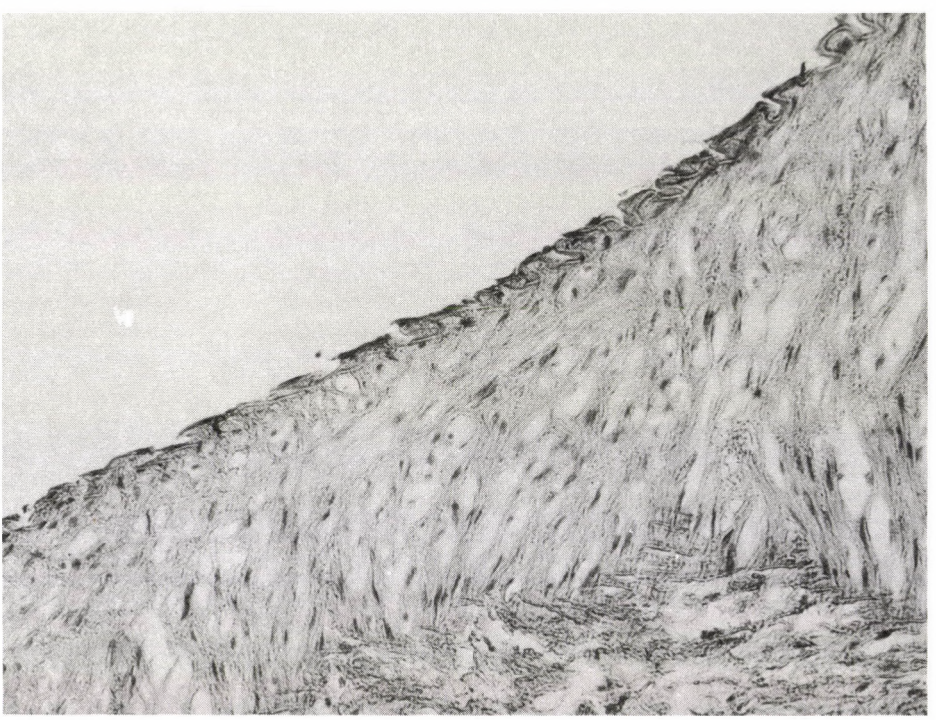

*Fig. 3.* Section of rabbit femoral artery wall after I. series of noradrenaline administration. Endothelial cells are well preserved. Hematoxylin and eosin (HE) ×1260

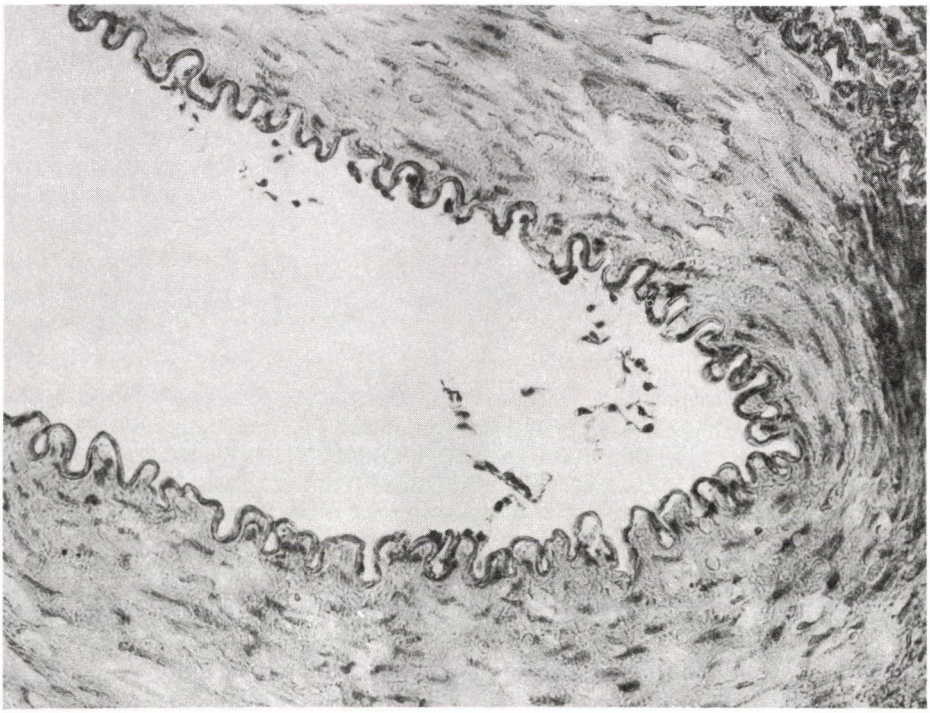

*Fig. 4.* Rabbit femoral artery following 4 consecutive noradrenaline application series. The vessel wall is constricted, the endothelial cells are mostly denuded. (HE) ×1260

As to the histological examination of the femoral artery an endothelium loss was found (in extent of 50–60%) following the I series of noradrenaline application (Fig. 3). Following the III noradrenaline application series the endothelium loss exceeded 80%. Sporadic endothelial cells were preserved only following four consecutive noradrenaline application series (Fig. 4).

The results of the evaluation of isolated ear artery responses to noradrenaline following four application series are shown in Fig. 5. Following the II noradrenaline application series the constrictive responses were already significantly increased. The last application series did not result in further increase of the responses. The acetylcholine test performed after the IV noradrenaline application series revealed a decrease of relaxing responses up to 26.5 ± 4.2%, indicating the loss of functional endothelium. Nearly complete deendothelization of vessel segments was confirmed by histological examination at the end of the experiment.

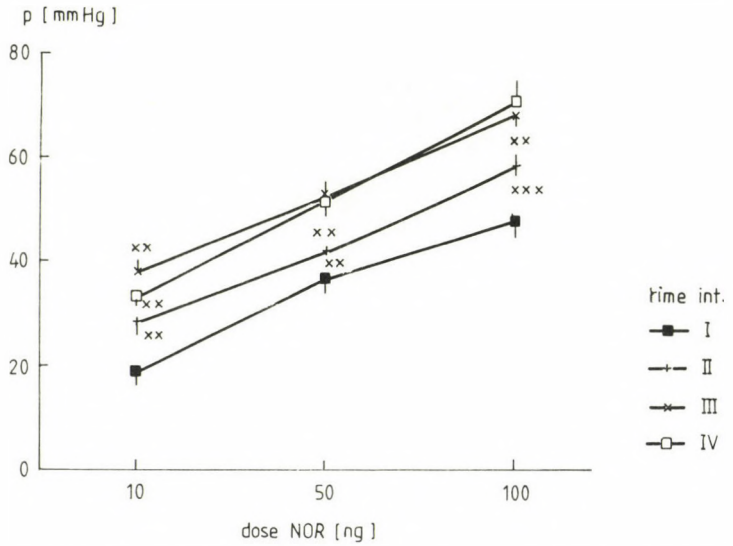


*Fig. 5.* Dose-response curves of isolated rabbit ear artery to noradrenaline administered in 4 time intervals (n = 7). Statistical significance was found between I–II and II–III intervals, $^{**}p < 0.01$, $^{***}p < 0.001$

## Discussion

A progressive increase of constrictive responses of rabbit femoral and ear arteries was found following repeated administration of submaximal noradrenaline doses. The rise in vessel reactivity occurred within a very short time after the application of vasoactive stimuli. Results of histological examination suggest a direct connection of endothelium loss during the experiment with the constrictive response enhancement. This is confirmed by data, showing that the catecholamines, noradrenaline above all, cannot only damage the endothelial cells but it may even cause cell death [7, 8].

Our results are very similar to those obtained by mechanic deendothelization stimulus (e.g. by stick, air bubbles) in various types of vessels [3, 9, 10]. There is an increase in reactivity not only to noradrenaline, but also to other substances, as histamine and KCl depolarization solution.

The mechanism of the vessel reactivity increase following deendothelization has not been sufficiently explained. The most plausible explanation can be in decreased production of vasodilating factors in endothelial cells, namely EDRF and $PGI_2$. Considering that the endothelial cells are the major source of $PGI_2$ synthesis the intactness of endothelium plays an important role in the local regulation of the

vessel tonus, especially regarding vasodilatation. Findings, that indomethacin increased the noradrenaline vessel responses in vitro (unpublished results) support the suggestion that $PGI_2$ participates in the reactivity of vessels.

A further possibility concerning of increased vessel reactivity can be the influence on the processes connected with $Ca^{2+}$ transport and with cyclic nucleotides. Ignarro et al. [6] found that deendothelization of intrapulmonary arteries induced decreased cGMP levels in smooth muscle. After cGMP had been inhibited by LY 83583 the sensitivity of intact vessels to vasoconstrictive substances rose similarly as in deendothelized vessels [10].

Another hypothetical explanation can be seen in increased production of vasoactive substances, namely of endothelin, produced not only in endothelial cells but also in smooth muscle cells of vessels [4]. The hypothesis that the secretion of endothelin in smooth muscle could participate, together with other mechanisms, in enhancing constrictive effects of vasoactive substances is to be proven experimentally.

The finding of adrenergic $alpha_2$ receptors on the endothelial cells, mediating the release of EDRF, can contribute to clarification of constrictive response in connection with endothelium loss. After the endothelium of coronary vessels in various animal species has been removed, the concentration-response curves to noradrenaline were shifted to the left and the maximal response was increased [1].

These results demonstrate that vasoactive stimuli significantly damage the endothelial layer in perfused vessels and their interpretation does not correspond in fact to physiological conditions. In evaluation of vessel reactivity to vasoconstrictive substances, maximal doses should not be used without checking the state of endothelium, above all, during a long-term comparative experiment. This factor should be considered in studies of this type. In experiments with perfused isolated vessels the addition of albumin into perfusion solution would be useful, the stability of endothelial layer could be so enhanced and a considerable endothelium loss during the experiment prevented [5].

Present results call attention to the fact, that if during pharmacotherapy vasoconstrictive substances are repeatedly applied, or in conditions with damaged endothelial lining integrity, increased readiness of vessels to contract can develop with consequent local disturbances of circulation.

## Acknowledgement

These studies were supported by grant N° 1 (990504) 92, Grant agency for sciences, Ministry of Education, Slovak Republic.

## REFERENCES


1. Angus, J. A., Cocks, T. M., Satoh, K.: The alpha adrenoceptor on endothelial cells. Federation Proc. **45**, 2355–2359 (1986).
2. Babál, P., Kriška, M., Kristová, V., Jakubovský, J., Caňová, R., Blahutová, V.: Changes of the vascular endothelium in rabbit fetuses under conditions of perfusion in vitro. Bratisl. Lek. Listy **91**, 335–340 (1990).
3. Carrier, G. O., White, R. E.: Enhancement of alpha-1 and alpha-2 adrenergic agonists induced vasoconstriction by removal of endothelium in rat aorta. J. Pharmacol. Exp. Ther. **232**, 682–687 (1985).
4. Coceani, F., Kelsey, L.: Endothelin-1 release from lamb ductus arteriosus: relevance to postnatal closure of the vessel. Can. J. Physiol. Pharmacol. **69**, 218–221 (1990).
5. Hoogerwerf, N., Zijlstra, E. J., Van der Linden, P. J. W., Westerhof, N., Sipkema, P.: Endothelium function is protected by albumin and flow-induced constriction is independent of endothelium and tone in isolated rabbit femoral artery. J. Vasc. Res. **29**, 367–375 (1992).
6. Ignarro, L. J., Burke, T. M., Wood, K. S, Woolin, M. S., Kadowitz, P. J.: Association between cyclic GMP accumulation and acetylcholine-elicited relaxation of bovine pulmonary artery. J. Pharmacol. Exp. Ther. **228**, 682–690 (1984).
7. Joris, I., Majno, G.: Endothelial changes induced by arterial spasm. Amer. J. Pathol. **102**, 346–358 (1981).
8. Makhmudov, R. M., Mamedov, J. D., Dolgov, V. V., Repin, V. S.: Catecholamine-mediated injury to endothelium in rabbit perfused aorta: A quantitative analysis by scanning electron microscopy. Cor Vasa **27**, 456–463 (1985).
9. Kriška, M., Babál, P., Kristová, V., Caňová, R.: Evaluation of perfused vessel reactivity in relation to the endothelium. Čs. Fysiol. **38**, 153 (1989).
10. Tesfamariam, B., Weisbrod, R. M., Cohen, R. A.: Cyclic GMP modulators on vascular adrenergic neurotransmission. J. Vasc. Res. **29**, 396–404 (1992).

*Acta Physiologica Hungarica, Volume 81 (4), pp. 371 – 393 (1993)*

# EFFECTS OF HYPERCALCEMIA ON KIDNEY FUNCTION IN ANESTHETIZED DOGS

G. KÖVÉR, Hilda TOST

DEPARTMENT OF PHYSIOLOGY, SEMMELWEIS UNIVERSITY MEDICAL SCHOOL BUDAPEST, HUNGARY

Received March 5, 1993
Accepted March 24, 1993

The effects of acute hypercalcemia on renal function were evaluated in anesthetized mongrel dogs. Calcium concentration was increased by infusion of $CaCl_2$ solution into the left renal artery at two different rates.

At the lower rate of infusion (0.010 mM/kg/min) the plasma total calcium concentration in the left kidney increased from 2.5 mM/l to 3.76 mM/l and the arterial plasma total calcium concentration to 2.94 mM/l. Renal vascular resistance in the left kidney did not change in association with a small decrement in the renal blood flow (9.5%). The glomerular filtration rate decreased from 82.9 ml/min to 65.9 ml/min in association with a small decrease in the urine output. The calcium excretion increased slightly from 3.3 μM/min to 4.05 μM/min.

When this amount of $CaCl_2$ was infused into the left renal artery the parameters of the right intact kidney did not change.

During the higher rate of infusion (0.020 mM/kg/min) in the left kidney the plasma total calcium concentration in the left kidney increased from 2.3 mM/l to 6.15 mM/l and in the arterial plasma to 3.4 mM/l. Renal vascular resistance increased considerably from 1.66 to 4.0 and the renal blood flow decreased from 482 ml/min to 311 ml/min. The glomerular filtration rate dropped from 78.7 ml/min to 43 ml/min with a significant decrease in the urine output. The calcium excretion increased from 4.35 μM/min to 7.5 μM/min.

In the right kidney during the $CaCl_2$ infusion the $C_{PAH}$ decreased from 304 ml/min to 239 ml/min showing that there was an increase in the vascular resistance in association with decrements in $C_{inulin}$ from 85 ml/min to 67.2 ml/min.

These data prove a direct, but not linear relationship between the total plasma calcium concentration and the renal vascular resistance.

We suppose that the distal tubular calcium load participates in the distal tubular feedback regulation, when the calcium ion concentration in the tubular fluid at the macula densa increases. This increment elicits vasoconstriction in the afferent arteriole decreasing the filtered calcium load in the glomeruli.

**Keywords:** renal vascular resistance, renal blood flow, plasma calcium concentration, calcium excretion, tubuloglomerular feedback

Correspondence should be addressed to
G. KÖVÉR
Department of Physiology, Semmelweis University Medical School
H – 1088 Budapest, Puskin u. 9, Hungary

*Akadémiai Kiadó, Budapest*

In previous studies, it has been reported that there is either no change or a decrease in glomerular filtration rate (GFR) after administration of calcium salts [2, 8, 9, 22]. In studies testing the effects of various cations on local vascular resistance, renal intra-arterial infusions of solutions containing $CaCl_2$ have caused marked increases in renal vascular resistance [10]. In our experiments the intravenous infusion of calcium chloride decreased the glomerular filtration rate and the excreting capacity of the kidneys [13, 23]. The acute hypercalcemia decreased the renal blood flow [6].

Calcium ion is known to have a significant role in the maintenance of stable membrane potentials and in the muscle contractile process. Since both of these factors are important determinants of smooth muscle tone the calcium ion could participate in the regulation of the renal vascular bed.

Several studies have provided a basis for understanding the mechanism by which calcium ion modulates the renal hemodynamics.

A well-supported and widely accepted hypothesis exists concerning the negative feedback control of GFR and renin release by a system that involves communication between a macula densa sensor of early distal tubular flow rate or composition and the afferent arteriole and renin releasing juxtaglomerular cells [3, 4, 20]. This negative feedback system may be responsible for the autoregulation of renal blood flow and glomerular filtration rate [24, 25].

It was reported that the presence of calcium ions in the luminal fluid is a necessary prerequisite to elicit a full feedback response [1, 16, 18]. Other results do not support the concept that luminal divalent cations participate in the initiation of tubulo-glomerular feedback response [19].

It has also been reported that calcium antagonists interfere with the ability of the kidney to autoregulate blood flow, suggesting a role for calcium in this process [17].

It is well established that tension development in vascular smooth muscle varies as a continuous function of cytosolic calcium activity, and that renin release is inversely related to the activity of calcium within the cytoplasma of the JG cells [7, 16]. Calcium acts as a link in stimulus-secretion coupling in a wide variety of secretory systems [18].

It is possible that the intracellular calcium activity alters the feedback control from the macula densa to the afferent arteriolar and JG cells. The changes of the plasma calcium ion concentration produce many extrarenal mechanism modulations besides the renal effects which can explain that specific quantitative relationship between the effective calcium concentration and the changes in renal hemodynamic function have not been described.

In our experiments we studied the effects of the acute hypercalcemia on the renal function, when the calcium chloride was infused into the left renal artery.

## Materials and methods

The experiments were performed on mongrel dogs of either sex weighing between 15 and 30 kg. For 24 hours prior to experiment the animals were kept on water only. Anesthesia was induced by intravenous administration of pentobarbital sodium (Nembutal, Abott 30 mg/kg body wt.) and maintained with periods of additional administration. After the anesthesia each animal received an infusion of Ringer solution equal to 1% of the body weight, containing para-amino-hippuric acid (PAH) and inulin, ensuring a plasma concentration of 2 mg and 30 mg per 100 ml respectively, followed by an intravenous infusion of 0.25 ml/kg of Ringer solution containing 154 mmol/l NaCl, 4 mmol/l KCl, 1.78 mmol/l $NaHCO_3$, 2.16 mmol/l $CaCl_2$ per min for the rest of the experiment.

Cannulation of the femoral arteries and veins on both sides was performed in all animals for arterial blood collections and infusions. Mean arterial blood pressure was measured by a Statham strain gauge transducer connected to a polyethylene catheter in the left femoral artery and recorded on a RADELKIS OH 814/1 recorder.

From a lower midline incision the bladder was exposed and the urethers were catheterized supravesically using fine polyethylene cannulas.

The left renal hilum was exposed from a left lumbar incision, and the left renal vein was anastomosed with the left external jugular vein by means of siliconized rubber tube. Its T extension allowed to measure directly renal venous blood flow ($RBF_{dir}$). Before establishing the anastomosis the animals were given 500 NE/kg heparin intravenously.

A thin cannula was inserted in the left renal artery and 1.0 ml Ringer solution per min was infused by means of a pump directly in the blood flowing to the left kidney during the experiment.

About 60 minutes after starting the intravenous infusion urine was collected separately from both kidneys in 10 min periods. At the middle of each period, arterial and renal venous blood samples were taken and renal venous blood flow was measured with the help of a graduated cylinder and a stopwatch.

The two control periods (periods 1 and 2) were followed by the calcium chloride infusion and 0.010 mM/kg or 0.020 mM/kg $CaCl_2$ dissolved 1.0 ml Ringer solution was infused per minute into the left renal artery.

After starting the infusion of the $CaCl_2$ 10 minutes were allowed for the equilibration and the urine was again collected in two 10 min periods (periods 3 and 4).

Following the completion of period 4 clearance measurements, the calcium chloride infusion into the left renal artery was discontinued and 10 minutes were allowed for the recovery.

After a 10-min interval two 10-min postinfusion control periods were made (periods 5 and 6).

PAH concentration in urine and plasma was determined by the method of Smith et al. [21] that of inulin by the method of Little [15]. Urinary and plasma calcium, sodium and potassium concentration was measured by flame photometry. Total osmolality of urine and plasma was measured by the method of freezing-point depression in a Fiske osmometer. Hematocrit was determined by means of Hawskley microhematocrit centrifuge, plasma protein concentration by the biuret method [11].

The clearance of PAH ($C_{PAH}$), the extraction of PAH ($E_{PAH}$) and the clearance of inulin ($C_{inulin}$), the extraction of inulin $E_{inulin}$ were determined by the usual formules. The data for renal blood flow ($RBF_{dir}$), $C_{PAH}$, $C_{inulin}$, urine flow, sodium excretion ($U_{Na^+} \times V$), potassium excretion ($U_{K^+} \times V$), calcium excretion ($U_{Ca^{\#}} \times V$), free water clearance ($C_{H_2O}$) were referred to 100 g kidney tissue weight. The total vascular resistance ($R_{kidney/kg}$) was calculated for 1000 g kidney weight.

Statistical analysis of the data was carried out by paired and unpaired analysis using Student's 't'-test. A p value of less than 0.05 was considered significant.

## Results

The first series of studies concerns the effects of Ringer solutions infusion in anesthetized dogs. The results of this group (the number of the animals is 10) are summarized in Table I and Table II. The averages of the individual periods are in good agreement with each other within the limits of error. Table II shows the parameters of the intact right kidney. The fact that parameters for the cannulated left kidney are in good agreement with those for the intact right kidney may lead to the conclusion that the anastomosis between the renal vein and the external jugular vein did not disturb markedly the function of the left kidney.

Table III shows the left renal parameters obtained in 10 dogs where following the control period 2. 0.010 mM/kg $CaCl_2$ was infused per minute into the left renal artery. The data of the renal parameters of this series in the control periods (periods 1 and 2) are in good agreement with those of the first series.

During the calcium infusion the arterial blood pressure did not change and the RBF decreased by about 10 per cent with a considerable reduction in the glomerular filtration rate. The $C_{inulin}$ decreased from 82.5 ml/min to 65.9 ml/min ($p < 0.01$).

The urine flow was reduced from 2.17 ml/min to 1.53 ml/min ($p > 0.05$). The renal venous plasma calcium concentration in the left kidney increased from the control value (2.51 mM/l to 3.70 mM/l) during the calcium chloride infusion and in the postinfusion periods returned to 2.70 mM/l value. During the calcium infusion the calcium excretion in the left kidney increased from 3.25 μM/min to 4.07 μM/min.

In Table IV the right kidney's parameters are summarized when 0.010 mM/kg/min $CaCl_2$ is infused into the left renal artery. We can observe that when the arterial plasma $Ca^{2+}$ concentration increased from 2.48 mM/l to 2.94 mM/l, the values of the $C_{PAH}$, $C_{inulin}$, the urine flow and the other parameters did not change in the right kidney.

Table V shows averages of the parameters obtained in the left kidney when following two control periods 0.020 mM/kg/min $CaCl_2$ was infused into the left renal artery.

**Table I**

*Renal parameters in the left kidney of the control animals*
*n = 10 (Mean ± S.E.M.)*

| Periods | 1 | 2 | 3 | 4 | 5 | 6 |
|---|---|---|---|---|---|---|
| Arterial blood pressure mmHg | 125 ± 2 | 122 ± 3 | 116 ± 3 | 116 ± 4 | 116 ± 4 | 113 ± 5 |
| RBF ml/min | 559 ± 24 | 571 ± 23 | 592 ± 21 | 568 ± 22 | 555 ± 25 | 530 ± 25 |
| $R_{kidney/kg}$ mmHg.s.ml$^{-1}$ | 1.37 ± 0.07 | 1.31 ± 0.07 | 1.25 ± 0.07 | 1.31 ± 0.08 | 1.34 ± 0.10 | 1.38 ± 0.12 |
| $C_{PAH}$ ml/min | 299 ± 10 | 260 ± 13 | 239 ± 17 | 263 ± 20 | 263 ± 17 | 257 ± 19 |
| $E_{PAH}$ | 0.73 ± 0.03 | 0.76 ± 0.01 | 0.76 ± 0.01 | 0.76 ± 0.01 | 0.75 ± 0.03 | 0.82 ± 0.02 |
| $C_{inulin}$ ml/min | 85.9 ± 2.9 | 81.2 ± 4.0 | 75.4 ± 4.1 | 82.3 ± 4.7 | 85.3 ± 3.8 | 78.5 ± 6.2 |
| $E_{inulin}$ | 0.28 ± 0.02 | 0.28 ± 0.02 | 0.30 ± 0.03 | 0.29 ± 0.03 | 0.29 ± 0.02 | 0.33 ± 0.03 |
| Urine flow ml/min | 2.09 ± 0.26 | 1.89 ± 0.27 | 1.67 ± 0.33 | 1.62 ± 0.36 | 1.90 ± 0.50 | 1.93 ± 0.56 |
| Venous plasma $Ca^{2+}$ conc. mM/l | 2.31 ± 0.06 | 2.31 ± 0.06 | 2.49 ± 0.08 | 2.55 ± 0.10 | 2.36 ± 0.10 | 2.25 ± 0.08 |
| $U_{Ca^{2+}} \times V$ $\mu$M/min | 3.43 ± 0.38 | 2.75 ± 0.30 | 2.13 ± 0.32 | 1.93 ± 0.36 | 1.74 ± 0.36 | 1.57 ± 0.33 |
| $U_{Na^+} \times V$ $\mu$M/min | 281 ± 37 | 220 ± 30 | 148 ± 25 | 127 ± 27 | 118 ± 24 | 106 ± 23 |
| $U_{K^+} \times V$ $\mu$M/min | 76 ± 10 | 71 ± 9 | 64 ± 10 | 66 ± 12 | 72 ± 13 | 69 ± 13 |
| Urine osm. conc. mosm/l | 429 ± 23 | 436 ± 26 | 424 ± 30 | 427 ± 36 | 414 ± 43 | 405 ± 44 |
| $C_{H_2O}$ ml/min | -0.68 ± 0.14 | -0.63 ± 0.18 | -0.33 ± 0.20 | -0.28 ± 26 | -0.06 ± 0.42 | +0.07 ± 0.47 |

**Table II**

*Renal parameters in the right kidney of the control animals*
*n = 10 (Mean ± S.E.M.)*

| Periods | 1 | 2 | 3 | 4 | 5 | 6 |
|---|---|---|---|---|---|---|
| $C_{PAH}$ ml/min | 319 ± 14 | 287 ± 14 | 258 ± 18 | 274 ± 14 | 268 ± 17 | 267 ± 16 |
| $C_{inulin}$ ml/min | 96.2 ± 3.1 | 93.3 ± 4.8 | 85.2 ± 3.9 | 92.4 ± 5.6 | 86.8 ± 4.1 | 83.3 ± 5.1 |
| Urine flow ml/min | 2.00 ± 0.28 | 1.63 ± 0.19 | 1.34 ± 0.22 | 1.27 ± 0.25 | 1.52 ± 0.40 | 1.58 ± 0.48 |
| Arterial plasma $Ca^{2+}$ conc. mM/l | 2.31 ± 0.06 | 2.33 ± 0.06 | 2.49 ± 0.11 | 2.47 ± 0.07 | 2.39 ± 0.10 | 2.33 ± 0.07 |
| $U_{Ca^{2+}} \times V$ $\mu$M/min | 3.18 ± 0.43 | 2.42 ± 0.31 | 1.69 ± 0.30 | 1.54 ± 0.40 | 1.43 ± 0.36 | 1.29 ± 0.32 |
| $U_{Na^{+}} \times V$ $\mu$M/min | 258 ± 39 | 185 ± 29 | 107 ± 16 | 78 ± 14 | 81 ± 17 | 77 ± 19 |
| $U_{K^{+}} \times V$ $\mu$M/min | 73 ± 8 | 73 ± 7 | 64 ± 8 | 62 ± 8 | 65 ± 11 | 64 ± 11 |
| Urine osm. conc. mosm/l | 449 ± 25 | 455 ± 28 | 457 ± 33 | 446 ± 36 | 421 ± 40 | 411 ± 42 |
| $C_{H_2O}$ ml/min | -0.79 ± 0.22 | -0.70 ± 0.18 | -0.45 ± 0.16 | -0.36 ± 0.20 | -0.16 ± 0.34 | -0.01 ± 0.43 |
| Haematocrit % | 42 ± 1.2 | 42 ± 1.1 | 43 ± 0.4 | 43 ± 1.0 | 44 ± 1.2 | 43 ± 1.1 |
| Plasma total protein conc. g/100 ml | 5.24 ± 0.38 | 5.21 ± 0.38 | 5.01 ± 0.36 | 4.79 ± 0.34 | 4.71 ± 0.31 | 4.57 ± 0.27 |

**Table III**

*Renal parameters in the left kidney during 0.010 mM/kg/min $CaCl_2$ infusion in the left renal artery*
*n = 10 (Mean ± S.E.M.)*

| Periods | 1 | 2 | 3 | 4 | 5 | 6 |
|---|---|---|---|---|---|---|
| Arterial blood pressure mmHg | 124 ± 5 | 119 ± 3 | 117 ± 6 | 116 ± 7 | 117 ± 6 | 116 ± 5 |
| RBF ml/min | 484 ± 54 | 502 ± 48 | 485 ± 49 | 447 ± 54 | 425 ± 50 | 419 ± 52 |
| $R_{kidney/kg}$ mmHg.s.ml$^{-1}$ | 1.62 ± 0.16 | 1.48 ± 0.14 | 1.51 ± 0.13 | 1.64 ± 0.16 | 1.74 ± 0.17 | 1.79 ± 0.20 |
| $C_{PAH}$ ml/min | 283 ± 30 | 246 ± 26 | 215 ± 27 | 198 ± 28 | 204 ± 28 | 206 ± 27 |
| $E_{PAH}$ | 0.76 ± 0.04 | 0.80 ± 0.03 | 0.76 ± 0.04 | 0.74 ± 0.05 | 0.77 ± 0.04 | 0.77 ± 0.05 |
| $C_{inulin}$ ml/min | 85.3 ± 9.3 | 80.4 ± 8.2 | 68.4 ± 6.4 | 63.3 ± 7.3 | 69.3 ± 7.4 | 74.9 ± 9.9 |
| $E_{inulin}$ | 0.27 ± 0.04 | 0.27 ± 0.05 | 0.28 ± 0.04 | 0.25 ± 0.04 | 0.30 ± 0.04 | 0.28 ± 0.02 |
| Urine flow ml/min | 2.23 ± 0.44 | 2.11 ± 0.41 | 1.64 ± 0.27 | 1.42 ± 0.21 | 1.45 ± 0.24 | 1.58 ± 0.24 |
| Venous plasma $Ca^{2+}$ conc. mM/l | 2.53 ± 0.08 | 2.49 ± 0.07 | 3.51 ± 0.13 | 3.88 ± 0.16 | 2.92 ± 0.10 | 2.65 ± 0.08 |
| $U_{Ca^{2+}} \times V$ $\mu$M/min | 3.51 ± 0.87 | 2.99 ± 0.46 | 4.03 ± 0.57 | 4.11 ± 0.55 | 2.99 ± 0.56 | 2.97 ± 0.46 |
| $U_{Na^+} \times V$ $\mu$M/min | 346 ± 78 | 312 ± 71 | 209 ± 49 | 177 ± 47 | 137 ± 36 | 148 ± 34 |
| $U_{K^+} \times V$ $\mu$M/min | 81 ± 8 | 76 ± 9 | 69 ± 5 | 64 ± 3 | 58 ± 5 | 64 ± 6 |
| Urine osm. conc. mosm/l | 504 ± 55 | 514 ± 65 | 507 ± 69 | 485 ± 58 | 462 ± 65 | 459 ± 68 |
| $C_{H_2O}$ ml/min | -1.17 ± 0.20 | -1.68 ± 0.30 | -0.82 ± 0.20 | -0.66 ± 0.20 | -0.56 ± 0.20 | -0.54 ± 0.30 |

**Table IV**

*Renal parameters in the right kidney during 0.010 mM/kg/min $CaCl_2$ infusion in the left renal artery*
*n = 10 (Mean ± S.E.M.)*

| Periods | 1 | 2 | 3 | 4 | 5 | 6 |
|---|---|---|---|---|---|---|
| $C_{PAH}$ ml/min | 287 ± 27 | 284 ± 34 | 286 ± 38 | 282 ± 44 | 256 ± 31 | 242 ± 26 |
| $C_{inulin}$ ml/min | 90.2 ± 6.2 | 91.0 ± 7.5 | 93.7 ± 9.3 | 92.7 ± 11.2 | 88.3 ± 10.9 | 90.9 ± 12.2 |
| Urine flow ml/min | 2.65 ± 0.75 | 2.38 ± 0.70 | 1.98 ± 1.52 | 1.72 ± 0.48 | 1.69 ± 0.45 | 1.61 ± 0.41 |
| Arterial plasma $Ca^{2+}$ conc. mM/l | 2.50 ± 0.10 | 2.47 ± 0.10 | 2.89 ± 0.12 | 2.98 ± 0.13 | 2.89 ± 0.10 | 2.82 ± 0.11 |
| $U_{Ca^{2+}} \times V$ $\mu$M/min | 3.77 ± 0.91 | 3.20 ± 0.68 | 3.50 ± 0.72 | 3.68 ± 0.73 | 3.10 ± 0.69 | 2.87 ± 0.66 |
| $U_{Na^+} \times V$ $\mu$M/min | 360 ± 108 | 315 ± 96 | 254 ± 83 | 206 ± 72 | 182 ± 62 | 158 ± 54 |
| $U_{K^+} \times V$ $\mu$M/min | 74 ± 8 | 81 ± 9 | 79 ± 7 | 68 ± 6 | 72 ± 10 | 69 ± 8 |
| Urine osm. conc. mosm/l | 523 ± 71 | 527 ± 76 | 529 ± 82 | 529 ± 82 | 530 ± 82 | 484 ± 57 |
| $C_{H_2O}$ ml/min | -1.11 ± 0.30 | -0.98 ± 0.40 | -0.90 ± 0.30 | -0.91 ± 0.30 | -0.79 ± 0.20 | -0.58 ± 0.10 |
| Haematocrit % | 40 ± 0.9 | 41 ± 1.0 | 42 ± 1.5 | 42 ± 1.4 | 41 ± 1.5 | 41 ± 1.6 |
| Plasma total protein conc. g/100 ml | 5.43 ± 0.57 | 4.87 ± 0.29 | 5.07 ± 0.35 | 4.77 ± 0.26 | 4.54 ± 0.33 | 4.45 ± 0.18 |

**Table V**

*Renal parameters in the left kidney during 0.020 mM/kg/min $CaCl_2$ infusion in the left renal artery*
*n = 10 (Mean ± S.E.M.)*

| Periods | 1 | 2 | 3 | 4 | 5 | 6 |
|---|---|---|---|---|---|---|
| Arterial blood pressure mmHg | 130 ± 5 | 125 ± 6 | 130 ± 7 | 131 ± 8 | 126 ± 10 | 125 ± 10 |
| RBF ml/min | 480 ± 47 | 485 ± 45 | 361 ± 64 | 262 ± 76 | 269 ± 87 | 278 ± 87 |
| $R_{kidney}$ mmHg.s.ml$^{-1}$ | 1.71 ± 0.15 | 1.61 ± 0.16 | 2.45 ± 0.33 | 5.60 ± 1.76 | 4.82 ± 1.21 | 4.80 ± 1.40 |
| $C_{PAH}$ ml/min | 299 ± 26 | 283 ± 25 | 197 ± 40 | 140 ± 39 | 146 ± 55 | 217 ± 80 |
| $E_{PAH}$ | 0.74 ± 0.02 | 0.76 ± 0.03 | 0.67 ± 0.03 | 0.59 ± 0.05 | 0.61 ± 0.05 | 0.62 ± 0.05 |
| $C_{inulin}$ ml/min | 77.1 ± 3.2 | 80.2 ± 3.0 | 53.2 ± 9.4 | 32.8 ± 7.2 | 32.7 ± 9.1 | 45.3 ± 11.7 |
| $E_{inulin}$ | 0.27 ± 0.02 | 0.26 ± 0.03 | 0.32 ± 0.05 | 0.30 ± 0.04 | 0.23 ± 0.03 | 0.20 ± 0.03 |
| Urine flow ml/min | 2.50 ± 0.32 | 2.81 ± 0.54 | 1.76 ± 0.36 | 0.99 ± 0.19 | 0.77 ± 0.25 | 1.14 ± 0.31 |
| Venous plasma $Ca^{2+}$ conc. mM/l | 2.33 ± 0.10 | 2.30 ± 0.10 | 5.41 ± 0.54 | 6.88 ± 0.89 | 3.51 ± 0.16 | 3.00 ± 0.09 |
| $U_{Ca^{2+}} \times V$ μM/min | 4.53 ± 0.51 | 4.21 ± 0.57 | 9.87 ± 2.16 | 5.19 ± 1.03 | 2.77 ± 0.65 | 2.52 ± 0.51 |
| $U_{Na^+} \times V$ μM/min | 368 ± 57 | 382 ± 69 | 214 ± 51 | 112 ± 32 | 83 ± 26 | 99 ± 28 |
| $U_{K^+} \times V$ μM/min | 82 ± 11 | 81 ± 8 | 73 ± 5 | 49 ± 11 | 39 ± 12 | 54 ± 18 |
| Urine osm. conc. mosm/l | 424 ± 20 | 416 ± 32 | 388 ± 27 | 402 ± 37 | 382 ± 33 | 359 ± 33 |
| $C_{H_2O}$ ml/min | -0.90 ± 0.10 | -0.85 ± 0.10 | -0.35 ± 0.10 | -0.30 ± 0.10 | -0.25 ± 0.08 | -0.24 ± 0.09 |

While the arterial blood pressure did not change the RBF decreased from 483 ml/min to 361 ml/min and 262 ml/min and remained on this value (273 ml/min) in the postinfusion control periods, in spite of the fact, that the venous plasma calcium concentration decreased considerably.

In these experiments during the calcium chloride infusion the venous plasma calcium concentration rose from 2.31 mM/l to 5.42 mM/l and 6.89 mM/l. In the postinfusion control periods the plasma calcium concentration was 3.50 mM/l and 3.00 mM/l. In these animals during the hypercalcemia the glomerular filtration rate fell considerably from 78.5 ml/min to 53.2 ml/min and 32.8 ml/min and remained on this low value during the postinfusion periods (32.7 ml/min and 45.3 ml/min). The hypercalcemia reduced the urine flow rate from 2.65 ml/min to 1.76 ml/min and 0.99 ml/min which remained on these lower values in the postinfusion control periods (0.77 ml/min and 1.14 ml/min).

As we can see in Table VI in these experiments the arterial plasma calcium concentration rose from 2.43 mM/l to 3.13 mM/l and 3.68 mM/l (the mean 3.40 mM/l) when 0.020 mM/kg/min $CaCl_2$ was infused into the left renal artery. The clearance of the PAH decreased in the intact right kidney from 304 ml/min to 239 ml/min and the glomerular filtration rate from 85 ml/min to 67 ml/min ($p < 0.01$) during the calcium chloride infusion into the left renal artery. The urine excretion decreased from 3.28 ml/min to 2.36 ml/min ($p > 0.1$).

Figure 1 depicts the relationships between $Ca^{2+}$ infusion into the left renal artery and arterial blood pressure, renal blood flow, as well as renal vascular resistance. At the higher rate of calcium chloride infusion the total renal vascular resistance increased considerably and the renal blood flow decreased. No consistent or significant changes in arterial blood pressure were observed.

In Fig 2. the changes of the plasma calcium concentration in the renal venous plasma and in the arterial plasma are shown. The total calcium concentration in the arterial plasma changed to a less extent than the total calcium concentration in the left renal venous plasma.

Figure 3 shows the modifications of the $C_{PAH}$, the $C_{inulin}$ as well as of the urine output in the left kidney during the calcium chloride infusion. As it can be seen in the figure during the lower rate of infusion the glomerular filtration rate decreased slightly and the reduction was more significant during the infusion of the higher calcium chloride dose. The concomitant changes in the sodium, potassium and calcium excretion are shown in Fig. 4. Both lower and higher rate of calcium chloride infusions reduce the sodium excretion in the left kidney, but there is a decrease in the control series too, which is due to the experimental technics. (The changes of sodium excretion are exactly the same in the intact right kidney. See Fig. 6.)

**Table VI**

*Renal parameters in the right kidney during 0.020 mM/kg/min $CaCl_2$ infusion in the left renal artery*
*n = 10 (Mean ± S.E.M.)*

| Periods | 1 | 2 | 3 | 4 | 5 | 6 |
|---|---|---|---|---|---|---|
| $C_{PAH}$ ml/min | 319 ± 23 | 289 ± 27 | 249 ± 30 | 228 ± 36 | 258 ± 27 | 256 ± 31 |
| $C_{inulin}$ ml/min | 86.7 ± 3.8 | 83.0 ± 6.2 | 68.1 ± 4.6 | 66.3 ± 7.7 | 78.3 ± 7.0 | 75.1 ± 6.1 |
| Urine flow ml/min | 3.24 ± 0.42 | 3.33 ± 0.71 | 2.69 ± 0.77 | 2.04 ± 0.58 | 2.73 ± 0.89 | 2.86 ± 1.05 |
| Arterial plasma $Ca^{2+}$ conc. mM/l | 2.44 ± 0.07 | 2.41 ± 0.06 | 3.13 ± 0.10 | 3.67 ± 0.16 | 3.26 ± 0.15 | 2.94 ± 0.09 |
| $U_{Ca^{2+}} \times V$ μM/min | 5.85 ± 1.15 | 4.83 ± 1.29 | 4.45 ± 1.41 | 4.13 ± 1.07 | 4.40 ± 0.99 | 3.55 ± 0.88 |
| $U_{Na^+} \times V$ μM/min | 475 ± 85 | 463 ± 112 | 290 ± 78 | 205 ± 60 | 255 ± 94 | 251 ± 105 |
| $U_{K^+} \times V$ μM/min | 95 ± 15 | 92 ± 15 | 76 ± 14 | 71 ± 15 | 93 ± 17 | 87 ± 20 |
| Urine osm. conc. mosm/l | 423 ± 25 | 414 ± 36 | 419 ± 39 | 422 ± 45 | 384 ± 43 | 373 ± 47 |
| $C_{H_2O}$ ml/min | -1.16 ± 0.20 | -0.81 ± 0.29 | -0.38 ± 0.17 | -0.31 ± 0.23 | -0.04 ± 0.36 | -0.25 ± 0.42 |
| Haematocrit % | 38 ± 1.0 | 40 ± 1.2 | 40 ± 1.1 | 40 ± 1.2 | 38 ± 1.3 | 38 ± 0.9 |
| Plasma total protein conc. g/100 ml | 4.90 ± 0.23 | 4.82 ± 0.26 | 4.57 ± 0.28 | 4.42 ± 0.24 | 4.30 ± 0.27 | 4.29 ± 0.21 |

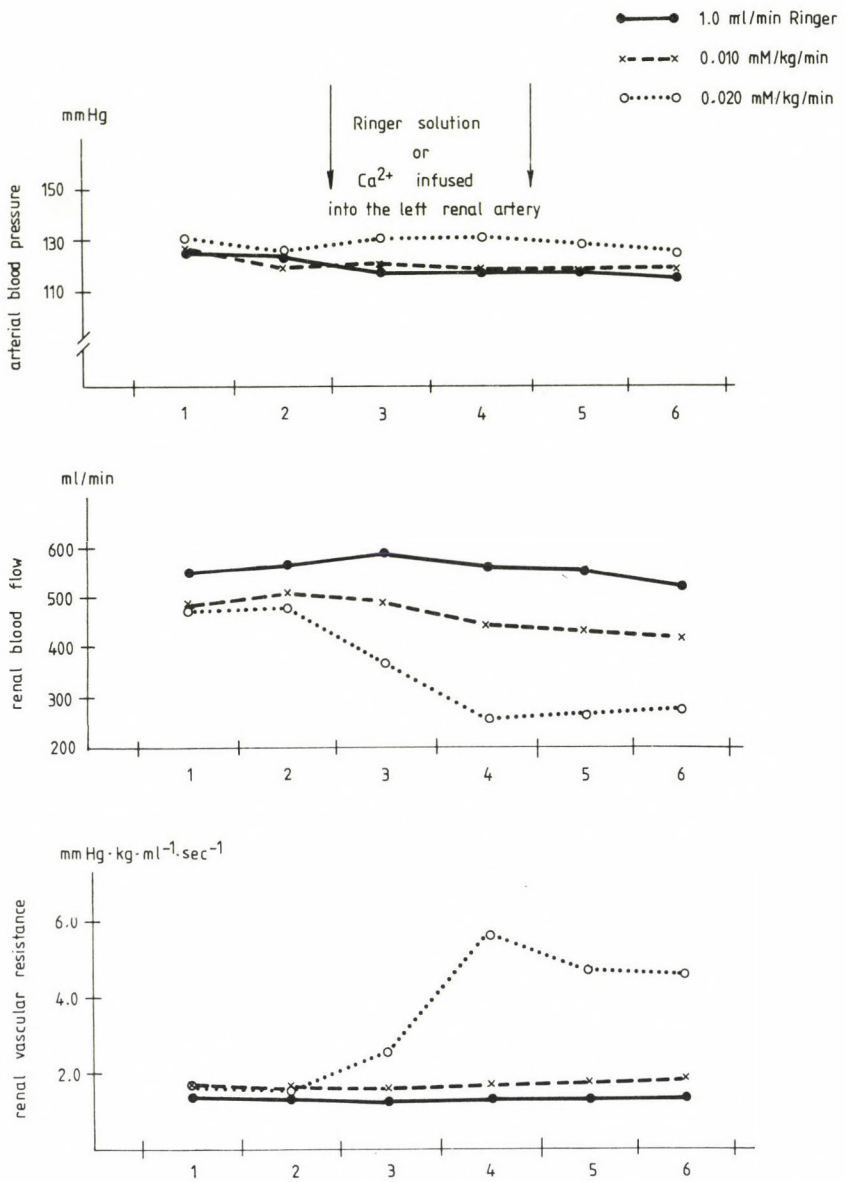


*Fig. 1.* Effects of calcium loading on the arterial blood pressure on the renal blood flow and renal vascular resistance in the left kidney. Each point represents mean data for the three series

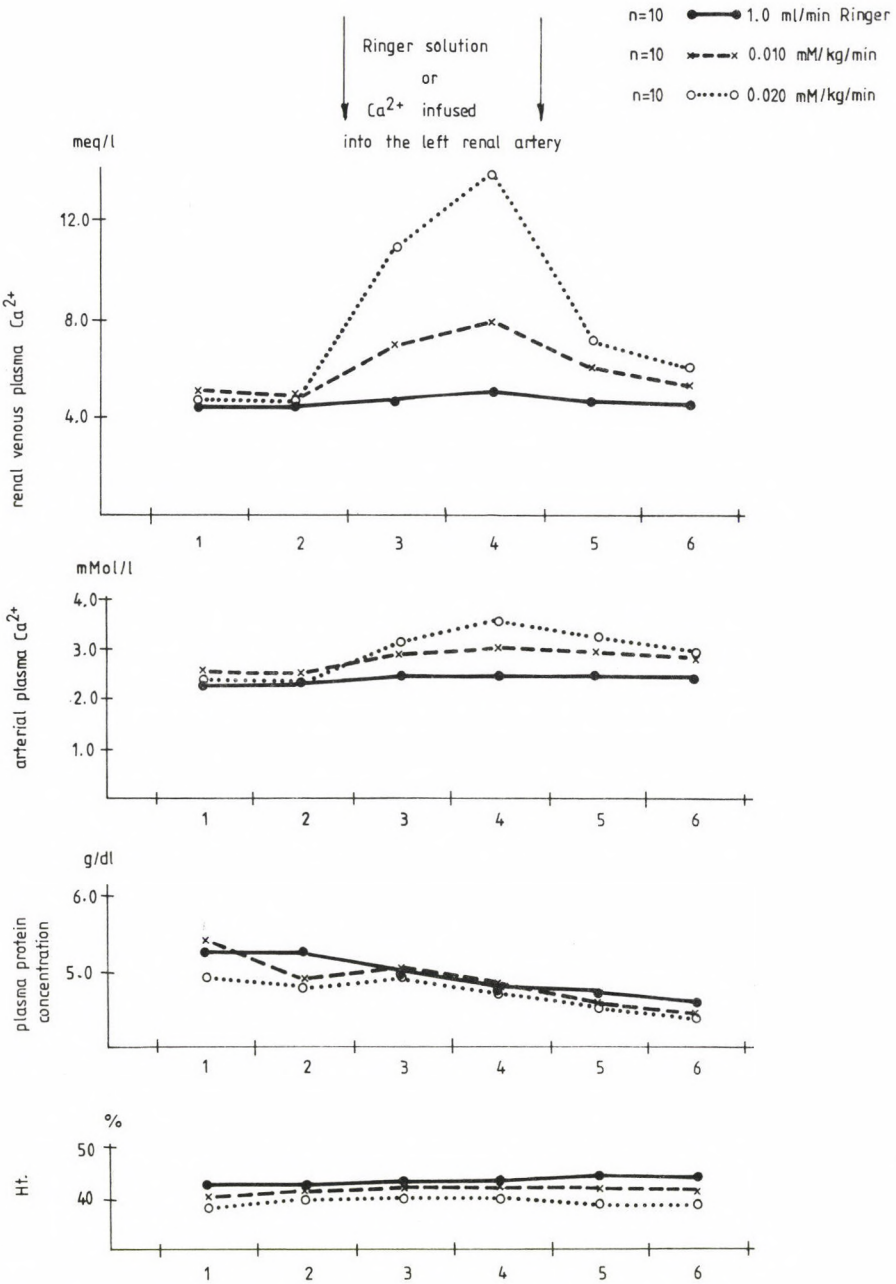


*Fig. 2.* Effects of calcium loading on the renal venous plasma $Ca^{2+}$ and arterial plasma $Ca^{2+}$ concentrations, the plasma protein concentration and hematocrit. Each point represents mean data for the three series

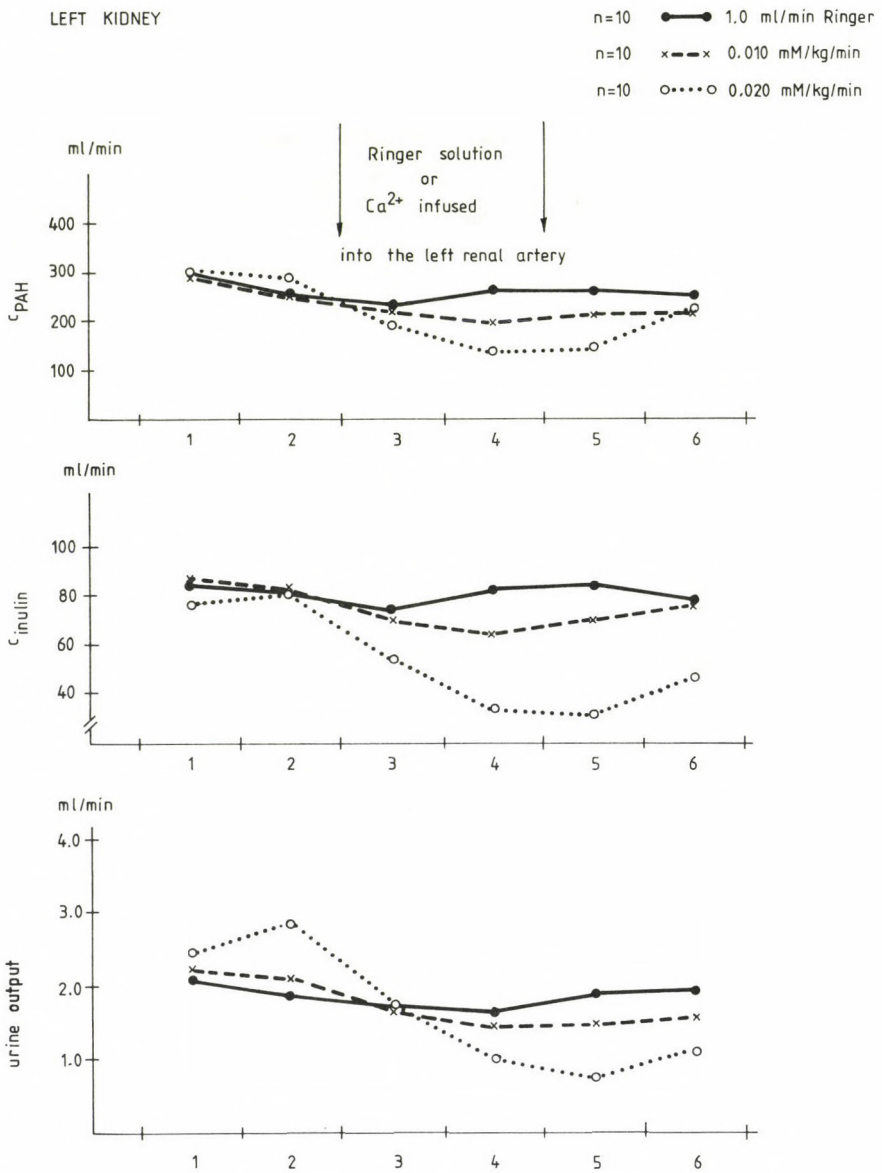


*Fig. 3.* Changes in the $C_{PAH}$, the $C_{inulin}$, and urine output in the left kidney during the calcium chloride infusion into the left renal artery. Each point represents average values in the three series of the experiments

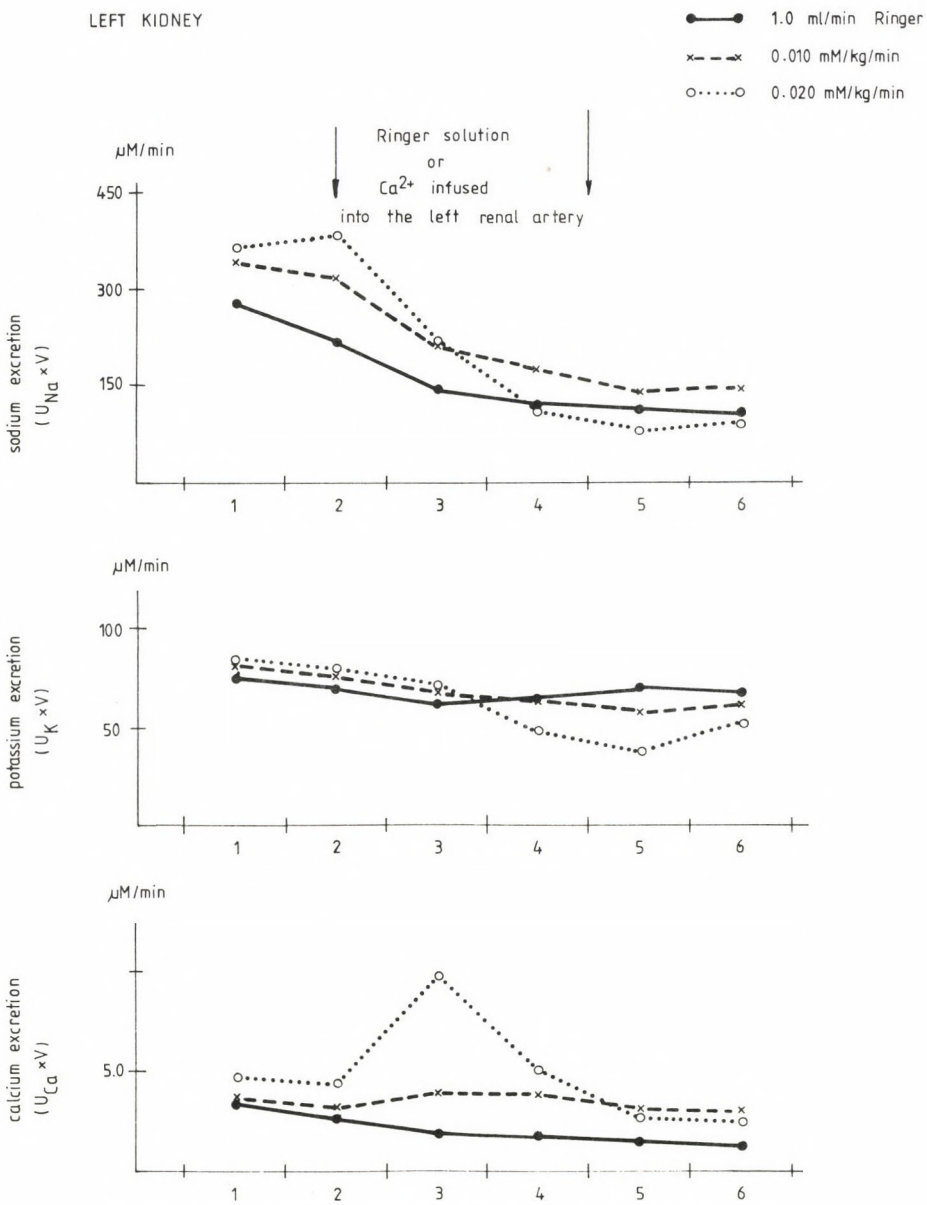


*Fig. 4.* Changes in the sodium, potassium and calcium excretion in the left kidney during the hypercalcemia induced by the $CaCl_2$ infusion into the left renal artery

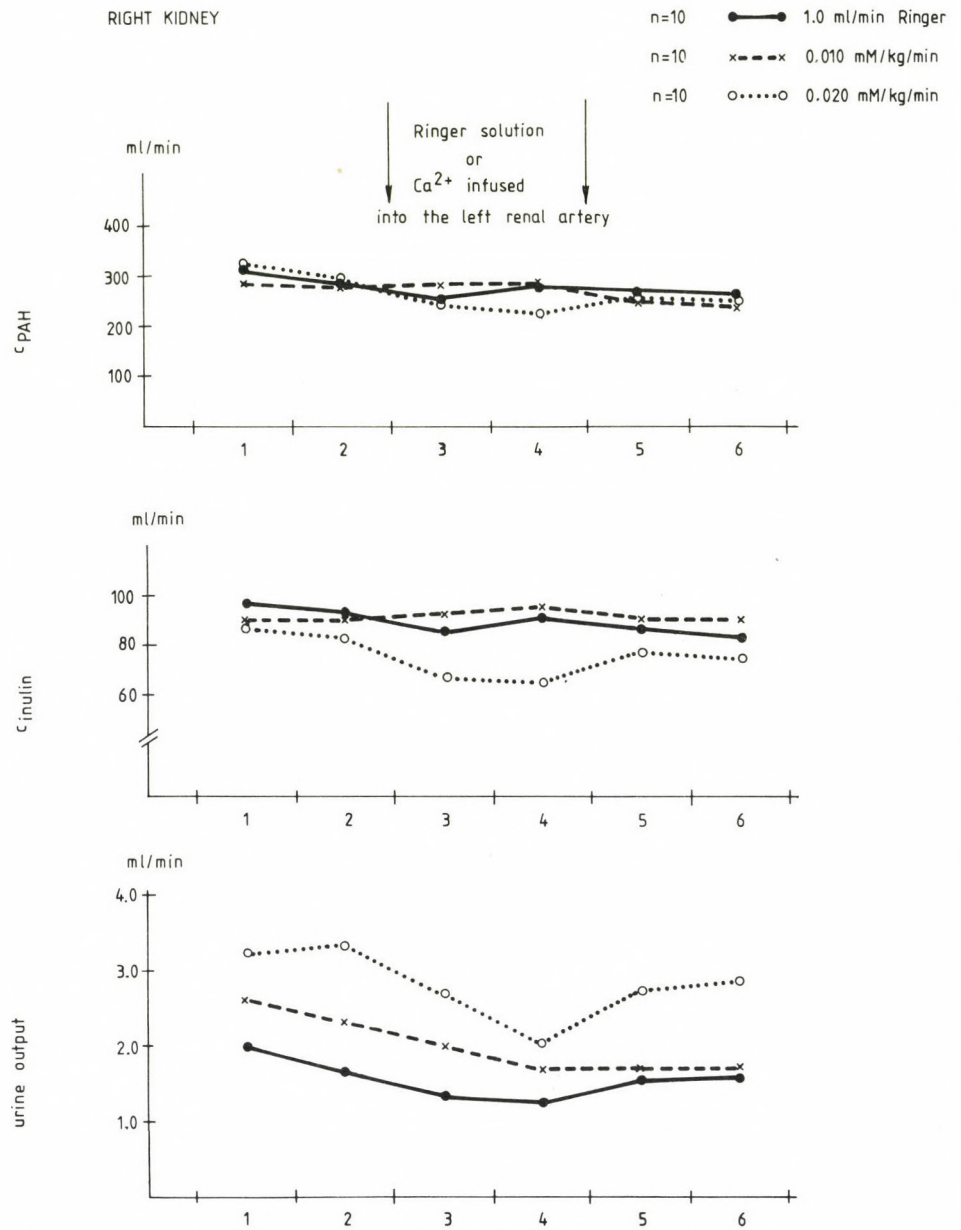


*Fig. 5.* The $C_{PAH}$, the $C_{inulin}$ and the urine output responses to hypercalcemia in the right kidney. Each point represents the average values in the three series of the experiments

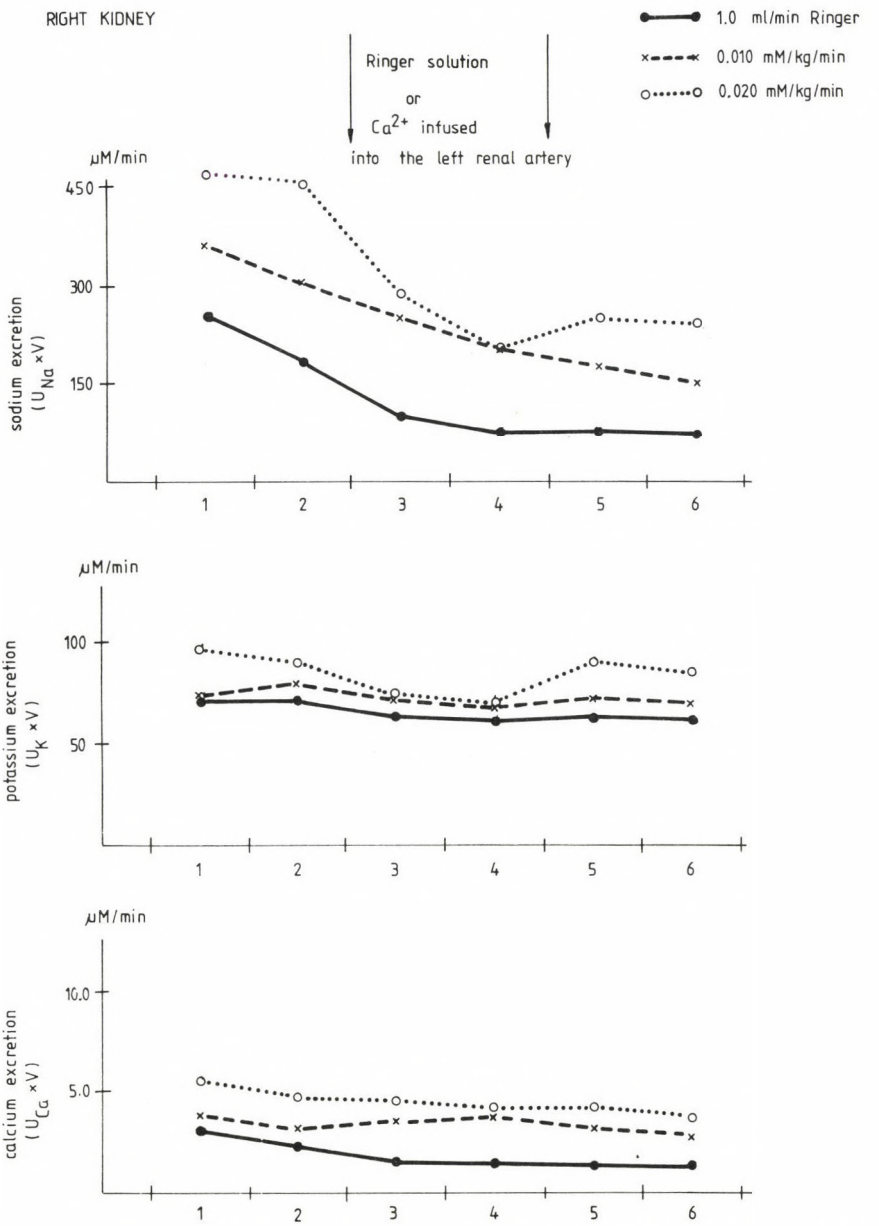


*Fig. 6.* Changes in sodium, potassium and calcium excretion in the intact right kidney during the $CaCl_2$ infusion into the left renal artery. The points represent the average values of the clearance periods

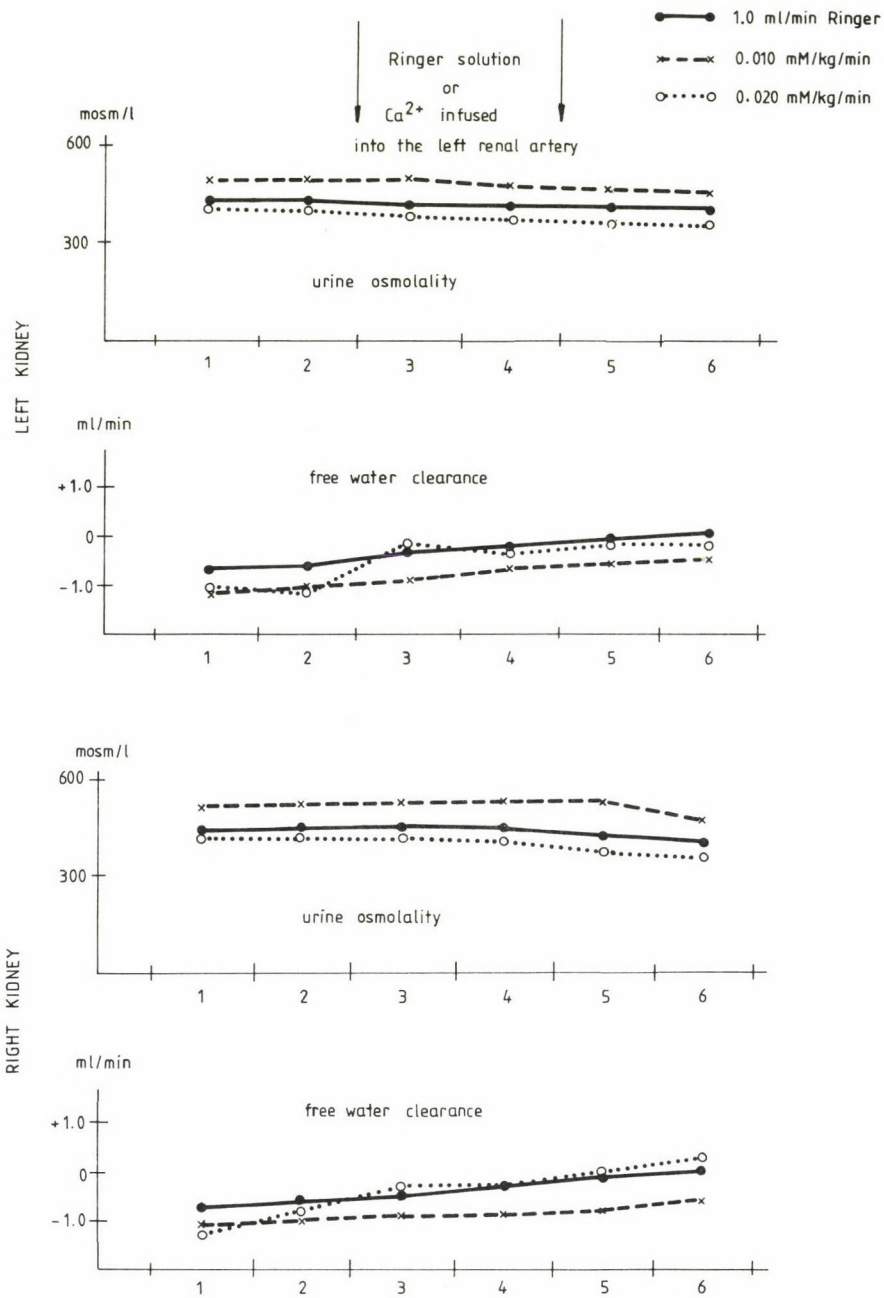


*Fig. 7.* Urine osmolality and free water clearance responses to hypercalcemia in the left and the right kidney

At the higher rate of calcium infusion the calcium excretion in the left kidney increases considerably, then GFR decreases while the plasma calcium concentration increases, thus leading to reduction of the calcium excretion because the filtered calcium load will be reduced.

In Fig 5. the changes of the $C_{PAH}$, the $C_{inulin}$ and the urine output of the three series of the experiments in the right kidney are shown. Average values of the $C_{PAH}$ are about the same in the three series and do not change considerably during the experiment. The mean values of the glomerular filtration rate are in good agreement in the two control periods (periods 1 and 2). The infusion of the high concentration chloride produces a definitive decrease of the $C_{inulin}$ in the right kidney.

The overall changes in the renal handling of sodium, potassium and calcium in the right kidney are shown in Fig. 6. No consistent or significant changes in these data were observed.

Figure 7 demonstrates the modifications of the urine osmolarity, the free water clearance in the left as well as in the right kidneys. In each series of the experiments in function of the time these parameters of the kidneys are changing parallel the urine osmolarity remains constant and the free water clearance slightly increases.

## Discussion

In the current study emphasis is placed on the effects of increased plasma calcium concentration induced by $CaCl_2$ solution infusion into the left renal artery. The direct renal blood flow measurement allowed to take renal venous blood samples and determine the total plasma calcium concentration in the perfusing renal blood.

In the blood samples taken from the femoral artery the arterial plasma total calcium concentration was determined, so the right intact kidney perfusing blood plasma calcium concentration was known.

The ultrafilterable calcium ion concentrations in our experiments were not determined. We have accepted the results of Chomdei et al. [6] to calculate the ultrafilterable calcium ion concentration from the total plasma calcium concentration.

During the control periods in our experiments the arterial plasma total calcium concentrations were 2.31 mM/l, 2.48 mM/l and 2.43 mM/l so the calculated ultrafilterable calcium ion concentration could be 1.35 mM/l, 1.45 mM/l and 1.40 mM/l.

When the lower amount of $CaCl_2$ (0.01 mM/kg/min) was infused into the left renal artery, the plasma total calcium concentration was 3.70 mM/l and the ultrafilterable calcium ion concentration was 4.85 mM/l while the arterial plasma ion concentration was 1.71 mM/l.

In the second series when the higher dose of $CaCl_2$ (0.020 mM/kg/min) was infused into the left renal artery the plasma calcium ion concentration was 2.3 mM/l in the left kidney perfusing blood and 1.8 mM/l in the arterial blood.

From our findings we can summarize, that the increase in ultrafilterable calcium ion concentration caused by the $CaCl_2$ infusion into the left renal artery, were less than the increases in total plasma calcium concentration.

The decreases in renal blood flow and glomerular filtration rate were not linearly related to the increases in the calcium ion concentration. The reduction of the RBF became progressively more marked as the ultrafilterable calcium concentration increased.

Since calcium ion has an important role in the smooth muscle contraction, the increase in renal vascular resistance (the decrease of the renal blood flow) is consistent with the theory that the elevation of the ultrafilterable plasma calcium concentration produces a vasoconstriction in the arterioles of renal vasculature [10, 17].

An alternative explanation is based on the previous suggestion that the distal calcium load may participate in the tubuloglomerular feedback regulation [1, 12, 16].

In the present study the filtration fraction (FF) remained relatively constant during $CaCl_2$ infusion. During the smaller amount $CaCl_2$ infusion the FF in the control periods was 0.31 when $CaCl_2$ was infused into the left renal artery, the FF was 0.31.

In the second series when 0.020 mM/kg/min $CaCl_2$ was infused into the left renal artery the FF was 0.28 in the control periods and 0.24 during the calcium infusion.

In the intact right kidney during the control periods the filtered calcium ion amount was 131 $\mu$M/min and when $CaCl_2$ was infused into the left renal artery (the arterial plasma calcium ion concentration was 1.6 mM/l, the filtered load was 144 $\mu$M/min) and the glomerular filtration did not change. At the lower calcium chloride infusion when the ultrafilterable calcium was elevated in the left kidney from 1.45 mM/l to 1.95 mM/l the glomerular filtration rate decreased from 83 ml/min to 66 ml/min and the filtered calcium ion amount was 123 $\mu$M/min in the control periods and about the same 128 $\mu$M/min during the $CaCl_2$ infusion. In lack of a decrease in the GFR the filtered calcium load would be 162 $\mu$M/min (1.95 mM/l $\times$ 89 ml/min). Supposing that the reabsorbed amount of calcium ion does not change in the proximal tubule the distal calcium delivery increases when the plasma calcium ion concentration is elevated.

On the basis of this hypothesis, changes in renal vascular resistance could be elicited by the alteration in distal calcium delivery as a consequence of the increased plasma calcium concentration or filtered calcium load. The renal vasoconstriction

produced by the $CaCl_2$ infusion maintained the constancy of the filtered calcium load.

The results of the higher infusion rate of calcium suggest a similar situation. In the second series the filtered calcium ion amount was 119 μM/min in the intact right kidney during the control periods and 121 μM/min when the arterial plasma total calcium concentration was elevated to 3.4 mM/l (calcium ion concentration: 1.8 mM/l).

At the higher rate of calcium infusion in the left kidney the renal blood flow was reduced by 36% from the control 482 ml/min to 311 ml/min and the filtered calcium load was 110 μM/min in the control periods and 103 μM/min during the $CaCl_2$ infusion.

In these experiments the calcium excretion did not increase considerably in spite of the serious elevation of the plasma total calcium concentration. Our results suggest that the changes in the distal nephron delivery of calcium could be responsible for the changes in glomerular filtration rate at elevated levels of plasma calcium concentration.

This suggestion is competible with the results of micropuncture experiment reported by Edwards et al. [9] in which calcium chloride was infused intravenously.

The decrease of the GFR during hypercalcemia is the consequence of the vasoconstriction in the glomerular vessels mainly in the afferent arterioles.

These studies certainly cannot provide definitive evidence that allows conclusion with respect to the possible mechanism of hypercalcemia produced increase in the renal vascular resistance.

However these results suggest the possibility that the effects of hypercalcemia may operate the glomerulo-tubular feedback mechanism.

**Acknowledgement**

The authors are grateful to Mrs. Éva Perjési for technical assistance.

## REFERENCES

1. Bell, P. D., Franco Martha, Navar, L. G.: Calcium as a mediator of tubuloglomerular feedback. Ann. Rev. Physiol. **49**, 275–293 (1987).
2. Bennet, C. M.: Urine concentration and dilution in hypocalcemic and hypercalcemic dogs. J. Cin. Invest. **49**, 1447–1457 (1970).
3. Briggs, J. P., Wright, F. S.: Feedback control of glomerular filtration rate: Site of the effector mechanisms. Am. J. Physiol. **236**, F40–F47 (1974).

4. Briggs, J. P., Schermann, J.: The tubulo-glomerular feedback mechanism: Functional and biochemical aspects. Am. Rev. Physiol. **49**, 251–273 (1987).
5. Burke, T. J., Navar, L. G., Clapp, J. R., Robinson, R. R.: Response of single nephron glomerular filtration rate to distal nephron microperfusion. Kidney Int. **6**, 230–240 (1974).
6. Chomdei, B., Bell, P. D., Navar, L. G.: Renal hemodynamic and autoregulatory responses to acute hypercalcemia. Am. J. Physiol. **232**, F490–F496 (1977).
7. Churchill, P. C.: Second messengers in renin secretion. Am. J. Physiol. **249**, F175–F184 (1985).
8. DiBona, G. F.: Effect of hypercalcemia on renal tubular sodium handling in the rat. Am. J. Physiol. **220**, 49–53 (1971).
9. Edwards, B. R., Sutton, R. A. L., Dirks, J. H.: Effect of calcium infusion on renal tubular reabsorption in the dog. Am. J. Physiol. **227**, 13–18 (1974).
10. Fröhlich, E. D., Scott, J. B., Haddy, F. J.: Effect of cations on resistance and responsiveness of the renal and forelimb vascular beds. Am. J. Physiol. **203**, 582–587 (1962).
11. Gornall, A. G., Bardawill, C. J., David, M. M.: Determination of serum proteins by means of the biuret reaction. J. Biol. Chem. **177**, 751–766 (1949).
12. Israelit, A. H., Rector, F. C., Seldin, D. W.: The influence of perfusate composition and perfusion rate on glomerular capillary hydrostatic pressure. Abstracts 6th Annual Meeting Amer. Soc. Nephrol. Washington p. 53 (1973).
13. Kövér, G.: Effect of hypercalcemia on tubular calcium and phosphate transport. Acta Physiol. Acad. Sci. Hung. **45**, 95–107 (1974).
14. Kövér, G., Tost Hilda, Darvasi Anna: The effect of Ringer solution induced extracellular volume expansion on kidney function. Acta Physiol. Acad. Sci. Hung. **74**, 141–160 (1989).
15. Little, L. M.: Modified diphenylamine procedure for determination of inulin. J. Biol. Chem. **180**, 747–754 (1949).
16. Naftilan, A. J., Oparil, S.: The role of calcium in the control of renin release. Hypertension Dallas **4**, 670–675 (1982).
17. Ono, H., Kokubun, H., Haskimoto, K.: Abolition by calcium antagonists of the autoregulation of renal blood flow. Arch. Exptl. Pathol. Pharmakol. **285**, 201–207 (1974).
18. Rubin, R. P.: The role of calcium in the release of neurotransmitter substances and hormones. Pharmacol. Rev. **22**, 389–428 (1970).
19. Schermann, J., Hermle, M.: Maintenance of feedback regulation of filtration dynamics in the absence of divalent cations in the lumen of the distal tubule. Pflügers Arch. **358**, 311–323 (1975).
20. Schermann, J., Briggs, J. P.: Role of the renin-angiotensin system in tubulo-glomerular feedback. Fed. Proc. **45**, 1426–1430 (1986).
21. Smith, H. W., Finkelstein, N., Aliminosa, L., Crawford, B., Graber, M.: The renal clearances of substituted hippuric acid derivates and other aromatic acids in dog and man. J. Clin. Invest. **24**, 388–404 (1945).
22. Suki, W. N., Eknoyan, G., Rector, F. C., Seldin, D. W.: The renal diluting and concentrating mechanism in hypercalcemia. Nephron **6**, 50–61 (1969).

23. Tarkovács, G., Mózes, T., Kövér, G., Tost, Hilda: Effect of hypercalcemia on renal function. Acta Physiol. Acad. Sci. Hung. **45**, 89–94 (1974).
24. Thurau, K., Schnermann, J. W., Nagel, M., Horster, M., Wahl, M.: Composition of tubular fluid in the macula densa segment as a factor regulating the function of the juxtaglomerular apparatus. Cirs. Res. **20**, II-79–II-81 (1967).
25. Wright, F. S., Briggs, J. P.: Feedback control of glomerular blood flow, pressure and filtration rate. Physiol. Rev. **59**, 958–1006 (1979).

*Acta Physiologica Hungarica, Volume 81 (4), pp. 395–408 (1993)*

# $TxA_2$-$PGI_2$-$PGF_{2\ alfa}$ RESPONSES IN THE KIDNEY TO BLOOD PRESSURE REDUCTION INDUCED BY VASODILATOR/VASORELAXING AGENTS WITH DIFFERENT ACTION IN PATIENTS WITH ESSENTIAL HYPERTENSION

B. SZÉKÁCS, I. JUHÁSZ, B. GACHÁLYI*, J. FEHÉR

SECOND DEPARTMENT OF MEDICINE, SEMMELWEIS UNIVERSITY MEDICAL SCHOOL, BUDAPEST, HUNGARY
* FIRST DEPARTMENT OF MEDICINE, POSTGRADUATE MEDICAL UNIVERSITY, BUDAPEST, HUNGARY

Received February 10, 1993
Accepted March 17, 1993

In blood pressure (BP) reduction induced by gallopamil, hydralazine and prazosin in patients with essential hypertension a common trend was found in renal prostanoid production which included increased $TxB_2$ excretion and/or augmented $TxB_2$/6-keto-$PGF_{1alfa}$ ratio and, with the exception of response to prazosin, enhanced $PGF_{2alfa}$ excretion. Role of direct biochemical actions by the drugs in these responses was excluded by in vitro experiments with kidney slices from rats. The clinical and in vitro experimental findings suggested a mediator role of sympathetic activation but not that of the increased renin release in the urinary eicosanoid responses. Significant correlation was observed between the changes in reabsorbed amounts of sodium and excreted amounts of $TxB_2$ and $PGF_{2alfa}$. The results suggest that the reactivity of pressure type prostanoids in the kidney could be considered as part of a more complex renal counteraction to BP decrease.

**Keywords**: essential hypertension, gallopamil, prazosin, hydralazine, urinary renal prostanoids, plasma renin activity, sodium reabsorption, renal counterregulation

Links which exist between renal eicosanoid metabolism and systemic/renal arterial blood pressure cannot be considered as ones sufficiently clarified and fully understood. Findings have been reported predominantly about the problems of prostaglandin responses in the kidney to the elevation of the arterial vascular tone. No data have been available on the effects of decreases in systemic blood pressure on prostanoid production in the kidney. In our previous clinical study [1, 2] we found

Correspondence should be addressed to
Béla SZÉKÁCS
Second Department of Medicine
Semmelweis University Medical School
H–1444 Budapest, P.O.Box 277, Szentkirályi u. 46, Hungary

*Akadémiai Kiadó, Budapest*

significant enhancement in the excretion rate of $TxB_2$ and $PGF_{2alfa}$ in urine to reduction of arterial blood pressure (BP) in patients with essential hypertension. Controlled relative hypotensive state was induced by intravenous infusion of sodium nitroprusside. $TxB_2$ and $PGF_{2alfa}$ responses in urine were considered as parts of the kidney's reaction to BP reduction.

To test our earlier findings and to get more information on "pressure type" prostanoid responses in the kidney we carried out a new clinical study in patients with essential hypertension. In this study other three vasodilator/vasorelaxing agents with different sites of peripheral vascular action were used to attenuate BP. These agents were hydralazine acting directly on vascular smooth muscle, $Ca^{++}$ entry blocker gallopamil and postsynaptic $alfa_1$-receptor blocker prazosin. In vitro experiments with kidney slices were carried out in parallel to differentiate the direct biochemical effects of these agents on the prostanoid release from renal tissue and to study directly the possibility of a mediator role of secondary sympathetic activation to systemic vasodilation (vasorelaxation) in inducing changes in renal prostanoid metabolism.

## Methods

Twenty-five patients with essential hypertension were involved in the study. They were without renal, cerebral or cardiac complications. Informed consent to participation was obtained from each individual. They were of both sexes and aged from 18 to 50 years. Any drug intake was stopped two weeks before the study.

The study was carried out during the morning hours while the patients were in a fasting state and supine position. Following a 150-minute control period, either hydralazine (Apresoline, CIBA), gallopamil (Procorum, Knoll AG) or prazosin (Minipress, Pfizer) was administered orally (according to a randomized schedule and with two-day washout periods) to the patients to decrease their blood pressure (BP) for another 150-minute period of observation.

The total dose of each drug was divided into two equal parts to produce a more uniform decrease of BP. The first part was taken at the onset of the second 150-minute period of observation. The doses and the time of the intake of the second one based on our preliminary experiences, were as follows. Gallopamil: first dose 0.6 mg/kg b.w. and 0.36 mg/kg b.w. as second dose (at 75 min), prazosin: first dose 0.016 mg/kg b.w. and the same as second dose (at 30 min), hydralazine: first dose 0.25 mg/kg b.w. and the same as second dose (at 30 min).

The arterial blood pressure was measured in 8-minute intervals by the Riva Rocci auscultation method, and a weighted mean was calculated for each period.

The patients drank water of 2.5 ml/kg b.w. divided into three equal parts during the first hour of each period to maintain urine flow rate sufficient to avoid catheterization. Urine was collected throughout each period for measurement of sodium, creatinine and prostanoid concentrations.

The urine aliqouts for prostanoid measurements were frozen below −20 °C. At the termination of each period peripheral venous blood samples were drawn for the measurement of sodium and creatinine levels and plasma renin activity (PRA, New England Nuclear $^{125}$J-Agt I RIA kit).

Urinary and plasma prostanoid levels were measured with sensitive and specific RIA kits developed by the Isotope Institute of the Hungarian Academy of Sciences ($^3$H-$TxB_2$ RIA kit, $^3$H-$PGF_{2alfa}$ RIA kit, $^{125}$J-6-keto-$PGF_{1alfa}$ RIA kit). The values of urinary $TxB_2$, $PGF_{2alfa}$, 6-keto-$PGF_{1alfa}$ excretion were regarded as indexes of renal $TxA_2$, $PGF_{2alfa}$, and $PGI_2$ production [3-5].

The lower limits of our RIA measurements were 5 pg.ml$^{-1}$ for $TxB_2$, 6 pg.ml$^{-1}$ for 6-keto-$PGF_{1alfa}$ and 10 pg.ml$^{-1}$ for $PGF_{2alfa}$. Cross reactivity of antisera at 50 percent binding ranged between 0.1–1.9% (tested for $TxB_2$. $PGF_{2alfa}$, $PGE_1$, $PGE_2$). Purification of samples was avoided, as it would introduce artifacts falsely elevating some results [10]. The sources of methodological errors were minimized by using the subjects as their own controls and suitably specific and sensitive RIA kits.

The in vitro experiments were carried out with rat kidney slices. The kidneys of Sprague-Dawley rats (b.w. 50–200 g) were removed after perfusion with 80 ml ice-cooled isotonic saline. Kidney slices (30–60 mg/test tubes) were incubated in test tubes containing 50 ml Krebs-Ringer medium gassed continuously with a mixture of 95% $O_2$ and 5% $CO_2$ placed in metabolic shaker at 37 °C. After a 15-min preincubation period the kidney slices were incubated with or without gallopamil, hydralazine and prazosin ($10^{-6}$ M) for another 15 min. Samples were drawn from media at the end of the latter incubation period and kept frozen below −20 °C until RIAs were performed. The same system was used to test the effect of the adrenergic agonist noradrenaline and isoproterenol ($10^{-6}$ M) on $TxA_2$, $PGI_2$ and $PGF_{2alfa}$ production in the kidney. Paired and unpaired Student's *t*-tests, variance analysis and regression analysis were used for statistical evaluation.

## Results

### *1. Blood pressure (BP) reduction induced by gallopamil, prazosin and hydralazine*

All the three vasodilator/vasorelaxing agents led to significant and comparable decreases in mean arterial blood pressure in the 25 patients with essential hypertension (gallopamil: from 122 ± 2.0 (mean ± SEM) to 110 ± 2.1 mmHg, prazosin: from 120 ± 1.6 to 110 ± 1.0 mmHg, hydralazine: from 120 ± 3.0 to 103 ± 2.1 mmHg, $p < 0.001$ in all cases (Fig. 1).

### *2. Effect of BP reduction on peripheral venous PRA*

PRA values significantly increased in response to BP reduction induced by any of the three peripheral hypotensive agents (gallopamil: from 1.2 ± 0.2 to 2.14 ± 0.4 ng Agt I/ml/h $p < 0.05$, prazosin: from 0.9 ± 0.2 to 1.8 ± 0.3 ng Agt I/ml/h $p < 0.02$, hydralazine: from 0.9 ± 0.2 to 2.03 ± 0.4 ng Agt I/ml/h $p < 0.001$ (Fig. 2).

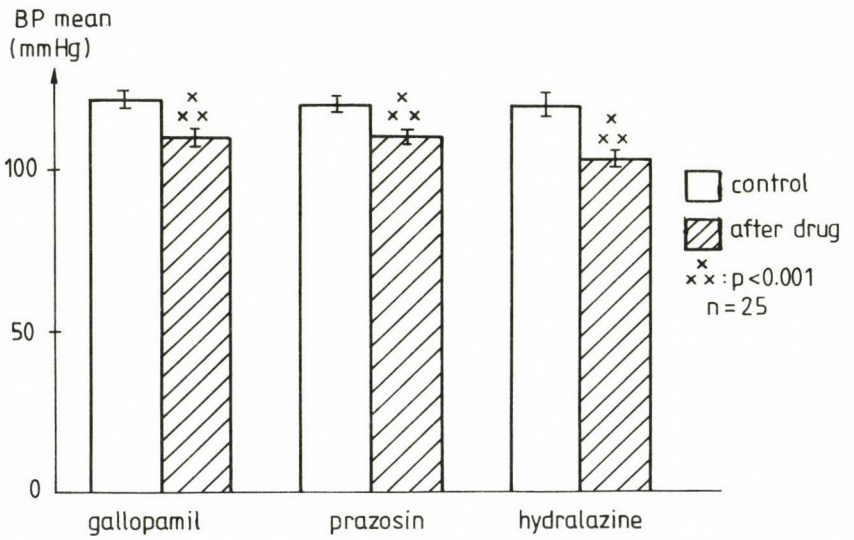


*Fig. 1.* Reduction in the arterial blood pressure of patients with essential hypertension in response to gallopamil, prazosin and hydralazine

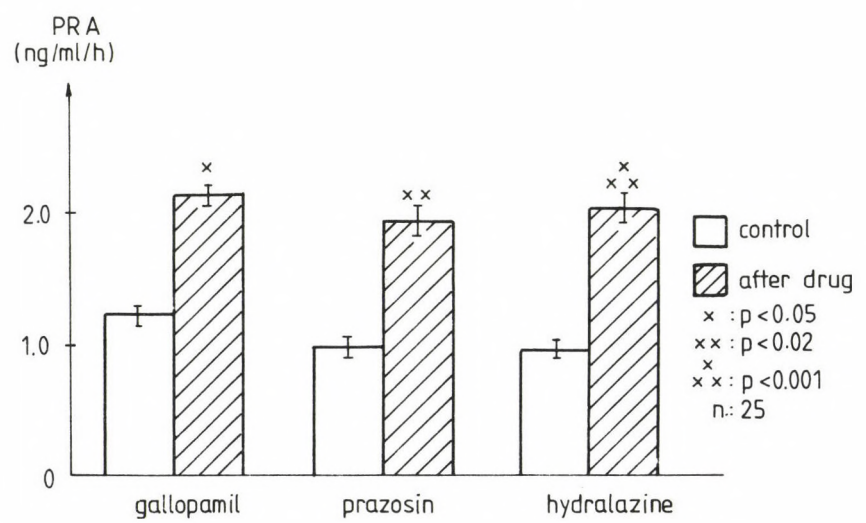


*Fig. 2.* Changes in peripheral venous PRA after the administration of gallopamil, prazosin and hydralazine

*3. Changes in sodium reabsorption in the action of the three hypotensive drugs*

The amount of the reabsorbed sodium was significantly enhanced in the systemic action of gallopamil and hydralazine but did not change significantly after the intake of prazosin (gallopamil: from 16.7 ± 1.2 to 20.2 ± 1.0 mmol/min $p < 0.05$, prazosin: from 18.7 ± 1.08 to 20.4 ± 1.06 mmol/min, n.s., hydralazine: from 17.7 ± 0.9 to 20.9 ± 1.2 mmol/min $p < 0.05$) (Fig. 3).

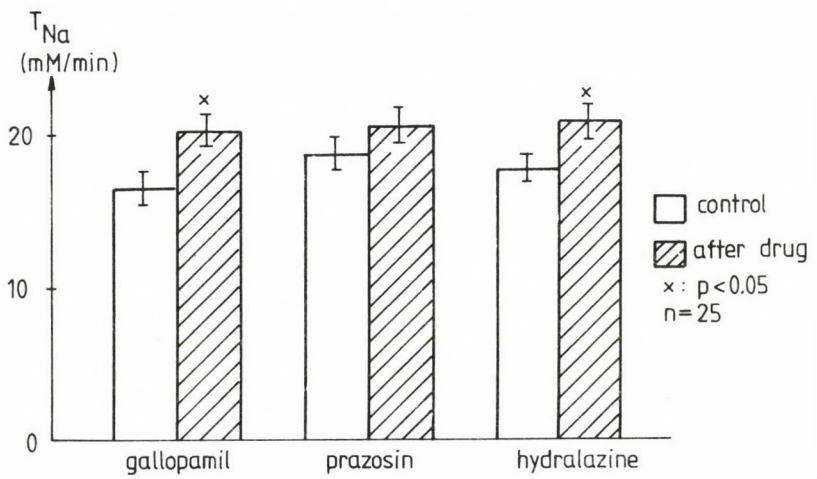


*Fig. 3.* Changes in the amount of reabsorbed sodium after gallopamil, prazosin and hydralazine

Glomerular filtration rate showed no increase after the intake of the three drugs (Table I).

**Table I**

*Endogenous creatinine clearance after the administration of gallopamil, prazosin and hydralazine (n = 25)*

| | $C_{creatinine}$ ml/min (mean ± SEM) | | |
|---|---|---|---|
| | control | after drug | |
| Gallopamil | 126.9 ± 11.7 | 144.9 ± 12.1 | n.s. |
| Prazosin | 135.2 ± 7.9 | 146.7 ± 7.4 | n.s. |
| Hydralazine | 125.1 ± 8.9 | 132.1 ± 0.3 | n.s. |

*4. Effect of the three hypotensive drugs on urinary excretion of $TxB_2$-$PGF_{2alfa}$ – 6-keto-$PGF_{1alfa}$*

The excreted amount of $TxB_2$ ($TxA_2$) in urine increased after the administration of gallopamil and hydralazine but not after prazosin (gallopamil: from 968 ± 104 to 1361 ± 192 pg/min, $p < 0.05$, prazosin: from 877 ± 112 to 1022 ± 108 pg/min, n.s., hydralazine: from 896 ± 93 to 1109 ± 100 pg/min, $p < 0.05$). Urinary $PGF_{2alfa}$ excretion showed the same trend of alterations (gallopamil: from 312 ± 50 to 493 ± 56 pg/min, $p < 0.001$, prazosin: from 288 ± 39 to 337 ± 55 pg/min, n.s., hydralazine: from 301 ± 39 to 387 ± 56 pg/min, $p < 0.05$). Blood pressure reduction induced by any of the three drugs did not cause significant change in the excretion of 6-keto-$PGF_{1alfa}$ ($PGI_2$) (gallopamil: from 294 ± 32 to 386 ± 78 pg/min, n.s., prazosin: from 315 ± 41 to 290 ± 51 pg/min, n.s., hydralazine: from 324 ± 52 to 254 ± 46 pg/min, n.s.) (Fig. 4).

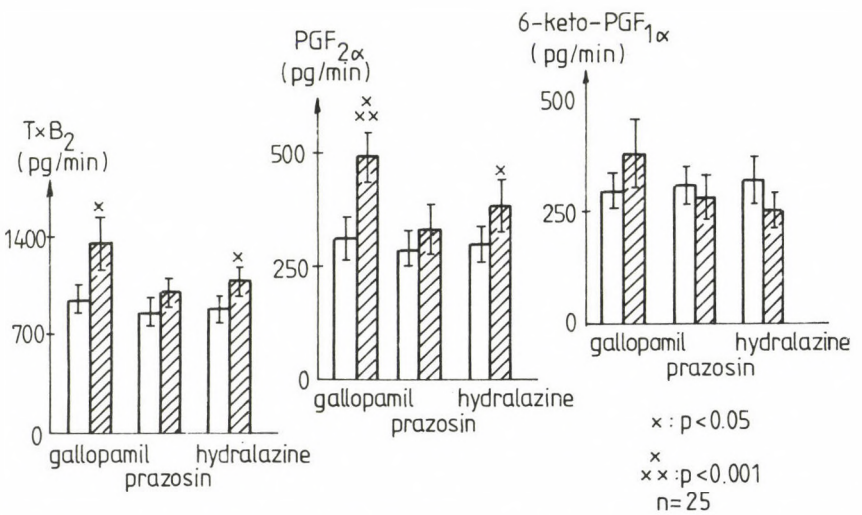


*Fig. 4.* Excretion of $TxB_2$, $PGF_{2alfa}$ and 6-keto-$PGF_{1alfa}$ in urine in control state and after the administration of gallopamil, prazosin, and hydralazine

*5. Urinary $TxB_2$/6-keto-$PGF_{1alfa}$ ratios during BP decrease*

$TxB_2$/6-keto-$PGF_{1alfa}$ ratio significantly increased after the intake of prazosin and hydralazine, while it remained unchanged in the action of gallopamil (prazosin: from 3.13 ± 0.4 to 5.49 ± 0.8, $p < 0.001$, hydralazine: from 3.2 ± 0.5 to 5.01 ± 0.1, $p < 0.001$, gallopamil: from 3.56 ± 0.4 to 3.8 ± 0.3, n.s.) (Fig. 5).

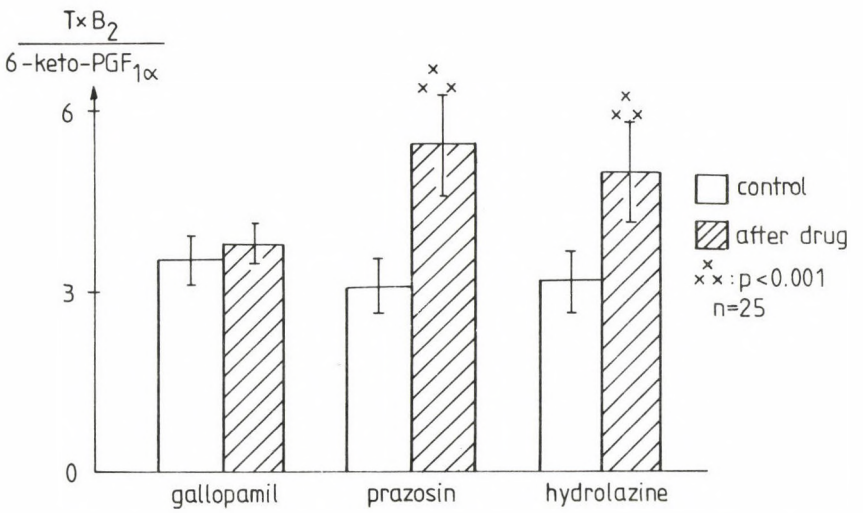


*Fig. 5.* $TxB_2/PGI_2$ indexes in the urine before and after the administration of gallopamil, prazosin and hydralazine

### *6. Release of $PGF_{2alfa}$, $PGI_2$ and $TxA_2$ from rat kidney slices incubated with gallopamil, prazosin and hydralazine ($10^{-6}$ M)*

Kidney slices produced significantly less $TxA_2$ ($TxB_2$), and the $TxB_2$/6-keto-$PGF_{1alfa}$ index was significantly lower in the presence of gallopamil compared to the control. Gallopamil did not cause change in $PGF_{2alfa}$ release. As shown in Table II no change was noted in the $PGF_{2alfa}$ – $TxA_2$ ($TxB_2$) and $PGI_2$ (6-keto-$PGF_{1alfa}$) generation and in $TxB_2$/6-keto-$PGF_{1alfa}$ index in kidney slices exposed to prazosin or hydralazine.

**Table II**

*Prostanoid synthesis in kidney slices under the effect of gallopamil, prazosin and hydralazine ($10^{-6}$ M). ($n$ = 8) (mean ± SEM)*

| | (ng/g wet tissue wt./min) | | | |
|---|---|---|---|---|
| | $PGF_{2alfa}$ | $TxB_2$ | 6-$KPGF_{1alfa}$ | $TxB_2$/6-$KPGF_{1alfa}$ |
| Control | 37 ± 5 | 19 ± 1 | 26 ± 3 | 0.7 ± 0.09 |
| Gallopamil | 44 ± 5 | 12 ± 1* | 33 ± 6 | 0.4 ± 0.05 |
| Prazosin | 40 ± 6 | 22 ± 2 | 35 ± 6 | 0.6 ± 0.13 |
| Hydralazine | 35 ± 5 | 23 ± 2 | 30 ± 4 | 0.8 ± 0.11 |

*:$p < 0.05$

### *7. Release of $PGF_{2alfa}$, $TxA_2$, $PGI_2$ from rat kidney slices under the effect of noradrenaline (NA) and isoproterenol (IP)*

Release of $PGF_{2alfa}$, $TxA_2$ ($TxB_2$) and $PGI_2$ (6-keto-$PGF_{1alfa}$) from kidney slices incubated with noradrenaline ($10^{-6}$ M) was increased. This alteration was more marked in the case of $PGI_2$ – derivate in comparison to the other two prostanoids. Significant change was found in $TxA_2$ generation of kidney slices upon isoproterenol ($10^{-6}$ M). $TxB_2$/6-keto-$PGF_{1alfa}$ ratio was diminished in the presence of NA, while an opposite but non-significant trend was noted.

Prostanoid responses in the kidney to hypotension under the effect of IP. See results in Table III.

**Table III**

*Prostanoid synthesis in rat kidney slices incubated with noradrenaline ($10^{-6}$ M) and isoproterenol ($10^{-6}$ M). ($n$ = 10) (mean ± SEM)*

| | (ng/g wet tissue wt./min) | | | |
|---|---|---|---|---|
| | $PGF_{2alfa}$ | $TxB_2$ | 6-$kpGF_{1alfa}$ | $TxB_2$/6-$kpGF_{1alfa}$ |
| Control | 34 ± 5 | 18 ± 2 | 29 ± 4 | 0.6 ± 0.09 |
| Noradrenaline | 53 ± 6* | 26 ± 2* | 71 ± 9*** | 0.4 ± 0.05* |
| Isoproterenol | 45 ± 6 | 30 ± 3** | 32 ± 5 | 0.9 ± 0.14 |

*:$p < 0.05$, **:$p < 0.01$, ***:$p < 0.001$

*8. Relationships between reabsorbed amounts of sodium and excreted amounts of $TxB_2$ and $PGF_{2alfa}$ during BP reduction*

Both changes in $TxB_2$ – and $PGF_{2alfa}$ – excretion showed significant correlation with the alterations in the reabsorbed amounts of sodium during BP reduction by hypotensive drugs (Figs 6, 7).

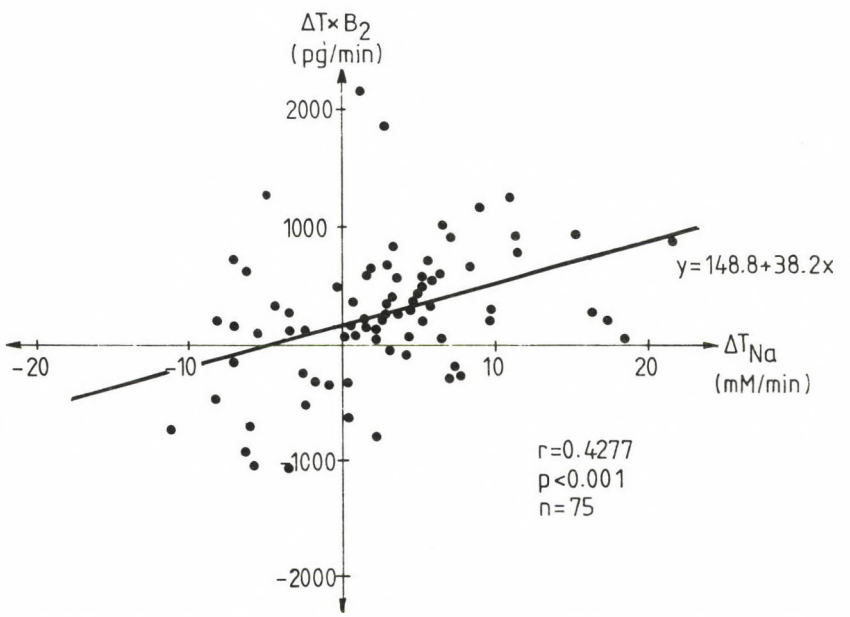


*Fig. 6.* Relationship between the changes of the amount of reabsorbed sodium and those of the excreted amounts of $TxB_2$ during drug-induced blood pressure reduction

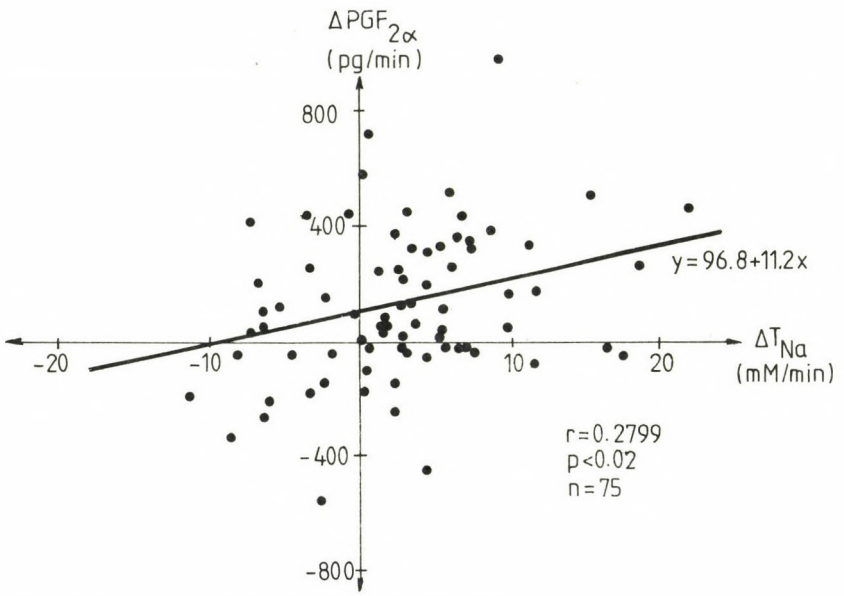


*Fig. 7.* Relationship between the alteration in the reabsorbed amounts of sodium and the changes in urinary $PGF_{2alfa}$ excretion during blood pressure reduction

## Discussion

Our previous clinical studies [1, 2] headlighted new aspect of existing or possibly existing links between alterations of systemic arterial blood pressure and eicosanoid production in the kidney. We demonstrated an increase in urinary $TxB_2$ and $PGF_{2alfa}$ excretion in response to arterial BP decrease induced by sodium nitroprusside in patients with essential hypertension. Those findings were supposed to be part of a more complex counterregulatory activity in the kidney [6] against drug-induced decrease in systemic arterial BP. The importance of the former makes it quite reasonable that one of our main aims in the present study was to demonstrate that the response in renal eicosanoid metabolism to vasodilator-induced BP fali cannot be considered solely as a special response to a given vasodilator agent but more likely as a characteristic reactivity of the kidney to BP decrease which can be induced by various vasodilator/vasorelaxing agents.

We found that treatment with either hydralazine, gallopamil or prazosin resulted in significant and comparable decrease in arterial BP in patients with essential hypertension.

Our finding of parallel and significant augmentation in peripheral venous PRA and significant increase in the amount of reabsorbed sodium (except in the effect of

prazosin) suggested a counterregulatory activity of the kidney against systemic vasodilation/relaxation. In consequence we could consider the parallel changes in renal $TxA_2$ – $PGI_2$ – and $PGF_{2alfa}$ production in those drug-induced relative hypotensive states as responses which predominantly are parts of "counteraction" of the kidney against BP fall.

A common trend was found in the changes of $TxA_2$ – $PGI_2$ – $PGF_{2alfa}$ production in kidneys after oral administration of hydralazine, gallopamil and prazosin. These prostanoid responses implied augmentation in $TxA_2$ release (urinary $TxB_2$ excretion) and/or increase in its ratio to the production of $PGI_2$ (urinary $TxB_2$/6-keto-$PGF_{1alfa}$ index). $PGF_{2alfa}$ excretion was enhanced by hydralazine and gallopamil but not by prazosin. Our parallel in vitro experiments with kidney slices from rats clearly demonstrated that these changes were not the result of direct biochemical effects of the three drugs on the renal tissue. Consequently the common tendency in the variety of changes in renal prostanoid production found after oral intake of vasodilating/vasorelaxing drugs could rather be due to effects of systemic vasodilation and relative hypotension.

The common trend in changes of renal prostanoid metabolism did not mean an unanimously uniform pattern of prostanoid responses after the intake of the three hypotensive drugs despite the fact that BP decreases induced by them were about the same. After the administration of gallopamil the characteristic trend in the $TxA_2$ and $PGI_2$ responses appeared partly indirectly. The amount of $TxB_2$ excreted in urine increased but the $TxB_2$/6-keto-$PGF_{1alfa}$ index did not change. We could only understand these findings with the help of additional in vitro experiments with kidney slices from rats incubated with or without gallopamil. The gallopamil – in agreement with similar direct biochemical effect [7, 8] of other $Ca^{++}$ entry blockers – resulted in a significant decrease in $TxB_2$/6-keto-$PGF_{1alfa}$ index in the medium. This change in endoperoxide metabolism induced by $Ca^{++}$ entry blockade was interpreted by some investigators [8] as a shift in endoperoxide metabolism from $TxA_2$ to $PGI_2$ generation. The lack of this change in the urinary $TxB_2$/6-keto-$PGF_{1alfa}$ index, and the enhancement of $TxB_2$ excretion in the urine when gallopamil was administered clearly proved other action(s) on endoperoxide metabolism induced directly or indirectly by the systemic arterial vasorelaxation and arterial BP reduction. That action(s) could oppose the direct biochemical effect of gallopamil in renal tissue.

On the basis of these considerations the unchanged $TxB_2$/6-keto-$PGF_{1alfa}$ index was just in line with the increased ratios found after hydralazine or prazosin, the two drugs which did not have any direct effect on prostanoid metabolism in kidney slices.

Variations in prostanoid responses following the administration of the three different hypotensive drugs provided basis to reveal mechanisms which could result in the common elements in prostanoid responses. The most important information

about such possible mechanism(s) comes from the findings got after the intake of prazosin. Administration of hydralazine or gallopamil yielded significant enhancement of urinary $TxB_2$ and $PGF_{2alfa}$ index. On the other hand, the intake of prazosin also caused a higher $TxB_2$/6-keto-$PGF_{1alfa}$ index in urine, but it did not increase the absolute amounts of either the $TxB_2$ or the $PGF_{2alfa}$ exerted (in the urine). It means that after the administration of prazosin some components of the "common trend" in prostanoid responses to the blood pressure decrease could not be found. Just this lack provided basis to conclude that secondary sympathetic activation [9, 10] should have some mediating role in producing the characteristic prostanoid response to BP decrease which plausibly appeared more definitely in the systemic action of the two other drugs. An increased liberation of free arachidonic acid (AA) available for the synthesis of prostanoids is responsible for mediating the adrenergic action on eicosanoids [11]. Noradrenaline facilitates phospholipase $A_2$ activity, which enzyme liberates AA from cellular membrane. In line with those results we also demonstrated in our parallel in vitro experiments that noradrenaline augmented the production of $TxA_2$ and $PGF_{2alfa}$ (and $PGI_2$) in kidney slices from rats. However, in the state of reflex sympathetic action caused by BP fall, the higher $TxB_2$/6-keto-$PGF_{1alfa}$ index in urine cannot be explained by alfa adrenergic mechanism because this alteration was also found in BP reduction induced by prazosin, while just the opposite change was noted in the ratio when kidney slices were incubated with NA. On the other hand, results obtained from incubations of renal tissue with isoproterenol let us conclude that beta-adrenergic activation probably could have a role in the production of the characteristic shift from $PGI_2$ to $TxA_2$ generation.

The question remains open which part along the nephron took place in these changes in prostanoid metabolism. It is known, that both glomeruli- and $alfa_1$-innervated [12] tubuli are capable of producing $TxA_2$ and other prostanoids [13]. So theoretically both of these sites could be involved in the kidney's prostanoid response to hypotension. The findings of significant relationships between the changes of excreted amounts of $TxB_2$ and $PGF_{2alfa}$ and that of the reabsorbed sodium suggest, that tubuli are involved at least in part in renal prostanoid responses found in the drug-induced hypotensive periods. This conclusion is also supported by other reports which demonstrated significant facilitating effect of tubular NaCl transport on tubular $TxA_2$ production [14] and also on $PGE_2$-9-ketoreductase activity [15], the enzyme of $PGE_2$ – $PGF_{2alfa}$ interconversion.

It must be pointed out that all the relationships discussed above can explain only the increases in the absolute amount of $TxA_2$- and $PGF_{2alfa}$- production. Except a certain role of beta-adrenerg activation they do not allow to understand the characteristic common change, the relative increase in $TxA_2$ production, i.e. the higher urinary $TxB_2$/6-keto-$PGF_{1alfa}$ index which was a uniform response after the administration of all the three drugs in spite of the fact that prazosin, probably by

inhibiting the alfa adrenergic effects on tubuli, did not lead to significant increase in tubular sodium reabsorption while GFR was not significantly changed by any of the three drugs. Thus we must suppose the existence of other mechanism(s) responsible for this $PGI_2$-$TxA_2$ shift in prostanoid synthesis in the kidney. Obviously this mechanism could not be defined in the present study.

Both $TxA_2$ [16] and $PGF_{2alfa}$ [17, 18] as vasoconstrictors can act locally on glomeruli and also on peritubular veins whose condition can influence transtubular transport processes, too. Moreover, $TxA_2$ has vasopressin-like activity on tubuli [19]. When the increase in $TxA_2$ production to enhanced tubular $Cl^-$ load is blocked, the typically joining autoregulative decrease of RBF and GFR to $Cl^-$ load also disappears [20]. Efficacy of furosemide can be potentiated with the inhibition of $TxA_2$ synthesis [21].

These already known biological activities seem to provide sufficient basis for the conclusion that $TxA_2$- and $PGF_{2alfa}$-responses located either at glomerular and/or tubular sites, are partial mechanisms in the counteraction of the kidney against the consequences of systemic and intrarenal vasodilation/vasorelaxation and arterial BP fall. However, this conclusion needs further support using other methodological approaches.

## Acknowledgements

This work was supported by grant of Hungarian Ministry of Health N° 7-434/J. The authors are thankful to Mrs Irén G. Kováts for her valuable assistance.

## REFERENCES

1. Székács, B., Mohácsi, E., Gachályi, B., Tihanyi, K., Juhász, I., Horváth, B.: Renal thromboxane response to blood pressure fall in essential hypertension: examination of a possible relationship with other urinary prostanoids and plasma renin activity. IRCS Med. Sci. **14**, 53-54 (1986).
2. Székács, B., Mohácsi, E., Gachályi, B., Tihanyi, K., Juhász, I.: $PGF_{2alfa}$ response to the reduction of blood pressure in essential hypertension. IRCS Med. Sci. **14**, 51-52 (1986).
3. Patrono, C., Ciabattoni, G., Patrignani, P., Filabozzi, P., Pinca, E., Satta, M. A., van Dorne, D., Cinotti, G. A., Pugliese, F., Pierucci, A., Simonetti, B. M.: Evidence for a renal origin of urinary thromboxane $B_2$ in health and disease. Adv. Prost. Thromb. Leuk. Res. **11**, 493-498 (1983).
4. Frölich, J. C., Wilson, T. W., Sweetman, B. J., Smiegel, M., Nies, A. S., Carr, K., Watson, J. T., Oates, J. A.: Urinary prostaglandins: Identification and origin. J. Clin. Invest. **55**, 763-770 (1975).
5. Sun, F. F., Taylor, B. M., McGuire, J. C., Wong, P. Y., Malik, K. U., McGiff, J. C.: Metabolic disposition of prostacyclin. In: Prostacyclin eds Vane, J. R., Gregstrom, L. Raven Press. N. Y. 1979, pp. 119-131
6. Guyton, A. C., Hall, J. E., Lohmeier, T. E., Jackson, T. E., Kastner, P. R.: Blood pressure regulation: basic concepts. Federation Proc. **40(8)**, 2252-2256 (1981).

7. Smallbone, B. W., Davies, B. J., Noulty, E. J., Pisters, L. L., Taylor, N. E., McDonald, J. W.: Effects of verapamil on thromboxane synthesis and pulmonary hypertension in sheep. Clin. Invest. Med. **9**, 145 – 149 (1986).
8. Mehta, J., Mehta, P., Ostrowski, N., Brigmon, L.: $Ca^{++}$ blocker diltiazem inhibits human platelet $TxA_2$ synthesis and increases vessel wall $PGI_2$ release (abstr.). Clin. Res. **31**, 25, 1A (1983).
9. Murphy, M. B., Scriven, A. J., Brown, M. J., Causon, R. C., Dollery, C. T.: The effects of nifedipine and hydralazine induced hypotension on sympathetic activity. Eur. J. Clin. Pharmacol. **23(6)**, 479 – 482 (1982).
10. Colucci, W. S.: Alpha-adrenergic receptor blockade with prazosin. Consideration of hypertension, heart failure, and potential new applications. Ann. Intern. Med. **97(1)**, 67 – 77 (1982).
11. Depydupont, G.: Arachidonic acid release during stress. In: New trends in atherosclerosis. Ed. By Malmendier, C. L., Polonowsky, J. Brussel, 1984, pp. 49 – 56
12. Gottschalk, C. W.: Renal nerves and sodium excretion. Ann. Rev. Physiol. **41**, 229 – 240 (1979).
13. Farman, N., Pradelles, P., Bonvalet, J.: $PGE_2$, $PGF_{2alfa}$, 6-keto $PGF_{1alfa}$ and $TxB_2$ synthesis along rabbit nephron. Am. J. Physiol. **252**, F53 – F59 (1987).
14. Kurtz, A., Pfeilschifter, J., Brown, C. D., Bauer, C.: NaCl transport stimulates prostaglandin release in cultured renal epithelial (MDCK) cells. Am. J. Physiol. **250** (Cell Physiol. 19) (5 Pt 1), C676 – C681 (1986).
15. Weber, P. C., Larsson, C., Scherer, B.: Prostaglandin $E_2$-9-ketoreductase as a mediator of salt intake-related prostaglandin renin interaction. Nature **266(5597)**, 64 – 66 (1977).
16. Dusting, G. J., Moncada, S., Vane, J. R.: Vascular actions of arachidonic acid and its metabolites in perfused mesenteric and femoral beds of the dog. Eur. J. Pharmacol. **49(1)**, 65 – 72 (1978).
17. Karim, S. M., Somers, K., Hillier, K.: Cardiovascular actions of prostaglandins $F_{2alfa}$ infusion in man. Eur. J. Pharmacol **5**, 117 – 120 (1969).
18. Malic, K. U., McGiff, J. C.: Modulation by prostaglandins of adrenergic transmission in the isolated perfused rabbit and rat kidney. Circ. Res. **36(5)**, 599 – 609 (1975).
19. Burch, R. M., Halushka, P. V.: Thromboxane and stable prostaglandin endoperoxide analogs stimulate water permeability in the toad urinary bladder. J. Clin. Invest. **66(6)**, 1251 – 1257 (1980).
20. Wilcox, C. S., Roddis, H., Peart, W. S., Gordon, D., Lewis, G. P.: Intrarenal prostaglandin release: effects of arachidonic acid and hyperchloraemia. Kidney Int. **28(1)**, 43 – 50 (1985).
21. Melki, T. S., Foegh, M. L., Ramwell, P. W.: Implication of thromboxane $A_2$ in furosemide diuresis in rats. Clin. Sci. **71(6)**, 647 – 650 (1986).

*Acta Physiologica Hungarica, Volume 81 (4), pp. 409–424 (1993)*

# 3-DIMENSIONAL (TYPE I) MICROCRYSTALS OF DETERGENT-SOLUBILIZED ($NA^+$, $K^+$)-ATPase ENZYME FROM PIG KIDNEY

S. VARGA

FRITZ VERZÁR INTERNATIONAL LABORATORY FOR EXPERIMENTAL GERONTOLOGY (VILEG), HUNGARIAN SECTION, UNIVERSITY MEDICAL SCHOOL, DEBRECEN, HUNGARY

Received May 7, 1993
Accepted June 2, 1993

3-dimensional crystalline arrays (Type I) of the ion transporting ($Na^+$, $K^+$)–ATPase enzyme from pig kidney develop in detergent-solubilized crude membrane-fragments or purified ($Na^+$, $K^+$)-ATPase preparations upon exposure to 0.1 M KCl and 0.1 M NaCl at pH 7.4 for several days at 2 °C in a crystallization medium that preserves the ATPase activity. Crystallization was obtained with non-ionic detergents; $C_{12}E_8$, $C_{12}E_9$, $C_{12}E_{10}$, and BRIJ 36 at a detergent: protein ratio ranging from 1.8:1 to 4.4:1 in purified ($Na^+$, $K^+$)-ATPase preparations. High concentration of glycerol (40% v/v), $Mg^{2+}$ ions and low temperature proved to be essential for crystallization and for protection of ATPase activity. Cross-linking of ($Na^+$, $K^+$)-ATPase crystals with glutaraldehyde protects the crystalline structure under conditions which otherwise disrupt the preformed crystals. The new crystals show close resemblance to the 3-dimensional crystals of the $Ca^{2+}$-ATPase [49] featuring the same structure of stacked lamellae. High-resolution electron microscopy of frozen-hydrated ($Na^+$, $K^+$)-ATPase samples is in progress to give unit cell dimensions and molecular packing of the new crystals.

**Keywords:** ($Na^+$, $K^+$)-ATPase, pig kidney, detergent-solubilized, 3-d crystals, electron microscopy.

Since the discovery [41] of the role of the ($Na^+$, $K^+$)-ATPase [ATP phosphohydrolase (EC.3.6.1.3.)] in the active transport mechanism of ions across the cell membrane large body of information on the structure and function of this enzyme has been accumulated (for review see: [13, 16, 42]). The physiological importance of the ($Na^+$, $K^+$)-ATPase (or the so-called sodium-pump) is the accomplishment of coupled active transport of $Na^+$ and $K^+$ across the cell

Correspondence should be addressed to
Sándor VARGA
Fritz Verzár International Laboratory for Experimental Gerontology,
Hungarian Section, University Medical School
H–4012 Debrecen, Nagyerdei krt. 98, Hungary

*Akadémiai Kiadó, Budapest*

membrane. The enzyme splits one molecule of ATP and transduces the energy to the coupled efflux of 3 $Na^+$ and influx of 2 $K^+$, both against their electrochemical gradients. This is the basis for vital cell functions such as regulation of cell volume, maintenance of transmembrane potential and excitability [48], transepithelial salt and water transport, regulation of transport via co- and counter-transport coupled to the $Na^+$- and $Ka^+$-gradients [17], and possibly more. The enzyme belongs to the so-called P-type of ion-transport ATPases. Other enzymes of this class are the $Ca^{2+}$-ATPase and the ($H^+$, $K^+$)-ATPase [35].

The enzyme consists of two subunits of integral membrane proteins, called α-subunit and β-subunit, with molecular weights of approx. 94–112 kDa and 35–58 kDa (depending on the source of material, method of preparation and evaluation [11, 13, 16, 18, 23]), and containing 1020 and 302 amino acids, respectively [21, 39, 40]. The catalytic properties are confined to the α-subunit, whereas the β-subunit, a sialoglycoprotein, seems to play a role in the in situ membrane-insertion process [16].

The spatial organization of the catalytic subunit in the membrane is not completely known. The N-terminus is located on the cytoplasmic side of the bilayer, while the location of the C-terminus is uncertain. The alfa-polypeptide was currently suggested, to include seven or eight transmembrane helical segments each of them consisting of 21–25 amino acids, mostly hydrophobic residues. Identification of the oligomeric organization of the ($Na^+$, $K^+$)-ATPase is uncertain for several reasons and apparent disagreements exist as to whether an αβ unit or an $(\alpha\beta)_2$ unit is the physiological organization in the cell membrane.

Inspite of the existing information about the structure and function of the ($Na^+$, $K^+$)-ATPase [13, 16, 17, 42], further advance is needed toward a molecular mechanism of the energy transduction and $Na^+$, $K^+$ translocation. This requires knowledge of the structure of the pump-protein at molecular level. Molecular models that couple the primary structure into a mechanistic model for the tertiary structure of the ($Na^+$, $K^+$)-ATPase are beginning to emerge [19]. A hypothetical model of the tertiary structure of $Ca^{2+}$-ATPase was suggested [3, 25], however, ($Na^+$, $K^+$)-ATPase segments on the α-chain have been assigned only to ATP-binding and ouabain-binding, but no domains for cation transport have yet been determined, even though a recent report suggests that it consists of two negatively charged residues in a non-aqueous environment [38].

Significant progress has been achieved in structural analysis of the ($Na^+$, $K^+$)-ATPase since the pioneer report of Skriver et al. [43] on the electron microscopic analysis of the two-dimensional membrane crystals of the pump-protein. Since then 2-dimensional crystalline sheets of the enzyme have been formed under a variety of conditions in a number of laboratories [14, 31, 32, 34, 51].

Structural organization of the enzyme has been studied by electron microscopy and electron diffraction, and resulted in the 3-dimensional reconstruction of the

overall shape of the molecules by image-processing techniques. However, due to the limited diffraction from these crystals (approx. 20–25 Å), the reconstructions only define the surface contours of the molecule, its disposition in the membrane, and some intermolecular contacts, and do not suggest any structural basis for the reaction mechanism and/or the ion-channel.

This paper serves as a starting-point for further advance in structural analysis of the ($Na^+$, $K^+$)-ATPase, providing one possible approach to the 3-d crystallization of the enzyme. These new crystals, like those of the $Ca^{2+}$-ATPase [6, 46, 49] are more suitable for structural analysis of higher resolution compared to the 2-d crystals known and analyzed so far. Refining the method of 3-d crystallization presented in this paper and/or exploring the conditions for growth of a more ordered Type II 3-d crystals (which would be suitable even for X-ray crystallography), one could expect a significant breakthrough in the resolution of structural analysis of the ($Na^+$, $K^+$)-ATPase.

## Materials and methods

($Na^+$, $K^+$)-ATPase was prepared from crude membrane fractions of tissue from the outer medulla of pig kidneys, according to Jorgensen [15, 18]. The specific activity of the crude microsome-fraction was in the range of 2.5–4.0 μmol Pi $min^{-1}$ $mg^{-1}$ protein. After incubation with SDS in presence of ATP at 20 °C, samples were applied on a discontinuous density gradient of successive 3 layers of sucrose: 12.5 ml of 29.4%, 7.5 ml of 15% and 5.0 ml of 10% (w/v) sucrose in 25 mM imidazole, 1 mM EDTA, pH: 7.5 (20 °C), and were centrifuged in Beckman Ti60 angle rotor at 60 000 rpm for 90 min or at 55 000 rpm for 105 min, at 4 °C. The pure enzyme-fractions were collected by pipetting and resuspended in large volume (typically 500 ml) of 25 mM imidazole, 1 mM EDTA, pH: 7.5 (20 °C) and sedimented in a Beckman Type 35 rotor at 30 000 rpm for 30 min, at 4 °C. The pellets were recollected and resuspended in a smaller volume of buffer and sedimented again in a Beckman Type 35 rotor at 30 000 rpm for 30 min, at 4 °C. After final homogenization in 25 mM imidazole, 1 mM EDTA, pH: 7.5 (20 °C) at a protein concentration of 2–6 mg/ml, protein was stored at −20 °C or −86 °C.

Protein concentrations were determined by the method of Lowry et al. [24] without extra detergent-treatment for demasking, using bovine serum albumine as a standard.

According to Cantley and Josephson [5], the coupled assay of Barnett [2], monitoring NADH oxidation, was employed to measure ATPase activities. The reaction was followed at 340 nm at 37 °C, in a Specord M40 UV/VIS double-beam spectrophotometer with a thermostated cell holder.

All assays were done in the presence of 10 mM HEPES-triethylamine, pH: 7.4, 100 mM NaCl, 20 mM KCl, 2.5 mM ATP, 2.5 mM $MgCl_2$, 10 μg/ml LDH (L-Lactic dehydrogenase), 10 μg/ml PK (Pyruvate kinase), 1.4 mM P(E)P (Phospho(enol)pyruvate), 0.26 mM NADH (β-nicotinamide adenine dinucleotide, reduced form); and 1-5 μg/ml ($Na^+$, $K^+$)-ATPase. After prolonged incubation of the crystalline specimens a 10-min pretreatment with Asolectin (in a concentration range of 50–100 mg/mg protein, at 37 °C) always preceeded the assay to recover the decreasing activities.

Gel-electrophoresis was performed according to Weber and Osborn [53], with minor modification, using Pharmacia low molecular weight kit for calibration.

*Crystallization experiments*

The basic crystallization medium used for successful crystallization of the crude microsomal fraction or of purified enzyme, consisted of: 100 mM NaCl, 100 mM KCl in 20 mM imidazole, supplemented with 40% (v/v) glycerol, 5 mM $MgCl_2$, 5 mM DTT (dithiotreitol), 3 mM $NaN_3$ 25, IU/ml Trasylol, 2 μg/ml BHT (2,[6]-di-tert-butil-p-cresol). The "working" pH-range for the crystallization media were between 7.2 and 7.5 (20 °C). Typical protein concentrations varied between 1 and 2 mg/ml. Countless variations of this crystallization medium were tested without success (see Results).

Detergents proved to be successful for crystallization were $C_{12}E_8$ (octaethylene glycol dodecyl monoether), $C_{12}E_9$ (polyoxyethylene 9-lauryl ether), $C_{12}E_{10}$ and BRIJ 36 (polyoxyethylene 10-lauryl ether), at a detergent: protein ratio of 1.8:1 – 2.25:1 for $C_{12}E_8$ and $C_{12}E_9$, and 3.8:1-4.4:1 for the latter two.

Samples were kept at 2 °C for weeks in a volume of 0.25 – 1.0 ml.

*Electron microscopy*

Samples for negative staining, with 1% uranyl acetate (pH: 4.3), were taken on the 0 – 60 days. Specimens were checked for crystals in a JEOL JEM 100 – B, and Philips 420 electron microscopes. Due to the nature of specimens the "screening"-magnification had to be at least x 50 – 60 000 (instrumental).

*Thin sections*

Selected samples were fixed with 1% glutaraldehyde for 24 hours at 2 °C, postfixed in 2% $OsO_4$ at room temperature for 1 h. After dehydration in a graded ethanol series, pellets were embedded in Araldite and sectioned. Thin sections were stained with uranyl acetate and lead citrate.

## Results

### *Factors influencing the crystallization*

The whole strategy of the crystallization trials based on the experiences and results with the successful crystallization of $Ca^{2+}$ATPase [6, 46, 49]. Despite of these experiences, and the several thousand conditions, tested so far for the ($Na^+$, $K^+$)-ATPase, only a few proved to be successful.

Buffers like MOPS (used for the $Ca^{2+}$-ATPase crystallization), TRIS – HCl, TES, HEPES did not work for ($Na^+$, $K^+$)-ATPase. The only buffer which helped crystallization was Imidazole in the pH-range of 7.2 – 7.5 (at 20 °C), at a concentration of 20 mM (in most cases).

Glycerol at higher concentrations seemed to be essential not only for crystal-formation, but for the preservation of the $Ca^{2+}$-ATPase activity. While the glycerol-concentration (between 20% and 40%) strongly modified the course of crystal-formation in the $Ca^{2+}$-ATPase experiments, we could not find ($Na^+$, $K^+$)-ATPase crystals either at lower (20 – 30%) or at higher concentration (50%) of glycerol, though the activities of these samples were fairly high at each glycerol-concentration.

The high concentration of the "crystallization-agent", $Ca^{2+}$ (20 mM) for the $Ca^{2+}$-ATPase, was mimicked in the ($Na^+$, $K^+$)-ATPase experiments, using high concentration of $Na^+$ and $K^+$. The concentration-ranges for both ions varied between from 10 mM up to molar concentrations, in every reasonable combinations. The actual concentrations of these crucial ions, in all successful experiments, were 100–100 mM, respectively.

$Mg^{2+}$ proved to be essential for crystallization. When it was omitted from the medium, even the successful combination did not produce crystals.

The low temperature (0–4 °C) also proved to be crucial for crystal-production. Samples at room-temperature (20–25 °C) or higher (37 °C) never yielded crystals. Exposure of crystalline samples to higher temperature (20 °C and 37 °C, respectively) for 2 hours destroyed the preformed crystals. Further incubation of these samples after cooling back to 0–4 °C never produced crystals again.

*Choice of detergent*

From the two dozen detergents tested for crystallization so far, only the non-ionic ethylene-ethers: $C_{12}E_8$, $C_{12}E_9$, $C_{12}E_{10}$ and BRIJ 36 proved to be successful, though tests with the rest were not really extensive. $C_{12}E_9$ and $C_{12}E_{10}$ only produced crystals for a few times at a detergent: protein ratio of 2:1 and 3.75–4.0:1, respectively.

The actual detergent: protein ratio in successful experiments for $C_{12}E_8$ and BRIJ 36 also varied from 1.8:1 to 2.25:1 for $C_{12}E_8$, and from 3.8:1 to 4.4:1 for BRIJ 36.

Repeated successful crystallization occurred, under otherwise identical conditions, only using the same starting material (either microsomal fraction or purified ($Na^+$, $K^+$)-ATPase). Using different batches of material, conditions used for successful trials, had to be changed. These observations strongly suggest that one of the crucial factor for crystal-production is the quality of the initial preparation, i.e., the "purity" of the crude microsomal fraction.

Though the author strictly followed the step-by-step instructions of the Jorgensen-method [15, 18] during preparation of the crude membrane fraction and for purification afterwards, the gel-patterns (which otherwise were very consistent for all trials) were different from those shown in his paper [15]. Besides the two characteristic bands of 112 kDa for the $\alpha$ subunit, and 58 kDa for the $\beta$ subunit (which are higher than his values [15]), we always had bands at 180 kDa and 360 kDa, respectively. It is very tempting to suppose these bands may be an $\alpha\beta$ and an $(\alpha\beta)_2$ unit, and to suggest that the presence of these "impurities" may play some special role in the crystallization process.

*Electron microscopy of crystalline specimens*

In control preparations of purified membrane-bound ($Na^+$, $K^+$)-ATPase, enzyme-molecules are observed by negative staining as surface particles randomly distributed in clusters and strands (Fig. 1), similar to those shown in the paper of Skriver et al. [44]. The average diameter of the membrane-fragments varied between 0.3–0.5 μm.

Crystal-growth in detergent solubilized crude membrane fraction was limited, though search for the optimal conditions was not really extensive. Conditions when crystallization occurred were similar to those for purified enzyme, except that higher detergent: protein ratio had to be used for crude enzyme preparation.

Typical condition for crystallization of the microsomal fraction was: 20 mM imidazole, pH: 7.4, 100 mM NaCl, 100 mM KCl, 40% glycerol, 5 mM $MgCl_2$, 5 mM DTT, 3 mM $NaN_3$, 25 IU/ml Trasylol, 2 μg/ml BHT. Protein concentrations varied between 1 and 2 mg/ml. The detergent: protein ratio for $C_{12}E_8$ was 2.25:1 and for BRIJ 36 4.2–4.4:1. Crystallization occurred after a couple of days of incubation at 2 °C.

Typical picture of negatively stained crystalline structure of ($Na^+$, $K^+$) ATPase molecules is shown in Fig. 2, superposed on the surface of aggregated clusters of detergent-solubilized materials. Crystals in the crude membrane system generally developed in association with these solubilized/aggregated clusters, making the observation very difficult. Individual crystals or groups of those (frequently seen in the $Ca^{2+}$-ATPase experiments [49]), growing separately has never been observed in this system. The average diameter of the crystals was about 1 μm.

In purified enzyme-preparation, using the same basic crystallization medium, but somewhat lower detergent: protein ratio (1.8–2.2:1 for $C_{12}E_8$ and 3.6–4.2:1 for BRIJ 36) larger crystals were growing. Crystals shown in Fig. 3, grown at a detergent: protein ratio of 4:1 with BRIJ 36, having a diameter of 2 μm, were easily recognizable not only due to their sizes, but they were grown separately form the disturbing background.

We have not found any noticeable difference between crystals grown in the presence of different detergents.

In Fig. 4 a crystal grown in the presence of $C_{12}E_8$ at a concentration of 2 mg/ml protein is shown. Though the general appearance of the background-material seems to be different in organization from that seen with BRIJ 36, it does not seem to influence the crystal-organization and order.

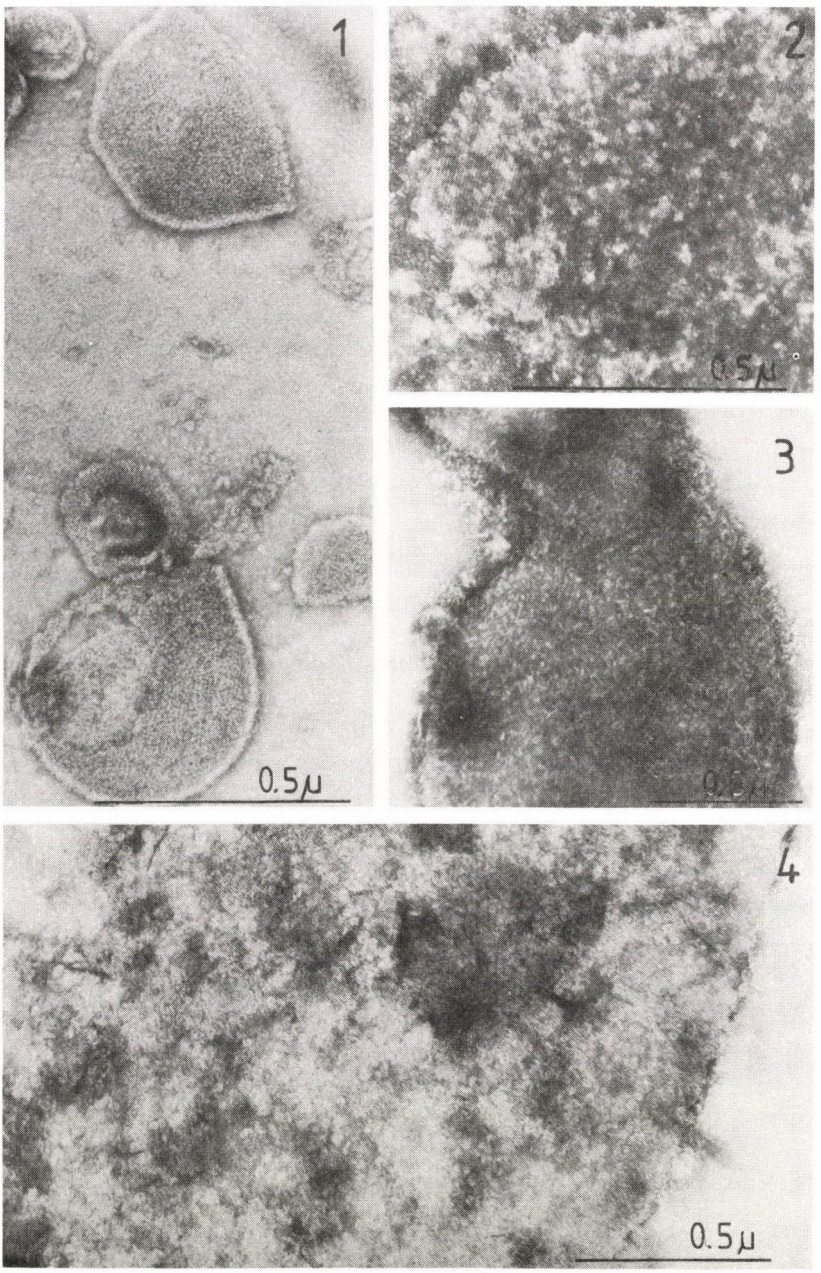


*Fig. 1.* Control purified ($Na^+$, $K^+$)-ATPase membrane fragments suspended in 25 mM imidazole pH: 7.5, 2 mM EDTA. The membrane-bound enzyme-molecules are randomly distributed in clusters and strands. Magnification: × 74 450

*Fig. 2.* Crystal growing in detergent–solubilized crude microsomal fraction at a protein concentration of 2 mg/ml and BRIJ 36 at 8 mg/ml in a standard crystallization medium, after 2 weeks of incubation at 2 °C. Magnification: × 78 750

*Fig. 3.* Purified ($Na^+$, $K^+$)-ATPase at a concentration of 1 mg/ml was solubilized with BRIJ 36 at a detergent: protein ratio of 4:1, and incubated at 2 °C for 7 days. Crystals with diameter of 2 μm grew in groups, separated from the solubilized materials. Magnification: × 35 450

*Fig. 4.* Purified ($Na^+$, $K^+$)-ATPase crystal growing in the presence 2 mg/ml $C_{12}E_8$ after 5 days of incubation at 2 °C. Magnification: × 55 880

Electronmicrographs of crystals growing on the surface and/or in association with the solubilized/aggregated material frequently suggest the presence of a single crystalline lamella, like in Fig. 5. However, thin sections prepared from these samples showed stacked multilamellar arrays of ATPase molecules (Fig. 6). In these multilamellar stacks the superimposed layers are seen in register, suggesting interactions between surface groups of ATPase molecules in the neighbouring layers. The number of the stacked lamellae varied from 2 to 30. There is a striking difference between the diameters of crystals measured on an in-plane image (viewed down the z-axes) or measured on micrographs taken from the sectioned material (side view). While the average for the in-plane view was about 2 μm, in sectioned material it was only about 0.3–0.4 μm. This difference suggests that the crystals of ($Na^+$, $K^+$)-ATPase may be more sensitive to the same mechanical stresses than the $Ca^{2+}$-ATPase crystals. Using identical procedures for handling the samples of both protein-crystals, diameters for $Ca^{2+}$-ATPase-crystals did not differ significantly in sectioned material and in negatively stained samples [49].

The projected view (normal to the plane of the lamellae) of the crystalline sheets of ($Na^+$, $K^+$)-ATPase shows ordered arrays of stain-excluding particles with two distinct periodicities (Fig. 7). One is about 80 Å (measured values: 73–88 Å), representing the half-period of the "a" cell dimensions, while the other is about 55 Å (measured values: 48–61 Å), representing the "b" cell dimensions.

Surprisingly low values were measured for the inter-lamellar distances in the sectioned materials (Fig. 6 and Fig. 8). Though the number of samples available might not be enough for a reliable statistical evaluation, the low values (an average of about 88 Å) were very consistent using different detergent ($C_{12}E_8$ for Fig. 6 and BRIJ 36 for Fig. 8), or using different embedded samples for thin sectioning. One cannot exclude limited shrinkage of the structure during embedding, yet these values are lower than it was expected, and those measured for $Ca^{2+}$-ATPase-crystals in similar specimens [6, 46, 49].

Presenting the first micrographs of the 3-d crystals of detergent-solubilized ($Na^+$, $K^+$)-ATPase, and comparing them to those of the $Ca^{2+}$-ATPase [6, 46, 49], one could say that these crystals seem to be indistinguishably identical. In lack of the appropriate instrumental background (in our laboratory) for the determination of unit cell dimensions, which unambiguously would show differences between the unit cell dimensions of the two crystals, we had set up several control experiments to exclude the possibility of accidental crystallization of the $Ca^{2+}$-ATPase which might be present as a cross-contamination in the ($Na^+$, $K^+$)-ATPase preparations.

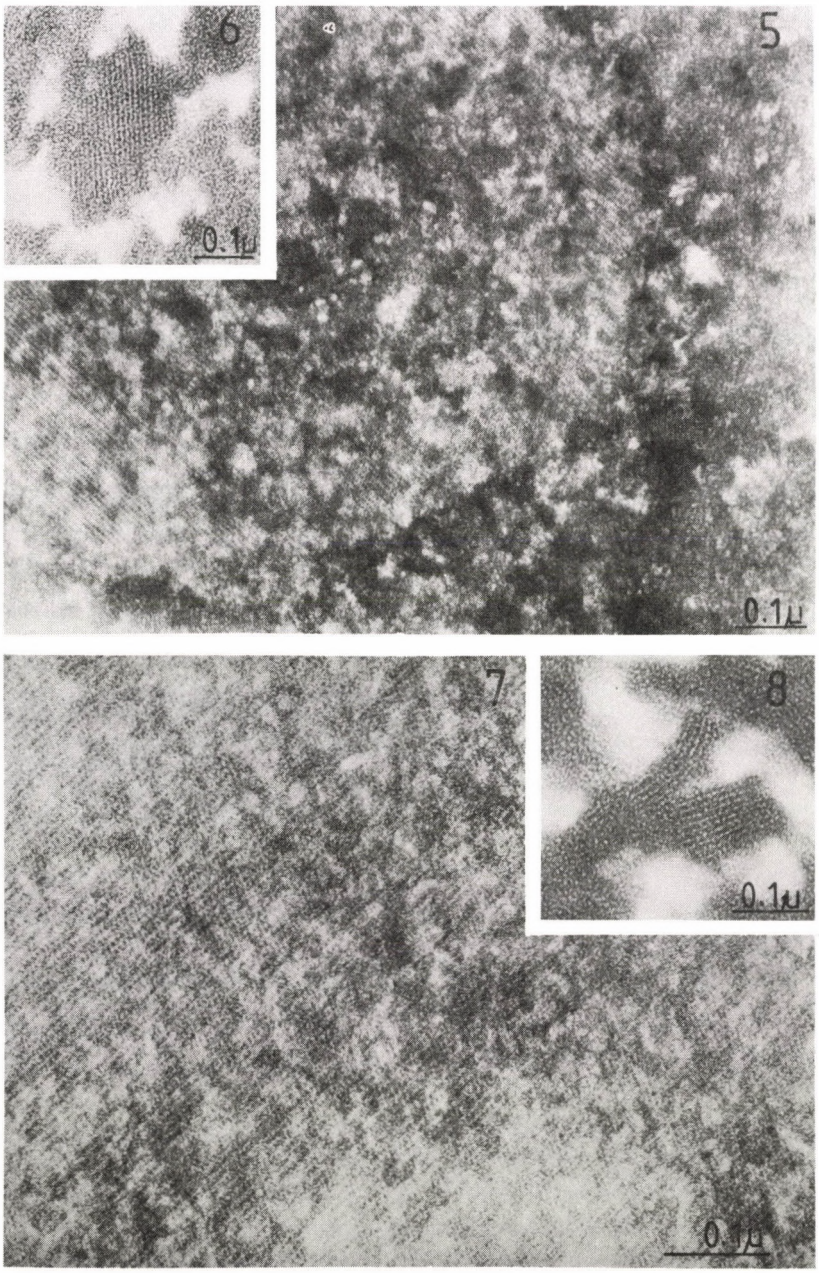


*Fig. 5.* Crystal growing on the surface of dissolved materials suggests a single-layer structure. Purified ($Na^+$, $K^+$)-ATPase was solubilized in BRIJ 36 at a detergent: protein ratio of 4:1. Magnification: × 114 720

*Fig. 6.* In sectioned material the stacked multilamellar arrays of molecules can be clearly seen. The average distance between neighbouring lamellae does not depend on the type of detergent used for crystallization. Magnification: × 77 780

*Fig. 7.* Purified ($Na^+$, $K^+$)-ATPase solubilized in $C_{12}E_8$ at a 2:1 detergent: protein ratio produced large, well-organized crystals. The stain-excluding ATPase molecules were redistributed in a highly organized fashion, showing two distinct periodicities. Magnification: × 145 800

*Fig. 8.* In sectioned material crystals show much smaller "diameter" than it could be measured on an im-plane projection (Fig. 7). Magnification: × 118 800

Countless control experiments had dispelled the suspicion of a possible cross-crystallization. Further indirect facts were previously presented by authors working with the $Ca^{2+}$-ATPases to exclude this possibility. None of these authors (Stokes and Green [45], Misra et al. [30] and the Martonosi-team [6, 36, 46, 47, 49] working with the sarcoplasmic reticulum $Ca^{2+}$-ATPase, and Pikula et al. [37] using erythrocyte plasma membrane ($Ca^{2+}+Mg^{2+}$)-ATPase observed crystallization of the $Ca^{2+}$-ATPases under those conditions which proved to be successful for ($Na^+$, $K^+$)-ATPase crystallization. According to these authors: crystals never grew at $Ca^{2+}$-concentration lower than 0.2 mM, and in the pH range of 7.2–7.5 without high concentration of $Ca^{2+}$.

## Discussion

The high-resolution structural analysis of the ($Na^+$, $K^+$)-ATPase has started with the pioneer work of Skriver et al. [43] on the two-dimensional crystals of the pump-protein. Since then dozens of papers dealing with different aspects of the structure have been published [26, 31, 34, 35, 42, 44, 45]. However, due to the nature of a 2-dimensional crystal, and the techniques used for analysis, only limited resolution (about 20–25 Å) of the structure has been achieved. Similar values were published for the 2-dimensional crystals of the $Ca^{2+}$-ATPase [47], probably as a resolution limit for these types of crystals. It was obvious, that further advance toward atomic resolution of the structure requires the 3-dimensional crystals of sufficient size and order. The first step in this direction, and reports on the further refinement of the 3-d crystallization-method for the $Ca^{2+}$-ATPase enzyme were provided by the Martonosi-team [6, 36, 46, 49], and years later by others [30, 37, 45].

To demonstrate the difficulties one encounters dealing with crystallization of macromolecules, we quote an expert of this field, McPherson [27]: "The reason that crystallization step has become the primary obstacle to expanded structural knowledge is the necessarily empirical nature of the method employed to overcome it. Macromolecules are extremely complex physical-chemical systems whose properties vary as a function of many environmental influences such as temperature, pH, ionic strength, contaminants and solvent composition to name only a few. They are structurally dynamic, microheterogenous, aggregating systems, and they change conformation in the presence of ligands. Superimposed on this is the poor state of our current understanding of macromolecular crystallization phenomena and the forces that promote and maintain protein and nucleic acid crystals.

As a substitute for the precise and reasoned approaches that we commonly apply to scientific problems, we are forced for the time being at least, to employ a strictly empirical methodology."

These words proved to be real when we (having no previous experience with the sodium-pump enzyme) started crystallization of the ($Na^+$, $K^+$)-ATPase, despite of the great body of experience we have collected while working with the $Ca^{2+}$-ATPase.

Solubilization of ($Na^+$, $K^+$)-ATPase by detergents is a prerequisite for the formation of 3-dimensional crystals. Since the detergent-solubilized enzyme is notoriously unstable at the high detergent concentrations used for solubilization/crystallization in these experiments, the first task was to find conditions that preserve the ATPase activity of the enzyme for several days or weeks.

It was evident to try those conditions first which already proved to be successful for the $Ca^{2+}$-ATPase. These were: the high glycerol-content, vital ions for the ($Na^+$, $K^+$)-ATPase, antioxidants, protease inhibitors, bacteriostatic agents, the proper protein concentration and detergent: protein ratio, to mention only a few.

We have tried different combinations of these ingredients before finding the successful version (see: Methods).

The first striking results were a much lower yield for the ($Na^+$, $K^+$)-ATPase crystals compared to those of the $Ca^{2+}$-ATPase. While, after longer incubation, the majority of the protein solubilized in "any" sample of the $Ca^{2+}$-ATPase experiments has been crystallized, only a very small portion of the ($Na^+$, $K^+$)-ATPase showed crystalline structures even after prolonged incubation. This difference could partially be explained with the differences between the purity of the two protein preparations. While the initial concentrations of these proteins in the lipid bilayers are almost the same (7 mM for the ($Na^+$, $K^+$)-ATPase [18] and 4–6 mM for the $Ca^{2+}$-ATPase [47], there is a significant difference between the efficiencies of different purification. (Our values could be even worse than 50–70% given for preparation of the ($Na^+$, $K^+$)-ATPase in an angle rotor [18]).

Using different batches of the starting material under otherwise identical "successful" conditions we could not reproduce crystallization without fitting the conditions again. These facts, and the known complicated behavior of protein in a detergent-solubilized system [12, 15, 22, 27, 29, 52], put emphasis on the "purity" of the starting material for crystallization.

As the crystallization strongly depends on the actual detergent: lipid (endogenous or added): protein ratio and on numerous other factors, which – in turn – could modify the interactions between the three major constituents of the crystals, no previously calculated conditions could be called successful until the first micrographs were taken.

In our case only persistent, repeated trials under (and around) those conditions, which once proved to be successful, produced crystals repeatedly. In those laboratories, where the preparation of the ($Na^+$, $K^+$)-ATPase has a long tradition,

hence a purer and much better characterized enzyme is available, faster development in the crystallization technique could be expected.

The other surprising result was the close resemblance of the new crystals to those of the $Ca^{2+}$-ATPase.

The theoretical background, and our present knowledge about the oligomeric organization of the ($Na^+$, $K^+$)-ATPase in the native membrane, is quite confusing [26, 32]. An apparent disagreement exists as to whether an $\alpha\beta$ or an $(\alpha\beta)_2$ unit is the physiological organization in the cell membrane. Studies on binding sites per unit mass of protein show one site per $(\alpha\beta)_2$ unit [13], or only one site per $(\alpha\beta)$ unit [18]. Binding studies of ATP and ouabain suggest cooperative interaction of the two sites at certain ligand combinations [1]. Dimeric interaction is also in accord with radiation inactivation studies [20, 33], sedimentation equilibrium analysis [15, 16] and cross-linking studies [1], however it has been demonstrated that the protomer has the capability of both hydrolytic activity [4, 8] and of occlusion of ions [7, 50], although with somewhat different kinetic parameters.

Similar contradicting conclusions were drawn from the 3-d reconstruction of the molecular structure [26, 32, 44]. The different crystal-forms of the 2-dimensional crystals induced by different ligands show a wide variety of unit cell dimensions [23, 26, 34, 43, 50]. Some of these data support the hypothesis of one protomer (an $(\alpha\beta)$ unit) per unit cell, while the others stand for a dimer (an $(\alpha\beta)_2$ unit) per unit cell, while the others stand for a dimer (an $(\alpha\beta)_2$) unit per unit cell. Both hypotheses are supported by indirect facts as they were the functional unit in the native membrane.

In the light of these pieces of information about the oligomeric organization of the ($Na^+$, $K^+$)-ATPase molecules, the interpretation of the electronmicrographs of the new 3-d crystals is even more difficult. In absence of the unit cell dimensions of these crystals no statement about the molecular packing can be made this time.

Knowing the unit cell dimensions of the 2-d crystals of the ($Na^+$, $K^+$)-ATPase protomers (59–70 Å for the a-axes, and 51–59 Å for the b-axes, [26]) and values for the dimeric crystals (135–148 Å for a-axes, and 44–56 Å for b-axes [26]), and the same values for the 2-d $Ca^{2+}$-ATPase crystals (62–72 Å and 51–55 Å for the protomer, and 66 Å and 114 Å for the dimer a- and b-axes, respectively [47]), one can meditate how these data are comparable to those of the 3-d crystals.

The unit cell dimensions of the known 3-d $Ca^{2+}$-ATPase crystals are: 164 Å and 55 Å for a- and b-axes, respectively, according to Taylor et al. [47], and 151 Å, 51 Å and 158 Å for a-, b- and c-axes, respectively, for one type of crystals and 166 Å, 58 Å and 164 Å, for a-, b- and c-axes, respectively, for another crystal-type, according to Stokes and Green [45]. These 3-d crystals show closer similarity in their protomeric organization to the $Ca^{2+}$-induced 2-d crystals of the $Ca^{2+}$-pump protein, stabilized in the $E_1$ conformation, than to the vanadate-stabilized dimeric $E_2$ conformation.

It is plausible to suppose a close correlation between the protomer's b-values: 51–55 Å for 2-d crystals, and 55 Å [47], and 51–58 Å [45], respectively, for the 3-d $Ca^{2+}$-ATPase. Values for a-axes of the 2-d protomers (62–72 Å), for the $Ca^{2+}$-ATPase, are also close enough to one of the periodicity-values of the 3-d protomers (82 Å [47], and 75 Å, 79 Å, respectively, [45]) which represent the half of the a-axes dimensions.

Using the same analogy, the values measured from the periodicities of the new 3-d crystals of the ($Na^+$, $K^+$)-ATPase: 80 Å and 55 Å, for the half of the a-, and for the b-axes, respectively, show the same close correlation to the values of the 2-d protomer crystals: 59–70 Å for the a- and 51–59 Å for the b-axes.

These possible correlations, if any, could partially explain the close resemblance of the two 3-d crystals.

The other important question whether only individual α-subunits or the whole αβ protomers are the building-units of the new crystals, could only be answered after successful crystallization trials of the separated detergent-solubilized α-subunit populations.

Experiments in this direction, and for further refinement of our crystallization techniques and to determine the unit cell dimensions of the new crystals, are in progress.

Further, more reliable details about the organization of the crystals and the submolecular structure of the pump-protein could be expected after successful Type II [12, 22, 28] crystallization of the ($Na^+$, $K^+$)-ATPase. These crystal-types would show a perfect order in the third dimension, and providing an appropriate overall size they were suitable for X-ray crystallography.

**Acknowledgement**

My thanks are due to Dr. Márton Szabolcs (Central Research Laboratory, Univ. Med. School, Debrecen) for his help with the gel-electrophoresis and reviewing the manuscript, and to Mr. Sándor Szabados (V.I.L.E.G., Univ. Med. School, Debrecen) for his excellent technical help. This work was supported by a research grant OTKA 1474.

## REFERENCES

1. Askari, A., Huang, W. H.: $Na^+$, $K^+$-ATPase: half of the subunits cross-linking reactivity suggests an oligomeric structure containing a minimum of four catalytic subunits. Biochem. Biophys. Res. Commun. **93**, 448–453 (1980).
2. Barnett, R. E.: Effect of monovalent cations on the quabain inhibition of the sodium and potassium ion activated adenosine triphosphate. Biochemistry **9**, 4644–4648 (1970).

3. Brandl, C. J., Green, N. M., Korczak, B., MacLennan, D. H.: Two $Ca^{2+}$-ATPase genes; homologies and mechanistic implications of deduced amino acid sequences. Cell **44**, 597–607 (1986).
4. Brotherus, J. R., Moller, J. V., Jorgensen, P. L.: Soluble and active renal $Na^+$, $K^+$-ATPase with maximum protein molecular mass 170 000 ± 9 000 daltons; formation of larger subunits by secondary aggregation. Biochem. Biophys. Res. Commun. **100**, 146–154 (1981).
5. Cantley, L. C. Jr., Josephson, L.: A slow interconversion between active and inactive states of the (Na–K)ATPase. Biochemistry **15**, 5280–5287 (1976).
6. Dux, L., Pikula, S., Mullner, N., Martonosi, A.: Crystallization of $Ca^{2+}$-ATPase in detergent-solubilized sarcoplasmic reticulum. J. Biol. Chem. **262**, 6439–6442 (1987).
7. Esmann, M.: Occlusion of $Rb^+$ by detergent-solubilized ($Na^+ + K^+$)-ATPase from shark salt glands. Biochim. Biophys. Acta **815**, 196–202 (1985).
8. Esmann, M.: Solubilized ($Na^+ + K^+$)-ATPase from shark rectal gland and ox kidney – an inactivation study. Biochim. Biophys. Acta **857**, 38–47 (1986).
9. Esmann, M., Skou, J. C., Christiansen, C.: Solubilization and molecular weight determination of the ($Na^+ + K^+$)-ATPase from rectal glands of Squalus acanthias. Biochim. Biophys. Acta **567**, 410–420 (1979).
10. Esmann, M., Christiansen, C., Karlsson, K. A., Hansson, G. C., Skou, J. C.: Hydrodynamic properties of solubilized ($Na^+K^+$)-ATPase from rectal glands of Squalus acanthias. Biochim. Biophys. Acta **603**, 1–12 (1990).
11. Forbush, B. III.: Characterization of right-side-out membrane vesicles rich in (Na, K)-ATPase and isolated from dog kidney outer medulla. J. Biol. Chem. **257**, 12678–12684 (1982).
12. Garavito, R. M., Rosenbush, J. P.: Isolation and crystallization of bacterial porin. Methods in Enzymol. **104**, 370–381 (1986).
13. Glynn, I. M.: The $Na^+$, $K^+$-transporting adenosinetriphosphatase. In: The enzymes of biological membranes, cd. Martonosi, A. M. Vol. 3, Plenum Press, New York 1985, pp. 35–114.
14. Hebert, H., Jorgensen, P. L., Skriver, E., Maunsbach, A. B.: Crystallization patterns of membrane-bound ($Na^+ + K^+$)-ATPase. Biochim. Biophys. Acta **689**, 571–574, (1982).
15. Jorgensen, P. L.: Purification and characterization of ($Na^+ + K^+$)-ATPase. III. Purification from the outer medulla of mammalian kidney after selective removal of membrane components by sodium dodecylsulphate. Biochim. Biophys. Acta **356**, 36–52 (1974).
16. Jorgensen, P. L.: Mechanism of the $Na^+$, $K^+$ pump. Protein structure and conformations of the pure ($Na^+ + K^+$)-ATPase. Biochim. Biophys. Acta **694**, 27–68 (1982).
17. Jorgensen, P. L.: Structure, function and regulation of Na, K-ATPase in the kidney. Kidney International **29**, 10–20 (1986).
18. Jorgensen, P. L.: Purification of $Na^+$, $K^+$-ATPase: Enzyme sources, preparative problems, and preparation from mammalian kidney. Methods in Enzymol. **156**, 29–43 (1988).
19. Jorgensen, P. L., Andersen, J. P.: Structural basis for E1–E2 conformational transition in Na, K-pump and Ca-pump proteins J. Membr. Biol. **103**, 95–120 (1988).
20. Karlish, S. J. D., Kempner, E.: Minimal functional unit for transport and enzyme activities of ($Na^+ + K^+$)-ATPase as determined by radiation inactivation. Biochim. Biophys. Acta **776**, 288–298 (1984).
21. Kawakami, K., Noguchi, S., Noda, M., Takahashi, H., Ohta, T., Kawamura, M., Nojima, H., Nagano, K., Hirose, T., Inayama, S., Hayashida, H., Miyata, T. and Numa, S.: Primary structure of the alfa-subunit of Torpedo californica ($Na^+ + K^+$)ATPase deduced from cDNA sequence. Nature **316**, 733–736 (1985).
22. Kuhlbrandt, W.: Three-dimensional crystallization of membrane proteins. Quart. Rev. Biophys. **21**, 429–477 (1988).

23. Kyte, J.: Purification of the sodium- and potassium-dependent adenosine triphosphatase from canine renal medulla. J. Biol. Chem. **246**, 4157–4165 (1971).
24. Lowry, O. H., Rosebrough, N. J., Farr, A. L., Randall, R. J.: Protein measurement with the Folin phenol reagent. J. Biol. Chem. **193**, 265–275 (1951).
25. MacLennan, D. H., Brandl, C. J., Korczak, B., Green, N. M.: Amino acid sequence of a $Ca^{2+}+Mg^{2+}$-dependent ATPase from rabbit muscle sarcoplasmic reticulum, deduced from its complementary DNA sequence. Nature **316**, 696–700 (1985).
26. Maunsbach, A. B., Skriver, E., Soderholm, M., Hebert, H.: Three-dimensional structure and topography of membrane-bound Na, K-ATPase. In: The $Na^+$, $K^+$-pump. Part A: Molecular Aspects. eds Skou, J. C., Norby, J. G., Maunsbach, A. B., Esmann, M., Alan R. Liss, Inc., New York 1988, pp. 39–56.
27. McPherson, A.: Current approaches to macromolecular crystallization. Eur. J. Biochem. **189**, 1–23 (1990).
28. Michel, H.: Crystallization of membrane proteins. TIBS **8**, 56–59 (1983).
29. Michel, H.: General and practical aspects of membrane protein crystallization. In: Crystallization of membrane proteins. ed.: Michel, H., CRC Press, Boca Raton 1988, pp. 73–88.
30. Misra, M., Taylor, D., Oliver, T., Taylor, K. A.: Effect of organic anions on the crystallization of the $Ca^{2+}$-ATPase of muscle sarcoplasmic reticulum. Biochim. Biophys. Acta **1077**, 107–118 (1991).
31. Mohraz, M., Smith, P. R.: Structure of ($Na^+$, $K^+$)-ATPase as revealed by electron microscopy and image processing. J. Cell Biol. **98**, 1836–1841 (1984).
32. Mohraz, M., Smith, P. R.: Three-dimensional structure of Na, K-ATPase and a model for the olygomeric form and the mechanism of the Na, K-pump. In: The $Na^+$, $K^+$-pump. Part A: Molecular Aspects. eds: Skou, J. C., Norby, J. G., Maunsbach, A. B., Esmann, M., Alan R. Liss, Inc., New York 1988, pp. 99–106.
33. Norby, J. G., Jensen, J.: A model for the stepwise radiation inactivation of the alpha 2-dimer of Na, K-ATPase. J. Biol. Chem. **264**, 19548–19558 (1989).
34. Ovchinnikov, Yu. A., Demin, V. V., Barnakov, A. N., Kuzin, A. P., Lunev, A. V., Modyanov, N. N., Dzhandzhugazyan, K. N.: Three-dimensional structure of ($Na^+ + K^+$)-ATPase revealed by electron microscopy of two-dimensional crystals. FEBS Lett. **190**, 73–76 (1985).
35. Pedersen, P. L., Carafoli, E.: Ion motive ATPases. I. Ubiquity, properties, and significance to cell function. TIBS **12**, 146–150 (1987).
36. Pikula, S., Mullner, N., Dux, L., Martonosi, A.: Stabilization and crystallization of $Ca^{2+}$-ATPase in detergent-solubilized sarcoplasmic reticulum. J. Biol. Chem. **263**, 5277–5286 (1988).
37. Pikula, S., Wrzosek, A., Famulski, K. S.: Long-term stabilization of ($Ca^{2+}+Mg^{2+}$)-ATPase of detergent-solubilized erythrocyte plasma membrane. Biochim. Biophys. Acta **1061**, 206–214 (1991).
38. Shani-Sekler, M., Goldshleger, R., Tal, D. M., Karlish, S. J. D.: Inactivation of $Rb^+$ and $Na^+$ occlusion on ($Na^+$, $K^+$)-ATPase by modification of carboxyl groups. J. Biol. Chem. **263**, 19331–19341 (1988).
39. Shull, G. E., Schwartz, A., Lingrel, J. B.: Amino-acid sequence of the catalytic subunit of the ($Na^+$, $K^+$)-ATPase deduced from a complementary DNA. Nature **316**, 691–695 (1985).
40. Shull, G. E., Lane, L. K. and Lingrel, J. B.: Amino-acid sequence of the beta-subunit of the ($Na^+ + K^+$) ATPase deduced from a cDNA. Nature **321**, 429–431 (1986).
41. Skou, J. C.: The influence of some cations on an adenosine triphosphatase from peripheral nerves. Biochim. Biophys. Acta **23**, 394–401 (1957).

42. Skou, J. C.: The energy coupled exchange of $Na^+$ for $K^+$ across the cell membrane. The $Na^+$, $K^+$-pump. FEBS Lett. **268**, 314–324 (1990).
43. Skriver, E., Maunsbach, A. B., Jorgensen, P. L.: Formation of two-dimensional crystals in pure membrane-bound $Na^+$, $K^+$-ATPase. FEBS Lett. **131**, 219–222 (1981).
44. Skriver, E., Hebert, H., Maunsbach, A. B.: Crystallization and structure of membrane-bound Na, K-ATPase In: The sodium pump. eds: Glynn, I., Ellory, C. The Company of Biologists Ltd., Cambridge 1985, pp. 37–45.
45. Stokes, D. L., Green, M.: Three-dimensional crystals of Ca-ATPase from sarcoplasmic reticulum. Biophys. J. **57**, 1–14 (1990).
46. Taylor, K. A., Mullner, N., Pikula, S., Dux, L., Peracchia, C., Varga, S., Martonosi, A.: Electron microscope observations on $Ca^{2+}$-ATPase microcrystals in detergent-solubilized sarcoplasmic reticulum. J. Biol. Chem. **263**, 5287–5294 (1988).
47. Taylor, K. A., Dux, L., Varga, S., Ting-Beall, H. P., Martonosi, A.: Analysis of two-dimensional crystals of $Ca^{2+}$-ATPase in sarcoplasmic reticulum. Methods in Enzymol. **157**, 271–289 (1988).
48. Thomas, R. C.: Electrogenic sodium pump in nerve and muscle cells. Physiological Rev. **52**, 563–594 (1972).
49. Varga, S., Taylor, K. A., Martonosi, A.: Effects of solutes on the formation of crystalline sheets of the $Ca^{2+}$-ATPase in detergent-solubilized sarcoplasmic reticulum. Biochim. Biophys. Acta **1068**, 374–386 (1991).
50. Vilsen, B., Andersen, J. P., Petersen, J., Jorgensen, P. L.: Occlusion of $22Na^+$ and $86Rb^+$ in membrane-bound and soluble protomeric alpha beta-units of Na, K-ATPase. J. Biol. Chem. **262**, 10511–10517 (1987).
51. Zampighi, G., Kyte, J., Freitag, W.: Structural organization of $(Na^+ + K^+)$-ATPase in purified membranes. J. Cell Biol. **98**, 1851–1864 (1984).
52. Zulauf, M.: Detergent phenomena in membrane protein crystallization. In: Crystallization of membrane proteins. ed.: Michel, H., CRC Press, Boca Raton 1988. pp. 53–72.
53. Weber, K., Osborn, M.: The reliability of molecular weight determinations by dodecyl sulphate-polyacrylamide gel electrophoresis. J. Biol. Chem. **244**, 4406–4412 (1969).

ACTA PHYSIOLOGICA HUNGARICA
VOLUME 81

# INDEX

## Number 1



## Number 2

Number 3

Number 4

# AUTHOR INDEX

# INSTRUCTIONS TO AUTHORS

*Form of manuscript*

Two complete copies of the manuscript including all tables and illustrations should be submitted. Manuscripts should be typed double-spaced with margins at least 3 cm wide. Pages should be numbered consecutively.

Manuscripts should include the title, authors' names and short postal address of the institution where the work was done.

An abstract of not more than 200 words should be supplied typed before the text of the paper. The abstract should be followed by (no more than) five key-words.

*Abbreviations* should be spelled out when first used in the text. *Drugs* should be referred to by their WHO code designation (Recommended International Nonproprietary Name): the use of proprietary names is unacceptable. The *International System of Units* (SI) should be used for all measurements.

*References*

References should be numbered in alphabetical order and only the numbers should appear in the text [in brackets]. The list of references should contain the name and initials of all authors (the use of et al. instead of authors' name in the reference list is not accepted): for journal articles the title of the paper, title of the journal abbreviated according to the style used in Index Medicus, volume number, first and last page number and year of publication, for books the title followed by the publisher and place of publication.

Examples:

Székely, M., Szelényi, Z.: Endotoxin fever in the rat. Acta physiol. hung. **53,** 265–277 (1979).

Schmidt, R. F.: Fundamentals of Sensory Physiology. Springer Verlag, New York–Heidelberg–Berlin 1978.

Dettler, J. C.: Biochemical variation. In: Textbook of Human Genetics, eds Fraser, O., Mayo, O., Blackwell Scientific Publications, Oxford 1975, p. 115.

*Tables and illustrations*

Tables should be comprehensible to the reader without reference to the text. The headings should be typed above the table.

Figures should be identified by number and authors' name. The top should be indicated on the back. Their approximate place should be indicated in the text. Captions should be provided on a separate page.

*Proofs and reprints*

Reprints and proofs will be sent to the first author unless otherwise indicated. Proofs should be returned within 48 hours of receipt. Fifty reprints of each paper will be supplied free of charge.